# ORGANOMETALLIC $P_n$-LIGAND COMPLEXES AS SUPRAMOLECULAR BUILDING BLOCKS

Dissertation zur Erlangung des
Doktorgrades der Naturwissenschaften (Dr. rer. nat.)
der Naturwissenschaftlichen Fakultät IV - Chemie und Pharmazie
der Universität Regensburg


vorgelegt von

**Laurence John Gregoriades**

aus Nicosia, Zypern

**Regensburg 2006**

Diese Arbeit wurde angeleitet von Prof. Dr. Manfred Scheer.

Promotionsgesuch eingereicht am: 2 Februar 2006
Tag der mündlichen Prüfung: 7 März 2006

Vorsitzender: Prof. Dr. Henri Brunner
Prüfungsausschuss: Prof. Dr. Manfred Scheer
Prof. Dr. Rainer Winter
Prof. Dr. Ruth Gschwind

Die vorliegende Arbeit wurde in der Zeit von September 2001 bis März 2004 am Institut für Anorganische Chemie der Universität Karlsruhe (TH) und von April 2004 bis Januar 2006 am Institut für Anorganische Chemie der Universität Regensburg unter Anleitung von Herrn Prof. Dr. Manfred Scheer angefertigt.

*To my two families*

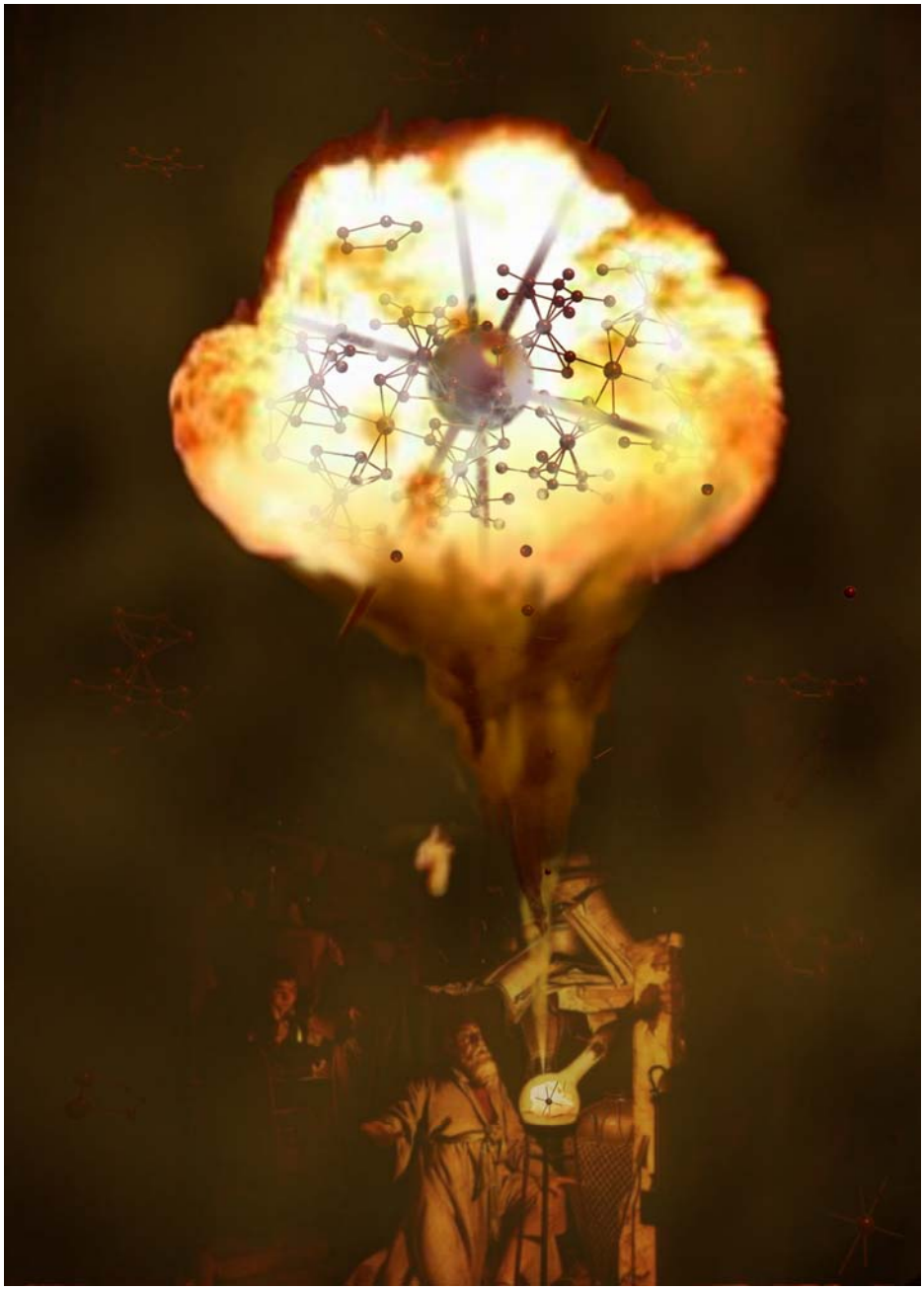

*Regensburger Alchemie*, Roswitha Neumann, **2006** (modified illustration of *The Alchymist, In Search of the Philosopher's Stone, Discovers Phosphorus, and prays for the successful Conclusion of his operation, as was the custom of the Ancient Chymical Astrologers*, Joseph Wright of Derby, **1771**, taken from http://www.ibiblio.org/wm/paint/auth/wright/).

*"One lesson we learn is that when pure science is being done, and sometimes long after it is done, it is usually impossible to predict what the consequences will be. This shows how important it is to support pure science even if it has no obvious consequences. The important criterion should be the quality of the work, not its possible practical applications."*

Keith J. Laidler, *To Light Such a Candle*, Oxford University Press, Oxford, **1998**

# Contents

# 1. Introduction

Supramolecular chemistry[1] has been masterfully implemented by Nature since the beginning of time and is most brilliantly embodied in the hydrogen-bonded structure of the substance that forms the essence of life itself, deoxyribonucleic acid (DNA, Figure 1.1). It is the chemistry involving the construction of molecular assemblies from discrete units by using weak, non-covalent interactions. In addition to hydrogen bonding, these interactions include van der Waals forces, Coulombic interactions and dipole-dipole interactions, and Nature skilfully manipulates these delicate tools to elegantly construct a plethora of other biomolecules and macromolecules. Furthermore, biological processes, for instance, oxygen transport and enzymolysis, are governed by the capacity of particular proteins to efficiently exercise control over metal coordination environments. In contrast to Nature, the scientific community's involvement with supramolecular systems spans a mere four decades and its contributions are relatively modest. Nevertheless, it soon became evident that the study of supramolecules is not only of great interest to biologists and chemists, but also to physicists and engineers, and that it clearly defies the traditional boundaries of science, emerging as a true interdisciplinary field which is at the vanguard of current scientific research.

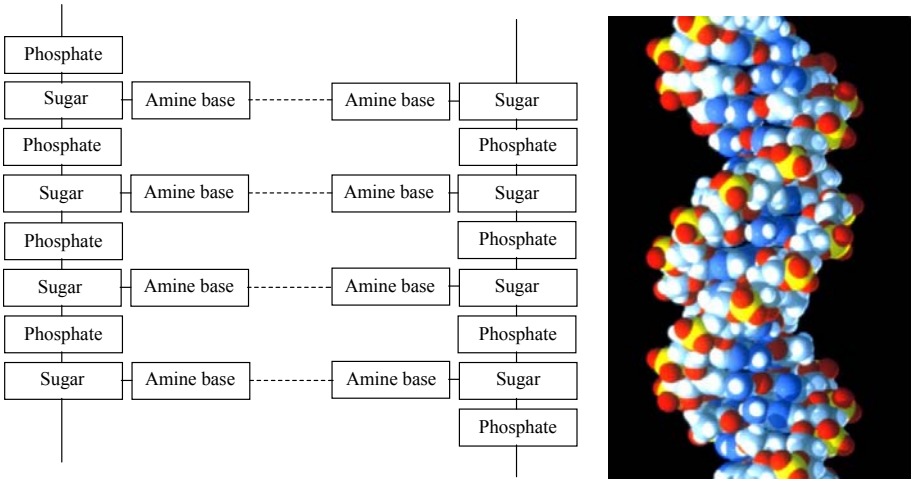


Figure 1.1. Schematic representation (left) and computer-generated structure (right, taken from http://de.wikipedia.org/wiki/Bild:DNA.jpg) of DNA. Hydrogen-bonding interactions between the amine bases of two separate sugar-phosphate strands result in the double helix structure.

Despite the infancy of this field, supramolecular chemists have succeeded in creating a vast array of remarkable architectures by using, in particular, a simple yet effective synthetic concept based on metal centres and coordination chemistry, and have demonstrated the potential of such structures in molecular recognition and transport, catalysis, light harvesting, molecular electronics and the construction of molecular machines.[2] The aforesaid concept, also referred to as 'metal-directed synthesis' or 'metal-mediated self-assembly,' is the most widely used strategy in the synthesis of supramolecules and involves the combination of coordinatively unsaturated metals and suitable ligands. In such reactions, weak dative bonding interactions generally lead to the often spontaneous self-assembly of a variety of coordination compounds ranging from discrete structures such as polygons, polyhedra, bowls and cages to extended arrays including 1D, 2D and 3D polymers, grids and networks (Figure 1.2). Moreover, this panoply of structures is usually accessible in high yields and under mild conditions, two decisive factors in synthetic chemistry.

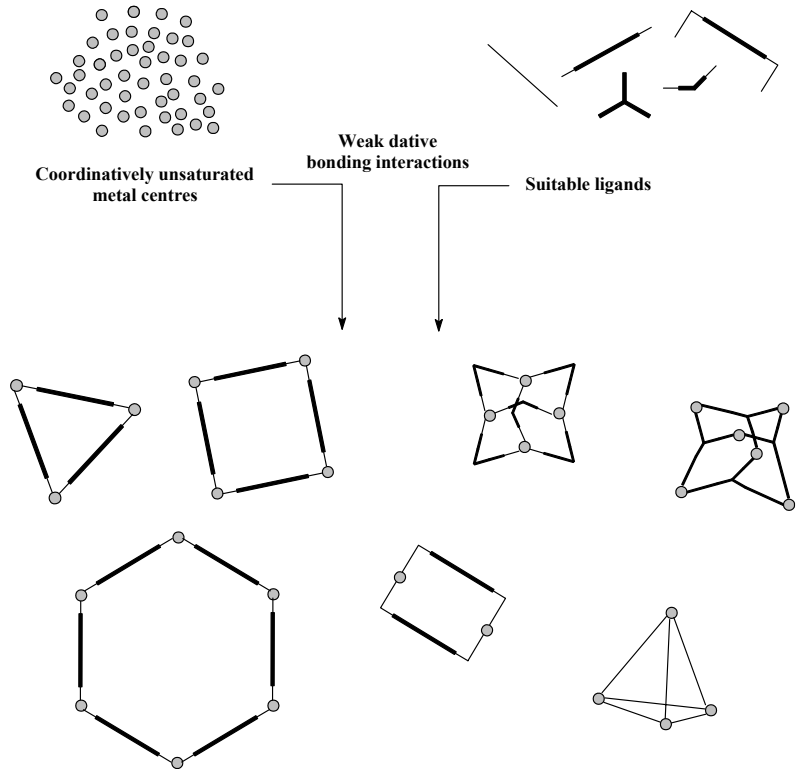


Figure 1.2. Selected structures accessible by weak dative bonding interactions between coordinatively unsaturated metals and suitable ligands.

The supramolecular structures mentioned above are most frequently synthesised using nitrogen, oxygen and sulphur donor ligands. The use of phosphorus donor ligands, on the other hand, is less common and generally limited to organophosphine ligands.[3] Organometallic $P_n$-ligand complexes,[4] that is, complexes containing substituent-free or 'naked' P atoms, have been shown to function as phosphorus donor ligands and are thus appealing candidates for use as building blocks in the construction of supramolecules. This fascinating class of compounds is a result of the pioneering work of Dahl and co-workers,[5] Ginsberg and Lindsell,[6] and Sacconi and co-workers.[7] Dahl and co-workers published their results at a time when dinitrogen complexes were already known and a subject of intense investigation, whereas analogous compounds of the heavier pnicogens were unknown. Although the published compounds $[Co(CO)_3(\eta^3\text{-}As_3)]$ **1**[5a] and $[Co_2(CO)_6(\mu,\eta^2\text{-}As_2)]$ **2**[5b] (Figure 1.3) are actually $As_n$-ligand complexes,[4c-g] they provided chemists with the incentive to synthesise analogous $P_n$-ligand complexes. The efforts of Ginsberg and Lindsell were soon rewarded in the early 1970s with the isolation of $[ClRh(L)_2(\eta^2\text{-}P_4)]$ **3a-d** (Figure 1.4), complexes containing a dihapto-coordinated, and thus distorted, tetraphosphorus unit. Shortly after, Markò and co-workers isolated the compound $[Co_2(CO)_6(\mu,\eta^2\text{-}P_2)]$ **4**,[8] the P analogue of compound **2**, and it was not until the end of the 1970s that Sacconi and co-workers were able to isolate $[(np_3)Ni(\eta^1\text{-}P_4)]$ **5**[7a] ($np_3$ = $N(CH_2CH_2PPh_2)_3$, Figure 1.4), a complex

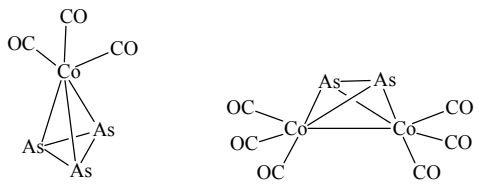


**1** **2**

Figure 1.3. The early $As_n$-ligand complexes of Dahl and co-workers.

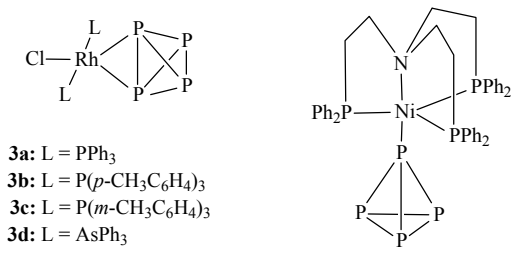


**3a:** L = $PPh_3$
**3b:** L = $P(p\text{-}CH_3C_6H_4)_3$
**3c:** L = $P(m\text{-}CH_3C_6H_4)_3$
**3d:** L = $AsPh_3$

**5**

Figure 1.4. The $P_4$-ligand complexes of Ginsberg and Lindsell (**3**) and Sacconi and co-workers (**5**).

containing an intact $P_4$ tetrahedron. Since then, the class of $P_n$-ligand complexes has developed into one rich with compounds of astonishing structural diversity and includes the tetrahedrane complexes $[Cp^x{}_2M_2(CO)_4(\mu,\eta^2\text{-}P_2)]$ **6a-e**[9] and $[Cp^xM(CO)_2(\eta^3\text{-}P_3)]$ **7a-f**,[9a-e,10] the complexes $[Cp^xM(CO)_2(\eta^4\text{-}P_4)]$ **8a**,**b**,[11] the sandwich complexes $[Cp^xM(\eta^5\text{-}P_5)]$ **9a-h**,[12] and the triple-decker sandwich complexes $[(Cp^xCr)_2(\mu,\eta^5\text{-}P_5)]$ **10a**,**b**[13] and $[(Cp^xM)_2(\mu,\eta^6\text{-}P_6)]$ **11a-d**[9e,g] (Table 1.1). The complexes **9a**, **10b** and **11c** were the first of their kind to be

Table 1.1. Selected examples of $P_n$-ligand complexes.

| Structure | $Cp^x$ | M | Compound[Reference] |
|---|---|---|---|
| 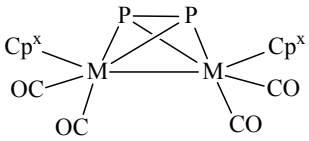 | Cp | Cr | **6a**[9a,b] |
| | Cp | Mo | **6b**[9c,d] |
| | Cp* | Mo | **6c**[9e] |
| | Cp | W | **6d**[9f] |
| | Cp* | W | **6e**[9g] |
| 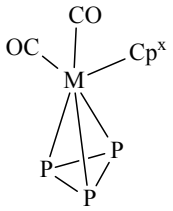 | Cp | Cr | **7a**[9a,b] |
| | Cp | Mo | **7b**[9c,d,10] |
| | Cp* | Mo | **7c**[9e] |
| | Cp´ | Mo | **7d**[10a] |
| | Cp´´ | Mo | **7e**[10a] |
| | Cp* | W | **7f**[9g,10b] |
| 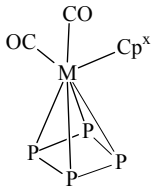 | Cp* | Nb | **8a**[11a] |
| | Cp´´ | Ta | **8b**[11b] |
| 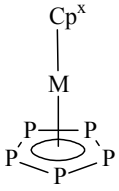 | Cp* | Fe | **9a**[12a-c] |
| | $Cp^{Et}$ | Fe | **9b**[12d] |
| | Cp´´ | Fe | **9c**[10a,12e] |
| | Cp´´´ | Fe | **9d**[12f] |
| | Cp* | Ru | **9e**[12d,g] |
| | $Cp^{Et}$ | Ru | **9f**[12d,g] |
| | Cp* | Os | **9g**[12g] |
| | $Cp^{Et}$ | Os | **9h**[12g] |

| | | | |
|---|---|---|---|
| 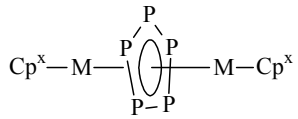 | Cp | Cr | **10a**[13a] |
| | Cp* | Cr | **10b**[13b] |
| 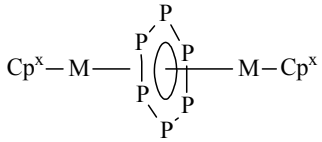 | Cp* | V | **11a**[9g] |
| | $Cp^{Et}$ | V | **11b**[9g] |
| | Cp* | Mo | **11c**[9e] |
| | Cp* | W | **11d**[9g] |

isolated and can undoubtedly be considered as milestones in the field of $P_n$-ligand complex research. Compounds **9a** and **10b** contain the *cyclo*-$P_5$ anion and **11c** hexaphosphabenzene, the all-phosphorus analogues of the cyclopentadienide anion and benzene, respectively, and thus beautifully demonstrate the isolobality of P atoms and CH fragments.

The compounds listed in Table 1.1 are all neutral, but there are also examples of ionic $P_n$-ligand complexes, such as the monocationic triple-decker sandwich complexes $[CpFe(\mu,\eta^5\text{-}P_5)FeCp^x]^+$ **12a**,**b**[14] and the recently reported dianionic sandwich complex $[Ti(\eta^5\text{-}P_5)_2]^{2-}$ **13**[15] (Figure 1.5) which, surprisingly, is described as air-stable although it is formally a 16VE $Ti^0$ complex. The discovery of the 'carbon-free' metallocene **13** is, without question, one of great significance and will undoubtedly fuel the efforts of chemists around the world who are striving to 'bake' new 'bread' for that 'old sandwich,' ferrocene.

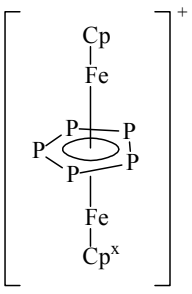

**12a:** $Cp^x = Cp^*$
**12b:** $Cp^x = Cp^{Et}$

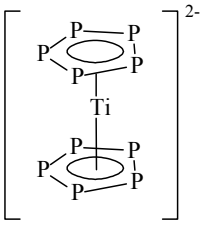

**13**

Figure 1.5. Examples of ionic $P_n$-ligand complexes.

As the family of $P_n$-ligand complexes began to expand, researchers in the field became interested in the reactivity of these intriguing compounds. Many $P_n$-ligand complexes have been isolated as adducts of the neutral Lewis-acidic 16 VE $M(CO)_5$ (M = Cr, Mo, W) fragments, thus revealing the Lewis basicity of the P atoms in these compounds.[16] The ligating potential of these complexes is also evidenced in examples of greater elegance. Scherer and co-workers have demonstrated that the reaction of **6b** with $[Re_2(CO)_6(\mu\text{-}Br)_2(THF)_2]$ in $CH_2Cl_2$ leads to **14**.[16b] Interestingly, in THF, **14** rearranges to **15** thus leading to the formation of a six-membered $Re_2P_4$ ring (Figure 1.6).

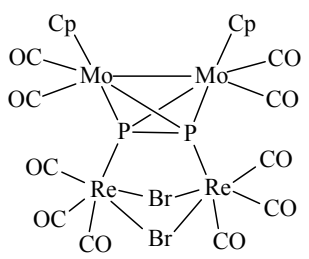


**14**

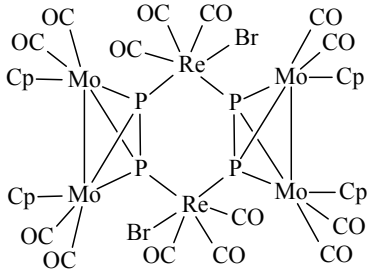


**15**

Figure 1.6. The first compounds reported containing the $P_n$-ligand complex **6b** as a ligand.

Stoppioni and co-workers have shown that the $P_n$-ligand complexes [(tppme)M($\eta^3$-$P_3$)] (tppme = $CH_3C(CH_2PPh_2)_3$; M = Co, Rh, Ir) react with $Cu^I$, $Ag^I$ and $Au^I$ salts of weakly coordinating anions (WCAs) to yield the trinuclear cationic complexes $[\{(tppme)M(\eta^3\text{-}P_3)\}_2M']^+$ **16a-f**[17] (M′ = Cu, Ag, Au; Figure 1.7) in which coordination of M′ to two P─P edges, each from a different *cyclo*-$P_3$ unit, is observed. Furthermore, reaction of [(tppme)Ir($\eta^3$-$P_3$)] with CuBr has been shown by Ghilardi and co-workers to lead to the remarkable ionic compound $[\{(tppme)Ir(\eta^3\text{-}P_3)\}_3Cu_5Br_4][CuBr_2]$ **17** (Figure 1.7), in which the Cu atoms are found in three different coordination environments.[18] In the cation of **17**, the Cu atoms are in trigonal and tetrahedral coordination modes, whereas in $[CuBr_2]^-$, the coordination mode is essentially linear. The same authors have also reported the 'super-sandwich' $[\{(tppme)Co(\eta^3\text{-}P_3)\}_2(CuBr)_6]$ **18** (Figure 1.7) in which a hexagonal $Cu_6Br_6$ moiety is sandwiched between two [(tppme)Co($\eta^3$-$P_3$)] complexes.[19]

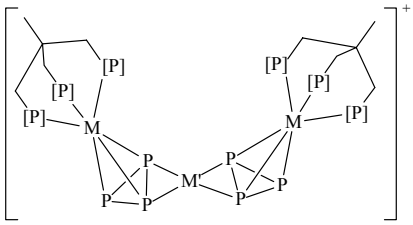

[P] = $PPh_2$

**16a:** M = Co, M' = Cu
**16b:** M = Co, M' = Ag
**16c:** M = Co, M' = Au
**16d:** M = Rh, M' = Ag
**16e:** M = Rh, M' = Au
**16f:** M = Ir, M' = Au

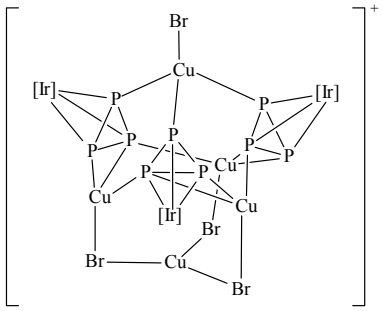

[Ir] = (tppme)Ir

**17**

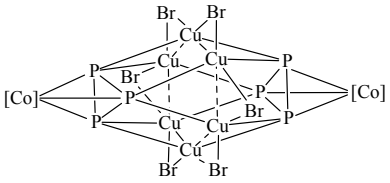

[Co] = (tppme)Co

**18**

Figure 1.7. Compounds containing the $P_n$-ligand complexes [(tppme)M($\eta^3$-$P_3$)] (M = Co, Rh, Ir).

$P_n$-ligand complexes have been subjected to various other reactivity studies. Due to their analogy with ferrocene, investigations on the complexes [$Cp^xFe(\eta^5$-$P_5)$] **9a-d** (Table 1.1) have been particularly intensive. Compounds **9a**,**b** react with [$CpFe(\eta^6$-$C_6H_6)$]$PF_6$ to yield the cationic triple-decker complexes **12a**,**b** (Figure 1.5).[14] In addition, **9a** has been shown to react with [$M(CO)_3(NCMe)_3$] (M = Cr, Mo) under formation of the binuclear complexes [$Cp^*Fe(\mu,\eta^5$-$P_5)M(CO)_3$] **19a**,**b**[20] (Scheme 1.1), while reaction with [{$Cp^*Ir(CO)$}$_2$] yields the compounds **20-22**[12c,21] (Scheme 1.1), depending on the reaction conditions. In complex **20**, the *cyclo*-$P_5$ unit coordinates in a $\eta^2$ side-on fashion to the Ir atom and the planarity of this unit is maintained, whereas in **21** and **22**, distortion from planarity and, in the case of **22**, even bond cleavage is observed. Distortion from planarity and bond cleavage of the *cyclo*-$P_5$ unit is also observed in **23-25**[21,22] (Scheme 1.1), the products resulting from the reaction of **9a** with [Cp´´$Ta(CO)_4$]. A range of polynuclear clusters has also been isolated by the reaction of **9a** with [{$Cp^xCo(CO)$}$_2$],[23] [$Cp^*Mo(CO)_3CH_3$][24] and [{Cp´´$Ru(CO)_2$}$_2$][25] and are shown in Scheme 1.2. Most of these clusters demonstrate that the *cyclo*-$P_5$ unit of **9a** has undergone fragmentation.

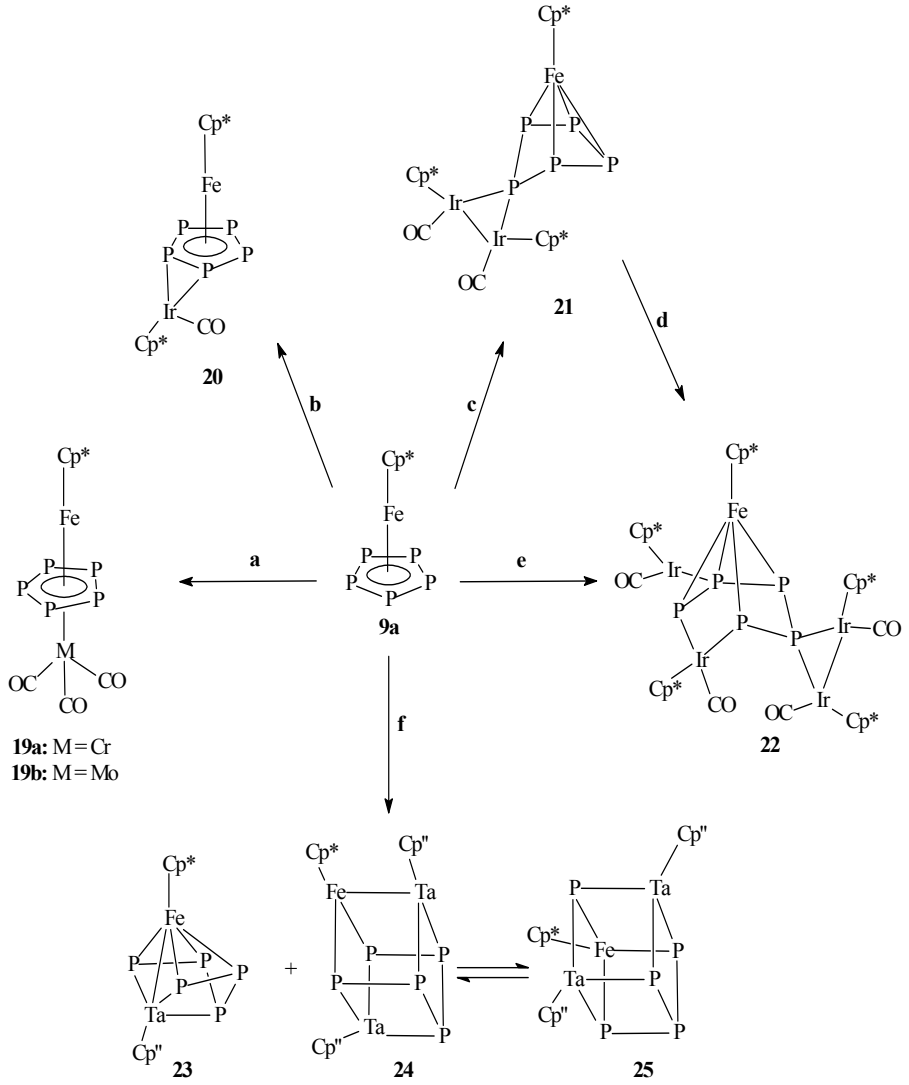


Scheme 1.1. Selected reactions of **9a** with organometallic compounds, demonstrating simple coordination, distortion and bond cleavage of the *cyclo*-$P_5$ moiety (**a**: $[M(CO)_3(NCMe)_3]$ (M = Cr, Mo), $CH_2Cl_2$; **b**: $[\{Cp^*Ir(CO)\}_2]$, toluene, *hv*; **c**: $[\{Cp^*Ir(CO)\}_2]$, toluene, 110 °C; **d**: $[\{Cp^*Ir(CO)\}_2]$, toluene, 25 °C; **e**: $2[\{Cp^*Ir(CO)\}_2]$, toluene, 25 °C; **f**: $[Cp''Ta(CO)_4]$, decalin, 190 °C).

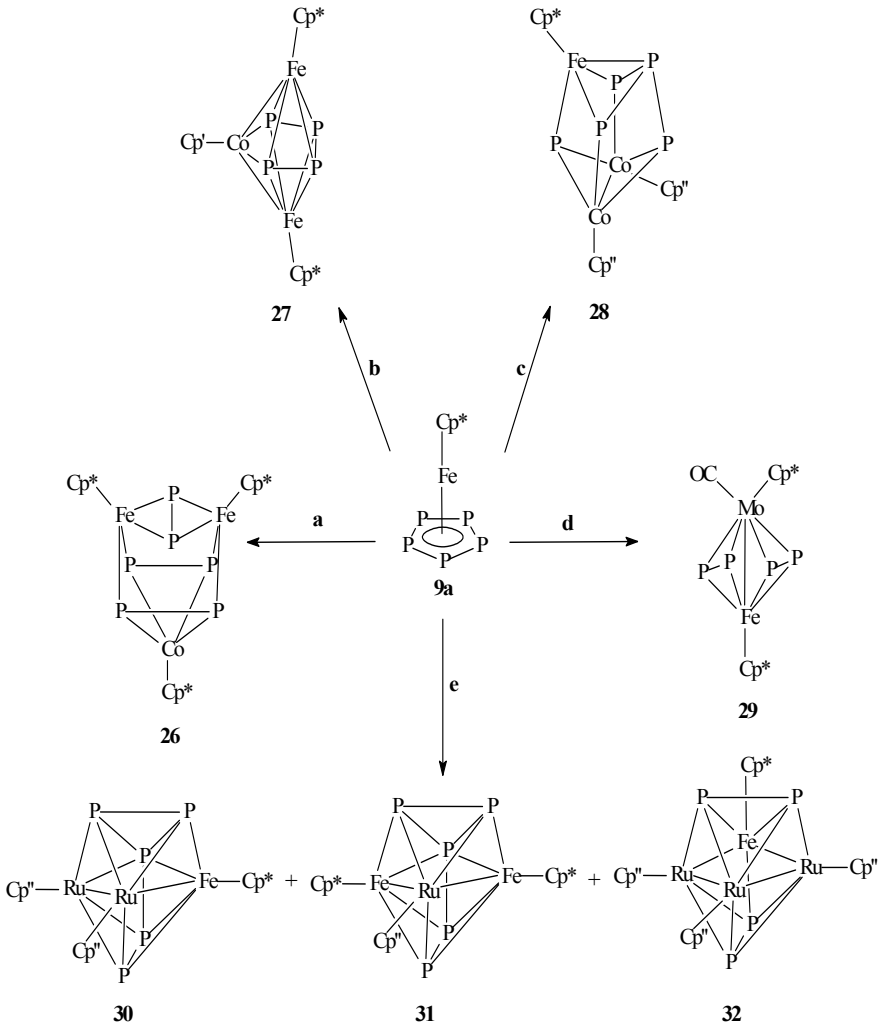


Scheme 1.2. Selected reactions of **9a** with organometallic compounds, demonstrating distortion, bond cleavage and fragmentation of the *cyclo*-$P_5$ moiety (**a**: [{Cp*Co(CO)}$_2$], decalin, 190 °C; **b**: [{Cp´Co(CO)}$_2$], decalin, 190 °C; **c**: [{Cp´´Co(CO)}$_2$], decalin, 190 °C; **d**: [Cp*Mo(CO)$_3$CH$_3$], xylene, reflux; **e**: [{Cp´´Ru(CO)$_2$}$_2$], decalin, 190 °C).

Winter and Geiger have explored the redox reactions of several $P_n$-ligand complexes by electrochemical methods[26] and the results of their investigations on **9a**[26a] suggest dimerisation upon oxidation and reduction to give a dication **33** and a dianion **34**, respectively, the proposed structures of which are shown in Figure 1.8.

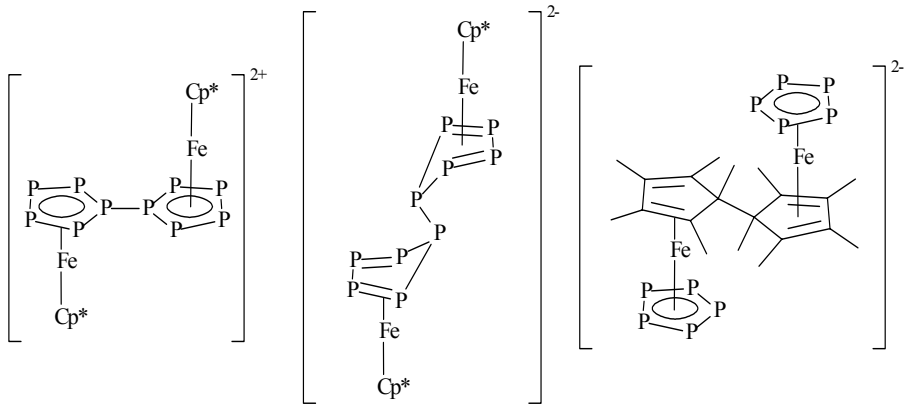

**33** **34a** **34b**

Figure 1.8. Structures proposed for the cationic (**33**) and anionic (**34**) species resulting from electrochemical oxidation and reduction, respectively, of the complex **9a**.

Mays and co-workers have demonstrated that the complexes **6b**,**d** react with alkali metal hydroxides and yield the phosphido complexes $[Cp_2M_2(CO)_4(\mu\text{-}PH_2)(\mu\text{-}H)]$ **35a**,**b** (M = Mo, W) upon protonation with $HBF_4$.[9f] The authors further demonstrated that the resulting phosphido complexes, after treatment with *t*-BuLi, can be reacted with Group 15 trichlorides $ECl_3$ (E = P, As, Sb) to yield the complexes **6b**,**d** when E = P, and the complexes $[Cp_2M_2(CO)_4(\mu,\eta^2\text{-}EP)]$ **36a-d** when E = As, Sb (Scheme 1.3).[27]

Reactivity studies conducted in the Scheer group on the complex **6a** with $LiBEt_3H$ have shown that in addition to compound **37**, the Cr analogue of **35**, the compounds $[Cp_2Cr_2(CO)_4(\mu\text{-}PH_2)_2]$ **38** and $[\{Cp_2Cr_2(CO)_4(\mu\text{-}PH_2)\}\{(CpCr)_2(\mu,\eta^1\text{:}\eta^1\text{:}\eta^5\text{:}\eta^5\text{-}P_5)\}]$ **39** (Scheme 1.3) can be isolated.[28] Compound **39** consists of a triple-decker sandwich structure with a distorted *cyclo*-$P_5$ middle deck. Furthermore, complex **6a** reacts with $PCl_3$ or $PCl_5$ to yield the known complex **7a**, whereas with $ECl_3$ (E = As, Sb) a mixture of **7a** and the new complexes $[CpCr(CO)_2(\eta^3\text{-}EP_2)]$ **40a**,**b** (Scheme 1.3) are isolated.[29] Besides, the mixed chalcogen-pnicogen trinuclear clusters **41a**,**b** (Figure 1.9) were obtained upon reaction of **7a** with $[Fe_3(CO)_9(\mu_3\text{-}Y)_2]$ (Y = S, Se) in the presence of trimethylamine oxide.[30]

Further reactivity studies on $P_n$-complexes have shown that these complexes can undergo a variety of functionalisation reactions in which alkylation of the P atoms, CO and carbene insertion across the P─P and P─M bonds of these complexes, and coupling of alkynes and phosphalkynes with $P_n$-units can occur.[31]

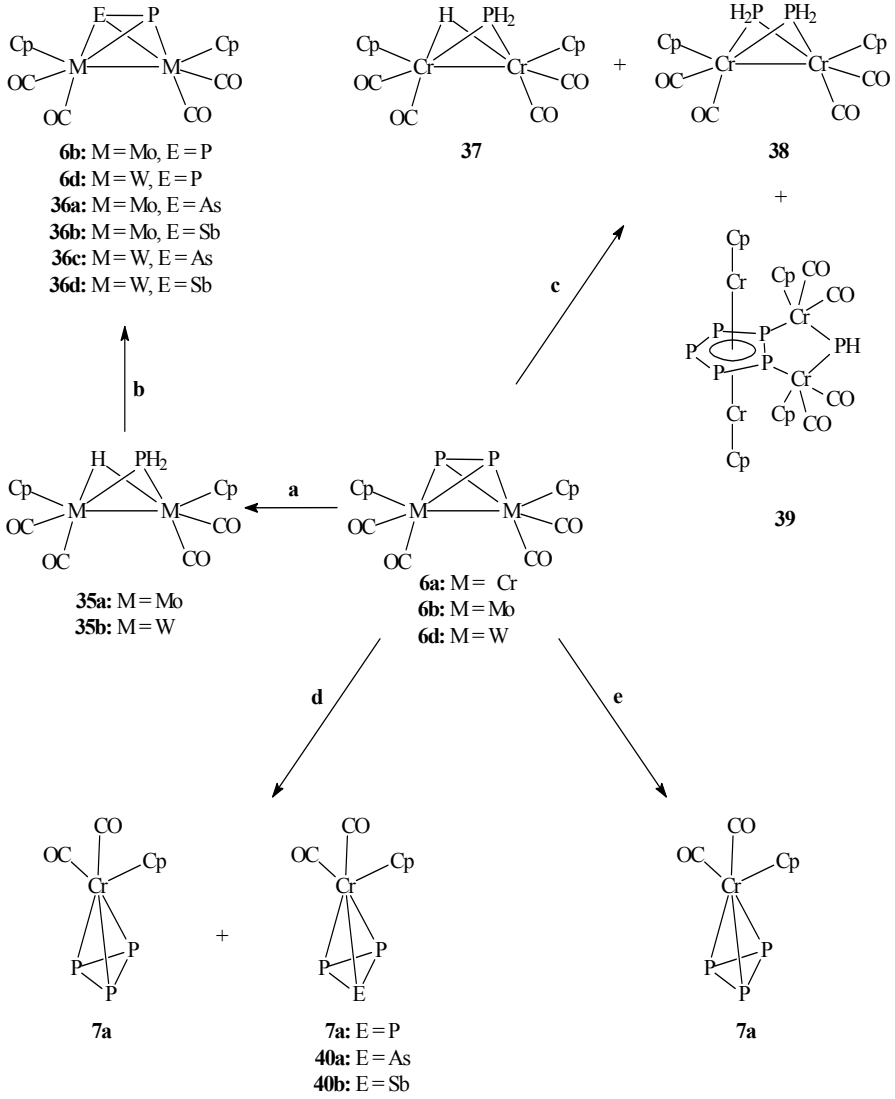


Scheme 1.3. Selected reactivity studies on the complexes **6a**,**b**,**d** (**a**: 1. $HO^-$, 80 °C; 2. $HBF_4$; **b**: 1. *t*-BuLi; 2. $ECl_3$; **c**: $LiBEt_3H$, THF, –78 °C; **d**: $ECl_3$, RT; **e**: $PCl_5$, $CH_2Cl_2$, RT).

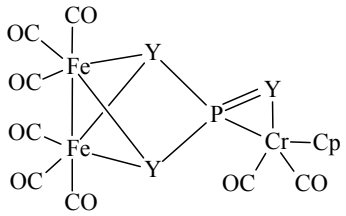


**41a:** Y = S
**41b:** Y = Se

Figure 1.9. The mixed chalcogen-pnicogen trinuclear clusters **41a**,**b** resulting from the reaction of **7a** with $[Fe_3(CO)_9(\mu_3\text{-}Y)_2]$ (Y = S, Se) in the presence of trimethylamine oxide.

The examples described so far lay bare the multi-faceted reactivity of $P_n$-ligand complexes. Surprisingly, even though the coordinating capacity of these complexes had been clearly demonstrated by the mid 1980s, their potential as supramolecular building blocks was not considered in earnest until the beginning of this millennium. By exploiting this potential, the Scheer group demonstrated that **6b** could be used to synthesise not only the discrete structures **42a-c**,[32] but also the well-defined 1D polymers **43a-c**[32a,33] and **44**[32a] (Figure 1.10). Compounds **42a-c**, formed upon reaction of **6b** with $CuPF_6$,[32b] $AgBF_4$[32b] and AgOTf,[32a] respectively, consist of dications which are the first examples of structures featuring units of **6b** in both a novel side-on and a bridging coordination mode. The polymers **43a-c** are formed by reaction of **6b** with CuX (X = Cl, Br, I) and display a 1D chain structure consisting of an alternating arrangement of four-membered $Cu_2X_2$ and six-membered $Cu_2P_4$ rings which are nearly perpendicular to one another. Reaction of **6b** with $AgNO_3$ leads to polymer **44**, which consists of a cationic undulated chain built up of six-membered $Ag_2P_4$ rings that are bridged by a unit of **6b** and a nitrate ion to form seven-membered $Ag_2NO_2P_2$ rings.

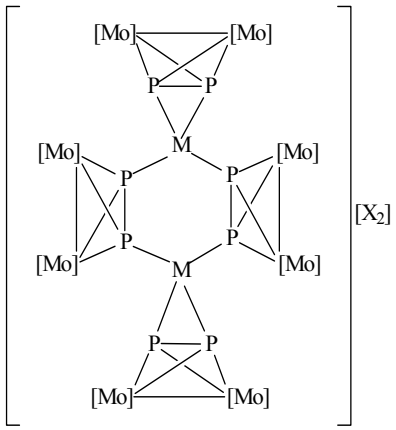


**42a:** M = Cu, X = $PF_6$
**42b:** M = Ag, X = $BF_4$
**42c:** M = Ag, X = OTf

[Mo] = $CpMo(CO)_2$

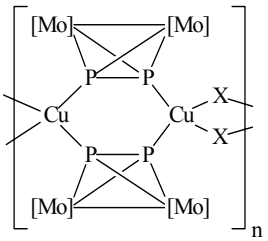


**43a:** X = Cl
**43b:** X = Br
**43c:** X = I

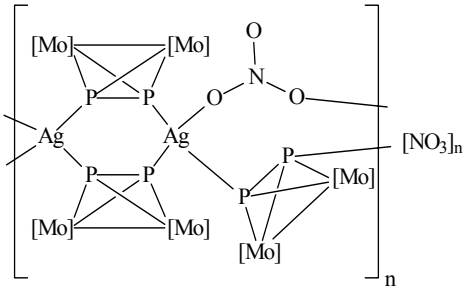


**44**

Figure 1.10. The supramolecular aggregates obtained by the Scheer group using **6b**.

The Scheer group have also investigated the reactivity of **9a** with $Cu^{I}$ halides[34] and found that with CuCl the 1D polymer **45** (Figure 1.11) is obtained,[34a] whose core structure is similar to that of the polymers **43a-c**. With CuBr and CuI, however, the corrugated 2D polymers **46a**,**b** (Figure 1.11), respectively, are obtained.[34a]

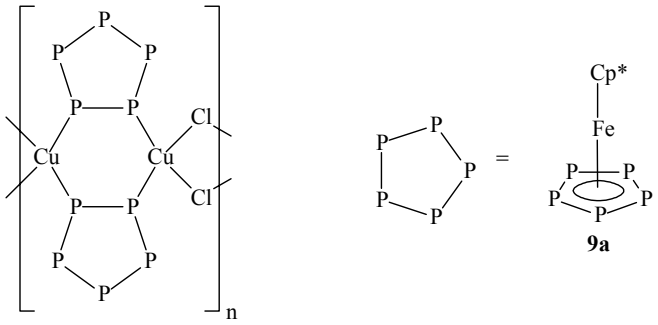


**45** **9a**

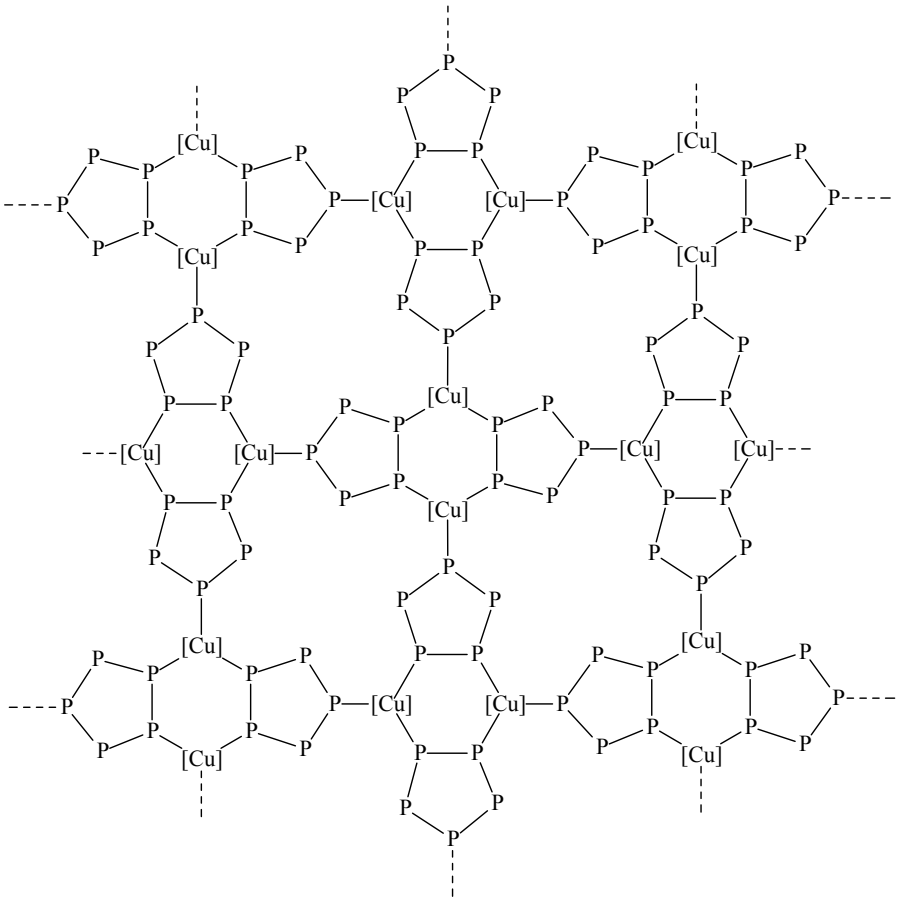


**46a:** X = Br
**46b:** X = I

Figure 1.11. The 1D and 2D polymers obtained by the Scheer group using **9a**.

Although the latter two halides provided essentially quantitative yields of the respective polymers, the yield in the case of the chloride derivative was about 50%. Eventually, the remarkable fullerene-like aggregate **47** (Figure 1.12) was isolated from the mother liquor.[34b] This compound consists of *cyclo*-$P_5$ moieties surrounded by six-membered $Cu_2P_4$ rings, a polygon arrangement characteristic of the fullerenes. The inner diameter of this coordination fullerene-like nanoball is about 13 Å and one could thus imagine the fullerene $C_{60}$ (outer diameter ≈ 7 Å) acting as a template for the construction of **47**.

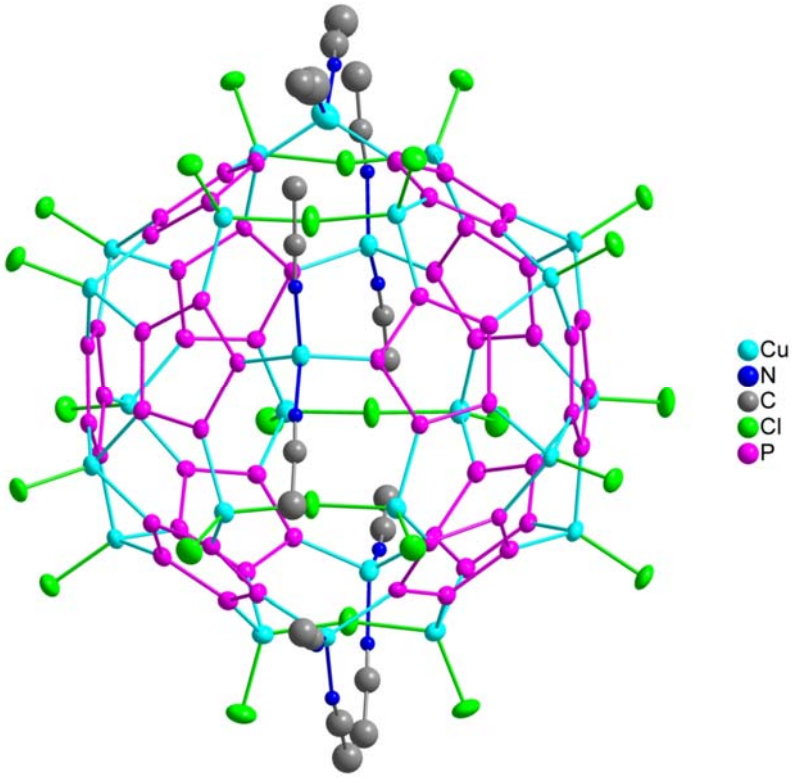


Figure 1.12. Structure of the coordination fullerene-like nanoball **47** (Cp*Fe fragments and hydrogen atoms omitted for clarity). Thermal ellipsoids are represented at the 50 % probability level.

Following appropriate alterations to the stoichiometry and dilution of the reactants, the reaction conditions for the synthesis of **47** could be optimised. These optimisations were important for the synthesis of another nanoball, with the same core structure as **47**, based on **9b** and CuBr.[35]

# 2. Research Objectives

The results obtained so far by the Scheer group[32-35] have demonstrated the potential of $P_n$-ligand complexes in supramolecular chemistry and have set new perspectives in $P_n$-ligand complex research. With this in mind, it was deemed exigent to investigate the aptitude of $P_n$-ligand complexes as supramolecular building blocks further and to examine the properties of the resulting aggregates in greater depth with the assistance of various techniques including NMR and IR spectroscopy, mass spectrometry and X-ray crystallography. Thus, the objectives of this work were as follows:

- Extension of the palette of coordination aggregates based on $[Cp_2Mo_2(CO)_4(\mu,\eta^2\text{-}P_2)]$ **6b** and $[Cp^*Fe(\eta^5\text{-}P_5)]$ **9a** by probing their reactivity in the presence of other transition metal salts and complexes.
- Use of the salt $Ag[Al\{OC(CF_3)_3\}_4]$[36] with the purpose of obtaining coordination aggregates with improved solubility and thus facilitating the investigation of the solution behaviour of such systems.
- Determination of the suitability of previously unexplored $P_n$-ligand complexes as building blocks for supramolecular architectures.
- Preliminary investigations into the potential of $As_n$-[4c-g] and $P_mS_n$-ligand[4e,37] complexes as connecting moieties in supramolecular chemistry.

# 3. Results and Discussion

## 3.1. The Tetrahedrane Cluster $[Cp_2Mo_2(CO)_4(\mu,\eta^2\text{-}P_2)]$ as a Ligand

The Scheer group began their investigations into the potential of $P_n$-ligand complexes as ligands in supramolecular chemistry with the tetrahedrane complex $[Cp_2Mo_2(CO)_4(\mu,\eta^2\text{-}P_2)]$[9c,d] **6b**. Reactions of **6b** with $CuPF_6$ and AgX (X = $BF_4$, OTf) yield the sparingly soluble products **42a-c** (Figure 1.10),[32] which, surprisingly, display only one singlet in their solution $^{31}$P-NMR spectra. Reactions of **6b** with CuX (X = Cl, Br, I) and $AgNO_3$ yield the insoluble polymers **42a-c**[32a,33] and **44**[32a] (Figure 1.10). It was therefore considered pertinent to investigate the reactivity of **6b** towards $Ag^I$ salts of other weakly coordinating anions (WCAs) and coordinating anions as well as coordinatively unsaturated transition metal species in order to establish whether novel supramolecular structures could be created.

### 3.1.1. Studies on the Reactivity of $[Cp_2Mo_2(CO)_4(\mu,\eta^2\text{-}P_2)]$ with $Ag^I$ Salts

Reactions of **6b** with AgX (X = $ClO_4$, $PF_6$, $SbF_6$, $[Al\{OC(CF_3)_3\}_4]$[36]) in a 2:1 stoichiometry in, depending on the anion, $CH_3CN$, $CH_2Cl_2$, or mixtures of these two solvents, yield the products **42d-g** (Equation 3.1) as air- and light-sensitive red-orange crystalline solids. Compounds **42d-f** are only sparingly soluble in polar solvents such as $CH_3CN$. In contrast, **42g** is readily soluble in solvents such as $CH_2Cl_2$, THF and $CH_3CN$, most likely due to the large perfluoroalkoxyaluminate anion.

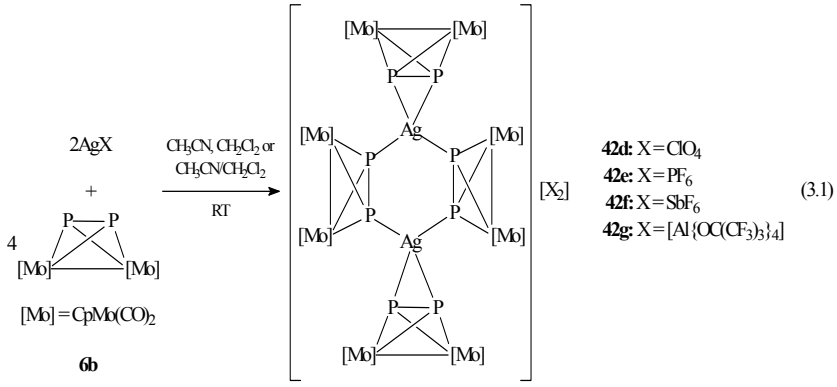


(3.1)

The compounds **42d-g** have all been characterised by single crystal X-ray crystallography and are similar to the previously synthesised complexes **42b**,**c**[32] in that they consist of a dication well-separated from the anions. The structure of the dication in **42g** is shown in Figure 3.1 and is representative of the structures of the dications in compounds **42d-f**. Selected structural details for the compounds **42b-g** are listed in Table 3.1. The P─P bond lengths of the bridging units of **6b** in the complexes are somewhat longer than that of uncoordinated **6b** (2.079(2) Å),[9c] whereas those of the side-on coordinated units of **6b** are significantly longer. The Ag─$P_s$ ($P_s$ = P atom of side-on coordinated unit of **6b**) bond lengths are comparable to the Ag─P bond lengths found in previously reported $[Ag(PPh_3)_4]^+$ salts (2.631(5)-2.746(5) Å)[38] whereas the Ag─$P_b$ ($P_b$ = P atom of bridging unit of **6b**) bond lengths are noticeably shorter. As in **42b**,**c**, the coordination mode of the Ag atoms in the compounds **42d-g** seems to be tetrahedral, but after consideration of the relevant bond angles ($P_b$─Ag─$P_b$ ≈ 120°; $P_s$─Ag─$P_s$ < 50°) and bond lengths ($P_s$─$P_s$ > $P_b$─$P_b$), it is best described as trigonal since the Ag atoms appear to be bonded to four P atoms via two $\sigma$-bonds and one $\pi$-bond.

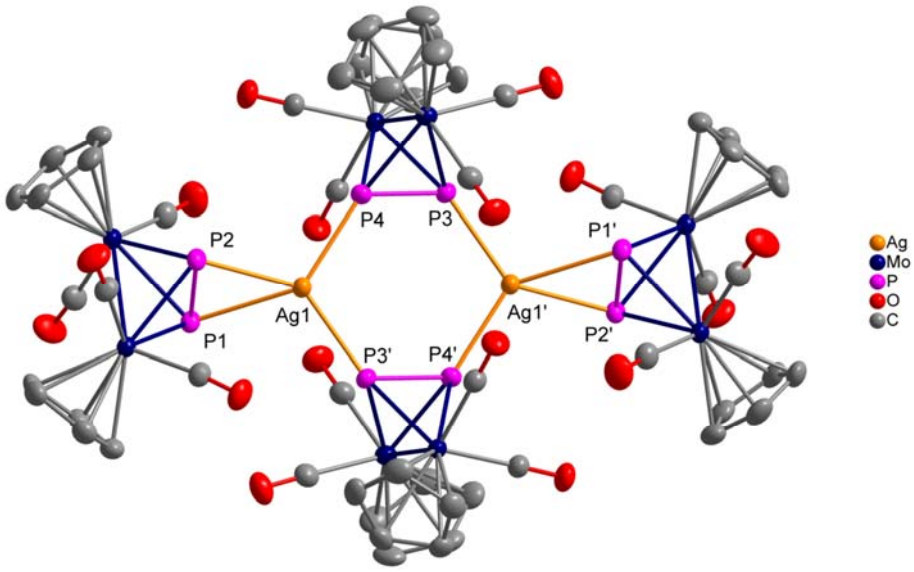


Figure 3.1. Structure of the dication in **42g** (hydrogen atoms omitted for clarity). Thermal ellipsoids are represented at the 50 % probability level.

Table 3.1. Selected bond lengths (Å) and angles (°) for compounds **42b-g**.

| Parameter | **42b**[32b] | **42c**[32a] | **42d** | **42e** | **42f** | **42g** |
|---|---|---|---|---|---|---|
| $P_b$─$P_b$[a] | 2.096(4) | 2.098(2) | 2.104(2) | 2.099(1) | 2.097(2) | 2.091(1) |
| $P_s$─$P_s$[a] | 2.136(6) | 2.137(2) | 2.150(1) | 2.145(1) | 2.133(2) | 2.143(1) |
| Ag─$P_b$ | 2.468(4) | 2.470(1) | 2.476(1) | 2.483(1) | 2.481(1) | 2.474(1) |
| | 2.487(4) | 2.489(1) | 2.489(1) | 2.485(1) | 2.502(1) | 2.478(1) |
| Ag─$P_s$ | 2.606(4) | 2.610(1) | 2.621(1) | 2.620(1) | 2.600(1) | 2.580(1) |
| | 2.699(5) | 2.727(2) | 2.676(1) | 2.704(1) | 2.774(1) | 2.685(1) |
| $P_b$─Ag─$P_b$ | 120.28(1) | 120.28(8) | 120.50(4) | 119.95(3) | 118.89(4) | 112.63(3) |
| $P_s$─Ag─$P_s$ | 47.46(1) | 47.45(7) | 47.87(3) | 47.50(3) | 46.63(4) | 47.99(3) |
| $P_b$─Ag─$P_s$ | 98.95(2) | 98.96(8) | 100.30(3) | 99.48(3) | 97.99(4) | 107.88(3) |
| | 108.34(1) | 108.32(8) | 106.80(4) | 106.98(3) | 111.39(4) | 109.28(4) |
| | 130.28(1) | 130.25(8) | 131.07(4) | 132.18(3) | 129.05(4) | 133.42(3) |
| | 131.01(2) | 131.04(8) | 131.68(3) | 132.73(4) | 134.00(4) | 134.43(3) |

$P_b$ = P atom of bridging unit of **6b**; $P_s$ = P atom of side-on coordinated unit of **6b**.
[a] P─P bond length in uncoordinated **6b** = 2.079(2) Å.[9c]

The cores of the dications in **42b-g** comprise six-membered $Ag_2P_4$ rings, which are in a slight chair-conformation. Close examination of the $Ag_2P_4$ rings reveals a dependence of the folding angle (angle between AgPP and PPPP planes) on anion size. The sizes of the folding angles and the radii of the corresponding anions[39] are tabulated below (Table 3.2) and demonstrate that as the size of the anion increases the folding angle decreases, a phenomenon most likely attributable to crystal packing effects.

Table 3.2. Comparison of the anionic radii (Å) and folding angles (°) of the $Ag_2P_4$ rings (angle between AgPP and PPPP planes) in compounds **42b-g**.

| Compound | Anion | Anion Radius | Folding Angle |
|---|---|---|---|
| **42b**[32b] | $BF_4^-$ | 2.05 | 6.05(3) |
| **42d** | $ClO_4^-$ | 2.25 | 6.74(3) |
| **42c**[32a] | $OTf^-$ | 2.30 | 7.08(2) |
| **42e** | $PF_6^-$ | 2.42 | 7.96(3) |
| **42f** | $SbF_6^-$ | 2.52 | 10.11(5) |
| **42g** | $[Al\{OC(CF_3)_3\}_4]^-$ | 6.25 | 20.69(2) |

The room temperature $^{31}$P-NMR spectra of the compounds **42b-g** in $CD_3CN$ display slightly broad singlets which are shifted by about 25-35 ppm upfield compared to uncoordinated **6b** (–43 ppm), depending on the anion, without any detectable coupling to $^{107/109}$Ag (Table 3.3). Considering the solid-state structures of these compounds, one would expect at least two signals in the $^{31}$P-NMR spectra if the integrity of the corresponding dications were maintained in solution. However, the experimental spectra suggest dynamic behaviour in solution which

could not be resolved in previous work for **42b**,**c** even at the lowest temperature possible for measurement with $CD_3CN$ (–30 °C).[32]

Table 3.3. $^{31}$P-NMR chemical shifts (ppm) of the compounds **42b-g** in $CD_3CN$ at room temperature.

| Compound | Chemical Shift | Compound | Chemical Shift |
|---|---|---|---|
| **42b**[32b] | –71.3 | **42e** | –64.2 |
| **42c**[32a] | –69.0 | **42f** | –71.3 |
| **42d** | –59.5 | **42g** | –77.5 |

Positive ion electrospray ionisation mass spectrometry (ESI-MS) measurements on the compounds **42d-g** in $CH_3CN$ at room temperature (Table 3.4) reveal that the peaks with 100 % relative abundance correspond to the monocation $[Ag\{Cp_2Mo_2(CO)_4P_2\}_2]^+$. Other larger fragments, detected in smaller amounts, allude to the presence of the dication observed in the solid state and thus the existence of a dynamic monomer/dimer equilibrium in solution.

Table 3.4. Selected fragments (mass/charge (relative abundance in %)) detected in the positive ion ESI-MS spectra of compounds **42d-g** in $CH_3CN$ and the proposed cations for these fragments.

| **42d** X = $ClO_4$ | **42e** X = $PF_6$ | **42f** X = $SbF_6$ | **42g** X = $Al\{OC(CF_3)_3\}_4$ | **Proposed Cations** |
|---|---|---|---|---|
| – | 3095.2 (0.1) | – | – | $[Ag_3\{Cp_2Mo_2(CO)_4P_2\}_5X_2]^+$ |
| 2298.9 (1.5) | 2346.8 (1) | 2436.9 (2) | 3164.2 (45) | $[Ag_2\{Cp_2Mo_2(CO)_4P_2\}_4X]^+$ |
| – | 2100.7 (0.5) | – | – | $[Ag_3\{Cp_2Mo_2(CO)_4P_2\}_3X_2]^+$ |
| 1804.9 (1) | 1847.6 (0.5) | 1941.1 (0.5) | 2670.6 (3.5) | $[Ag_2\{Cp_2Mo_2(CO)_4P_2\}_3X]^+$ |
| 1593.9 (4) | 1595.0 (10) | 1596.7 (4) | – | $[Ag\{Cp_2Mo_2(CO)_4P_2\}_3]^+$ |
| 1100.8 (100) | 1100.7 (100) | 1100.8 (100) | 1100.7 (100) | $[Ag\{Cp_2Mo_2(CO)_4P_2\}_2]^+$ |
| 643.8 (60) | 645.8 (50) | 643.9 (30) | 643.8 (35) | $[Ag\{Cp_2Mo_2(CO)_4P_2\}(NCCH_3)]^+$ |

In the case of **42e**, the ESI-MS spectra even suggest the presence of the trication $[Ag_3\{Cp_2Mo_2(CO)_4P_2\}_5]^{3+}$, albeit in minute amounts. In the negative ion ESI-MS spectra of the compounds **42d-g**, only peaks attributable to the corresponding anions are observed.

Due to the greater solubility of **42g**, positive ion ESI-MS spectra of this complex were also recorded in $CH_2Cl_2$ at room temperature. The spectra display only one fragment attributable to the monocation $[Ag\{Cp_2Mo_2(CO)_4P_2\}_2]^+$. Furthermore, vapour pressure osmometric (VPO) measurements on **42g** in $CH_2Cl_2$ at 28 °C suggest the virtually exclusive presence of the monomer $[Ag\{Cp_2Mo_2(CO)_4P_2\}_2][Al\{OC(CF_3)_3\}_4]$ **48**. The slightly overestimated molecular mass value for **48** (2257 ± 113 g mol$^{-1}$ as opposed to 2067 g mol$^{-1}$) is indicative of the existence of a small

amount of larger species and, therefore, of a monomer/dimer equilibrium, albeit almost exclusively in favour of the monocation.

Density functional theory (DFT) calculations have shown that the structure of lowest energy for the monocation in **48** in $CH_2Cl_2$ at room temperature is one in which the two units of **6b** are bound to the Ag cation in a $\eta^2$ coordination mode (**I**, Figure 3.2), and is hence reminiscent of that of the cation $[Ag(\eta^2\text{-}P_4)_2]^+$.[40] However, the monocation **I** is only 9 kJ mol$^{-1}$ more stable than the $\eta^1$:$\eta^2$ monocation (**II**, Figure 3.2) and the enthalpy of formation of the calculated dication **III** (Figure 3.2) from **I** is only mildly exothermic (–6.8 kJ mol$^{-1}$). One could thus envisage the equilibria displayed in Scheme 3.1 existing in solutions of the compound **42g**: one between the monocations **I** and **II**, and one between **II** and the dication **III**.

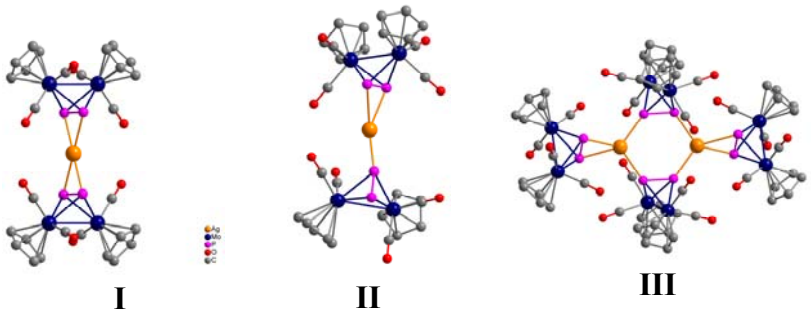


Figure 3.2. Calculated structures (in $CH_2Cl_2$ at room temperature) for the monocations **I** and **II** and the dication **III**. The structure of the crystallographically determined dication in **42g** was used as the basis for the optimisation of the structure of **III**.

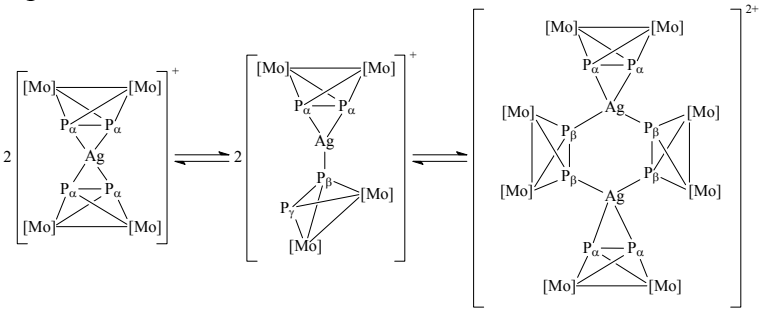


Scheme 3.1. Proposed cation equilibria in solutions of **42g**, with labelling scheme.

In order to gain further insight into the equilibria proposed in Scheme 3.1, variable temperature $^{31}$P-NMR spectra of **42g** were recorded. The spectrum of the compound in $CD_2Cl_2$ at room temperature displays a slightly broadened singlet at –96.1 ppm which becomes broader and shifts to lower field as the temperature is reduced, but nevertheless shows no splitting even at –80 °C. $^{31}$P-NMR measurements on **42g** were thus performed in a 4:1 mixture of THF-$d_8$ and $CD_2Cl_2$ since it was expected that the splitting of the signal would occur at a temperature below the freezing point of $CD_2Cl_2$. At room temperature in this mixture, the compound displays a singlet at –82.0 ppm which can be resolved into two broad signals at –80 °C centred at –77.2 and –90.4 ppm with an integration ratio of approximately 1:2 (Figure 3.3). At –100 °C, two broad signals are observed centred at –77.4 and –94.7 ppm in an integration ratio of about 1:2.

The calculated $^{31}$P-NMR chemical shifts for the P atoms in the cations **I**, **II** and **III** (Figure 3.2) in $CD_2Cl_2$ at 0 K are tabulated below (Table 3.5). The calculated shifts are overestimated compared to the experimental values, but the peak separations are somewhat in agreement. Furthermore, the integration ratios of the signals in the experimental spectra of **42g**, which do not correspond to any of those that would be expected for the proposed cations (singlet for **I**; 1:2:1 for **II**; 1:1 for **III**), suggest that a mixture of these three cations might in fact be present in solutions of **42g**, as might be expected from the small energy differences calculated for these species.

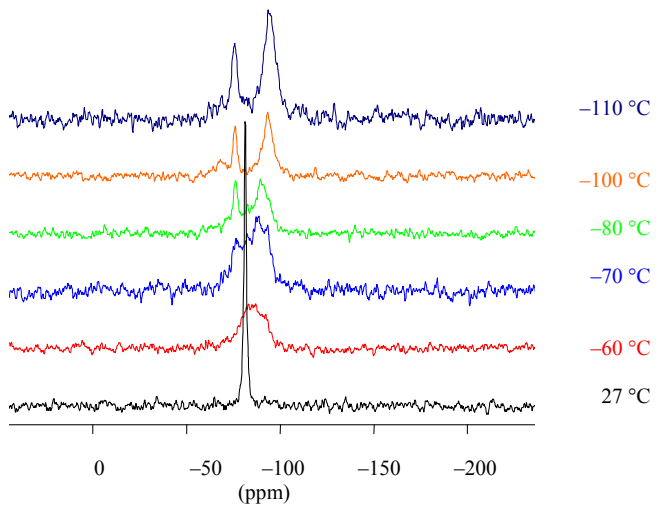


Figure 3.3. Variable temperature $^{31}$P-NMR spectra of **42g** in a 4:1 mixture of THF-$d_8$ and $CD_2Cl_2$.

Table 3.5. Calculated $^{31}$P-NMR chemical shifts (ppm) for the cations **I**, **II** and **III** in $CD_2Cl_2$ at 0 K (see Scheme 3.1 for clarification of labelling scheme).

| Cation | P Atom | Chemical Shift |
|---|---|---|
| **I** | $P_\alpha$ | -117 |
| **II** | $P_\alpha$ | -122 |
| | $P_\beta$ | -133 |
| | $P_\gamma$ | -115 |
| **III** | $P_\alpha$ | -124 |
| | $P_\beta$ | -155 |

The solution equilibrium proposed above for **42g** (Scheme 3.1) and, by extension, for **42b-f**, raises the question of why the dimer **42g**, rather than the monomer **48**, is the species observed in the solid state. The Born-Haber cycle for **42g**, illustrated in Scheme 3.2, sheds light on this query and demonstrates that crystallisation of the dimer is favoured due to the greater lattice energy (909 kJ mol$^{-1}$ as opposed to 305 kJ mol$^{-1}$ for the monomer **48**), whereas dissolution of **42g** under essentially complete dissociation to **48** is driven by entropy ($\Delta H_{Diss}$ = 6.8 kJ mol$^{-1}$, but $\Delta G_{Diss} < 0$ kJ mol$^{-1}$[41]).

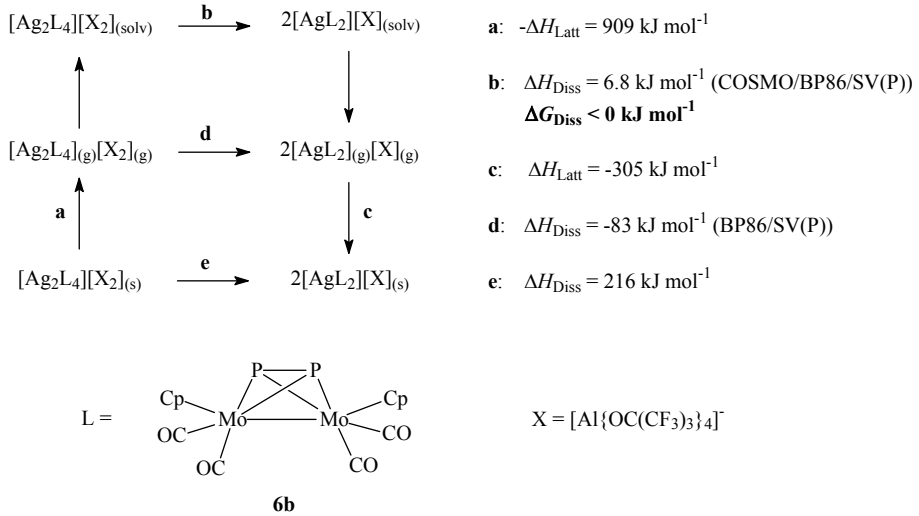


**6b**

Scheme 3.2. Born-Haber cycle for **42g**.

Interestingly, reaction of **6b** with $Ag[Al\{OC(CF_3)_3\}_4]$ in a 1:1 stoichiometry in $CH_2Cl_2$ leads, nevertheless, to the isolation of **42g**, confirming that the 2:1 product is a thermodynamic minimum in the solid state. Furthermore, ESI-MS spectra of this reaction solution suggest that the only species present, containing both $Ag^+$ cations and

units of **6b**, is the cation $[Ag\{Cp_2Mo_2(CO)_4P_2\}_2]^+$, thus implying that a 2:1 stoichiometry presents a thermodynamic minimum in solution as well.

As the compounds described above demonstrate, reactions of $Ag^I$ salts of WCAs with **6b** yield complex salts consisting of a dication with the same basic structure, regardless of the WCA. Minor variations of the dication geometry appear to depend on the size of the anion and hence on crystal packing effects. In contrast, the coordinating potential of the $NO_3^-$ ion and thus its effect on the resulting structure is clearly demonstrated in the product obtained from the reaction of $AgNO_3$ with **6b**, the undulated polymer **44** (Figure 1.10).[32a] In the light of this observation, it was considered to be of interest to investigate the ligating potential of **6b** in the presence of other $Ag^I$ salts of coordinating anions. Reaction of **6b** with $AgNO_2$ (Equation 3.2) in $CH_3CN$ or mixtures of $CH_3CN$ and $CH_2Cl_2$ at room temperature leads to the dimer **49** as an insoluble air- and light-sensitive dark brown microcrystalline powder. This compound consists of two Ag cations bridged by two units of **6b** to form a six-membered $Ag_2P_4$ ring and the coordination sphere of the $Ag^I$ centres is completed by $\eta^2$ coordination of the $NO_2^-$ anions through the O atoms.

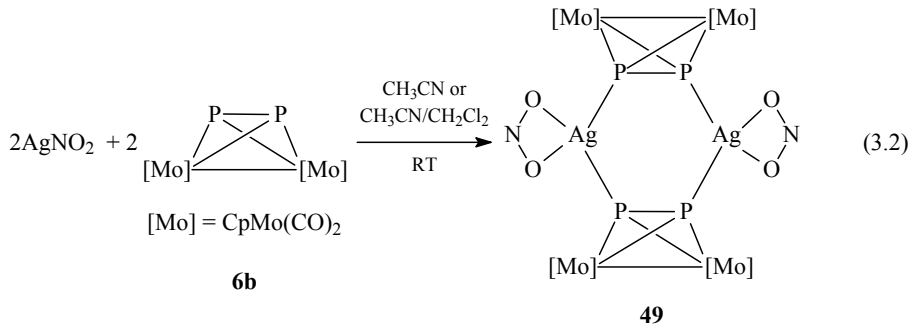


(3.2)

The structure of **49** is illustrated in Figure 3.4. The P─P bond lengths of the units of **6b** in **49** (2.110(1) Å) are appreciably longer than that in uncoordinated **6b** (2.079(2) Å).[9c] The Ag─P bond lengths (2.417(8), 2.560(8) Å) lie within and above the range defined by those of the complexes $[(AgNO_2)_m(R_2P(R')PR_2)]_n$ (R = Ph, R′ = $CH_2$ (m = 1, n = 2); R = Ph, R′ = $(CH_2)_3$ (m = 1, n = 2); R = Ph, R′ = CH═CH (m = 2, n = 2); R = *p*-Tol, R′ = (R)-(+)-1,1-binaphthyl (m = 1, n = 1)) (2.365(1)-2.490(2) Å).[3d] The O─Ag─O angle (51.6(1)°) is within the range defined by the reference compounds (41.0(5)-54.2(5)°).

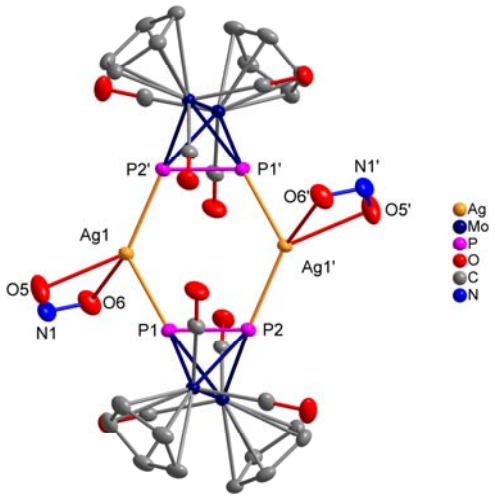


Figure 3.4. Structure of compound **49** (hydrogen atoms omitted for clarity). Thermal ellipsoids are represented at the 50 % probability level. Selected bond lengths (Å) and angles (°): P1─P2 2.110(1), Ag1─P1 2.560(8), Ag1─P2′ 2.417(8), Ag1─O5 2.439(3), Ag1─O6 2.379(3), P1─Ag1─P2′ 118.58(3), O5─Ag1─O6 51.55(10), P1─Ag1─O5 96.94(10), P1─Ag1─O6 94.71(8), P2′─Ag1─O5 136.30(9), P2′─Ag1─O6 138.71(7).

Although dimer **49** is insoluble in most common solvents, it dissolves in trace amounts in polar solvents such as $CH_3CN$. Peaks detected in the positive ion ESI-MS spectra of **49** in this solvent are listed in Table 3.6 and suggest the presence of even higher aggregates in solution than observed in the solid state. Unfortunately, the solubility is not sufficient for the acquisition of NMR spectra.

Table 3.6. Selected fragments (mass/charge (relative abundance in %)) detected in the positive ion ESI-MS spectra of compound **49** in $CH_3CN$ and the proposed cations for these fragments.

| **Fragments** | **Proposed Cations** |
|---|---|
| 2249.8 (8) | $[Ag_2\{Cp_2Mo_2(CO)_4P_2\}_4(NO_2)]^+$ |
| 1904.7 (20) | $[Ag_3\{Cp_2Mo_2(CO)_4P_2\}_3(NO_2)_2]^+$ |
| 1748.9 (38) | $[Ag_2\{Cp_2Mo_2(CO)_4P_2\}_3(NO_2)]^+$ |
| 1596.8 (11) | $[Ag\{Cp_2Mo_2(CO)_4P_2\}_3]^+$ |
| 1255.8 (5) | $[Ag_2\{Cp_2Mo_2(CO)_4P_2\}_2(NO_2)]^+$ |
| 1100.7 (100) | $[Ag\{Cp_2Mo_2(CO)_4P_2\}_2]^+$ |
| 643.8 (40) | $[Ag\{Cp_2Mo_2(CO)_4P_2\}(NCCH_3)]^+$ |

## 3.1.2. Studies on the Reactivity of $[Cp_2Mo_2(CO)_4(\mu,\eta^2\text{-}P_2)]$ with $Au^I$ Salts

Since the interaction of $Cu^I$ and $Ag^I$ salts with **6b** seemed to present a favourable combination for the synthesis of well-defined aggregates, extension of this concept to $Au^I$ salts appeared attractive and plausible, especially after considering that Stoppioni and co-workers were able to isolate the complexes **16c**,**e**,**f** (Figure 1.7).[17b] Indeed, reaction of $[AuPPh_3][PF_6]$[17b] with **6b** in a 1:2 stoichiometry, in a mixture of $CH_2Cl_2$ and THF, leads to the formation of **42h** which can be isolated as an air-sensitive wine-red crystalline solid (Equation 3.3). This complex salt is insoluble in most common solvents and only sparingly soluble in $CH_2Cl_2$ and THF.

Compound **42h** consists of a dication structurally similar to the Ag-containing dications found in the complexes **42b**-**g**, in which the $Au^+$ cations are found in a pseudo-tetrahedral coordination mode and whose structure is illustrated in Figure 3.5. The P─P bond lengths of the bridging units of **6b** (2.089(3) Å) are only marginally longer than that of uncoordinated **6b** (2.079(2) Å),[9c] whereas those of the side-on coordinated units of **6b** are significantly longer (2.186(3) Å). The Au─P bond lengths in the dication of **42h** (2.349(2)-2.536(3) Å) compare well with those of complexes **16c**,**e**,**f** (2.39(1)-2.54(1) Å),[17b] $[Au(PPh_3)_4][BPh_4]$ (2.392(4)-2.610(9) Å)[42] and $[Au(Ph_2PCH_2CH_2PPh_2)Cl\bullet 2H_2O]$ (2.384(2)-2.412(2) Å).[43]

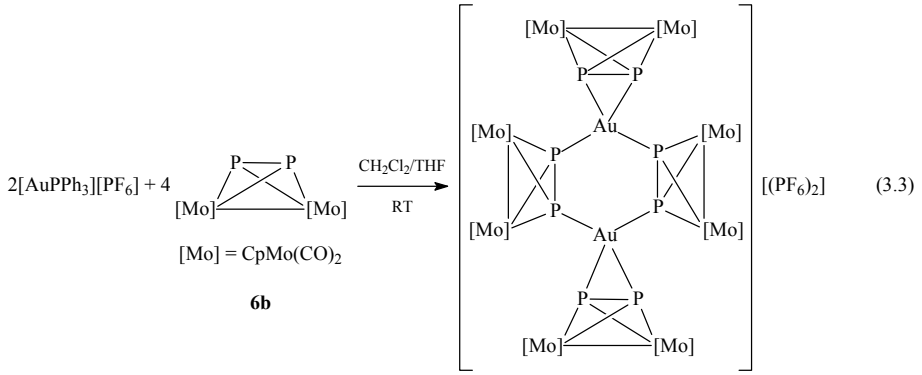

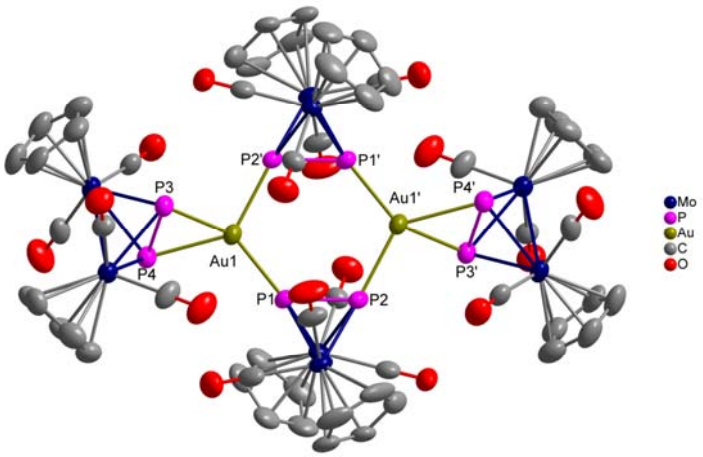


Figure 3.5. Structure of the dication in **42h** (hydrogen atoms omitted for clarity). Thermal ellipsoids are represented at the 50 % probability level. Selected bond lengths (Å) and angles (°): P1─P2 2.089(3), P3─P4 2.186(3), Au1─P1 2.349(3), Au1─P2′ 2.437(3), Au1─P3 2.536(3), Au1─P4 2.509(3), P1─Au1─P2′ 111.15(9), P3─Au1─P4 51.36(8), P1─Au1─P3 142.13(10), P1─Au1─P4 113.65(8), P2′─Au1─P3 99.74(9), P2′─Au1─P4 131.44(8).

The $^{31}$P-NMR spectrum of **42h** in $CD_2Cl_2$ at room temperature exhibits a slightly broadened singlet at –52.7 ppm and a septet at –143.9 ppm ($PF_6^-$, $^1J_{FP}$ = 710 Hz). In the ESI-MS spectra of the compound in $CH_2Cl_2$, the fragments with the highest relative abundance are attributable to the cations $[Au\{Cp_2Mo_2(CO)_4P_2\}_2(THF)_2]^+$ and $[Au\{Cp_2Mo_2(CO)_4P_2\}_2]^+$. In addition, the fragments detected in the positive ion ESI-MS spectra of the reaction solution for the synthesis of **42h** display further peaks attributable to the cations $[Au\{Cp_2Mo_2(CO)_4P_2\}(PPh_3)]^+$ and $[Au(PPh_3)_2]^+$. These data demonstrate, as in the case of the analogous $Ag^I$ complexes, that a monomer/dimer equilibrium most likely exists in solution. In parallel with the observations made for **42g**, which showed that its synthesis appears to be independent of reactant stoichiometry, reaction of $[AuPPh_3][PF_6]$ and **6b** in a 1:1 stoichiometry also demonstrates this independence and leads to the formation of **42h**.

As in the case of $Cu^I$ and $Ag^I$, it was of interest to investigate the reactivity of **6b** with $Au^I$ salts of coordinating anions. Reaction with [LAuCl] (L = CO,[44] tetrahydrothiophene (THT)[45]) in a 1:1 stoichiometry in $CH_2Cl_2$ or a mixture of $CH_2Cl_2$ and toluene, at room temperature when L = THT and at –78 °C when L = CO, results in ligand exchange and yields the complex **50** as an air-sensitive, red-

orange microcrystalline powder (Equation 3.4). Compound **50** is only sparingly soluble in solvents such as $CH_2Cl_2$ and THF, and can be stored indefinitely under an inert atmosphere at ambient conditions.

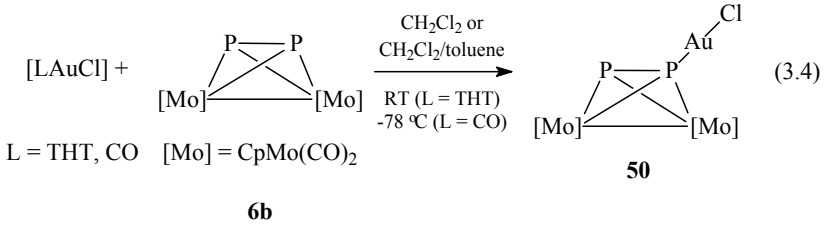


The structure of **50** is illustrated in Figure 3.6 and consists of a unit of **6b** with the Lewis-acidic fragment [AuCl] coordinated to one of the P atoms. The P─P bond length (2.095(8) Å) is only slightly longer than that in the uncoordinated complex **6b** (2.079(2) Å).[9c] The Au─P bond length (2.235(5) Å) compares well with that found in $[Au(PPh_3)Cl]$ (2.233 Å), whereas the Au─Cl bond length (2.325(5) Å) is noticeably longer than that in the same compound (2.278 Å).[46] Although the coordination mode of the $Au^I$ centre in $[Au(PPh_3)Cl]$ is essentially linear (P─Au─Cl 179.71°), the P─Au─Cl angle in **50** deviates appreciably from linearity (170.4(2)°).

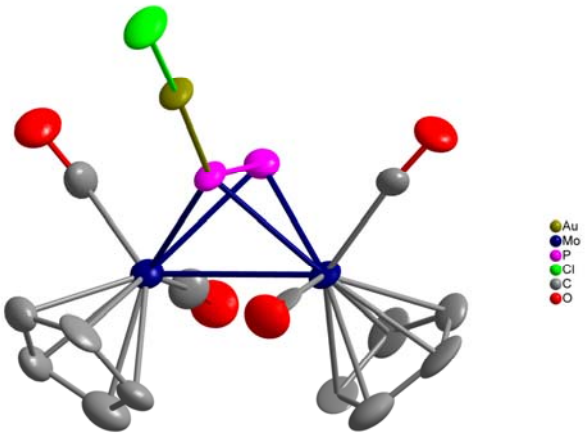


Figure 3.6. Structure of the compound **50** (hydrogen atoms omitted for clarity). Thermal ellipsoids are represented at the 50 % probability level. Selected bond lengths (Å) and angles (°): P─P 2.095(8), Au─P 2.235(5), Au─Cl 2.325(5), P─Au─Cl 170.4(2).

The $^{31}$P-NMR spectrum of **50** in THF-$d_8$ at room temperature displays a somewhat broadened peak at –77.2 ppm, thus suggesting

dynamic behaviour in solution. Interestingly, the fragments detected in the positive and negative ion ESI-MS spectra of **50** in a mixture of $CH_3CN$ and $CH_2Cl_2$ suggest that the species in solution might be $[Au\{Cp_2Mo_2(CO)_4P_2\}_2][AuCl_2]$ **51**. It is likely that the structure of the cation of **51** in solution is similar to that calculated for the monocation in solutions of **42g** (Figure 3.2).

## 3.1.3. Studies on the Reactivity of $[Cp_2Mo_2(CO)_4(\mu,\eta^2\text{-}P_2)]$ with Group 9 Transition Metal Complexes

In view of the versatility of $P_n$-ligand complexes as building blocks for supramolecular assemblies it was decided to extend this synthetic methodology to cationic transition metal complexes which have been shown to react favourably with conventional ligands used in supramolecular chemistry. Amouri and co-workers have shown that the Group 9 transition metal complexes $[Cp^*M\{OC(CH_3)_2\}_3][BF_4]_2$ (M = Rh, Ir)[47] function as efficient 'tripod connectors' in the construction of the metallocryptands **52a-d** (Figure 3.7).[48] Using multinuclear NMR, the authors were also able to demonstrate that one of the $BF_4^-$ anions of **52c**,**d** is encapsulated within the iridocryptand, thus revealing the property of these cationic assemblies to act as hosts.

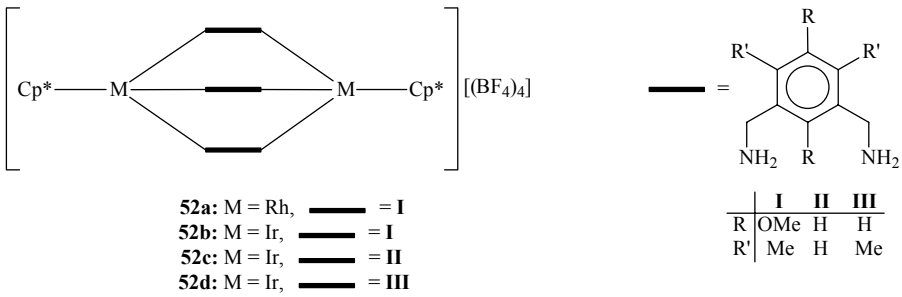


Figure 3.7. The metallocryptands **52a-d** isolated by Amouri and co-workers.

Attempts to exploit the 'tripod connector' potential of the complexes $[Cp^*M(NCCH_3)_3][(SbF_6)_2]$ (M = Rh, Ir)[47] in the presence of **6b**, by applying a reactant stoichiometry of 2:3, were not successful and led instead to the formation of the air-sensitive complexes **53a**,**b** (Equation 3.5). The structure illustrated in Equation 3.5 is based on the results of elemental analyses of the compounds and X-ray crystallographic data obtained for **53b**, whose crystals were of sufficient quality for the determination of the connectivity of atoms heavier than carbon. Compound **53a** can be isolated as fine dark brown

needles and **53b** as shimmering ruby red needles, and both can be stored indefinitely at ambient conditions under an inert atmosphere. Both compounds are readily soluble in polar solvents such as $CH_3CN$ and acetone, and sparingly soluble in solvents such as $CH_2Cl_2$ and THF.

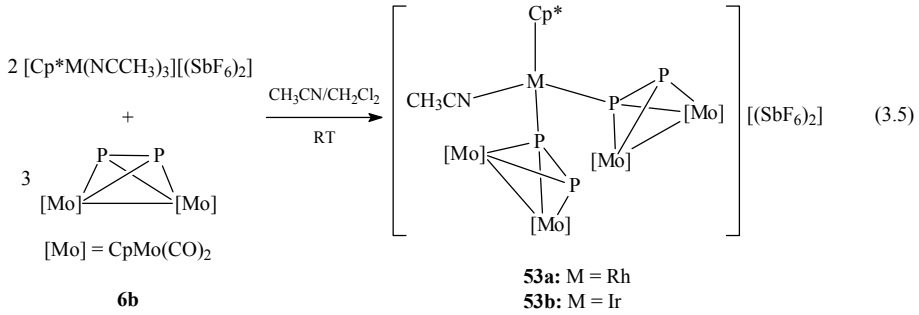


(3.5)

The fragments detected in the positive ion ESI-MS spectra of **53a**,**b** in $CH_3CN$ at room temperature along with the proposed cations for these fragments are listed in Table 3.7 and demonstrate that cations of lower molecular mass than those in the parent compounds are most likely present in solution. The presence of cations of lower molecular mass is supported by the $^{31}$P-NMR spectra of the compounds in $CD_3CN$ at room temperature (Figure 3.8), which also suggest that extensive dissociation to the starting materials takes place upon dissolution, particularly in the case of the Rh derivative **53a**. The spectrum of **53a** displays a singlet at –41.3 ppm, attributable to uncoordinated **6b**, and two weak broad signals, with an integration ratio of 1:1, at 7.3 and –126.3 ppm. Complex **53b** also exhibits a peak attributable to uncoordinated **6b**, at –41.2 ppm, in addition to two distinct doublets, with an integration ratio of 1:1, at –27.9 ($^1J_{PP}$ = 495 Hz) and –147.0 ($^1J_{PP}$ = 498 Hz) ppm, and a weak broad signal and broad multiplet, also in a ratio of 1:1, at –68.6 and –108.0 ($^1J_{PP}$ = 495 Hz) ppm, respectively.

Table 3.7. Selected fragments (mass/charge (relative abundance in %)) detected in the positive ion ESI-MS spectra of compounds **53a**,**b** in $CH_3CN$ and the proposed cations for these fragments.

| **53a** (M = Rh) | **53b** (M = Ir) | **Proposed Cations** |
|---|---|---|
| – | 1555.2 (0.5) | $[Cp^*M\{Cp_2Mo_2(CO)_4P_2\}_2(NCCH_3)(SbF_6)]^+$ |
| 1012.0 (0.5) | 1100.1 (0.5) | $[Cp^*M\{Cp_2Mo_2(CO)_4P_2\}(NCCH_3)(SbF_6)]^+$ |
| 968.8 (1) | 1059.0 (1) | $[Cp^*M\{Cp_2Mo_2(CO)_4P_2\}(SbF_6)]^+$ |
| 768.9 (3) | – | $[Cp^*M\{Cp_2Mo_2(CO)_4P_2\}(NCCH_3)]^+$ |
| 752.9 (6) | 843.1 (13) | $[Cp^*M\{Cp_2Mo_2(CO)_3P_2\}(NCCH_3)]^+$ |
| 734.0 (7) | – | $[Cp^*M\{Cp_2Mo_2(CO)_4P_2\}]^+$ |
| 703.9 (2) | 794.1 (21) | $[Cp^*M\{Cp_2Mo_2(CO)_3P_2\}]^+$ |
| 677.8 (1) | 766.0 (10) | $[Cp^*M\{Cp_2Mo_2(CO)_2P_2\}]^+$ |
| 649.9 (2) | 740.1 (43) | $[Cp^*M\{Cp_2Mo_2(CO)P_2\}]^+$ |
| – | 712.0 (4) | $[Cp^*M\{Cp_2Mo_2P_2\}]^+$ |
| – | 680.7 (0.5) | $[Cp^*M\{Cp_2Mo_2(CO)_4P_2\}_2(NCCH_3)]^{2+}$ |
| – | 660.6 (2) | $[Cp^*M\{Cp_2Mo_2(CO)_4P_2\}_2]^{2+}$ |
| – | 646.1 (6) | $[Cp^*M\{Cp_2Mo_2(CO)_{3.5}P_2\}_2]^{2+}$ |
| – | 618.6 (8) | $[Cp^*M\{Cp_2Mo_2(CO)_{2.5}P_2\}_2]^{2+}$ |
| – | 606.2 (2) | $[Cp^*M\{Cp_2Mo_2(CO)_2P_2\}_2]^{2+}$ |
| – | 590.1 (14) | $[Cp^*M\{Cp_2Mo_2(CO)_{1.5}P_2\}_2]^{2+}$ |
| – | 575.6 (10) | $[Cp^*M\{Cp_2Mo_2(CO)P_2\}_2]^{2+}$ |
| – | 561.1 (9) | $[Cp^*M\{Cp_2Mo_2(CO)_{0.5}P_2\}_2]^{2+}$ |
| – | 546.7 (3) | $[Cp^*M\{Cp_2Mo_2P_2\}_2]^{2+}$ |
| 408.1 (36) | – | $[Cp^*M\{Cp_2Mo_2(CO)_4P_2\}(NCCH_3)_2]^{2+}$ |
| 388.1 (7) | – | $[Cp^*M\{Cp_2Mo_2(CO)_4P_2\}(NCCH_3)]^{2+}$ |
| 380.1 (27) | 425.1 (63) | $[Cp^*M\{Cp_2Mo_2(CO)_2P_2\}(NCCH_3)_2]^{2+}$ |
| 367.0 (100) | 412.1 (43) | $[Cp^*M\{Cp_2Mo_2(CO)_4P_2\}]^{2+}$ |
| 352.1 (13) | 397.1 (100) | $[Cp^*M\{Cp_2Mo_2(CO)_3P_2\}]^{2+}$ |

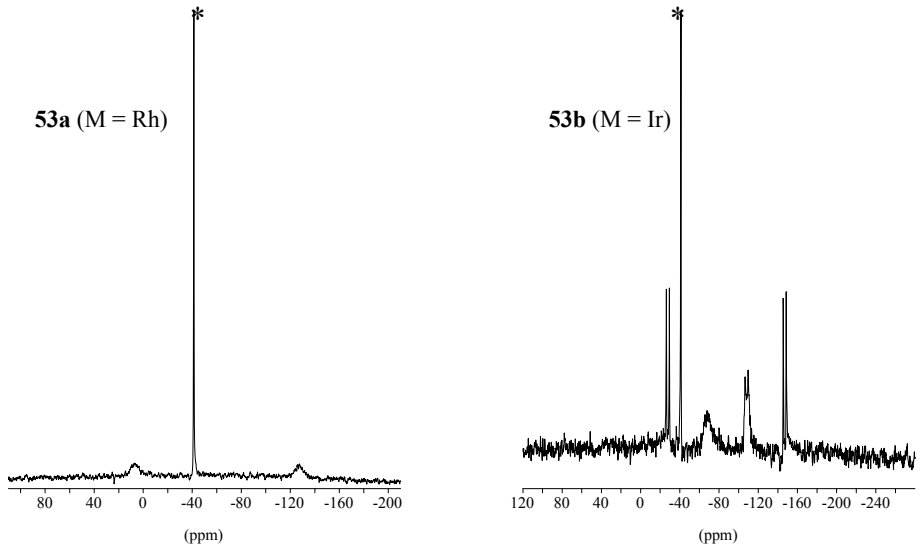


Figure 3.8. $^{31}$P-NMR spectra of the compounds **53a**,**b** in $CD_3CN$ at room temperature (peaks marked with an asterisk are due to uncoordinated **6b**). Coupling constants for **53b**: $^1J_{PP}$ = 498 Hz ($\delta$ = –147.0 ppm); $^1J_{PP}$ = 495 Hz ($\delta$ = –108.0 ppm); $^1J_{PP}$ = 495 Hz ($\delta$ = –27.9 ppm).

Scheme 3.3 illustrates the equilibria which are most probably existent in solutions of the complexes **53a**,**b** and should be considered before interpretation of the spectra. Upon dissolution of the compounds in $CH_3CN$, the parent dication $[Cp^*M\{Cp_2Mo_2(CO)_4P_2\}_2(NCCH_3)]^{2+}$ **IV** most probably loses a unit of **6b** and forms the dication $[Cp^*M\{Cp_2Mo_2(CO)_4P_2\}(NCCH_3)_2]^{2+}$ **V**, which could exchange its last unit of **6b** for $CH_3CN$ to form the dication $[Cp^*M(NCCH_3)_3]^{2+}$ **VI**. However, the solution would then contain uncoordinated **6b**, which could combine with **IV** to form the dication $[Cp^*M\{Cp_2Mo_2(CO)_4P_2\}_3]^{2+}$ **VII**. Of the three P-containing cations, **V** would be expected to display the simpler $^{31}$P-NMR spectrum (AX spin system), namely a pair of well-separated doublets of equal intensity. In fact, the spectrum of **53b** exhibits such a pair of peaks (–27.9 ppm, $^1J_{PP}$ = 495 Hz and –147.0 ppm, $^1J_{PP}$ = 498 Hz), the low field signal being assigned to the uncoordinated P atom and the high field signal to the coordinated one. The sharpness and fine structure of these signals indicate that the conversion of **V** to either **IV** or **VI** is slow on the NMR time scale. The parent dication **IV** and the dication **VII** would be expected to present more complicated spectra (**IV**: AA′XX′ spin system; **VII**: AA′A″XX′X″ spin system) each displaying two multiplets of equal intensity with chemical shifts comparable to those of **V**. The spectrum of **53b** displays two further broad peaks at –68.6 and –108.0 ppm, the higher field signal demonstrating some fine structure ($^1J_{PP}$ = 495 Hz). The breadth and poor structure of these peaks as well as their smaller separation compared to that of the peaks assigned to **V** (39.4 ppm as opposed to 119.1 ppm) are indicative of fast exchange processes, which may be in the form of fluxional behaviour, a fast equilibrium between **IV** and **VII**, rapid conversion of **IV** to **V**, or a combination of all of these phenomena. Regrettably, the spectrum of **53a** does not permit one to draw many conclusions, save that the two peaks are probably due to a dication of the type defined by **V**. This assignment is based on the difference in the chemical shifts of these peaks (133.6 ppm), which is comparable to that of the likewise assigned peaks in **53b** (119.06 ppm).

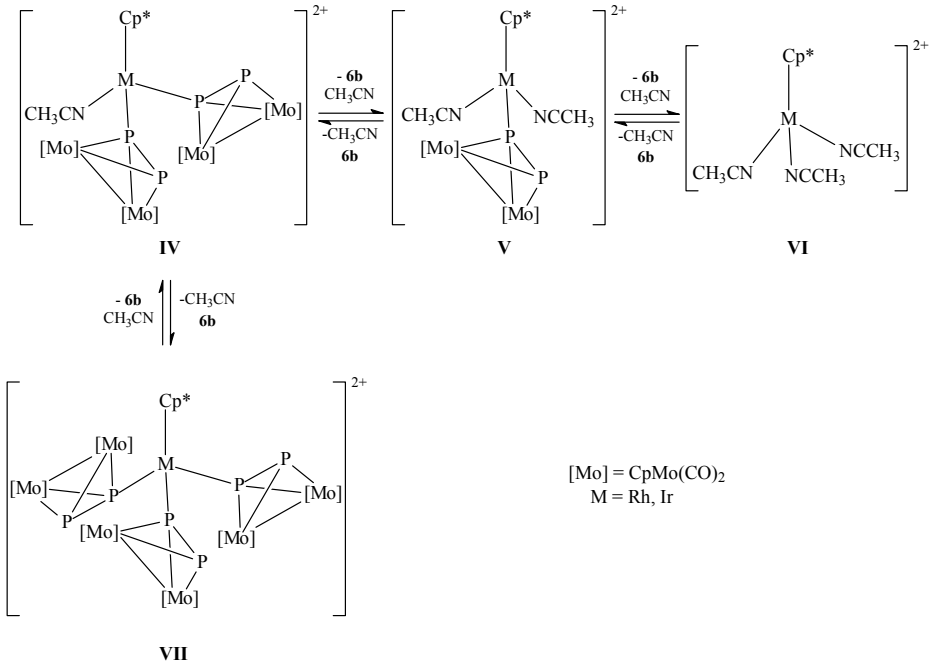


Scheme 3.3. Proposed cation equilibria in solutions of **53a**,**b**.

The reactivity of **6b** was also investigated in the presence of the complex $[Cp''RhCl(NCCH_3)_2][BF_4]$.[47b] A 1:1 reaction of these two complexes in a mixture of THF and $CH_2Cl_2$ at room temperature resulted in the isolation of a small amount of **54** in the form of air-sensitive dark brown needles (Equation 3.6).

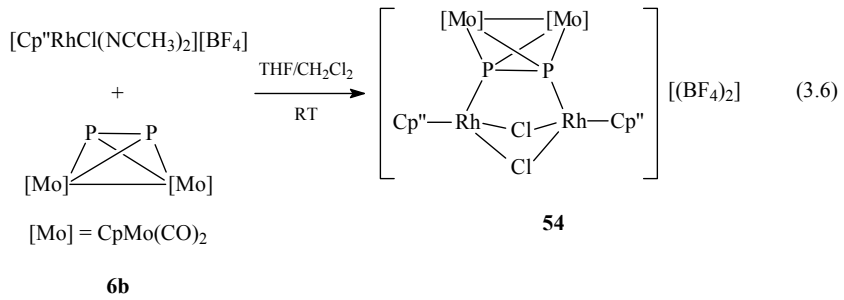


(3.6)

Crystals of **54** were characterised by X-ray crystallography and the structure of the dication in **54** is depicted in Figure 3.9. The Rh centres in this dication are bridged by a unit of **6b** as well as by the two Cl ligands, thus leading to a core comprising a four-membered $Rh_2Cl_2$ ring and two five-membered $Rh_2P_2Cl$ rings. This core structure is reminiscent of that observed in the neutral complex **14** (Figure 1.6)

reported by Scherer and co-workers, which consists of a four-membered $Re_2Br_2$ ring and two five-membered $Re_2P_2Br$ rings.[16b]

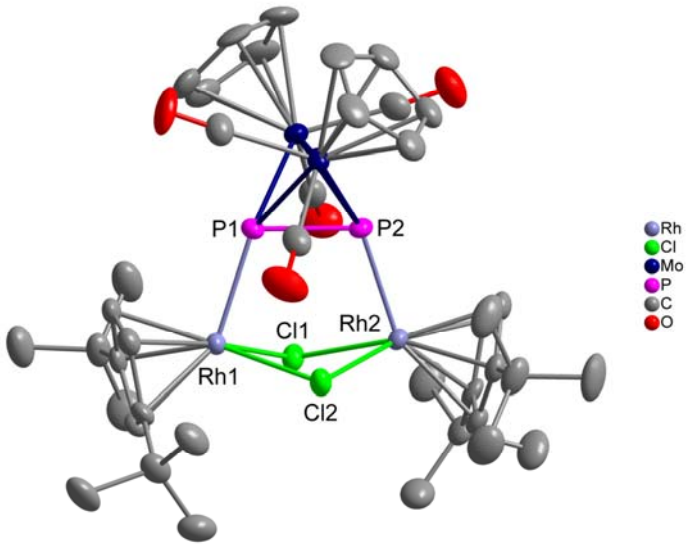


Figure 3.9. Structure of the dication in **54** (hydrogen atoms omitted for clarity). Thermal ellipsoids are represented at the 50 % probability level. Selected bond lengths (Å) and angles (°): P1─P2 2.112(2), Rh1─P1 2.365(2), Rh2─P2 2.360(2), Rh1─Cl1 2.432(2), Rh1─Cl2 2.443(2), Rh2─Cl1 2.448(2), Rh2─Cl2 2.423(2), P1─Rh1─Cl1 88.10(6), P1─Rh1─Cl2 90.51(6), P2─Rh2─Cl1 90.47(6), P2─Rh2─Cl2 87.68(6), Cl1─Rh1─Cl2 79.00(5), Cl1─Rh2─Cl2 79.07(5), Rh1─Cl1─Rh2 94.70(5), Rh1─Cl2─Rh2 95.06(5).

The P─P bond length of the unit of **6b** in **54** (2.112(2) Å) is noticeably longer than that in uncoordinated **6b** (2.079(2) Å),[9c] while the Rh─P and Rh─Cl bond lengths (2.360(2)-2.365(2) and 2.423(2)-2.448(2) Å, respectively) are within the ranges defined by the complexes $[Rh_2Cl_6(\mu\text{-}Ph_2PCHPPh_2)_2]$ (2.368(1)-2.399(2) and 2.369(1)-2.375(1) Å, respectively)[49] and $[Rh_2(NO)_2(\mu\text{-}Ph_2PCHPPh_2)_2(\mu\text{-}Cl)_2]$ (2.354(1)-2.369(1) and 2.425(1)-2.454(1) Å, respectively).[50] The Rh─Cl─Rh bond angles (94.70(5)-95.06(5)°) are also comparable to those of the reference compounds (92.43(4)°,[49] 94.25(5)°[50]), whereas the Cl─Rh─Cl bond angles (79.00(5), 79.07(5)°) are appreciably smaller (87.57(4)°,[49] 85.76(4)°[50]).

## 3.1.4. Studies on the Reactivity of $[Cp_2Mo_2(CO)_4(\mu,\eta^2\text{-}P_2)]$ with Platinum Aryl Complexes

Stang and co-workers have been successful in using Pt aryl complexes in combination with suitable N-donor ligands to construct a number of molecular squares and rectangles.[51] For example, 4,4′-bipyridyl and the organometallic 'clip' **55** self-assemble to form the molecular rectangle **56** (Equation 3.7).[51c,d]

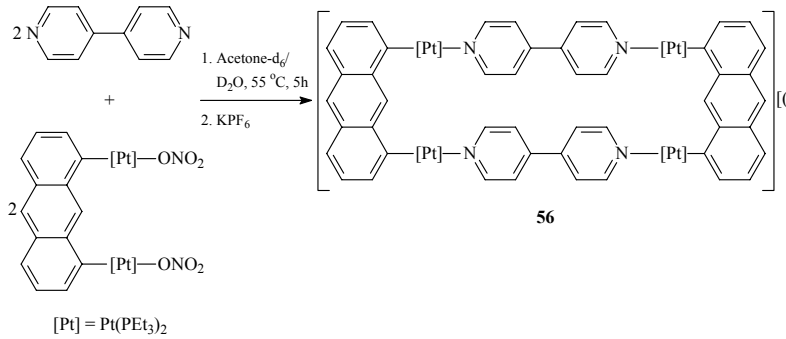


(3.7)

Bimetallic aryl compounds such as **55** appeared to be promising starting materials for the construction of supramolecules with $P_n$-ligand complexes. Reaction of **6b** with **55** in a 2:1 ratio, in a mixture of water, acetone and excess $KPF_6$, under ultrasonic agitation, results in the precipitation of **57** as an air-sensitive bright orange powder (Equation 3.8). Interestingly, the same product is obtained if **6b** and **55** are allowed to react in a 1:1 stoichiometry, thus indicating that **57** presents a thermodynamic minimum in the solid state. Complex **57** is readily soluble in solvents such as $CH_2Cl_2$ and $CH_3CN$, albeit under almost complete dissociation, as $^{31}$P-NMR experiments have shown.

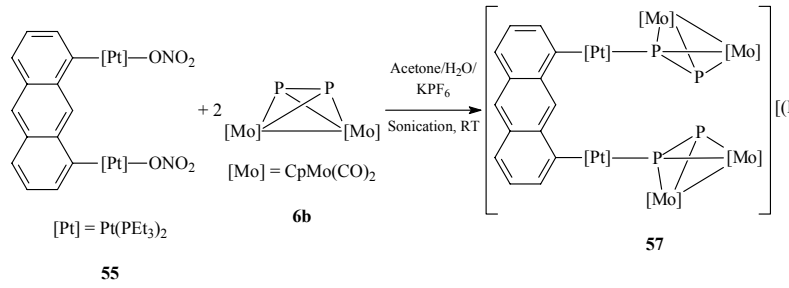


(3.8)

Crystals of **57** can be obtained as red needles by allowing hexane to slowly diffuse into a $CH_2Cl_2$ solution of the compound. The structure of the dication in **57**, which consists of the diplatinum aryl dication

derived from **55** and two units of **6b**, each bound to a separate Pt atom in a $\eta^1$ coordination mode, is depicted in Figure 3.10.

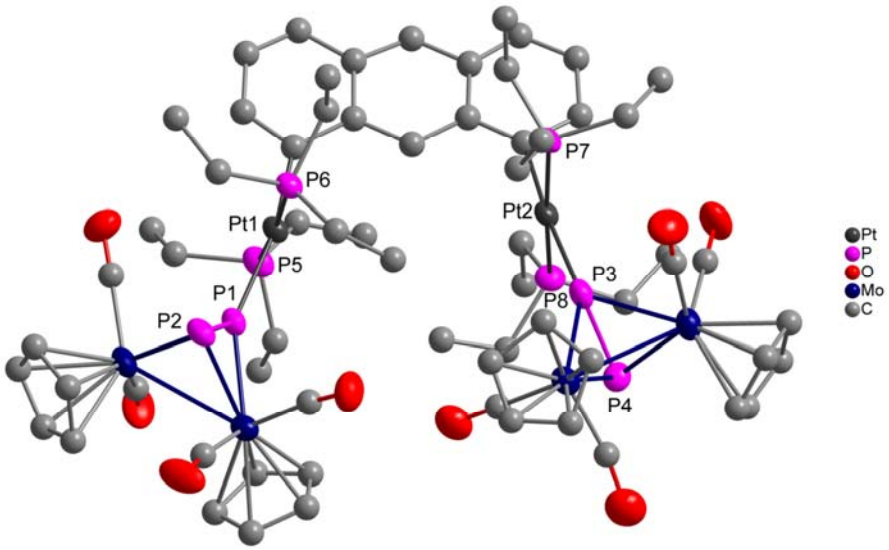


Figure 3.10. Structure of the dication in **57** (hydrogen atoms omitted for clarity). Thermal ellipsoids are represented at the 50% probability level. Selected bond lengths (Å) and angles (°): P1─P2 2.099(7), P3─P4 2.081(7), Pt1─P1 2.383(4), Pt1─P5 2.329(6), Pt1─P6 2.320(4), Pt2─P3 2.403(4), Pt2─P7 2.335(4), Pt2─P8 2.343(5), Pt1─C9 1.98(2), Pt2─C17 2.05(2), P1─Pt1─P5 92.4(2), P1─Pt1─P6 92.8(2), P5─Pt1─C9 85.6(5), P6─Pt1─C9 88.7(5), P3─Pt2─P7 92.1(2), P3─Pt2─P8 93.3(2), P7─Pt2─C17 86.9(5), P8─Pt2─C17 87.3(5), P5─Pt1─P6 173.6(2), P1─Pt1─C9 169.4(5), P7─Pt2─P8 172.5(2), P3─Pt2─C17 175.3(5).

The entire cation in **57** assumes a minor dihedral twist (dihedral angle Pt1─C9─C17─Pt2 ≈ 16.26°), which is comparable to that found in the starting material **55** (≈ 15°) and most likely due to steric crowding of the $PEt_3$ ligands.[51d] The P─P bond lengths of the units of **6b** in **57** (P1─P2 2.099(7), P3─P4 2.081(7) Å) are slightly longer than that in uncoordinated **6b** (2.079(2) Å).[9c] The bond lengths between the Pt atoms and the P atoms of the $PEt_3$ ligands (2.320(4)-2.343(5) Å) are slightly elongated compared to those in **55** (2.306(2)-2.323(2) Å).[51d] The bond lengths between the Pt atoms and the P atoms of the units of **6b** (Pt1─P1 2.383(4), Pt2─P3 2.403(4) Å) are considerably longer than the aforementioned Pt─P bond lengths. As the bond angles about the Pt atoms indicate (Σ ≈ 359.5°), the coordination geometry at the Pt atoms deviates slightly from square planar, as observed in **55** (Σ ≈ 361.5°).[51d]

The $^{31}$P-NMR spectra of **57** in $CD_2Cl_2$ at room temperature indicate that this complex dissolves under essentially complete dissociation. In addition to the peaks attributable to $PF_6^-$, uncoordinated **6b** and the **6b**-free Pt aryl dication, two broad signals of low intensity are observed at –102.9 and –98.3 ppm. These signals may arise from both the P1 and the P3 atoms in **57**, but an unambiguous assignment is impossible since equilibria between **57**, a monomeric species comprising the Pt aryl dication and one unit of **6b**, and oligomeric species in which the units of **6b** are in a bridging coordination mode are highly likely in solution.[51d] ESI-MS measurements of **57** in $CH_3CN/CH_2Cl_2$ also suggest that the compound dissolves under complete dissociation, as only fragments arising from the dication in **55** and no fragments containing **6b** are detected.

The procedure used for the synthesis of **55**[51c,d] can also be used to prepare the monoplatinum derivative **58**, reaction of which with **6b** in a 1:1 ratio yields **59** as an air-sensitive bright orange powder (Equation 3.9). Compound **59** is soluble in solvents such as $CH_2Cl_2$ and $CH_3CN$ and can be crystallised in the form of red needles by controlled diffusion of hexane into a $CH_2Cl_2$ solution of the compound.

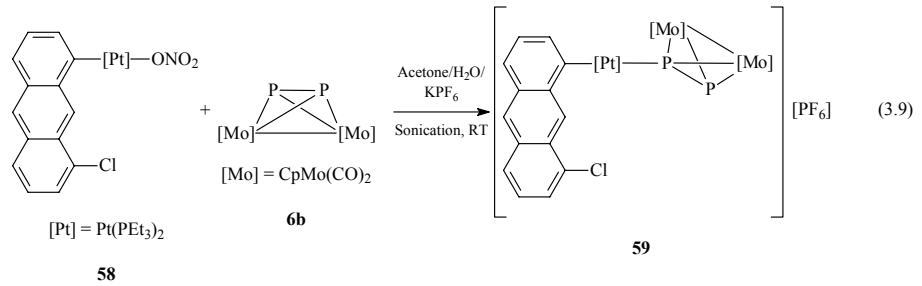


(3.9)

The structure of the monocation in **59**, comprising the Pt aryl monocation derived from **58** and a unit of **6b** coordinated to the Pt atom in a $\eta^1$ fashion, is illustrated in Figure 3.11. Unlike the anthracene moiety in **57**, the one in **59** is essentially planar (dihedral angle Pt─C1─C11─Cl ≈ 0.22°). The P─P bond length of the unit of **6b** in **59** (2.089(2) Å) is slightly longer than that in uncoordinated **6b** (2.079(2) Å)[9c] and the Pt─P bond lengths (2.314(2)-2.389(2) Å) are comparable to those in **57**. Furthermore, the coordination mode at the Pt centre deviates slightly from planarity, as illustrated by the sum of the bond angles about this atom (Σ ≈ 360.5°).

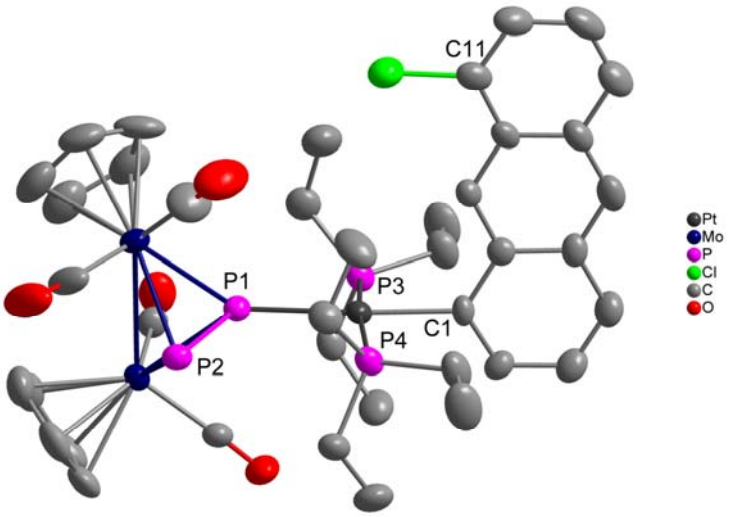


Figure 3.11. Structure of the cation in **59** (hydrogen atoms omitted for clarity). Thermal ellipsoids are represented at the 50% probability level. Selected bond lengths (Å) and angles (°): P1─P2 2.089(2), Pt─P1 2.389(2), Pt─P3 2.314(2), Pt─P4 2.331(2), Pt─C1 2.043(5), C11─Cl 1.734(8), P1─Pt─P3 92.33(5), P1─Pt─P4 93.57(5), C1─Pt─P3 86.62(17), C1─Pt─P4 87.76(17), P3─Pt─P4 171.33(6), P1─Pt─C1 177.20(18).

The capacity of **6b** to act as a ligand for other cationic Pt aryl complexes, such as the benzene derivatives **60** and **61**,[51a,b,52] the fluorene derivative **62** and the anthracene derivative **63** (Figure 3.12), was also investigated, but experiments invariably led to the isolation of red oils which could not be adequately characterised.

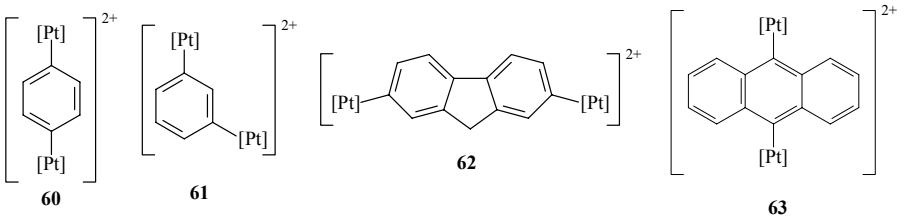


[Pt] = $Pt(PEt_3)_2$

Figure 3.12. Other cationic Pt aryl complexes subjected to reactivity studies with **6b**.

## 3.1.5. Studies on the Reactivity of $[Cp_2Mo_2(CO)_4(\mu,\eta^2\text{-}P_2)]$ with Mixed Transition Metal Salts

Experiments were performed in which **6b** was allowed to react with a 1:1 mixture of $CuPF_6$ and CuCl (Scheme 3.4). It was hoped that a method could be developed by which the 1D polymer **64** could be synthesised, whose length could be controlled simply by varying the stoichiometry of the two Cu salts. However, only the dimer **42a**[32b] and the polymer **43a**[33] could be isolated, as evidenced by X-ray crystallography, probably due to the strongly differing affinities of the salts for **6b**.

Another set of experiments involved reaction of **6b** with a 1:1 mixture of $CuPF_6$ and $AgPF_6$, the objective of which was to obtain the mixed metal aggregate **65** comprising a dication with a six-membered $CuAgP_4$ core (Scheme 3.5). Unfortunately, the outcome of these experiments was not the desired one, since only the oligomers **42a**[32b] and **42e** could be isolated, as demonstrated by X-ray crystallography, again most likely because of the differing affinities of the $Cu^I$ and $Ag^I$ centres for **6b**.

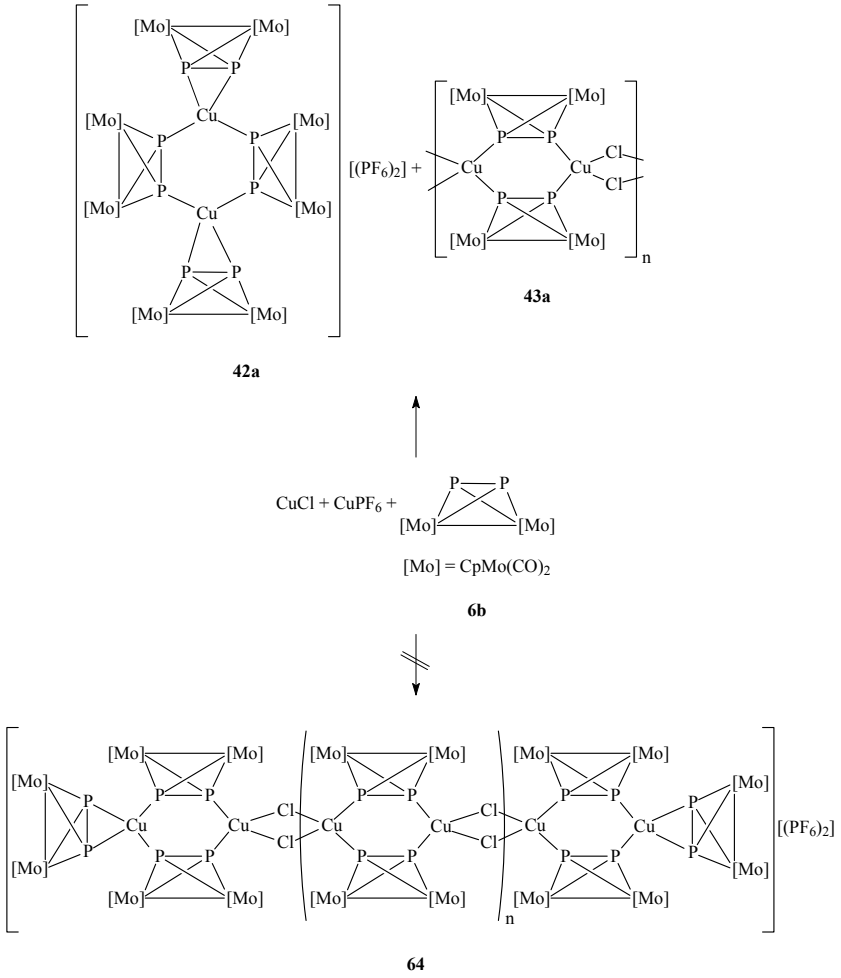


Scheme 3.4. Reaction of **6b** with a 1:1 mixture of $CuPF_6$ and CuCl.

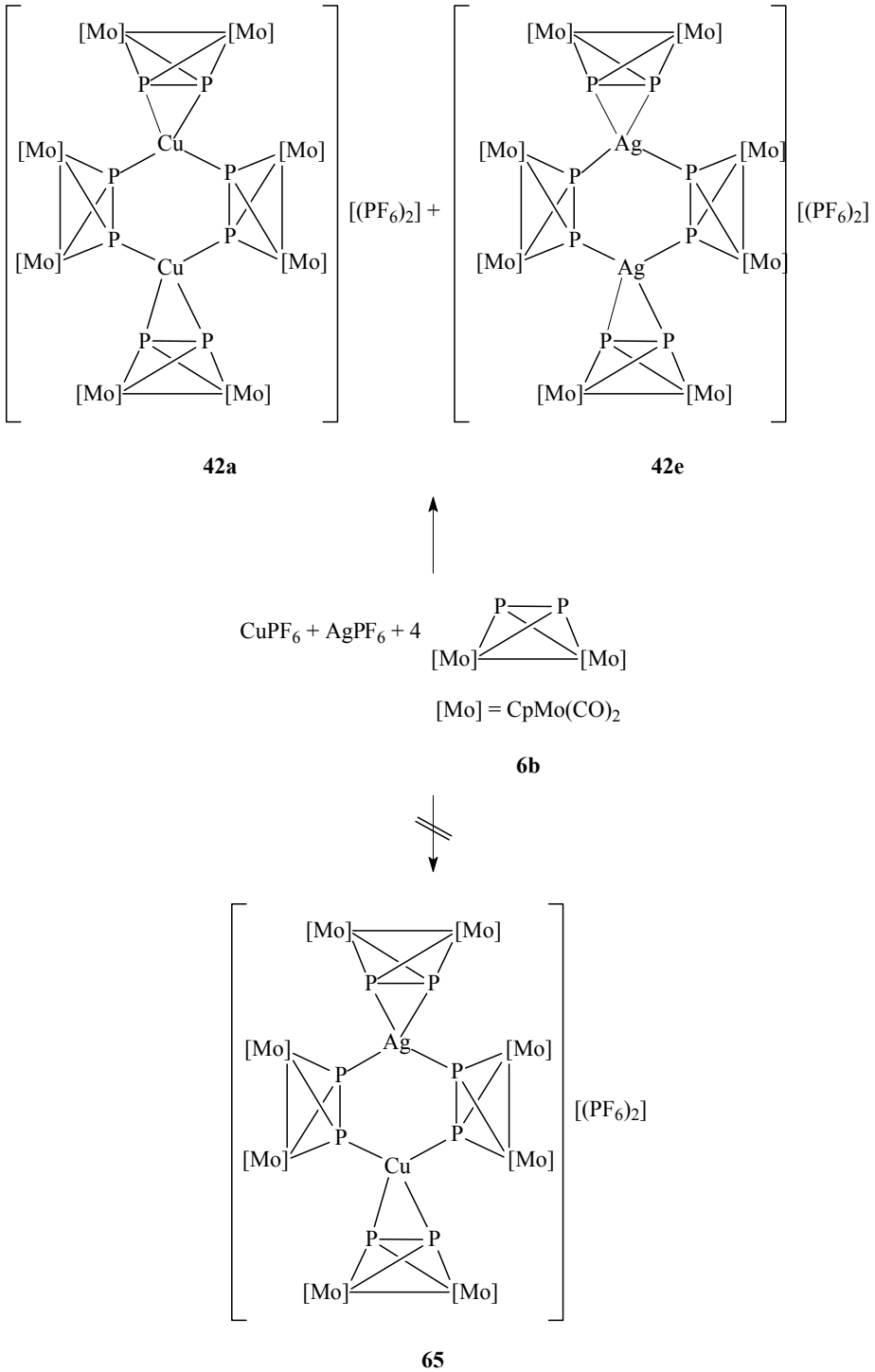


Scheme 3.5. Reaction of **6b** with a 1:1 mixture of $CuPF_6$ and $AgPF_6$.

## 3.2. The Tetrahedrane Cluster $[Cp_2Cr_2(CO)_4(\mu,\eta^2\text{-}P_2)]$ as a Ligand

Although the compound $[Cp_2Cr_2(CO)_4(\mu,\eta^2\text{-}P_2)]$[9a,b] **6a** is less stable than its Mo analogue **6b** and has been shown to readily undergo fragmentation reactions,[28,53] its properties as a supramolecular building block were nevertheless investigated. It was of particular interest to determine whether reaction of **6a** with CuX (X = Cl, Br, I) would yield compounds structurally comparable with the 1D polymers **43a-c**[32a,33] (Figure 1.10) obtained from the reaction of **6b** with the same $Cu^I$ salts. The structures of **43a-c** consist of an alternating arrangement of four-membered $Cu_2X_2$ rings and six-membered $Cu_2P_4$ rings, which are nearly orthogonal to one another. At first sight, the P atoms in the crystal structures of **43a-c** appear to be quite similar, despite being crystallographically distinct, and one would expect perhaps a single broad peak in the solid-state $^{31}$P MAS-NMR spectra of all three polymers. $^{31}$P MAS-NMR investigations on these polymers, undertaken during the course of this work, revealed that the spectrum of **43c** does indeed display a broad multiplet, centred at –87 ppm. The spectra of **43a**,**b** are, however, strikingly different and both exhibit two distinct multiplets separated by about 150 ppm (Figure 3.13). Upon closer scrutiny of the crystal structures (Figure 3.13), it was revealed that the unanticipated spectra are most likely a result of subtle differences in the arrangement of the Cp and particularly the CO ligands at the Mo atoms of the units of **6b**. In **43a**,**b**, the average interatomic distance between the P1 atoms and the carbonyl C atoms of the corresponding units of **6b** (**43a**: 3.283(1) Å; **43b**: 3.261(1) Å) is markedly shorter than that observed for the P2 atoms (**43a**: 3.424(1) Å; **43b**: 3.400(1) Å). The P1 atoms in these two polymers are thus more deshielded than the P2 atoms and resonate at a lower field. In contrast to **43a**,**b**, the same interatomic distances in **43c** are essentially identical (3.196(1) and 3.180(1) Å, respectively) and therefore both the P1 and the P2 atoms are shielded to approximately the same extent by the CO ligands.

In order to rationalise these observations, DFT calculations were performed on the model compounds **66a′**,**b′**,[33] whose calculated structures are depicted in Figure 3.14. The calculated $^{31}$P-NMR shifts for the P atoms in the central $Cr_2P_4$ rings of these compounds (**66a′**: 78, –147 ppm; **66b′**: 73, –160 ppm) demonstrate a similar pattern to that observed in the experimental spectra of **43a**,**b**, that is, two well-separated signals ($\Delta\delta$ > 200 ppm), the low field signals arising from the

P atoms which are closer, on average, to the carbonyl C atoms of the corresponding units of **6a**.

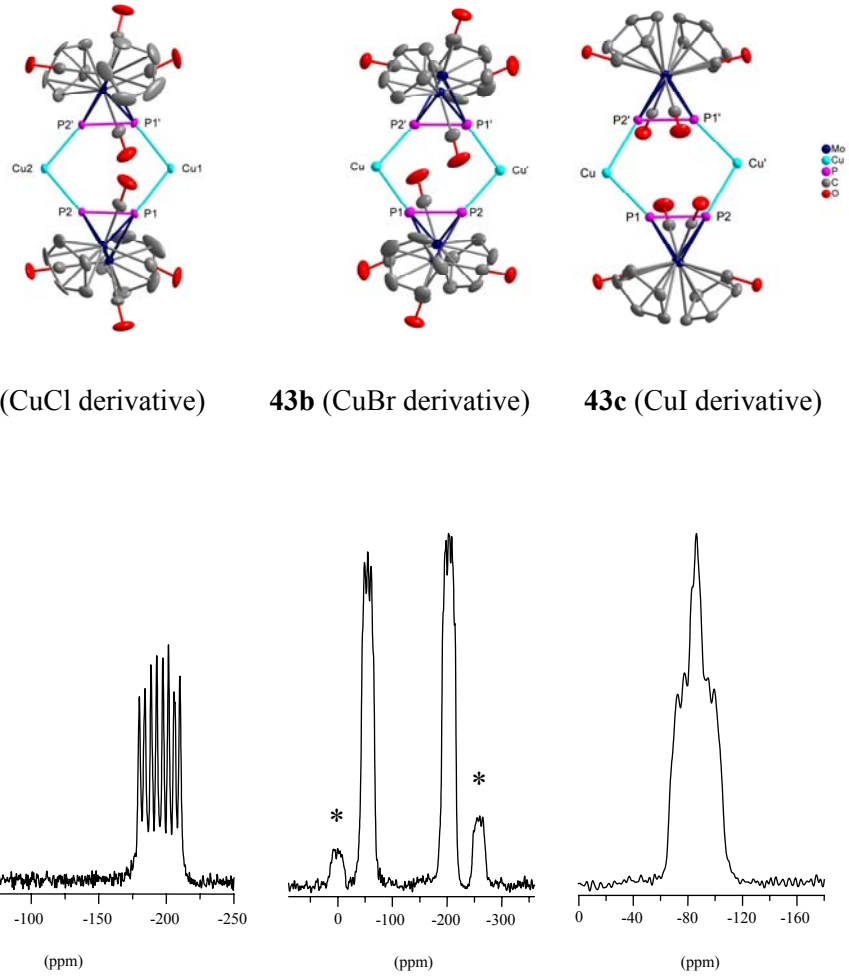


**43a** (CuCl derivative) **43b** (CuBr derivative) **43c** (CuI derivative)

Figure 3.13. View of the $Cu_2P_4$ rings found in the 1D polymers **43a-c** (**43a** perpendicular to the Cu1─P1─P1´ plane, **43b**,**c** perpendicular to the P1─P2─P1´─P2´ planes; hydrogen and halogen atoms omitted for clarity; thermal ellipsoids are represented at the 50 % probability level), demonstrating the subtle differences in the arrangement of the Cp and CO ligands at the Mo atoms with respect to the different P atoms, and the $^{31}$P MAS-NMR spectra of the compounds (spinning side-bands marked with an asterisk; **43a**: P1 –53.0 ppm ($^1J_{CuP}$ = 1040 ($^{63}$Cu), 1108 ($^{65}$Cu) Hz; $^1J_{PP}$ = 517 Hz); P2 –193.6 ppm ($^1J_{CuP}$ = 1042 ($^{63}$Cu), 1109 ($^{65}$Cu) Hz; $^1J_{PP}$ = 504 Hz); **43b**: P1 –55.0 ppm ($^1J_{CuP}$ = 968 Hz; $^1J_{PP}$ = 605 Hz); P2 –203.4 ppm ($^1J_{CuP}$ = 1032 Hz; $^1J_{PP}$ = 592 Hz); **43c**: P1 –78.2 ppm ($^1J_{CuP}$ = 897 Hz; $^1J_{PP}$ = 485 Hz); P2 –93.8 ppm ($^1J_{CuP}$ = 911 Hz; $^1J_{PP}$ = 542 Hz)).

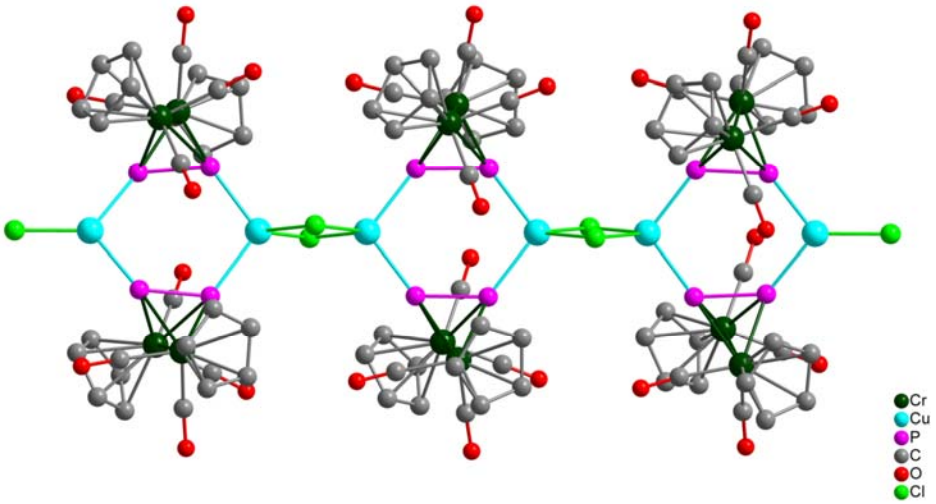


**66a´**

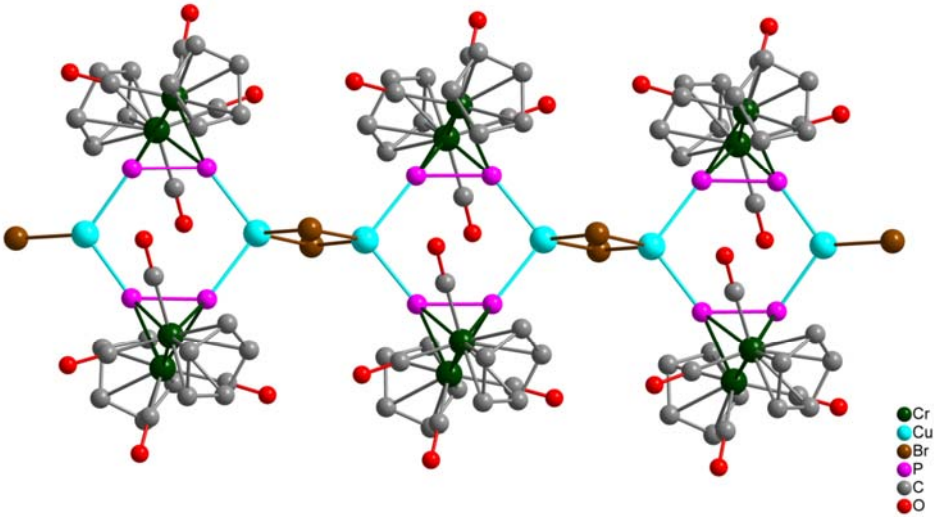


**66b´**

Figure 3.14. Calculated structures of the model compounds **66a´**,**b´**, optimised using the crystal structures of **43a**,**b** as a basis.

## 3.2.1. Studies on the Reactivity of $[Cp_2Cr_2(CO)_4(\mu,\eta^2\text{-}P_2)]$ with CuX (X = Cl, Br, I)

Reaction of **6a** with CuX (X = Cl, Br, I) in a mixture of $CH_3CN$ and $CH_2Cl_2$ at room temperature leads to the formation of the 1D polymers **66a-c** (Equation 3.10) as air-sensitive moss-green microcrystalline powders, which can be stored indefinitely at ambient conditions under an inert atmosphere. They are insoluble in most common solvents and soluble in trace amounts in polar solvents such as $CH_3CN$, and then only under dissociation to the starting materials, as evidenced by $^{31}$P-NMR spectroscopy.

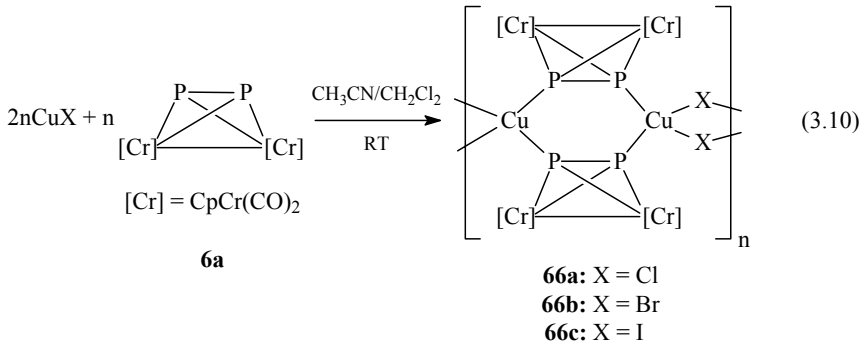


(3.10)

The structures of the compounds **66a-c** (Figure 3.15) display a polymeric core-structure reminiscent of that in the Mo analogues **43a-c**. The $Cu^I$ centres in **66a-c** are found in a distorted tetrahedral coordination mode and are bridged by the P atoms of **6a** and the halogen atoms in such a way, that structures consisting of an alternating arrangement of planar four-membered $Cu_2X_2$ rings and six-membered $Cu_2P_4$ rings in a slight chair-like conformation result, in which these rings are nearly orthogonal to each other. Compounds **66b**,**c** and their Mo analogues **43b**,**c** are structurally similar, whereas polymers **66a** and **43a** are not. Unlike **43a**, the $Cu_2P_4$ rings in **66a** possess an inversion centre situated at the centre of these rings.

Selected structural details for the compounds **66a-c** are listed in Table 3.8. The P─P bond lengths of the units of **6a** in **66a**,**b** are unchanged compared to uncoordinated **6a** (2.060(1) Å),[9a] whereas those in **66c** are marginally longer. Although the Cu─P bond lengths are generally longer than those found in the complexes $[Cu_2X_2(PPh_3)_3]$ (X = Cl[54a] 2.183(4)-2.245(5) Å, Br[54b] 2.190(3)-2.260(3) Å, I[54c] 2.219(3)-2.267(3) Å), the Cu─X bond lengths are within the ranges defined by these compounds (X = Cl[54a] 2.298(4)-2.454(4) Å, Br[54b] 2.370(2)-2.610(2) Å, I[54c] 2.500(2)-2.819(1) Å).

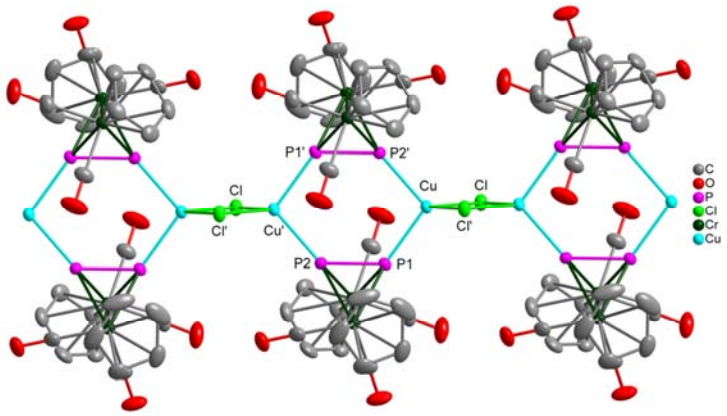


**66a**

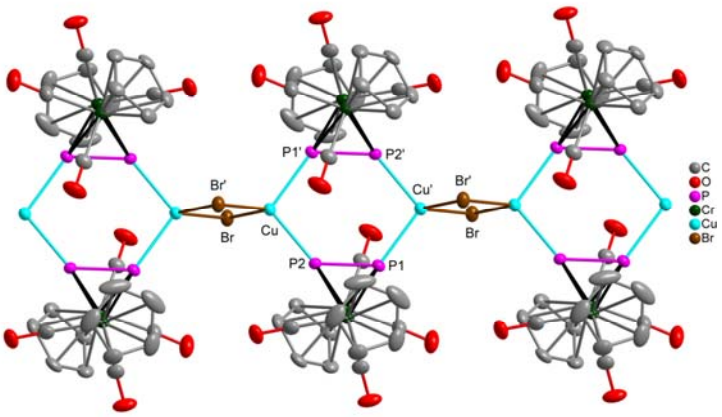


**66b**

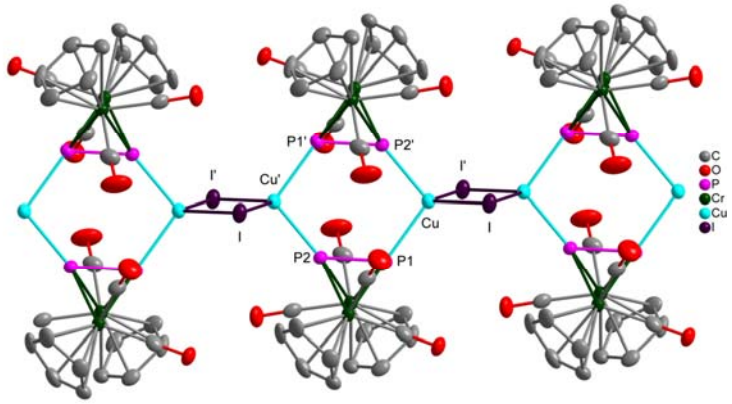


**66c**

Figure 3.15. Portions of the 1D polymeric structures of **66a-c** (hydrogen atoms omitted for clarity). Thermal ellipsoids are represented at the 50 % probability level.

Table 3.8. Selected bond lengths(Å) and angles (°) for compounds **66a-c**.

| Parameter | 66a | 66b | 66c |
|---|---|---|---|
| P─P | 2.061(1) | 2.061(1) | 2.073(2) |
| Cu─P | 2.289(1), 2.296(1) | 2.297(1), 2.305(1) | 2.323(2), 2.333(2) |
| Cu─X | 2.344(1), 2.363(1) | 2.467(4), 2.479(4) | 2.611(1), 2.675(1) |
| P─Cu─P | 103.17(2) | 104.07(2) | 104.95(7) |
| P1─Cu─X | 111.41(2), 114.53(2) | 111.97(2), 112.84(2) | 106.77(6), 116.81(6) |
| P2─Cu─X | 112.02(2), 115.58(2) | 110.77(2), 113.81(2) | 106.42(6), 113.17(6) |
| X─Cu─X | 100.49(2) | 103.62(2) | 108.10(4) |
| Cu─X─Cu | 79.51(2) | 76.38(1) | 71.90(3) |
| Cu···Cu···Cu | 174.86(1) | 176.48(2) | 170.50(1) |

A further interesting structural feature observed in all three polymers is that the Cu atoms are alternately distributed along two parallel lines, as illustrated by the Cu···Cu···Cu angles given in Table 3.8 and the representation of the polymers in Figure 3.16. Moreover, the folding angle of the $Cu_2P_4$ rings, that is, the angle between the CuP1P2 and P1P2P1P2 planes (**66a**: 3.81(1)°; **66b**: 2.48(1)°; **66c**: 0.97(1)°) decreases as the size of the halogen increases.

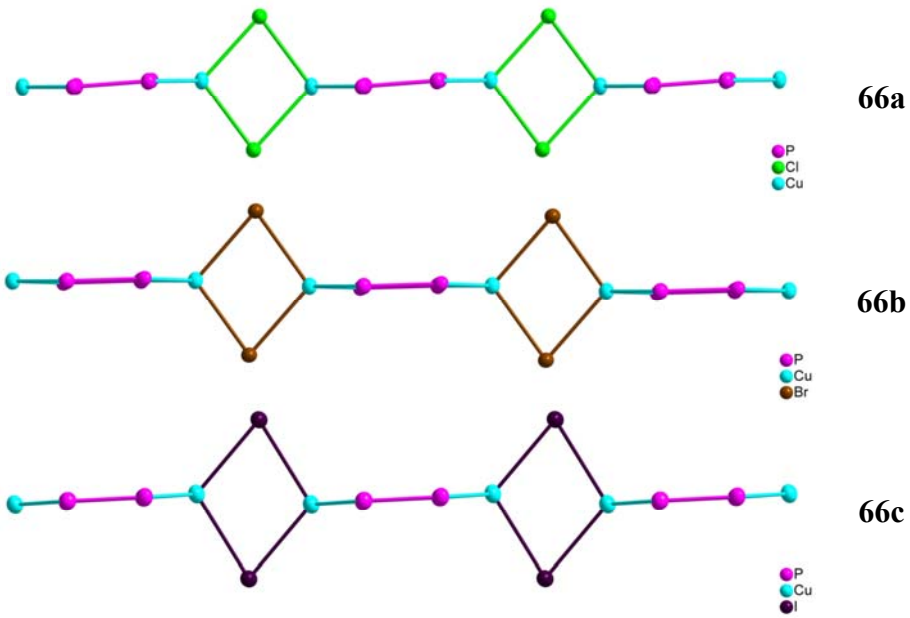


Figure 3.16. View of the structures of **66a-c** perpendicular to the faces of the $Cu_2X_2$ rings (Cr atoms and their supporting ligands omitted for clarity). Thermal ellipsoids are represented at the 50% probability level.

Solid-state $^{31}P$ MAS-NMR measurements were performed on the polymers **66a-c** at room temperature and the spectra obtained are

depicted in Figure 3.17. The chloride and bromide derivatives exhibit identical spectra and display two multiplets at –100 and 81 ppm, whereas the iodide derivative displays one broad signal at about 48 ppm with no analysable fine structure. The low field signals in the spectra of the chloride and bromide derivatives are assigned to the P1 atoms since the average interatomic distance between these atoms and the carbonyl C atoms of the respective units of **6a** (**66a**: 3.128(1) Å; **66b**: 3.129(1) Å) is shorter than that of the P2 atoms (**66a**: 3.286(1) Å; **66b**: 3.279(1) Å), and they are therefore more deshielded. The same average interatomic distances in **66c** are 3.065(1) and 3.079(1) Å and hence P1 and P2 in this compound are essentially identical, as suggested by its spectrum.

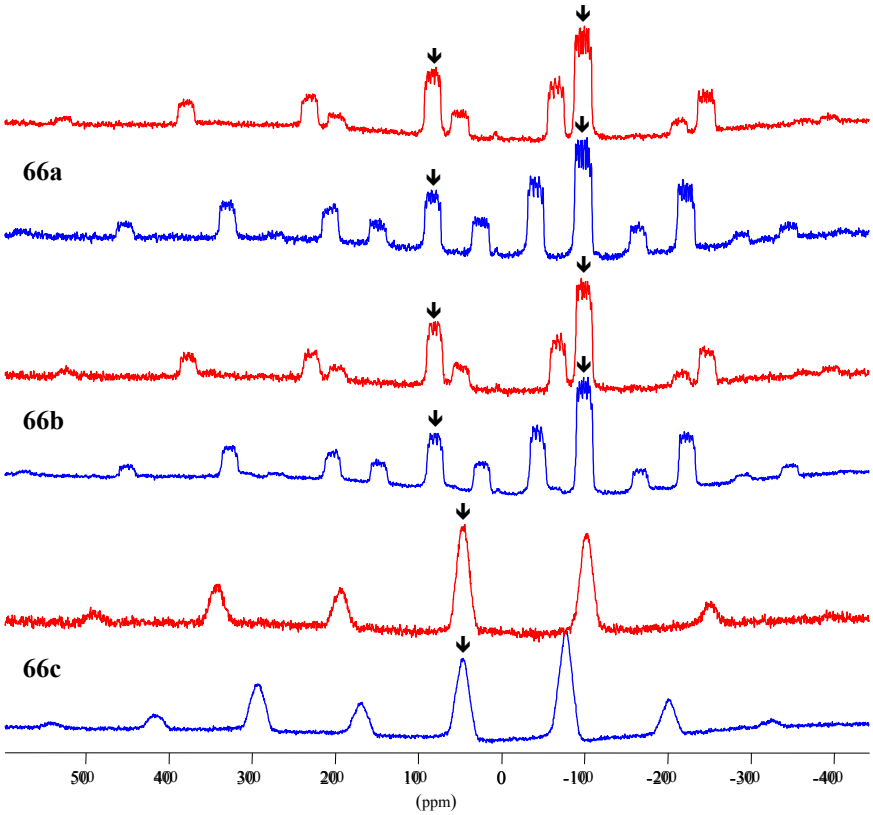


Figure 3.17. Solid state $^{31}$P MAS-NMR spectra of polymers **66a-c**, recorded with a spinning rate of 25 kHz (blue) and 30 kHz (red). The peaks marked with arrows are the sample peaks and the unmarked peaks are the spinning side-bands (**66a**: P1 83.0 ppm ($^{1}J_{CuP}$ = 1110 Hz; $^{1}J_{PP}$ = 505 Hz; $^{2}J_{PP}$ = 220 Hz); P2 –97.0 ppm ($^{1}J_{CuP}$ = 1080 Hz; $^{1}J_{PP}$ = 543 Hz; $^{2}J_{PP}$ = 240 Hz); **66b**: P1 81.0 ppm; P2 –100.0 ppm; **66c**: 48.0 ppm).

The spectra of **66a-c** thus demonstrate a pattern very similar to that of the Mo analogues **43a-c** (Figure 3.13).[33] Furthermore, the experimental chemical shifts observed for **66a**,**b** are in good agreement with the calculated values for the model compounds **66a´** and **66b´** (Figure 3.14).

As already mentioned above, complexes **66a-c** dissolve in $CH_3CN$ in trace amounts, apparently under complete dissociation to the starting materials according to $^{31}$P-NMR measurements. However, the fragments detected in the positive ion ESI-MS spectra of the compounds in $CH_3CN$ at room temperature (Table 3.9) suggest that oligomeric species are most likely present in solution.

Table 3.9. Selected fragments (mass/charge (relative abundance in %)) detected in the positive ion ESI-MS spectra of compounds **66a-c** in $CH_3CN$ and the proposed cations for these fragments.

| **66a** (X = Cl) | **66b** (X = Br) | **66c** (X = I) | **Proposed Cation** |
|---|---|---|---|
| 1076.7 (3) | 1166.6 (9) | 1260.7 (12) | $[(Cu_3X_2)\{Cp_2Cr_2(CO)_4P_2\}_2]^+$ |
| 1022.6 (2) | 1110.5 (4) | 1204.6 (7) | $[(Cu_3X_2)\{Cp_2Cr_2(CO)_3P_2\}_2]^+$ |
| 978.7 (16) | 1022.7 (18) | 1070.6 (10) | $[(Cu_2X)\{Cp_2Cr_2(CO)_4P_2\}_2]^+$ |
| 922.7 (8) | 966.6 (11) | 1014.6 (10) | $[(Cu_2X)\{Cp_2Cr_2(CO)_3P_2\}_2]^+$ |

## 3.2.2. Studies on the Reactivity of $[Cp_2Cr_2(CO)_4(\mu,\eta^2\text{-}P_2)]$ with $Ag[Al\{OC(CF_3)_3\}_4]$

As a result of the extensive investigations on the reactivity of **6b** with Ag salts of various WCAs, it was decided to study the reaction of **6a** with $Ag[Al\{OC(CF_3)_3\}_4]$, since this salt generally offers the advantage of solubility, even in non-coordinating solvents. This reaction, carried out in $CH_2Cl_2$ at room temperature, leads to the isolation of the complex salt **67** as a dark wine-red powder (Equation 3.11), elemental analysis of which confirms a 2:1 stoichiometry of **6a** and the Ag salt. Complex **67** is light- and air-sensitive, and is soluble in solvents such as $CH_2Cl_2$, THF and $CH_3CN$. Solutions of the compound undergo slow decomposition, even at freezer temperatures (–28 °C), and solid samples should be stored under an inert atmosphere below room temperature, preferably in a freezer. The structure of compound **67** is most probably similar to that of the Mo derivative **42g** (Figure 3.1), since **6a** has been shown to react with CuX (X = Cl, Br, I) in a manner identical to that of its Mo analogue **6b**.

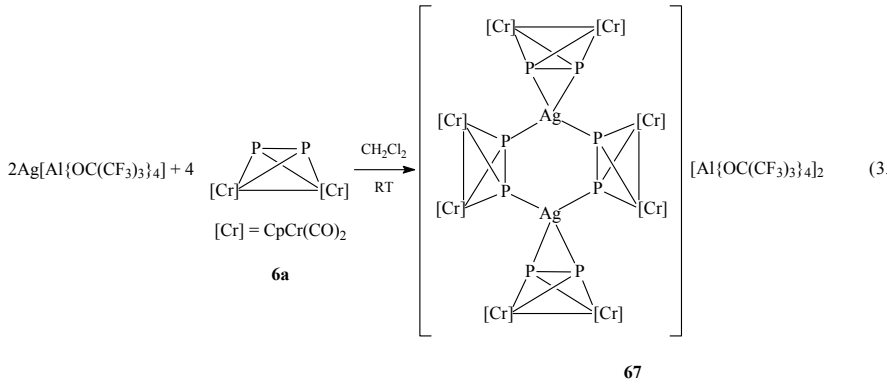


(3.11)

In the positive ion ESI-MS spectra of **67**, the most abundant fragment detected is attributable to the cation $[Ag\{Cp_2Cr_2(CO)_4P_2\}_2]^+$, regardless of whether the measurements are made in $CH_2Cl_2$ or $CH_3CN$. A fragment of low abundance, assigned to the cation $[Ag_2\{Cp_2Cr_2(CO)_4P_2\}\{Cp_2Cr_2(CO)_3P_2\}]^{2+}$, is also detected. These two fragments suggest the existence of an equilibrium similar to that proposed for **42g** (Scheme 3.1) in solutions of **67**, involving the dimer **67** and the monomer $[Ag\{Cp_2Cr_2(CO)_4P_2\}_2][Al\{OC(CF_3)_3\}_4]$ **68**.

Variable temperature $^{31}$P-NMR measurements in $CD_2Cl_2$ (Figure 3.18) also support dynamic behaviour in solutions of **67**, and therefore the existence of a monomer/dimer equilibrium. At room temperature, a singlet without any detectable coupling to $^{107/109}$Ag is observed at 43.3 ppm, which is shifted by about 70 ppm upfield relative to uncoordinated **6a**.[9a,b] As the temperature is reduced, the signal becomes broader and, at –40 °C, is resolved into two signals, one at 62.2 ppm and one centred at approximately 20 ppm. The high field signal is particularly broad and the integration ratio of the two signals is approximately 2:1.

VPO measurements on **67** in $CH_2Cl_2$ at 28 °C reveal a molecular mass of 3060 ± 153 g mol$^{-1}$ for the species in solution (expected: **67**: 3784 g mol$^{-1}$; **68**: 1892 g mol$^{-1}$) and therefore suggest a monomer to dimer ratio of approximately 5:6. Here, it is interesting to note that the presence of a monomer in solutions of the Mo derivative **42g** is virtually exclusive. Considering the ESI-MS, $^{31}$P-NMR and VPO data as well as the previous discussion on the solution behaviour of **42g**, it is not unlikely that the equilibria illustrated in Scheme 3.6 exist in solutions of **67**, involving the monocations **VIII** and **IX**, and the dication **X**.

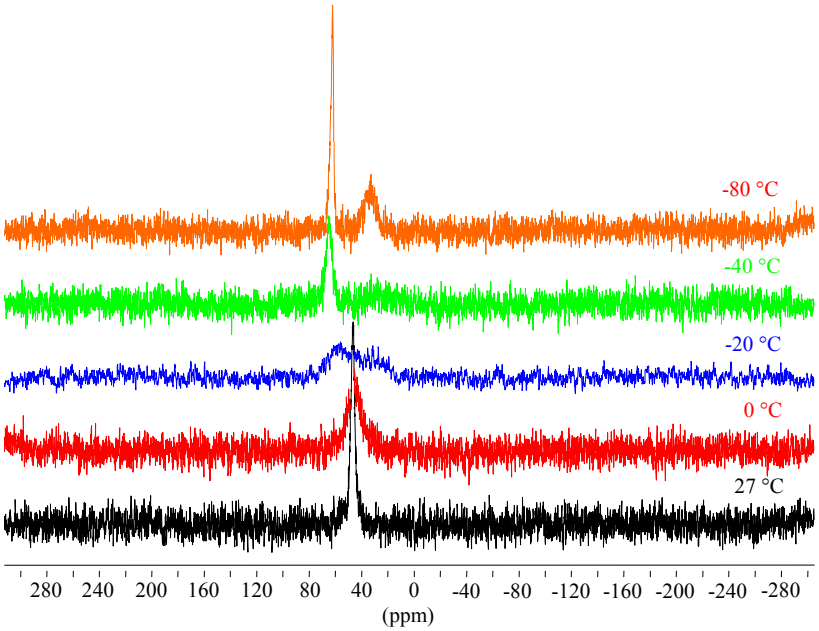


Figure 3.18. Variable temperature $^{31}$P-NMR spectra of **67** in $CD_2Cl_2$.

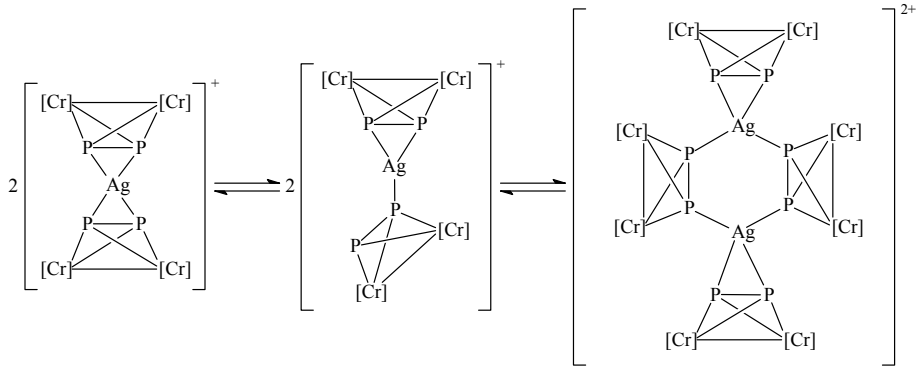


Scheme 3.6. Proposed cation equilibria in solutions of **67**.

## 3.3. The Tetrahedrane Complex $[CpCr(CO)_2(\eta^3\text{-}P_3)]$ as a Ligand

The compound $[CpCr(CO)_2(\eta^3\text{-}P_3)]$ **7a**[9a,b] is even less stable than **6a** and solutions of this complex tend to slowly decompose, particularly under the influence of light. Even solid samples of **7a** are unstable at room temperature and should be stored under an inert atmosphere at typical freezer temperatures. The investigations on the suitability of this complex as a supramolecular building block were thus limited.

### 3.3.1. Studies on the Reactivity of $[CpCr(CO)_2(\eta^3\text{-}P_3)]$ with $Ag[Al\{OC(CF_3)_3\}_4]$

The reaction of complex **7a** with $Ag[Al\{OC(CF_3)_3\}_4]$ in a 2:1 stoichiometry in $CH_2Cl_2$ at room temperature leads to the isolation of the complex **69** as an ochre coloured solid (Equation 3.12). Elemental analysis confirms that the product comprises **7a** and the Ag salt in a 2:1 stoichiometry, and the solid-state structure most probably consists of a cationic 1D polymer chain as illustrated in Equation 3.12. This suggested structure is based on the results obtained from similar investigations on the Mo analogue of **7a** (see section **3.4.1**). Compound **69** is air- and light-sensitive and readily dissolves in solvents such as $CH_2Cl_2$, THF and $CH_3CN$, its solutions being unstable even under an inert atmosphere at –28 °C. In the solid state, it should be stored under an inert atmosphere at low temperatures.

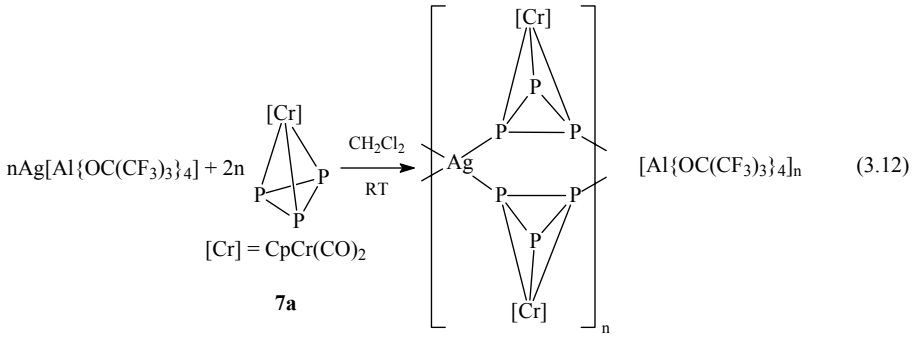


Assuming that the proposed structure for **69** is correct, $^{31}$P-NMR spectroscopy suggests the existence of dynamic behaviour in its solutions. The room temperature spectrum of **69** in $CD_2Cl_2$ displays a

singlet at –299.9 ppm, which is approximately 15 ppm upfield-shifted with respect to uncoordinated **7a**, and exhibits no coupling to $^{107/109}$Ag. Low temperature NMR measurements in the same solvent did not lead to resolution of this signal, even at –80 °C. Spectra recorded in a 1:3 mixture of $CD_2Cl_2$ and THF-$d_8$ at –120 °C show significant broadening, but no signal splitting.

In the room temperature ESI-MS spectra of **69**, acquired in either $CH_2Cl_2$ or $CH_3CN$, fragments attributable to the cation $[Ag\{CpCr(CO)_2P_3\}_2]^+$ are detected, albeit with a very low relative abundance. These peaks demonstrate the likely existence of dynamic behaviour in solution and the spectra in general reflect the low stability of the species in solution. VPO measurements on **69** in $CH_2Cl_2$ at 28 °C reveal a molecular mass of 1904 ± 95 g mol$^{-1}$ for the species in solution (expected for the monomer $[Ag\{CpCr(CO)_2P_3\}_2][Al\{OC(CF_3)_3\}_4]$ **70**: 1608 g mol$^{-1}$), which is indicative of a dynamic equilibrium. The possible solution equilibria will be discussed in more detail in the next section.

## 3.4. The Tetrahedrane Complex $[CpMo(CO)_2(\eta^3\text{-}P_3)]$ as a Ligand

The compound $[CpMo(CO)_2(\eta^3\text{-}P_3)]$ **7b**[9c,d] is considerably more stable than its Cr analogue **7a**, but its solutions are nevertheless susceptible to slow decomposition under the influence of light. On account of the greater stability of **7b**, investigations on this complex were more extensive. Experiments with CuX (X = Cl, Br, I) have so far resulted in the isolation of amorphous powders, which could not be adequately characterised.

### 3.4.1. Studies on the Reactivity of $[CpMo(CO)_2(\eta^3\text{-}P_3)]$ with $Ag[Al\{OC(CF_3)_3\}_4]$

Reaction of **7b** with $Ag[Al\{OC(CF_3)_3\}_4]$ in a 2:1 stoichiometry in $CH_2Cl_2$ at room temperature leads to the isolation of **71** as air- and light-sensitive canary-yellow needles after storage of the reaction mixture at –28 °C (Equation 3.13). Complex **71** is readily soluble in solvents such as $CH_2Cl_2$, THF and $CH_3CN$, and can be stored indefinitely under an inert atmosphere.

Compound **71** has been crystallographically characterised and the structure of the polycation is depicted in Figure 3.19. This cation possesses a 1D polymeric structure consisting of Ag cations bridged

pairwise by two units of **7b**, thus forming a chain of six-membered $Ag_2P_4$ rings.

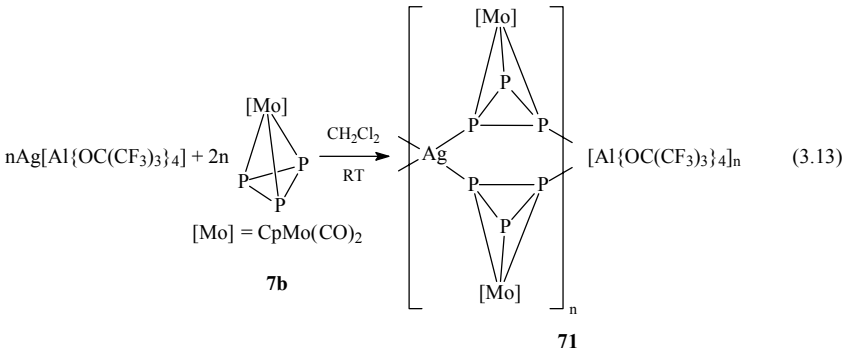


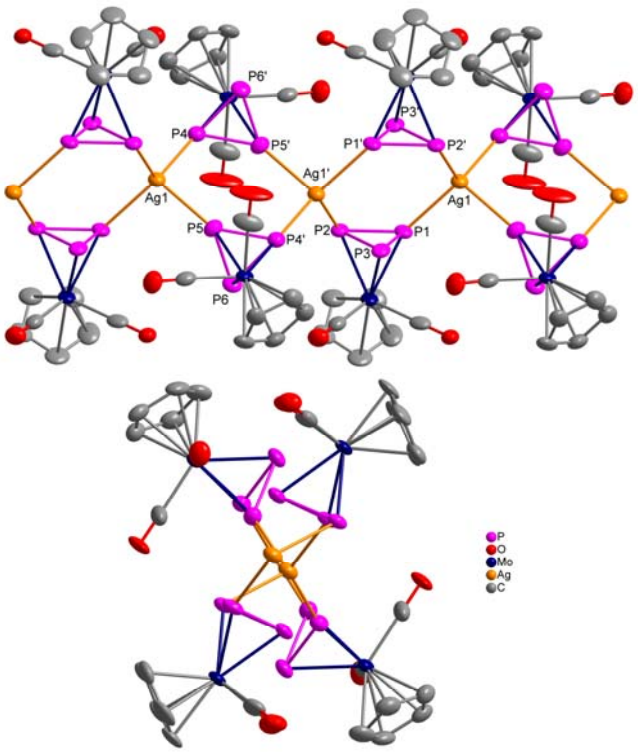


Figure 3.19. Section of the structure of the 1D polycationic chain in **71** (hydrogen atoms omitted for clarity). The bottom illustration is a view of the chain along the crystallographic *a*-axis. Thermal ellipsoids are represented at the 50 % probability level. Selected bond lengths (Å) and angles (°): P1─P2 2.146(3), P1─P3 2.155(3), P2─P3 2.203(3), P4─P5′ 2.144(3), P4─P6′ 2.161(3), P5─P6 2.134(3), Ag1─P1 2.571(2), Ag1─P2′ 2.641(2), Ag1─P4 2.522(2), Ag1─P5 2.577(2), P1─Ag1─P2′ 106.19(7), P1─Ag1─P4 129.20(7), P1─Ag1─P5 100.15(7), P2′─Ag1─P4 112.78(6), P2′─Ag1─P5 105.60(7), P4─Ag1─P5 99.42(8).

The $Ag^I$ centres in **71** are in a distorted tetrahedral coordination mode and are alternately distributed along two parallel lines (Ag1···Ag1´···Ag1 165.15(2)°). Although only alternate $Ag_2P_4$ rings are identical, all assume a chair conformation (angle between Ag1P1P2´ and P1P2P1´P2´ planes: 23.03(7)°; angle between Ag1P4P5 and P4P5P4´P5´ planes: 1.05(7)°). The average P─P bond lengths of the two different $P_3$ rings in **71** (2.146(3) and 2.168(3) Å) are somewhat longer than those reported for the two independent molecules found in the crystal structure of **7b** (2.127(3) and 2.134(2) Å).[55] The Ag─P bond lengths (2.522(2)-2.641(2) Å) are within the range defined by the compounds **42b**,**c**[32] and **42d-g** (2.468-2.774 Å). A further structural feature of interest is the arrangement of the Cp and particularly the CO ligands with respect to the $P_3$ rings. In the units of **7b** containing the P atoms P1, P2 and P3, the carbonyl C atom and P atom interatomic distances are shortest for the non-coordinated P3 atoms (average interatomic distance 2.910(9) Å), whereas in the units containing the P atoms P4, P5 and P6, these distances are shortest for the coordinated P5 atoms (average interatomic distance 2.89(1) Å).

In the positive ion ESI-MS spectra of polymer **71** in $CH_2Cl_2$ at room temperature, only one fragment is detected, which can be ascribed to the cation $[Ag\{CpMo(CO)_2P_3\}_2]^+$, and this suggests that **71** dissolves under depolymerisation. This is confirmed by VPO measurements on **71** in $CH_2Cl_2$ at 28 °C, which reveal that the molecular mass of the species in solution is 2440 ± 122 g $mol^{-1}$. If one considers the monomeric species $[Ag\{CpMo(CO)_2P_3\}_2]$ $[Al\{OC(CF_3)_3\}_4]$ **72** (1695 g $mol^{-1}$) and the dimeric species $[Ag_2\{CpMo(CO)_2P_3\}_4]$ $[\langle Al\{OC(CF_3)_3\}_4\rangle_2]$ **73** (3390 g $mol^{-1}$), the experimentally determined molecular mass of **71** is slightly lower than that that would be expected for a 1:1 mixture of **72** and **73** (2543 $gmol^{-1}$), suggesting that a monomer/dimer equilibrium exists in solution, slightly in favour of the monomer (monomer:dimer = 7:5). It is indeed quite likely that this equilibrium is similar to that already described above for **42g** (Scheme 3.1) and most probably involves the monocations **XI** and **XII**, and the dication **XIII**, as outlined in Scheme 3.7. An analogous equilibrium could be postulated for solutions of the proposed Cr derivative **69** (see section **3.3.1**).

The $^{31}$P-NMR spectrum of the polymer **71** in $CD_2Cl_2$ at room temperature is also indicative of dynamic behaviour, as only a singlet at –365.4 ppm is observed, 15 ppm upfield-shifted relative to uncoordinated **7b**,[9c,d] without any coupling to $^{107/109}$Ag. This signal could not be resolved, even at –80 °C, and therefore further measurements in a 3:1 mixture of THF-$d_8$ and $CD_2Cl_2$ were performed

(Figure 3.20). At room temperature in this mixture, **71** exhibits

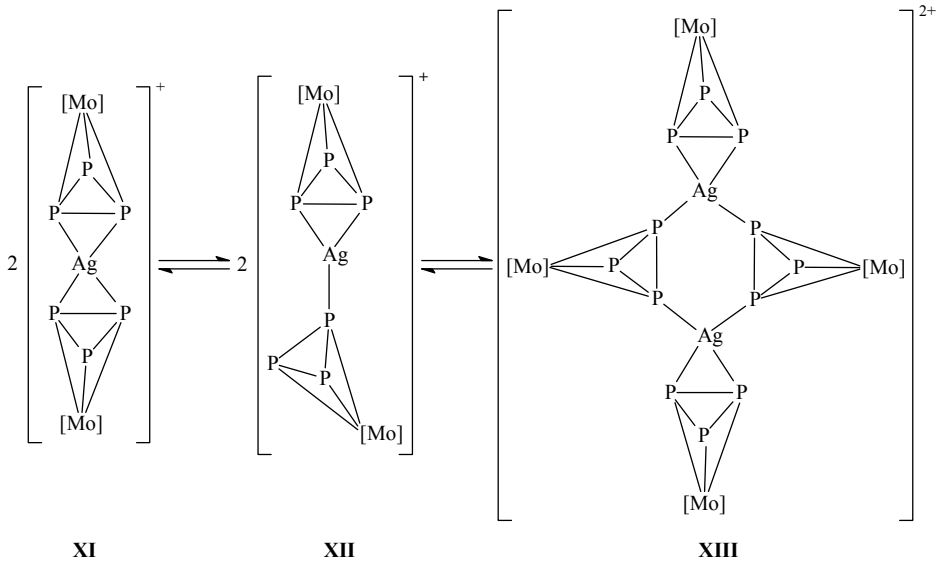


Scheme 3.7. Proposed cation equilibria in solutions of **71**.

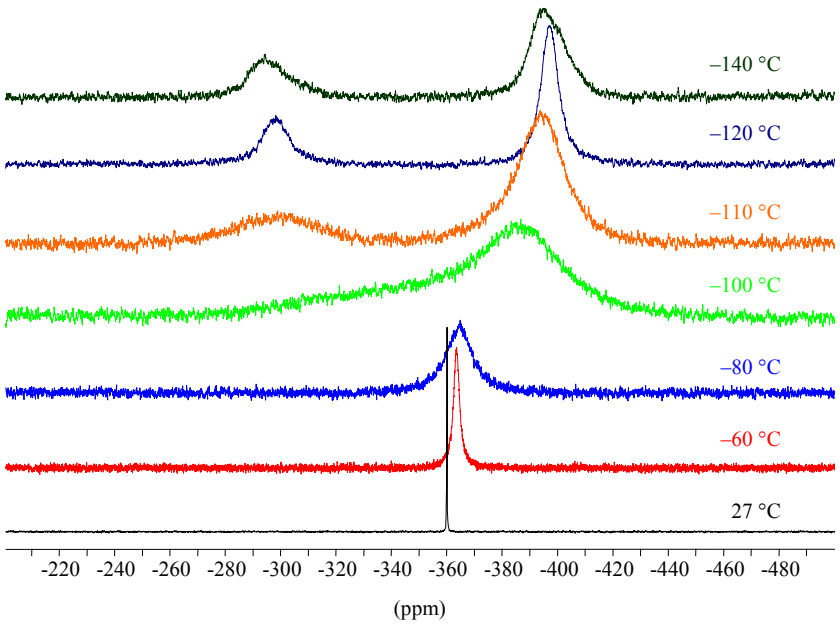


Figure 3.20. Variable temperature $^{31}$P-NMR spectra of **71** in a 3:1 mixture of THF-$d_8$ and $CD_2Cl_2$.

a singlet at –360.2 ppm and as the temperature is reduced, a slight upfield shift and broadening of the peak is observed. At –100 °C the peak becomes extremely flat and broad and at –110 °C two distinct broad signals emerge at –299.0 and –393.7 ppm with an integration ratio of 1:2. Considering the cations in Scheme 3.7, one would expect **XI** and **XIII** to be the most likely species to yield spectra consisting of two well separated peaks with an integration ratio of 1:2, since in these species, the ratio of non-coordinated P atoms to coordinated ones is 1:2, as observed in the solid-state structure of **71**. Assuming that the equilibria in Scheme 3.7 are valid, the experimental spectra suggest that, at low temperature, the conversion of **XII** to either **XI** or **XIII** is fast, whereas the reverse reactions are slow. At higher temperatures, these reverse reactions become fast on the NMR timescale and thus a singlet is observed.

Another dynamic process which would be expected to lead to the observed spectra, and which does not necessitate the existence of a fast monomer/dimer equilibrium, is fast rotation of the $P_3$ rings in the cations depicted in Scheme 3.7. According to VPO measurements, solutions of **71** consist of the monomer **72** and the dimer **73** in a ratio of approximately 7:5. Fast rotation of the $P_3$ rings in these species would render all P atoms within a species equivalent and the chemical shifts of **72** and **73** should be comparable. Hence, a singlet would be expected at room temperature, even though both monomeric and dimeric species would be present in solution, which do not necessarily undergo rapid interconversion. If this rotational motion could be 'frozen' by reducing the temperature, and the resulting 'frozen' cations had the structures of **XI** and **XIII**, the spectral characteristics of both of these cations should resemble those demonstrated experimentally at low temperature by solutions of **71**. One would expect two well-separated signals with an integration ratio of 1:2, corresponding to the ratio of non-coordinated and coordinated P atoms.

At this point, it should be stressed that the choice of the monomer/dimer equilibrium illustrated in Scheme 3.7 as the basis of the discussion of the solution dynamics of **71** arises from the previous discussion on **42g**, the results of the VPO measurements and from a desire to illustrate the lability of the Ag─P bonds of the species in solution using an easily comprehensible system. Furthermore, larger systems are particularly difficult or impossible to investigate theoretically. It is recognised that solutions of **71** may contain minute amounts of even larger cations, which are more representative of the polymeric solid-state structure.

Solid-state $^{31}$P MAS-NMR measurements have also been performed on polymer **71** and, remarkably, suggest the existence of

dynamic behaviour in the solid state (Figure 3.21). Considering the solid state structure of the polymer, one would expect at least two broad signals, one at a lower field relative to **7b** due to the uncoordinated P atoms (P3 and P6), and one at a higher field relative to **7b** due to the coordinated P atoms (P1, P2, P4 and P5), with an integration ratio of 1:2. However, at room temperature, a singlet at –369.4 ppm is observed which can be resolved into the two expected broad signals at –304.2 and –413.2 ppm at –133 °C. The solid-state spectra are thus very similar to the solution spectra and this raises the question of the nature of the dynamic behaviour in solid **71**. Fast rotation of the $P_3$ rings is most probably occurring in the solid state at room temperature, which would render the P atoms equivalent on the NMR timescale. Since fast rotation of the $P_3$ rings in **71** seems to explain the appearance of the solid-state spectra of this compound at room temperature, it is not unlikely that the solution spectral characteristics of **71** are the result of such ring rotation rather than fast equilibrium processes as outlined in Scheme 3.7.

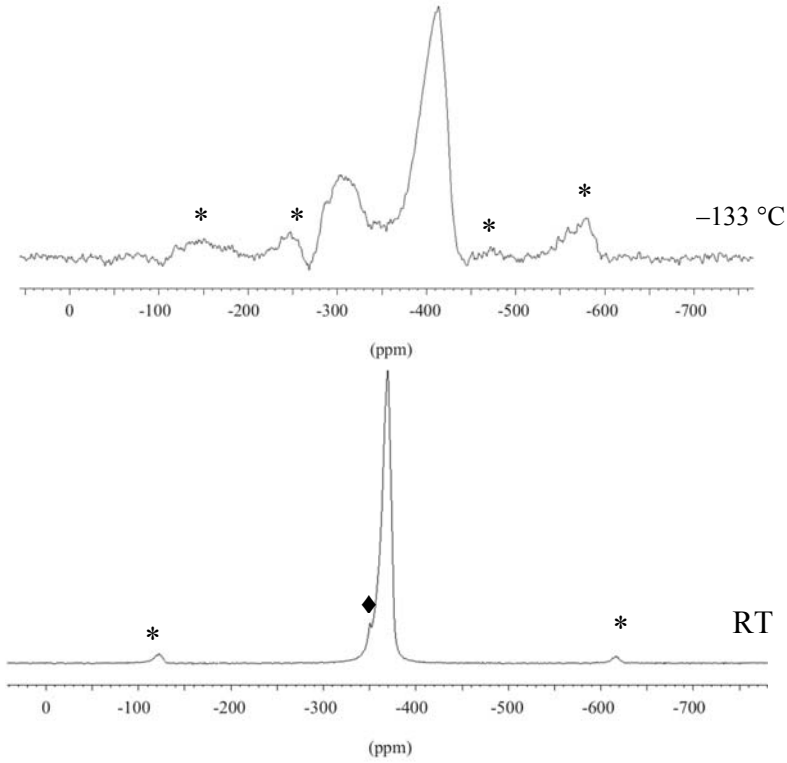


Figure 3.21. Solid-state $^{31}$P MAS-NMR spectra of **71** at room temperature and –133 °C (peaks marked with an asterisk are the spinning side-bands; peak marked with a diamond is due to impurity).

In view of the apparent dynamic behaviour in solutions of **71**, it was of interest to determine whether reactions of **7b** with $Ag[Al\{OC(CF_3)_3\}_4]$ in different proportions would lead to the isolation of different supramolecular architectures. Reaction of the starting materials in a 3:1 stoichiometry in $CH_2Cl_2$ at room temperature results nevertheless in the 2:1 polymer **71**, indicating that this product presents a thermodynamic minimum in the solid state. Changing the reactant stoichiometry to 6:1 leads to the isolation of the 3:1 product **74** as yellow-orange plates (Equation 3.14). Compound **74** is air- and light-sensitive and dissolves readily in solvents such as $CH_2Cl_2$, THF and $CH_3CN$. Solid samples of **74** can be stored indefinitely under an inert atmosphere at room temperature.

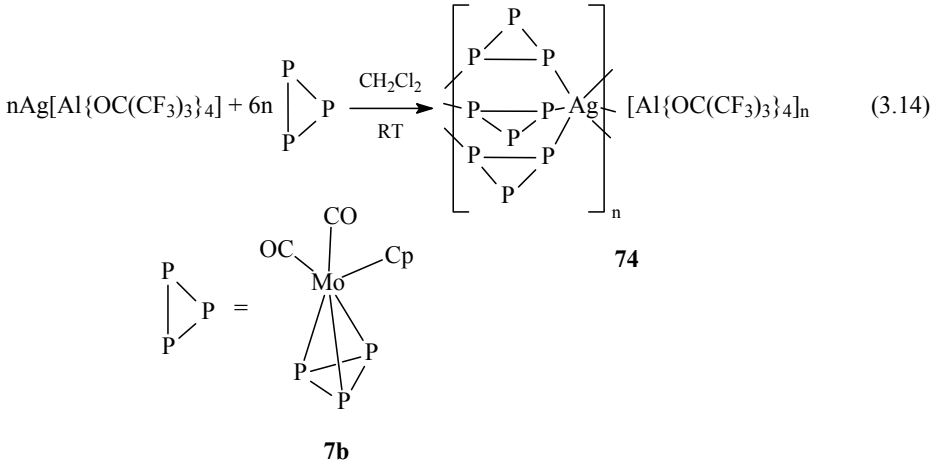


(3.14)

Attempts to obtain crystals of **74** suitable for a satisfactory X-ray crystallographic analysis have so far been unsuccessful, but the quality of the crystals was adequate for determining the connectivity of the atoms heavier than carbon. The structure of the cation in **74** is illustrated in Figure 3.22 and comprises a chain of Ag atoms in an octahedral coordination mode[56] bridged pairwise by three units of **7b**. Thus, a 1D polymer results whose core consists of a chain of $Ag_2P_6$ cages or capsules. Complex **74** is the first example of a compound in which Ag atoms are found octahedrally coordinated to six P atoms.

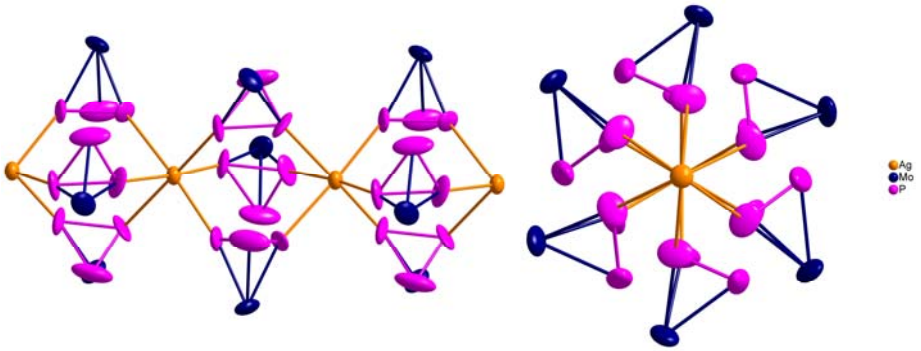


Figure 3.22. View of a portion of the cationic chain in the 1D polymer **74** perpendicular to (left) and along (right) the crystallographic *c*-axis (Cp and CO ligands omitted for clarity). Thermal ellipsoids are represented at the 50 % probability level.

The ESI-MS spectra of **74** in $CH_2Cl_2$ at room temperature display fragments attributable to the cation $[Ag\{CpMo(CO)_2P_3\}_3]^+$ as well as the cations $[Ag\{CpMo(CO)_2P_3\}_2]^+$ and $[Ag\{CpMo(CO)_2P_3\}_4]^+$, which imply that **74** dissolves under depolymerisation and demonstrates dynamic behaviour in solution. VPO measurements on **74** in $CH_2Cl_2$ at 28 °C suggest that only the monomer $[Ag\{CpMo(CO)_2P_3\}_3][Al\{OC(CF_3)_3\}_4]$ **75** (2005 $gmol^{-1}$) is present in solution since a molecular mass of 1916 ± 96 $gmol^{-1}$ is obtained. However, this is not to say that the presence of larger aggregates can be entirely excluded and it is highly likely that equilibria involving the monocations **XIV** and **XV**, and the dication **XVI**, as described in Scheme 3.8, may be in progress in solutions of **74**. The structure of the cation **XIV** seems probable considering the essentially trigonal planar $[Ag(\eta^2\text{-}C_2H_4)_3]^+$ cation of Krossing and Reisinger.[57]

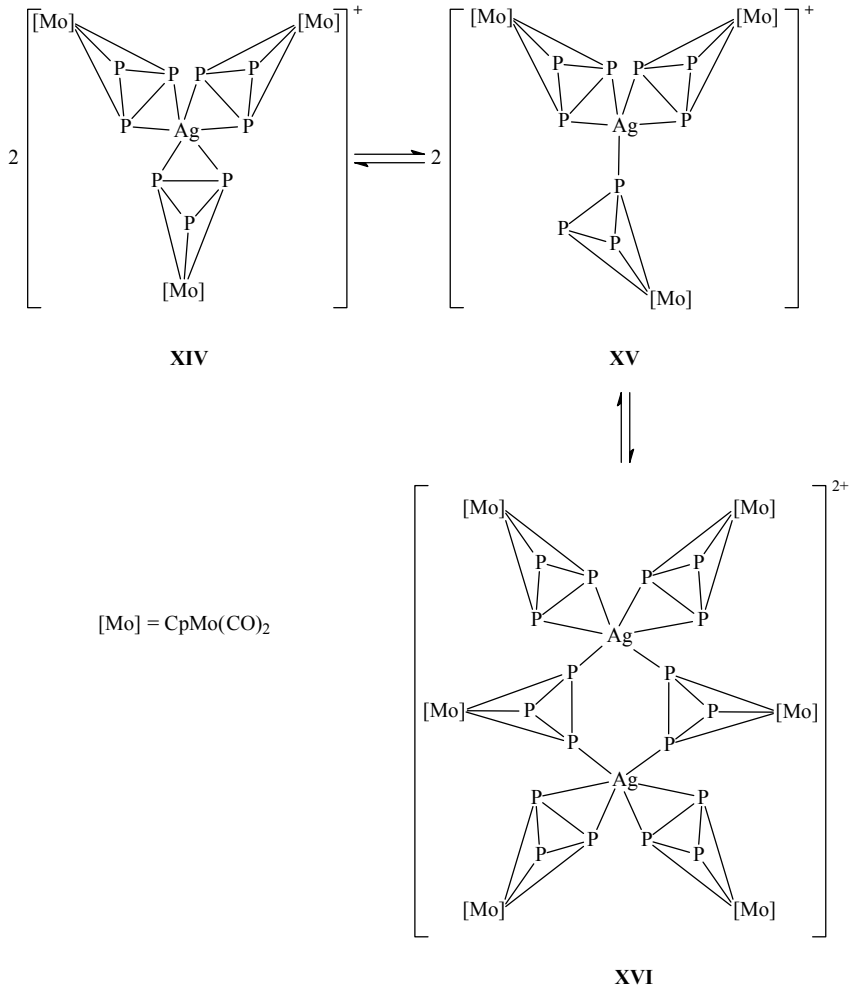


**XIV** **XV** **XVI**

Scheme 3.8. Proposed cation equilibria in solutions of **74**.

In the $^{31}$P-NMR spectrum of polymer **74** in $CD_2Cl_2$ at room temperature, a singlet at –359.6 ppm is observed, without any detectable coupling to $^{107/109}$Ag, which also suggests dynamic behaviour in solutions of **74**. As low temperature measurements in $CD_2Cl_2$ were not conclusive, a 3:1 mixture of THF-$d_8$ and $CD_2Cl_2$ was chosen. At room temperature in this mixture, a singlet at –359.0 ppm is observed, while at –120 °C two well-separated broad peaks are observed at –293.8 and –396.2 ppm with an integration ratio of 1:2, a pattern already observed in the case of polymer **71**. The cations **XIV** and **XVI** would be expected to display spectra resembling the low temperature spectrum of **74**, that is, spectra with two well-separated peaks in an integration ratio of 1:2, corresponding to the ratio of non-coordinated and coordinated P atoms. If the equilibria in Scheme 3.8 are valid, the spectra suggest that the interconversion between **XIV** and

**XVI** over **XV** is fast in both directions at room temperature, whereas at low temperature only the conversion of **XV** to **XIV** or **XVI** is fast while the reverse reactions are slow.

Alternatively, as also suggested for **71**, fast rotation of the $P_3$ rings in the cations illustrated in Scheme 3.8 would also be expected to give rise to simple spectra, since this rotation would render all P atoms within a cation equivalent, and the chemical shifts of all three cations should be essentially identical. 'Freezing' this motion in the cations **XIV** and **XVI** would be expected to result in spectra similar to that observed at low temperature for **74**. If this $P_3$ ring rotation really does govern the appearance of the spectra, the rate constants of the equilibria in Scheme 3.8 as well as the presence of larger cations are irrelevant.

Remarkably, room temperature $^{31}$P MAS-NMR measurements on **74** reveal dynamic behaviour in the solid state, as in the case of **71**, with a singlet being observed at –350.70 ppm. Thus, rotational motion of the $P_3$ rings can most probably be inferred for **74** in the solid state at room temperature. Since such motion appears to be occurring in the solid state, it is most likely that this dynamic process is responsible for the appearance of the solution $^{31}$P-NMR spectra of **74**, and not fast monomer/dimer/oligomer equilibria.

## 3.5. The Tetrahedrane Complex [Cp*Mo(CO)$_2$($\eta^3$-P$_3$)] as a Ligand

It was also of interest to investigate the compound [Cp*Mo(CO)$_2$($\eta^3$-P$_3$)] **7c**[9e] and its potential as a supramolecular building block since, unlike **7b**, it possesses a Cp* instead of a Cp ligand. Compared to Cp, Cp* is a stronger $\pi$-donor, is sterically more demanding and often enhances solubility,[58] and it was thought that these properties might have an influence on the structure of the products resulting from reactions with transition metal salts and complexes.

### 3.5.1. Studies on the Reactivity of [Cp*Mo(CO)$_2$($\eta^3$-P$_3$)] with CuX (X = Cl, Br, I)

Reactions of **7c** with CuX (X = Cl, Br) in a 1:3 stoichiometry in mixtures of $CH_3CN$ and $CH_2Cl_2$ at room temperature lead to the dimeric products **76a**,**b** (Equation 3.15).[59] The complex **76a** can be isolated as air- and light-sensitive lemon yellow plates after storage of the reaction mixture at –28 °C, whereas **76b** crystallises at room temperature as air- and mildly light-sensitive yellow prisms. Both

products can be stored indefinitely under an inert atmosphere at ambient conditions and are insoluble in common solvents. They are, however, sparingly soluble in polar solvents such as $CH_3CN$, and then only under dissociation to the starting materials as evidenced by $^{31}P$-NMR spectroscopy.

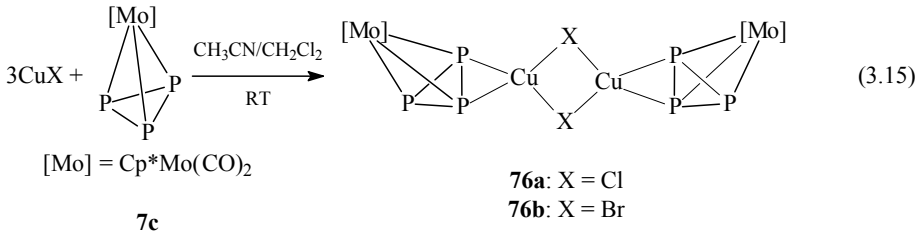


(3.15)

[Mo] = $Cp^*Mo(CO)_2$

**7c**

**76a**: X = Cl
**76b**: X = Br

The structures of **76a**,**b** are illustrated in Figures 3.23 and 3.24, respectively. Each compound consists of two units of **7c** linked by a planar four-membered $Cu_2X_2$ ring. Each Cu centre is bound to two halogen atoms and a P─P edge of a $P_3$ ring of a unit of **7c** and, as the relevant angles suggest (Figures 3.23 and 3.24), is thus in a pseudotetrahedral coordination mode. The coordinated P─P edge of each *cyclo*-$P_3$ unit (**76a**: 2.291(1) Å; **76b**: 2.279(1) Å) is, as expected, longer than the other two edges (**76a**: 2.118(1), 2.153(1) Å; **76b**: 2.152(1) Å), and longer than the P─P bond lengths in uncoordinated **7c** (2.141(1)-2.170(1) Å) as determined crystallographically during the course of this work. The Cu─P bond lengths of **76a** (2.246(1), 2.347(1) Å) lie above and below the range defined by the polymers based on **6a** (**66a**: 2.289(1), 2.296(1) Å) and **6b** (**43a**: 2.282(2), 2.304(2) Å)[33], while those of **76b** (2.310(1), 2.331(1) Å) are somewhat longer than those of the Br derivatives of these polymers (**66b**: 2.297(1), 2.305(1) Å; **43b**: 2.294(2), 2.300(2) Å).[32a] The Cu─Cl bond lengths of **76a** (2.262(1), 2.395(1) Å) are also outside the range defined by those of **43a** (2.348(2), 2.360(2) Å)[33] and **66a** (2.344(1), 2.363(1) Å), while the lengths of the Cu─Br bonds in **76b** (2.402(1), 2.472(1) Å) are such that one falls outside and one within the range defined by those of **43b** (2.472(1), 2.481(1) Å)[32a] and **66b** (2.467(4), 2.479(4) Å).

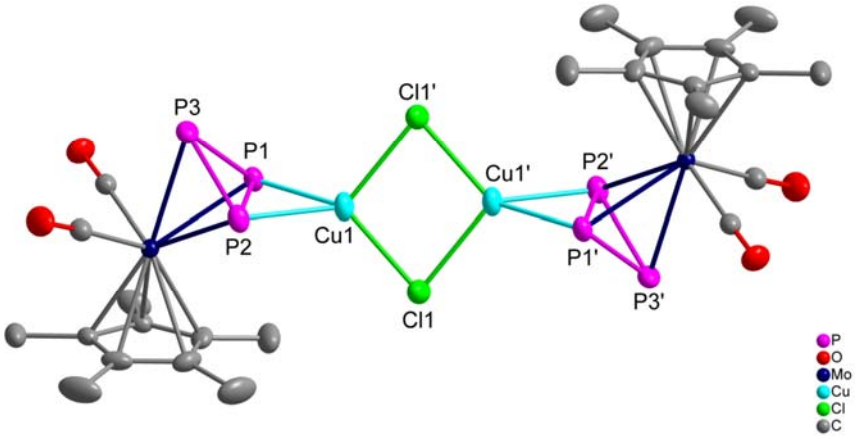


Figure 3.23. Structure of **76a** (hydrogen atoms omitted for clarity). Thermal ellipsoids are represented at the 50 % probability level. Selected bond lengths (Å) and angles (°):P1─P2 2.291(1), P1─P3 2.118(1), P2─P3 2.153(1), Cu1─P1 2.347(1), Cu1─P2 2.246(1), Cu1─Cl1 2.262(1), Cu1─Cl1′ 2.395(4), Cl1─Cu1─Cl1′ 99.17(4), Cl1─Cu1─P1 132.43(4), Cl1′─Cu1─P1 116.75(4), Cl1─Cu1─P2 123.19(4), Cl1′─Cu1─P2 124.68(4), P1─Cu1─P2 59.79(4), Cu1─Cl1─Cu1′ 80.83(4).

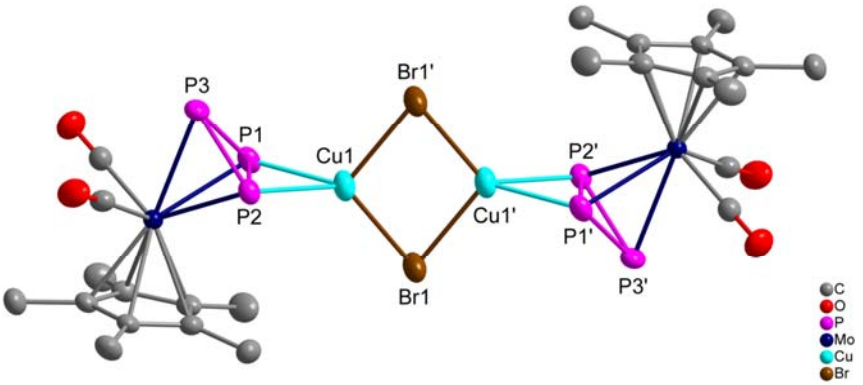


Figure 3.24. Structure of **76b** (hydrogen atoms omitted for clarity). Thermal ellipsoids are represented at the 50 % probability level. Selected bond lengths (Å) and angles (°): P1─P2 2.279(1), P1─P3 2.152(1), P2─P3 2.152(1), Cu1─P1 2.310(1), Cu1─P2 2.331(1), Cu1─Br1 2.402(1), Cu1─Br1′ 2.472(4), Br1─Cu1─Br1′ 104.62(1), Br1─Cu1─P1 124.32(2), Br1′─Cu1─P1 120.08(2), Br1─Cu1─P2 130.95(2), Br1′─Cu1─P2 113.29(2), P1─Cu1─P2 58.81(2), Cu1─Br1─Cu1′ 75.38(1).

Unlike the reactions of **7c** with CuCl and CuBr, in which dimeric products are obtained, reaction of **7c** with CuI in a 1:3 stoichiometry in a mixture of $CH_3CN$ and $CH_2Cl_2$ at room temperature leads to the polymeric product **77** (Equation 3.16).[59] The complex **77** crystallises as air-sensitive red-orange prisms following addition of diethyl ether to the reaction mixture and storage at –28 °C. Solid samples of **77** can be stored indefinitely under an inert atmosphere at ambient conditions and the compound is insoluble in most common solvents. However, it is sparingly soluble in polar solvents such as $CH_3CN$, but then only under dissociation to the starting materials as evidenced by $^{31}$P-NMR spectroscopy.

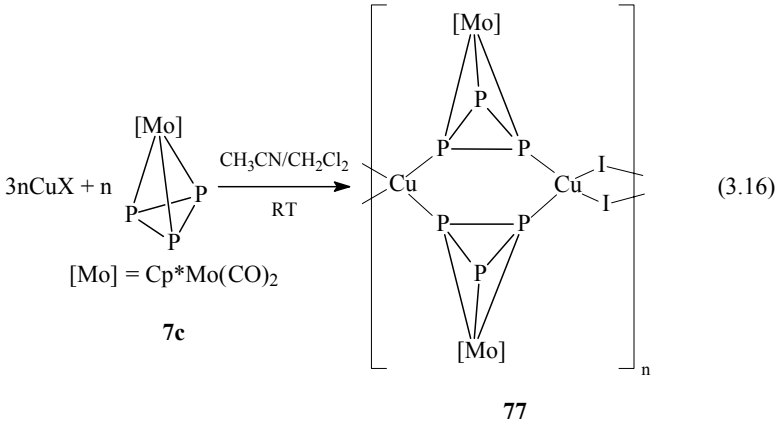


(3.16)

The structure of **77** is depicted in Figure 3.25. The $Cu^I$ centres in this polymer are alternately distributed along two parallel lines (Cu1···Cu1′···Cu1 178.13(8)°) and are in a distorted tetrahedral coordination mode. The core of the polymer consists of an alternating arrangement of four-membered $Cu_2I_2$ and six-membered $Cu_2P_4$ rings, which are nearly orthogonal to each other, and this structural arrangement is essentially identical to that of the 1D polymers based on **6a** (**66c)** and **6b** (**43c**[33]). As opposed to the $P_3$ triangle in the uncoordinated complex **7c** (P─P 2.141(1)-2.170(1) Å), the $P_3$ triangles in **77** are effectively equilateral (P─P 2.140(6)-2.143(5) Å), and, astonishingly, the average P─P bond length is shorter in **77** than in uncoordinated **7c**, an effect that may be due to a combination of the strong $\pi$-donor capacity of the Cp* ligand[58] and the $\pi$-acceptor properties of the P atoms. The Cu─P bond lengths (2.330(4), 2.332(4) Å) are somewhat longer than those of **43c**[33] (2.312(1) Å), but comparable to those of **66c** (2.323(2), 2.333(2) Å). The Cu─I bond lengths (2.618(2), 2.621(3) Å) lie within the range defined by those of

the reference polymers (**43c**: 2.606(1), 2.668(1) Å; **66c**: 2.611(1), 2.675(1) Å).

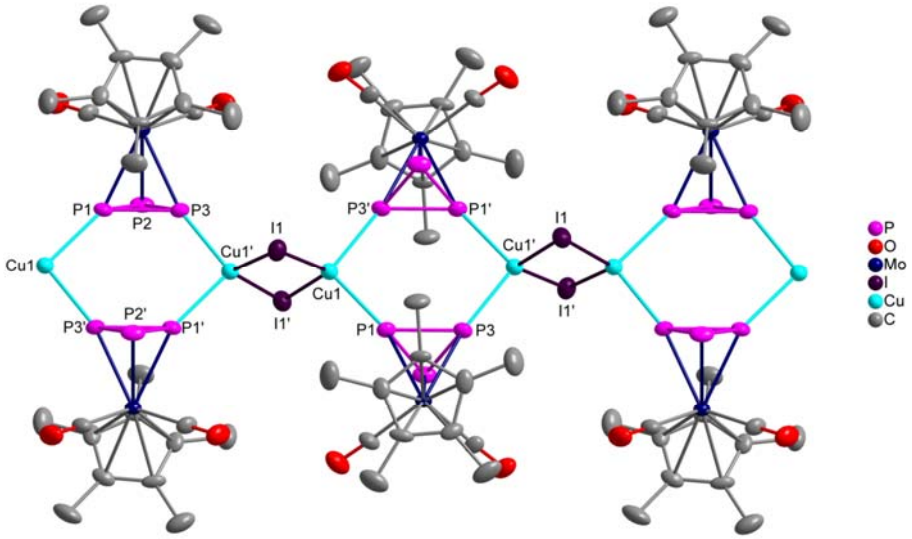


Figure 3.25. Section of the 1D polymeric structure of **77** (hydrogen atoms omitted for clarity). Thermal ellipsoids are represented at the 50 % probability level. Selected bond lengths (Å) and angles (°): P1─P3 2.140(6), P1─P2 2.142(7), P2─P3 2.143(5), Cu1─P1 2.330(4), Cu1─P3′ 2.332(4), Cu1─I1 2.621(3), Cu1─I1′ 2.618(2), I1─Cu1─I1′ 115.90(9), I1─Cu1─P1 111.29(14), I1′─Cu1─P1 107.33(12), I1─Cu1─P3′ 109.35(14), I1′─Cu1─P3′ 112.70(12), P1─Cu1─P3′ 98.96(16), Cu1─I1─Cu1′ 63.83(7).

The products **76a**,**b** and **77** all consist of **7c** and the appropriate $Cu^{I}$ halide in a ratio of 1:1, yet the lighter halide derivatives are both dimers while the iodide derivative is a 1D polymer. It is unclear what the cause of this apparent discrepancy is, but it may be due to the size of the halide. In the case of CuCl and CuBr, the steric demand of the Cp* ligand of **7c** probably excludes the formation of polymers and forces dimerisation to **76a**,**b**. On moving to CuI, the larger iodide may lift the steric restrictions imposed by the Cp* ligand in the case of the smaller halides, and thus permit polymerisation. A more definitive method to investigate the interplay of the Cp* ligand and the halide, and how it determines the structure of the products, would be to carry out similar experiments using the Cp derivative **7b**. As already mentioned at the beginning of this section, these experiments have so far led to the formation of amorphous products which could not be adequately characterised.

## 3.5.2. Studies on the Reactivity of [Cp*Mo(CO)$_2$($\eta^3$-P$_3$)] with Ag[Al{OC(CF$_3$)$_3$}$_4$]

Reaction of **7c** with Ag[Al{OC(CF$_3$)$_3$}$_4$] in $CH_2Cl_2$ at room temperature leads to the isolation of the product **78**, following storage at –28 °C, in the form of air- and light-sesitive bright yellow needles (Equation 3.17). Regardless of whether a 2:1 or 3:1 reactant stoichiometry is employed, spectroscopic data and elemental analysis have shown that the 2:1 product is obtained in both cases. Compound **78** is soluble in solvents such as $CH_2Cl_2$, THF and $CH_3CN$, though to a lesser extent than the **7b**-based **71**, and can be stored indefinitely at ambient conditions under an inert atmosphere.

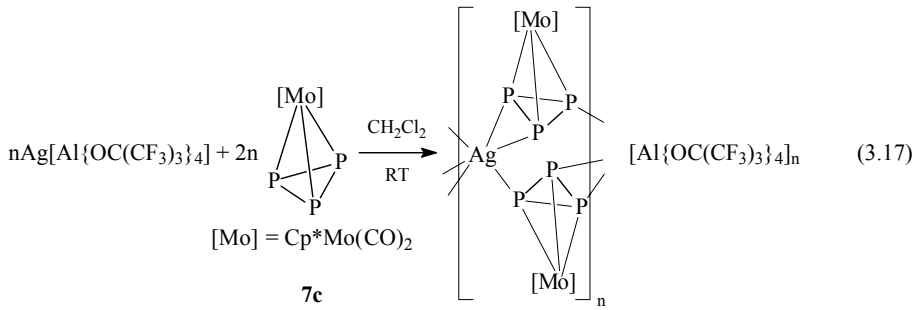


Although only poor quality crystals of **78** could be obtained, X-ray crystallographic analysis nevertheless revealed that it consists of a 1D polycation (Figure 3.26). This polycation comprises a chain of $Ag^+$ ions, each being tetrahedrally coordinated to six P atoms of four units of **7c** via two $\pi$- and two $\sigma$-bonds, and thus all the P atoms in **78** are coordinated.

The structure illustrated in Figure 3.26 is supported by $^{31}$P MAS-NMR measurements on **78** at room temperature, which yield spectra displaying two broad peaks, without any analysable coupling to $^{107/109}$Ag, at –344.5 and –360.0 ppm (Figure 3.27), in an integration ratio of 1:2. Considering the structure of the cation in **78** (Figure 3.26), one might in fact expect the $^{31}$P MAS-NMR spectrum observed experimentally, since each *cyclo*-P$_3$ unit is coordinated to two $Ag^I$ centres via a P─P edge (P1─P2 or P5─P6) and the lone-pair of electrons of the P atom not involved in these edges (P3 or P4). The chemical shifts of the P1, P2, P5 and P6 atoms would be expected to be similar, but appreciably different from those of the P3 and P4 atoms. The P3 and P4 atoms, however, would most likely also be similar and

therefore a $^{31}$P MAS-NMR spectrum would result consisting of two broad peaks with an integration ratio of 1:2, corresponding to the ratio of P atoms coordinated via their lone-pairs and P atoms contained in coordinated P─P edges. It is interesting to note that, according to the $^{31}$P MAS-NMR results, no solid-state dynamic behaviour is displayed by polymer **78**, as opposed to polymers **71** and **74** (section **3.4**).

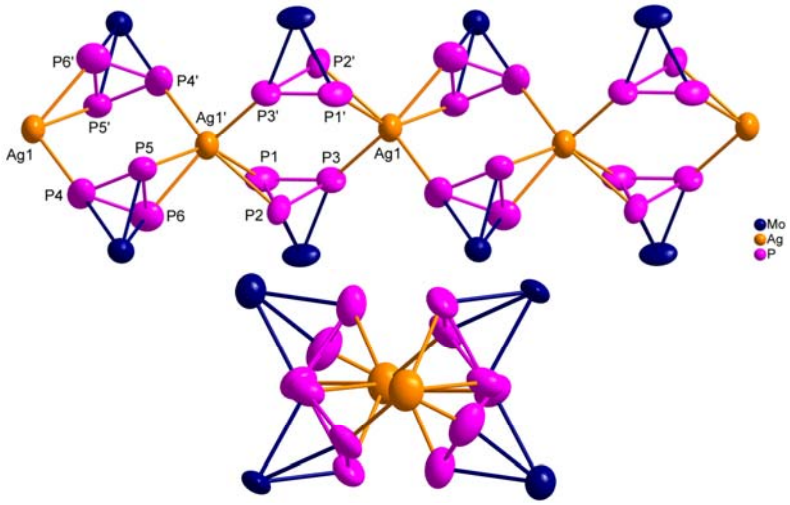


Figure 3.26. Section of the structure of the 1D polycationic chain in **78** (Cp* and CO ligands omitted for clarity). The bottom illustration is a view of the chain along the crystallographic *a*-axis. Thermal ellipsoids are represented at the 50 % probability level.

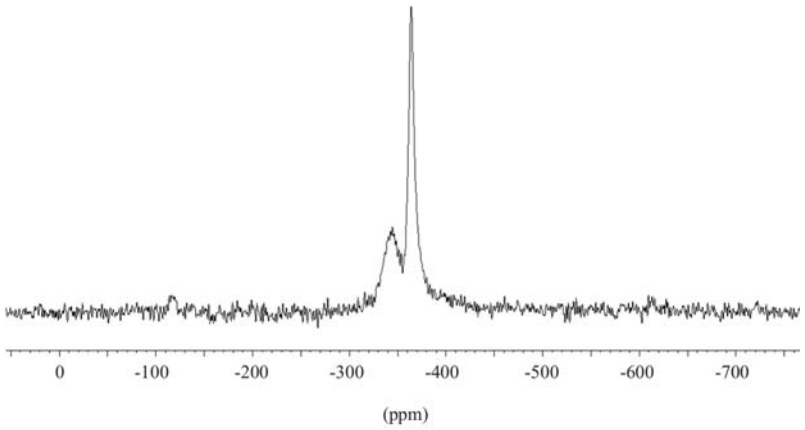


Figure 3.27. Solid-state $^{31}$P MAS-NMR spectrum of **78** at room temperature.

The positive ion ESI-MS spectra of **78** in $CH_2Cl_2$ at room temperature suggest that the compound dissolves under depolymerisation, since only fragments attributable to the cation $[Ag\{Cp^*Mo(CO)_2P_3\}_2]^+$ are detected. This species also displays the highest relative abundance in ESI-MS spectra of **78** obtained in $CH_3CN$. VPO measurements on **78** in $CH_2Cl_2$ at 28 °C confirm dissolution under depolymerisation since a molecular mass of 1953 ± 98 g $mol^{-1}$ is obtained, a value only slightly higher than that expected for the monomer $[Ag\{Cp^*Mo(CO)_2P_3\}_2][Al\{OC(CF_3)_3\}_4]$ **79** (1835 g $mol^{-1}$). This is indicative of a dynamic equilibrium between **79** and higher aggregates, albeit strongly in favour of **79**. Thus, equilibria comparable to those proposed for **71** may be in progress in solutions of **78**, involving the monocations **XVII** and **XVIII** and the dication **XIX**, as illustrated in Scheme 3.9.

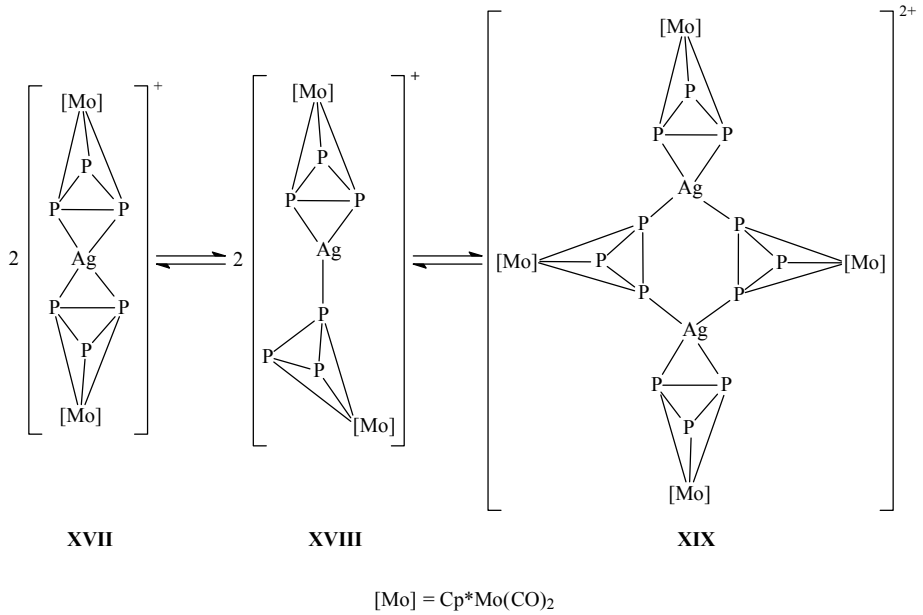


Scheme 3.9. Proposed cation equilibria in solutions of **78**.

The $^{31}$P-NMR spectrum of **78** in $CD_2Cl_2$ at room temperature supports the existence of a dynamic equilibrium in solutions of the compound. Only a singlet without any coupling to $^{107/109}$Ag is observed at –348.0 ppm, shifted by almost 15 ppm upfield relative to uncoordinated **7c**, which can not be resolved even at –80 °C. Variable temperature spectra were thus recorded in a 3:1 mixture of THF-$d_8$ and $CD_2Cl_2$ (Figure 3.28) and revealed a pattern very similar to that already observed for **71**. At room temperature in this mixture, a singlet at –

346.6 ppm is detected, which, at –100 °C, splits into two broad peaks centred at –275.6 and –387.4 ppm with an integration ratio of 1:2. The separation of these two peaks is much greater than that observed in the solid-state room temperature spectrum of **78** (111.8 ppm as opposed to 16 ppm). It thus appears that in solutions of **78** species comparable to those in solutions of **71** are present, as illustrated in Scheme 3.9. Larger cations may, of course, also be at hand, but the VPO measurements suggest that if this is the case, they are present in negligible concentrations. Both the monocation **XVII** and the dication **XIX** would be expected to exhibit spectra resembling the low temperature spectra of **78**, since the ratio of the uncoordinated and coordinated P atoms in these cations is 1:2. Provided that the equilibria in Scheme 3.9 hold, the low temperature spectra of **78** suggest that the conversion of **XVIII** to **XVII** and to **XIX** is fast, whereas the reverse processes are slow.

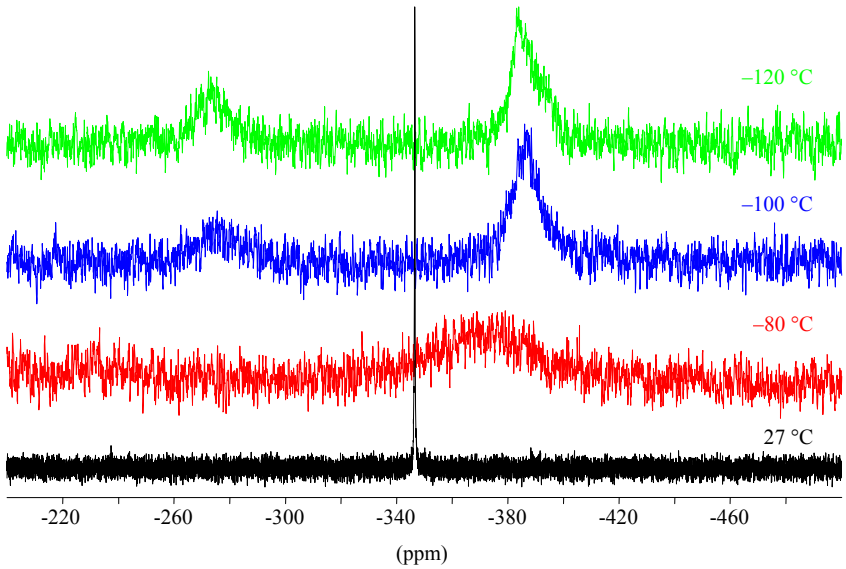


Figure 3.28. Variable temperature $^{31}$P-NMR spectra of **78** in a 3:1 mixture of THF-$d_8$ and $CD_2Cl_2$.

However, as was also suggested for the species in solutions of **71** and **74**, rotation of the $P_3$ rings in **XVII** and **XIX**, which is fast at room temperature and slow at lower temperatures, may be the more likely explanation for the appearance of the solution spectra of **78**. According to $^{31}$P MAS-NMR measurements, **71** and **74**, but not **78**, demonstrate dynamic behaviour in the solid state, most probably attributable to fast $P_3$ ring rotation. Since this dynamic process seems to be occurring in the solid state and to be governing the appearance of the solid-state spectra of **71** and **74**, it is most likely responsible for the appearance of the solution spectra of the polymers **71**, **74** and **78** as well.

## 3.6. An Excursion in the Realm of $As_n$-Ligand Complexes: the Tetrahedrane Complex $[Cp^*Mo(CO)_2(\eta^3\text{-}As_3)]$ as a Ligand

It was already mentioned in the introductory chapter that the development of the field of $P_n$-ligand complexes was prompted by the $As_n$-ligand complexes **1** and **2** (Figure 1.3), isolated by Dahl and co-workers.[5] The area of $As_n$-ligand complexes[4c-g] flourished alongside that of $P_n$-ligand complexes and an equally impressive arsenal of structures has been obtained. The apparent suitability of $P_n$-ligand complexes as supramolecular building blocks led to the question of whether $As_n$-ligand complexes would be appropriate as such. In order to investigate this matter, experiments were performed with the complex $[Cp^*Mo(CO)_2(\eta^3\text{-}As_3)]$ **80** (Figure 3.29),[60] which was particularly appealing since, being the heavier analogue of the complex **7c**, the effect of exchanging P for its heavier homologue on the structure of the products obtained could be explored. Single crystal X-ray diffraction analysis of the products obtained from reactions of **80** with CuX (X = Cl, Br, I)[61] revealed that all three products are dimers and structurally similar to the compounds **76a**,**b** (Figures 3.23 and 3.24). It has already been shown that **7c** reacts with CuI to form the 1D polymer **77** (Figure 3.25) and not a dimer, a discrepancy which may be due to the higher *s*-character of the lone-pair electrons at As in **80**.[58]

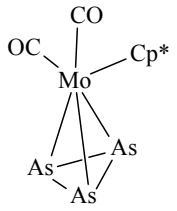


Figure 3.29. Structure of the $As_n$-ligand complex **80**.

### 3.6.1. Studies on the Reactivity of $[Cp^*Mo(CO)_2(\eta^3\text{-}As_3)]$ with $Ag[Al\{OC(CF_3)_3\}_4]$

Reaction of **80** with $Ag[Al\{OC(CF_3)_3\}_4]$ in either a 1:1 or 2:1 ratio in $CH_2Cl_2$ leads to the isolation of the oligomer **81** as air- and light sensitive bright orange needles (Equation 3.18). The complex **81** is

soluble in solvents such as $CH_2Cl_2$, THF and $CH_3CN$ and can be stored indefinitely at ambient conditions under an inert atmosphere.

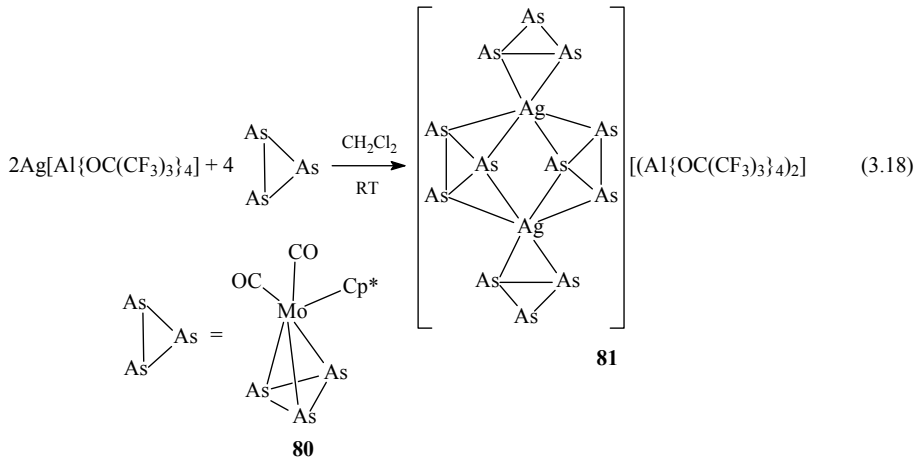


Compound **81** has been characterised by single crystal X-ray diffraction and the structure of the dication is illustrated in Figure 3.30. It consists of four units of **80** and two $Ag^+$ cations, these being doubly bridged by two units of **80** in a $\eta^2$:$\eta^2$ fashion. Each of the remaining units of **80** coordinates to an $Ag^I$ centre in a $\eta^2$ mode. The $Ag^I$ centres are thus coordinated to six As atoms via three $\pi$-bonds and the coordination geometry is probably best described as trigonal pyramidal especially after consideration of the appropriate bond angles (Figure 3.30). As would be expected from the $\pi$-coordination mode, the edges As1─As2 (2.452(2) Å), As2─As3 (2.464(2) Å) and As4─As5 (2.528(2) Å) are noticeably longer than the As─As bonds in uncoordinated **80** (2.372(1), 2.377(2) Å),[60] whereas the uncoordinated edges remain essentially unchanged. The Ag─As bond lengths (2.665(1)-2.828(1) Å) are, on average, longer than those found in previously reported $[Ag(AsPh_3)_4]^+$ salts (2.643(4)-2.700(5) Å).[62]

It is interesting to reflect upon the solid-state structure of the dimeric assembly **81**. In the previous section it was shown that the *cyclo*-$P_3$ analogue of **80**, complex **7c**, yields the product **78** whose solid-state structure consists of a 1D polymeric polycation. The Ag atoms in **78** are bonded to both single P atoms via their lone pairs as well as to P─P edges via $\pi$-bonds. This difference in coordination mode of the *cyclo*-$E_3$ (E = P, As) units is most likely due to the increase in *s*-character of the lone-pair electrons at the E atom on moving from P to As.[58] The *cyclo*-$As_3$ unit in **80** thus coordinates via its edges and probably no polymerisation can occur as a result of steric crowding.

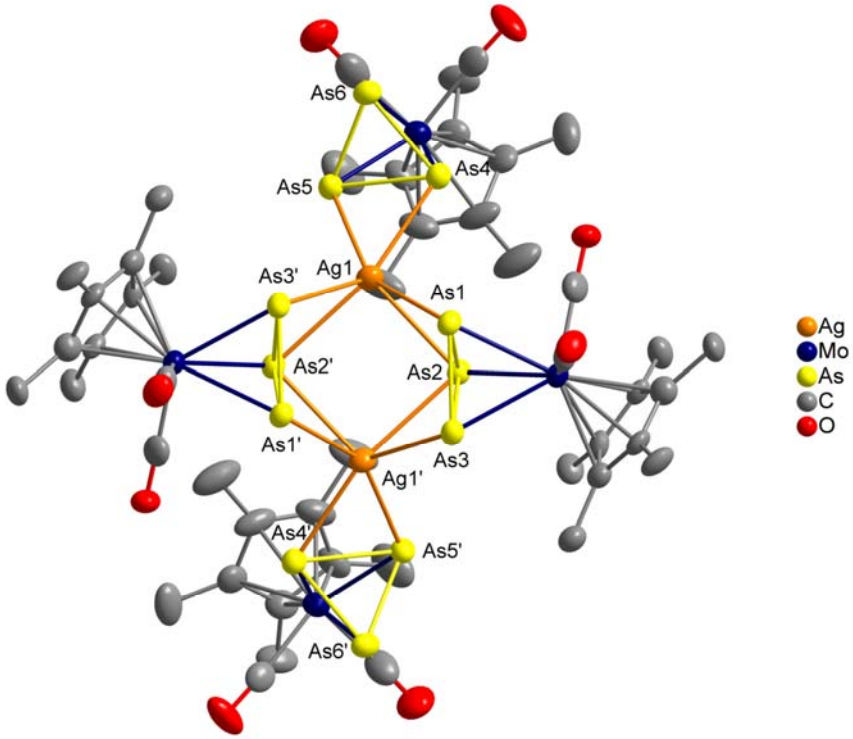


Figure 3.30. Structure of the dication in **81** (hydrogen atoms omitted for clarity). Thermal ellipsoids are represented at the 50 % probability level. Selected bond lengths (Å) and angles (°): As1─As2 2.452(2), As1─As3 2.368(2), As2─As3 2.464(2), As4─As5 2.528(2), As4─As6 2.371(2), As5─As6 2.369(2), Ag1─As1 2.828(1), Ag1─As2 2.806(1), Ag1─As2′ 2.823(1), Ag1─As3′ 2.780(1), Ag1─As4 2.704(2), Ag1─As5 2.665(1), As1─Ag1─As2 51.59(4), As1─Ag1─As2′ 105.02(4), As1─Ag1─As3′ 82.26(4), As1─Ag1─As4 96.65(4), As1─Ag1─As5 151.49(5), As2─Ag1─As2′ 90.09(4), As2′─Ag1─As3′ 52.16(4), As2─Ag1─As3′ 111.33(4), As2─Ag1─As4 101.54(4), As2′─Ag1─As4 158.17(5), As2─Ag1─As5 135.13(5), As2′─Ag1─As5 102.72(4), As3′─Ag1─As4 135.69(5), As3′─Ag1─As5 110.35(5), As4─Ag1─As5 56.17(4).

In the positive ion ESI-MS spectra of compound **81**, the fragment with the highest relative abundance is attributable to the cation $[Ag\{Cp^*Mo(CO)_2As_3\}_2]^+$. VPO measurements (28 °C, $CH_2Cl_2$) yield a molecular mass of 2756 ± 138 g mol$^{-1}$ for the species in solution, which suggests an equilibrium between the monomer $[Ag\{Cp^*Mo(CO)_2As_3\}_2]$ $[Al\{OC(CF_3)_3\}_4]$ **82** (2099 g mol$^{-1}$) and the dimer **81** (4198 g mol$^{-1}$), noticeably in favour of the monomer (monomer:dimer ≈ 3:1).

The structures of the respective cations (monocation **XX**; dication **XXI**) in $CH_2Cl_2$ solution at room temperature have been calculated by DFT methods and are illustrated in Figure 3.31. In the monocation, the $Ag^I$ centre is coordinated to two units of **80** via two As─As edges in a linear fashion and these five atoms are coplanar. The structure of the dication differs slightly from that of the dication in the solid state (Figure 3.30), particularly in the way that the bridging units of **80** are coordinated to the $Ag^I$ centres. In the calculated dication, each *cyclo*-$As_3$ moiety of these units is bonded to one $Ag^I$ centre via an As─As edge and to the other via a rather long Ag─As contact (3.008 Å), which is shorter than the sum of the van der Waals radii of the two elements (3.55 Å),[63] whereas in the dication in the solid state, these moieties coordinate to both $Ag^I$ centres exclusively via As─As edges. The dication in solution can thus be viewed as two weakly associated monocations.

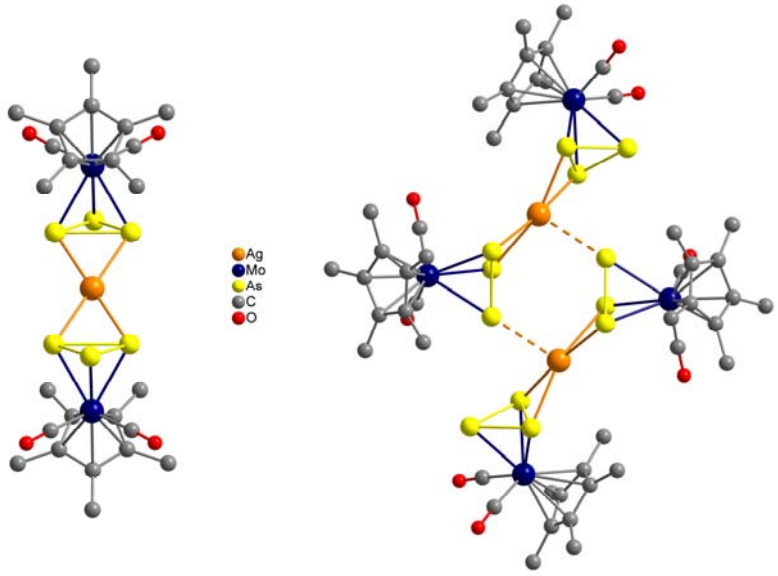


**XX** **XXI**

Figure 3.31. Calculated structures of the monocation **XX** and the dication **XXI** in $CH_2Cl_2$ at room temperature.

Calculations have shown that the formation of the dication **XXI** from the monocation **XX** is endothermic in the gas phase (111.4 kJ $mol^{-1}$),[64] but exothermic in $CH_2Cl_2$ solution (–19.2 kJ $mol^{-1}$).[65] The endothermic nature of the formation of **XXI** in the gas phase as well as the two somewhat long Ag─As contacts therein, are probably the reasons why only the monocation is detected in the ESI-MS spectra, whereas the exothermic nature of its formation in solution explains the

crystallisation of the dimer rather than the monomer. Based on the theoretical calculations, the experimental data, and the results of the investigations on $P_n$-ligand complexes discussed in the previous sections, an equilibrium between the monocation **XX** and the dication **XXI** can most certainly be postulated for solutions of the dimer **81**.

## 3.7. The Sandwich Complex [Cp*Fe($\eta^5$-$P_5$)] as a Ligand

The potential of the sandwich complex [Cp*Fe($\eta^5$-$P_5$)] **9a**[12a-c] to act as a building block for supramolecular architectures has been clearly demonstrated by the Scheer group.[34] Reactions of **9a** with CuX (X = Cl, Br, I) yield 1D and 2D coordination polymers[34a] as well as a remarkable fullerene-like nanoball.[34b] In view of the diversity of structures obtained using $Cu^I$ halides, it was of interest to examine the reactivity of **9a** with $CuPF_6$ as well as various $Ag^I$ and $Au^I$ salts. Unfortunately, experiments with $CuPF_6$ resulted in the formation of insoluble, amorphous solids, which could not be adequately characterised. The investigations involving $Ag^I$ and $Au^I$ salts are discussed below.

### 3.7.1. Studies on the Reactivity of [Cp*Fe($\eta^5$-$P_5$)] with $Ag^I$ Salts

Initial investigations on the reactivity of **9a** with $Ag^I$ involved experiments with the salts of the WCAs $TfO^-$ and $ClO_4^-$. However, these experiments yielded amorphous compounds which could not be satisfactorily characterised. In contrast, a 2:1 reaction of **9a** and $Ag[Al\{OC(CF_3)_3\}_4]$ in $CH_2Cl_2$ at room temperature led to the isolation of the novel 1D polymer **83** in the form of air- and light-sensitive dark brown needles, following storage of the concentrated reaction solution at –28 °C (Equation 3.19). Complex **83** is readily soluble in solvents such as toluene, $CH_2Cl_2$ and THF, and can be stored indefinitely under an inert atmosphere at ambient conditions.

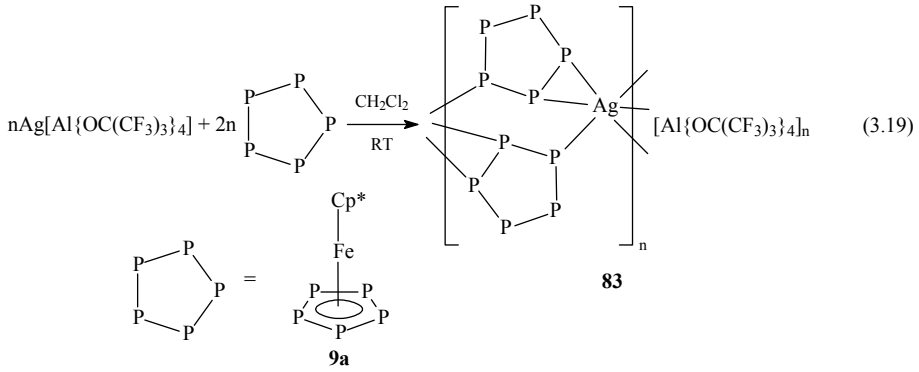


Crystals of **83** have been characterised by X-ray diffraction and a section of the polycation therein is illustrated in Figure 3.32. The core of this cation consists of a chain of $Ag^{I}$ cations alternately distributed along two parallel lines (Ag···Ag′···Ag 165.58(1)°), and these are in turn doubly bridged by the *cyclo*-$P_5$ moieties of two units of **9a** in a novel $\eta^2$:$\eta^1$ fashion (1,2,3 coordination mode).[66] Through this unusual coordination mode, a complex results in which the $Ag^{I}$ centres are tetrahedrally coordinated to six P atoms via two $\sigma$- and two $\pi$-bonds. Formally, the polycation in **83** may be viewed as being built up of a chain of six-membered $Ag_2P_4$ rings, which are fused to two three-membered $AgP_2$ rings through two opposite Ag─P edges. The P─P bond lengths in the $Ag_2P_4$ rings (P11─P15 2.124(4) Å; P21─P22 2.118(4) Å) are essentially unaltered compared to those in the uncoordinated complex **9a** as determined crystallographically during the course of this work (2.116(2)-2.127(2) Å) and by electron diffraction (2.117(4) Å),[67] but somewhat longer than those in the complex **9b** (2.088(3)-2.108(3) Å), as determined by X-ray crystallography.[12d] The P─P edges coordinated to the $Ag^{I}$ centres are, in contrast, significantly longer (P11─P12 2.156(4) Å; P22─P23 2.155(4) Å), as would be expected from the $\pi$-coordination mode. The edges P12─P13 (2.141(4) Å) and P23─P24 (2.129(4) Å) are also elongated, but to a lesser extent, and the remaining P─P bond lengths are within the range defined by **9a** and **9b**. As expected due to the $\sigma$-coordination mode, the Ag─P15 (2.590(2) Å) and Ag─P21 (2.615(3) Å) bonds are shorter than the other Ag─P bonds (2.758(2)-2.824(3) Å).

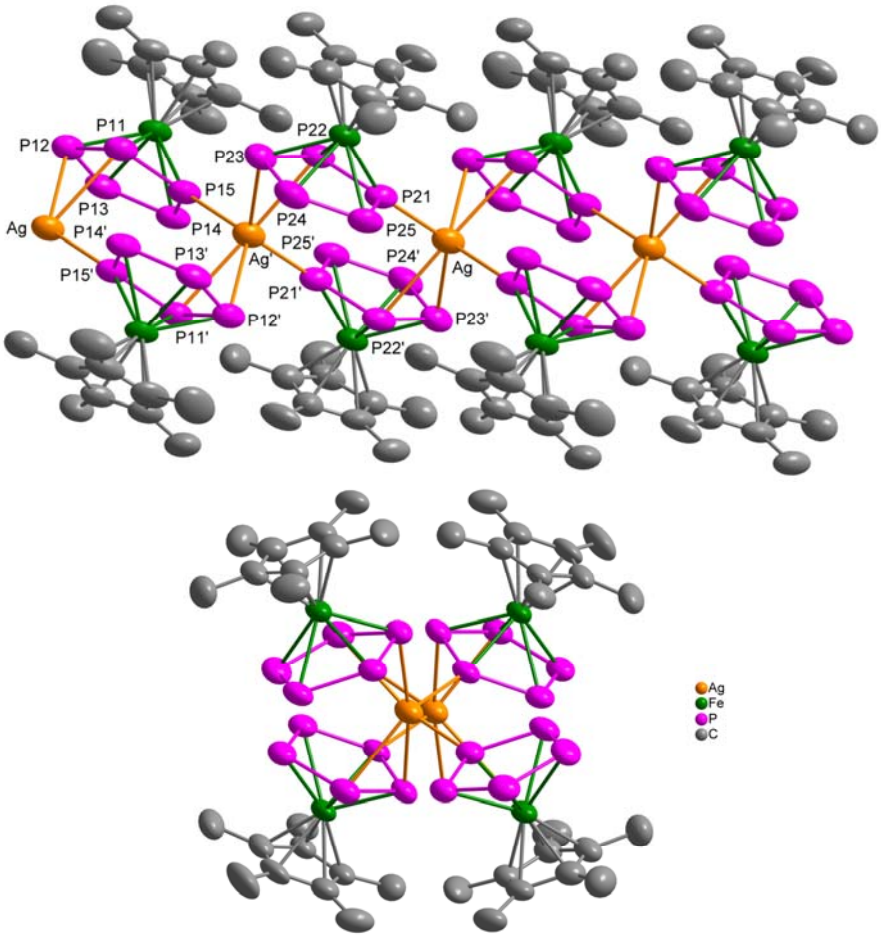


Figure 3.32. View of a section of the polycation in **83** perpendicular to (top) and along (bottom) the crystallographic *a*-axis (hydrogen atoms omitted for clarity). Thermal ellipsoids are represented at the 50 % probability level. Selected bond lengths (Å) and angles (°): P11─P12 2.156(4), P11─P15 2.124(4), P12─P13 2.141(4), P13─P14 2.112(4), P14─P15 2.111(4), P21─P22 2.118(4), P21─P25 2.110(4), P22─P23 2.155(4), P23─P24 2.129(4), P24─P25 2.107(5), Ag─P11 2.824(3), Ag─P12 2.758(2), Ag─P15′ 2.590(2), Ag─P21 2.615(3), Ag─P22′ 2.775(3), Ag─P23′ 2.809(3), P11─Ag─P12 45.41(8), P11─Ag─P15′ 83.05(8), P11′─Ag′─P21′ 97.96(8), P11′─Ag′─P22 171.86(8), P11′─Ag′─P23 127.11(9), P12─Ag─P15′ 125.75(8), P12′─Ag′─P21′ 98.76(8), P12′─Ag′─P22 128.29(8), P12′─Ag′─P23 99.78(9), P15─Ag′─P21′ 105.06(9), P15─Ag′─P22 100.89(8), P15─Ag′─P23 100.34(9), P21─Ag─P22′ 87.96(9), P21─Ag─P23′ 130.43(9), P22─Ag′─P23 45.39(8).

In the positive ion ESI-MS spectra of **83** in $CH_2Cl_2$ at room temperature, only fragments attributable to the cation $[Ag(Cp^*FeP_5)_2]^+$ are detected. The sole existence of the monomer $[Ag(Cp^*FeP_5)_2][Al\{OC(CF_3)_3\}_4]$ **84** (1767 g mol$^{-1}$) in $CH_2Cl_2$ solutions of **83** at 28 °C is confirmed by VPO measurements, as a molecular mass value of 1725 ± 86 g mol$^{-1}$ is found for the species in solution. Since the polymer **83**, rather than the monomer **84**, is isolated in the solid state, the existence of equilibria in solution cannot be excluded. Possible structures for the monocation $[Ag(Cp^*FeP_5)_2]^+$ **XXII** and the dication $[Ag_2(Cp^*FeP_5)_4]^{2+}$ **XXIII** have been calculated by DFT methods. The potential energy surfaces of these cations were found to be quite flat and at least four structures could be localised for the dication (**XXIIIa-d**), all within 16 kJ mol$^{-1}$ of each other. The structures of the cations are depicted in Figure 3.33. In the monocation **XXII**, both units of **9a** are bonded to the $Ag^I$ centre in a $\eta^2$ coordination mode. In **XXIIIa**, the most stable dication, two units of **9a** bridge the two $Ag^I$ cations via their *cyclo*-$P_5$ moieties in a $\eta^2$:$\eta^1$ fashion, but in a 1,2,4-coordination mode rather than the 1,2,3-coordination mode observed in the solid state, while two further units of **9a**, one per Ag atom, are coordinated in a $\eta^2$ fashion. The four dications **XXIIIa-d** differ in the way the bridging as well as the terminal units of **9a** are coordinated to the Ag atoms, and these structural differences and the energy of each dication relative to **XXIIIa** are summarised in Table 3.10.

Dynamic behaviour in solutions of **83** is also supported by variable temperature $^{31}$P-NMR spectroscopy of the compound in $CD_2Cl_2$ (Figure 3.34). At room temperature only a singlet at 154.2 ppm is observed, shifted marginally upfield relative to uncoordinated **9a**,[12a] with no detectable coupling to $^{107/109}$Ag. As the temperature is reduced, the signal is shifted gradually to higher field and becomes broader, and at –90 °C the signal is resolved into two distinct broad signals, centred at 150.9 and 123.2 ppm, with an approximate integration ratio of 1:1.

The $^{31}$P-NMR spectra are best interpreted by considering the equilibria illustrated in Scheme 3.10. According to VPO data, the monomer **84**, and thus the monocation **XXII**, is present exclusively in $CH_2Cl_2$ solutions of **83** at room temperature and the equilibrium can be seen as being entirely in favour of **XXII**. If, at room temperature, **XXII** existed in solution as depicted in Figure 3.33, one would expect at least two broad signals in the $^{31}$P-NMR spectrum with an approximate ratio of 2:3 ($(AA'BMM')_2$ spin system), since four P atoms are coordinated and six are not, but only a sharp singlet is observed at this temperature instead. This is not surprising since calculations have revealed that several structures of similar energy are possible for **XXII**. One would

thus expect fast exchange between these structures in solution on the NMR timescale, which may alternatively be viewed as fast rotation of the *cyclo*-$P_5$ moieties in **XXII**, and this would render all P atoms equivalent. At low temperature, splitting of the signal is observed, but the new signals are in an approximate integration ratio of 1:1 and not 2:3.

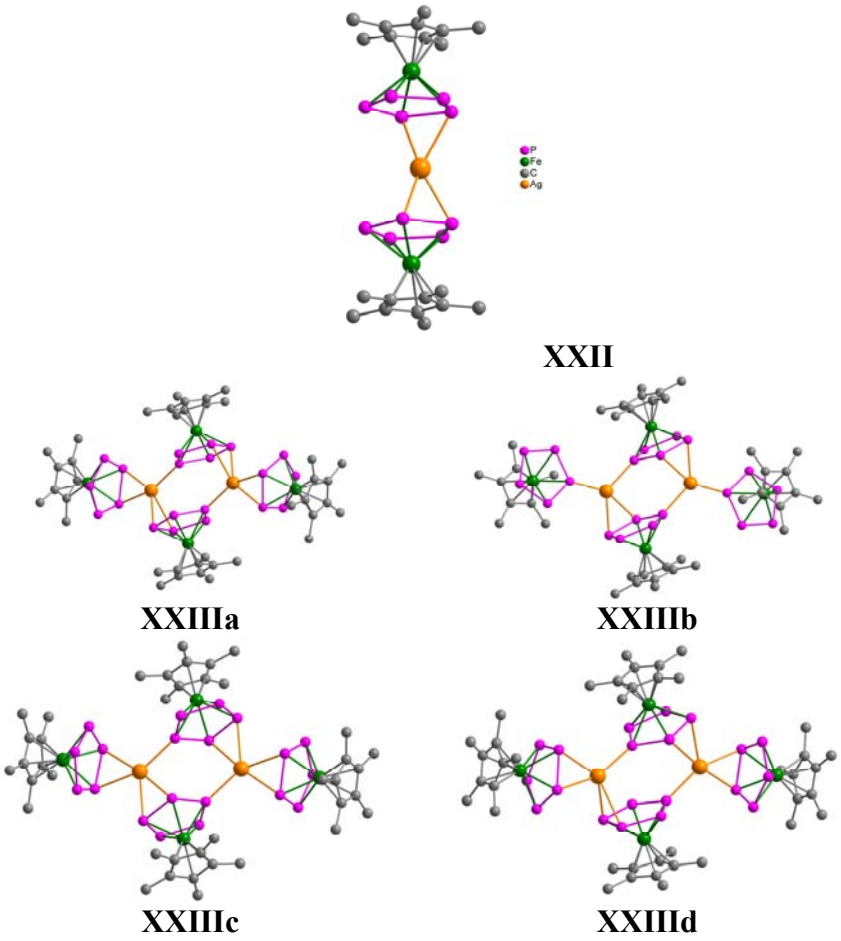


Figure 3.33. Calculated structures for the monocation **XXII** and the dication **XXIII** at room temperature.

Table 3.10. Summary of the structural differences between the calculated dications **XXIIIa-d** and their energies (kJ mol$^{-1}$) relative to **XXIIIa**.

| Dication XXIII | Coordination mode of bridging units of 9a | Coordination mode of terminal units of 9a | Energy relative to XXIIIa |
|---|---|---|---|
| **a** | 1,2,4; 1,2,4 | 1,2; 1,2 | 0 |
| **b** | 1,2,3; 1,2,3 | 1; 1 | 7 |
| **c** | 1,2,3; 1,2,3 | 1,2; 1,2 | 8 |
| **d** | 1,2,3; 1,2,4 | 1,2; 1,2 | 16 |

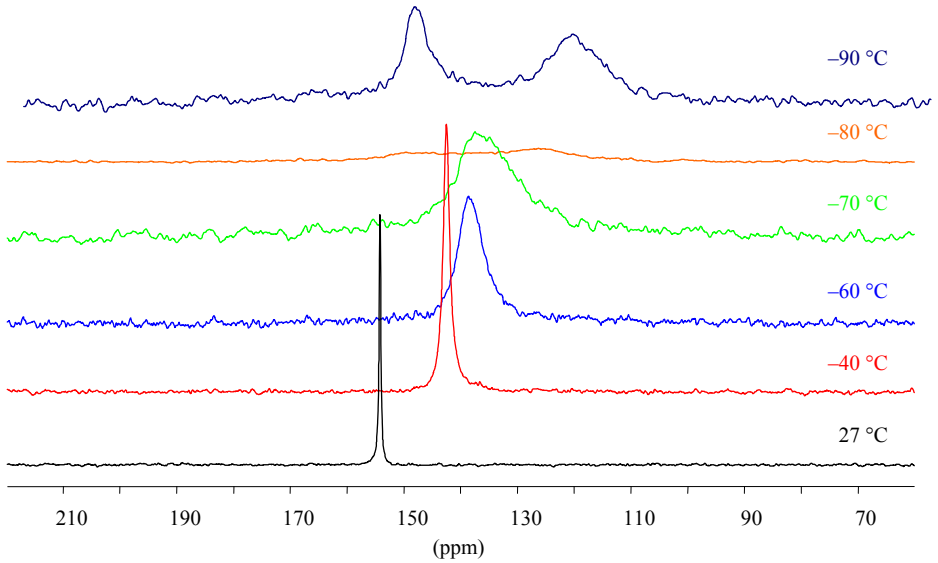


Figure 3.34. Variable temperature $^{31}$P-NMR spectra of **83** in $CD_2Cl_2$.

The $^{31}$P-NMR shifts for **XXII** and **XXIIIa**,**b** have been calculated and the average chemical shift for each species determined by adding the corresponding calculated chemical shifts and dividing the result by the number of P atoms in the respective species. This was deemed as a valid procedure, since the aforementioned low energy differences would be expected to facilitate fast exchange processes, which would in turn render all P atoms within a species equivalent. Again, these exchange processes are probably best viewed as fast rotation of the *cyclo*-$P_5$ moieties in the respective cations. For **XXII**, an average chemical shift of 159 ppm was determined, a value comparable to that observed at room temperature (154.2 ppm). For **XXIIIa**,**b**, values of 149 and 127 ppm, respectively, were determined, and after consideration of the experimental spectra at –90 °C, which exhibit two peaks at 150.9 and 123.2 ppm in an approximate 1:1 integration ratio, one could postulate the existence of an equilibrium between **XXIIIa**

and **XXIIIb** at this temperature. However, the presence of **XXII** at low temperature cannot be excluded, since its average chemical shift is essentially the same as that of **XXIIIa** and the energy difference between **XXII** and **XXIIIa** is small (calculated enthalpy of dissociation of **XXIIIa** to **XXII** at –90 °C: 12 kJ $mol^{-1}$). The existence of at least all three of these cations, if not even larger aggregates, is likely at low temperature. In addition, rotational motion of the *cyclo*-$P_5$ units in the proposed cations, which is fast at room temperature and slow at low temperatures, rather than fast monomer/dimer/oligomer equilibria, most probably determines the appearance of the spectra.

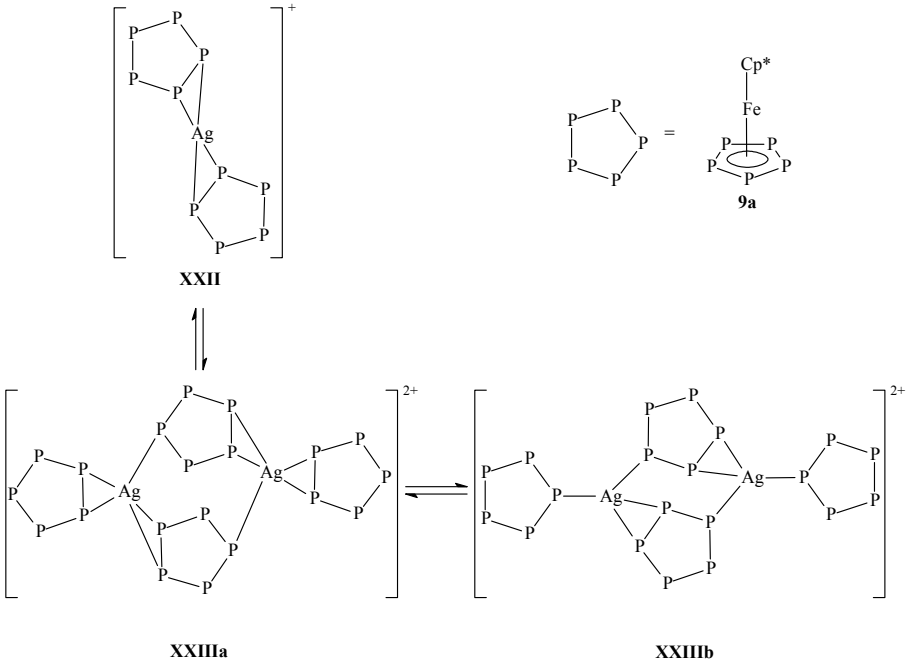


Scheme 3.10. Proposed cation equilibria in solutions of **83**.

In order to understand the reasons why the polymer **83** is isolated in the solid state, rather than the monomer **84**, it is useful to consider the Born-Haber cycle in Scheme 3.11. This includes calculated thermodynamic data as well as qualitative thermodynamic assessments based on inferences drawn from experimental observations. In solution, even though oligomerisation is enthalpically slightly favoured, particularly at lower temperatures, the effect of entropy outweighs the enthalpic effect and **83** thus dissolves under complete depolymerisation. In the solid state, however, entropic effects are insignificant and lattice enthalpy gains the upper hand, which leads to crystallisation of the polymer. This strange behaviour is most likely a

result of the low lattice enthalpy induced by the large size of the $[Al\{OC(CF_3)_3\}_4]^-$ anion (diameter = 1.25 nm[39b]).

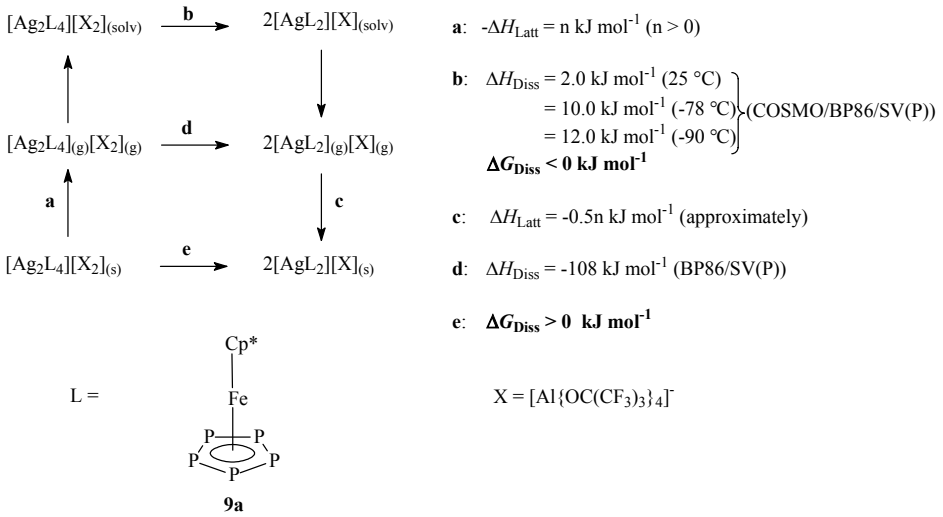


Scheme 3.11. Born-Haber cycle for the oligomeric system used to explain the properties of polymer **83** (in steps **a** and **c**: n is a number greater than 0).

Interestingly, solid-state dynamic behaviour in **83** is suggested by variable temperature $^{31}$P MAS-NMR measurements (Figure 3.35). At room temperature, the spectrum displays two broad peaks at 152.3 and 149.7 ppm with an integration ratio of approximately 3:7. As the temperature is reduced, these signals become even broader and merge at approximately –75 °C. At –100 °C, the peak appears to display some splitting into two very broad and closely spaced signals, but, regrettably, spectra could not be recorded at lower temperatures. Provided that the solid state structure of the polymer **83** were rigid at room temperature, at least two well-separated broad signals would be expected in the $^{31}$P MAS-NMR spectrum, one at lower field due to the uncoordinated P atoms and one at higher field due to the coordinated P atoms, with an integration ratio of 2:3. In contrast, if a dynamic process such as fast rotation of the *cyclo*-$P_5$ rings were occurring at room temperature, a singlet would be expected.

It was also of interest to investigate the reactivity of **9a** with $Ag^I$ salts of coordinating anions, but so far experiments with $AgNO_2$ in mixtures of $CH_3CN$ and $CH_2Cl_2$ at room temperature led to the formation of an amorphous, highly insoluble brown powder **85**, which could not be comprehensively characterised. Although fragments attributable to $[Ag(Cp^*FeP_5)(NO_2)(NCCH_3)_3]^+$ and fragments thereof

were detected in the positive ion ESI-MS spectra of trace amounts of **85** in $CH_3CN$, attempts to establish the stoichiometry of the product by elemental analysis were inconclusive.

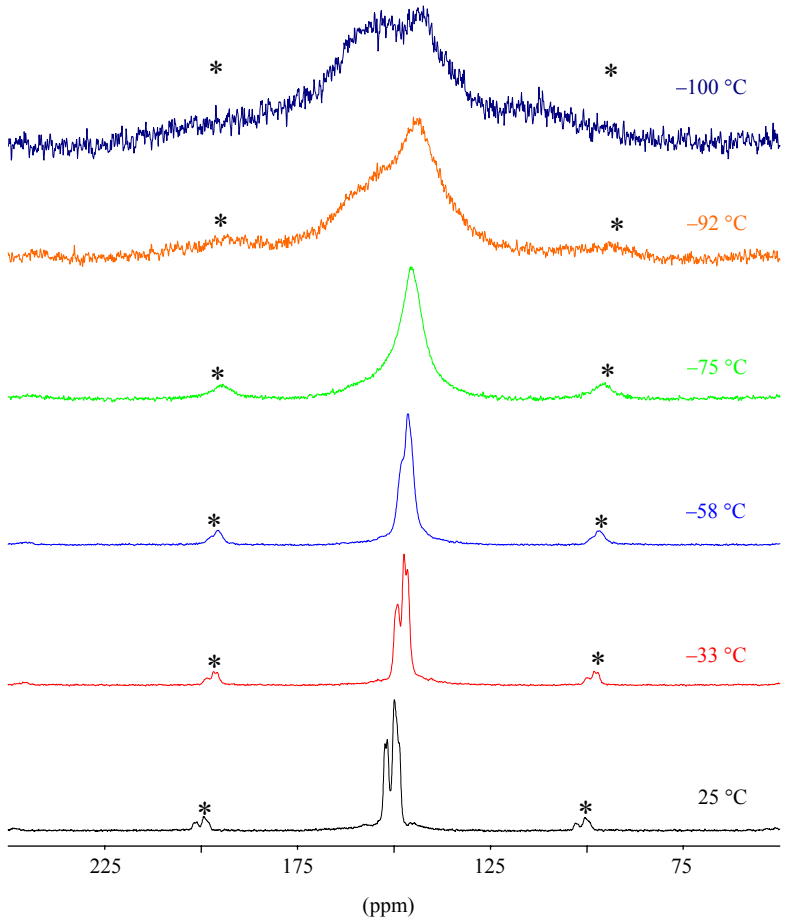


Figure 3.35. Variable temperature solid-state $^{31}P$ MAS-NMR spectra of **83** (peaks marked with an asterisk are the spinning side-bands).

## 3.7.2. Studies on the Reactivity of [Cp*Fe($\eta^5$-$P_5$)] with $Au^I$ Salts

Reaction of **9a** with $[Au(PPh_3)][PF_6]$ in a mixture of THF and $CH_2Cl_2$ at room temperature led to the formation of a brown, amorphous powder **86**, even if the reactants were allowed to mix by slow diffusion. This product is insoluble in common solvents and does not appear to be particularly sensitive. Elemental analysis suggests that the chemical formula of the compound is $[Au_5(Cp^*FeP_5)_2]_n[(PF_6)_5]_n$.

Experiments were also performed in which the salt [(THT)AuCl] was allowed to react with **9a** in a mixture of THF and $CH_2Cl_2$ at room temperature, but this led to the formation of the product **87** as a brown powder, which is insoluble in common solvents and could only be poorly characterised. According to the results of an elemental analysis, the chemical formula $[Au_3(Cp^*FeP_5)Cl_3]_n$ could be proposed for **87**.

## 3.8. The Triple-Decker Sandwich Complex $[(Cp^*Mo)_2(\mu,\eta^6\text{-}P_6)]$ as a Ligand

The isolation of the triple-decker sandwich complex $[(Cp^*Mo)_2(\mu,\eta^6\text{-}P_6)]$ **11c**[9e] in the mid-1980s was one of the most remarkable developments in the field of $P_n$-ligand complexes, since it incorporates the all-P analogue of benzene, hexaphosphabenzene. It was thus particularly intriguing to investigate the capacity of this highly interesting complex to act as a supramolecular building block. However, since **11c** can only be prepared in very low yields, investigations were not extensive and were conducted on a small scale.

### 3.8.1. Studies on the Reactivity of $[(Cp^*Mo)_2(\mu,\eta^6\text{-}P_6)]$ with CuCl

Room temperature reaction of **11c** with a large excess of CuCl in a mixture of $CH_3CN$, $CH_2Cl_2$ and $Et_2O$ led to the isolation of thin amber plates of the air- and light-sensitive compound **88** (Equation 3.20). In the schematic illustration of compound **88** depicted in Equation 3.20, Cu´ denotes Cu atoms which are disordered over two non-equivalent positions in a ratio of 3:1 and here the major position is shown. In the minor position, the Cu´ atoms shift in such a way so that they may coordinate with the $P_a$─$P_b$ edges. Complex **88** is insoluble in common solvents and can be stored indefinitely at ambient conditions under an inert atmosphere.

Single crystal X-ray diffraction analysis of **88** revealed that it forms corrugated sheets, as depicted in Figure 3.36. The repeat unit of this polymer consists of one unit of **11c**, three $CH_3CN$ ligands and five units of CuCl, with one $Cu^I$ centre being disordered over two non-equivalent positions in a ratio of 3:1. These positions are illustrated in Figure 3.36 as Cu5 and Cu6, respectively. The Cu atoms are found in both distorted tetrahedral (Cu1, Cu3-Cu6) and distorted trigonal pyramidal (Cu2) coordination modes and are coordinated to the units of **11c** in a $\eta^1$ fashion, with the exception of the disordered Cu atoms in the Cu6 positions, which are coordinated in a $\eta^2$ fashion to the P2─P3

edges. The $CH_3CN$ ligands are borne by the Cu1, Cu4 and the disordered Cu atoms ($CH_3CN$ ligand of Cu6 not shown in Figure 3.36). All Cl atoms are present as simple bridging ligands, except Cl5, which acts as a $\mu_3$ ligand. The 2D sheet structure thus comprises, in addition to the essentially planar $P_6$ rings of **11c** (mean deviation from planarity: 0.002(2) Å), four-membered $Cu_2Cl_2$, five-membered $Cu_2P_2Cl$, 24-membered $Cu_{10}P_8Cl_6$, and, depending on the positions of the disordered Cu atoms, ten-membered $Cu_4P_4Cl_2$, 11-membered $Cu_4P_5Cl_2$ and 12-membered $Cu_4P_6Cl_2$ rings. The geometry of the $Cu_2Cl_2$ rings incorporating Cl1 and Cl2 depends on the position of the disordered Cu atom. Selected bond lengths and angles for **88** are listed in Table 3.11.

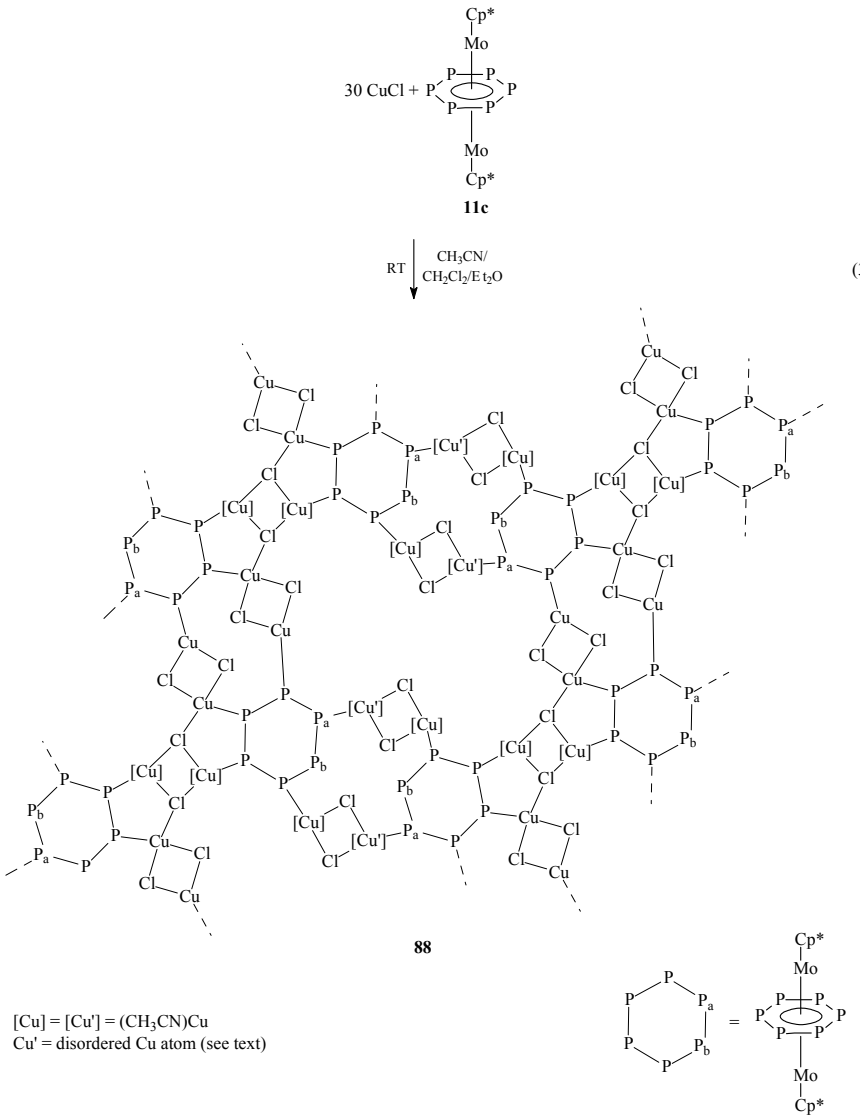

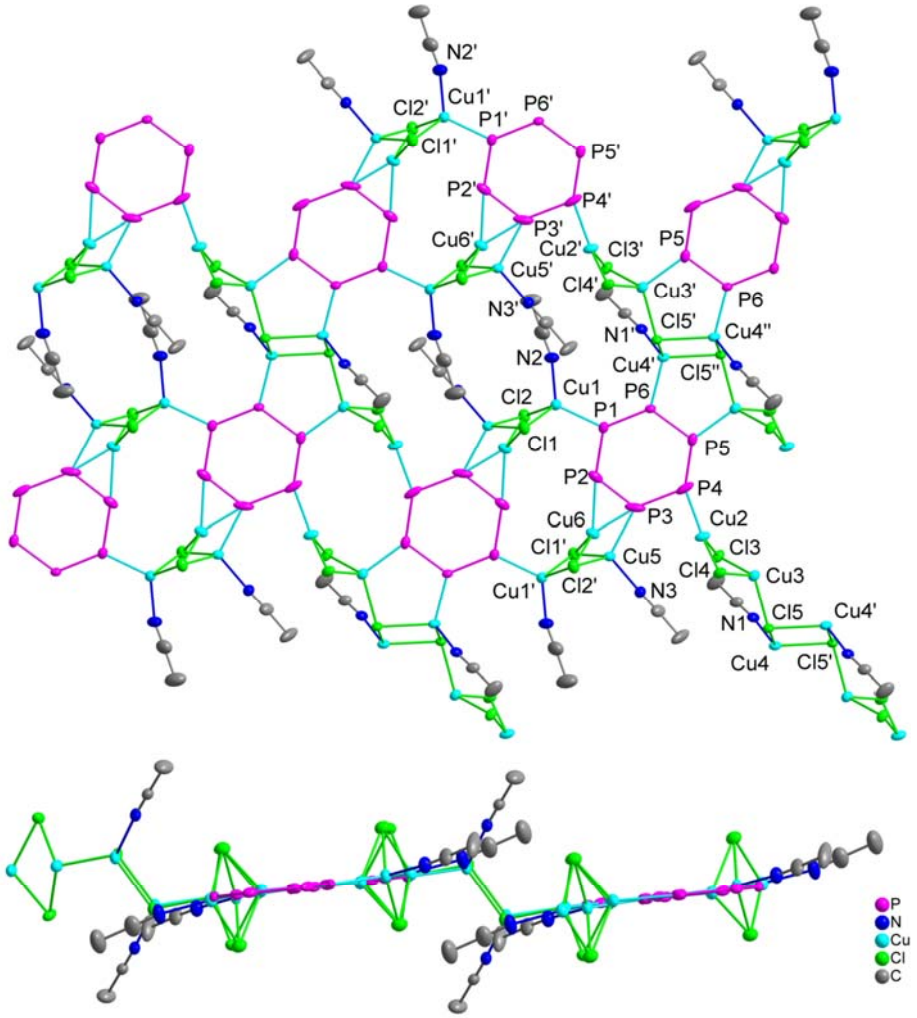


Figure 3.36.View of a section of the 2D structure of **88** along the crystallographic *a*-axis (top) and *c*-axis (bottom) (Cp*Mo fragments, $CH_3CN$ molecule attached to Cu6 and H atoms omitted for clarity). Atoms Cu5 and Cu6 denote the two non-equivalent positions over which one of the five Cu atoms in the repeat unit of **88** is disordered, in a ratio of 3:1. Thermal ellipsoids are represented at the 50 % probability level. Selected bond lengths and angles for **88** are collected in Table 3.11.

Table 3.11. Selected bond lengths (Å) and angles (°) for **88**.

| | | | |
|---|---|---|---|
| P1─P2[a] | 2.188(2) | Cl4─Cu2─P4 | 127.05(6) |
| P1─P6[a] | 2.140(2) | Cl3─Cu3─Cl4 | 98.36(5) |
| P2─P3[a] | 2.134(2) | Cl3─Cu3─Cl5 | 114.33(5) |
| P3─P4[a] | 2.261(3) | Cl3′─Cu3′─P5 | 112.31(6) |
| P4─P5[a] | 2.151(2) | Cl4─Cu3─Cl5 | 107.31(5) |
| P5─P6[a] | 2.229(2) | Cl4′─Cu3′─P5 | 112.09(6) |
| Cu1─Cl1 | 2.371(2) | Cl5′─Cu3′─P5 | 111.64(6) |
| Cu1─Cl2 | 2.376(2) | Cl5─Cu4─N1 | 110.47(1) |
| Cu2─Cl3 | 2.285(2) | Cl5′─Cu4′─P6 | 114.85(5) |
| Cu2─Cl4 | 2.280(2) | Cl5─Cu4─Cl5′ | 98.10(5) |
| Cu3─Cl3 | 2.378(2) | P6─Cu4′─N1′ | 111.80(1) |
| Cu3─Cl4 | 2.386(2) | Cl5′─Cu4─N1 | 114.47(1) |
| Cu3─Cl5 | 2.360(2) | Cl5′′─Cu4′─P6 | 106.49(5) |
| Cu4─Cl5 | 2.369(2) | P3─Cu5─N3 | 111.57(2) |
| Cu4─Cl5′ | 2.435(1) | Cl1′─Cu5─P3 | 111.53(6) |
| Cu5─Cl1′ | 2.402(2) | Cl2′─Cu5─P3 | 111.06(7) |
| Cu5─Cl2′ | 2.350(2) | Cl1′─Cu5─N3 | 114.4(2) |
| Cu6─Cl1′ | 2.243(4) | Cl2′─Cu5─N3 | 108.1(2) |
| Cu6─Cl2′ | 2.338(3) | Cl1′─Cu5─Cl2′ | 99.52(6) |
| Cu1─P1 | 2.241(2) | Cl1′─Cu6─Cl2′ | 104.68(1) |
| Cu2─P4 | 2.189(2) | Cl1′─Cu6─P2 | 125.82(1) |
| Cu3′─P5 | 2.259(2) | Cl2′─Cu6─P2 | 115.98(1) |
| Cu4′─P6 | 2.256(1) | P2─Cu6─P3 | 55.63(9) |
| Cu5─P3 | 2.328(2) | Cl2′─Cu6─P3 | 120.32(2) |
| Cu6─P2 | 2.427(3) | Cl1′─Cu6─P3 | 128.08(2) |
| Cu6─P3 | 2.105(4) | Cu1′─Cl1′─Cu5 | 78.12(5) |
| Cl1─Cu1─Cl2 | 99.66(5) | Cu1′─Cl1′─Cu6 | 76.50(9) |
| Cl1─Cu1─P1 | 111.48(6) | Cu1′─Cl2′─Cu5 | 79.04(5) |
| Cl1─Cu1─N2 | 109.30(2) | Cu1′─Cl2′─Cu6 | 74.63(9) |
| Cl2─Cu1─P1 | 112.38(6) | Cu2─Cl3─Cu3 | 72.62(5) |
| Cl2─Cu1─N2 | 100.85(2) | Cu2─Cl4─Cu3 | 72.55(5) |
| P1─Cu1─N2 | 120.71(2) | Cu4─Cl5─Cu4′ | 81.90(5) |
| Cl3─Cu2─Cl4 | 104.35(6) | Cu3─Cl5─Cu4 | 116.38(6) |
| Cl3─Cu2─P4 | 127.19(6) | Cu3─Cl5─Cu4′ | 102.51(5) |

[a] P─P bond lengths in uncoordinated **11c** = 2.167(3)-2.175(3) Å.[9e]

The P─P bond lengths in **88** (2.134(2)-2.229(2) Å) span a larger range than those of the uncoordinated complex **11c** (2.167(3)-2.175(3) Å).[9e] The Cu─Cl bond lengths (2.243(4)-2.435(1) Å) are comparable to those found in the complex $[Cu_2Cl_2(PPh_3)_3]$[54a] (2.298(4)-2.454(4) Å), while the range covered by the Cu─P bond lengths (2.105(4)-2.427(3) Å) is larger than that of the reference compound (2.183(4)-2.245(5) Å).

Although **88** is practically insoluble in common solvents, sufficient amounts of the compound dissolve in $CH_3CN$ for the

acquisition of ESI-MS spectra. Selected fragments detected in the positive ion ESI-MS spectrum are tabulated below (Table 3.12) and illustrate that **88** probably dissolves under depolymerisation.

Table 3.12. Selected fragments (mass/charge (relative abundance in %)) detected in the positive ion ESI-MS spectrum of **88** in $CH_3CN$ at room temperature and the proposed cations for these fragments.

| Fragments | Proposed Cations |
|---|---|
| 1787.8 (0.01) | $[(Cu_5Cl_4)\{(Cp^*Mo)_2P_6\}_2(NCCH_3)]^+$ |
| 1745.2 (0.10) | $[(Cu_5Cl_4)\{(Cp^*Mo)_2P_6\}_2]^+$ |
| 1645.4 (0.45) | $[(Cu_4Cl_3)\{(Cp^*Mo)_2P_6\}_2]^+$ |
| 1547.4 (0.10) | $[(Cu_3Cl_2)\{(Cp^*Mo)_2P_6\}_2]^+$ |
| 1449.3 (0.20) | $[(Cu_2Cl)\{(Cp^*Mo)_2P_6\}_2]^+$ |
| 1353.4 (0.60) | $[Cu\{(Cp^*Mo)_2P_6\}_2]^+$, $[(Cu_5Cl_4)\{(Cp^*Mo)_2P_6\}(NCCH_3)_6]^+$ |
| 1324.4 (0.30) | $[(Cu_6Cl_5)\{(Cp^*Mo)_2P_6\}(NCCH_3)_3]^+$ |
| 1297.4 (0.23) | $[(Cu_4Cl_3)\{(Cp^*Mo)_2P_6\}(NCCH_3)_7]^+$ |
| 1187.1 (0.03) | $[(Cu_5Cl_4)\{(Cp^*Mo)_2P_6\}(NCCH_3)_2]^+$ |
| 1087.2 (0.10) | $[(Cu_4Cl_3)\{(Cp^*Mo)_2P_6\}(NCCH_3)_2]^+$ |
| 1005.0 (0.06) | $[(Cu_4Cl_3)\{(Cp^*Mo)_2P_6\}]^+$ |
| 848.1 (1) | $[(Cu_2Cl)\{(Cp^*Mo)_2P_6\}(NCCH_3)]^+$ |
| 746.1 (10) | $[Cu\{(Cp^*Mo)_2P_6\}(NCCH_3)]^+$ |
| 716.2 (1) | $[Cu\{(Cp^*Mo)_2P_6\}]^+$ |

## 3.8.2. Studies on the Reactivity of $[(Cp^*Mo)_2(\mu,\eta^6\text{-}P_6)]$ with $Ag[Al\{OC(CF_3)_3\}_4]$

Reaction of a 1:1 mixture of **11c** and $Ag[Al\{OC(CF_3)_3\}_4]$ in $CH_2Cl_2$ or a mixture of $CH_2Cl_2$ and $CH_3CN$ at room temperature results in oxidation of **11c** and formation of the complex salt **89** (Equation 3.21). Compound **89** can be isolated as a dark teal solid, which is soluble in most common solvents except alkanes. It can be stored indefinitely under an inert atmosphere at ambient conditions and it even appears to be air-stable, since acetone solutions of the compound stored under air retain their original colour for several weeks.

The apparently facile oxidation of **11c** in the conditions described above was initially quite surprising. Scherer and co-workers have studied **11c** by electrochemical methods in 1,2-dichloroethane and have determined that this complex undergoes irreversible oxidation at 0.90 V versus the aqueous saturated calomel electrode (SCE), with retention of the triple-decker sandwich structure.[9g] Since $Ag^+$, a commonly utilised one-electron oxidant, has a formal potential of 1.11 V versus SCE in $CH_2Cl_2$,[68] it functions as a strong oxidising agent for **11c**.

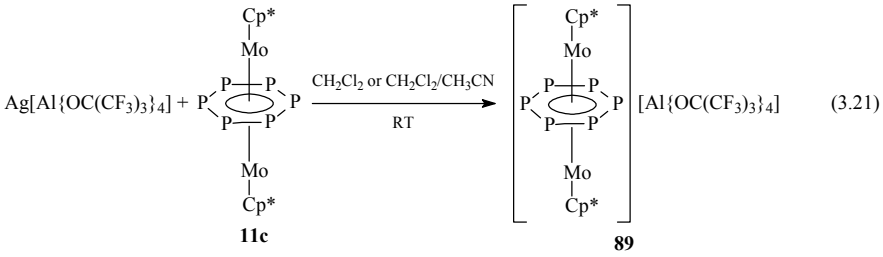


(3.21)

As electrochemical studies have shown, oxidation and reduction of the complex [Cp*Fe($\eta^5$-$P_5$)] **9a** both result in dimerisation and the formation of a dication and a dianion (Figure 1.8), respectively.[26a] ESI-MS, crystallographic and VPO analyses demonstrate that the 27 VE cation in **89** does not dimerise. In the positive ion ESI-MS spectra of **89** in $CH_2Cl_2$ at room temperature, only peaks attributable to the monocation $[(Cp^*Mo)_2P_6]^+$ are detected.[69] The existence of only this cation in $CH_2Cl_2$ solution is confirmed by VPO measurements, which revealed a molecular mass of 1524 ± 76 g mol$^{-1}$ (expected: 1615 g mol$^{-1}$). Single crystal X-ray diffraction analysis of **89** demonstrates its monomeric nature, but the quality of the crystallographic data set is too low for a detailed structural discussion. The reluctance of the cation in **89** to dimerise is probably a result of the steric demand imposed on the triple-decker sandwich structure by the Cp* ligands.

Interestingly, reaction of **11c** and Ag[Al{OC(CF$_3$)$_3$}$_4$] in $CH_2Cl_2$ at room temperature in a 2:1 stoichiometry leads to the formation of a mixture of the compounds **89** and **90** (Equation 3.22). Complex **90** crystallises as air- and light-sensitive red-orange plates, following storage of the reaction mixture at –28 °C. Solid samples of **90** are quite stable and can be stored indefinitely at ambient conditions under an inert atmosphere. The solubility of the compound is generally poor and solutions tend to decompose to **89** as illustrated by ESI-MS and $^{31}$P-NMR spectroscopy.

Crystals of **90** have been characterised by X-ray diffraction analysis and the structure of the cation in the compound, which consists of two units of **11c** coordinated to the Ag$^I$ centre in a $\eta^2$ coordination mode, is shown in Figure 3.37. The Ag cation and the four P atoms of the two coordinated P─P edges are coplanar, whereas the *cyclo*-$P_6$ moieties deviate marginally from planarity (mean deviation from planarity: 0.004(3) Å). The coordinated P─P edges (2.305(1) Å) are considerably longer than those in uncoordinated **11c** (2.167(3)-2.175(3) Å),[9e] while the remaining edges (2.173(1)-2.187(1) Å) are, on average, only marginally longer. The Ag─P bond lengths (2.596(1), 2.635(1) Å) lie just outside or just within the lower end of the range defined by previously reported $[Ag(PPh_3)_4]^+$ salts (2.631(5)-2.746(5) Å).[38]

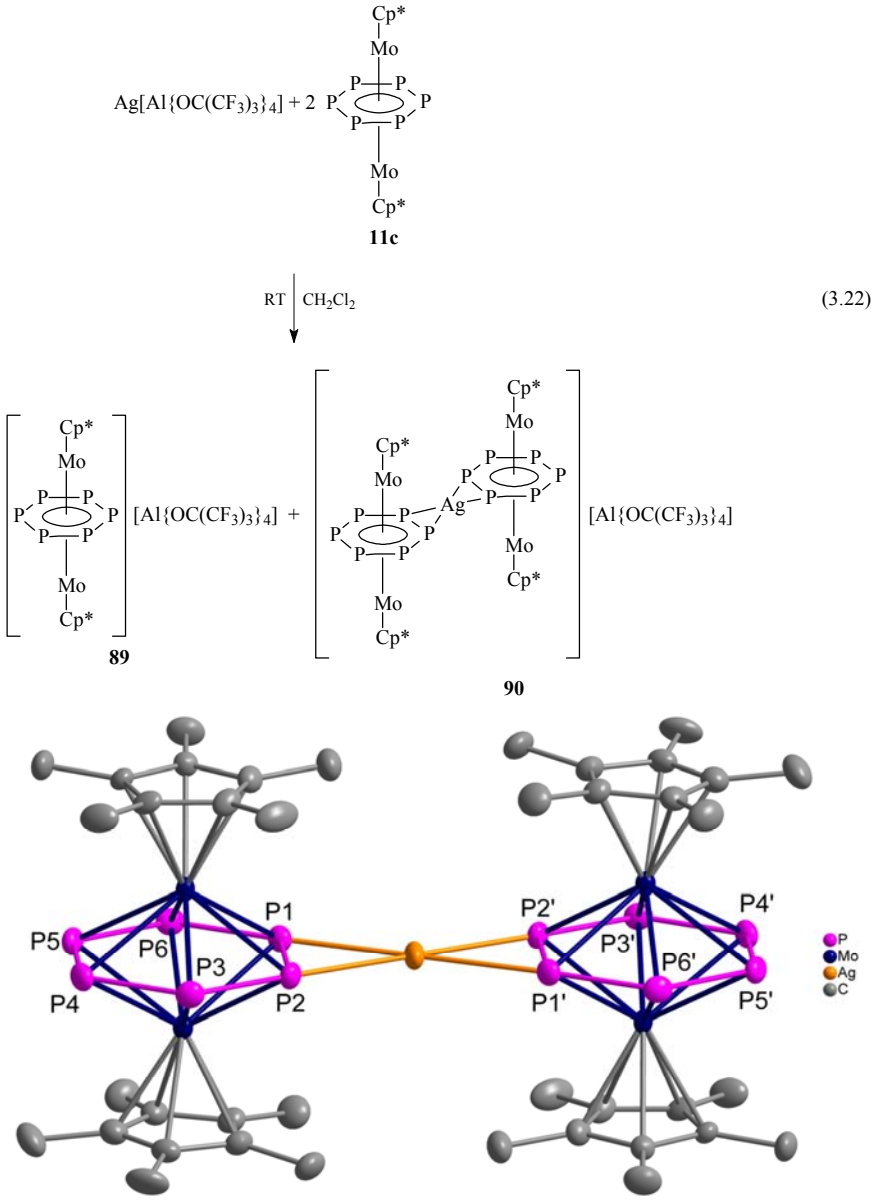


Figure 3.37. Structure of the cation in **90** (hydrogen atoms omitted for clarity). Thermal ellipsoids are represented at the 50% probability level. Selected bond lengths (Å) and angles (°): P1─P2 2.305(1), P1─P6 2.181(1), P2─P3 2.185(1), P3─P4 2.187(1), P4─P5 2.173(1), P5─P6 2.185(1), Ag─P1 2.596(1), Ag─P2 2.635(1), P1─Ag─P2 52.3(1), P1─Ag─P1′ 180.0(1), P1─Ag─P2′ 127.7(1), P2─Ag─P2′ 180.0(1).

# 3.9. An Excursion in the Realm of Mixed Group 15/16 Element Ligand Complexes: the Cluster $[(Cp^*Mo)_2(\mu,\eta^3\text{-}P_3)(\mu,\eta^2\text{-}PS)]$ as a Ligand

The synthesis of organometallic $P_n$-ligand complexes is typically achieved using a suitable metal complex and the homoatomic cage molecule $P_4$.[4a] If, instead, heteroatomic cage compounds of the type $E_mX_n$ (E = P, As; X = S, Se) are used, a fascinating variety of complexes incorporating both Group 15 and Group 16 atoms can be obtained.[4e,37] Such $P_mS_n$-ligand complexes are particularly intriguing candidates for supramolecular chemistry since the pnicogen and chalcogen atoms may either compete for coordination sites or may both coordinate.[70] Preliminary investigations involved the complex $[(Cp^*Mo)_2(\mu,\eta^3\text{-}P_3)(\mu,\eta^2\text{-}PS)]$ **91** (Figure 3.38), which contains a bent $P_3$ and a linear PS ligand.[71]

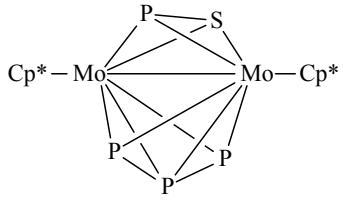


Figure 3.38. Structure of the $P_mS_n$-ligand complex **91**.

## 3.9.1. Studies on the Reactivity of $[(Cp^*Mo)_2(\mu,\eta^3\text{-}P_3)(\mu,\eta^2\text{-}PS)]$ with CuX (X = Cl, Br, I)

Reaction of **91** and CuX (X = Cl, Br, I) in a 1:2 stoichiometry in a mixture of $CH_3CN$ and $CH_2Cl_2$ at room temperature leads to the isolation of the compounds **92a-c** as air-sensitive ruby-red crystalline solids (Equation 3.23). These complexes are insoluble in common solvents and can be stored indefinitely under an inert atmosphere at ambient conditions.

Compound **92c** has been crystallographically characterised (Figure 3.39) and shown to be a 1D polymer, which consists of a stack of distorted $Cu_3I_3$ rings bridged by units of **91**. A further unit of **91** is coordinated to each $Cu_3I_3$ ring in a terminal fashion. Although discrete $Cu_3X_3$ rings are apparently the predominant species in CuX vapours,[72] such rings present a structural rarity in the solid state[73] and have not been observed for X = I until the present work. Thus the $Cu_3I_3$ rings in **92c** are certainly one of its most remarkable structural features.

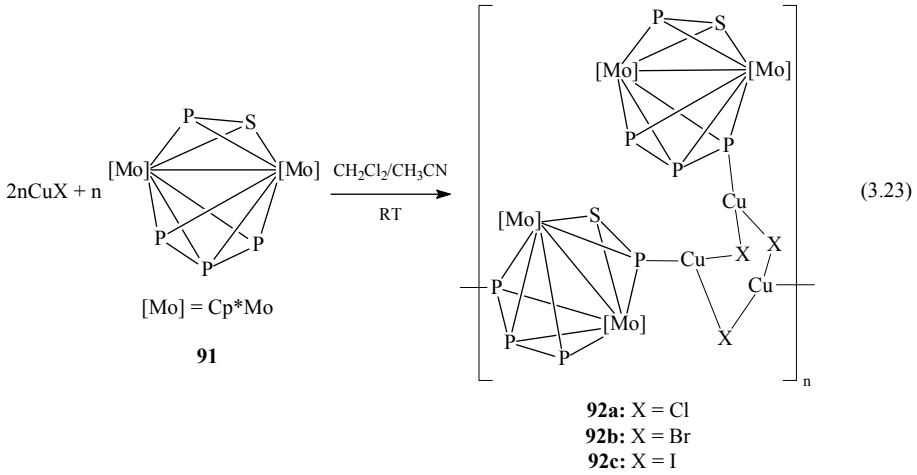


(3.23)

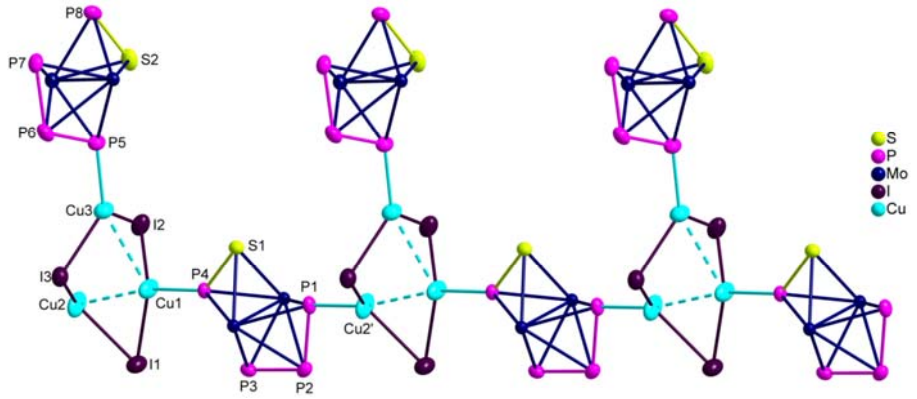


Figure 3.39. Section of the 1D polymeric structure of **92c** (Cp* ligands omitted for clarity). Thermal ellipsoids are represented at the 50% probability level. Selected bond lengths (Å), interatomic distances (Å) and angles (°): P1─P2 2.187(1), P2─P3 2.155(2), P5─P6 2.191(1), P6─P7 2.149(1), S1─P4 2.088(1), S2─P8 2.081(1), Cu1─P4 2.220(1), Cu2´─P1 2.218(1), Cu3─P5 2.211(1), Cu1─I1 2.616(1), Cu2─I1 2.583(1), Cu1─I2 2.671(1), Cu3─I2 2.557(1), Cu2─I3 2.689(1), Cu3─I3 2.556(1), Cu1···Cu2 2.554(7), Cu1···Cu3 2.79(2), I1─Cu1─I2 109.40(3), I1─Cu1─P4 111.96(4), I2─Cu1─P4 121.45(4), I1─Cu2─I2 96.78(2), I1─Cu2─P1 124.28(4), I3─Cu2─P1 116.80(4), I2─Cu3─I3 111.78(2), I2─Cu3─P5 121.00(4), I3─Cu3─P5 125.04(4), Cu1─I1─Cu2 58.85(2), Cu1─I2─Cu3 64.58(2), Cu2─I3─Cu3 81.81(2).

The elements P and S are essentially indistinguishable by X-ray crystallography and the assignment of these elements in the PS ligands of both the bridging and pendant units of **91** as shown in Figure 3.39 is based on crystallographic data obtained for compound **93** (Figure 3.40),[71] the $Cr(CO)_5$ adduct of **91**, and on solid state $^{31}P$ MAS-NMR data of **92c** (see below). In **93**, the $Cr(CO)_5$ fragment is bound to the $P_3$ ligand of **91** via the P4 atom and the length of the P3─P4 bond (2.286(6) Å) is longer than that of the P2─P3 bond (2.109(7) Å). Correspondingly, in **92c**, the P1─P2 (2.187(1) Å) and P5─P6 (2.191(1) Å) bonds are longer than the P2─P3 (2.155(2) Å) and P6─P7 (2.149(1) Å) bonds, respectively, and therefore the P and S atoms can be assigned based on the structure of **93**. The S─P bonds in **92c** (2.088(1), 2.081(1) Å) are longer than that in **93** (2.023(5) Å). The lengths of the Cu─P (2.211(1)-2.220(1) Å) and Cu─I (2.556(1)-2.689(1) Å) bonds are comparable to the corresponding bond lengths found in the complex $[Cu_2I_2(PPh_3)_3]$ (2.219(3)-2.267(3) Å and 2.500(2)-2.819(1) Å, respectively).[54c] Considering the interatomic distances Cu1···Cu2 (2.554(7) Å) and Cu1···Cu3 (2.79(2) Å), the existence of weak interactions between the atom Cu1 and the atoms Cu2 and Cu3, respectively, is likely, since these contacts are shorter than or equal to twice the van der Waals radius of Cu (1.40 Å).[63]

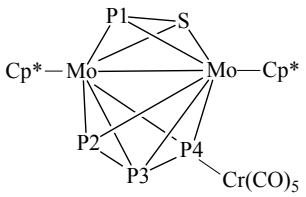


Figure 3.40. Structure of the complex **93**, the $Cr(CO)_5$ adduct of **91**, with labelling scheme.

It is helpful to consider the solution $^{31}P$-NMR spectral properties of the starting complex **91** in $CHCl_3$ (Table 3.13),[71] before discussing the solid-state $^{31}P$ MAS-NMR spectrum of **92c**. The P resonances exhibited in the spectrum of **91** are typical of an ABMX spin system and, by following the labelling scheme given in Table 3.13, $P_A$ resonates at 343.3 ppm, $P_B$ at 320.8 ppm, $P_M$ at –132.0 ppm and $P_X$ at –366.5 ppm.

As demonstrated by X-ray crystallography, **92c** contains both bridging and pendant units of **91**, which are therefore chemically distinct. Furthermore, the bridging units coordinate via the $P_3$ as well as the PS ligand, while the pendant units are bound via the $P_3$ ligand only. The $^{31}P$ MAS-NMR spectrum of **92c** (Figure 3.41) displays two signals

in the region where the $P_M$ resonances would be expected, one at lower field with coupling to $^{63/65}$Cu (–107.5 ppm, $^1J_{CuP}$ = 1500 Hz) and one at higher field (–132.8 ppm) without such coupling. This does not only demonstrate that the $P_M$ atoms of the bridging and pendant units of **91** are electronically distinct, but also that the P atoms, and not the S atoms, of the PS ligands in the bridging units of **91** are coordinated. This in turn confirms that the $P_B$ atoms of the $P_3$ ligands

Table 3.13. Structure of **91**, with labelling scheme, and the $^{31}$P-NMR chemical shifts (ppm) of the compound in $CHCl_3$.

| Structure | P Atom | Chemical Shift[a] |
|---|---|---|
| 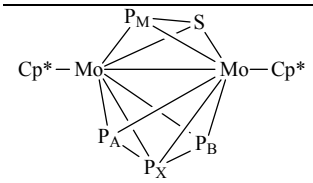 | $P_A$ | 343.3 |
| | $P_B$ | 320.8 |
| | $P_M$ | –132.0 |
| | $P_X$ | –366.5 |



[a] Simulated coupling constants, $J_{PP}$ (Hz): $J_{AX}$ = 375; $J_{BX}$ = 392; $J_{AM}$ = 64; $J_{MX}$ = 19; $J_{AB}$ = 15; $J_{BM}$ < 10[71]

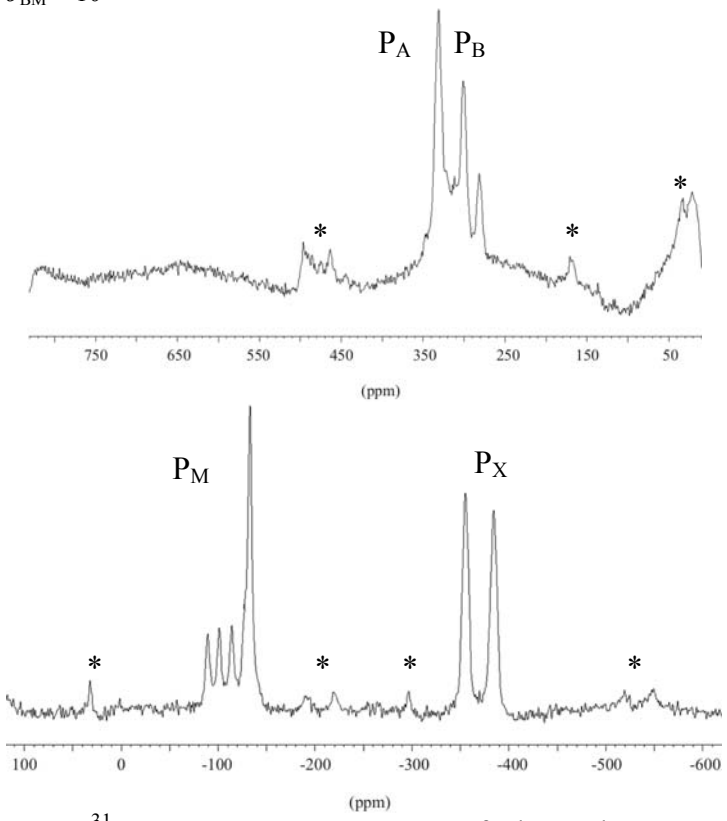


Figure 3.41. $^{31}$P MAS-NMR spectrum of the polymer **92c**, with labelling scheme (peaks marked with an asterisk are the spinning side-bands; $P_M$ –107.5 ppm ($^1J_{CuP}$ = 1500 Hz)).

of the bridging units of **91** are coordinated. Two signals are observed in the region where the $P_X$ resonances would be expected, the higher field one (–384.2 ppm) probably being due to the pendant units of **91** and the lower field one (–354.8 ppm) due to the bridging units, as is the case with the $P_M$ resonances. The region in which the $P_A$ and $P_B$ resonances would be expected displays a group of broad signals, with no resolvable coupling to $^{63/65}$Cu, and therefore it cannot be determined whether the pendant units of **91** are bound via the $P_A$ or the $P_B$ atoms. Although coordination via the $P_B$ atoms was chosen for the structural representation in Figure 3.39, based on bond length comparisons with **93** (Figure 3.40),[71] a statistical distribution is not unlikely. Such a distribution and the marginally differing chemical shifts of the corresponding P atoms of the bridging units of **91** might explain why broad signals with no resolvable coupling to $^{63/65}$Cu are observed in the corresponding region of the spectrum.

Although practically insoluble in common solvents, sufficient amounts of the compounds **92a-c** are soluble in $CH_3CN$ for the acquisition of ESI-MS spectra. Selected fragments are listed in Table 3.14 and indicate that the compounds most probably dissolve under depolymerisation. Since all three compounds display similar fragmentation patterns, it is believed that the compounds **92a**,**b**, which could not be characterised crystallographically, are similar in structure to **92c**.

Table 3.14. Selected fragments (mass/charge (relative abundance in %)) detected in the positive ion ESI-MS spectra of the compounds **92a-c** in $CH_3CN$ and the proposed cations for these fragments.

| **92a** (X = Cl) | **92b** (X = Br) | **92c** (X = I) | **Proposed Cations** |
|---|---|---|---|
| 1491.0 (4) | 1588.0 (3) | 1682.4 (2) | $[(Cu_3X_2)\{(Cp^*Mo)_2P_4S\}_2]^+$ |
| 1398.1 (8) | 1444.1 (15) | 1491.1 (26) | $[(Cu_2X)\{(Cp^*Mo)_2P_4S\}_2]^+$ |
| 1301.1 (10) | 1300.1 (13) | 1300.0 (17) | $[Cu\{(Cp^*Mo)_2P_4S\}_2]^+$ |
| 913.8 (6) | 1011.7 (4) | 1103.8 (2) | $[(Cu_3X_2)\{(Cp^*Mo)_2P_4S\}(NCCH_3)]^+$ |
| – | 968.7 (15) | – | $[(Cu_3X_2)\{(Cp^*Mo)_2P_4S\}]^+$ |
| 821.9 (10) | 865.9 (58) | 913.9 (74) | $[(Cu_2X)\{(Cp^*Mo)_2P_4S\}(NCCH_3)]^+$ |
| – | 822.9 (3) | 874.8 (6) | $[(Cu_2X)\{(Cp^*Mo)_2P_4S\}]^+$ |
| 722.0 (100) | 722.1 (100) | 722.0(100) | $[Cu\{(Cp^*Mo)_2P_4S\}(NCCH_3)]^+$ |
| 681.0 (2) | 683.0 (1) | 681.0 (2) | $[Cu\{(Cp^*Mo)_2P_4S\}]^+$ |

## 3.9.2. Studies on the Reactivity of $[(Cp^*Mo)_2(\mu,\eta^3\text{-}P_3)(\mu,\eta^2\text{-}PS)]$ with $Ag[Al\{OC(CF_3)_3\}_4]$

Reaction of **91** and $Ag[Al\{OC(CF_3)_3\}_4]$ in a 2:1 stoichiometry in a mixture of toluene and $CH_2Cl_2$ at room temperature leads to the formation of the complex **94** as an air- and light-sensitive red-brown crystalline solid (Equation 3.24). This compound is sparingly soluble in polar solvents such as $CH_3CN$ and can be stored indefinitely under an inert atmosphere at ambient conditions.

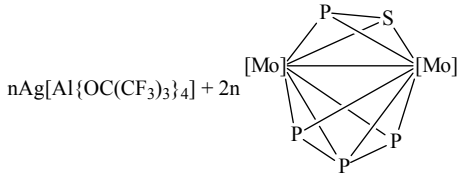


**91**

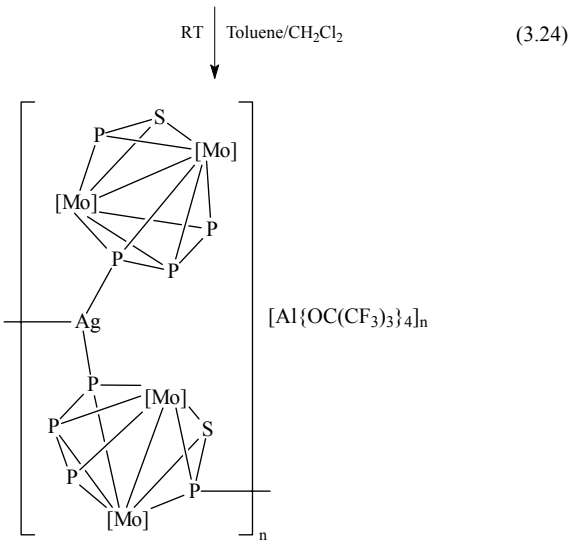


**94**

The undulated 1D polymeric structure of **94** (Figure 3.42) was revealed by single crystal X-ray diffraction analysis and consists of a chain of $Ag^I$ centres singly bridged by units of **91**. Each Ag atom is coordinated to a further unit of **91** in a terminal fashion and is thus in a trigonal coordination mode. The assignment of the elements phosphorus and sulphur in the PS ligands of both the bridging and pendant units of **91** as shown in Figure 3.42 is based on solution $^{31}$P-

NMR data of **94** (see below), on the $^{31}$P MAS-NMR spectra of polymer **92c**, which suggest that the S atoms are not involved in coordination with the Cu atoms, and on crystallographic data obtained for compound **93** (Figure 3.40),[71] the $Cr(CO)_5$ adduct of **91**.

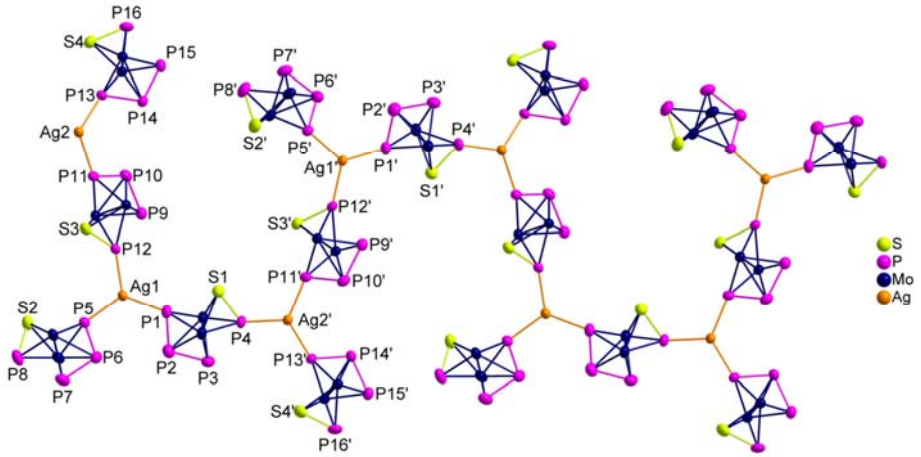


Figure 3.42. View of a section of the undulated cationic chain structure of **94** along the crystallographic *b*-axis (Cp* ligands omitted for clarity). Thermal ellipsoids are represented at the 50% probability level. Selected bond lengths (Å) and angles (°): P1─P2 2.173(9), P2─P3 2.15(1), P5─P6 2.163(8), P6─P7 2.162(9), P9─P10 2.141(8), P10─P11 2.189(8), P13─P14 2.182(6), P14─P15 2.160(8), S1─P4 2.100(8), S2─P8 2.09(1), S3─P12 2.097(7), S4─P16 2.069(9), Ag1─P1 2.477(5), Ag1─P5 2.477(5), Ag1─P12 2.489(6), Ag2′─P4 2.481(5), Ag2─P11 2.489(6), Ag2─P13 2.464(5), P1─Ag1─P5 123.5(2), P1─Ag1─P12 119.6(2), P5─Ag1─P12 117.0(2), P4─Ag2′─P11′ 113.7(2), P4─Ag2′─P13′ 119.7(2), P11─Ag2─P13 126.6(2).

In **93**, the $Cr(CO)_5$ fragment is bound to the $P_3$ ligand of **91** via the P4 atom and the length of the P3─P4 bond (2.286(6) Å) is longer than that of the P2─P3 bond (2.109(7) Å). Correspondingly, in **94**, the P1─P2 (2.173(9) Å), P5─P6 (2.163(8) Å), P10─P11 (2.189(8) Å) and P13─P14 (2.182(8) Å) bonds are longer than the P2─P3 (2.15(2) Å), P6─P7 (2.162(9) Å), P9─P10 (2.141(8) Å) and P14─P15 (2.160(8) Å) bonds, respectively, and therefore the P and S atoms can be assigned based on the structure of **93**. The P─S bonds in **94** (2.069(9)-2.100(8) Å) are longer than that in **93** (2.023(5) Å). The lengths of the Ag─P bonds (2.464(5)-2.489(6) Å) are within the range defined by those found in the tricoordinate Ag complex $[Ag\{(PPh_2)_2C_2B_9H_{10}\}(PPh_3)]$ (2.397(1)-2.494(1) Å).[74]

In the room temperature positive ion ESI-MS spectrum of **94** in $CH_3CN$, the most abundant fragment, which also happens to be the

largest fragment observed, is attributable to the cation $[Ag\{(Cp^*Mo)_2P_4S\}_2]^+$. Unfortunately, the solubility of **94** in common solvents is too low for a reliable determination of the molecular mass of the species in solution.

The $^{31}$P-NMR spectrum of **94** in $CD_3CN$ is illustrated in Figure 3.43 and is characteristic of an ABMX spin system, as is that of the starting complex **91** (Table 3.13). All resonances are shifted 10-15 ppm upfield with respect to those of uncoordinated **91**, with the exception of the signal attributable to $P_M$ (P atom of the PS ligand, Table 3.13), whose chemical shift is essentially identical to that of the $P_M$ atom in uncoordinated **91**, and none of the signals demonstrate coupling to $^{107/109}$Ag. Thus, assuming that only the cation $[Ag\{(Cp^*Mo)_2P_4S\}_2]^+$ **XXIV** is present in solution, the NMR data imply that coordination of the two units of **91** to the $Ag^I$ centre is exclusively via the $P_3$ ligands, which is the reason for believing that the S atoms of the PS ligands of **91** are not involved in coordination with the $Ag^I$ centres in the solid state, and that the resulting complex is fluxional. Consequently, one could envisage two possible structural variations of the cation **XXIV**, depicted schematically as **XXIVa** and **XXIVb** in Figure 3.44. Both consist of an $Ag^+$ cation, 'sandwiched' between the two $P_3$ edges of the two units of **91**, but differ in the way the $P_3$ edges are arranged with respect to each other. As illustrated, one $P_3$ ligand in **XXIVa** is the reflection of the other, whereas in **XXIVb**, the $Ag^+$ cation can be regarded as an inversion centre. In both variations, the $P_3$ ligands can essentially 'slip' back and forth with respect to the $Ag^+$ cation, as indicated by the double-headed arrows, and at any one time, the ligands may both be $\eta^1$-coordinated or $\eta^2$-coordinated, or one ligand may be $\eta^1$-coordinated while the other is $\eta^2$-coordinated. Interconversion between **XXIVa** and **XXIVb** could occur following appropriate rotation of one of the $P_3$ ligands about the axis of its bond to $Ag^+$.

It is obvious that several structures are possible for **XXIV**, which, energetically speaking, are most probably indistinguishable, and thus interconversion between these structures is likely to be facile. This would in turn lead to all three P resonances of the $P_3$ ligand being shifted upfield, albeit without any detectable coupling to $^{107/109}$Ag.

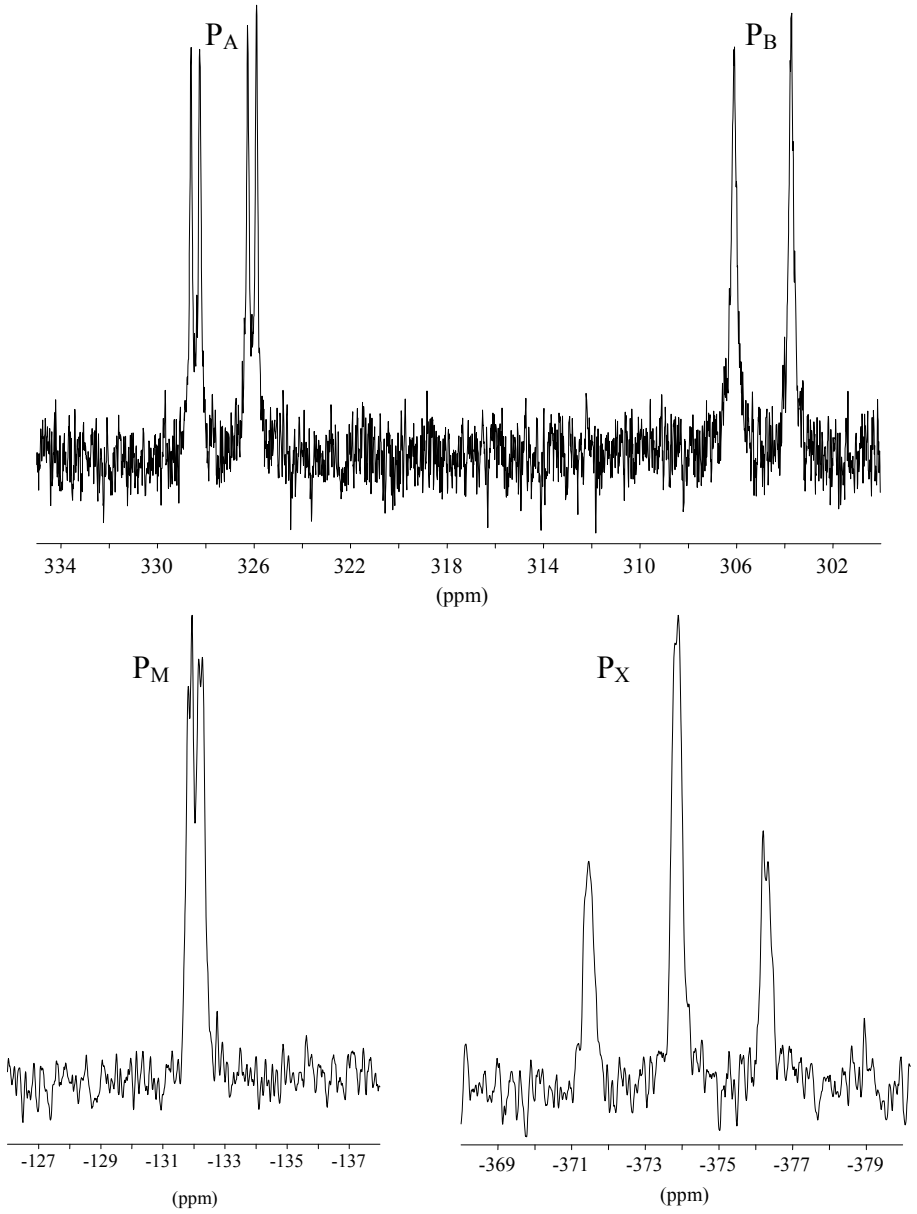


Figure 3.43. Room temperature $^{31}$P-NMR spectrum of **94** in $CD_3CN$, with labelling scheme ($P_X$: –373.8 ($^1J_{AX}$ = 375 Hz, $^1J_{BX}$ = 386 Hz, $^2J_{MX}$ = 22 Hz); $P_M$: –132.1 ($^2J_{AM}$ = 57 Hz, $^2J_{XM}$ = 18 Hz); $P_B$: 304.9 ($^1J_{XB}$ = 384 Hz); $P_A$: 327.3 ($^1J_{XA}$ = 380 Hz, $^2J_{MA}$ = 57 Hz)).

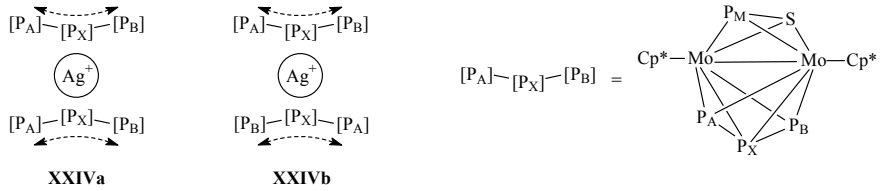


Figure 3.44. Schematic representation of the two structural variations proposed for the cation **XXIV**.

# 4. Experimental

## 4.1. General Remarks

### 4.1.1. Preparative Procedures

All manipulations were performed using standard Schlenk and dry-box techniques under an atmosphere of nitrogen or argon. Traces of oxygen and moisture were removed from the inert gases by passing them over a BASF R 3-11 ($CuO/MgSiO_3$) catalyst, through concentrated $H_2SO_4$, over coarsely granulated silica gel and over $P_4O_{10}$ supported on pumice gravel, in that order.

### 4.1.2. Solvent Purification

All solvents were degassed and distilled from appropriate drying agents under an atmosphere of dry, oxygen-free nitrogen prior to use. Boiling the solvents under reflux for at least four hours preceded the distillation process. Pentane and hexane were distilled from $LiAlH_4$, toluene, xylene and decahydronaphthalene from Na, $Et_2O$ and THF from Na/benzophenone, and $CH_2Cl_2$ and $CH_3CN$ from $CaH_2$. Acetone was doubly distilled, first from $P_4O_{10}$ and then from $K_2CO_3$.

All deuterated solvents were degassed and stored over molecular sieves, which had previously been dried for several hours under high vacuum at 200 °C. In the case of THF-$d_8$, this was additionally distilled from Na/benzophenone and then stored over molecular sieves treated in the aforementioned manner.

### 4.1.3. Starting Materials

The compounds **6a**,**b**,[9b,d] **7a-c**,[9b,d,e] **9a**,[12c] **11c**,[9e] **55**,[51d] **58**,[51d] **60-63**,[51,52] $Ag[Al\{OC(CF_3)_3\}_4]$,[36] $[Au(PPh_3)][PF_6]$,[17b] [LAuCl] (L = CO,[44] THT,[45] $PPh_3$[75]) and $[Cp^*M(NCCH_3)_3][(SbF_6)_2]$ (M = Rh, Ir)[47b] were prepared according to literature procedures. Samples of $Ag[Al\{OC(CF_3)_3\}_4]$ for preliminary investigations were generously donated by Prof. Ingo Krossing and co-workers (EPFL, Lausanne, Switzerland). The complex $[Cp''RhCl(NCCH_3)_2][BF_4]$[47b] was kindly donated by Dr. Sergei Konchenko (Russian Academy of Sciences (Siberian Division), Novosibirsk, Russia). The compounds **80**[60] and **91**[71] were munificently provided by Dr. Joachim Wachter (University of Regensburg).

$[Cu(CH_3CN)_4][PF_6]$ (Aldrich), AgOTf (Fluka), $AgClO_4$ (Strem), $AgPF_6$ (Aldrich), $AgSbF_6$ (Lancaster), $AgNO_2$ (Fluka), $AgNO_3$ (Aldrich) and $TlPF_6$ (Strem) were transferred to a dry-box for storage and used as received. CuCl (Strem) and CuBr (Strem) were purified before use, under a nitrogen atmosphere, by washing with the appropriate, degased aqueous hydrohalic acid (half-concentrated), followed by $H_2O$, EtOH and $Et_2O$. The resulting solids were then dried at room temperature under high vacuum and stored in a dry box. CuI (Aldrich) was purified and stored in a similar manner, the only difference being that a mixture of aqueous HCl (half-concentrated) and KI was used as the first washing medium.

The polymers **43a-c** for the solid-state MAS-NMR investigations were prepared according to the literature procedures.[32a,33]

## 4.1.4. Characterisation Methods

Solution NMR spectra were obtained by the NMR departments of the universities of Karlsruhe and Regensburg using either a Bruker AC250 (University of Karlsruhe) or a Bruker AVANCE400 or 600 (University of Regensburg) spectrometer. Samples were referenced against TMS ($^1H$, $^{13}C$), $Al(NO_3)_3$ in $D_2O$ ($^{27}Al$), $CFCl_3$ ($^{19}F$) and 85% $H_3PO_4$ ($^{31}P$) as external standards. Chemical shifts are reported in ppm, according to the $\delta$-scale, and the coupling constants $J$ in Hz. The NMR spectra were processed using the 1D-WINNMR programme.[76]

The solid-state $^{31}P$ MAS-NMR spectra of polymers **43a-c**[33] were recorded by Dr. Gunther Brunklaus (research group of Prof. Hellmut Eckert, University of Münster) on a Bruker DSX400 solid-state spectrometer in a 2.5 mm probe. The spectrum of **43a** was acquired at 121.49 MHz using a spinning rate of 30 kHz and those of **43b**,**c** at 162.01 MHz using spinning rates of 33 kHz. A rotor-synchronised Hahn spin-echo sequence, generated with 90° pulse lengths of about 4 μs and relaxation delays of 3 minutes (280 scans), was used to record the spectra and samples were referenced against 85% $H_3PO_4$ as an external standard.

The solid-state $^{31}P$ MAS-NMR spectra of polymers **66a-c** and **83** were recorded by Dr. Long Zhang (research group of Prof. Hellmut Eckert, University of Münster) on a Bruker DSX400 solid-state spectrometer in 2.5 mm probes. The spectra were acquired at 162.01 MHz using spinning rates of 25 and 30 kHz. A rotor synchronised Hahn spin-echo sequence, generated with 90° pulse lengths of about 4 μs and relaxation delays of 3 minutes (280 scans), was used to record the spectra and samples were referenced against 85% $H_3PO_4$ as an external standard. The $^{65}Cu$ MAS-NMR spectra were acquired at

106.01 MHz using single-pulse acquisition with short pulses of 1 μs at spinning rates of 30-33 kHz.

The solid-state $^{31}P$ MAS-NMR spectra of compounds **71**, **74**, **78** and **92c** were recorded by Dipl. Phys. Christian Gröger (research group of Prof. Eike Brunner, University of Regensburg) on a Bruker AVANCE300 solid-state spectrometer in 2.5 mm probes. All spectra were acquired at 121.50 MHz using a solid echo sequence and spinning rates of 20 and 30 kHz, and samples were referenced against $NaH_2PO_4$ as an external standard.

ESI-MS spectra were acquired by the MS departments of the universities of Karlsruhe and Regensburg either on an Ionspec ULTIMA FT-ICR (University of Karlsruhe) or a ThermoQuest Finnigan TSQ 7000 (University of Regensburg) spectrometer. The identity of the observed fragments was assigned according to the mass/charge (m/z) ratio and by comparison of the experimental spectra with simulated spectra, which were generated using software available on the Internet.[77] The peak with the highest relative abundance is reported for each isotopic band.

IR spectra were recorded either on a Bruker IFS 280 (University of Karlsruhe) or a Varian FTS 2000 (University of Regensburg) spectrometer, in the form of KBr discs or $CH_2Cl_2$ solutions. Spectra at the University of Regensburg were recorded with the assistance of Mrs. Petra Lugauer. Signals are reported in $cm^{-1}$.

Molecular mass determinations were performed under the supervision of Dr. Roland Neueder (Institute of Physical Chemistry, University of Regensburg) using a Knauer K-7000 vapour pressure osmometer, at 28 °C. The osmometer was calibrated using 0.01, 0.03, 0.05 and 0.1 M solutions of benzil in $CH_2Cl_2$.

Elemental analyses were performed by the microanalytical laboratories of the universities of Karlsruhe and Regensburg.

Melting and decomposition points were determined with the assistance of Mrs. Petra Lugauer using a Büchi S, Büchi 510 or Büchi SMP-20 melting point apparatus, and are uncorrected.

All X-ray crystallographic analyses were performed either by Prof. Manfred Scheer, the X-ray crystallography department of the University of Regensburg or Dr. Alexander V. Virovets (Russian Academy of Sciences (Siberian Division), Novosibirsk, Russia). The data were collected either on a STOE IPDS or an Oxford Diffraction Xcalibur 3 CCD diffractometer. The structures were solved using either SIR-97[78] or SHELXS-97[79] and refined using SHELXL-97[80] with anisotropic displacements for non-hydrogen atoms. Hydrogen atoms were located in idealised positions and refined isotropically according

to the riding model. Pictorial representations of the structures were generated using the Diamond programme.[81]

## 4.1.5. Theoretical Calculations

Theoretical calculations related to compounds **42g** and **83** were executed by Prof. Ingo Krossing (EPFL, Lausanne, Switzerland) at the density functional theory (DFT) level using the TURBOMOLE programme package.[82] The 28 and 46 electron cores of Mo and Ag were replaced by a quasi-relativistic effective core potential.[83] All species were fully optimised using the BP86[84] exchange-correlation functional along with the SV(P) basis set,[85] and solvation energies were calculated using the conductor-like screening model (COSMO) approach.[86] $^{31}$P-NMR shift calculations, performed at the BP86/SV(P) level for **42g** (Mo and Ag: SVPalls2 all-electron basis set optimised for NMR calculations) and at the BP86/TZVPP level for **83** (Ag: TZVPPalls2 all-electron basis set optimised for NMR calculations),[87] were done as single points on the BP86/SV(P) optimised geometries. The Born-Haber cycles for **42g** and **83** were generated based on the theoretical results by Prof. Krossing.

Theoretical calculations on the model compounds **66a´**,**b´** (related to polymers **43a**,**b** and **66a**,**b**) and calculations related to compound **81** were performed by Dr. Marek Sierka (Humboldt University, Berlin) at the DFT level using the TURBOMOLE programme package.[82] The BP86[84] exchange-correlation functional was employed along with the TZVP basis and auxiliary basis sets[85,87,88] for the structure optimisations. In order to speed up calculations, the Coulomb part was evaluated by using the MARI-J method.[85,89] The $^{31}$P chemical shifts of the model compounds **66a´**,**b´** were calculated within the GIAO approach[90] using a more extended TZP basis set on P, which is known to yield reasonably accurate NMR chemical shielding constants.[87b,90,91] In the calculations related to compound **81**, quasi-relativistic pseudopotentials were used for the elements Mo and Ag[83,92] and solvation energies were calculated using the COSMO approach.[86]

Pictorial representations of calculated structures were prepared using the Diamond programme.[81]

## 4.2. Synthesis of the Complexes Based on $[Cp_2Mo_2(CO)_4(\mu,\eta^2\text{-}P_2)]$

### 4.2.1. $[Ag_2\{Cp_2Mo_2(CO)_4(\mu_3,\eta^2\text{:}\eta^2\text{:}\eta^2\text{-}P_2)\}_2\{Cp_2Mo_2(CO)_4(\mu_4,\eta^2\text{:}\eta^2\text{:}\eta^1\text{:}\eta^1\text{-}P_2)\}_2][(ClO_4)_2]$ (42d)

A solution of $AgClO_4$ (24 mg, 0.12 mmol) in $CH_3CN$ (10 ml) was carefully layered over a solution of $[Cp_2Mo_2(CO)_4(\mu,\eta^2\text{-}P_2)]$ **6b** (100 mg, 0.20 mmol) in $CH_2Cl_2$ (10 ml) at room temperature. The vessel was then placed in a refrigerator (4 °C) and red prism-shaped crystals of **42d**•2$CH_3CN$ appeared within a week. These crystals were filtered, washed with $CH_3CN$ (2 × 3 ml) and dried under vacuum. The solvent of crystallisation was not lost during the drying process.

**Yield**: 111 mg (89 %).
**$^1$H-NMR** ($CD_3CN$, 400.13 MHz, 27 °C): $\delta$ = 5.35 (s; $C_5H_5$) ppm.
**$^{13}$C{$^1$H}-NMR** ($CD_3CN$, 100.63 MHz, 27 °C): $\delta$ = 87.83 (s; $C_5H_5$) ppm.
**$^{31}$P{$^1$H}-NMR** ($CD_3CN$, 161.98 MHz, 27 °C): $\delta$ = –59.5 (s) ppm.
**Positive ion ESI-MS** ($CH_3CN$, RT): *m/z* (%) = 2298.9 (1.5) $[\langle Ag_2\{Cp_2Mo_2(CO)_4P_2\}_4\rangle(ClO_4)]^+$, 1804.9 (1) $[\langle Ag_2\{Cp_2Mo_2(CO)_4P_2\}_3\rangle(ClO_4)]^+$, 1593.9 (4) $[Ag\{Cp_2Mo_2(CO)_4P_2\}_3]^+$, 1100.8 (100) $[Ag\{Cp_2Mo_2(CO)_4P_2\}_2]^+$, 643.8 (60) $[Ag\{Cp_2Mo_2(CO)_4P_2\}(NCCH_3)]^+$, 597.7 (0.5) $[Ag\{Cp_2Mo_2(CO)_4P_2\}]^+$.
**Negative ion ESI-MS** ($CH_3CN$, RT): *m/z* (%) = 99.0 (100) $ClO_4^-$.
**IR** (KBr): $\tilde{\nu}$ = 3114 (w), 1947 (vs; CO), 1919 (vs; CO), 1420 (m), 1104 (s), 1058 (m), 1011 (w), 828 (m), 624 (w), 562 (w), 520 (w), 491 (w), 455 (m) $cm^{-1}$.
**Elemental analysis**: Calculated (%) for $C_{60}H_{46}Ag_2Cl_2Mo_8N_2O_{24}P_8$ (2480.97): C 29.05, H 1.87, N 1.13; found: C 29.02, H 2.12, N 1.33.
**Melting point**: 160 °C (explosive decomposition).

### 4.2.2. $[Ag_2\{Cp_2Mo_2(CO)_4(\mu_3,\eta^2\text{:}\eta^2\text{:}\eta^2\text{-}P_2)\}_2\{Cp_2Mo_2(CO)_4(\mu_4,\eta^2\text{:}\eta^2\text{:}\eta^1\text{:}\eta^1\text{-}P_2)\}_2][(PF_6)_2]$ (42e)

A mixture of $AgPF_6$ (29 mg, 0.11 mmol), $[Cp_2Mo_2(CO)_4(\mu,\eta^2\text{-}P_2)]$ **6b** (100 mg, 0.20 mmol) and $CH_3CN$ (30 ml) was stirred in the dark at room temperature for 1 h. The reaction vessel was then placed overnight in a freezer (–28°C), during which time **42e** precipitated as a bright orange microcrystalline powder. The solid was filtered, washed

with $CH_3CN$ (2 × 3 ml) and dried under vacuum. Crystals of **42e**•2$CH_3CN$ suitable for X-ray diffraction analysis were obtained as red prisms by controlled diffusion of a $CH_3CN$ solution of $AgPF_6$ into a $CH_2Cl_2$ solution of **6b** at room temperature in the absence of light.

**Yield**: 70 mg (56 %).
**$^1$H-NMR** ($CD_3CN$, 600.13 MHz, 27 °C): $\delta$ = 5.38 (s; $C_5H_5$) ppm.
**$^{13}$C{$^1$H}-NMR** ($CD_3CN$, 150.92 MHz, 27 °C): $\delta$ = 88.45 (s; $C_5H_5$), 226.22 (s; CO) ppm.
**$^{19}$F-NMR** ($CD_3CN$, 376.47 MHz, 27 °C): $\delta$ = –71.74 (d; $^1J_{PF}$ = 706 Hz; $PF_6^-$) ppm.
**$^{31}$P{$^1$H}-NMR** ($CD_3CN$, 161.98 MHz, 27 °C): $\delta$ = –143.1 (m; $^1J_{FP}$ = 706 Hz; $PF_6$), –64.2 (s) ppm.
**Positive ion ESI-MS** ($CH_3CN$, RT): *m/z* (%) = 3095.2 (0.1) $[\langle Ag_3\{Cp_2Mo_2(CO)_4P_2\}_5\rangle (PF_6)_2]^+$, 2346.8 (1) $[\langle Ag_2\{Cp_2Mo_2(CO)_4P_2\}_4\rangle(PF_6)]^+$, 2100.7 (0.5) $[\langle Ag_3\{Cp_2Mo_2(CO)_4P_2\}_3\rangle (PF_6)_2]^+$, 1847.6 (0.5) $[\langle Ag_2\{Cp_2Mo_2(CO)_4P_2\}_3\rangle(PF_6)]^+$, 1595.0 (10) $[Ag\{Cp_2Mo_2(CO)_4P_2\}_3]^+$, 1100.7 (100) $[Ag\{Cp_2Mo_2(CO)_4P_2\}_2]^+$, 645.8 (60) $[Ag\{Cp_2Mo_2(CO)_4P_2\}(NCCH_3)]^+$, 600.7 (8) $[Ag\{Cp_2Mo_2(CO)_4P_2\}]^+$.
**Negative ion ESI-MS** ($CH_3CN$, RT): *m/z* (%) = 145.0 (100) $PF_6^-$.
**IR** (KBr): $\tilde{\nu}$ = 2926 (w), 1953 (vs; CO), 1915 (vs; CO), 1420 (m), 1108 (w), 1063 (w), 1012 (w), 868 (s), 846 (s), 831 (s), 558 (m), 530 (m), 520 (m), 493 (w), 457 (m), 442 (m) $cm^{-1}$.
**Elemental analysis**: Calculated (%) for $C_{56}H_{40}Ag_2F_{12}Mo_8O_{16}P_{10}$ (2489.90): C 27.01, H 1.62; found: C 27.25, H 1.58.
**Melting point**: 180 °C (decomposition).

## 4.2.3. $[Ag_2\{Cp_2Mo_2(CO)_4(\mu_3,\eta^2:\eta^2:\eta^2\text{-}P_2)\}_2\{Cp_2Mo_2(CO)_4(\mu_4,\eta^2:\eta^2:\eta^1:\eta^1\text{-}P_2)\}_2][(SbF_6)_2]$ (42f)

A mixture of $AgSbF_6$ (40 mg, 0.12 mmol), $[Cp_2Mo_2(CO)_4(\mu,\eta^2\text{-}P_2)]$ **6b** (100 mg, 0.20 mmol) and $CH_3CN$ (30 ml) was stirred in the absence of light at room temperature for 1 h. The reaction vessel was then placed overnight in a freezer (–28°C), during which time **42f** precipitated as a bright orange microcrystalline powder. The solid was filtered, washed with $CH_3CN$ (2 × 3 ml) and dried under vacuum. Crystals of **42f**•4.5$CH_3CN$ suitable for X-ray diffraction analysis were obtained as orange-red prisms by controlled diffusion of a $CH_3CN$ solution of $AgSbF_6$ into a $CH_2Cl_2$ solution of **6b** at room temperature in the dark.

**Yield**: 85 mg (63 %).
**$^{1}$H-NMR** ($CD_3CN$, 400.13 MHz, 27 °C): $\delta$ = 5.34 (s; $C_5H_5$) ppm.
**$^{13}$C{$^{1}$H}-NMR** ($CD_3CN$, 100.63 MHz, 27 °C): $\delta$ = 88.06 (s; $C_5H_5$), 225.08 (s; CO) ppm.
**$^{19}$F-NMR** ($CD_3CN$, 376.47 MHz, 27 °C): $\delta$ = –122.82 (m; $^{1}J_{SbF}$ = 1050 Hz; $^{123}SbF_6^-$), –122.81 (m; $^{1}J_{SbF}$ = 1934 Hz; $^{121}SbF_6^-$) ppm.
**$^{31}$P{$^{1}$H}-NMR** ($CD_3CN$, 161.98 MHz, 27 °C): $\delta$ = –71.3 (s) ppm.
**Positive ion ESI-MS** ($CH_3CN$, RT): *m/z* (%) = 2436.9 (2) $[\langle Ag_2\{Cp_2Mo_2(CO)_4P_2\}_4\rangle(SbF_6)]^+$, 1941.1 (0.5) $[\langle Ag_2\{Cp_2Mo_2(CO)_4P_2\}_3\rangle(SbF_6)]^+$, 1596.7 (4) $[Ag\{Cp_2Mo_2(CO)_4P_2\}_3]^+$, 1100.8 (100) $[Ag\{Cp_2Mo_2(CO)_4P_2\}_2]^+$, 643.9 (30) $[Ag\{Cp_2Mo_2(CO)_4P_2\}(NCCH_3)]^+$, 601.9 (0.5) $[Ag\{Cp_2Mo_2(CO)_4P_2\}]^+$.
**Negative ion ESI-MS** ($CH_3CN$, RT): *m/z* (%) = 234.8 (100) $SbF_6^-$.
**IR** (KBr): $\tilde{\nu}$ = 3121 (w), 1965 (vs; CO), 1946 (vs; CO), 1422 (m), 1109 (w), 1063 (w), 1012 (w), 837 (m), 829 (m), 660 (s), 560 (m), 519 (m), 490 (m), 456 (m) $cm^{-1}$.
**Elemental analysis**: Calculated (%) for $C_{56}H_{40}Ag_2F_{12}Mo_8O_{16}P_8Sb_2$ (2671.45): C 25.18, H 1.51; found: C 25.17, H 1.68.
**Melting point**: 170 °C (decomposition).

## 4.2.4. $[Ag_2\{Cp_2Mo_2(CO)_4(\mu_3,\eta^2:\eta^2:\eta^2\text{-}P_2)\}_2\{Cp_2Mo_2(CO)_4(\mu_4,\eta^2:\eta^2:\eta^1:\eta^1\text{-}P_2)\}_2][\langle Al\{OC(CF_3)_3\}_4\rangle_2]$ (42g)

A mixture of $Ag[Al\{OC(CF_3)_3\}_4]\bullet CH_2Cl_2$ (117 mg, 0.10 mmol), $[Cp_2Mo_2(CO)_4(\mu,\eta^2\text{-}P_2)]$ **6b** (100 mg, 0.20 mmol) and $CH_2Cl_2$ (10 ml) was stirred in the absence of light for 8 h at room temperature. The solution was filtered over diatomaceous earth, which was subsequently washed with $CH_2Cl_2$ (2 × 2 ml). The combined filtrate and washings were stored in a freezer (–28 °C) and crystals of **42g**•$CH_2Cl_2$ appeared within two days in the form of orange-red needles. These crystals were isolated by filtration at –30 °C, washed with pentane (2 × 3 ml) at room temperature and dried under vacuum. The solvent of crystallisation was completely removed during the drying process. Addition of an equal volume of pentane to the mother liquor led to the isolation of a further crop of **42g** as a bright orange powder. Alternatively, **42g**•$CH_2Cl_2$ can be prepared in the form of red prisms by controlled diffusion of a toluene solution of **6b** into a $CH_2Cl_2$ solution of $Ag[Al\{OC(CF_3)_3\}_4]$ at room temperature in the absence of light.

**Yield**: 168 mg (81%).
**$^{1}$H-NMR** ($CD_2Cl_2$, 400.13 MHz, 27 °C): $\delta$ = 5.36 (s; $C_5H_5$) ppm.

**$^{13}C\{^1H\}$-NMR** ($CD_2Cl_2$, 62.90 MHz, 27 °C): $\delta$ = 87.81 (s; $C_5H_5$), 121.66 (q; $^1J_{FC}$ = 291 Hz; $CF_3$), 223.09 (s; CO) ppm.
**$^{27}Al$-NMR** ($CD_2Cl_2$, 78.21 MHz, 27 °C): $\delta$ = 33.77 (s; $[Al\{OC(CF_3)_3\}_4]^-$) ppm.
**$^{19}F$-NMR** ($CD_2Cl_2$, 376.50 MHz, 25 °C): $\delta$ = –75.32 (s; $CF_3$) ppm.
**$^{31}P\{^1H\}$-NMR** ($CD_2Cl_2$, 161.98 MHz, 27 °C): $\delta$ = –96.1 (s) ppm.
**$^{31}P\{^1H\}$-NMR** ($CD_3CN$, 161.98 MHz, 27 °C): $\delta$ = –77.5 (s) ppm.
**$^{31}P\{^1H\}$-NMR** (THF-$d_8$/$CD_2Cl_2$ (4:1), 161.98 MHz, 27 °C): $\delta$ = –82.0 (s) ppm.
**$^{31}P\{^1H\}$-NMR** (THF-$d_8$/$CD_2Cl_2$ (4:1), 161.98 MHz, –110 °C): $\delta$ = –95.2 (b), –77.3 (b) ppm.
**Positive ion ESI-MS** ($CH_2Cl_2$, RT): *m/z* (%) = 1100.8 (100) $[Ag\{Cp_2Mo_2(CO)_4P_2\}_2]^+$.
**Negative ion ESI-MS** ($CH_2Cl_2$, RT): *m/z* (%) = 967.1 (100) $[Al\{OC(CF_3)_3\}_4]^-$.
**Positive ion ESI-MS** ($CH_3CN$, RT): *m/z* (%) = 3164.2 (45) $[\langle Ag_2\{Cp_2Mo_2(CO)_4P_2\}_4\rangle\langle Al\{OC(CF_3)_3\}_4\rangle]^+$, 2670.6 (3.5) $[\langle Ag_2\{Cp_2Mo_2(CO)_4P_2\}_3\rangle\langle Al\{OC(CF_3)_3\}_4\rangle]^+$, 1100.7 (100) $[Ag\{Cp_2Mo_2(CO)_4P_2\}_2]^+$, 643.8 (35) $[Ag\{Cp_2Mo_2(CO)_4P_2\}(NCCH_3)]^+$.
**Negative ion ESI-MS** ($CH_3CN$, RT): *m/z* (%) = 967.1 (100) $[Al\{OC(CF_3)_3\}_4]^-$.
**IR** ($CH_2Cl_2$): $\tilde{\nu}$ = 1987 (s; CO), 1943 (s; CO), 1420 (w), 1352 (m), 1300 (s), 1278 (s), 1264 (s), 1241 (vs), 1224 (vs), 976 (vs) $cm^{-1}$.
**IR** (KBr): $\tilde{\nu}$ = 1985 (vs; CO), 1951 (vs; CO), 1423 (m), 1352 (s), 1302 (vs), 1277 (vs), 1242 (vs), 1219 (vs), 1169 (m), 1066 (w), 1014 (w), 974 (vs), 829 (s), 756 (w), 728 (vs), 561 (m), 537 (m), 520 (m), 488 (m), 444 (s) $cm^{-1}$.
**Molecular mass**: Theoretical for $C_{88}H_{40}Ag_2Al_2F_{72}Mo_8O_{24}P_8$ = 4134.17 g $mol^{-1}$; found (osmometric, $CH_2Cl_2$, 28 °C) = 2257 ± 113 g $mol^{-1}$.
**Elemental analysis**: Calculated (%) for $C_{88}H_{40}Ag_2Al_2F_{72}Mo_8O_{24}P_8$ (4134.17): C 25.57, H 0.98; found: C 25.72, H 1.04.
**Melting point**: 179 °C (decomposition).

## 4.2.5. $[Au_2\{Cp_2Mo_2(CO)_4(\mu_3,\eta^2:\eta^2:\eta^2\text{-}P_2)\}_2\{Cp_2Mo_2(CO)_4(\mu_4,\eta^2:\eta^2:\eta^1:\eta^1\text{-}P_2)\}_2][(PF_6)_2]$ (42h)

A mixture of $[(Ph_3P)AuCl]$ (46 mg, 0.09 mmol), $TlPF_6$ (35 mg, 0.10 mmol), THF (5 ml) and $CH_2Cl_2$ (5 ml) was stirred at room temperature in the dark for 8 h, during which time TlCl was formed as a fine pale grey precipitate. The $[(Ph_3P)Au][PF_6]$ solution was filtered over diatomaceous earth, which was subsequently washed with THF (2 × 2 ml). The combined filtrate and washings were added to a solution

of $[Cp_2Mo_2(CO)_4(\mu,\eta^2\text{-}P_2)]$ **6b** (100 mg, 0.20 mmol) in $CH_2Cl_2$ (10 ml). This new mixture was stirred overnight and then filtered over diatomaceous earth, which was subsequently washed with $CH_2Cl_2$ (2 × 3 ml). The combined filtrate and washings were concentrated under reduced pressure and at room temperature to about a quarter of the original volume and stored at –28 °C. Ruby red plates of **42h**•$2C_4H_8O$•$2CH_2Cl_2$ crystallised within a week and were filtered, washed with pentane (2 × 3 ml) and dried under vacuum. The drying process did not lead to loss of the solvent of crystallisation.

**Yield**: 45 mg (32 %).
**$^1$H-NMR** ($CD_2Cl_2$, 400.13 MHz, 27 °C): $\delta$ = 1.82 (m; THF), 3.68 (m; THF), 5.39 (s; $C_5H_5$) ppm.
**$^{13}$C{$^1$H}-NMR** ($CD_2Cl_2$, 100.63 MHz, 27 °C): $\delta$ = 25.99 (s; THF), 68.18 (s; THF), 88.45 (s; $C_5H_5$), 222.67 (s; CO) ppm.
**$^{19}$F-NMR** ($CD_2Cl_2$, 376.47 MHz, 27 °C): $\delta$ = –73.35 (d; $^1J_{PF}$ = 710 Hz; $PF_6^-$) ppm.
**$^{31}$P{$^1$H}-NMR** ($CD_2Cl_2$, 161.98 MHz, 27 °C): $\delta$ = –143.9 (m; $^1J_{FP}$ = 710 Hz; $PF_6^-$), –52.7 (s) ppm.
**Positive ion ESI-MS** ($CH_2Cl_2$, RT): *m/z* (%) = 1340.5 (100) $[Au\{Cp_2Mo_2(CO)_4P_2\}_2(THF)_2]^+$, 1190.8 (98) $[Au\{Cp_2Mo_2(CO)_4P_2\}_2]^+$, 1161.7 (15) $[Au\{Cp_2Mo_2(CO)_{3.5}P_2\}_2]^+$, 1134.7 (94) $[Au\{Cp_2Mo_2(CO)_3P_2\}_2]^+$, 1105.7 (100) $[\langle Au_2\{Cp_2Mo_2(CO)_4P_2\}\{THF\}\rangle(PF_6)]^+$, 1077.8 (6) $[\langle Au_2\{Cp_2Mo_2(CO)_3P_2\}\{THF\}\rangle(PF_6)]^+$, 1048.6 (4) $[\langle Au_2\{Cp_2Mo_2(CO)_2P_2\}(THF)\rangle(PF_6)]^+$.
**Negative ion ESI-MS** ($CH_2Cl_2$, RT): *m/z* (%) = 144.9 (100) $PF_6^-$.
**IR** (KBr): $\tilde{\nu}$ = 1975 (vs; CO), 1942 (vs; CO), 1637 (m), 1559 (m), 1420 (m), 1357 (w), 1262 (w), 1063 (w), 1012 (w), 845 (s), 830 (s), 668 (m), 558 (s), 518 (m), 488 (m), 456 (m) $cm^{-1}$.
**Elemental analysis**: Calculated (%) for $C_{66}H_{60}Au_2Cl_4F_{12}Mo_8O_{18}P_{10}$ (2982.17): C 26.58, H 2.03; found: C 26.74, H 1.98.
**Melting point**: 166 °C (decomposition).

## 4.2.6. $[Ag_2\{Cp_2Mo_2(CO)_4(\mu_4,\eta^2\text{:}\eta^2\text{:}\eta^1\text{:}\eta^1\text{-}P_2)\}_2(\eta^2\text{-}NO_2)_2]$ (49)

A mixture of $AgNO_2$ (35 mg, 0.23 mmol), $[Cp_2Mo_2(CO)_4(\mu,\eta^2\text{-}P_2)]$ **6b** (100 mg, 0.20 mmol) and $CH_3CN$ (30 ml) was stirred in the absence of light at room temperature for 1 h, during which time **49** was formed as a microcrystalline dark brown powder. The solid was filtered, washed with $CH_3CN$ (2 × 3 ml) and dried under vacuum.

Crystals of **49** suitable for X-ray diffraction analysis were obtained as dark brown plates by controlled diffusion of a $CH_3CN$ solution of $AgNO_2$ into a $CH_2Cl_2$ solution of **6b** at room temperature in the dark.

**Yield**: 121 mg (92 %).
**Positive ion ESI-MS** ($CH_3CN$, RT): *m/z* (%) = 2249.8 (8) $[\langle Ag_2\{Cp_2Mo_2(CO)_4P_2\}_4\rangle(NO_2)]^+$, 1904.7 (20) $[\langle Ag_3\{Cp_2Mo_2(CO)_4P_2\}_3\rangle(NO_2)_2]^+$, 1748.9 (38) $[\langle Ag_2\{Cp_2Mo_2(CO)_4P_2\}_3\rangle (NO_2)]^+$, 1596.8 (11) $[Ag\{Cp_2Mo_2(CO)_4P_2\}_3]^+$, 1255.8 (5) $[\langle Ag_2\{Cp_2Mo_2(CO)_4P_2\}_2\rangle(NO_2)]^+$, 1100.7 (100) $[Ag\{Cp_2Mo_2(CO)_4P_2\}_2]^+$, 643.8 (40) $[Ag\{Cp_2Mo_2(CO)_4P_2\}(NCCH_3)]^+$, 599.9 (1) $[Ag\{Cp_2Mo_2(CO)_4P_2\}]^+$.
**IR** (KBr): $\tilde{\nu}$ = 3115 (w), 1997 (vs; CO), 1954 (vs; CO), 1919 (vs; CO), 1419 (m), 1264 (m), 1241 (m), 1103 (w), 1061 (w), 1010 (w), 867 (w), 828 (m), 669 (w), 559 (w), 514 (w), 483 (w), 455 (m) $cm^{-1}$.
**Elemental analysis**: Calculated (%) for $C_{28}H_{20}Ag_2Mo_4N_2O_{12}P_4$ (1299.86): C 25.87, H 1.55, N 2.16; found: C 25.41, H 1.83, N 2.07.
**Melting point**: 103 °C (decomposition).

## 4.2.7. [Au{$Cp_2Mo_2(CO)_4(\mu_3,\eta^2:\eta^2:\eta^1$-$P_2$)}Cl] (50)

A room temperature solution of $[Cp_2Mo_2(CO)_4(\mu,\eta^2\text{-}P_2)]$ **6b** (100 mg, 0.20 mmol) in toluene (10 ml) was layered over a frozen solution of [(OC)AuCl] (52 mg, 0.20 mmol) in toluene (10 ml) submerged in a Dewar flask containing liquid nitrogen. The vessel was left in the Dewar flask, connected to a mercury valve, and allowed to gradually reach room temperature in the absence of light. Crystals of **50** were formed within two weeks as red needles, which were filtered, washed with pentane (2 × 3 ml) and dried under vacuum. Alternatively, **50** can be prepared as an orange powder by mixing [(THT)AuCl] (THT = $C_4H_8S$) and **6b** in $CH_2Cl_2$ at room temperature.

**Yield**: 130 mg (89 %).
**$^1$H-NMR** (THF-$d_8$, 400.13 MHz, 27 °C): $\delta$ = 5.55 (s; $C_5H_5$) ppm.
**$^{31}$P{$^1$H}-NMR** (THF-$d_8$, 161.98 MHz, 27 °C): $\delta$ = –77.2 (b) ppm.
**Positive ion ESI-MS** ($CH_3CN/CH_2Cl_2$, RT): *m/z* (%) = 1915.0 (2.5) $[Au_2Cl\{Cp_2Mo_2(CO)_4\ P_2\}_3]^+$, 1425.0 (1.5) $[Au_2Cl\{Cp_2Mo_2(CO)_4P_2\}_2]^+$, 1189.0 (100) $[Au\{Cp_2Mo_2(CO)_4P_2\}_2]^+$.
**Negative ion ESI-MS** ($CH_3CN/CH_2Cl_2$, RT): *m/z* (%) = 996.9 (2.5) $[Au_2Cl_3\{Cp_2Mo_2(CO)_4\ P_2\}]^-$, 266.8 (100) $[AuCl_2]^-$.
**IR** (KBr): $\tilde{\nu}$ = 3098 (w), 2006 (vs; CO), 1984 (vs; CO), 1946 (vs; CO), 1924 (vs; CO), 1630 (w), 1418 (m), 1356 (w), 1263 (w), 1105 (w),

1060 (w), 928 (w), 854 (w), 839 (m), 829 (m), 818 (m), 735 (w), 605 (w), 561 (m), 519 (s), 485 (m), 456 (s), 447 (s) $cm^{-1}$.
**Elemental analysis**: Calculated (%) for $C_{14}H_{10}AuClMo_2O_4P_2$ (728.48): C 23.08, H 1.38; found: C 22.65, H 1.43.
**Melting point**: 160 °C (decomposition).

## 4.2.8. [Cp*Rh{$Cp_2Mo_2(CO)_4(\mu_3,\eta^2:\eta^2:\eta^1$-$P_2$)}$_2$ ($NCCH_3$)][($SbF_6$)$_2$] (53a)

A mixture of [Cp*Rh($NCCH_3$)$_3$][($SbF_6$)$_2$] (119 mg, 0.14 mmol), [$Cp_2Mo_2(CO)_4(\mu,\eta^2$-$P_2$)] **6b** (106 mg, 0.21 mmol), $CH_3CN$ (5 ml) and $CH_2Cl_2$ (20 ml) was stirred at room temperature for 1 h. The resulting dark red-brown solution was filtered and concentrated to about half the original volume (~ 10 ml) under reduced pressure at room temperature. After addition of hexane (3 ml) to the concentrated solution, the vessel was stored in a freezer (–28 °C) and red-brown needles of **53a** appeared within four days. These crystals were filtered at –30 °C, washed with pentane (2 × 3 ml) and dried under vacuum.

**Yield**: 53 mg (28 %).
**$^1$H-NMR** ($CD_3CN$, 400.13 MHz, 27 °C): $\delta$ = 1.75-1.76 ($CH_3$; Cp*), 1.97 (s; $CH_3CN$), 5.31 (s; $C_5H_5$; **6b**), 5.53 (s; $C_5H_5$), 5.58 (s; $C_5H_5$) ppm.
**$^{13}$C{$^1$H}-NMR** ($CD_3CN$, 100.63 MHz, 27 °C): $\delta$ = 9.47 (s; $CH_3$; Cp*), 86.43 (s; $C_5H_5$), 87.85 (s; $C_5H_5$), 88.75 (s; $C_5H_5$; **6b**), 104.03 (s; Cp*), 104.11 (s; Cp*), 222.72 (s; CO; **6b**), 225.93 (s; CO) ppm.
**$^{19}$F-NMR** ($CD_3CN$, 376.47 MHz, 27 °C): $\delta$ = –122.68 (m; $^1J_{SbF}$ = 1050 Hz; $^{123}SbF_6^-$), –122.67 (m; $^1J_{SbF}$ = 1934 Hz; $^{121}SbF_6^-$) ppm.
**$^{31}$P{$^1$H}-NMR** ($CD_3CN$, 161.98 MHz, 27 °C): $\delta$ = –126.3 (b), –41.3 (s; **6b**), 7.3 (b) ppm.
**Positive ion ESI-MS** ($CH_3CN$, RT): *m/z* (%) = 1012.0 (0.5) [⟨Cp*Rh{$Cp_2Mo_2(CO)_4P_2$} ($NCCH_3$)⟩($SbF_6$)]$^+$, 968.8 (1) [⟨Cp*Rh{$Cp_2Mo_2(CO)_4P_2$}⟩($SbF_6$)]$^+$, 768.9 (3) [Cp*Rh{$Cp_2Mo_2(CO)_4P_2$}($NCCH_3$)]$^+$, 752.9 (6) [Cp*Rh{$Cp_2Mo_2(CO)_3P_2$}($NCCH_3$)]$^+$, 734.0 (7) [Cp*Rh{$Cp_2Mo_2(CO)_4P_2$}]$^+$, 703.9 (2) [Cp*Rh{$Cp_2Mo_2(CO)_3P_2$}]$^+$, 677.8 (1) [Cp*Rh{$Cp_2Mo_2(CO)_2P_2$}]$^+$, 649.9 (2) [Cp*Rh{$Cp_2Mo_2(CO)P_2$}]$^+$, 408.1 (36) [Cp*Rh{$Cp_2Mo_2(CO)_4P_2$} ($NCCH_3$)$_2$]$^{2+}$, 388.1 (7) [Cp*Rh{$Cp_2Mo_2(CO)_4P_2$}($NCCH_3$)]$^{2+}$, 380.1 (27) [Cp*Rh{$Cp_2Mo_2(CO)_2P_2$}($NCCH_3$)$_2$]$^{2+}$, 367.0 (100) [Cp*Rh{$Cp_2Mo_2(CO)_4P_2$}]$^{2+}$, 352.1 (13) [Cp*Rh{$Cp_2Mo_2(CO)_3P_2$}]$^{2+}$.
**Negative ion ESI-MS** ($CH_3CN$, RT): *m/z* (%) = 234.8 (100) $SbF_6^-$.

**IR** (KBr): $\tilde{\nu}$ = 2961 (w), 1980 (vs; CO), 1932 (vs; CO), 1636 (w), 1473 (w), 1424 (m), 1375 (w), 1362 (w), 1261 (w), 1161 (w), 1063 (w), 1015 (w), 873 (w), 838 (m), 826 (m), 660 (s), 560 (w), 519 (m), 489 (w), 455 (m) $cm^{-1}$.
**Elemental analysis**: Calculated (%) for $C_{40}H_{38}F_{12}Mo_4NO_8P_4RhSb_2$ (1742.78): C 27.57, H 2.20, N 0.80; found: C 28.14, H 2.74, N 0.68.
**Melting point**: 210 °C (decomposition).

## 4.2.9. [Cp*Ir{$Cp_2Mo_2(CO)_4(\mu_3,\eta^2:\eta^2:\eta^1$-$P_2)$}$_2$ ($NCCH_3$)][($SbF_6$)$_2$] (53b)

A mixture of [Cp*Ir($NCCH_3$)$_3$][($SbF_6$)$_2$] (220 mg, 0.24 mmol), [$Cp_2Mo_2(CO)_4(\mu,\eta^2$-$P_2)$] **6b** (220 mg, 0.44 mmol), $CH_3CN$ (10 ml) and $CH_2Cl_2$ (20 ml) was stirred at room temperature for 1 h. The resulting ruby-red solution was filtered and concentrated to about half the original volume (~ 15 ml) under reduced pressure at room temperature. After addition of hexane (5 ml) to the concentrated solution, the vessel was stored in a freezer (–28 °C) and shimmering ruby-red needles of **53b** appeared within three days. These crystals were filtered at –30 °C, washed with pentane (2 × 3 ml) and dried under vacuum. A further crop of **53b** was obtained as a wine-red powder by addition of an equal volume of $Et_2O$ to the mother liquor.

**Yield**: 340 mg (84 %).
**$^1$H-NMR** ($CD_3CN$, 400.13 MHz, 27 °C): $\delta$ = 1.79 ($CH_3$; Cp*), 1.80 ($CH_3$; Cp*), 1.84 ($CH_3$; Cp*), 1.97 (s; $CH_3CN$), 5.31 (s; $C_5H_5$; **6b**), 5.54 (s; $C_5H_5$), 5.58 (b; $C_5H_5$) ppm.
**$^{13}$C{$^1$H}-NMR** ($CD_3CN$, 100.63 MHz, 27 °C): $\delta$ = 9.77 (s; $CH_3$; Cp*), 10.44 (s; $CH_3$; Cp*), 87.49 (s; $C_5H_5$), 88.77 (s; $C_5H_5$; **6b**), 89.88 (s; $C_5H_5$), 98.51 (s; Cp*), 101.93 (s; Cp*), 222.72 (s; CO; **6b**), 227.01 (s; CO) ppm.
**$^{19}$F-NMR** ($CD_3CN$, 376.47 MHz, 27 °C): $\delta$ = –122.69 (m; $^1J_{SbF}$ = 1049 Hz; $^{123}SbF_6^-$), –122.68 (m; $^1J_{SbF}$ = 1934 Hz; $^{121}SbF_6^-$) ppm.
**$^{31}$P{$^1$H}-NMR** ($CD_3CN$, 161.98 MHz, 27 °C): $\delta$ = –147.0 (d; $^1J_{PP}$ = 498 Hz), –108.0 (d; $^1J_{PP}$ = 495 Hz), –68.61 (b), –41.2 (s; **6b**), –27.9 (d; $^1J_{PP}$ = 495 Hz) ppm.
**Positive ion ESI-MS** ($CH_3CN$, RT): *m/z* (%) = 1555.2 (0.5) [⟨Cp*Ir{$Cp_2Mo_2(CO)_4P_2$}$_2$ {$NCCH_3$}⟩($SbF_6$)]$^+$, 1100.1 (0.5) [⟨Cp*Ir{$Cp_2Mo_2(CO)_4P_2$}($NCCH_3$)⟩($SbF_6$)]$^+$, 1059.0 (1) [⟨Cp*Ir{$Cp_2Mo_2(CO)_4P_2$}⟩($SbF_6$)]$^+$, 843.1 (13) [Cp*Ir{$Cp_2Mo_2(CO)_3P_2$}($NCCH_3$)]$^+$, 794.1 (21) [Cp*Ir{$Cp_2Mo_2(CO)_3P_2$}]$^+$, 766.0 (10) [Cp*Ir{$Cp_2Mo_2(CO)_2P_2$}]$^+$,

740.1 (43) $[Cp^*Ir\{Cp_2Mo_2(CO)P_2\}]^+$, 712.0 (4) $[Cp^*Ir\{Cp_2Mo_2P_2\}]^+$, 680.7 (0.5) $[Cp^*Ir\{Cp_2Mo_2(CO)_4\ P_2\}_2(NCCH_3)]^{2+}$, 660.6 (2) $[Cp^*Ir\{Cp_2Mo_2(CO)_4P_2\}_2]^{2+}$, 646.1 (6) $[Cp^*Ir\{Cp_2Mo_2(CO)_{3.5}\ P_2\}_2]^{2+}$, 618.6 (8) $[Cp^*Ir\{Cp_2Mo_2(CO)_{2.5}P_2\}_2]^{2+}$, 606.2 (2) $[Cp^*Ir\{Cp_2Mo_2(CO)_2P_2\}_2]^{2+}$, 590.1 (14) $[Cp^*Ir\{Cp_2Mo_2(CO)_{1.5}P_2\}_2]^{2+}$, 575.6 (10) $[Cp^*Ir\{Cp_2Mo_2(CO)P_2\}_2]^{2+}$, 561.1 (9) $[Cp^*Ir\{Cp_2Mo_2(CO)_{0.5}P_2\}_2]^{2+}$, 546.7 (3) $[Cp^*Ir\{Cp_2Mo_2P_2\}_2]^{2+}$, 425.1 (63) $[Cp^*Ir\{Cp_2Mo_2\ (CO)_2P_2\}(NCCH_3)_2]^{2+}$, 412.1 (43) $[Cp^*Ir\{Cp_2Mo_2(CO)_4P_2\}]^{2+}$, 397.1 (100) $[Cp^*Ir\{Cp_2Mo_2\ (CO)_3P_2\}]^{2+}$.
**Negative ion ESI-MS** ($CH_3CN$, RT): *m/z* (%) = 234.8 (100) $SbF_6^-$.
**IR** (KBr): $\tilde{\nu}$ = 2960 (w), 2253 (w; CN), 1980 (vs; CO), 1931 (vs; CO), 1654 (w), 1648 (w), 1637 (w), 1560 (w), 1508 (w), 1474 (w), 1458 (w), 1421 (m), 1378 (w), 1363 (w), 1160 (w), 1110 (w), 1064 (w), 1015 (w), 838 (m), 827 (m), 660 (s), 560 (m), 520 (m), 490 (m), 455 (m) $cm^{-1}$.
**Elemental analysis**: Calculated (%) for $C_{40}H_{38}F_{12}IrMo_4NO_8P_4Sb_2$ (1832.08): C 26.22, H 2.09, N 0.76; found: C 26.22, H 2.31, N 0.96.
**Melting point**: 141 °C (decomposition).

### 4.2.10. $[(Cp''Rh)_2\{Cp_2Mo_2(CO)_4(\mu_4,\eta^2:\eta^2:\eta^1:\eta^1\text{-}P_2)\}(\mu\text{-}Cl)_2][(BF_4)_2]$ (54)

A solution of $[Cp_2Mo_2(CO)_4(\mu,\eta^2\text{-}P_2)]$ **6b** (64 mg, 0.13 mmol) in THF (5 ml) was carefully layered over a solution of $[Cp''Rh(NCCH_3)_2Cl][BF_4]$ (50 mg, 0.12 mmol) in $CH_2Cl_2$ (5 ml) and left at room temperature in the dark. A small amount of **54**•$1.5CH_2Cl_2$ was deposited as dark brown needles within a month.

### 4.2.11. $[(C_{14}H_8)Pt_2\{Cp_2Mo_2(CO)_4(\mu_3,\eta^2:\eta^2:\eta^1\text{-}P_2)\}_2(PEt_3)_4][(PF_6)_2]$ (57)

A mixture of $[(C_{14}H_8)Pt_2(PEt_3)_4(\eta^1\text{-}NO_3)_2]$ **55** (117 mg, 0.10 mmol), $[Cp_2Mo_2(CO)_4(\mu,\eta^2\text{-}P_2)]$ **6b** (100 mg, 0.20 mmol), $KPF_6$ (100 mg, 0.54 mmol), acetone (5 ml) and water (5 ml) was sonicated at room temperature for 6 h. The resulting solid was filtered and extracted with $CH_2Cl_2$ (3 × 4 ml). Addition of pentane (25 ml) to the $CH_2Cl_2$ solution led to the precipitation of **57** as a bright orange powder, which was filtered, washed with pentane (2 × 3 ml) and dried under vacuum. A further crop of **57** was obtained by placing the $CH_2Cl_2$/pentane mother liquor in a freezer (–28 °C). Crystals of **57** suitable for X-ray diffraction analysis were grown by controlled diffusion of hexane into $CH_2Cl_2$ solutions of **57**.

**Yield**: 172 mg (74 %).
**$^{1}$H-NMR** ($CD_2Cl_2$, 400.13 MHz, 27 °C): $\delta$ = 0.78-1.21 (b; $CH_3$), 1.43-1.89 (b; $CH_2$), 5.31-5.56 ($C_5H_5$), 7.02-9.09 ([($\mu$,$\eta^2$-$C_{14}H_8$)$Pt_2$]) ppm.
**$^{13}$C{$^{1}$H}-NMR** ($CD_2Cl_2$, 100.63 MHz, 27 °C): $\delta$ = 7.76-8.96 ($CH_3$), 14.28-17.59 ($CH_2$), 86.79-89.21 ($C_5H_5$), 124.86 (b; [($\mu$,$\eta^2$-$C_{14}H_8$)$Pt_2$]), 226.40 (s; CO) ppm.
**$^{19}$F-NMR** ($CD_2Cl_2$, 376.47 MHz, 27 °C): $\delta$ = –72.83 (d; $^{1}J_{PF}$ = 711 Hz; $PF_6^-$) ppm.
**$^{31}$P{$^{1}$H}-NMR** ($CD_2Cl_2$, 161.98 MHz, 27 °C): $\delta$ = –143.8 (m; $^{1}J_{FP}$ = 711 Hz; $PF_6^-$), –100.6 (d; $^{1}J_{PP}$ = 747 Hz), –43.1 (s; **6b**), –1.0-20.8 ([$Pt(PEt_3)_2$]) ppm.
**Positive ion ESI-MS** ($CH_3CN/CH_2Cl_2$, RT): *m/z* (%) = 1265.7 (11) [{($C_{14}H_8$)$Pt_2$($P_4Et_{12}$) ($NCCH_3$)$_2$}($PF_6$)]$^+$, 1224.6 (2) [{($C_{14}H_8$)$Pt_2$($P_4Et_{12}$)($NCCH_3$)}($PF_6$)]$^+$, 1169.7 (1) [{($C_{14}H_8$) $Pt_2$($P_4Et_{10}$)($NCCH_3$)}($PF_6$)]$^+$, 1155.6 (14) [{($C_{14}H_8$)$Pt_2$($P_4Et_{11}$)}($PF_6$)]$^+$, 1138.6 (5) [{($C_{14}H_8$) $Pt_2$($P_4Et_9$)($NCCH_3$)}($PF_6$)]$^+$, 1126.5 (1.5) [{($C_{14}H_8$)$Pt_2$($P_4Et_{10}$)}($PF_6$)]$^+$, 1114.4 (1.5) [{($C_{14}H_8$)$Pt_2$($P_4Et_8$)($NCCH_3$)}($PF_6$)]$^+$, 1096.7 (0.5) [{($C_{14}H_8$)$Pt_2$($P_4Et_9$)}($PF_6$)]$^+$, 560.4 (100) [($C_{14}H_8$)$Pt_2$($P_4Et_{12}$)($NCCH_3$)$_2$]$^{2+}$.
**Negative ion ESI-MS** ($CH_3CN/CH_2Cl_2$, RT): *m/z* (%) = 145.0 (100) $PF_6^-$.
**IR** (KBr): $\tilde{\nu}$ = 3127 (w), 3046 (w), 2968 (w), 2938 (w), 2882 (w), 1971 (vs; CO), 1923 (vs; CO), 1636 (w), 1518 (w), 1458 (m), 1420 (m), 1384 (w), 1359 (w), 1279 (w), 1261 (w), 1108 (w), 1036 (m), 1014 (w), 845 (s), 756 (m), 711 (w), 668 (w), 640 (w), 558 (m), 525 (w), 492 (w), 456 (m) cm$^{-1}$.
**Elemental analysis**: Calculated (%) for $C_{66}H_{88}F_{12}Mo_4O_8P_{10}Pt_2$ (2321.06): C 34.15, H 3.82; found: C 34.02, H 3.84.
**Melting point**: 174 °C (decomposition).

## 4.2.12. [($C_{14}H_8Cl$)Pt{$Cp_2Mo_2(CO)_4$($\mu_3$,$\eta^2$:$\eta^2$:$\eta^1$-$P_2$)} ($PEt_3$)$_2$][$PF_6$] (59)

A mixture of [($C_{14}H_8Cl$)Pt($PEt_3$)$_2$($\eta^1$-$NO_3$)] **58** (25 mg, 0.04 mmol), [$Cp_2Mo_2(CO)_4$($\mu$,$\eta^2$-$P_2$)] **6b** (18 mg, 0.04 mmol), $KPF_6$ (50 mg, 0.27 mmol), acetone (3 ml) and water (3 ml) was sonicated at room temperature for 6 h. The resulting solid was filtered and extracted with $CH_2Cl_2$ (3 × 3 ml). The $CH_2Cl_2$ solution was then carefully layered with hexane (15 ml) and left at room temperature. A small amount of **59**•$CH_2Cl_2$ crystallised in the form of bright red needles within a week.

## 4.3. Synthesis of the Complexes Based on $[Cp_2Cr_2(CO)_4(\mu,\eta^2\text{-}P_2)]$

### 4.3.1. $[Cu(\mu\text{-}Cl)\{Cp_2Cr_2(CO)_4(\mu_4,\eta^2\text{:}\eta^2\text{:}\eta^1\text{:}\eta^1\text{-}P_2)\}]_n$ (66a)

A solution of CuCl (49 mg, 0.49 mmol) in $CH_3CN$ (10 ml) was carefully layered over a solution of $[Cp_2Cr_2(CO)_4(\mu,\eta^2\text{-}P_2)]$ **6a** (100 mg, 0.25 mmol) in $CH_2Cl_2$ (10 ml) at room temperature. The vessel was left at room temperature in the dark and insoluble moss green needles of **66a** were deposited within a month. These were filtered, washed with $CH_3CN$ (2 × 3 ml) and pentane (2 × 3 ml), in that order, and dried under vacuum.

**Yield**: 100 mg (80 %).
**$^{65}$Cu MAS-NMR** (106.01 MHz, RT): $\delta$ = 500.0 (b), 593.0 (b) ppm.
**$^{31}$P MAS-NMR** (162.01 MHz, RT): $\delta$ = –97.0 (m; $^1J_{CuP}$ = 1080 Hz (simulated); $^1J_{PP}$ = 543 Hz; $^2J_{PP}$ = 240 Hz) 83.0 (m; $^1J_{CuP}$ = 1110 Hz (simulated); $^1J_{PP}$ = 505 Hz; $^2J_{PP}$ = 220 Hz) ppm.
**Positive ion ESI-MS** ($CH_3CN$, RT): *m/z* (%) = 1076.7 (3) $[Cu_3Cl_2\{Cp_2Cr_2(CO)_4P_2\}_2]^+$, 1022.6 (2) $[Cu_3Cl_2\{Cp_2Cr_2(CO)_3P_2\}_2]^+$, 978.7 (16) $[Cu_2Cl\{Cp_2Cr_2(CO)_4P_2\}_2]^+$, 922.7 (8) $[Cu_2Cl\{Cp_2Cr_2(CO)_3P_2\}_2]^+$, 878.8 (33) $[Cu\{Cp_2Cr_2(CO)_4P_2\}_2]^+$, 864.7 (2) $[Cu_2Cl\{Cp_2Cr_2\ (CO)_2P_2\}_2]^+$, 822.8 (43) $[Cu\{Cp_2Cr_2(CO)_3P_2\}_2]^+$, 794.8 (1) $[Cu\{Cp_2Cr_2(CO)_{2.5}P_2\}_2]^+$, 766.8 (22) $[Cu\{Cp_2Cr_2(CO)_2P_2\}_2]^+$, 712.7 (1) $[Cu\{Cp_2Cr_2(CO)P_2\}_2]^+$, 751.8 (1) $[Cu_2Cl\{Cp_2Cr_2\ (CO)P_2\}_2]^+$, 695.9 (1) $[Cu_2Cl\{Cp_2Cr_2P_2\}_2]^+$, 654.7 (1) $[Cu\{Cp_2Cr_2P_2\}_2]^+$, 511.8 (60) $[Cu\ \{Cp_2Cr_2(CO)_4P_2\}(NCCH_3)]^+$, 496.9 (2) $[Cu\{Cp_2Cr_2(CO)_2P_2\}(NCCH_3)_2]^+$, 471.6 (1) $[Cu\{Cp_2Cr_2(CO)_4P_2\}]^+$, 455.8 (100) $[Cu\{Cp_2Cr_2(CO)_2P_2\}(NCCH_3)]^+$, 442.9 (9) $[Cu\{Cp_2Cr_2\ P_2\}(NCCH_3)_2]^+$ or $[Cu\{Cp_2Cr_2(CO)_3P_2\}]^+$, 427.8 (17) $[Cu\{Cp_2Cr_2(CO)P_2\}(NCCH_3)]^+$.
**IR** (KBr): $\tilde{\nu}$ = 3118 (w), 1993 (vs; CO), 1951 (vs; CO), 1914 (vs; CO), 1880 (vs; CO), 1851 (s; CO), 1424 (m), 1363 (w), 1264 (w), 1116 (w), 1062 (m), 1013 (m), 957 (w), 932 (w), 886 (m), 867 (m), 854 (s), 846 (s), 669 (w), 621 (m), 603 (m), 596 (m), 560 (s), 551 (s), 523 (m), 506 (m), 489 (m), 479 (m), 446 (w), 427 (w) $cm^{-1}$.
**Elemental analysis**: Calculated (%) for $C_{14}H_{10}ClCr_2CuO_4P_2$ (507.17): C 33.16, H 1.99; found: C 32.83, H 1.99.
**Melting point**: 167 °C (decomposition).

## 4.3.2. $[Cu(\mu\text{-Br})\{Cp_2Cr_2(CO)_4(\mu_4,\eta^2{:}\eta^2{:}\eta^1{:}\eta^1\text{-}P_2)\}]_n$ (66b)

A solution of CuBr (70 mg, 0.49 mmol) in $CH_3CN$ (10 ml) was carefully layered over a solution of $[Cp_2Cr_2(CO)_4(\mu,\eta^2\text{-}P_2)]$ **6a** (100 mg, 0.25 mmol) in $CH_2Cl_2$ (10 ml) at room temperature. The vessel was left at room temperature in the dark and insoluble moss green needles of **66b** were deposited within a month. These were filtered, washed with $CH_3CN$ (2 × 3 ml) and pentane (2 × 3 ml), in that order, and dried under vacuum.

**Yield**: 120 mg (89 %).
**$^{65}$Cu MAS-NMR** (106.01 MHz, RT): $\delta$ = 514.0 (b) ppm.
**$^{31}$P MAS-NMR** (162.01 MHz, RT): $\delta$ = –100.0 (m), 81.0 (m) ppm.
**Positive ion ESI-MS** ($CH_3CN$, RT): *m/z* (%) = 1166.6 (9) $[Cu_3Br_2\{Cp_2Cr_2(CO)_4P_2\}_2]^+$, 1110.5 (4) $[Cu_3Br_2\{Cp_2Cr_2(CO)_3P_2\}_2]^+$, 1022.7 (18) $[Cu_2Br\{Cp_2Cr_2(CO)_4P_2\}_2]^+$, 1007.6 (2) $[Cu_2Br\{Cp_2Cr_2(CO)_3P_2\}_2(NCCH_3)]^+$, 966.6 (11) $[Cu_2Br\{Cp_2Cr_2(CO)_3P_2\}_2]^+$, 910.6 (1) $[Cu_2Br\{Cp_2Cr_2(CO)_2P_2\}_2]^+$, 878.8 (40) $[Cu\{Cp_2Cr_2(CO)_4P_2\}_2]^+$, 822.8 (17) $[Cu\{Cp_2Cr_2(CO)_3P_2\}_2]^+$, 799.5 (1) $[Cu_2Br\{Cp_2Cr_2\ (CO)P_2\}_2]^+$, 766.8 (6) $[Cu\{Cp_2Cr_2(CO)_2P_2\}_2]^+$, 743.6 (1) $[Cu_2Br\{Cp_2Cr_2P_2\}_2]^+$, 655.7 (2) $[Cu\{Cp_2Cr_2P_2\}_2]^+$, 599.8 (5) $[Cu_2Br\{Cp_2Cr_2(CO)_2P_2\}\ (NCCH_3)]^+$, 511.8 (100) $[Cu\{Cp_2Cr_2(CO)_4P_2\}(NCCH_3)]^+$, 496.8 (8) $[Cu\{Cp_2Cr_2(CO)_2P_2\}\ (NCCH_3)_2]^+$, 468.9 (2) $[Cu\{Cp_2Cr_2(CO)_4P_2\}]^+$, 455.8 (45) $[Cu\{Cp_2Cr_2(CO)_2P_2\}(NCCH_3)]^+$, 440.8 (9) $[Cu\{Cp_2Cr_2P_2\}(NCCH_3)_2]^+$ or $[Cu\{Cp_2Cr_2(CO)_3P_2\}]^+$, 427.8 (5) $[Cu\{Cp_2Cr_2(CO)\ P_2\}(NCCH_3)]^+$.
**IR** (KBr): $\tilde{\nu}$ = 3113 (w), 1995 (vs; CO), 1951 (vs; CO), 1915 (vs; CO), 1881 (vs; CO), 1851 (s; CO), 1424 (m), 1363 (w), 1265 (w), 1116 (w), 1060 (w), 1005 (w), 956 (w), 930 (w), 886 (w), 867 (m), 852 (s), 669 (w), 620 (m), 602 (m), 596 (m), 559 (s), 550 (s), 521 (m), 504 (m), 488 (m), 478 (s), 445 (w) $cm^{-1}$.
**Elemental analysis**: Calculated (%) for $C_{14}H_{10}BrCr_2CuO_4P_2$ (551.62): C 30.48, H 1.83; found: C 30.13, H 1.81.
**Melting point**: 202 °C (decomposition).

## 4.3.3. $[Cu(\mu\text{-I})\{Cp_2Cr_2(CO)_4(\mu_4,\eta^2{:}\eta^2{:}\eta^1{:}\eta^1\text{-}P_2)\}]_n$ (66c)

A solution of CuI (93 mg, 0.49 mmol) in $CH_3CN$ (10 ml) was carefully layered over a solution of $[Cp_2Cr_2(CO)_4(\mu,\eta^2\text{-}P_2)]$ **6a** (100 mg, 0.25 mmol) in $CH_2Cl_2$ (10 ml) at room temperature. The vessel was left at room temperature in the dark and insoluble moss green

needles of **66c**•n$CH_3CN$ were deposited within a month. These were filtered, washed with $CH_3CN$ (2 × 3 ml) and pentane (2 × 3 ml), in that order, and dried under vacuum at room temperature. The solvent of crystallisation was not lost during the drying process.

**Yield**: 140 mg (89 %).
**$^{65}$Cu MAS-NMR** (106.01 MHz, RT): $\delta$ = 429.0 (b) ppm.
**$^{31}$P MAS-NMR** (162.01 MHz, RT): $\delta$ = 48.0 (b) ppm.
**Positive ion ESI-MS** ($CH_3CN$, RT): *m/z* (%) = 1260.7 (12) $[Cu_3I_2\{Cp_2Cr_2(CO)_4P_2\}_2]^+$, 1204.6 (7) $[Cu_3I_2\{Cp_2Cr_2(CO)_3P_2\}_2]^+$, 1070.6 (10) $[Cu_2I\{Cp_2Cr_2(CO)_4P_2\}_2]^+$, 1055.6 (1) $[Cu_2I\{Cp_2Cr_2(CO)_3P_2\}_2(NCCH_3)]^+$, 1014.6 (11) $[Cu_2I\{Cp_2Cr_2(CO)_3P_2\}_2]^+$, 958.6 (2) $[Cu_2I\{Cp_2Cr_2(CO)_2P_2\}_2]^+$, 878.8 (35) $[Cu\{Cp_2Cr_2(CO)_4P_2\}_2]^+$, 822.8 (17) $[Cu\{Cp_2Cr_2(CO)_3P_2\}_2]^+$, 766.7 (5) $[Cu\{Cp_2Cr_2(CO)_2P_2\}_2]^+$, 647.7 (4) $[Cu_2I\{Cp_2Cr_2(CO)_2P_2\}(NCCH_3)]^+$, 511.8 (100) $[Cu\{Cp_2Cr_2(CO)_4P_2\}(NCCH_3)]^+$, 496.8 (8) $[Cu\{Cp_2Cr_2(CO)_2P_2\}(NCCH_3)_2]^+$, 468.9 (2) $[Cu\{Cp_2Cr_2(CO)_4P_2\}]^+$, 455.8 (42) $[Cu\{Cp_2Cr_2(CO)_2P_2\}(NCCH_3)]^+$, 440.8 (8) $[Cu\{Cp_2Cr_2P_2\}(NCCH_3)_2]^+$ or $[Cu\{Cp_2Cr_2(CO)_3P_2\}]^+$, 427.8 (6) $[Cu\{Cp_2Cr_2(CO)P_2\}(NC\,CH_3)]^+$.
**IR** (KBr): $\tilde{\nu}$ = 3123 (w), 3099 (w), 2254 (w; CN), 1992 (vs; CO), 1975 (vs; CO), 1918 (vs; CO), 1425 (m), 1363 (w), 1264 (w), 1116 (w), 1064 (m), 1016 (w), 927 (w), 843 (m), 833 (m), 606 (m), 599 (m), 563 (s), 540 (m), 490 (m), 425 (w) $cm^{-1}$.
**Elemental analysis**: Calculated (%) for $C_{16}H_{13}Cr_2CuINO_4P_2$ (639.67): C 30.04, H 2.05, N 2.19; found: C 29.61, H 2.05, N 2.08.
**Melting point**: 184 °C (decomposition).

## 4.3.4. $[Ag_2\{Cp_2Cr_2(CO)_4(\mu_3,\eta^2:\eta^2:\eta^2\text{-}P_2)\}_2\{Cp_2Cr_2(CO)_4(\mu_4,\eta^2:\eta^2:\eta^1:\eta^1\text{-}P_2)\}_2][\langle Al\{OC(CF_3)_3\}_4\rangle_2]$ (67)

A mixture of $Ag[Al\{OC(CF_3)_3\}_4]$•$CH_2Cl_2$ (142 mg, 0.12 mmol), $[Cp_2Cr_2(CO)_4(\mu,\eta^2\text{-}P_2)]$ **6a** (100 mg, 0.25 mmol) and $CH_2Cl_2$ (5 ml) was stirred in the absence of light for 4 h at room temperature. The solution was filtered over diatomaceous earth, which was subsequently washed with $CH_2Cl_2$ (2 × 2 ml). Addition of pentane (10 ml) to the combined filtrate and washings led to the isolation of **67** as a microcrystalline wine-red powder, which was filtered, washed with hexane (2 × 3 ml) and dried under vacuum at room temperature.

**Yield**: 205 mg (82 %).
**$^1$H-NMR** ($CD_2Cl_2$, 400.13 MHz, 27 °C): $\delta$ = 5.05 (s; $C_5H_5$) ppm.

**$^{13}$C{$^{1}$H}-NMR** ($CD_2Cl_2$, 100.63 MHz, 27 °C): $\delta$ = 88.86 (s; $C_5H_5$), 121.68 (q; $^{1}J_{FC}$ = 291 Hz; $CF_3$), 234.31 (s; CO) ppm.
**$^{27}$Al-NMR** ($CD_2Cl_2$, 104.26 MHz, 27 °C): $\delta$ = 33.66 (s; $[Al\{OC(CF_3)_3\}_4]^-$) ppm.
**$^{19}$F-NMR** ($CD_2Cl_2$, 376.47 MHz, 25 °C): $\delta$ = –75.60 (s; $CF_3$) ppm.
**$^{31}$P{$^{1}$H}-NMR** ($CD_2Cl_2$, 161.98 MHz, 27 °C): $\delta$ = 43.3 (s) ppm.
**$^{31}$P{$^{1}$H}-NMR** ($CD_2Cl_2$, 161.98 MHz, –80 °C): $\delta$ = 59.0 (b), 29.7 (b) ppm.
**Positive ion ESI-MS** ($CH_2Cl_2$, RT): *m/z* (%) = 924.9 (100) $[Ag\{Cp_2Cr_2(CO)_4P_2\}_2]^+$, 868.9 (30) $[Ag\{Cp_2Cr_2(CO)_3P_2\}_2]^+$, 812.8 (17) $[Ag\{Cp_2Cr_2(CO)_2P_2\}_2]^+$, 756.8 (5) $[Ag\{Cp_2Cr_2(CO)\ P_2\}_2]^+$,.
**Negative ion ESI-MS** ($CH_2Cl_2$, RT): *m/z* (%) = 967.1 (100) $[Al\{OC(CF_3)_3\}_4]^-$.
**IR** ($CH_2Cl_2$): $\tilde{\nu}$ = 3114 (s), 1977 (s; CO), 1928 (s; CO), 1426 (w), 1352 (m), 1300 (s), 1278 (s), 1264 (s), 1241 (s), 1224 (s), 1167 (w), 843 (w), 976 (s), 561 (w), 537 (w), 489 (w), 447 (w) cm$^{-1}$.
**IR** (KBr): $\tilde{\nu}$ = 3131 (w), 1976 (vs; CO), 1942 (vs; CO), 1429 (w), 1353 (m), 1302 (vs), 1278 (vs), 1243 (vs), 1220 (vs), 1169 (m), 1067 (w), 1017 (w), 975 (vs), 846 (m), 756 (w), 728 (vs), 595 (m), 558 (s), 536 (m), 485 (m), 447 (m) cm$^{-1}$.
**Molecular mass**: Theoretical for $C_{88}H_{40}Ag_2Al_2Cr_8F_{72}O_{24}P_8$ = 3782.61 g mol$^{-1}$; found (osmometric, $CH_2Cl_2$, 28 °C) = 3060 ± 153 g mol$^{-1}$.
**Elemental analysis**: Calculated (%) for $C_{88}H_{40}Ag_2Al_2Cr_8F_{72}O_{24}P_8$ (3782.61): C 27.94, H 1.07; found: C 27.59, H 1.28.
**Melting point**: 158 °C (decomposition).

## 4.4. Synthesis of the Complex Based on $[CpCr(CO)_2(\eta^3\text{-}P_3)]$

### 4.4.1. $[Ag\{CpCr(CO)_2(\mu_3,\eta^3\text{:}\eta^1\text{:}\eta^1\text{-}P_3)\}_2]_n[Al\{OC(CF_3)_3\}_4]_n$ (69)

A mixture of $Ag[Al\{OC(CF_3)_3\}_4]\bullet CH_2Cl_2$ (218 mg, 0.19 mmol), $[CpCr(CO)_2(\eta^3\text{-}P_3)]$ **7a** (100 mg, 0.38 mmol) and $CH_2Cl_2$ (5 ml) was stirred in the absence of light for 4 h at room temperature. The solution was filtered over diatomaceous earth, which was subsequently washed with $CH_2Cl_2$ (2 × 2 ml). Addition of hexane (10 ml) to the combined filtrate and washings led to the isolation of **69** as a microcrystalline ochre powder, which was filtered, washed with hexane (2 × 3 ml) and dried under vacuum at room temperature.

**Yield**: 290 mg (96 %).
**$^{1}$H-NMR** ($CD_2Cl_2$, 400.13 MHz, 27 °C): $\delta$ = 5.14 (s; $C_5H_5$) ppm.

**$^{13}$C{$^{1}$H}-NMR** ($CD_2Cl_2$, 100.63 MHz, 27 °C): $\delta$ = 78.92 (b; $C(CF_3)_3$), 87.85 (s; $C_5H_5$), 121.71 (q; $^{1}J_{FC}$ = 294 Hz; $CF_3$), 230.13 (s; CO) ppm.
**$^{27}$Al-NMR** ($CD_2Cl_2$, 104.26 MHz, 27 °C): $\delta$ = 33.68 (s; $[Al\{OC(CF_3)_3\}_4]^-$) ppm.
**$^{19}$F-NMR** ($CD_2Cl_2$, 376.47 MHz, 27 °C): $\delta$ = –75.55 (s; $CF_3$) ppm.
**$^{31}$P{$^{1}$H}-NMR** ($CD_2Cl_2$, 161.98 MHz, 27 °C): $\delta$ = –299.9 (s) ppm.
**$^{31}$P{$^{1}$H}-NMR** (THF-$d_8$/$CD_2Cl_2$ (3:1), 161.98 MHz, 27 °C): $\delta$ = –290.6 (s) ppm.
**$^{31}$P{$^{1}$H}-NMR** (THF-$d_8$/$CD_2Cl_2$ (3:1), 161.98 MHz, –120 °C): $\delta$ = –310.5 (b) ppm.
**Positive ion ESI-MS** ($CH_3CN$, RT): *m/z* (%) = 638.9 (0.3) $[Ag\{CpCr(CO)_2P_3\}_2]^+$, 610.3 (0.1) $[Ag\{CpCr(CO)_{1.5}P_3\}_2]^+$, 555.9 (0.2) $[Ag\{CpCr(CO)_{0.5}P_3\}_2]^+$, 517.4 (0.9) $[Ag\{Cp_{0.5}Cr(CO)\ P_3\}_2]^+$, 467.1 (0.5) $[Ag\{CpCr(CO)P_3\}(NCCH_3)_3]^+$, 415.8 (0.8) $[Ag\{CpCr(CO)_2P_3\}(NC\ CH_3)]^+$, 188.8 (100) $[Ag(NCCH_3)_2]^+$.
**Negative ion ESI-MS** ($CH_3CN$, RT): *m/z* (%) = 967.2 (100) $[Al\{OC(CF_3)_3\}_4]^-$.
**IR** ($CH_2Cl_2$): $\tilde{\nu}$ = 3053 (w), 1990 (m; CO), 1937 (m; CO), 1423 (w), 1352 (w), 1300 (w), 1241 (m), 1224 (m), 976 (m), 569 (w), 537 (w) $cm^{-1}$.
**IR** (KBr): $\tilde{\nu}$ = 2018 (s; CO), 1980 (s; CO), 1428 (w), 1352 (m), 1303 (vs), 1279 (vs), 1242 (vs), 1220 (vs), 1168 (m), 1067 (w), 1013 (w), 975 (vs), 847 (m), 755 (w), 728 (s), 669 (w), 589 (w), 557 (m), 537 (m), 485 (w), 447 (m) $cm^{-1}$.
**Molecular mass**: Theoretical for $C_{30}H_{10}AgAlCr_2F_{36}O_8P_6$ = 1607.03 g $mol^{-1}$; found (osmometric, $CH_2Cl_2$, 28 °C) = 1904 ± 95 g $mol^{-1}$.
**Elemental analysis**: Calculated (%) for $C_{30}H_{10}AgAlCr_2F_{36}O_8P_6$ (1607.03): C 22.42, H 0.63; found: C 23.00, H 0.92.
**Melting point**: 124 °C (decomposition).

## 4.5. Synthesis of the Complexes Based on $[CpMo(CO)_2(\eta^3\text{-}P_3)]$

### 4.5.1. $[Ag\{CpMo(CO)_2(\mu_3,\eta^3\text{:}\eta^1\text{:}\eta^1\text{-}P_3)\}_2]_n[Al\{OC(CF_3)_3\}_4]_n$ (71)

A mixture of $Ag[Al\{OC(CF_3)_3\}_4]\bullet CH_2Cl_2$ (374 mg, 0.32 mmol), $[CpMo(CO)_2(\eta^3\text{-}P_3)]$ **7b** (200 mg, 0.65 mmol) and $CH_2Cl_2$ (30 ml) was stirred in the absence of light for 8 h at room temperature. The yellow solution was filtered over diatomaceous earth, which was subsequently washed with $CH_2Cl_2$ (2 × 3 ml), and the combined filtrate and washings were stored in a freezer (–28 °C). Bright yellow needles of **71**•n$CH_2Cl_2$ crystallised within a week and these were filtered at –30 °C, washed

with pentane (2 × 3 ml) and dried under vacuum at room temperature. The solvent of crystallisation was lost during the drying process. Addition of pentane (30 ml) to the mother liquor led to the isolation of a further crop of **71** as a microcrystalline yellow powder.

**Yield**: 460 mg (84 %).
**$^{1}$H-NMR** ($CD_2Cl_2$, 400.13 MHz, 27 °C): $\delta$ = 5.54 (s; $C_5H_5$) ppm.
**$^{13}$C{$^{1}$H}-NMR** ($CD_2Cl_2$, 100.63 MHz, 27 °C): $\delta$ = 88.71 (s; $C_5H_5$), 121.65 (q; $^{1}J_{FC}$ = 293 Hz; $CF_3$), 217.31 (s; CO) ppm.
**$^{27}$Al-NMR** ($CD_2Cl_2$, 78.21 MHz, 27 °C): $\delta$ = 33.83 (s; $[Al\{OC(CF_3)_3\}_4]^-$) ppm.
**$^{19}$F-NMR** ($CD_2Cl_2$, 376.47 MHz, 27 °C): $\delta$ = –75.56 (s; $CF_3$) ppm.
**$^{31}$P{$^{1}$H}-NMR** ($CD_2Cl_2$, 101.26 MHz, 27 °C): $\delta$ = –365.4 (s) ppm.
**$^{31}$P{$^{1}$H}-NMR** (THF-$d_8$/$CD_2Cl_2$ (3:1), 161.98 MHz, 27 °C): $\delta$ = –360.2 (s) ppm.
**$^{31}$P{$^{1}$H}-NMR** (THF-$d_8$/$CD_2Cl_2$ (3:1), 161.98 MHz, –140 °C): $\delta$ = –394.9 (b), –294.4 (b) ppm.
**$^{31}$P MAS-NMR** (121.50 MHz, RT): $\delta$ = –369.4 (b) ppm.
**$^{31}$P MAS-NMR** (121.50 MHz, –133 °C): $\delta$ = –413.2 (b), –304.2 (b) ppm.
**Positive ion ESI-MS** ($CH_2Cl_2$, RT): *m/z* (%) = 728.6 (100) $[Ag\{CpMo(CO)_2P_3\}_2]^+$.
**Negative ion ESI-MS** ($CH_2Cl_2$, RT): *m/z* (%) = 967.1 (100) $[Al\{OC(CF_3)_3\}_4]^-$.
**Positive ion ESI-MS** ($CH_3CN$, RT): *m/z* (%) = 726.7 (20) $[Ag\{CpMo(CO)_2P_3\}_2]^+$, 459.8 (100) $[Ag\{CpMo(CO)_2P_3\}(NCCH_3)]^+$, 418.7 (6) $[Ag\{CpMo(CO)_2P_3\}]^+$.
**Negative ion ESI-MS** ($CH_3CN$, RT): *m/z* (%) = 967.1 (100) $[Al\{OC(CF_3)_3\}_4]^-$.
**IR** ($CH_2Cl_2$): $\tilde{\nu}$ = 2004 (m; CO), 1945 (m; CO), 1421 (w), 1352 (w), 1301 (m), 1273 (s), 1259 (s), 1241 (s), 1224 (s), 1168 (w), 976 (s), 896 (m), 825 (w), 760 (s), 714 (s), 561 (w), 537 (w), 517 (w), 447 (w) cm$^{-1}$.
**IR** (KBr): $\tilde{\nu}$ = 2033 (s; CO), 1988 (s; CO), 1423 (w), 1353 (m), 1303 (vs), 1278 (vs), 1242 (vs), 1218 (vs), 1168 (m), 1011 (w), 974 (vs), 839 (m), 755 (w), 728 (s), 560 (w), 537 (m), 493 (m), 446 (m) cm$^{-1}$.
**Molecular mass**: Theoretical for $C_{30}H_{10}AgAlF_{36}Mo_2O_8P_6$ = 1694.92 g mol$^{-1}$; found (osmometric, $CH_2Cl_2$, 28 °C) = 2440 ± 122 g mol$^{-1}$.
**Elemental analysis**: Calculated (%) for $C_{30}H_{10}AgAlF_{36}Mo_2O_8P_6$ (1694.92): C 21.26, H 0.59; found: C 21.12, H 0.99.
**Melting point**: 147 °C (decomposition).

## 4.5.2. $[Ag\{CpMo(CO)_2(\mu_3,\eta^3:\eta^1:\eta^1\text{-}P_3)\}_3]_n[Al\{OC(CF_3)_3\}_4]_n$ (74)

A mixture of $Ag[Al\{OC(CF_3)_3\}_4]\bullet CH_2Cl_2$ (63 mg, 0.05 mmol), $[CpMo(CO)_2(\eta^3\text{-}P_3)]$ **7b** (100 mg, 0.32 mmol) and $CH_2Cl_2$ (10 ml) was stirred in the absence of light for 8 h at room temperature. The yellow solution was filtered over diatomaceous earth, which was subsequently washed with $CH_2Cl_2$ (2 × 2 ml), and the combined filtrate and washings were concentrated to approximately one third of the original volume (~ 5 ml) and stored in a freezer (–28 °C). Dark yellow plates of **74** were deposited within a week and these were filtered at –30 °C, washed with pentane (2 × 3 ml) and dried under vacuum at room temperature. Addition of pentane (5 ml) to the mother liquor led to the isolation of a further crop of **74** as a microcrystalline yellow powder.

**Yield**: 85 mg (72 %).
**$^1$H-NMR** ($CD_2Cl_2$, 400.13 MHz, 27 °C): $\delta$ = 5.47 (s; $C_5H_5$) ppm.
**$^{13}$C{$^1$H}-NMR** ($CD_2Cl_2$, 100.63 MHz, 27 °C): $\delta$ = 87.92 (s; $C_5H_5$), 121.64 (q; $^1J_{FC}$ = 291 Hz; $CF_3$), 219.06 (s; CO) ppm.
**$^{31}$P{$^1$H}-NMR** ($CD_2Cl_2$, 161.98 MHz, 27 °C): $\delta$ = –359.6 (s) ppm.
**$^{31}$P{$^1$H}-NMR** (THF-$d_8$/$CD_2Cl_2$ (3:1), 161.98 MHz, 27 °C): $\delta$ = –359.0 (s) ppm.
**$^{31}$P{$^1$H}-NMR** (THF-$d_8$/$CD_2Cl_2$ (3:1), 161.98 MHz, –140 °C): $\delta$ = –396.2 (b), –293.8 (b) ppm.
**$^{31}$P MAS-NMR** (121.50 MHz, RT): $\delta$ = –350.7 (b) ppm.
**Positive ion ESI-MS** ($CH_2Cl_2$, RT): *m/z* (%) = 1038.6 (11) $[Ag\{CpMo(CO)_2P_3\}_3]^+$, 728.7 (100) $[Ag\{CpMo(CO)_2P_3\}_2]^+$.
**Negative ion ESI-MS** ($CH_2Cl_2$, RT): *m/z* (%) = 967.2 (100) $[Al\{OC(CF_3)_3\}_4]^-$.
**IR** (KBr): $\tilde{\nu}$ = 2965 (w), 2031 (s; CO), 1988 (s; CO), 1422 (w), 1352 (m), 1303 (s), 1280 (s), 1241 (s), 1219 (vs), 1168 (m), 1010 (w), 975 (vs), 829 (m), 756 (w), 728 (s), 551 (w), 537 (w), 498 (m), 468 (w), 452 (m), 443 (m) $cm^{-1}$.
**Molecular mass**: Theoretical for $C_{37}H_{15}AgAlF_{36}Mo_3O_{10}P_9$ = 2004.90 g $mol^{-1}$; found (osmometric, $CH_2Cl_2$, 28 °C) = 1916 ± 96 g $mol^{-1}$.
**Elemental analysis**: Calculated (%) for $C_{37}H_{15}AgAlF_{36}Mo_3O_{10}P_9$ (2004.90): C 22.16, H 0.75; found: C 22.48, H 1.05.
**Melting point**: 189 °C (decomposition).

## 4.6. Synthesis of the Complexes Based on [Cp*Mo(CO)$_2$($\eta^3$-P$_3$)]

### 4.6.1. [Cu$_2$($\mu$-Cl)$_2${Cp*Mo(CO)$_2$($\mu$,$\eta^3$:$\eta^2$-P$_3$)}$_2$] (76a)

A solution of CuCl (78 mg, 0.79 mmol) in $CH_3CN$ (10 ml) was added to a solution of [Cp*Mo(CO)$_2$($\eta^3$-P$_3$)] **7c** (100 mg, 0.26 mmol) in $CH_2Cl_2$ (8 ml) at room temperature. The vessel was stored in a freezer (–28 °C) and crystals of **76a** were deposited as lemon yellow plates within three weeks. These were filtered at –30 °C, washed with $Et_2O$ (2 × 3 ml) and dried under vacuum at room temperature.

**Yield**: 100 mg (79 %).
**Positive ion ESI-MS** ($CH_3CN$, RT): *m/z* (%) = 1020.8 (1) $[Cu_3Cl_2\{Cp^*Mo(CO)_2P_3\}_2]^+$, 922.9 (3) $[Cu_2Cl\{Cp^*Mo(CO)_2P_3\}_2]^+$, 823.1 (9) $[Cu\{Cp^*Mo(CO)_2P_3\}_2]^+$, 486.0 (6) $[Cu\{Cp^*Mo(CO)_2P_3\}(NCCH_3)]^+$, 145.0 $[Cu(NCCH_3)_2]^+$.
**Negative ion ESI-MS** ($CH_3CN$, RT): *m/z* (%) = 728.4 (1) $[Cu_7Cl_8]^-$, 674.3 (0.5) $[Cu_6Cl_7(NC\,CH_3)]^-$, 630.5 (2) $[Cu_6Cl_7]^-$, 574.6 (1) $[Cu_5Cl_6(NCCH_3)]^-$, 530.7 (14) $[Cu_5Cl_6]^-$, 476.7 (0.5) $[Cu_4Cl_5(NCCH_3)]^-$, 430.7 (3) $[Cu_4Cl_5]^-$, 378.5 (0.5) $[Cu_3Cl_4(NCCH_3)]^-$, 332.7 (3) $[Cu_3Cl_4]^-$, 313.0 (1) $[Cu_2Cl_3(NCCH_3)_2]^-$, 276.6 (1) $[Cu_2Cl_3(NCCH_3)]^-$, 232.8 (20) $[Cu_2Cl_3]^-$, 223.8 (12) $[CuCl_2(NCCH_3)_2]^-$, 178.8 (5) $[CuCl_2(NCCH_3)]^-$, 134.9 (100) $[CuCl_2]^-$.
**IR** (KBr): $\tilde{\nu}$ = 2983 (w), 2962 (w), 2908 (w), 2858 (w), 2000 (vs; CO), 1951 (vs; CO), 1935 (vs; CO), 1478 (m), 1451 (w), 1425 (w), 1382 (s), 1072 (w), 1030 (m), 802 (w), 560 (w), 506 (s), 477 (m), 460 (m), 450 (m), 425 (w), 417 (w) $cm^{-1}$.
**Elemental analysis**: Calculated (%) for $C_{12}H_{15}ClCuMoO_2P_3$ (479.11): C 30.08, H 3.16; found: C 30.17, H 3.04.
**Melting point**: 167 °C (decomposition).

### 4.6.2. [Cu$_2$($\mu$-Br)$_2${Cp*Mo(CO)$_2$($\mu$,$\eta^3$:$\eta^2$-P$_3$)}$_2$] (76b)

A solution of CuBr (113 mg, 0.79 mmol) in $CH_3CN$ (10 ml) was carefully layered over a solution of [Cp*Mo(CO)$_2$($\eta^3$-P$_3$)] **7c** (100 mg, 0.26 mmol) in $CH_2Cl_2$ (8 ml) at room temperature. The vessel was left at room temperature in the dark and yellow prisms of **76b** crystallised within two weeks. These were filtered, washed with $Et_2O$ (2 × 3 ml) and dried under vacuum at room temperature.

**Yield**: 50 mg (36 %).

**Positive ion ESI-MS** ($CH_3CN/CH_2Cl_2$, RT): *m/z* (%) = 1110.7 (1) $[Cu_3Br_2\{Cp^*Mo(CO)_2P_3\}_2]^+$, 968.8 (3) $[Cu_2Br\{Cp^*Mo(CO)_2P_3\}_2]^+$, 823.0 (10) $[Cu\{Cp^*Mo(CO)_2P_3\}_2]^+$, 485.9 (8) $[Cu\{Cp^*Mo(CO)_2P_3\}(NCCH_3)]^+$, 145.0 (100) $[Cu(NCCH_3)_2]^+$.
**Negative ion ESI-MS** ($CH_3CN/CH_2Cl_2$, RT): *m/z* (%) = 798.2 (0.5) $[Cu_5Br_6]^-$, 652.5 (0.5) $[Cu_4Br_5]^-$, 510.6 (2) $[Cu_3Br_4]^-$, 366.6 (8) $[Cu_2Br_3]^-$, 222.8 (100) $[CuBr_2]^-$.
**IR** (KBr): $\tilde{\nu}$ = 2983 (w), 2961 (w), 2907 (w), 2859 (w), 2000 (vs; CO), 1953 (vs; CO), 1936 (vs; CO), 1478 (m), 1450 (w), 1426 (w), 1381 (s), 1159 (w), 1073 (w), 1029 (m), 800 (w), 559 (m), 505 (s), 475 (m), 460 (m), 449 (m), 433 (m), 424 (m), 416 (m) $cm^{-1}$.
**Elemental analysis**: Calculated (%) for $C_{12}H_{15}BrCuMoO_2P_3$ (523.56): C 27.53, H 2.89; found: C 27.69, H 2.76.
**Melting point**: 153 °C (decomposition).

## 4.6.3. $[Cu(\mu\text{-I})\{Cp^*Mo(CO)_2(\mu_3,\eta^3:\eta^1:\eta^1\text{-}P_3)\}]_n$ (77)

A mixture of CuI (150 mg, 0.79 mmol), $[Cp^*Mo(CO)_2(\eta^3\text{-}P_3)]$ **7c** (100 mg, 0.26 mmol), $CH_3CN$ (15 ml) and $CH_2Cl_2$ (8 ml) was carefully layered with $Et_2O$ (10 ml) at room temperature. After storage of the vessel in a freezer (–28 °C) for three weeks, colourless prisms of $[CuI(CH_3CN)]_2$ and bright orange rods of **77** were deposited. These crystals were filtered, washed with pentane (2 × 2 ml) and dried under vacuum at room temperature. The crystals of **77** were separated manually from those of $[CuI(NCCH_3)]_2$ in a glove box.

**Yield**: 100 mg (67 %).
**Positive ion ESI-MS** ($CH_3CN$, RT): *m/z* (%) = 1204.7 (1) $[Cu_3I_2\{Cp^*Mo(CO)_2P_3\}_2]^+$, 1014.8 (4) $[Cu_2I\{Cp^*Mo(CO)_2P_3\}_2]^+$, 823.0 (20) $[Cu\{Cp^*Mo(CO)_2P_3\}_2]^+$, 485.9 (10) $[Cu\{Cp^*Mo(CO)_2P_3\}\{NCCH_3\}]^+$, 145.0 (100) $[Cu(NCCH_3)_2]^+$.
**Negative ion ESI-MS** ($CH_3CN$, RT): *m/z* (%) = 2221.7 (0.1) $[Cu_{11}I_{12}]^-$, 2031.8 (0.1) $[Cu_{10}I_{11}]^-$, 1842.0 (0.4) $[Cu_9I_{10}]^-$, 1650.0 (0.2) $[Cu_8I_9]^-$, 1460.3 (0.2) $[Cu_7I_8]^-$, 1270.3 (1.5) $[Cu_6I_7]^-$, 1078.3 (1) $[Cu_5I_6]^-$, 888.4 (6) $[Cu_4I_5]^-$, 698.6 (24) $[Cu_3I_4]^-$, 506.8 (30) $[Cu_2I_3]^-$, 316.8 (100) $[CuI_2]^-$.
**IR** (KBr): $\tilde{\nu}$ = 2985 (w), 2963 (w), 2910 (w), 1984 (vs; CO), 1929 (vs; CO), 1476 (m), 1450 (w), 1421 (w), 1381 (s), 1072 (w), 1029 (m), 800 (w), 623 (w), 594 (w), 549 (m), 500 (s), 463 (m), 440 (w), 421 (m) $cm^{-1}$.
**Elemental analysis**: Calculated (%) for $C_{12}H_{15}CuIMoO_2P_3$ (570.56): C 25.26, H 2.65; found: C 25.28, H 2.63.
**Melting point**: 180-187 °C.

### 4.6.4. $[Ag\{Cp^*Mo(CO)_2(\mu_3,\eta^3:\eta^2:\eta^1\text{-}P_3)\}_2]_n[Al\{OC(CF_3)_3\}_4]_n$ (78)

A mixture of $Ag[Al\{OC(CF_3)_3\}_4]\bullet CH_2Cl_2$ (134 mg, 0.12 mmol), $[Cp^*Mo(CO)_2(\eta^3\text{-}P_3)]$ **7c** (88 mg, 0.23 mmol) and $CH_2Cl_2$ (15 ml) was stirred in the absence of light for 8 h at room temperature. The yellow solution was filtered over diatomaceous earth, which was subsequently washed with $CH_2Cl_2$ (2 × 3 ml), and the combined filtrate and washings were stored in a freezer (–28 °C). Bright yellow needles of **78** were deposited within a week and these were filtered at –30 °C, washed with pentane (2 × 3 ml) and dried under vacuum at room temperature. Addition of pentane (20 ml) to the mother liquor led to the isolation of a further crop of **78** as a microcrystalline yellow powder.

**Yield**: 195 mg (92 %).
**$^1$H-NMR** ($CD_2Cl_2$, 400.13 MHz, 27 °C): $\delta$ = 2.06 (s; $CH_3$) ppm.
**$^{13}$C{$^1$H}-NMR** ($CD_2Cl_2$, 100.63 MHz, 27 °C): $\delta$ = 12.27 (s; $CH_3$), 103.88 (s; Cp*), 121.67 (q; $^1J_{FC}$ = 293 Hz; $CF_3$), 221.01 (s; CO) ppm.
**$^{27}$Al-NMR** ($CD_2Cl_2$, 104.26 MHz, 27 °C): $\delta$ = 33.65 (s; $[Al\{OC(CF_3)_3\}_4]^-$) ppm.
**$^{19}$F-NMR** ($CD_2Cl_2$, 376.47 MHz, 27 °C): $\delta$ = –75.60 (s; $CF_3$) ppm.
**$^{31}$P{$^1$H}-NMR** ($CD_2Cl_2$, 161.98 MHz, 27 °C): $\delta$ = –348.02 (s) ppm.
**$^{31}$P{$^1$H}-NMR** (THF-$d_8$/$CD_2Cl_2$ (3:1), 161.98 MHz, 27 °C): $\delta$ = –346.61 (s) ppm.
**$^{31}$P{$^1$H}-NMR** (THF-$d_8$/$CD_2Cl_2$ (3:1), 161.98 MHz, –120 °C): $\delta$ = –384.04 (b), –271.12 (b) ppm.
**$^{31}$P MAS-NMR** (121.50 MHz, RT): $\delta$ = –364.0 (b), –344.5 (b) ppm.
**Positive ion ESI-MS** ($CH_2Cl_2$, RT): *m/z* (%) = 866.9 (100) $[Ag\{Cp^*Mo(CO)_2P_3\}_2]^+$, 840.9 (10) $[Ag\{Cp^*Mo(CO)_{1.5}P_3\}_2]^+$, 810.8 (3) $[Ag\{Cp^*Mo(CO)P_3\}_2]^+$, 754.8 (1) $[Ag\{Cp^*Mo\ P_3\}_2]^+$.
**Negative ion ESI-MS** ($CH_2Cl_2$, RT): *m/z* (%) = 967.1 (100) $[Al\{OC(CF_3)_3\}_4]^-$.
**Positive ion ESI-MS** ($CH_3CN$, RT): *m/z* (%) = 880.0 (16) $[Ag\{Cp^*Mo(CO)_{1.5}P_3\}_2(NC\ CH_3)]^+$, 866.9 (100) $[Ag\{Cp^*Mo(CO)_2P_3\}_2]^+$, 840.9 (2) $[Ag\{Cp^*Mo(CO)_{1.5}P_3\}_2]^+$, 812.9 (6) $[Ag\{Cp^*Mo(CO)P_3\}_2]^+$, 797.9 (4) $[Ag\{Cp^*MoP_3\}_2(NCCH_3)]^+$, 529.9 (74) $[Ag\{Cp^*Mo\ (CO)_2P_3\}(NCCH_3)]^+$.
**Negative ion ESI-MS** ($CH_3CN$, RT): *m/z* (%) = 967.1 (100) $[Al\{OC(CF_3)_3\}_4]^-$.
**IR** (KBr): $\tilde{\nu}$ = 2965 (w), 2035 (s; CO), 2017 (s; CO), 1983 (s; CO), 1971 (s; CO), 1352 (m), 1303 (vs), 1279 (vs), 1242 (vs), 1220 (vs), 1168 (m), 1027 (w), 975 (vs), 830 (w), 799 (w), 756 (w), 728 (s), 684

(w), 668 (s), 655 (w), 617 (w), 561 (w), 537 (w), 492 (w), 462 (w), 443 (w), 419 (w) $cm^{-1}$.
**Molecular mass**: Theoretical for $C_{40}H_{30}AgAlF_{36}Mo_2O_8P_6$ = 1835.19 g $mol^{-1}$; found (osmometric, $CH_2Cl_2$, 28 °C) = 1953 ± 98 g $mol^{-1}$.
**Elemental analysis**: Calculated (%) for $C_{40}H_{30}AgAlF_{36}Mo_2O_8P_6$ (1835.19): C 26.18, H 1.65; found: C 26.19, H 1.74.
**Melting point**: 190 °C (decomposition).

## 4.7. Synthesis of the Complex Based on $[Cp^*Mo(CO)_2(\eta^3\text{-}As_3)]$

### 4.7.1. $[Ag_2\{Cp^*Mo(CO)_2(\mu,\eta^3:\eta^2\text{-}As_3)\}_2\{Cp^*Mo(CO)_2(\mu_3,\eta^3:\eta^2:\eta^2\text{-}As_3)\}_2][\langle Al\{OC(CF_3)_3\}_4\rangle_2]$ (81)

A mixture of $Ag[Al\{OC(CF_3)_3\}_4]\bullet CH_2Cl_2$ (113 mg, 0.10 mmol), $[Cp^*Mo(CO)_2(\eta^3\text{-}As_3)]$ **80** (100 mg, 0.20 mmol) and $CH_2Cl_2$ (10 ml) was stirred in the absence of light for 8 h at room temperature. The yellow solution was filtered over diatomaceous earth, which was subsequently washed with $CH_2Cl_2$ (2 × 3 ml), and the combined filtrate and washings were stored in a freezer (–28 °C). Bright yellow-orange needles of **81**•$2.5CH_2Cl_2$ were deposited within a week and these were filtered at –30 °C, washed with pentane (2 × 3 ml) and dried under vacuum at room temperature. The solvent of crystallisation was completely removed during the drying process.

**Yield**: 180 mg (88 %).
**$^1$H-NMR** ($CD_2Cl_2$, 400.13 MHz, 27 °C): $\delta$ = 2.09 (s; $CH_3$) ppm.
**$^{13}$C{$^1$H}-NMR** ($CD_2Cl_2$, 100.63 MHz, 27 °C): $\delta$ = 12.89 (s; $CH_3$), 102.66 (s; Cp*), 121.68 (q; $^1J_{FC}$ = 293 Hz; $CF_3$), 220.79 (s; CO) ppm.
**$^{27}$Al-NMR** ($CD_2Cl_2$, 104.26 MHz, 27 °C): $\delta$ = 33.66 (s; $[Al\{OC(CF_3)_3\}_4]^-$) ppm.
**$^{19}$F-NMR** ($CD_2Cl_2$, 376.47 MHz, 27 °C): $\delta$ = –75.58 (s; $CF_3$) ppm.
**Positive ion ESI-MS** ($CH_2Cl_2$, RT): *m/z* (%) = 1644.7 (0.1) $[Ag\{Cp^*Mo(CO)_2As_3\}_3]^+$, 1130.8 (100) $[Ag\{Cp^*Mo(CO)_2As_3\}_2]^+$, 1102.7 (20) $[Ag\{Cp^*Mo(CO)_{1.5}As_3\}_2]^+$, 1076.7 (7) $[Ag\{Cp^*Mo(CO)P_3\}_2]^+$, 1046.6 (1) $[Ag\{Cp^*Mo(CO)_{0.5}As_3\}_2]^+$, 1020.6 (2) $[Ag\{Cp^*Mo\ As_3\}_2]^+$.
**Negative ion ESI-MS** ($CH_2Cl_2$, RT): *m/z* (%) = 967.1 (100) $[Al\{OC(CF_3)_3\}_4]^-$.
**Positive ion ESI-MS** ($CH_3CN$, RT): *m/z* (%) = 1143.7 (8) $[Ag\{Cp^*Mo(CO)_{1.5}As_3\}_2(NC\ CH_3)]^+$, 1132.8 (100) $[Ag\{Cp^*Mo(CO)_2As_3\}_2]^+$, 1102.7 (20) $[Ag\{Cp^*Mo(CO)_{1.5}As_3\}_2]^+$,

1074.6 (7) $[Ag\{Cp^*Mo(CO)P_3\}_2]^+$, 1059.7 (10) $[Ag\{Cp^*MoAs_3\}_2(NCCH_3)]^+$, 1046.8 (2) $[Ag\{Cp^*Mo(CO)_{0.5}As_3\}_2]^+$, 1018.7 (3) $[Ag\{Cp^*MoAs_3\}_2]^+$, 939.9 (3) $[Ag\{Cp^*_{0.5}Mo(CO)\ As_3\}_2]^+$, 909.8 (5) $[Ag\{Cp^*_{0.5}Mo(CO)_{0.5}As_3\}_2]^+$, 674.8 (8) $[Ag\{Cp^*Mo(CO)As_3\}(NC\ CH_3)_2]^+$, 661.8 (86) $[Ag\{Cp^*Mo(CO)_2As_3\}(NCCH_3)]^+$, 620.7 (10) $[Ag\{Cp^*Mo(CO)_2As_3\}]^+$, 605.7 (2) $[Ag\{Cp^*MoAs_3\}(NCCH_3)]^+$.
**Negative ion ESI-MS** ($CH_3CN$, RT): *m/z* (%) = 967.2 (100) $[Al\{OC(CF_3)_3\}_4]^-$.
**IR** ($CH_2Cl_2$): $\tilde{\nu}$ = 2006 (m; CO), 1952 (m; CO), 1382 (w), 1352 (w), 1301 (m), 1279 (m), 1241 (s), 1224 (s), 1168 (w), 1112 (w), 1080 (w), 976 (s), 830 (w), 557 (w), 537 (w), 508 (w), 449 (w) $cm^{-1}$.
**IR** (KBr): $\tilde{\nu}$ = 2966 (w), 2922 (w), 2018 (s; CO), 2007 (s; CO), 1974 (s; CO), 1958 (s; CO), 1941 (s; CO), 1559 (w), 1540 (w), 1507 (w), 1480 (w), 1457 (w), 1384 (w), 1353 (m), 1303 (vs), 1278 (vs), 1241 (vs), 1220 (vs), 1167 (m), 974 (vs), 831 (w), 801 (w), 756 (w), 728 (vs), 668 (w), 571 (w), 559 (w), 554 (w), 537 (m), 497 (m), 466 (w), 447 (m) $cm^{-1}$.
**Molecular mass**: Theoretical for $C_{80}H_{60}Ag_2Al_2As_{12}F_{72}Mo_4O_{16}$ = 4197.75 g $mol^{-1}$; found (osmometric, $CH_2Cl_2$, 28 °C) = 2756 ± 138 g $mol^{-1}$.
**Elemental analysis**: Calculated (%) for $C_{40}H_{30}AgAlAs_6F_{36}Mo_2O_8$ (2098.88): C 22.89, H 1.44; found: C 22.99, H 1.49.
**Melting point**: 200 °C (decomposition).

## 4.8. Synthesis of the Complexes Based on [Cp*Fe($\eta^5$-$P_5$)]

### 4.8.1. $[Ag\{Cp^*Fe(\mu_3,\eta^5:\eta^2:\eta^1\text{-}P_5)\}_2]_n[Al\{OC(CF_3)_3\}_4]_n$ (83)

A mixture of $Ag[Al\{OC(CF_3)_3\}_4]\bullet CH_2Cl_2$ (168 mg, 0.14 mmol), [Cp*Fe($\eta^5$-$P_5$)] **9a** (100 mg, 0.29 mmol) and $CH_2Cl_2$ (10 ml) was stirred in the absence of light for 8 h at room temperature. The brown solution was filtered over diatomaceous earth, which was subsequently washed with $CH_2Cl_2$ (2 × 3 ml). The combined filtrate and washings were concentrated under reduced pressure to about one fourth of the original volume (~ 5 ml) and stored in a freezer (–28 °C). Dark brown needles of **83**•$CH_2Cl_2$ were deposited within three days and these were filtered at –30 °C, washed with pentane (2 × 3 ml) and dried under vacuum at room temperature. The solvent of crystallisation was lost during the drying process. Addition of pentane (5 ml) to the mother

liquor led to the isolation of a further crop of **83** as a microcrystalline dark brown powder.

**Yield**: 230 mg (90 %).
**$^{1}$H-NMR** ($CD_2Cl_2$, 600.13 MHz, 27 °C): $\delta$ = 1.38 (s; $CH_3$) ppm.
**$^{13}$C{$^{1}$H}-NMR** ($CD_2Cl_2$, 150.92 MHz, 27 °C): $\delta$ = 11.11 (s; $CH_3$), 79.37 (b; $OC(CF_3)_3$), 95.41 (s; Cp*), 121.64 (q; $^{1}J_{FC}$ = 293 Hz; $CF_3$) ppm.
**$^{27}$Al-NMR** ($CD_2Cl_2$, 104.26 MHz, 27 °C): $\delta$ = 33.63 (s; $[Al\{OC(CF_3)_3\}_4]^-$) ppm.
**$^{19}$F-NMR** ($CD_2Cl_2$, 376.47 MHz, 27 °C): $\delta$ = –75.61 (s; $CF_3$) ppm.
**$^{31}$P{$^{1}$H}-NMR** ($CD_2Cl_2$, 161.98 MHz, 27 °C): $\delta$ = 154.2 (s) ppm.
**$^{31}$P{$^{1}$H}-NMR** ($CD_2Cl_2$, 161.98 MHz, –90 °C): $\delta$ = 123.2 (b), 150.9 (b) ppm.
**$^{31}$P MAS-NMR** (162.01 MHz, RT): $\delta$ = 149.7 (b), 152.3 (b) ppm.
**$^{31}$P MAS-NMR** (162.01 MHz, –100 °C): $\delta$ = 150.0 (b) ppm.
**Positive ion ESI-MS** ($CH_2Cl_2$, RT): *m/z* (%) = 798.8 (100) $[Ag(Cp^*FeP_5)_2]^+$.
**Negative ion ESI-MS** ($CH_2Cl_2$, RT): *m/z* (%) = 967.2 (100) $[Al\{OC(CF_3)_3\}_4]^-$.
**Positive ion ESI-MS** ($CH_3CN$, RT): *m/z* (%) = 798.9 (100) $[Ag(Cp^*FeP_5)_2]^+$, 493.9 (19) $[Ag(Cp^*FeP_5)(NCCH_3)]^+$, 451.1 (35) $[Ag(Cp^*FeP_5)]^+$.
**Negative ion ESI-MS** ($CH_3CN$, RT): *m/z* (%) = 967.1 (100) $[Al\{OC(CF_3)_3\}_4]^-$.
**IR** ($CH_2Cl_2$): $\tilde{\nu}$ = 1478 (w), 1428 (w), 1377 (w), 1352 (w), 1300 (m), 1278 (s), 1272 (vs), 1241 (vs), 1224 (vs), 1167 (w), 1022 (w), 976 (vs), 808 (w), 561 (w), 537 (w), 445 (w) $cm^{-1}$.
**IR** (KBr): $\tilde{\nu}$ = 2967 (w), 2921 (w), 1617 (m), 1599 (m), 1480 (m), 1450 (m), 1429 (m), 1380 (s), 1354 (s), 1304 (vs), 1278 (vs), 1242 (vs), 1219 (vs), 1166 (s), 1101 (m), 1074 (m), 1021 (s), 974 (vs), 862 (w), 828 (m), 820 (m), 756 (w), 727 (vs), 560 (m), 537 (m), 443 (m) $cm^{-1}$.
**Molecular mass**: Theoretical for $C_{36}H_{30}AgAlF_{36}Fe_2O_4P_{10}$ = 1766.86 g $mol^{-1}$; found (osmometric, $CH_2Cl_2$, 28 °C) = 1725 ± 86 g $mol^{-1}$.
**Elemental analysis**: Calculated (%) for $C_{36}H_{30}AgAlF_{36}Fe_2O_4P_{10}$ (1766.86): C 24.47, H 1.71; found: C 24.53, H 1.71.
**Melting point**: 200 °C (decomposition).

## 4.8.2. $[Ag_x\{Cp^*Fe(\eta^5\text{-}P_5)\}_y(NO_2)_x(NCCH_3)_z]$ (85)

A mixture of $AgNO_2$ (46 mg, 0.30 mmol), $[Cp^*Fe(\eta^5\text{-}P_5)]$ **9a** (100 mg, 0.29 mmol), $CH_3CN$ (5 ml) and $CH_2Cl_2$ (5 ml) was stirred at room temperature in the dark for 1 h. The resulting brown precipitate was filtered, washed with $CH_3CN$ (2 × 4 ml) and dried under vacuum at room temperature.

**Yield**: 85 mg.
**IR** (KBr): $\tilde{\nu}$ = 2965 (w), 2904 (w), 1823 (m), 1636 (w), 1476 (m), 1450 (m), 1429 (m), 1380 (m), 1261 (m), 1155 (s), 1073 (vs), 1025 (vs), 922 (s), 840 (s), 814 (s), 519 (m), 503 (m) $cm^{-1}$.
**Elemental analysis**: C 14.81, H 3.46, N 1.23.
**Melting point**: 138 °C (decomposition).

## 4.8.3. $[Au_5\{Cp^*Fe(\eta^5\text{-}P_5)\}_2]_n[(PF_6)_5]_n$ (86)

A mixture of $[(Ph_3P)AuCl]$ (66 mg, 0.13 mmol), $TlPF_6$ (50 mg, 0.14 mmol), THF (5 ml) and $CH_2Cl_2$ (5 ml) was stirred at room temperature in the dark for 8 h, during which time TlCl was formed as a fine pale grey precipitate. The $[(Ph_3P)Au][PF_6]$ solution was filtered over diatomaceous earth, which was subsequently washed with THF (2 × 2 ml). The combined filtrate and washings were added to a solution of $[Cp^*Fe(\eta^5\text{-}P_5)]$ **9a** (100 mg, 0.29 mmol) in $CH_2Cl_2$ (10 ml). This new mixture was stirred overnight and the resulting brown precipitate was filtered, washed with $CH_2Cl_2$ (2 × 3 ml) and dried under vacuum at room temperature.

**Yield**: 64 mg (100 %).
**IR** (KBr): $\tilde{\nu}$ = 2970 (w), 2902 (w), 1636 (w), 1476 (m), 1377 (m), 1155 (w), 1098 (w), 1073 (w), 1020 (m), 919 (m), 868 (m), 842 (s), 740 (m), 558 (m), 532 (w), 505 (w), 471 (w), 437 (w) $cm^{-1}$.
**Elemental analysis**: Calculated (%) for $C_{20}H_{30}Au_5F_{30}Fe_2P_{15}$ (2401.54): C 10.00, H 1.26; found: C 10.27, H 1.46.
**Melting point**: 152 °C (decomposition).

## 4.8.4. $[(AuCl)_3\{Cp^*Fe(\eta^5\text{-}P_5)\}]_n$ (87)

A mixture of [(THT)AuCl] (96 mg, 0.30 mmol), $[Cp^*Fe(\eta^5\text{-}P_5)]$ **9a** (100 mg, 0.29 mmol) and $CH_2Cl_2$ (20 ml) was stirred at room temperature in the dark for 8 h. The resulting brown precipitate was

filtered, washed with $CH_2Cl_2$ (2 × 3 ml) and dried under vacuum at room temperature.

**Yield**: 104 mg (100 %).
**IR** (KBr): $\tilde{\nu}$ = 2962 (w), 2904 (w), 1638 (m), 1476 (m), 1448 (m), 1426 (m), 1376 (m), 1262 (m), 1154 (w), 1074 (m), 1022 (m), 875 (w), 811 (m), 803 (m), 730 (w), 696 (w), 468 (w) $cm^{-1}$.
**Elemental analysis**: Calculated (%) for $C_{10}H_{15}Au_3Cl_3FeP_5$ (1043.20): C 11.51, H 1.45; found: C 11.99, H 1.87.
**Melting point**: > 220 °C.

## 4.9. Synthesis of the Complexes Based on $[(Cp^*Mo)_2(\mu,\eta^6\text{-}P_6)]$

### 4.9.1. $[Cu_{20}(\mu\text{-}Cl)_{16}(\mu_3\text{-}Cl)_4\{(Cp^*Mo)_2(\mu_7,\eta^6\text{:}\eta^6\text{:}\eta^1\text{:}\eta^1\text{:}\eta^1\text{:}\eta^1\text{-}P_6)\}_3\{(Cp^*Mo)_2(\mu_7,\eta^6\text{:}\eta^6\text{:}\eta^2\text{:}\eta^1\text{:}\eta^1\text{:}\eta^1\text{:}\eta^1\text{-}P_6)\}(NCCH_3)_{12}]_n$ (88)

A mixture of CuCl (30 mg, 0.30 mmol), $[(Cp^*Mo)_2(\mu,\eta^6\text{-}P_6)]$ **11c** (6 mg, 0.01 mmol), $CH_3CN$ (15 ml) and $CH_2Cl_2$ (15 ml) was carefully layered with $Et_2O$ (30 ml) at room temperature. The vessel was left at room temperature in the dark and amber plates of **88**•2n$CH_2Cl_2$ were deposited within a month. These crystals were filtered, washed with pentane (2 × 3 ml) and dried under vacuum at room temperature.

**Yield**: 10 mg (91 % if the solvent of crystallisation was retained; 92 % if the solvent of crystallisation was lost).
**Positive ion ESI-MS** ($CH_3CN$, RT): *m/z* (%) = 1787.8 (0.01) $[Cu_5Cl_4\{(Cp^*Mo)_2P_6\}_2(NC\,CH_3)]^+$, 1745.2 (0.10) $[Cu_5Cl_4\{(Cp^*Mo)_2P_6\}_2]^+$, 1645.4 (0.45) $[Cu_4Cl_3\{(Cp^*Mo)_2P_6\}_2]^+$, 1547.4 (0.10) $[Cu_3Cl_2\{(Cp^*Mo)_2P_6\}_2]^+$, 1449.3 (0.20) $[Cu_2Cl\{(Cp^*Mo)_2P_6\}_2]^+$, 1353.4 (0.60) $[Cu\{(Cp^*Mo)_2P_6\}_2]^+$ or $[Cu_5Cl_4\{(Cp^*Mo)_2P_6\}(NCCH_3)_6]^+$, 1324.4 (0.30) $[Cu_6Cl_5\{(Cp^*Mo)_2P_6\}(CH_3CN)_3]^+$, 1297.4 (0.23) $[Cu_4Cl_3\{(Cp^*Mo)_2P_6\}(NCCH_3)_7]^+$, 1187.1 (0.03) $[Cu_5Cl_4\{(Cp^*Mo)_2P_6\}(NCCH_3)_2]^+$, 1087.2 (0.10) $[Cu_4Cl_3\{(Cp^*Mo)_2P_6\}(NCCH_3)_2]^+$, 1005.0 (0.06) $[Cu_4Cl_3\{(Cp^*Mo)_2P_6\}]^+$, 848.1 (1) $[Cu_2Cl\{(Cp^*Mo)_2P_6\}(NCCH_3)]^+$, 746.1 (10) $[Cu\{(Cp^*Mo)_2P_6\}(NCCH_3)]^+$, 716.2 (1) $[Cu\{(Cp^*Mo)_2P_6\}]^+$, 185.9 (6) $[Cu(NCCH_3)_3]^+$, 144.9 (100) $[Cu(NCCH_3)_2]^+$.
**Negative ion ESI-MS** ($CH_3CN$, RT): *m/z* (%) = 626.5 (0.5) $[Cu_6Cl_7]^-$, 528.5 (2) $[Cu_5Cl_6]^-$, 430.6 (1) $[Cu_4Cl_5]^-$, 330.6 (2) $[Cu_3Cl_4]^-$, 312.8 (1)

$[Cu_2Cl_3(NCCH_3)_2]^-$, 232.8 (10) $[Cu_2Cl_3]^-$, 223.8 (12) $[CuCl_2(NCCH_3)_2]^-$, 134.9 (100) $[CuCl_2]^-$.
**IR** (KBr): $\tilde{\nu}$ = 2974 (w), 2901 (w), 1480 (m), 1449 (w), 1422 (w), 1392 (m), 1379 (s), 1309 (w), 1245 (m), 1028 (m), 985 (w), 803 (w), 734 (m), 702 (w), 670 (w) $cm^{-1}$.
**Melting point**: >220 °C.

## 4.9.2. $[(Cp^*Mo)_2(\mu,\eta^6\text{-}P_6)][Al\{OC(CF_3)_3\}_4]$ (89)

A mixture of $Ag[Al\{OC(CF_3)_3\}_4]\bullet CH_2Cl_2$ (135 mg, 0.12 mmol), $[(Cp^*Mo)_2(\mu,\eta^6\text{-}P_6)]$ **11c** (75 mg, 0.12 mmol) and $CH_2Cl_2$ (20 ml) was stirred for 72 h at room temperature in the dark. The dark teal solution was filtered over diatomaceous earth, which was subsequently washed with $CH_2Cl_2$ (2 × 2 ml), and the combined filtrate and washings were concentrated to about one fifth of the original volume (~ 5 ml). The concentrated solution was carefully layered with pentane (5 ml) and stored in a freezer (–28 °C). Dark teal plates of **89**•$2CH_2Cl_2$ crystallised within three weeks and these crystals were filtered, washed with pentane (2 × 3 ml) and dried under vacuum at room temperature. The solvent of crystallisation was not lost during the drying process. Addition of pentane (10 ml) to the mother liquor led to the isolation of a further crop of **89**.

**Yield**: 160 mg (86 %).
**$^1$H-NMR** ($CD_2Cl_2$, 400.13 MHz, 27 °C): $\delta$ = 4.16 (b; $CH_3$) ppm.
**$^{13}$C{$^1$H}-NMR** ($CD_2Cl_2$, 100.63 MHz, 27 °C): $\delta$ = 15.22 (s; $CH_3$), 90.22 (s; Cp*), 121.68 (q; $^1J_{FC}$ = 292 Hz; $CF_3$) ppm.
**$^{27}$Al-NMR** ($CD_2Cl_2$, 104.26 MHz, 27 °C): $\delta$ = 33.64 (s; $[Al\{OC(CF_3)_3\}_4]^-$) ppm.
**$^{19}$F-NMR** ($CD_2Cl_2$, 376.47 MHz, 27 °C): $\delta$ = –75.43 (s; $CF_3$) ppm.
**Positive ion ESI-MS** ($CH_2Cl_2$, RT): *m/z* (%) = 647.9 (100) $[(Cp^*Mo)_2P_6]^+$.
**Negative ion ESI-MS** ($CH_2Cl_2$, RT): *m/z* (%) = 966.9 (100) $[Al\{OC(CF_3)_3\}_4]^-$.
**IR** (KBr): $\tilde{\nu}$ = 2983 (w), 2924 (w), 1482 (w), 1451 (w), 142 (w), 1383 (m), 1353 (m), 1302 (s), 1277 (s), 1242 (s), 1220 (s), 1170 (m), 1101 (m), 1028 (m), 974 (s), 838 (w), 756 (w), 728 (s), 560 (w), 537 (m), 448 (m) $cm^{-1}$.
**Molecular mass**: Theoretical for $C_{36}H_{30}AlF_{36}Mo_2O_4P_6$ = 1615.28 g $mol^{-1}$; found (osmometric, $CH_2Cl_2$, 28 °C) = 1524 ± 76 g $mol^{-1}$.
**Elemental analysis**: Calculated (%) for $C_{38}H_{34}AlCl_4F_{36}Mo_2O_4P_6$ (1785.14): C 25.57, H 1.92; found: C 25.70, H 1.82.
**Melting point**: >220 °C.

### 4.9.3. $[Ag\{(Cp^*Mo)_2(\mu_3,\eta^6:\eta^6:\eta^2\text{-}P_6)\}_2][Al\{OC(CF_3)_3\}_4]$ (90)

A mixture of $Ag[Al\{OC(CF_3)_3\}_4]\bullet CH_2Cl_2$ (32 mg, 0.03 mmol), $[(Cp^*Mo)_2(\mu,\eta^6\text{-}P_6)]$ **11c** (36 mg, 0.06 mmol) and $CH_2Cl_2$ (10 ml) was stirred for 8 h at room temperature in the dark. The yellow-green solution was filtered over diatomaceous earth, which was subsequently washed with $CH_2Cl_2$ (2 × 2 ml). The combined filtrate and washings were stored in a freezer (–28 °C) and red-orange prisms of **90**$\bullet CH_2Cl_2$ crystallised within a day. These were filtered at –30 °C, washed with pentane (2 × 3 ml) and dried under vacuum at room temperature. The solvent of crystallisation was completely removed during the drying process.

**Yield**: 15 mg (23 %).
**IR** (KBr): $\tilde{\nu}$ = 2968 (w), 2912 (w), 1637 (w), 1618 (w), 1482 (w), 1425 (w), 1378 (m), 1353 (m), 1301 (s), 1277 (s), 1241 (s), 1220 (vs), 1165 (w), 1026 (w), 974 (vs), 830 (w), 728 (m), 560 (w), 537 (w), 445 (w) $cm^{-1}$.
**Elemental analysis**: Calculated (%) for $C_{56}H_{60}AgAlF_{36}Mo_4O_4P_{12}$ (2371.33): C 28.36, H 2.55; found: C 28.42, H 2.61.
**Melting point**: 160 °C (decomposition).

## 4.10. Synthesis of the Complexes Based on $[(Cp^*Mo)_2(\mu,\eta^3\text{-}P_3)(\mu,\eta^2\text{-}PS)]$

### 4.10.1. $[\{Cu(\mu\text{-}Cl)\}_3\{(Cp^*Mo)_2(\mu_3,\eta^3:\eta^3:\eta^1\text{-}P_3)(\mu,\eta^2\text{-}PS)\}\{(Cp^*Mo)_2(\mu_3,\eta^3:\eta^3:\eta^1\text{-}P_3)(\mu_3,\eta^2:\eta^2:\eta^1\text{-}PS)\}]_n$ (92a)

A solution of CuCl (16 mg, 0.16 mmol) in $CH_3CN$ (10 ml) was carefully layered over a solution of $[(Cp^*Mo)_2(\mu,\eta^3\text{-}P_3)(\mu,\eta^2\text{-}PS)]$ **91** (50 mg, 0.08 mmol) in $CH_2Cl_2$ (7 ml) at room temperature. The vessel was left at room temperature in the dark and **92a** was deposited as dark red prisms within a month. These crystals were filtered, washed with $CH_2Cl_2$ (2 × 3 ml) and dried under vacuum at room temperature.

**Yield**: 50 mg (83 %).
**Positive ion ESI-MS** ($CH_3CN$, RT): *m/z* (%) = 1592.0 (0.5) $[Cu_4Cl_3\{(Cp^*Mo)_2P_4S\}_2]^+$, 1491.0 (4) $[Cu_3Cl_2\{(Cp^*Mo)_2P_4S\}_2]^+$, 1398.1 (8) $[Cu_2Cl\{(Cp^*Mo)_2P_4S\}_2]^+$, 1301.1 (10)

$[Cu\{(Cp^*Mo)_2P_4S\}_2]^+$, 913.8 (7) $[Cu_3Cl_2\{(Cp^*Mo)_2P_4S\}(NCCH_3)]^+$, 821.9 (9) $[Cu_2Cl\ \{(Cp^*Mo)_2P_4S\}(NCCH_3)]^+$, 722.0 (100) $[Cu\{(Cp^*Mo)_2P_4S\}(NCCH_3)]^+$, 681.0 (3) $[Cu\ \{(Cp^*Mo)_2P_4S\}]^+$.
**Negative ion ESI-MS** ($CH_3CN$, RT): *m/z* (%) = 432.7 (1) $[Cu_4Cl_5]^-$, 369.2 (3) $[Cu_3Cl_4(NC\ CH_3)]^-$,332.7 (5) $[Cu_3Cl_4]^-$, 232.7 (11) $[Cu_2Cl_3]^-$, 223.7 (15) $[CuCl_2(NCCH_3)_2]^-$, 134.8 (100) $[CuCl_2]^-$.
**IR** (KBr): $\tilde{\nu}$ = 2972 (w), 2953 (w), 2903 (m), 2853 (w), 1637 (m), 1560 (w), 1542 (w), 1478 (m), 1448 (m), 1422 (m), 1406 (m), 1377 (s), 1303 (w), 1263 (w), 1241 (w), 1223 (w), 1160 (w), 1071 (w), 1027 (m), 976 (w), 802 (w), 730 (w), 669 (w), 654 (w), 626 (w), 552 (w), 506 (w), 431 (w) $cm^{-1}$.
**Elemental analysis**: Calculated (%) for $C_{40}H_{60}Cl_3Cu_3Mo_4P_8S_2$ (1533.59): C 31.33, H 3.94, S 4.18; found: C 30.94, H 4.13, S 3.75.
**Melting point**: 184 °C (decomposition).

### 4.10.2. $[\{Cu(\mu\text{-}Br)\}_3\{(Cp^*Mo)_2(\mu_3,\eta^3\!:\!\eta^3\!:\!\eta^1\text{-}P_3)(\mu,\eta^2\text{-}PS)\}\{(Cp^*Mo)_2(\mu_3,\eta^3\!:\!\eta^3\!:\!\eta^1\text{-}P_3)(\mu_3,\eta^2\!:\!\eta^2\!:\!\eta^1\text{-}PS)\}]_n$ (92b)

A solution of CuBr (23 mg, 0.16 mmol) in $CH_3CN$ (10 ml) was carefully layered over a solution of $[(Cp^*Mo)_2(\mu,\eta^3\text{-}P_3)(\mu,\eta^2\text{-}PS)]$ **91** (50 mg, 0.08 mmol) in $CH_2Cl_2$ (10 ml) at room temperature. The vessel was left at room temperature in the dark and **92b** was deposited as dark red prisms within a month. These crystals were filtered, washed with $CH_2Cl_2$ (2 × 3 ml) and dried under vacuum at room temperature.

**Yield**: 60 mg (67 %).
**Positive ion ESI-MS** ($CH_3CN$, RT): *m/z* (%) = 2061.4 (1) $[Cu_2Br\{(Cp^*Mo)_2P_4S\}_3]^+$, 1872 (0.5) $[Cu_5Br_4\{(Cp^*Mo)_2P_4S\}_2]^+$, 1731.0 (1) $[Cu_4Br_3\{(Cp^*Mo)_2P_4S\}_2]^+$, 1588.0 (3) $[Cu_3Br_2\{(Cp^*Mo)_2P_4S\}_2]^+$, 1444.1 (15) $[Cu_2Br\{(Cp^*Mo)_2P_4S\}_2]^+$, 1300.1 (13) $[Cu\ \{(Cp^*Mo)_2P_4S\}_2]^+$, 1153.8 (1) $[Cu_4Br_3\{(Cp^*Mo)_2P_4S\}(NCCH_3)]^+$, 1112.6 $[Cu_4Br_3\ \{(Cp^*Mo)_2P_4S\}]^+$, 1011.7 (6) $[Cu_3Br_2\{(Cp^*Mo)_2P_4S\}(NCCH_3)]^+$, 968.7 (14) $[Cu_3Br_2\ \{(Cp^*Mo)_2P_4S\}]^+$, 865.9 (56) $[Cu_2Br\{(Cp^*Mo)_2P_4S\}(NCCH_3)]^+$, 822.9 (2) $[Cu_2Br\ \{(Cp^*Mo)_2P_4S\}]^+$, 722.1 (100) $[Cu\{(Cp^*Mo)_2P_4S\}(NCCH_3)]^+$, 683.0 (1) $[Cu\{(Cp^*Mo)_2\ P_4S\}]^+$.
**Negative ion ESI-MS** ($CH_3CN$, RT): *m/z* (%) = 1513.9 (0.5) $[Cu_{10}Br_{11}]^-$, 1369.6 (0.5) $[Cu_9Br_{10}]^-$, 1228.1 (0.5) $[Cu_8Br_9]^-$, 1086.0 (0.5) $[Cu_7Br_8]^-$, 940.3 (1) $[Cu_6Br_7]^-$, 798.5 (1) $[Cu_5Br_6]^-$, 654.6 (2) $[Cu_4Br_5]^-$, 510.6 (10) $[Cu_3Br_4]^-$, 366.6 (33) $[Cu_2Br_3]^-$, 222.7 (100) $[CuBr_2]^-$.
**IR** (KBr): $\tilde{\nu}$ = 2973 (w), 2954 (w), 2902 (m), 2853 (w), 1629 (m), 1561 (w), 1542 (w), 1509 (w), 1478 (m), 1448 (m), 1422 (m), 1378 (s), 1264

(w), 1224 (w), 1161 (w), 1071 (w), 1027 (m), 803 (w), 737 (w), 703 (w), 625 (w), 553 (w), 510 (w), 427 (w), 407 (w) $cm^{-1}$.
**Melting point**: 215 °C (decomposition).

### 4.10.3. $[\{Cu(\mu\text{-}I)\}_3\{(Cp^*Mo)_2(\mu_3,\eta^3\text{:}\eta^3\text{:}\eta^1\text{-}P_3)(\mu,\eta^2\text{-}PS)\}\{(Cp^*Mo)_2(\mu_3,\eta^3\text{:}\eta^3\text{:}\eta^1\text{-}P_3)(\mu_3,\eta^2\text{:}\eta^2\text{:}\eta^1\text{-}PS)\}]_n$ (92c)

A solution of CuI (20 mg, 0.10 mmol) in $CH_3CN$ (10 ml) was carefully layered over a solution of $[(Cp^*Mo)_2(\mu,\eta^3\text{-}P_3)(\mu,\eta^2\text{-}PS)]$ **91** (33 mg, 0.05 mmol) in $CH_2Cl_2$ (10 ml) at room temperature. The vessel was left at room temperature in the dark and **92c** was deposited as dark red prisms within a month. These crystals were filtered, washed with $CH_2Cl_2$ (2 × 3 ml) and dried under vacuum at room temperature.

**Yield**: 40 mg (63 %).
**$^{31}$P MAS-NMR** (121.50 MHz, RT): –384.2 (b), –354.8 (b), –132.8 (b), –107.5 (m; $^1J_{CuP}$ = 1500 Hz), 281.7 (b), 301.3 (b), 331.1 (b).
**Positive ion ESI-MS** ($CH_3CN$, RT): *m/z* (%) = 2304.0 (0.5) $[Cu_3I_2\{(Cp^*Mo)_2P_4S\}_3]^+$, 2111.1 (1) $[Cu_2I\{(Cp^*Mo)_2P_4S\}_3]^+$, 1870.7 (1) $[Cu_4I_3\{(Cp^*Mo)_2P_4S\}_2]^+$, 1682.4 (2) $[Cu_3I_2\{(Cp^*Mo)_2P_4S\}_2]^+$, 1491.1 (26) $[Cu_2I\{(Cp^*Mo)_2P_4S\}_2]^+$, 1300.0 (16) $[Cu\{(Cp^*Mo)_2P_4S\}_2]^+$, 1103.8 (2) $[Cu_3I_2\{(Cp^*Mo)_2P_4S\}(NCCH_3)]^+$, 1062.8 (12) $[Cu_3I_2\{(Cp^*Mo)_2P_4S\}]^+$, 913.9 (72) $[Cu_2I\{(Cp^*Mo)_2P_4S\}(NCCH_3)]^+$, 874.8 (4) $[Cu_2I\{(Cp^*Mo)_2P_4S\}]^+$, 722.0 (100) $[Cu\{(Cp^*Mo)_2P_4S\}(NCCH_3)]^+$, 681.0 (3) $[Cu\{(Cp^*Mo)_2P_4S\}]^+$.
**Negative ion ESI-MS** ($CH_3CN$, RT): *m/z* (%) = 2220.1 (0.1) $[Cu_{11}I_{12}]^-$, 2033.8 (0.1) $[Cu_{10}I_{11}]^-$, 1843.8 (0.1) $[Cu_9I_{10}]^-$, 1649.9 (0.1) $[Cu_8I_9]^-$, 1460.0 (0.1) $[Cu_7I_8]^-$, 1270.3 (0.5) $[Cu_6I_7]^-$, 1078.3 (0.5) $[Cu_5I_6]^-$, 888.4 (1) $[Cu_4I_5]^-$, 698.6 (11) $[Cu_3I_4]^-$, 506.7 (26) $[Cu_2I_3]^-$, 316.7 (100) $[CuI_2]^-$.
**IR** (KBr): $\tilde{\nu}$ = 2972 (w), 2952 (w), 2902 (m), 2850 (w), 1629 (w), 1561 (w), 1542 (w), 1477 (m), 1446 (m), 1422 (m), 1377 (s), 1262 (w), 1160 (w), 1070 (w), 1026 (m), 801 (w), 736 (w), 625 (w), 556 (w), 540 (w), 507 (w), 427 (w) $cm^{-1}$.
**Elemental analysis**: Calculated (%) for $C_{40}H_{60}Cu_3I_3Mo_4P_8S_2$ (1807.95): C 26.57, H 3.34, S 3.55; found: C 26.45, H 3.49, S 3.56.
**Melting point**: 168 °C (decomposition).

### 4.10.4. $[Ag\{(Cp^*Mo)_2(\mu_3,\eta^3:\eta^3:\eta^1\text{-}P_3)(\mu,\eta^2\text{-}PS)\}\{(Cp^*Mo)_2(\mu_3,\eta^3:\eta^3:\eta^1\text{-}P_3)(\mu_3,\eta^2:\eta^2:\eta^1\text{-}PS)\}]_n[Al\{OC(CF_3)_3\}_4]_n$ (94)

A solution of $[(Cp^*Mo)_2(\mu,\eta^3\text{-}P_3)(\mu,\eta^2\text{-}PS)]$ **91** (25 mg, 0.04 mmol) in toluene (5 ml) was carefully layered over a solution of $Ag[Al\{OC(CF_3)_3\}_4]\bullet CH_2Cl_2$ (24 mg, 0.02 mmol) in $CH_2Cl_2$ (3 ml) at room temperature. The vessel was left at room temperature in the dark and brown needles of **94**•0.25n$C_7H_8$ appeared within a month. These crystals were filtered, washed with pentane (2 × 3 ml) and dried under vacuum at room temperature. The solvent of crystallisation was completely removed during the drying process.

**Yield**: 30 mg (64 %).
**$^1$H-NMR** ($CD_3CN$, 400.13 MHz, 27 °C): $\delta$ = 1.93 (s; $CH_3$) ppm.
**$^{13}$C{$^1$H}-NMR** ($CD_3CN$, 100.63 MHz, 27 °C): $\delta$ = 14.00 (s; $CH_3$), 107.00 (s; Cp*) ppm.
**$^{27}$Al-NMR** ($CD_3CN$, 104.26 MHz, 27 °C): $\delta$ = 34.38 (s; $[Al\{OC(CF_3)_3\}_4]^-$) ppm.
**$^{19}$F-NMR** ($CD_3CN$, 376.47 MHz, 27 °C): $\delta$ = –74.74 (s; $CF_3$) ppm.
**$^{31}$P{$^1$H}-NMR** ($CD_3CN$, 161.93 MHz, 27 °C): ABMX spin system $\delta$ = –373.8 (m; $^1J_{AX}$ = 375 Hz, $^1J_{BX}$ = 386 Hz, $^2J_{MX}$ = 22 Hz; $P_X$), –132.1 (dd; $^2J_{AM}$ = 57 Hz, $^2J_{XM}$ = 18 Hz; $P_M$), 304.9 (d; $^1J_{XB}$ = 384 Hz; $P_B$), 327.3 (dd; $^1J_{XA}$ = 380 Hz, $^2J_{MA}$ = 57 Hz; $P_A$) ppm.
**Positive ion ESI-MS** ($CH_3CN$, RT): *m/z* (%) = 1345.2 (100) $[Ag\{(Cp^*Mo)_2P_4S\}_2]^+$, 767.9 (19) $[Ag\{(Cp^*Mo)_2P_4S\}(NCCH_3)]^+$, 726.9 (3) $[Ag\{(Cp^*Mo)_2P_4S\}]^+$.
**Negative ion ESI-MS** ($CH_3CN$, RT): *m/z* (%) = 967.2 (100) $[Al\{OC(CF_3)_3\}_4]^-$.
**IR** (KBr): $\tilde{\nu}$ = 2972 (w), 2914 (w), 1481 (w), 1449 (w), 1425 (w), 1378 (m), 1353 (m), 1302 (s), 1278 (s), 1242 (s), 1220 (vs), 1167 (w), 1135 (w), 1103 (m), 1027 (w), 975 (vs), 830 (w), 805 (w), 756 (w), 728 (m), 560 (w), 537 (w), 447 (w) $cm^{-1}$.
**Elemental analysis**: Calculated (%) for $C_{56}H_{60}AgAlF_{36}Mo_4O_4P_8S_2$ (2311.56): C 29.10, H 2.62, S 2.77; found: C 29.30, H 2.49, S 3.06.
**Melting point**: >220 °C.

# 5. Conclusions

Following preliminary investigations performed in the Scheer group, a palette of supramolecular aggregates could be created (Figures 1.10-1.12)[32-34] based on the $P_n$-ligand complexes $[Cp_2Mo_2(CO)_4(\eta^2\text{-}P_2)]$ **6b**[9c] and $[Cp^*Fe(\eta^5\text{-}P_5)]$ **9a**[12a] (Figure 5.1). The objectives of the present work were to expand the collection of supramolecules based on **6b** and **9a** in order to establish structural trends, to assess the potential of other $P_n$-ligand complexes ($[Cp_2Cr_2(CO)_4(\eta^2\text{-}P_2)]$ **6a**,[9a] $[Cp^xM(CO)_2(\eta^3\text{-}P_3)]$ **7a-c**,[9a,c,e] $[(Cp^*Mo)_2(\eta^6\text{-}P_6)]$ **11c**,[9e] Figure 5.1) as supramolecular building blocks, and to determine whether the $As_n$-ligand complex $[Cp^*Mo(CO)_2(\eta^3\text{-}As_3)]$ **80**[60] and the $P_mS_n$-ligand complex $[(Cp^*Mo)_2(\mu,\eta^3\text{-}P_3)(\mu,\eta^2\text{-}PS)]$ **91**[71] (Figure 5.1) could function as efficient connecting units in the synthesis of well-defined aggregates.

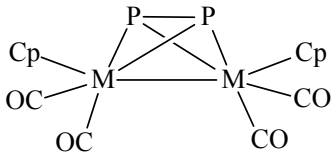


**6a**: M = Cr
**6b**: M = Mo

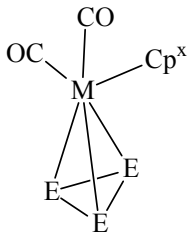


**7a**: M = Cr; $Cp^x$ = Cp; E = P
**7b**: M = Mo; $Cp^x$ = Cp; E = P
**7c**: M = Mo; $Cp^x$ = Cp*; E = P
**80**: M = Mo; $Cp^x$ = Cp*; E = As

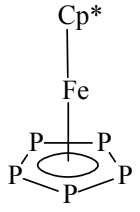


**9a**

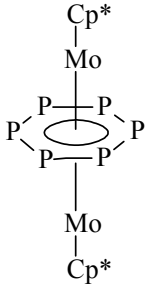


**11c**

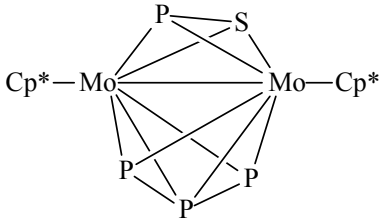


**91**

Figure 5.1. The complexes investigated for their potential as supramolecular building blocks.

## 5.1. Complexes Based on $[Cp_2M_2(CO)_4(\eta^2\text{-}P_2)]$ (M = Cr, Mo)

The complexes obtained using $[Cp_2M_2(CO)_4(\eta^2\text{-}P_2)]$ **6a**,**b** (Figure 5.1) as ligands are illustrated in Scheme 5.1. Reaction of **6a** and **6b** with $Ag^I$ and $Au^I$ salts of weakly coordinating anions (WCAs) invariably leads to the formation of dimeric complex salts (**42d-h**, **67**). The structures of all of these compounds, save **67**, have been confirmed by single crystal X-ray crystallography and consist of a dication whose six-membered ring core is constructed from two M´ (Ag, Au) centres and four P atoms. For the Ag-containing products **42d-g**, it could be shown that the folding angle of these $Ag_2P_4$ rings depends on anion size.

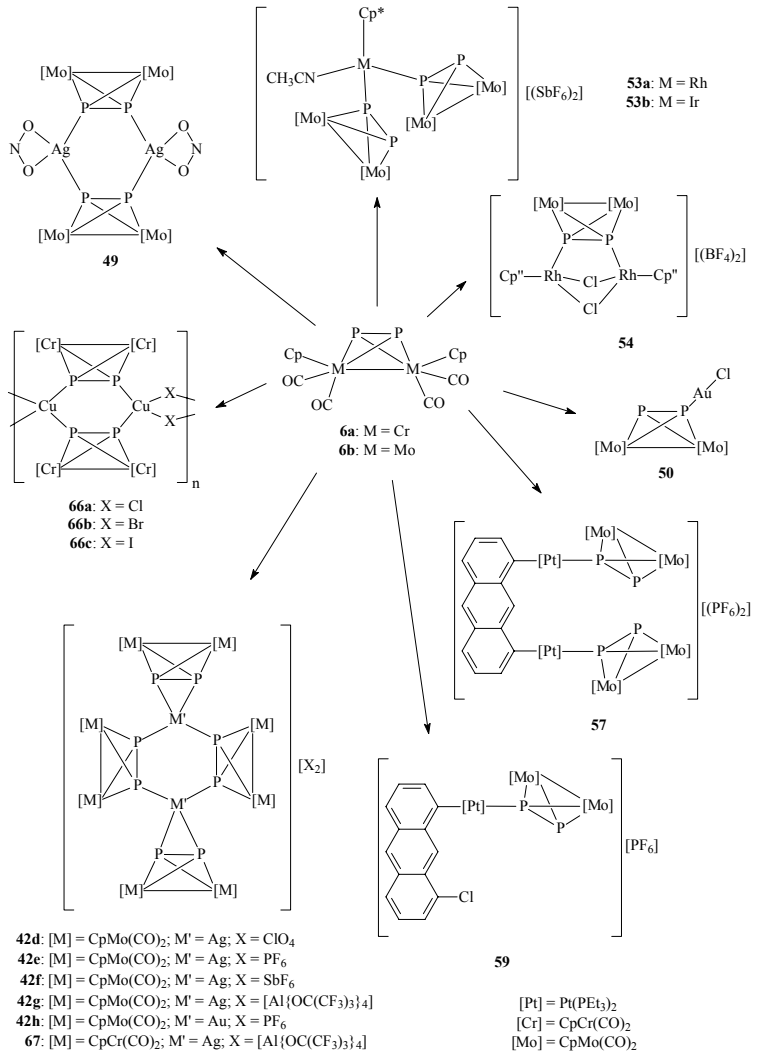


Scheme 5.1. Complexes based on $[Cp_2M_2(CO)_4(\eta^2\text{-}P_2)]$ (M = Cr, Mo).

Although these complex salts, with the exception of the Mo derivative **42g** and the Cr derivative **67** (anion: $[Al\{OC(CF_3)_3\}_4]^-$[36]), are only poorly soluble, ESI-MS and solution $^{31}$P-NMR spectroscopic evidence could nevertheless be obtained, which suggests that solutions of these complex salts demonstrate dynamic behaviour. The greatly improved solubility characteristics imparted to **42g** and **67** by the $[Al\{OC(CF_3)_3\}_4]^-$ anion permitted a much more extensive examination of the dynamic behaviour in solutions of these compounds, which included low temperature solution $^{31}$P-NMR and vapour pressure osmometric (VPO) measurements. Using **42g** as an example, it was thus revealed that an equilibrium between the monomeric species $[Ag\{Cp_2Mo_2(CO)_4P_2\}_2][Al\{OC(CF_3)_3\}_4]$ **48** and the dimeric species **42g** exists in solutions of **42g**, which is almost entirely in favour of **48** at room temperature and appears to shift in favour of **42g** as the temperature is reduced. Comparable results were obtained for **67**. In the case of **42g**, these findings are further supported by theoretical calculations, which demonstrate that the energy difference between **42g** and **48** is small, and therefore that dissolution of the dimer **42g** under dissociation to the monomer **48** is driven by entropy, while crystallisation of **42g** rather than **48** is driven by its greater lattice enthalpy.

The reactivity of **6b** towards $Ag^I$ and $Au^I$ salts of coordinating anions was also investigated and the complexes **49** and **50** could be isolated and characterised by single crystal X-ray diffraction. Despite their low solubilities, ESI-MS spectra could be obtained for both compounds, which suggest dynamic behaviour in solutions of these compounds and, in the case of **49**, the presence of larger aggregates in solution than that observed in the solid state. Furthermore, solution $^{31}$P-NMR spectra could also be acquired for **50**, which confirm dynamic behaviour in solutions of this compound.

It was of interest to explore the reactivity of **6b** with cationic organometallic transition metal fragments and therefore experiments with $[Cp^*M(NCCH_3)_3][(SbF_6)_2]$ (M = Rh, Ir),[47b] $[Cp''RhCl(NCCH_3)_2][BF_4]$,[47b] and the Pt aryl complexes $[(C_{14}H_8)Pt_2(PEt_3)_4(\eta^1\text{-}NO_3)_2]$ **55**[51d] and $[(C_{14}H_8Cl)Pt(PEt_3)_2(\eta^1\text{-}NO_3)_2]$ **58**[51d] were performed. The compounds **53a**,**b**, **54**, **57** and **59** (Scheme 5.1) could thus be isolated and the solid state structures of **54**, **57** and **59** were established unambiguously by single crystal X-ray crystallography. Unfortunately, due to poor crystal quality, the connectivity of the atoms in **53b** could only be established for atoms heavier than carbon. ESI-MS and solution $^{31}$P-NMR studies on the compounds **53a**,**b**, **57** and **59** demonstrate that these complexes dissolve under extensive dissociation and display dynamic behaviour.

The 1D polymers **43a-c** (Figure 1.10),[32a,33] obtained previously in the Scheer group, were characterised by solid-state $^{31}$P MAS-NMR spectroscopy in the present work.[33] This investigation revealed that the spectrum of **43c** meets one's expectations, whereas those of **43a**,**b** are astonishingly different. Each of the solid state structures of **43a-c** contains two types of crystallographically distinct P atoms, which, nevertheless, appear chemically similar. Closer scrutiny of these structures reveals that the experimental spectra are most likely the result of subtle differences in the arrangement of the Cp and, particularly, the CO ligands about the Mo atoms. This is supported by theoretical calculations on the model compounds $[Cu_6X_2(\mu\text{-}X)_4\{Cp_2Cr_2(CO)_4(\mu_4,\eta^2{:}\eta^2{:}\eta^1{:}\eta^1\text{-}P_2)\}_6]$ (X = Cl **66a´**, Br **66b´**; Figure 3.14),[33] in which Mo is substituted by its lighter homologue Cr. The calculated $^{31}$P-NMR spectra of these model compounds display peak patterns comparable to those of **43a**,**b**. As a result of this investigation, it was considered to be of significance to obtain compounds analogous to **43a-c** experimentally, with the Cr complex **6a** as the bridging ligand instead of the Mo complex **6b**. Complex **6a** indeed reacts with CuX (X = Cl, Br, I) to form the insoluble 1D polymers **66a-c** (Scheme 5.1), which have been characterised by single crystal X-ray crystallography and shown to possess structures akin to those of polymers **43a-c**. In addition, the solid state $^{31}$P MAS-NMR spectra of complexes **66a-c** exhibit patterns comparable to those of their Mo analogues, and those of **66a**,**b** compare well with those of the calculated compounds **66a´**,**b´**.

## 5.2. Complexes Based on $[Cp^xM(CO)_2(\eta^3\text{-}E_3)]$ ($Cp^x$ = Cp, Cp*;M = Cr, Mo; E = P, As)

An overview of the compounds obtained using $[Cp^xM(CO)_2(\eta^3\text{-}E_3)]$ **7a-c**, **80** (Figure 5.1) as ligands is presented in Scheme 5.2. The complexes **7a**,**b** react with $Ag[Al\{OC(CF_3)_3\}_4]$ to yield the polymers **69** and **71**. The solid state structure of **71** was confirmed by single crystal X-ray crystallography and it is assumed that **69** is structurally comparable to **71** due to the similarity of their spectral characteristics. ESI-MS, solution $^{31}$P-NMR and VPO measurements indicate that these compounds dissolve under depolymerisation and most likely establish equilibria between the monomeric species $[Ag\{CpM(CO)_2P_3\}_2][Al\{OC(CF_3)_3\}_4]$ and the dimeric species $[Ag_2\{CpM(CO)_2P_3\}_4]$ $[\langle Al\{OC(CF_3)_3\}_4\rangle_2]$ (M = Cr, Mo). The solid-state structure of **71** has also been investigated by $^{31}$P MAS-NMR and, surprisingly, dynamic behaviour was also revealed, which is probably attributable to fast rotation of the *cyclo*-$P_3$ rings in this polymer. This

ring rotation most likely gives rise to the solution $^{31}$P-NMR spectra observed for both **69** and **71**.

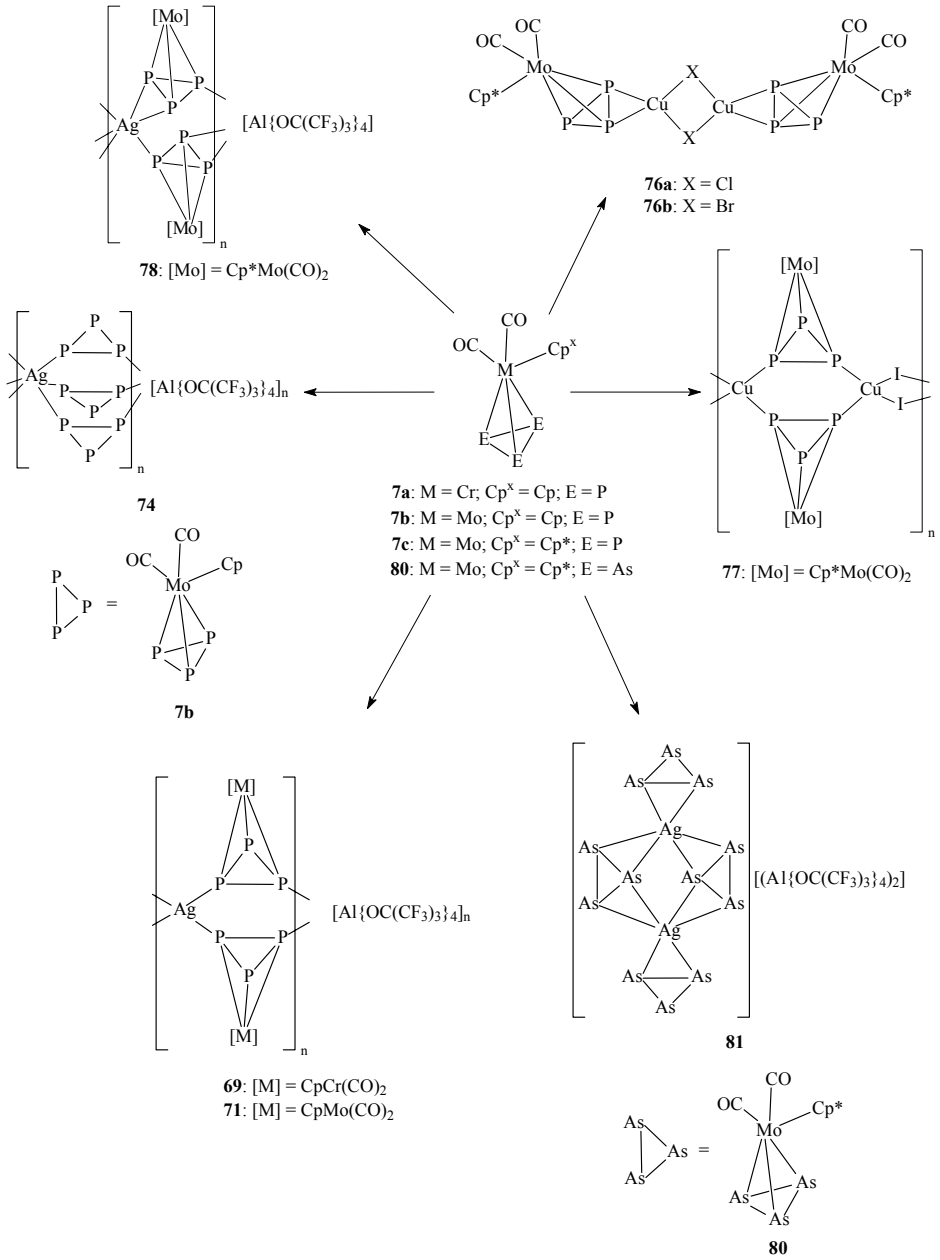


Scheme 5.2. Complexes based on $[Cp^xM(CO)_2(\eta^3\text{-}E_3)]$ ($Cp^x$ = Cp, Cp*; M = Cr, Mo; E = P, As).

The polymer **74** (Scheme 5.2) can be synthesised by reaction of **7b** with $Ag[Al\{OC(CF_3)_3\}_4]$ under the same conditions that **71** is synthesised, but a 6:1 reactant stoichiometry seems to be necessary. In

**71**, the $Ag^I$ centres are tetrahedrally coordinated to four **7b** ligands, while in **74** they are octahedrally coordinated to six of these ligands. Polymer **74** is the first example of a complex in which Ag is octahedrally coordinated to six P atoms. In parallel with polymer **71**, spectroscopic and VPO data suggest that **74** dissolves under depolymerisation to the monomer $[Ag\{CpMo(CO)_2P_3\}_3][Al\{OC(CF_3)_3\}_4]$ and exhibits dynamic behaviour. Unlike room temperature solutions of **71**, in which the corresponding monomer and dimer are present in a nearly 1:1 ratio, the presence of a monomer in solutions of **74** appears to be exclusive. An equilibrium between this monomer and a dimer or even larger oligomers is, however, not unlikely, particularly at lower temperatures. Polymer **74** also exhibits dynamic behaviour in the solid state, as evidenced by $^{31}P$ MAS-NMR spectroscopy. As with **71**, this most probably entails fast rotation of the *cyclo*-$P_3$ rings in **74**.

Complex **7c**, the Cp* analogue of **7b** (Figure 5.1), reacts with $Ag[Al\{OC(CF_3)_3\}_4]$ to yield the 1D polymer **78** (Scheme 5.2) in which all the P atoms of the *cyclo*-$P_3$ units of the **7c** ligands are involved in coordination, as opposed to **71** wherein two P atoms per *cyclo*-$P_3$ unit are coordinated. The structure of **78** depicted in Scheme 5.2 was confirmed by X-ray crystallography and $^{31}P$ MAS-NMR measurements. Complex **78** also dissolves under depolymerisation and displays dynamic behaviour, as evidenced by ESI-MS, $^{31}P$-NMR and VPO. In addition, no solid-state dynamic behaviour was revealed for **78** at room temperature.

Investigations on the reactivity of **7c** with CuX (X = Cl, Br, I) revealed that the insoluble products **76a**,**b** and **77** (Scheme 5.2) are obtained. The solid state structures of all three compounds could be determined by X-ray diffraction analysis and interestingly, the chloride and bromide derivatives **76a**,**b** are dimeric, while the iodide derivative **77** is polymeric. Moreover, the coordination mode of the *cyclo*-$P_3$ rings in these compounds is different in that these moieties are coordinated side-on to the Cu atoms in **76a**,**b** whereas in **77** they are in a bridging coordination mode. This discrepancy is thought to arise from an interplay of the steric demand of the Cp* ligand in **7c** and the size of the halogen atom.

As a consequence of the apparent suitability of $P_n$-ligand complexes as supramolecular building blocks, the potential of the $As_n$-ligand complex **80** (Figure 5.1) as such was investigated. This complex was particularly intriguing since it is the As analogue of **7c** and the effect of exchanging P for its heavier homologue on the resulting structures could be explored. Indeed, reaction of **80** with $Ag[Al\{OC(CF_3)_3\}_4]$ yields the dimer **81** (Scheme 5.2) and not a

polymer as in the case of **7c**. Single crystal X-ray crystallographic analysis revealed that the dication in **81** contains two $Ag^+$ cations and four units of **80**, two in a bridging and two in a terminal coordination mode. Unlike the **7c**-based polymer **78**, the units of **80** in **81** coordinate exclusively via As─As edges. According to ESI-MS and VPO measurements, the dimer **81** exhibits dynamic behaviour in solution, and an equilibrium between the monomer $[Ag\{Cp^*Mo(CO)_2As_3\}_2][Al\{OC(CF_3)_3\}_4]$ and the dimer $[Ag_2\{Cp^*Mo(CO)_2As_3\}_4]$ $[\langle Al\{OC(CF_3)_3\}_4\rangle_2]$ is most likely established, somewhat in favour of the monomer. Theoretical calculations suggest that dimerisation is actually favoured in solution, which may explain why crystallisation of the dimer rather than the monomer is observed.

## 5.3. Complexes Based on [Cp*Fe($\eta^5$-$P_5$)]

Experiments involving the $P_n$-ligand complex [Cp*Fe($\eta^5$-$P_5$)] **9a** (Figure 5.1) yielded the products illustrated in Scheme 5.3. Reaction of **9a** with $Ag[Al\{OC(CF_3)_3\}_4]$ yields the complex **83** whose 1D polymeric structure was ascertained by single crystal X-ray crystallography. Polymer **83** dissolves under depolymerisation and displays dynamic behaviour, as indicated by ESI-MS, solution $^{31}$P-NMR and VPO measurements. Equilibria are most likely established between the monomeric species $[Ag\{Cp^*FeP_5\}_2][Al\{OC(CF_3)_3\}_4]$ and the dimeric species $[Ag_2\{Cp^*FeP_5\}_4][\langle Al\{OC(CF_3)_3\}_4\rangle_2]$, albeit entirely in favour of the monomer at room temperature. Theoretical calculations on the monocation (**XXII**) in the monomer and the dication (**XXIII**) in the dimer demonstrate that the structural minima of these species lie on relatively flat potential energy surfaces and thus that other structures of comparable energy are readily accessible. Furthermore, the energy difference between the monomer of lowest energy and the dimer of lowest energy is small. Fast exchange processes are therefore likely in solution, which would explain the appearance of the solution $^{31}$P-NMR spectra. Besides, polymer **83** appears to demonstrate dynamic behaviour in the solid state, as suggested by solid state $^{31}$P MAS-NMR measurements, which is most likely attributable to fast rotation of the *cyclo*-$P_5$ moieties in the compound. This rotational motion is most likely responsible for the appearance of the solution $^{31}$P-NMR spectra.

The complexes **85**-**87** (Scheme 5.3) could also be obtained, but due to poor solubility could not be adequately characterised. For **86** and **87**, the stoichiometry of the compounds was established by elemental analysis. This was not possible for **85**.

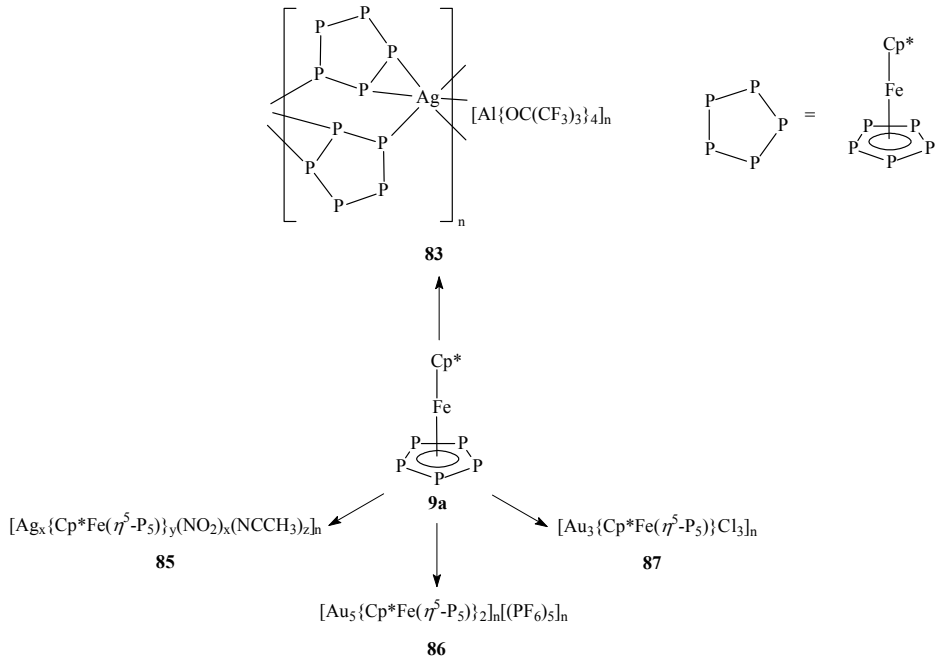


Scheme 5.3. Complexes based on [Cp*Fe($\eta^5$-$P_5$)].

## 5.4. Complexes Based on [(Cp*Mo)$_2$($\mu$,$\eta^6$-$P_6$)]

The complexes derived from [(Cp*Mo)$_2$($\mu$,$\eta^6$-$P_6$)] **11c** are depicted in Scheme 5.4. Reaction of **11c** with CuCl yields the product **88**, X-ray diffraction analysis of which revealed a corrugated sheet structure. The repeat unit of this 2D polymer consists of one unit of **11c**, three $CH_3CN$ ligands and five units of CuCl, with one $Cu^I$ centre being disordered over two non-equivalent positions in a ratio of 3:1. The position with 75% occupancy (Cu′) is shown in Scheme 5.4.

A 1:1 reaction of **11c** and Ag[Al{OC(CF$_3$)$_3$}$_4$] results in oxidation of the $P_n$-ligand complex to yield the salt **89** (Scheme 5.4), as demonstrated by ESI-MS and VPO data. Remarkably, a complex of $Ag^I$ and **11c** (**90**, Scheme 5.4) can be obtained if a reaction stoichiometry of 2:1 instead of 1:1 is applied and the reaction solution is stored at –28 °C. Although stable in the solid state, solutions of **90** decompose to yield **89** and the starting material **11c**.

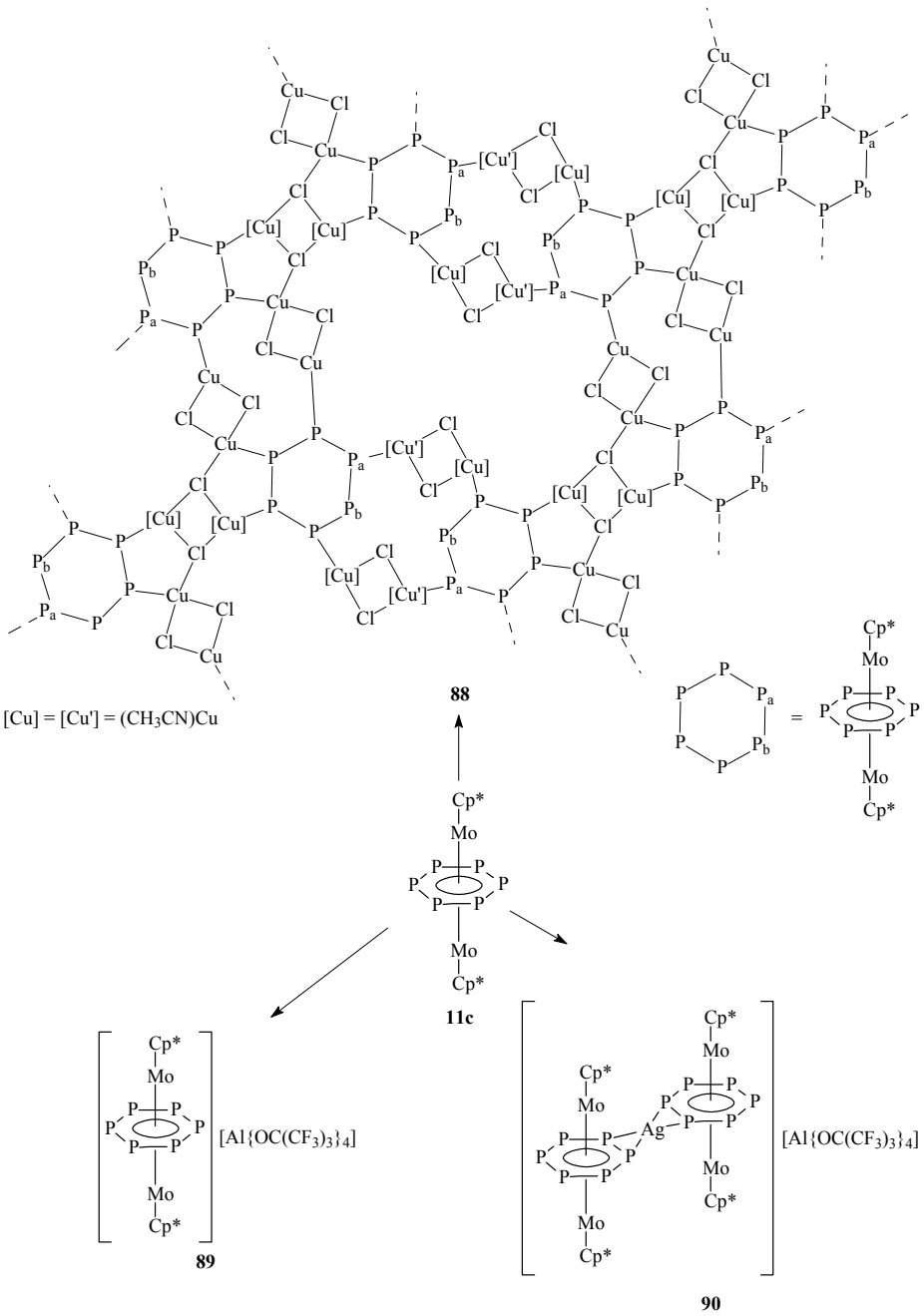


Scheme 5.4. Complexes based on $[(Cp^*Mo)_2(\mu,\eta^6\text{-}P_6)]$. In the schematic representation of **88**, Cu´ denotes the Cu atoms which are disordered over two non-equivalent positions in a ratio of 3:1 and here the major position is shown. In the minor position, Cu´ shifts in such a way so that it may coordinate with the $P_a$─$P_b$ edge.

## 5.5. Complexes Based on $[(Cp^*Mo)_2(\mu,\eta^3\text{-}P_3)(\mu,\eta^2\text{-}PS)]$

The results obtained from the investigations on the $P_mS_n$-ligand complex $[(Cp^*Mo)_2(\mu,\eta^3\text{-}P_3)(\mu,\eta^2\text{-}PS)]$ **91** (Figure 5.1) are given in Scheme 5.5. Reaction of **91** with CuX (X = Cl, Br, I) yields the practically insoluble compounds **92a-c**. The structure of the iodide derivative **92c** could be elucidated by single crystal X-ray crystallography and reveals a 1D polymeric architecture consisting of a stack of distorted six-membered $Cu_3I_3$ rings singly bridged by units of **91**. A further unit of **91** per $Cu_3I_3$ ring acts as a pendant ligand. The $Cu_3I_3$ rings are one of the most notable structural features of **92c** since discrete $Cu_3X_3$ rings are rarely observed in the solid state and have not been reported for X = I until the present work. It is impossible to distinguish between phosphorus and sulphur by X-ray diffraction and the assignment of these two elements in the PS ligands in **92c** was achieved with the assistance of solid state $^{31}P$ MAS-NMR spectroscopy. The spectra demonstrate that sulphur is not involved at all in coordination. It is believed that the lighter halide derivatives also possess a structure similar to that of the iodide derivative since all three compounds display similar fragmentation patterns in their ESI-MS spectra.

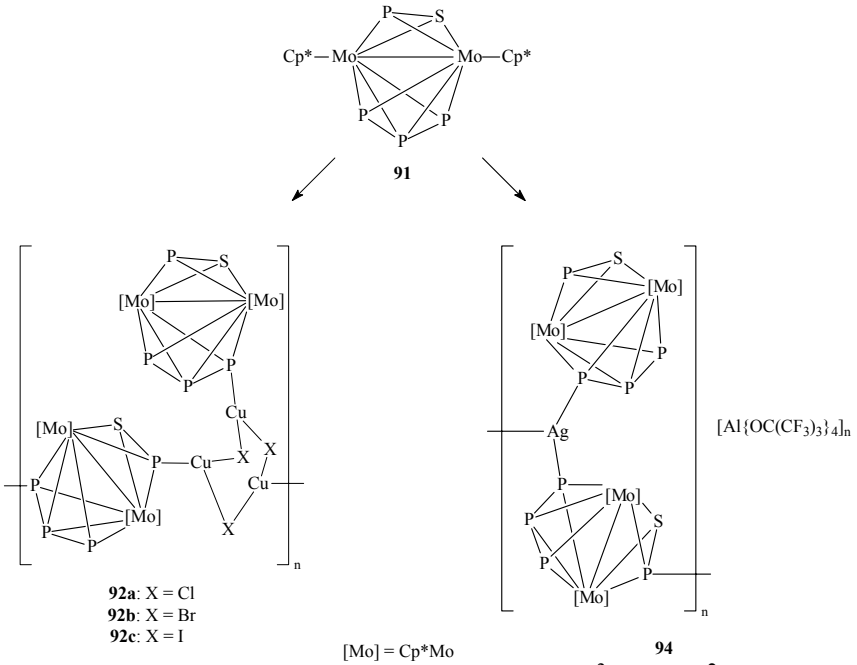


Scheme 5.5. Complexes based on $[(Cp^*Mo)_2(\mu,\eta^3\text{-}P_3)(\mu,\eta^2\text{-}PS)]$.

Complex **91** reacts with $Ag[Al\{OC(CF_3)_3\}_4]$ to yield the undulated 1D polymer **94** (Scheme 5.5), as shown by X-ray diffraction analysis. It consists of a chain of $Ag^I$ centres bridged singly by units of **91**, and the trigonal environment of each Ag cation is completed by a further unit of **91** coordinating as a pendant ligand. Polymer **94** dissolves under depolymerisation and demonstrates dynamic behaviour in solution, as evidenced by ESI-MS and $^{31}$P-NMR spectroscopy. The species in solution is most likely the monomer $[Ag\{(Cp^*Mo)_2P_4S\}_2][Al\{OC(CF_3)_3\}_4]$ and the solution $^{31}$P-NMR spectra suggest that the units of **91** in this species are coordinated to the Ag cation via the $P_3$ ligands and not via the PS ligands. The assignment of the P and S atoms in the PS ligands of **94** is based on the solution $^{31}$P-NMR spectra of the compound.

## 5.6. Outlook

The results described in the present work demonstrate that $P_n$-ligand complexes can undoubtedly be considered as efficient and interesting ligands for the construction of well-defined architectures. Although the significance of X-ray crystallography in supramolecular chemistry is unquestionable, solid state MAS-NMR and VPO were shown to be invaluable tools for the comprehensive characterisation of the resulting compounds. Moreover, the importance of theoretical calculations is reflected in the deeper understanding gained not only for the systems subjected to these calculations, but also for those not treated theoretically.

Compared to the typical nitrogen, oxygen and sulphur donor ligands employed in the synthesis of supramolecules, $P_n$-ligand complexes are still 'strangers' in the 'strange land' of supramolecular science. Nevertheless, these complexes have gained a firm foothold in this field and the preliminary results obtained for $As_n$-ligand and $P_mS_n$-ligand complexes in this work as well as a recent report describing the use of an $Sb_n$-ligand complex as a connecting unit in supramolecular chemistry[93] signify that $P_n$-ligand complexes will soon rid themselves of this label.

# 6. Notes and References


[1] a) J. -M. Lehn, *Supramolecular Chemistry*, VCH, Weinheim, **1995**; b) *Comprehensive Supramolecular Chemistry* (Ed: J. -M. Lehn), Pergamon, Oxford, **1996**.

[2] Recent reviews: a) N. C. Gianneschi, M. S. Masar III, C. A. Mirkin, *Acc. Chem. Res.*, **2005**, *38*, 825-837; b) M. Ruben, J. Rojo, F. J. Romero-Salguero, L. H. Uppadine, J. -M. Lehn, *Angew. Chem.*, **2004**, *116*, 3728-3747; *Angew. Chem. Int. Ed.* **2004**, *43*, 3644-3662; c) L. Carlucci, G. Ciani, D. M. Proserpio, *Coord. Chem. Rev.* **2003**, *246*, 247-289; d) B. J. Holliday, C. A. Mirkin, *Angew. Chem.*, **2001**, *113*, 2076-2097; *Angew. Chem. Int. Ed.* **2001**, *40*, 2022-2043; e) S. Leininger, B. Olenyuk, P. J. Stang, *Chem. Rev.* **2000**, *100*, 853-908.

[3] See, for example: a) C. Di Nicola, Effendy, F. Fazaroh, C. Pettinari, B. W. Skelton, N. Somers, A. H. White, *Inorg. Chim. Acta*, **2005**, *358*, 720-734; b) L. Zhang, X.-Q. Lü, C.-L. Chen, H.-Y. Tan, H.-X. Zhang, B.-S. Kang, *Cryst. Growth Des.*, **2005**, *5*, 283-287; c) P. D. Harvey, *Macromol. Symp.*, **2004**, *209*, 81-95; d) Effendy, J. V. Hanna, F. Marchetti, D. Martini, C. Pettinari, R. Pettinari, B. W. Skelton, A. H. White, *Inorg. Chim. Acta*, **2004**, *357*, 1523-1537; e) J. Zhang, M. Nieuwenhuyzen, J. P. H. Charmant, S. L. James, *Chem. Commun.*, **2004**, 2808-2809; f) P. D. Harvey, *Macromol. Symp.*, **2003**, *196*, 173-185; g) C. J. Blake, V. C. Cook, M. A. Keniry, H. J. Kitto, A. D. Rae, G. F. Swiegers, A. C. Willis, J. Zank, S. B. Wild, *Inorg. Chem.*, **2003**, *42*, 8709-8715; h) C. D. Delfs, H. J. Kitto, R. Stranger, G. F. Swiegers, S. B. Wild, A. C. Willis, G. J. Wilson, *Inorg. Chem.*, **2003**, *42*, 4469-4478; i) M.-C. Brandys, R. J. Puddephatt, *J. Am. Chem. Soc.*, **2002**, *124*, 3946-3950; j) P. D. Harvey, *Coord. Chem. Rev.*, **2001**, *219-221*, 17-52; k) E. Lozano, M. Nieuwenhuyzen, S. L. James, *Chem. Eur. J.*, **2001**, *7*, 2644-2651; l) F. Harrington, M. L. Matthews, B. Patel, G. Reid, *Polyhedron*, **2001**, *20*, 2741-2746; m) S. L. James, E. Lozano, M. Nieuwenhuyzen, *Chem. Commun.*, **2000**, 617-618; n) S. J. Berners-Price, R. J. Bowen, P. Galettis, P. C. Healy, M. J. McKeage, *Coord. Chem. Rev.*, **1999**, *185-186*, 823-836; o) S. J. Berners-Price, R. J. Bowen, T. W. Hambley, P. C. Healy, *J. Chem. Soc., Dalton Trans.*, **1999**, 1337-1346; p) S. J. Berners-Price, R. J. Bowen, P. J. Harvey, P. C. Healy, G. A. Koutsantonis, *J. Chem. Soc. Dalton Trans.*, **1998**, 1743-1750; q) B.-L. Chen, K.-F. Mok, S.-C. Ng, *J. Chem. Soc. Dalton Trans.*, **1998**, 2861-2866; r) A. L. Airey, G. F. Swiegers, A. C. Willis, S. B. Wild, *Inorg. Chem.*, **1997**, *36*, 1588-1597; s) A. L. Airey, G. F.

Swiegers, A. C. Willis, S. B. Wild, *J. Chem. Soc. Chem. Commun.*, **1995**, 695-696; t) V. Saboonchian, G. Wilkinson, B. Hussain-Bates, M. B. Hursthouse, *Polyhedron*, **1991**, *10*, 737-739; u) A. L. Balch, E. Y. Fung, *Inorg. Chem.*, **1990**, *29*, 4764-4768.

[4] Selected reviews: a) M. Ehses, A. Romerosa, M. Peruzzini, *Top. Curr. Chem.*, **2002**, *220*, 107-140; b) O. J. Scherer, *Angew. Chem.*, **2000**, *112*, 1069-1071; *Angew. Chem. Int. Ed.*, **2000**, *39*, 1029-1030; c) O. J. Scherer, *Acc. Chem. Res.*, **1999**, *32*, 751-762; d) K. H. Whitmire, *Adv. Organomet. Chem.*, **1998**, *42*, 1-145; e) M. Di Vaira, P. Stoppioni, *Coord. Chem. Rev.*, **1992**, *120*, 259-279; f) O. J. Scherer, C. Blath, J. Braun, B. Höbel, K. Pfeiffer, B. Rink, H. Slodzyk, P. Walther, B. Werner, R. Winter, in *Studies in Inorganic Chemistry 14: The Chemistry of Inorganic Ring Systems* (Ed: R. Steudel), 193-208, Elsevier, Amsterdam, **1992**; g) O. J. Scherer, *Angew. Chem.*, **1990**, *102*, 1137-1155; *Angew. Chem. Int. Ed. Engl.*, **1990**, *29*, 1104-1122; h) M. Scheer, E. Herrmann, *Z. Chem.*, **1990**, *29*, 41-55; i) M. Di Vaira, P. Stoppioni, *Polyhedron*, **1987**, *6*, 351-382.

[5] a) A. S. Foust, M. S. Foster, L. F. Dahl, *J. Am. Chem. Soc.*, **1969**, *91*, 5631-5633; b) A. S. Foust, M. S. Foster, L. F. Dahl, **1969**, *91*, 5633-5635.

[6] A. P. Ginsberg, W. E. Lindsell, *J. Am. Chem. Soc.*, **1971**, *93*, 2082-2084; b) W. E. Lindsell, *J. Chem. Soc., Chem. Commun.*, **1982**, 1422-1424.

[7] a) P. Dapporto, S. Midollini, L. Sacconi, *Angew. Chem.*, **1979**, *91*, 510; *Angew. Chem. Int. Ed. Engl.*, **1979**, *18*, 469; b) P. Dapporto, L. Sacconi, P. Stoppioni, F. Zanobini, *Inorg. Chem.*, **1981**, *20*, 3834-3839.

[8] A. Vizi-Orosz, G. Pàlyi, L. Markò, *J. Organomet. Chem.*, **1973**, *60*, C25-C26.

[9] a) L. Y. Goh, C. K. Chu, R. C. S. Wong, T. W. Hambley, *J. Chem. Soc. Dalton Trans.*, **1989**, 1951-1956; b) L. Y. Goh, R. C. S. Wong, *Inorg. Synth.*, **1992**, *29*, 247-250; c) O. J. Scherer, H. Sitzmann, G. Wolmershäuser, *J. Organomet. Chem.*, **1984**, *268*, C9-C12; d) O. J. Scherer, J. Schwalb, H. Sitzmann, *Inorg. Synth.*, **1990**, *27*, 224-227; e) O. J. Scherer, H. Sitzmann, G. Wolmershäuser, *Angew. Chem.*, **1985**, *97*, 358-359; *Angew. Chem. Int. Ed. Engl.*, **1985**, *24*, 115-117; f) J. E. Davies, M. J. Mays, P. R. Raithby, G. P. Shields, P. K. Tompkin, *Chem. Commun.*, **1997**, 361-362; g) O. J. Scherer, J. Schwalb, H.

Swarowsky, G. Wolmershäuser, W. Kaim, R. Gross, *Chem. Ber.*, **1988**, *121*, 443-449.

[10] a) M. Scheer, G. Friedrich, K. Schuster, *Angew. Chem.*, **1993**, *105*, 641-643; *Angew. Chem. Int. Ed. Engl.*, **1993**, *32*, 593-594; b) P. Jutzi, R. Kroos, *Chem. Ber.*, **1988**, *121*, 1399-1401.

[11] a) O. J. Scherer, J. Vondung, G. Wolmershäuser, *Angew. Chem.*, **1989**, *101*, 1395-1397; *Angew. Chem. Int. Ed.*, **1989**, *28*, 1355-1357; b) O. J. Scherer, R. Winter, G. Wolmershäuser, *Z. Anorg. Allg. Chem.*, **1993**, *619*, 827-835.

[12] a) O. J. Scherer, T. Brück, *Angew. Chem.*, **1987**, *99*, 59; *Angew. Chem. Int. Ed. Engl.*, **1987**, *26*, 59; b) M. Baudler, S. Akpapoglou, D. Ouzounis, F. Wasgestian, B. Meinigke, H. Budzikiewicz, H. Münster, *Angew. Chem.*, **1988**, *100*, 288-289; *Angew. Chem. Int. Ed. Engl.*, **1988**, *27*, 280-281; c) M. Detzel, G. Friedrich, O. J. Scherer, G. Wolmershäuser, *Angew. Chem.*, **1995**, *107*, 1454-1456; *Angew. Chem. Int. Ed. Engl.*, **1995**, *34*, 1321-1323; d) O. J. Scherer, T. Brück, G. Wolmershäuser, *Chem. Ber.*, **1988**, *121*, 935-938; e) V. A. Miluykov, O. G. Sinyashin, O. Scherer, E. Hey-Hawkins, *Mendeleev Comm.*, **2002**, 1-2; f) O. J. Scherer, T. Hilt, G. Wolmershäuser, *Organometallics*, **1998**, *17*, 4110-4112; g) B. Rink, O. J. Scherer, G. Wolmershäuser, *Chem. Ber.*, **1995**, *128*, 71-73.

[13] a) L. Y. Goh, R. C. S. Wong, C. K. Chu, T. W. Hambley, *J. Chem. Soc., Dalton Trans.*, **1990**, 977-982; b) O. J. Scherer, J. Schwalb, G. Wolmershäuser, W. Kaim, R. Gross, *Angew. Chem.*, **1986**, *98*, 349-350; *Angew. Chem. Int. Ed. Engl.*, **1986**, *25*, 363-364.

[14] O. J. Scherer, T. Brück, G. Wolmershäuser, *Chem. Ber.*, **1989**, *122*, 2049-2054.

[15] E. Urnėžius, W. W. Brennessel, C. J. Cramer, J. E. Ellis, P. von R. Schleyer, *Science*, **2002**, *295*, 832-834.

[16] See, for example: a) Ref. [14]; b) O. J. Scherer, H. Sitzmann, G. Wolmershäuser, *Angew. Chem.*, **1984**, *96*, 979-980; *Angew. Chem. Int. Ed. Engl.*, **1984**, *23*, 968-969; c) A. Vizi-Orosz, G. Pàlyi, L. Markò, *J. Organomet. Chem.*, **1985**, *288*, 179-187; d) L. Y. Goh, R. C. S. Wong, T. C. W. Mak, *J. Organomet. Chem.*, **1989**, *364*, 363-371; e) M. Scheer, M. Dargatz, A. Rufińska, *J. Organomet. Chem.*, **1992**, *440*, 327-333; f) M. Scheer, C. Troitzsch, P. G. Jones, *Angew. Chem.*, **1992**, *104*, 1395-1397; *Angew. Chem. Int. Ed. Engl.*, **1992**, *31*, 1377-1379; g) O. J. Scherer, J. Braun, P. Walther, G. Wolmershäuser, *Chem. Ber.*, **1992**, *125*, 2661-2665; h) M. Scheer, U. Becker, J. C. Huffman,

M. H. Chisholm, *J. Organomet. Chem.*, **1993**, *461*, C1-C3; i) M. Scheer, C. Troitzsch, L. Hilfert, M. Dargatz, E. Kleinpeter, P. G. Jones, J. Sieler, *Chem. Ber.*, **1995**, *128*, 251-257; j) M. Scheer, U. Becker, E. Matern, *Chem. Ber.*, **1996**, *129*, 721-724; k) M. Scheer, U. Becker, J. Magull, *Polyhedron*, **1998**, *17*, 1983-1989.

[17] a) M. Di Vaira, M. P. Ehses, M. Peruzzini, P. Stoppioni, *Polyhedron*, **1999**, *18*, 2331-2336; b) M. Di Vaira, P. Stoppioni, M. Peruzzini, *J. Chem. Soc., Dalton Trans.*, **1990**, 109-113.

[18] F. Cecconi, C. A. Ghilardi, S. Midollini, A. Orlandini, *Angew. Chem.*, **1983**, *95*, 554-555; *Angew. Chem. Int. Ed. Engl.*, **1983**, *22*, 554-555.

[19] F. Cecconi, C. A. Ghilardi, S. Midollini, A. Orlandini, *J. Chem. Soc., Chem. Commun.*, **1982**, 229-230.

[20] B. Rink, O. J. Scherer, G. Heckmann, G. Wolmershäuser, *Chem. Ber.*, **1992**, *125*, 1011-1016.

[21] M. Detzel, T. Mohr, O. J. Scherer, G. Wolmershäuser, *Angew. Chem.*, **1994**, *106*, 1142-1144; *Angew. Chem. Int. Ed. Engl.*, **1994**, *33*, 1110-1112.

[22] O. J. Scherer, T. Mohr, G. Wolmershäuser, *J. Organomet. Chem.*, **1997**, *529*, 379-385.

[23] a) G. Friedrich, O. J. Scherer, G. Wolmershäuser, *Z. Anorg. Allg. Chem.*, **1996**, *622*, 1478-1486; b) O. J. Scherer, S. Weigel, G. Wolmershäuser, *Chem. Eur. J.*, **1998**, *4*, 1910-1916.

[24] C. Hofmann, O. J. Scherer, G. Wolmershäuser, *J. Organomet. Chem.*, **1998**, *559*, 219-222.

[25] B. Koch, O. J. Scherer, G. Wolmershäuser, *Z. Anorg. Allg. Chem.*, **2000**, *626*, 1797-1802.

[26] a) R. F. Winter, W. E. Geiger, *Organometallics*, **1999**, *18*, 1827-1833; b) R. F. Winter, W. E. Geiger, *Organometallics*, **2003**, *22*, 1948-1952.

[27] J. E. Davies, M. C. Klunduk, M. J. Mays, P. R. Raithby, G. P. Shields, P. K. Tompkin, *J. Chem. Soc., Dalton Trans.*, **1997**, 715-719.

[28] P. Sekar, M. Scheer, A. Voigt, R. Kirmse, *Organometallics*, **1999**, *18*, 2833-2837.

[29] S. Umbarkar, P. Sekar, M. Scheer, *J. Chem. Soc., Dalton Trans.*, **2000**, 1135-1137.

[30] M. Scheer, S. B. Umbarkar, S. Chatterjee, R. Trivedi, P. Mathur, *Angew. Chem.*, **2001**, *113*, 399-401; *Angew. Chem. Int. Ed.*, **2001**, *40*, 376-378.

[31] Review: M. Peruzzini, R. R. Abdreimova, Y. Budnikova, A. Romerosa, O. J. Scherer, H. Sitzmann, *J. Organomet. Chem.*, **2004**, *689*, 4319-4331.

[32] a) J. Bai, E. Leiner, M. Scheer, *Angew. Chem.*, **2002**, *114*, 820-823; *Angew. Chem. Int. Ed.*, **2002**, *41*, 783-786; b) J. Bai, M. Scheer, unpublished results.

[33] M. Scheer, L. Gregoriades, J. Bai, M. Sierka, G. Brunklaus, H. Eckert, *Chem. Eur. J.*, **2005**, *11*, 2163-2169.

[34] a) J. Bai, A. V. Virovets, M. Scheer, *Angew. Chem.*, **2002**, *114*, 1808-1811; *Angew. Chem. Int. Ed.*, **2002**, *41*, 1737-1740; b) J. Bai, A. V. Virovets, M. Scheer, *Science*, **2003**, *300*, 781-783

[35] M. Scheer, J. Bai, B. P. Johnson, R. Merkle, A. V. Virovets, C. E. Anson, *Eur. J. Inorg. Chem.*, **2005**, 4023-4026.

[36] I. Krossing, *Chem. Eur. J.*, **2001**, *7*, 490-502.

[37] Review: J. Wachter, *Angew. Chem.*, **1998**, *110*, 782-800; *Angew. Chem. Int. Ed.*, **1998**, *37*, 750-768.

[38] a) C. Pelizzi, G. Pelizzi, P. Tarasconi, *J. Organomet. Chem.*, **1984**, *277*, 29-35; b) L. M. Engelhardt, C. Pakawatchai, A. H. White, P. C. Healy, *J. Chem. Soc., Dalton Trans.*, **1985**, 125-133; c) P. F. Barron, J. C. Dyason, P. C. Healy, L. M. Engelhardt, B. W. Skelton, A. H. White, *J. Chem. Soc., Dalton Trans.*, **1986**, 1965-1970; d) F. A. Cotton, R. L. Luck, *Acta Cryst.*, **1989**, *C45*, 1222-1224; e) D. D. Ellis, A. L. Spek, *Acta Cryst.*, **2000**, *C56*, e547-e548.

[39] a) H. K. Roobottom, H. D. B. Jenkins, J. Passmore, L. Glasser, *J. Chem. Ed.*, **1999**, *76*, 1570-1573; b) I. Krossing, H. Brands, R. Feuerhake, S. Koenig, *J. Fluorine Chem.* **2001**, *112*, 83-90.

[40] a) I. Krossing, *J. Am. Chem. Soc.*, **2001**, *123*, 4603-4604; b) I. Krossing, L. van Wüllen, *Chem. Eur. J.*, **2002**, *8*, 700-711; c) A. Bihlmeier, M. Gonsior, I. Raabe, N. Trapp, I. Krossing, *Chem. Eur. J.*, **2004**, *10*, 5041-5051.

[41] For technical reasons, $\Delta S_{Diss}$ could not be calculated. It is however reasonable to expect that dissociation of a dication to two monocations would lead to a large increase in entropy and therefore to $\Delta G_{Diss} < 0$ kJmol$^{-1}$.

[42] P. G. Jones, *J. Chem. Soc., Chem. Commun.*, **1980**, 1031-1033 ($[Au(PPh_3)_4][BPh_4]$ can be crystallised in three modifications (**I**, **II** and **III**). In **I**, the Au atom is actually in a trigonal coordination mode since the Au···P contact with the fourth $PPh_3$ ligand is markedly longer (3.946 Å). In **II** and **III**, the Au atoms are found in both trigonal and tetrahedral coordination environments. The

range quoted is defined by the Au─P bond lengths found in all three modifications, excluding the aforementioned long contact.).
[43] P. A. Bates, J. M. Waters, *Inorg. Chim. Acta*, **1984**, *81*, 151-156.
[44] D. Belli Dell'Amico, F. Calderazzo, *Inorg. Synth.*, **1986**, *24*, 236-238.
[45] R. Uson, A. Laguna, M. Laguna, *Inorg. Synth.*, **1989**, *26*, 85-91.
[46] N. C. Baenziger, W. E. Bennett, D. M. Soboroff, *Acta Cryst.*, **1976**, *B32*, 962-963.
[47] a) C. White, S. J. Thompson, P. M. Maitlis, *J. Chem. Soc., Dalton Trans.*, **1977**, 1654-1661; b) C. White, A. Yates, P. M. Maitlis, *Inorg. Synth.*, **1992**, *29*, 228-234.
[48] H. Amouri, M. N. Rager, F. Cagnol, J. Vaissermann, *Angew. Chem.*, **2001**, *113*, 3748-3750; *Angew. Chem. Int. Ed.*, **2001**, *40*, 3636-3638.
[49] F. A. Cotton, K. R. Dunbar, C. T. Eagle, L. R. Falvello, A. C. Price, *Inorg. Chem.*, **1989**, *28*, 1754-1757 (Only bond lengths and angles involving the bridging Cl ligands have been quoted from this reference.).
[50] Y. -W. Ge, P. R. Sharp, *Inorg. Chem.*, **1991**, *30*, 1671-1674.
[51] a) J. Manna, C. J. Kuehl, J. A. Whiteford, P. J. Stang, *Organometallics*, **1997**, *16*, 1897-1905; b) J. Manna, C. J. Kuehl, J. A. Whiteford, P. J. Stang, D. C. Muddiman, S. A. Hofstadler, R. D. Smith, *J. Am. Chem. Soc.*, **1997**, *119*, 11611-11619; c) C. J. Kuehl, C. L. Mayne, A. M. Arif, P. J. Stang, *Org. Lett.*, **2000**, *2*, 3727-3729; d) C. J. Kuehl, S. D. Huang, P. J. Stang, *J. Am. Chem. Soc.*, **2001**, *123*, 9634-9641.
[52] A. Albinati, U. von Gunten, P. S. Pregosin, H. J. Ruegg, *J. Organomet. Chem.*, **1985**, *295*, 239-256.
[53] P. Sekar, S. Umbarkar, M. Scheer, A. Voigt, R. Kirmse, *Eur. J. Inorg. Chem.*, **2000**, 2585-2589.
[54] a) V. G. Albano, P. L. Bellon, G. Ciani, M. Manassero, *J. Chem. Soc. Dalton Trans.*, **1972**, 171-175; b) H. Negita, M. Hiura, Y. Kushi, M. Kuramoto, T. Okuda, *Bull. Chem. Soc. Jpn.*, **1981**, *54*, 1247-1248; c) P. G. Eller, G. J. Kubas, R. R. Ryan, *Inorg. Chem.*, **1977**, *16*, 2454-2462 (The relatively wide ranges quoted for the Cu─P and Cu─X bond lengths are due to the fact that the Cu atoms in the complexes $[Cu_2X_2(PPh_3)_3]$ are found in both trigonal and tetrahedral coordination modes.).
[55] O. J. Scherer, H. Sitzmann, G. Wolmershäuser, *Acta Cryst.*, **1985**, *C41*, 1761-1763.
[56] Hexacoordinate, that is, octahedral and trigonal prismatic, Ag complexes are not very common. See, for example: a) J.

Clarkson, R. Yagbasan, P. J. Blower, S. C. Rawle, S. R. Cooper, *J. Chem. Soc., Chem. Commun.*, **1987**, 950-951; b) F. A. Cotton, G. Wilkinson, *Advanced Inorganic Chemistry*, 5th ed., Wiley-Interscience, New York, **1988**; c) G. Ouvrard, R. Brec, *Mat. Res. Bull.*, **1988**, *23*, 1199-1209; d) A. J. Blake, R. O. Gould, A. J. Holder, T. I. Hyde, M. Schröder, *Polyhedron*, **1989**, *8*, 513-518; e) A. S. Craig, R. Kataky, R. C. Matthews, D. Parker, G. Ferguson, A. Lough, H. Adams, N. Bailey, H. Schneider, *J. Chem. Soc., Perkin Trans. 2*, **1990**, 1523-1531; f) A. J. Blake, G. Reid, M. Schröder, *J. Chem. Soc., Dalton Trans.*, **1991**, 615-620; g) P. K.-K. Ho, S.-M. Peng, K.-Y. Wong, C.-M. Che, *J. Chem. Soc., Dalton Trans.*, **1996**, 1829-1834; h) T. Gyr, H. R. Mäcke, M. Hennig, *Angew. Chem.*, **1997**, *109*, 2869-2871; *Angew. Chem. Int. Ed. Engl.*, **1998**, *36*, 2786-2788; i) K. A. Hirsch, S. R. Wilson, J. S. Moore, *Inorg. Chem.*, **1997**, *36*, 2960-2968; j) M. Wagner, U. Drutkowski, P. Jörchel, R. Kempe, E. Hoyer, R.-M. Olk, *Chem. Ber./ Recueil*, **1997**, *130*, 425-429; k) D. Venkataraman, Y. Du, S. R. Wilson, K. A. Hirsch, P. Zhang, J. S. Moore, *J. Chem. Ed.*, **1997**, *74*, 915-918; l) R. Kniep, H. Engelhardt, *Z. Anorg. Allg. Chem.*, **1998**, *624*, 1291-1297; m) I. Belharouak, H. Aouad, M. Mesnaoui, M. Maazaz, C. Parent, B. Tanguy, P. Gravereau, G. Le Flem, *J. Solid State Chem.*, **1999**, *145*, 97-103; n) N. J. Melcer, G. D. Enright, J. A. Ripmeester, G. K. H. Shimizu, *Inorg. Chem.*, **2001**, *40*, 4641-4648; o) M. Wen, M. Munakata, Y. Suenaga, T. Kuroda-Sowa, M. Maekawa, *Inorg. Chim. Acta*, **2002**, *332*, 18-24.

[57] I. Krossing, A. Reisinger, *Angew. Chem.*, **2003**, *115*, 5903-5906; *Angew. Chem. Int. Ed.*, **2003**, *42*, 5725-5728.

[58] C. Elschenbroich, A. Salzer, *Organometallics: a Concise Introduction*, 2nd ed., VCH, Weinheim, **1992**.

[59] Reactions of **7c** and CuX (X = Cl, Br, I) in a 1:1 stoichiometry in mixtures of $CH_3CN$ and $CH_2Cl_2$ or pure $CH_3CN$ lead to the crystallisation of the starting material **7c**.

[60] I. Bernal, H. Brunner, W. Meier, H. Pfisterer, J. Wachter, M. L. Ziegler, *Angew. Chem.*, **1984**, *96*, 428-429; *Angew. Chem. Int. Ed. Engl.*, **1984**, *23*, 438-439.

[61] H. Kraus, *Diploma Thesis*, University of Regensburg, in preparation.

[62] a) M. Nardelli, C. Pelizzi, G. Pelizzi, P. Tarasconi, *J. Chem. Soc., Dalton Trans.*, **1985**, 321-331; b) A. Bonardi, A. Cantoni, C. Pelizzi, G. Pelizzi, P. Tarasconi, *J. Organomet. Chem.*, **1991**, *402*, 281-288; c) U. M. Tripathi, A. Bauer, H. Schmidbaur, *J.*

*Chem. Soc., Dalton Trans.*, **1997**, 2865-2868; d) G. A. Bowmaker, Effendy, R. D. Hart, J. D. Kildea, E. N. da Silva, B. W. Skelton, A. H. White, *Aust. J. Chem.*, **1997**, *50*, 539-552.

[63] J. E. Huheey, E. A. Keiter, R. L. Keiter, *Inorganic Chemistry: Principles of Structure and Reactivity*, 4th ed., Harper Collins, **1993**.

[64] This value is reduced to 72.6 kJ $mol^{-1}$ upon consideration of the effects of vibrational enthalpy and vibrational entropy at 298 K.

[65] Translational and rotational contributions negelected.

[66] For NMR evidence of such a coordination mode, see: a) G. Friedrich, *PhD Thesis*, University of Kaiserslautern, **1995**; b) M. Detzel, *PhD Thesis*, University of Kaiserslautern, **1995**.

[67] R. Blom, T. Brück, O. J. Scherer, *Acta Chem. Scand.*, **1989**, *43*, 458-462.

[68] N. G. Connelly, W. E. Geiger, *Chem. Rev.*, **1996**, *96*, 877-910.

[69] Positive ion ESI-MS spectra of the solution resulting from the 1:1 reaction of **11c** and $AgSbF_6$ in $CH_2Cl_2$ at room temperature appear identical to those of **89**.

[70] For the first examples of complexes in which the P atoms as well as the S atoms of the intact $P_4S_3$ cage molecule are involved in coordination, see: A. Adolf, M. Gonsior, I. Krossing, *J. Am. Chem. Soc.*, **2002**, *124*, 7111-7116.

[71] H. Brunner, U. Klement, W. Meier, J. Wachter, O. Serhadle, M. L. Ziegler, *J. Organomet. Chem.*, **1987**, *335*, 339-352.

[72] a) G. Krabbes, H. Oppermann, *Z. Anorg. Allg. Chem.*, **1977**, *435*, 33-44; b) T. P. Martin, H. Schaber, *J. Chem. Phys.*, **1980**, *73*, 3541-3546.

[73] For examples of crystallographically characterised compounds containing discrete $Cu_3X_3$ rings, see: a) P. C. Healy, B. W. Skelton, A. H. White, *J. Chem. Soc., Dalton Trans.*, **1989**, 971-976; b) L. Chen, L. K. Thompson, S. S. Tandon, J. N. Bridson, *Inorg. Chem.*, **1993**, *32*, 4063-4068; c) C. Näther, I. Jeß, *Z. Naturforsch.*, **2002**, *57b*, 1133-1140; d) G. Kickelbick, D. Rutzinger, T. Gallauner, *Monatshe. Chem.*, **2002**, *133*, 1157-1164.

[74] O. Crespo, M. C. Gimeno, P. G. Jones, A. Laguna, *J. Chem. Soc., Dalton Trans.,* **1996**, 4583-4588.

[75] P. Braunstein, H. Lehner, D. Matt, *Inorg. Synth.*, **1990**, *27*, 218-221.

[76] Bruker Daltonik GmbH, *WIN-NMR Version 6.2*, **2000**.

[77] http://www.shef.ac.uk/chemistry/chemputer/isotopes.html.

[78] A. Altomare, G. Cascarano, C. Giacovazzo, A. Guagliardi, *J. Appl. Cryst.*, **1993**, *26*, 343-350.
[79] G. M. Sheldrick, *SHELXS-97*, University of Göttingen, **1997**.
[80] G. M. Sheldrick, *SHELXL-97*, University of Göttingen, **1997**.
[81] Crystal Impact GbR, *Diamond Version 2.1e*, **2001**.
[82] a) R. Ahlrichs, M. Bär, M. Häser, H. Horn, C. Kölmel, *Chem. Phys. Lett.*, **1989**, *162*, 165-169; b) O. Treutler, R. Ahlrichs, *J. Chem. Phys.*, **1995**, *102*, 346-354.
[83] W. Küchle, M. Dolg, H. Stoll, H. Preuss, *Mol. Phys.*, **1991**, *74*, 1245-1263.
[84] a) A. D. Becke, *Phys. Rev.*, *A* **1988**, *38*, 3098-3100; b) S. H. Vosko, L. Wilk, M. Nusair, *Can. J. Phys.*, **1980**, *58*, 1200-1211; c) J. P. Perdew, *Phys. Rev. B*, **1986**, *33*, 8822-8824; erratum: J. P. Perdew, *Phys. Rev. B,* **1986**, *34*, 7406.
[85] K. Eichkorn, O. Treutler, H. Öhm, M. Häser, R. Ahlrichs, *Chem. Phys. Lett.*, **1995**, *242*, 652-660.
[86] A. Klamt, G. Schürmann, *J. Chem. Soc., Perkin. Trans.*, **1993**, *2*, 799-805.
[87] a) A. Schäfer, H. Horn, R. Ahlrichs, *J. Chem. Phys.*, **1992**, *97*, 2571-2577; b) A. Schäfer, C. Huber, R. Ahlrichs, *J. Chem. Phys.*, **1994**, *100*, 5829-5835.
[88] K. Eichkorn, F. Weigend, O. Treutler, R. Ahlrichs, *Theor. Chem. Acc.* **1997**, *97*, 119-124.
[89] M. Sierka, A. Hogekamp, R. Ahlrichs, *J. Chem. Phys.*, **2003**, *118*, 9136-9148.
[90] G. Schreckenbach, T. Ziegler, *J. Phys. Chem.*, **1995**, *99*, 606-611.
[91] T. Helgaker, P. J. Wilson, R. D. Amos, N. C. Handy, *J. Chem. Phys.*, **2000**, *113*, 2983-2989.
[92] a) D. Andrae, U. Häußermann, M. Dolg, H. Stoll, H. Preuss, *Theor. Chim. Acta*, **1990**, *77*, 123-141; b) A. Bergner, M. Dolg, W. Küchle, H. Stoll, H. Preuss, *Mol. Phys.*, **1993**, *80*, 1431-1441.
[93] H. V. Ly, M. Parvez, R. Roesler, *Inorg. Chem.*, **2006**, *45*, 345-351.

# 7. Appendix

## 7.1. List of Abbreviations

| | |
|---|---|
| *t*-Bu | tertiary (*tert*) butyl |
| $C_{14}H_8$ | anthracen-1,8-diyl |
| $C_{14}H_8Cl$ | 1-chloroanthracen-8-yl |
| Cp | cyclopentadienyl |
| Cp* | 1,2,3,4,5-pentamethylcyclopentadienyl |
| $Cp^{Et}$ | 1-ethyl-2,3,4,5-tetramethylcyclopentadienyl |
| Cp´ | 1-*tert*-butylcyclopentadienyl |
| Cp´´ | 1,4-di-*tert*-butylcyclopentadienyl |
| Cp´´´ | 1,2,4-tri-*tert*-butylcyclopentadienyl |
| d (NMR) | doublet |
| 1,2 or 3D | one-, two- or three-dimensional |
| Et | ethyl |
| IR | infra-red |
| m (IR) | medium |
| m (NMR) | multiplet |
| MAS | magic angle spinning |
| Me | methyl |
| NMR | nuclear magnetic resonance |
| OTf | trifluoromethanesulfonate |
| Ph | phenyl |
| q (NMR) | quartet |
| s (IR) | strong |
| s (NMR) | singlet |
| t (NMR) | triplet |
| THF | tetrahydrofuran |
| TMS | tetramethylsilane |
| *p*-Tol | *para*-tolyl |
| VE | valence electron |
| vs (IR) | very strong |
| w (IR) | weak |

## 7.2. List of the Reported Compounds

### 7.2.1. Compounds Based on $[Cp_2M_2(CO)_4(\mu,\eta^2\text{-}P_2)]$ (M = Cr, Mo)

**42d** $[Ag_2\{Cp_2Mo_2(CO)_4(\mu_3,\eta^2:\eta^2:\eta^2\text{-}P_2)\}_2\{Cp_2Mo_2(CO)_4(\mu_4,\eta^2:\eta^2:\eta^1:\eta^1\text{-}P_2)\}_2][(ClO_4)_2]$

**42e** $[Ag_2\{Cp_2Mo_2(CO)_4(\mu_3,\eta^2:\eta^2:\eta^2\text{-}P_2)\}_2\{Cp_2Mo_2(CO)_4(\mu_4,\eta^2:\eta^2:\eta^1:\eta^1\text{-}P_2)\}_2][(PF_6)_2]$

**42f** $[Ag_2\{Cp_2Mo_2(CO)_4(\mu_3,\eta^2:\eta^2:\eta^2\text{-}P_2)\}_2\{Cp_2Mo_2(CO)_4(\mu_4,\eta^2:\eta^2:\eta^1:\eta^1\text{-}P_2)\}_2][(SbF_6)_2]$

**42g** $[Ag_2\{Cp_2Mo_2(CO)_4(\mu_3,\eta^2:\eta^2:\eta^2\text{-}P_2)\}_2\{Cp_2Mo_2(CO)_4(\mu_4,\eta^2:\eta^2:\eta^1:\eta^1\text{-}P_2)\}_2]\langle Al\{OC(CF_3)_3\}_4\rangle_2]$

**42h** $[Au_2\{Cp_2Mo_2(CO)_4(\mu_3,\eta^2:\eta^2:\eta^2\text{-}P_2)\}_2\{Cp_2Mo_2(CO)_4(\mu_4,\eta^2:\eta^2:\eta^1:\eta^1\text{-}P_2)\}_2][(PF_6)_2]$

**49** $[Ag_2\{Cp_2Mo_2(CO)_4(\mu_4,\eta^2:\eta^2:\eta^1:\eta^1\text{-}P_2)\}_2(\eta^2\text{-}NO_2)_2]$

**50** $[Au\{Cp_2Mo_2(CO)_4(\mu_3,\eta^2:\eta^2:\eta^1\text{-}P_2)\}Cl]$

**53a** $[Cp^*Rh\{Cp_2Mo_2(CO)_4(\mu_3,\eta^2:\eta^2:\eta^1\text{-}P_2)\}_2(NCCH_3)][(SbF_6)_2]$

**53b** $[Cp^*Ir\{Cp_2Mo_2(CO)_4(\mu_3,\eta^2:\eta^2:\eta^1\text{-}P_2)\}_2(NCCH_3)][(SbF_6)_2]$

**54** $[(Cp''Rh)_2\{Cp_2Mo_2(CO)_4(\mu_4,\eta^2:\eta^2:\eta^1:\eta^1\text{-}P_2)\}(\mu\text{-}Cl)_2][(BF_4)_2]$

**57** $[(C_{14}H_8)Pt_2\{Cp_2Mo_2(CO)_4(\mu_3,\eta^2:\eta^2:\eta^1\text{-}P_2)\}_2(PEt_3)_4][(PF_6)_2]$

**59** $[(C_{14}H_8Cl)Pt\{Cp_2Mo_2(CO)_4(\mu_3,\eta^2:\eta^2:\eta^1\text{-}P_2)\}(PEt_3)_2][PF_6]$

**66a** $[Cu(\mu\text{-}Cl)\{Cp_2Cr_2(CO)_4(\mu_4,\eta^2:\eta^2:\eta^1:\eta^1\text{-}P_2)\}]_n$

**66b** $[Cu(\mu\text{-}Br)\{Cp_2Cr_2(CO)_4(\mu_4,\eta^2:\eta^2:\eta^1:\eta^1\text{-}P_2)\}]_n$

**66c** $[Cu(\mu\text{-}I)\{Cp_2Cr_2(CO)_4(\mu_4,\eta^2:\eta^2:\eta^1:\eta^1\text{-}P_2)\}]_n$

**67** $[Ag_2\{Cp_2Cr_2(CO)_4(\mu_3,\eta^2:\eta^2:\eta^2\text{-}P_2)\}_2\{Cp_2Cr_2(CO)_4(\mu_4,\eta^2:\eta^2:\eta^1:\eta^1\text{-}P_2)\}_2][\langle Al\{OC(CF_3)_3\}_4\rangle_2]$

### 7.2.2. Compounds Based on $[Cp^xM(CO)_2(\eta^3\text{-}E_3)]$ ($Cp^x$ = Cp, Cp*; M = Cr, Mo; E = P, As)

**69** $[Ag\{CpCr(CO)_2(\mu_3,\eta^3:\eta^1:\eta^1\text{-}P_3)\}_2]_n[Al\{OC(CF_3)_3\}_4]_n$

**71** $[Ag\{CpMo(CO)_2(\mu_3,\eta^3:\eta^1:\eta^1\text{-}P_3)\}_2]_n[Al\{OC(CF_3)_3\}_4]_n$

**74** $[Ag\{CpMo(CO)_2(\mu_3,\eta^3:\eta^1:\eta^1\text{-}P_3)\}_3]_n[Al\{OC(CF_3)_3\}_4]_n$

**76a** $[Cu_2(\mu\text{-}Cl)_2\{Cp^*Mo(CO)_2(\mu,\eta^3:\eta^2\text{-}P_3)\}_2]$

**76b** $[Cu_2(\mu\text{-}Br)_2\{Cp^*Mo(CO)_2(\mu,\eta^3:\eta^2\text{-}P_3)\}_2]$

**77** $[Cu(\mu\text{-}I)\{Cp^*Mo(CO)_2(\mu_3,\eta^3:\eta^1:\eta^1\text{-}P_3)\}]_n$

**78** $[Ag\{Cp^*Mo(CO)_2(\mu_3,\eta^3:\eta^2:\eta^1\text{-}P_3)\}_2]_n[Al\{OC(CF_3)_3\}_4]_n$

**81** $[Ag_2\{Cp^*Mo(CO)_2(\mu,\eta^3:\eta^2\text{-}As_3)\}_2\{Cp^*Mo(CO)_2(\mu_3,\eta^3:\eta^2:\eta^2\text{-}As_3)\}_2][\langle Al\{OC(CF_3)_3\}_4\rangle_2]$

## 7.2.3. Compounds Based on [Cp*Fe($\eta^5$-$P_5$)]

**83** $[Ag\{Cp^*Fe(\mu_3,\eta^5:\eta^2:\eta^1\text{-}P_5)\}_2]_n[Al\{OC(CF_3)_3\}_4]_n$
**85** $[Ag_x\{Cp^*Fe(\eta^5\text{-}P_5)\}_y(NO_2)_x(NCCH_3)_z]$
**86** $[Au_5\{Cp^*Fe(\eta^5\text{-}P_5)\}_2]_n[(PF_6)_{5n}]$
**87** $[(AuCl)_3\{Cp^*Fe(\eta^5\text{-}P_5)\}]_n$

## 7.2.4. Compounds Based on [(Cp*Mo)$_2$($\mu$,$\eta^6$-$P_6$)]

**88** $[Cu_{20}(\mu\text{-}Cl)_{16}(\mu_3\text{-}Cl)_4\{(Cp^*Mo)_2(\mu_7,\eta^6:\eta^6:\eta^1:\eta^1:\eta^1:\eta^1:\eta^1\text{-}P_6)\}_3\{(Cp^*Mo)_2(\mu_7,\eta^6:\eta^6:\eta^2:\eta^1:\eta^1:\eta^1:\eta^1\text{-}P_6)\}(NCCH_3)_{12}]_n$
**89** $[(Cp^*Mo)_2(\mu,\eta^6\text{-}P_6)][Al\{OC(CF_3)_3\}_4]$
**90** $[Ag\{(Cp^*Mo)_2(\mu_3,\eta^6:\eta^2\text{-}P_6)\}_2][Al\{OC(CF_3)_3\}_4]$

## 7.2.5. Compounds Based on [(Cp*Mo)$_2$($\mu$,$\eta^3$-$P_3$)($\mu$,$\eta^2$-PS)]

**92a** $[\{Cu(\mu\text{-}Cl)\}_3\{(Cp^*Mo)_2(\mu_3,\eta^3:\eta^3:\eta^1\text{-}P_3)(\mu,\eta^2\text{-}PS)\}\{(Cp^*Mo)_2(\mu_3,\eta^3:\eta^3:\eta^1\text{-}P_3)(\mu_3,\eta^2:\eta^2:\eta^1\text{-}PS)\}]_n$
**92b** $[\{Cu(\mu\text{-}Br)\}_3\{(Cp^*Mo)_2(\mu_3,\eta^3:\eta^3:\eta^1\text{-}P_3)(\mu,\eta^2\text{-}PS)\}\{(Cp^*Mo)_2(\mu_3,\eta^3:\eta^3:\eta^1\text{-}P_3)(\mu_3,\eta^2:\eta^2:\eta^1\text{-}PS)\}]_n$
**92c** $[\{Cu(\mu\text{-}I)\}_3\{(Cp^*Mo)_2(\mu_3,\eta^3:\eta^3:\eta^1\text{-}P_3)(\mu,\eta^2\text{-}PS)\}\{(Cp^*Mo)_2(\mu_3,\eta^3:\eta^3:\eta^1\text{-}P_3)(\mu_3,\eta^2:\eta^2:\eta^1\text{-}PS)\}]_n$
**94** $[Ag\{(Cp^*Mo)_2(\mu_3,\eta^3:\eta^3:\eta^1\text{-}P_3)(\mu,\eta^2\text{-}PS)\{(Cp^*Mo)_2(\mu_3,\eta^3:\eta^3:\eta^1\text{-}P_3)(\mu_3,\eta^2:\eta^2:\eta^1\text{-}PS)\}]_n[Al\{OC(CF_3)_3\}_4]_n$

# 7.3. Crystallographic Data for the Reported Structures

## 7.3.1. [Cp*Mo(CO)$_2$($\eta^3$-P$_3$)] (7c)

The complex **7c** was crystallised from a concentrated $CH_3CN$ solution of the compound at room temperature in the dark.

Table 7.1. Crystal data and structure refinement for **7c**.

| | |
|---|---|
| Empirical formula | $C_{12}H_{15}MoO_2P_3$ |
| Formula weight | 380.09 g mol$^{-1}$ |
| Crystal size | 0.200 × 0.200 × 0.180 mm |
| Crystal description | prism |
| Crystal colour | yellow |
| Crystal system | monoclinic |
| Space group | $P2_1/n$ |
| Unit cell dimensions | $a$ = 12.147(1) Å, $\alpha$ = 90° |
| | $b$ = 9.232(1) Å, $\beta$ = 95.27(1)° |
| | $c$ = 13.547(1) Å, $\gamma$ = 90° |
| Volume | 1512.8(2) Å$^3$ |
| Z, Calculated density | 4, 1.669 Mg m$^{-3}$ |
| Absorption coefficient | 1.175 mm$^{-1}$ |
| F(000) | 760 |
| Measurement device type | STOE-IPDS |
| Measurement method | rotation |
| Temperature | 173(1) K |
| Wavelength | 0.71073 Å |
| Monochromator | graphite |
| $\theta$ range for data collection | 2.16 to 26.86° |
| Index ranges | $-15 \le h \le 15$, $-11 \le k \le 11$, $-17 \le l \le 17$ |
| Reflections collected / unique | 13881 / 3242 [R(int) = 0.0253] |
| Reflections greater I>2\s(I) | 2774 |
| Absorption correction | numerical |
| Max. and min. transmission | 0.8662 and 0.7656 |
| Refinement method | Full-matrix least-squares on F$^2$ |
| Data / restraints / parameters | 3242 / 0 / 163 |
| Goodness-of-fit on F$^2$ | 0.979 |
| Final R indices [I>2sigma(I)] | R1 = 0.0196, wR2 = 0.0459 |
| R indices (all data) | R1 = 0.0256, wR2 = 0.0471 |
| Largest diff. peak and hole | 0.426 and -0.228 e Å$^{-3}$ |

Table 7.2. Atomic coordinates ( $\times 10^4$) and equivalent isotropic displacement parameters ($Å^2 \times 10^3$) for **7c**. $U_{eq}$ is defined as one third of the trace of the orthogonalised $U_{ij}$ tensor.

| **Atom** | **x** | **y** | **z** | $U_{eq}$ |
|---|---|---|---|---|
| Mo1 | 336(1) | 859(1) | 2372(1) | 19(1) |
| P1 | -293(1) | -1679(1) | 2712(1) | 33(1) |
| P2 | -303(1) | -1107(1) | 1157(1) | 36(1) |
| P3 | 1219(1) | -1611(1) | 2017(1) | 34(1) |
| O1 | 2161(1) | 607(2) | 4175(1) | 42(1) |
| O2 | 2170(1) | 1790(2) | 987(1) | 40(1) |
| C1 | -24(2) | 3208(2) | 2844(1) | 25(1) |
| C2 | -628(2) | 2249(2) | 3440(1) | 26(1) |
| C3 | -1441(2) | 1512(2) | 2799(1) | 26(1) |
| C4 | -1354(2) | 2002(2) | 1800(1) | 25(1) |
| C5 | -480(2) | 3045(2) | 1832(1) | 24(1) |
| C6 | 801(2) | 4328(2) | 3233(2) | 39(1) |
| C7 | -520(2) | 2193(3) | 4560(2) | 42(1) |
| C8 | -2354(2) | 562(2) | 3116(2) | 41(1) |
| C9 | -2145(2) | 1637(2) | 917(2) | 37(1) |
| C10 | -183(2) | 3960(2) | 972(2) | 35(1) |
| C11 | 1515(2) | 672(2) | 3508(1) | 27(1) |
| C12 | 1520(2) | 1424(2) | 1487(1) | 26(1) |

Table 7.3. Anisotropic displacement parameters ($Å^2 \times 10^3$) for **7c**. The anisotropic displacement factor exponent takes the form: $-2\pi^2[h^2a^{*2}U_{11} + ... + 2hka^*b^*U_{12}]$.

| **Atom** | $U_{11}$ | $U_{22}$ | $U_{33}$ | $U_{23}$ | $U_{13}$ | $U_{12}$ |
|---|---|---|---|---|---|---|
| Mo1 | 20(1) | 18(1) | 19(1) | 2(1) | 3(1) | 1(1) |
| P1 | 39(1) | 21(1) | 42(1) | 3(1) | 9(1) | -4(1) |
| P2 | 43(1) | 32(1) | 32(1) | -9(1) | -6(1) | 3(1) |
| P3 | 32(1) | 25(1) | 47(1) | -3(1) | 5(1) | 7(1) |
| O1 | 42(1) | 49(1) | 33(1) | 5(1) | -11(1) | -3(1) |
| O2 | 30(1) | 56(1) | 37(1) | 9(1) | 12(1) | -2(1) |
| C1 | 28(1) | 19(1) | 30(1) | -1(1) | 7(1) | 3(1) |
| C2 | 29(1) | 25(1) | 25(1) | 1(1) | 9(1) | 6(1) |
| C3 | 23(1) | 24(1) | 32(1) | 6(1) | 9(1) | 4(1) |
| C4 | 23(1) | 25(1) | 26(1) | 4(1) | 3(1) | 7(1) |
| C5 | 26(1) | 20(1) | 28(1) | 5(1) | 10(1) | 6(1) |
| C6 | 40(1) | 26(1) | 52(1) | -6(1) | 3(1) | -3(1) |
| C7 | 52(1) | 49(1) | 25(1) | 2(1) | 11(1) | 9(1) |
| C8 | 26(1) | 38(1) | 60(1) | 18(1) | 13(1) | 2(1) |
| C9 | 33(1) | 40(1) | 38(1) | -2(1) | -6(1) | 7(1) |
| C10 | 41(1) | 30(1) | 36(1) | 14(1) | 17(1) | 9(1) |
| C11 | 29(1) | 24(1) | 28(1) | 2(1) | 4(1) | -1(1) |
| C12 | 24(1) | 29(1) | 26(1) | 3(1) | 2(1) | 3(1) |

## 7.3.2. [Cp*Fe($\eta^5$-$P_5$)] (9a)

The complex **9a** was crystallised from a concentrated $CH_2Cl_2$ solution of the compound at –28 °C.

Table 7.4. Crystal data and structure refinement for **9a**.

| | |
|---|---|
| Empirical formula | $C_{10}H_{15}FeP_5$ |
| Formula weight | 345.92 g $mol^{-1}$ |
| Crystal size | 0.44 × 0.38 × 0.16 mm |
| Crystal description | flat prism |
| Crystal colour | dark green |
| Crystal system | monoclinic |
| Space group | $P2_1/n$ |
| Unit cell dimensions | $a$ = 9.0443(8) Å, $\alpha$ = 90° |
| | $b$ = 13.8767(16) Å, $\beta$ = 97.07(1)° |
| | $c$ = 11.8595(10) Å, $\gamma$ = 90° |
| Volume | 1477.1(3) $Å^3$ |
| Z, Calculated density | 4, 1.556 Mg $m^{-3}$ |
| Absorption coefficient | 1.534 $mm^{-1}$ |
| F(000) | 704 |
| Measurement device type | STOE-IPDS |
| Measurement method | rotation |
| Temperature | 123(1) K |
| Wavelength | 0.71073 A |
| Monochromator | graphite |
| $\theta$ range for data collection | 2.27 to 25.82° |
| Index ranges | $-11 \le h \le 11$, $-16 \le k \le 16$, $-14 \le l \le 14$ |
| Reflections collected / unique | 20374 / 2749 [R(int) = 0.1628] |
| Reflections greater I>2\s(I) | 2466 |
| Absorption correction | none |
| Refinement method | Full-matrix least-squares on $F^2$ |
| Data / restraints / parameters | 2749 / 0 / 145 |
| Goodness-of-fit on $F^2$ | 1.055 |
| Final R indices [I>2sigma(I)] | R1 = 0.0556, wR2 = 0.1540 |
| R indices (all data) | R1 = 0.0586, wR2 = 0.1567 |
| Largest diff. peak and hole | 0.987 and -0.626 e $Å^{-3}$ |

Table 7.5. Atomic coordinates ( $\times 10^4$) and equivalent isotropic displacement parameters ($Å^2 \times 10^3$) for **9a**. $U_{eq}$ is defined as one third of the trace of the orthogonalised $U_{ij}$ tensor.

| **Atom** | **x** | **y** | **z** | $U_{eq}$ |
|---|---|---|---|---|
| Fe1 | 1397(1) | 2918(1) | 3501(1) | 26(1) |
| P1 | 920(1) | 2942(1) | 5419(1) | 45(1) |
| P2 | 2114(1) | 1733(1) | 4900(1) | 49(1) |
| P3 | 3807(1) | 2254(1) | 3968(1) | 44(1) |
| P4 | 3668(1) | 3775(1) | 3921(1) | 37(1) |
| P5 | 1876(1) | 4200(1) | 4804(1) | 37(1) |
| C1 | 1118(4) | 3230(2) | 1745(3) | 29(1) |
| C2 | -6(4) | 3712(2) | 2284(3) | 29(1) |
| C3 | -863(4) | 2995(2) | 2793(3) | 30(1) |
| C4 | -250(4) | 2068(2) | 2566(3) | 30(1) |
| C5 | 969(4) | 2213(2) | 1925(3) | 28(1) |
| C6 | 2197(4) | 3699(3) | 1048(3) | 36(1) |
| C7 | -338(4) | 4772(3) | 2233(3) | 38(1) |
| C8 | -2217(4) | 3189(3) | 3371(4) | 40(1) |
| C9 | -863(4) | 1115(3) | 2888(3) | 38(1) |
| C10 | 1869(4) | 1430(2) | 1454(3) | 34(1) |

Table 7.6. Anisotropic displacement parameters ($Å^2 \times 10^3$) for **9a**. The anisotropic displacement factor exponent takes the form: $-2\pi^2[h^2a^{*2}U_{11} + ... + 2hka^*b^*U_{12}]$.

| **Atom** | $U_{11}$ | $U_{22}$ | $U_{33}$ | $U_{23}$ | $U_{13}$ | $U_{12}$ |
|---|---|---|---|---|---|---|
| Fe1 | 22(1) | 25(1) | 32(1) | -1(1) | -1(1) | 0(1) |
| P1 | 37(1) | 62(1) | 34(1) | 2(1) | 2(1) | -12(1) |
| P2 | 54(1) | 36(1) | 51(1) | 12(1) | -19(1) | -8(1) |
| P3 | 31(1) | 41(1) | 57(1) | -10(1) | -11(1) | 11(1) |
| P4 | 26(1) | 39(1) | 44(1) | -2(1) | -1(1) | -6(1) |
| P5 | 36(1) | 35(1) | 39(1) | -9(1) | -1(1) | 1(1) |
| C1 | 28(2) | 29(2) | 29(2) | 0(1) | -2(1) | 2(1) |
| C2 | 24(2) | 28(2) | 33(2) | -2(1) | -4(1) | 3(1) |
| C3 | 24(2) | 34(2) | 30(2) | -2(1) | -3(1) | 2(1) |
| C4 | 26(2) | 30(2) | 32(2) | 0(1) | -2(1) | -3(1) |
| C5 | 25(2) | 27(2) | 31(2) | -3(1) | -2(1) | 1(1) |
| C6 | 33(2) | 34(2) | 41(2) | 2(1) | 6(2) | -4(1) |
| C7 | 39(2) | 27(2) | 47(2) | -5(2) | -4(2) | 7(1) |
| C8 | 26(2) | 51(2) | 43(2) | -6(2) | 6(2) | 0(2) |
| C9 | 37(2) | 32(2) | 42(2) | 3(2) | -3(2) | -10(2) |
| C10 | 33(2) | 29(2) | 41(2) | -4(1) | 1(2) | 7(1) |

## 7.3.3. $[Ag_2\{Cp_2Mo_2(CO)_4(\mu_3,\eta^2:\eta^2:\eta^2\text{-}P_2)\}_2\{Cp_2Mo_2(CO)_4(\mu_4,\eta^2:\eta^2:\eta^1:\eta^1\text{-}P_2)\}_2][(ClO_4)_2]\bullet 2CH_3CN$ (**42d**•2CH$_3$CN)

Crystals of **42d**•2CH$_3$CN were obtained by controlled diffusion of a CH$_3$CN solution of AgClO$_4$ into a CH$_2$Cl$_2$ solution of [Cp$_2$Mo$_2$(CO)$_4$($\mu$,$\eta^2$-P$_2$)] **6b** at 4 °C.

Table 7.7. Crystal data and structure refinement for **42d**•2CH$_3$CN.

| | |
|---|---|
| Empirical formula | $C_{60}H_{46}Ag_2Cl_2N_2Mo_8O_{24}P_8$ |
| Formula weight | 2481.20 g mol$^{-1}$ |
| Crystal size | 0.260 x 0.100 x 0.040 mm |
| Crystal description | prism |
| Crystal colour | red |
| Crystal system | triclinic |
| Space group | $P\ \overline{1}$ |
| Unit cell dimensions | $a$ = 12.006(2) Å, $\alpha$ = 114.39(1)° |
| | $b$ = 13.484(1) Å, $\beta$ = 100.88(1)° |
| | $c$ = 15.538(2) Å, $\gamma$ = 95.61(1)° |
| Volume | 2205.8(5) Å$^3$ |
| Z, Calculated density | 1, 1.868 Mg m$^{-3}$ |
| Absorption coefficient | 1.800 mm^-1 |
| F(000) | 1196 |
| Measurement device type | STOE-IPDS |
| Measurement method | rotation |
| Temperature | 123(1) K |
| Wavelength | 0.71073 Å |
| Monochromator | graphite |
| $\theta$ range for data collection | 2.00 to 25.80 deg. |
| Index ranges | $-14 \le h \le 14$, $-16 \le k \le 16$, $-18 \le l \le 18$ |
| Reflections collected / unique | 19958 / 7892 [R(int) = 0.0256] |
| Reflections greater I>2\s(I) | 6821 |
| Absorption correction | numerical |
| Max. and min. transmission | 0.9384 and 0.6906 |
| Refinement method | Full-matrix least-squares on F$^2$ |
| Data / restraints / parameters | 7892 / 0 / 476 |
| Goodness-of-fit on F^2 | 1.041 |
| Final R indices [I>2sigma(I)] | R1 = 0.0280, wR2 = 0.0789 |
| R indices (all data) | R1 = 0.0327, wR2 = 0.0806 |
| Largest diff. peak and hole | 1.356 and -0.777 e Å$^{-3}$ |

Table 7.8. Atomic coordinates ( × $10^4$) and equivalent isotropic displacement parameters (Å$^2$ × $10^3$) for **42d**•2$CH_3CN$. $U_{eq}$ is defined as one third of the trace of the orthogonalised $U_{ij}$ tensor.

| **Atom** | **x** | **y** | **z** | $U_{eq}$ |
|---|---|---|---|---|
| Ag1 | 3961(1) | 1349(1) | 586(1) | 32(1) |
| Mo1 | 2561(1) | 3945(1) | 2591(1) | 23(1) |
| Mo2 | 2858(1) | 4454(1) | 901(1) | 21(1) |
| Mo3 | 2597(1) | -1449(1) | -2523(1) | 24(1) |
| Mo4 | 4359(1) | 201(1) | -2691(1) | 21(1) |
| P1 | 2398(1) | 2601(1) | 826(1) | 23(1) |
| P2 | 4098(1) | 3508(1) | 1716(1) | 23(1) |
| P3 | 3720(1) | 311(1) | -1196(1) | 25(1) |
| P4 | 4755(1) | -858(1) | -1746(1) | 25(1) |
| O1 | -103(2) | 3320(3) | 1575(2) | 43(1) |
| O2 | 2386(3) | 1659(3) | 2699(2) | 44(1) |
| O3 | 4872(3) | 6436(3) | 2422(2) | 38(1) |
| O4 | 4573(3) | 3653(3) | -434(2) | 42(1) |
| O5 | 2798(3) | -2495(3) | -1040(2) | 52(1) |
| O6 | 3761(3) | -3373(3) | -3760(2) | 44(1) |
| O7 | 6319(3) | 2145(3) | -1063(2) | 42(1) |
| O8 | 2663(3) | 1895(3) | -2345(2) | 42(1) |
| C1 | 3983(4) | 5396(4) | 3870(3) | 35(1) |
| C2 | 3061(4) | 5891(4) | 3632(3) | 37(1) |
| C3 | 2066(4) | 5426(4) | 3806(3) | 46(2) |
| C4 | 2380(4) | 4661(4) | 4173(3) | 46(2) |
| C5 | 3570(4) | 4631(4) | 4207(3) | 40(2) |
| C6 | 878(3) | 3528(3) | 1917(3) | 32(1) |
| C7 | 2439(3) | 2469(3) | 2633(3) | 31(1) |
| C8 | 2240(3) | 5366(3) | -16(3) | 33(1) |
| C9 | 1924(3) | 5886(3) | 882(3) | 31(1) |
| C10 | 1088(3) | 5105(4) | 935(3) | 35(1) |
| C11 | 902(3) | 4094(4) | 75(3) | 37(1) |
| C12 | 1603(4) | 4252(4) | -507(3) | 37(1) |
| C13 | 4157(3) | 5694(3) | 1886(3) | 28(1) |
| C14 | 3957(3) | 3937(3) | 62(3) | 30(1) |
| C15 | 1239(3) | -969(4) | -3542(3) | 37(1) |
| C16 | 1030(4) | -523(4) | -2599(3) | 39(1) |
| C17 | 702(4) | -1432(4) | -2390(3) | 41(1) |
| C18 | 721(3) | -2431(4) | -3200(3) | 39(1) |
| C19 | 1061(4) | -2137(4) | -3906(3) | 39(1) |
| C20 | 2745(3) | -2101(3) | -1564(3) | 34(1) |
| C21 | 3355(4) | -2664(3) | -3306(3) | 33(1) |
| C22 | 3866(4) | -35(4) | -4296(3) | 34(1) |

| | | | | |
|---|---|---|---|---|
| C23 | 3939(3) | -1109(3) | -4372(2) | 32(1) |
| C24 | 5102(4) | -1074(4) | -3916(3) | 35(1) |
| C25 | 5742(4) | 7(4) | -3582(3) | 38(1) |
| C26 | 4979(4) | 657(4) | -3814(3) | 38(1) |
| C27 | 5589(3) | 1445(3) | -1637(3) | 29(1) |
| C28 | 3270(3) | 1277(3) | -2452(3) | 29(1) |
| Cl1 | 8958(1) | 1950(1) | 6702(1) | 41(1) |
| O9 | 7902(4) | 2021(4) | 7018(3) | 72(2) |
| O10 | 8685(8) | 1704(10) | 5716(7) | 92(2) |
| O11 | 9723(8) | 3026(9) | 7162(7) | 92(2) |
| O12 | 9651(8) | 1246(9) | 6968(7) | 92(2) |
| O13 | 9826(10) | 2298(11) | 7476(9) | 92(2) |
| O14 | 8875(10) | 955(11) | 5842(9) | 92(2) |
| O15 | 9044(10) | 2662(12) | 6208(9) | 92(2) |
| N1 | 3273(4) | 2709(4) | 5249(3) | 60(2) |
| C31 | 2507(5) | 2269(5) | 5230(4) | 52(2) |
| C32 | 1374(5) | 1635(6) | 5334(5) | 86(3) |

Table 7.9. Anisotropic displacement parameters ($Å^2 \times 10^3$) for **42d**•2$CH_3CN$. The anisotropic displacement factor exponent takes the form: $-2\pi^2[h^2a^{*2}U_{11} + ... + 2hka^*b^*U_{12}]$.

| **Atom** | $U_{11}$ | $U_{22}$ | $U_{33}$ | $U_{23}$ | $U_{13}$ | $U_{12}$ |
|---|---|---|---|---|---|---|
| Ag1 | 44(1) | 33(1) | 20(1) | 9(1) | 9(1) | 22(1) |
| Mo1 | 26(1) | 22(1) | 18(1) | 7(1) | 7(1) | 3(1) |
| Mo2 | 22(1) | 20(1) | 20(1) | 9(1) | 4(1) | 5(1) |
| Mo3 | 28(1) | 22(1) | 20(1) | 9(1) | 7(1) | 3(1) |
| Mo4 | 28(1) | 21(1) | 16(1) | 9(1) | 9(1) | 6(1) |
| P1 | 27(1) | 19(1) | 19(1) | 7(1) | 5(1) | 4(1) |
| P2 | 24(1) | 24(1) | 21(1) | 9(1) | 5(1) | 8(1) |
| P3 | 34(1) | 23(1) | 17(1) | 9(1) | 10(1) | 5(1) |
| P4 | 31(1) | 23(1) | 20(1) | 10(1) | 6(1) | 6(1) |
| O1 | 24(2) | 54(2) | 53(2) | 29(2) | 8(1) | 0(1) |
| O2 | 67(2) | 31(2) | 39(2) | 21(2) | 11(1) | 6(1) |
| O3 | 39(2) | 32(2) | 35(1) | 13(1) | 3(1) | -4(1) |
| O4 | 52(2) | 39(2) | 39(2) | 14(2) | 28(1) | 10(1) |
| O5 | 55(2) | 61(2) | 51(2) | 43(2) | 6(2) | -7(2) |
| O6 | 54(2) | 30(2) | 34(2) | 1(1) | 7(1) | 13(2) |
| O7 | 41(2) | 34(2) | 37(2) | 10(2) | 3(1) | -8(1) |
| O8 | 47(2) | 37(2) | 45(2) | 18(2) | 10(1) | 19(2) |
| C1 | 37(2) | 34(2) | 19(2) | 3(2) | 4(2) | -4(2) |
| C2 | 51(2) | 25(2) | 24(2) | 0(2) | 14(2) | 3(2) |
| C3 | 48(3) | 39(3) | 33(2) | -5(2) | 20(2) | 7(2) |
| C4 | 64(3) | 44(3) | 18(2) | 2(2) | 20(2) | -10(2) |

| | | | | | | |
|---|---|---|---|---|---|---|
| C5 | 56(3) | 39(3) | 15(2) | 8(2) | 3(2) | -4(2) |
| C6 | 35(2) | 29(2) | 33(2) | 14(2) | 14(2) | 3(2) |
| C7 | 36(2) | 35(2) | 21(2) | 12(2) | 7(2) | 4(2) |
| C8 | 37(2) | 34(2) | 33(2) | 22(2) | 3(2) | 10(2) |
| C9 | 32(2) | 24(2) | 37(2) | 16(2) | 3(2) | 9(2) |
| C10 | 29(2) | 37(2) | 47(2) | 25(2) | 8(2) | 15(2) |
| C11 | 27(2) | 33(2) | 47(2) | 23(2) | -9(2) | 2(2) |
| C12 | 42(2) | 36(2) | 29(2) | 18(2) | -8(2) | 6(2) |
| C13 | 32(2) | 27(2) | 27(2) | 13(2) | 8(2) | 8(2) |
| C14 | 35(2) | 26(2) | 28(2) | 12(2) | 8(2) | 5(2) |
| C15 | 27(2) | 49(3) | 39(2) | 26(2) | 4(2) | 8(2) |
| C16 | 32(2) | 40(3) | 49(2) | 21(2) | 14(2) | 12(2) |
| C17 | 29(2) | 49(3) | 48(2) | 22(2) | 16(2) | 6(2) |
| C18 | 26(2) | 37(3) | 48(2) | 19(2) | 4(2) | -4(2) |
| C19 | 31(2) | 44(3) | 33(2) | 14(2) | -2(2) | 1(2) |
| C20 | 36(2) | 31(2) | 31(2) | 13(2) | 6(2) | -2(2) |
| C21 | 38(2) | 27(2) | 24(2) | 7(2) | 0(2) | 2(2) |
| C22 | 51(2) | 40(3) | 18(2) | 16(2) | 14(2) | 17(2) |
| C23 | 41(2) | 36(2) | 17(2) | 9(2) | 12(2) | 7(2) |
| C24 | 43(2) | 42(3) | 24(2) | 13(2) | 20(2) | 18(2) |
| C25 | 37(2) | 52(3) | 23(2) | 12(2) | 18(2) | 5(2) |
| C26 | 59(3) | 33(2) | 25(2) | 12(2) | 22(2) | 3(2) |
| C27 | 36(2) | 30(2) | 28(2) | 15(2) | 16(2) | 7(2) |
| C28 | 38(2) | 27(2) | 23(2) | 11(2) | 7(2) | 5(2) |
| Cl1 | 52(1) | 32(1) | 34(1) | 10(1) | 9(1) | 8(1) |
| O9 | 70(3) | 65(3) | 77(3) | 21(2) | 35(2) | 6(2) |
| O10 | 82(3) | 97(4) | 88(3) | 31(3) | 26(2) | 21(3) |
| O11 | 82(3) | 97(4) | 88(3) | 31(3) | 26(2) | 21(3) |
| O12 | 82(3) | 97(4) | 88(3) | 31(3) | 26(2) | 21(3) |
| O13 | 82(3) | 97(4) | 88(3) | 31(3) | 26(2) | 21(3) |
| O14 | 82(3) | 97(4) | 88(3) | 31(3) | 26(2) | 21(3) |
| O15 | 82(3) | 97(4) | 88(3) | 31(3) | 26(2) | 21(3) |
| N1 | 51(3) | 63(3) | 56(3) | 14(2) | 20(2) | 17(2) |
| C31 | 66(4) | 52(3) | 40(2) | 19(3) | 16(2) | 27(3) |
| C32 | 58(4) | 84(5) | 69(4) | -2(3) | -20(3) | 44(4) |

## 7.3.4. $[Ag_2\{Cp_2Mo_2(CO)_4(\mu_3,\eta^2:\eta^2:\eta^2\text{-}P_2)\}_2\{Cp_2Mo_2(CO)_4(\mu_4,\eta^2:\eta^2:\eta^1:\eta^1\text{-}P_2)\}_2][(PF_6)_2]\bullet 2CH_3CN$ (**42e**•2CH$_3$CN)

Crystals of **42e**•2CH$_3$CN were obtained by controlled diffusion of a CH$_3$CN solution of $AgPF_6$ into a $CH_2Cl_2$ solution of $[Cp_2Mo_2(CO)_4(\mu,\eta^2\text{-}P_2)]$ **6b** at room temperature in the dark.

Table 7.10. Crystal data and structure refinement for **42e**•2CH$_3$CN.

| | |
|---|---|
| Empirical formula | $C_{60}H_{46}Ag_2F_{12}N_2Mo_8O_{16}P_{10}$ |
| Formula weight | 2571.95 g mol$^{-1}$ |
| Crystal size | 0.400 × 0.320 × 0.220 mm |
| Crystal description | prism |
| Crystal colour | red |
| Crystal system | triclinic |
| Space group | $P\ \overline{1}$ |
| Unit cell dimensions | $a$ = 12.193(1) Å, $\alpha$ = 112.96(1)° |
| | $b$ = 13.420(1) Å, $\beta$ = 100.11(1)° |
| | $c$ = 15.3915(17) Å, $\gamma$ = 94.27(1)° |
| Volume | 2254.5(5) Å$^3$ |
| Z, Calculated density | 1, 1.894 Mg m$^{-3}$ |
| Absorption coefficient | 1.753 mm$^{-1}$ |
| F(000) | 1236 |
| Measurement device type | STOE-IPDS |
| Measurement method | rotation |
| Temperature | 173(1) K |
| Wavelength | 0.71073 Å |
| Monochromator | graphite |
| $\theta$ range for data collection | 2.20 to 25.87° |
| Index ranges | $-14 \le h \le 14$, $-16 \le k \le 16$, $-18 \le l \le 18$ |
| Reflections collected/ unique | 31811 / 8068 [R(int) = 0.0242] |
| Reflections greater I>2\s(I) | 7528 |
| Absorption correction | numerical |
| Max. and min. transmission | 0.7791 and 0.7058 |
| Refinement method | Full-matrix least-squares on F$^2$ |
| Data / restraints / parameters | 8068 / 0 / 496 |
| Goodness-of-fit on F$^2$ | 1.103 |
| Final R indices [I>2sigma(I)] | R1 = 0.0283, wR2 = 0.0864 |
| R indices (all data) | R1 = 0.0304, wR2 = 0.0877 |
| Largest diff. peak and hole | 1.224 and -0.499 e Å$^{-3}$ |

Table 7.11. Atomic coordinates ( $\times 10^4$) and equivalent isotropic displacement parameters ($Å^2 \times 10^3$) for **42e**•2$CH_3CN$. $U_{eq}$ is defined as one third of the trace of the orthogonalised $U_{ij}$ tensor.

| **Atom** | **x** | **y** | **z** | $\boldsymbol{U_{eq}}$ |
|---|---|---|---|---|
| Ag1 | -1036(1) | 1364(1) | 5596(1) | 41(1) |
| Mo1 | -2113(1) | 4503(1) | 5918(1) | 24(1) |
| Mo2 | -2391(1) | 3998(1) | 7642(1) | 27(1) |
| Mo3 | -630(1) | 262(1) | 2353(1) | 25(1) |
| Mo4 | -2369(1) | -1392(1) | 2490(1) | 27(1) |
| P1 | 290(1) | 840(1) | 6708(1) | 30(1) |
| P2 | -2546(1) | 2679(1) | 5893(1) | 29(1) |
| P3 | -894(1) | 3518(1) | 6729(1) | 30(1) |
| P4 | -1344(1) | 319(1) | 3817(1) | 30(1) |
| O1 | -4989(2) | 3495(3) | 6734(2) | 51(1) |
| O2 | -2598(3) | 1729(3) | 7788(2) | 57(1) |
| O3 | -434(3) | 3664(3) | 4562(2) | 55(1) |
| O4 | -166(2) | 6405(2) | 7366(2) | 49(1) |
| O5 | -2313(2) | 1983(3) | 2653(2) | 52(1) |
| O6 | 1232(2) | 2105(2) | 3969(2) | 49(1) |
| O7 | -2266(3) | -2537(3) | 3927(2) | 62(1) |
| O8 | -1160(3) | -3265(2) | 1258(2) | 54(1) |
| C1 | -3840(3) | 5207(3) | 5963(3) | 40(1) |
| C2 | -4018(3) | 4205(3) | 5128(3) | 40(1) |
| C3 | -3332(3) | 4317(3) | 4513(3) | 41(1) |
| C4 | -2711(3) | 5416(3) | 4970(3) | 39(1) |
| C5 | -3033(3) | 5947(3) | 5862(3) | 37(1) |
| C6 | -2561(4) | 4691(4) | 9228(3) | 48(1) |
| C7 | -2856(4) | 5484(4) | 8867(3) | 49(1) |
| C8 | -1906(4) | 5907(3) | 8648(3) | 43(1) |
| C9 | -995(3) | 5379(3) | 8875(2) | 41(1) |
| C10 | -1400(4) | 4634(3) | 9232(2) | 44(1) |
| C11 | -4035(3) | 3664(3) | 7032(3) | 35(1) |
| C12 | -2523(3) | 2537(3) | 7704(2) | 38(1) |
| C13 | -1030(3) | 3962(3) | 5066(3) | 36(1) |
| C14 | -856(3) | 5686(3) | 6857(2) | 34(1) |
| C15 | 161(3) | -979(4) | 1159(3) | 43(1) |
| C16 | 783(3) | 86(4) | 1508(3) | 48(1) |
| C17 | 62(4) | 760(4) | 1262(3) | 49(1) |
| C18 | -1008(4) | 101(3) | 768(2) | 42(1) |
| C19 | -944(3) | -960(3) | 693(2) | 38(1) |
| C20 | -3943(3) | -487(4) | 2403(3) | 44(1) |
| C21 | -3672(3) | -850(3) | 1484(3) | 40(1) |
| C22 | -3791(3) | -2003(4) | 1092(3) | 44(1) |

| | | | | |
|---|---|---|---|---|
| C23 | -4151(3) | -2366(4) | 1764(3) | 46(1) |
| C24 | -4248(3) | -1406(4) | 2584(3) | 47(1) |
| C25 | -1715(3) | 1347(3) | 2561(3) | 35(1) |
| C26 | 534(3) | 1437(3) | 3404(2) | 35(1) |
| C27 | -2276(3) | -2103(3) | 3418(3) | 39(1) |
| C28 | -1580(3) | -2571(3) | 1713(2) | 37(1) |
| P5 | 5928(1) | 8247(1) | 8261(1) | 40(1) |
| F1 | 6610(3) | 8849(4) | 9350(2) | 99(2) |
| F2 | 4835(3) | 8705(4) | 8558(3) | 89(2) |
| F3 | 5592(4) | 7207(4) | 8444(4) | 118(2) |
| F4 | 5283(4) | 7653(3) | 7168(3) | 102(2) |
| F5 | 7057(3) | 7824(3) | 7966(3) | 84(1) |
| F6 | 6298(3) | 9311(3) | 8091(2) | 71(1) |
| N1 | 8516(4) | 2804(4) | 374(3) | 72(2) |
| C29 | 7634(4) | 2333(4) | 170(3) | 44(1) |
| C30 | 6508(4) | 1740(5) | -104(5) | 73(2) |

Table 7.12. Anisotropic displacement parameters ($Å^2 \times 10^3$) for **42e**•2$CH_3CN$. The anisotropic displacement factor exponent takes the form: $-2\pi^2[h^2a^{*2}U_{11} + ... + 2hka^*b^*U_{12}]$.

| **Atom** | $U_{11}$ | $U_{22}$ | $U_{33}$ | $U_{23}$ | $U_{13}$ | $U_{12}$ |
|---|---|---|---|---|---|---|
| Ag1 | 57(1) | 42(1) | 25(1) | 11(1) | 8(1) | 27(1) |
| Mo1 | 26(1) | 25(1) | 23(1) | 11(1) | 5(1) | 5(1) |
| Mo2 | 31(1) | 28(1) | 23(1) | 11(1) | 7(1) | 6(1) |
| Mo3 | 29(1) | 27(1) | 21(1) | 10(1) | 6(1) | 4(1) |
| Mo4 | 32(1) | 25(1) | 24(1) | 11(1) | 5(1) | 3(1) |
| P1 | 36(1) | 29(1) | 25(1) | 12(1) | 3(1) | 7(1) |
| P2 | 36(1) | 26(1) | 26(1) | 10(1) | 8(1) | 6(1) |
| P3 | 30(1) | 34(1) | 30(1) | 16(1) | 8(1) | 12(1) |
| P4 | 39(1) | 28(1) | 22(1) | 9(1) | 9(1) | 4(1) |
| O1 | 33(1) | 66(2) | 57(2) | 30(2) | 11(1) | 2(1) |
| O2 | 91(2) | 39(2) | 51(2) | 28(1) | 18(2) | 12(2) |
| O3 | 66(2) | 52(2) | 55(2) | 19(1) | 40(2) | 15(2) |
| O4 | 50(2) | 42(2) | 43(2) | 15(1) | -4(1) | -12(1) |
| O5 | 49(2) | 41(2) | 67(2) | 23(1) | 10(1) | 19(1) |
| O6 | 45(2) | 43(2) | 47(2) | 13(1) | -1(1) | -8(1) |
| O7 | 81(2) | 63(2) | 53(2) | 40(2) | 9(2) | -2(2) |
| O8 | 68(2) | 40(2) | 40(2) | 2(1) | 11(1) | 19(1) |
| C1 | 33(2) | 46(2) | 47(2) | 26(2) | 6(1) | 14(2) |
| C2 | 30(2) | 38(2) | 52(2) | 26(2) | -6(2) | 4(2) |
| C3 | 49(2) | 40(2) | 32(2) | 18(2) | -6(2) | 9(2) |
| C4 | 46(2) | 39(2) | 38(2) | 25(2) | 4(2) | 8(2) |
| C5 | 39(2) | 30(2) | 44(2) | 19(2) | 4(1) | 10(1) |

| | | | | | | |
|---|---|---|---|---|---|---|
| C6 | 65(3) | 47(2) | 26(2) | 7(2) | 18(2) | -2(2) |
| C7 | 53(2) | 45(2) | 37(2) | 0(2) | 17(2) | 13(2) |
| C8 | 62(2) | 31(2) | 27(2) | 4(1) | 9(2) | 3(2) |
| C9 | 44(2) | 42(2) | 25(2) | 6(1) | 4(1) | -1(2) |
| C10 | 60(2) | 44(2) | 22(2) | 12(2) | 1(2) | 1(2) |
| C11 | 37(2) | 37(2) | 36(2) | 18(2) | 14(1) | 5(2) |
| C12 | 48(2) | 40(2) | 29(2) | 16(2) | 9(1) | 8(2) |
| C13 | 42(2) | 31(2) | 36(2) | 14(1) | 12(2) | 4(2) |
| C14 | 36(2) | 34(2) | 34(2) | 16(1) | 7(1) | 5(2) |
| C15 | 45(2) | 52(2) | 34(2) | 15(2) | 19(2) | 18(2) |
| C16 | 41(2) | 64(3) | 36(2) | 13(2) | 19(2) | 1(2) |
| C17 | 71(3) | 45(2) | 34(2) | 16(2) | 25(2) | -3(2) |
| C18 | 56(2) | 49(2) | 27(2) | 21(2) | 12(2) | 11(2) |
| C19 | 49(2) | 42(2) | 22(2) | 11(1) | 12(1) | 6(2) |
| C20 | 33(2) | 45(2) | 53(2) | 21(2) | 9(2) | 9(2) |
| C21 | 30(2) | 50(2) | 44(2) | 27(2) | -1(1) | 2(2) |
| C22 | 35(2) | 48(2) | 39(2) | 14(2) | -4(2) | 1(2) |
| C23 | 37(2) | 42(2) | 54(2) | 21(2) | -2(2) | -6(2) |
| C24 | 35(2) | 57(3) | 57(2) | 30(2) | 15(2) | 6(2) |
| C25 | 37(2) | 31(2) | 36(2) | 15(1) | 5(1) | 3(2) |
| C26 | 38(2) | 34(2) | 34(2) | 16(2) | 8(1) | 5(2) |
| C27 | 45(2) | 37(2) | 36(2) | 17(2) | 7(2) | -1(2) |
| C28 | 46(2) | 30(2) | 27(2) | 7(1) | 2(1) | 3(2) |
| P5 | 41(1) | 39(1) | 39(1) | 16(1) | 7(1) | 8(1) |
| F1 | 91(2) | 148(4) | 45(2) | 34(2) | -2(2) | 21(2) |
| F2 | 62(2) | 116(3) | 116(3) | 63(2) | 42(2) | 42(2) |
| F3 | 119(3) | 85(3) | 186(5) | 94(3) | 39(3) | 8(2) |
| F4 | 101(3) | 99(3) | 60(2) | 6(2) | -19(2) | -15(2) |
| F5 | 77(2) | 80(2) | 99(2) | 29(2) | 39(2) | 38(2) |
| F6 | 78(2) | 55(2) | 88(2) | 36(2) | 21(2) | 5(2) |
| N1 | 58(3) | 80(3) | 70(3) | 27(2) | 13(2) | -4(2) |
| C29 | 52(2) | 45(2) | 36(2) | 16(2) | 10(2) | 14(2) |
| C30 | 53(3) | 58(3) | 95(4) | 21(3) | 15(3) | 4(2) |

## 7.3.5. $[Ag_2\{Cp_2Mo_2(CO)_4(\mu_3,\eta^2:\eta^2:\eta^2\text{-}P_2)\}_2\{Cp_2Mo_2(CO)_4(\mu_4,\eta^2:\eta^2:\eta^1:\eta^1\text{-}P_2)\}_2][(SbF_6)_2]\bullet 4.5CH_3CN$ (**42f**$\bullet 4.5CH_3CN$)

Crystals of **42f**$\bullet 4.5CH_3CN$ were obtained by controlled diffusion of a $CH_3CN$ solution of $AgSbF_6$ into a $CH_2Cl_2$ solution of $[Cp_2Mo_2(CO)_4(\mu,\eta^2\text{-}P_2)]$ **6b** at room temperature in the dark.

Table 7.13. Crystal data and structure refinement for **42f**$\bullet 4.5CH_3CN$.

| | |
|---|---|
| Empirical formula | $C_{65}H_{53.5}Ag_2F_{12}N_{4.5}Mo_8O_{16}P_8Sb_2$ |
| Formula weight | 2844.14 |
| Crystal size | $0.32 \times 0.15 \times 0.10$ mm |
| Crystal description | prism |
| Crystal colour | orange to red |
| Crystal system | triclinic |
| Space group | $P\ \overline{1}$ |
| Unit cell dimensions | $a$ = 12.112(1) Å, $\alpha$ = 113.73(1)° |
| | $b$ = 13.733(1) Å, $\beta$ = 99.30(1)° |
| | $c$ = 15.671(1) Å, $\gamma$ = 93.50(1)° |
| Volume | 2332.0(4) $Å^3$ |
| Z, Calculated density | 1, 2.025 Mg $m^{-3}$ |
| Absorption coefficient | 2.231 $mm^{-1}$ |
| F(000) | 1357 |
| Measurement device type | STOE-IPDS |
| Measurement method | rotation |
| Temperature | 173(1) K |
| Wavelength | 0.71073 Å |
| Monochromator | graphite |
| $\theta$ range for data collection | 2.01 to 25.81° |
| Index ranges | $-14 \le h \le 14$, $-16 \le k \le 16$, $-19 \le l \le 19$ |
| Reflections collected / unique | 20232 / 8344 [R(int) = 0.0286] |
| Reflections greater I>2\s(I) | 6385 |
| Absorption correction | numerical |
| Max. and min. transmission | 0.8499 and 0.5143 |
| Refinement method | Full-matrix least-squares on $F^2$ |
| Data / restraints / parameters | 8344 / 0 / 496 |
| Goodness-of-fit on $F^2$ | 0.916 |
| Final R indices [I>2sigma(I)] | R1 = 0.0280, wR2 = 0.0708 |
| R indices (all data) | R1 = 0.0392, wR2 = 0.0731 |
| Largest diff. peak and hole | 0.940 and -0.649 e $Å^{-3}$ |

Table 7.14. Atomic coordinates ( $\times 10^4$) and equivalent isotropic displacement parameters ($Å^2 \times 10^3$) for **42f**•4.5$CH_3CN$. $U_{eq}$ is defined as one third of the trace of the orthogonalised $U_{ij}$ tensor.

| **Atom** | **x** | **y** | **z** | $U_{eq}$ |
|---|---|---|---|---|
| Ag1 | 1069(1) | -1364(1) | 4423(1) | 57(1) |
| Mo1 | -577(1) | 244(1) | 2381(1) | 37(1) |
| Mo2 | -2263(1) | -1384(1) | 2551(1) | 40(1) |
| Mo3 | 2082(1) | -4511(1) | 4069(1) | 34(1) |
| Mo4 | 2378(1) | -4047(1) | 2361(1) | 39(1) |
| P1 | -176(1) | -845(1) | 3282(1) | 41(1) |
| P2 | -1247(1) | 289(1) | 3843(1) | 42(1) |
| P3 | 2504(1) | -2739(1) | 4083(1) | 41(1) |
| P4 | 867(1) | -3544(1) | 3276(1) | 43(1) |
| O1 | 1292(3) | 2040(3) | 3921(3) | 71(1) |
| O2 | -2255(4) | 1957(3) | 2791(3) | 80(2) |
| O3 | -1072(4) | -3237(3) | 1261(3) | 76(1) |
| O4 | -2084(4) | -2499(3) | 3958(3) | 87(2) |
| O5 | 369(4) | -3651(3) | 5400(3) | 75(2) |
| O6 | 173(4) | -6376(3) | 2664(3) | 74(1) |
| O7 | 4965(3) | -3576(4) | 3227(3) | 76(2) |
| O8 | 2555(5) | -1833(3) | 2217(3) | 85(2) |
| C1 | 174(5) | -972(4) | 1136(3) | 60(2) |
| C2 | 803(6) | 48(5) | 1480(4) | 71(2) |
| C3 | 82(7) | 738(5) | 1294(4) | 75(2) |
| C4 | -989(6) | 134(4) | 838(3) | 65(2) |
| C5 | -933(5) | -926(4) | 732(3) | 55(2) |
| C6 | 600(4) | 1388(4) | 3383(3) | 48(1) |
| C7 | -1671(4) | 1331(4) | 2657(3) | 53(2) |
| C8 | -3611(4) | -852(4) | 1605(4) | 59(2) |
| C9 | -3713(4) | -1980(4) | 1215(4) | 62(2) |
| C10 | -4039(5) | -2323(5) | 1894(5) | 70(2) |
| C11 | -4127(5) | -1388(5) | 2705(4) | 69(2) |
| C12 | -3855(4) | -493(4) | 2519(4) | 62(2) |
| C13 | -1480(5) | -2549(4) | 1736(3) | 53(1) |
| C14 | -2129(5) | -2074(4) | 3464(4) | 57(2) |
| C15 | 3022(4) | -5920(4) | 4131(4) | 52(2) |
| C16 | 2656(5) | -5402(4) | 4999(3) | 56(2) |
| C17 | 3257(5) | -4335(4) | 5450(3) | 58(2) |
| C18 | 3970(4) | -4225(4) | 4856(4) | 58(2) |
| C19 | 3818(4) | -5216(4) | 4036(4) | 53(2) |
| C20 | 980(4) | -3958(3) | 4905(3) | 50(2) |
| C21 | 846(4) | -5677(4) | 3153(3) | 51(2) |
| C22 | 1913(6) | -5905(4) | 1367(3) | 62(2) |

| | | | | |
|---|---|---|---|---|
| C23 | 2867(6) | -5524(4) | 1155(4) | 68(2) |
| C24 | 2575(6) | -4750(4) | 801(3) | 68(2) |
| C25 | 1407(6) | -4682(5) | 797(3) | 66(2) |
| C26 | 1014(5) | -5384(4) | 1148(3) | 63(2) |
| C27 | 4010(5) | -3731(4) | 2946(3) | 51(2) |
| C28 | 2491(5) | -2619(4) | 2297(3) | 61(2) |
| Sb1 | 4174(1) | 1692(1) | 1708(1) | 54(1) |
| F1 | 4557(6) | 2910(5) | 1566(8) | 241(6) |
| F2 | 2833(3) | 2171(3) | 2066(3) | 101(2) |
| F3 | 4919(5) | 2326(5) | 2956(3) | 169(3) |
| F4 | 3398(5) | 1032(7) | 475(3) | 194(4) |
| F5 | 3760(4) | 474(3) | 1880(4) | 130(2) |
| F6 | 5485(3) | 1183(4) | 1334(3) | 107(2) |
| N1 | 1516(7) | 7168(6) | 9599(5) | 120(3) |
| C29 | 3513(7) | 8072(7) | 10203(6) | 111(3) |
| C30 | 2366(6) | 7558(5) | 9854(4) | 69(2) |

Table 7.15. Anisotropic displacement parameters ($Å^2 \times 10^3$) for **42f**•4.5$CH_3CN$. The anisotropic displacement factor exponent takes the form: $-2\pi^2[h^2a^{*2}U_{11} + ... + 2hka^*b^*U_{12}]$.

| **Atom** | $U_{11}$ | $U_{22}$ | $U_{33}$ | $U_{23}$ | $U_{13}$ | $U_{12}$ |
|---|---|---|---|---|---|---|
| Ag1 | 82(1) | 57(1) | 34(1) | 19(1) | 15(1) | 39(1) |
| Mo1 | 46(1) | 38(1) | 29(1) | 16(1) | 7(1) | 7(1) |
| Mo2 | 47(1) | 39(1) | 34(1) | 16(1) | 7(1) | 7(1) |
| Mo3 | 38(1) | 32(1) | 33(1) | 15(1) | 6(1) | 7(1) |
| Mo4 | 48(1) | 39(1) | 32(1) | 15(1) | 12(1) | 11(1) |
| P1 | 50(1) | 41(1) | 35(1) | 18(1) | 4(1) | 12(1) |
| P2 | 57(1) | 39(1) | 29(1) | 12(1) | 11(1) | 10(1) |
| P3 | 55(1) | 33(1) | 38(1) | 15(1) | 15(1) | 10(1) |
| P4 | 43(1) | 48(1) | 44(1) | 24(1) | 12(1) | 18(1) |
| O1 | 69(2) | 61(2) | 66(2) | 20(2) | -5(2) | -13(2) |
| O2 | 73(3) | 58(2) | 101(3) | 28(2) | 5(2) | 29(2) |
| O3 | 97(3) | 55(2) | 58(2) | 4(2) | 15(2) | 26(2) |
| O4 | 121(4) | 92(3) | 77(3) | 64(3) | 21(3) | 8(3) |
| O5 | 89(3) | 72(2) | 78(3) | 30(2) | 54(2) | 21(2) |
| O6 | 76(3) | 62(2) | 66(2) | 23(2) | -10(2) | -26(2) |
| O7 | 47(2) | 102(3) | 80(3) | 38(2) | 17(2) | 4(2) |
| O8 | 144(4) | 58(2) | 79(3) | 46(2) | 43(3) | 23(2) |
| C1 | 78(4) | 65(3) | 43(3) | 19(2) | 33(3) | 19(3) |
| C2 | 67(4) | 95(4) | 48(3) | 22(3) | 29(3) | 1(3) |
| C3 | 116(6) | 69(3) | 44(3) | 25(3) | 30(3) | -10(4) |
| C4 | 95(5) | 74(3) | 35(2) | 31(2) | 13(3) | 18(3) |
| C5 | 73(4) | 59(3) | 28(2) | 14(2) | 11(2) | 4(2) |

| | | | | | | |
|---|---|---|---|---|---|---|
| C6 | 54(3) | 48(2) | 42(2) | 21(2) | 6(2) | 8(2) |
| C7 | 58(3) | 48(2) | 49(3) | 21(2) | 1(2) | 7(2) |
| C8 | 41(3) | 82(3) | 64(3) | 44(3) | 1(2) | 11(2) |
| C9 | 51(3) | 65(3) | 53(3) | 18(2) | -12(2) | -2(2) |
| C10 | 55(3) | 66(3) | 85(4) | 37(3) | -2(3) | -8(3) |
| C11 | 47(3) | 98(4) | 70(4) | 42(3) | 17(3) | 4(3) |
| C12 | 44(3) | 67(3) | 76(4) | 31(3) | 11(3) | 14(2) |
| C13 | 66(3) | 47(2) | 41(2) | 16(2) | 4(2) | 8(2) |
| C14 | 66(3) | 51(3) | 54(3) | 24(2) | 11(3) | -1(2) |
| C15 | 56(3) | 41(2) | 62(3) | 26(2) | 6(2) | 16(2) |
| C16 | 72(3) | 53(3) | 51(3) | 35(2) | 1(2) | 12(2) |
| C17 | 71(4) | 55(3) | 41(2) | 21(2) | -12(3) | 10(2) |
| C18 | 41(3) | 60(3) | 71(3) | 35(3) | -11(3) | 7(2) |
| C19 | 49(3) | 56(3) | 64(3) | 33(2) | 10(2) | 23(2) |
| C20 | 60(3) | 43(2) | 51(3) | 21(2) | 17(2) | 8(2) |
| C21 | 54(3) | 50(2) | 50(3) | 24(2) | 6(2) | 4(2) |
| C22 | 94(4) | 43(2) | 40(3) | 7(2) | 18(3) | 8(3) |
| C23 | 85(4) | 55(3) | 46(3) | -1(2) | 23(3) | 24(3) |
| C24 | 105(5) | 57(3) | 40(3) | 12(2) | 32(3) | 2(3) |
| C25 | 85(4) | 73(3) | 34(2) | 19(2) | 2(3) | 14(3) |
| C26 | 73(4) | 59(3) | 36(2) | 5(2) | 1(2) | -5(3) |
| C27 | 52(3) | 58(3) | 47(3) | 23(2) | 18(2) | 8(2) |
| C28 | 92(4) | 58(3) | 40(2) | 23(2) | 25(3) | 23(3) |
| Sb1 | 60(1) | 53(1) | 51(1) | 23(1) | 9(1) | 15(1) |
| F1 | 165(6) | 186(6) | 545(16) | 277(9) | 183(8) | 90(5) |
| F2 | 83(3) | 91(2) | 130(3) | 36(2) | 46(3) | 32(2) |
| F3 | 118(4) | 219(6) | 74(3) | -18(3) | -16(3) | -13(4) |
| F4 | 126(4) | 377(10) | 60(3) | 69(4) | 5(3) | 88(6) |
| F5 | 127(4) | 83(3) | 206(5) | 81(3) | 46(4) | 18(3) |
| F6 | 84(3) | 140(3) | 117(3) | 61(3) | 39(2) | 55(3) |
| N1 | 83(5) | 139(6) | 96(5) | 11(4) | 8(4) | 3(4) |
| C29 | 106(6) | 100(5) | 112(6) | 25(5) | 37(5) | 5(5) |
| C30 | 67(4) | 70(3) | 61(3) | 18(3) | 14(3) | 10(3) |

## 7.3.6. $[Ag_2\{Cp_2Mo_2(CO)_4(\mu_3,\eta^2:\eta^2:\eta^2\text{-}P_2)\}_2\{Cp_2Mo_2(CO)_4(\mu_4,\eta^2:\eta^2:\eta^1:\eta^1\text{-}P_2)\}_2][\langle Al\{OC(CF_3)_3\}_4\rangle_2]\bullet CH_2Cl_2$ (**42g**•$CH_2Cl_2$)

The compound **42g**•$CH_2Cl_2$ was crystallised from a concentrated $CH_2Cl_2$ solution of **42g** at –28 °C.

Table 7.16. Crystal data and structure refinement for **42g**•$CH_2Cl_2$.

| | |
|---|---|
| Empirical formula | $C_{44.5}H_{21}AgAlClF_{36}Mo_4O_{12}P_4$ |
| Formula weight | 2109.55 g $mol^{-1}$ |
| Crystal size | 0.30 × 0.20 × 0.10 mm |
| Crystal description | plate |
| Crystal colour | red |
| Crystal system | triclinic |
| Space group | $P\ \bar{1}$ |
| Unit cell dimensions | $a$ = 13.838(3) Å, $\alpha$ = 105.90(3)° |
| | $b$ = 14.597(3) Å, $\beta$ = 100.30(3)° |
| | $c$ = 18.576(4) Å, $\gamma$ = 111.27(3)° |
| Volume | 3196.8(11) $Å^3$ |
| Z, Calculated density | 2, 2.192 Mg $m^{-3}$ |
| Absorption coefficient | 1.381 $mm^{-1}$ |
| F(000) | 2026 |
| Measurement device type | STOE-IPDS |
| Measurement method | rotation |
| Temperature | 150(1) K |
| Wavelength | 0.71073 Å |
| Monochromator | graphite |
| $\theta$ range for data collection | 1.61 to 27.14° |
| Limiting indices | $-17 \le h \le 16$, $-15 \le k \le 18$, $-23 \le l \le 23$ |
| Reflections collected / unique | 22151 / 12619 [R(int) = 0.0385] |
| Reflections greater I>2\s(I) | 11722 |
| Refinement method | Full-matrix least-squares on $F^2$ |
| Data / restraints / parameters | 12619 / 0 / 939 |
| Goodness-of-fit on $F^2$ | 1.029 |
| Final R indices [I>2sigma(I)] | R1 = 0.0348, wR2 = 0.0937 |
| Absorption correction | none |
| R indices (all data) | R1 = 0.0372, wR2 = 0.0958 |
| Extinction coefficient | 0.0084(5) |
| Largest diff. peak and hole | 0.690 and -0.998 e $Å^{-3}$ |

Table 7.17. Atomic coordinates ( × $10^4$) and equivalent isotropic displacement parameters (Å$^2$ × $10^3$) for **42g**•$CH_2Cl_2$. $U_{eq}$ is defined as one third of the trace of the orthogonalised $U_{ij}$ tensor.

| **Atom** | **x** | **y** | **z** | $U_{eq}$ |
|---|---|---|---|---|
| Ag | 4470(1) | 1233(1) | 749(1) | 25(1) |
| Mo1 | 3949(1) | 3219(1) | 2668(1) | 23(1) |
| Mo2 | 2160(1) | 2571(1) | 1154(1) | 25(1) |
| Mo3 | 2934(1) | -189(1) | -1956(1) | 23(1) |
| Mo4 | 5304(1) | 1315(1) | -1604(1) | 25(1) |
| P1 | 3107(1) | 1511(1) | 1558(1) | 25(1) |
| P2 | 4041(1) | 2822(1) | 1278(1) | 25(1) |
| P3 | 4527(1) | -399(1) | -1366(1) | 25(1) |
| P4 | 4397(1) | 901(1) | -643(1) | 27(1) |
| O1 | 6188(2) | 3105(2) | 2901(2) | 44(1) |
| O2 | 4919(2) | 5433(2) | 2504(2) | 47(1) |
| O3 | 1094(2) | 467(2) | -316(2) | 52(1) |
| O4 | 588(2) | 1368(3) | 1952(2) | 53(1) |
| O5 | 2527(2) | 1800(2) | -1225(1) | 44(1) |
| O6 | 1688(2) | -1269(2) | -939(2) | 45(1) |
| O7 | 7458(2) | 1502(2) | -547(2) | 47(1) |
| O8 | 5394(2) | -443(2) | -2978(1) | 44(1) |
| C1 | 5380(2) | 3160(3) | 2782(2) | 31(1) |
| C2 | 4565(2) | 4618(3) | 2544(2) | 32(1) |
| C3 | 1506(2) | 1216(3) | 230(2) | 36(1) |
| C4 | 1194(2) | 1795(3) | 1676(2) | 37(1) |
| C5 | 2686(2) | 1085(3) | -1481(2) | 32(1) |
| C6 | 2166(2) | -850(3) | -1282(2) | 33(1) |
| C7 | 6662(2) | 1405(3) | -928(2) | 34(1) |
| C8 | 5358(2) | 186(3) | -2473(2) | 33(1) |
| C9 | 3730(3) | 4168(3) | 3809(2) | 37(1) |
| C10 | 4530(3) | 3814(3) | 4021(2) | 37(1) |
| C11 | 3994(3) | 2686(3) | 3730(2) | 36(1) |
| C12 | 2886(3) | 2363(3) | 3348(2) | 35(1) |
| C13 | 2720(3) | 3277(3) | 3399(2) | 36(1) |
| C14 | 2335(3) | 4326(3) | 1498(2) | 41(1) |
| C15 | 1238(3) | 3630(3) | 1306(2) | 44(1) |
| C16 | 871(3) | 2948(3) | 498(2) | 46(1) |
| C17 | 1776(3) | 3240(3) | 212(2) | 45(1) |
| C18 | 2675(3) | 4090(3) | 827(2) | 42(1) |
| C19 | 1767(3) | -1808(3) | -2932(2) | 39(1) |
| C20 | 2720(3) | -1444(3) | -3151(2) | 36(1) |
| C21 | 2841(2) | -515(3) | -3292(2) | 33(1) |
| C22 | 1967(2) | -286(3) | -3153(2) | 34(1) |

| | | | | |
|---|---|---|---|---|
| C23 | 1297(2) | -1081(3) | -2928(2) | 37(1) |
| C24 | 4593(3) | 2366(3) | -2078(2) | 41(1) |
| C25 | 5365(3) | 2234(3) | -2447(2) | 43(1) |
| C26 | 6390(3) | 2708(3) | -1872(2) | 45(1) |
| C27 | 6255(3) | 3135(3) | -1134(2) | 43(1) |
| C28 | 5150(3) | 2926(3) | -1257(2) | 41(1) |
| Al1 | 9806(1) | 6700(1) | 3190(1) | 22(1) |
| O9 | 9036(2) | 5491(2) | 2425(1) | 29(1) |
| O10 | 10740(2) | 6549(2) | 3845(1) | 27(1) |
| O11 | 10439(2) | 7600(2) | 2785(1) | 27(1) |
| O12 | 9050(2) | 7180(2) | 3690(1) | 27(1) |
| F1 | 8770(2) | 3473(2) | 1385(2) | 61(1) |
| F2 | 7136(2) | 3202(2) | 820(1) | 56(1) |
| F3 | 7677(2) | 3527(2) | 2056(1) | 61(1) |
| F4 | 6929(2) | 4977(2) | 749(1) | 57(1) |
| F5 | 6692(2) | 4782(2) | 1827(1) | 63(1) |
| F6 | 7753(2) | 6294(2) | 1852(2) | 62(1) |
| F7 | 10065(2) | 5315(2) | 1347(1) | 54(1) |
| F8 | 9228(2) | 6208(2) | 1082(1) | 60(1) |
| F9 | 8602(2) | 4575(2) | 365(1) | 58(1) |
| F10 | 12986(2) | 6400(2) | 4960(1) | 53(1) |
| F11 | 11527(2) | 6259(2) | 5275(1) | 48(1) |
| F12 | 12471(2) | 7648(2) | 5086(1) | 47(1) |
| F13 | 11354(2) | 4461(2) | 4049(1) | 49(1) |
| F14 | 10413(2) | 4362(2) | 2955(1) | 49(1) |
| F15 | 9891(2) | 4679(2) | 3974(2) | 51(1) |
| F16 | 12685(2) | 5626(2) | 3375(1) | 47(1) |
| F17 | 12976(2) | 7254(2) | 3741(1) | 47(1) |
| F18 | 11653(2) | 6111(2) | 2719(1) | 42(1) |
| F19 | 8295(2) | 5400(2) | 3992(1) | 44(1) |
| F20 | 7436(2) | 5929(2) | 4742(1) | 47(1) |
| F21 | 6909(2) | 5613(2) | 3505(1) | 49(1) |
| F22 | 10212(2) | 8579(2) | 5135(1) | 52(1) |
| F23 | 8968(2) | 7966(2) | 5654(1) | 51(1) |
| F24 | 9825(2) | 7070(2) | 5234(1) | 44(1) |
| F25 | 8467(2) | 8825(2) | 4477(1) | 53(1) |
| F26 | 7107(2) | 7593(2) | 4565(2) | 56(1) |
| F27 | 7318(2) | 7536(2) | 3438(1) | 50(1) |
| F28 | 12768(2) | 8900(2) | 3299(2) | 69(1) |
| F29 | 11900(2) | 8955(2) | 4177(1) | 53(1) |
| F30 | 12431(2) | 10261(2) | 3786(2) | 63(1) |
| F31 | 10216(2) | 8477(2) | 1568(1) | 59(1) |
| F32 | 11909(2) | 9639(2) | 2200(2) | 58(1) |

| | | | | |
|---|---|---|---|---|
| F33 | 11497(2) | 7974(2) | 1803(1) | 54(1) |
| F34 | 10281(2) | 9469(2) | 3845(1) | 53(1) |
| F35 | 10496(2) | 10087(2) | 2915(2) | 55(1) |
| F36 | 9165(2) | 8575(2) | 2655(1) | 49(1) |
| C29 | 8406(2) | 4982(2) | 1663(2) | 29(1) |
| C30 | 7985(3) | 3779(3) | 1478(2) | 42(1) |
| C31 | 7432(3) | 5269(3) | 1518(2) | 45(1) |
| C32 | 9084(3) | 5262(3) | 1102(2) | 40(1) |
| C33 | 11414(2) | 6085(2) | 3949(2) | 27(1) |
| C34 | 12109(3) | 6604(3) | 4831(2) | 37(1) |
| C35 | 10758(3) | 4880(3) | 3731(2) | 37(1) |
| C36 | 12195(2) | 6276(3) | 3440(2) | 33(1) |
| C37 | 8545(2) | 7161(2) | 4251(2) | 27(1) |
| C38 | 7787(2) | 6015(3) | 4126(2) | 33(1) |
| C39 | 9397(3) | 7703(3) | 5081(2) | 36(1) |
| C40 | 7849(3) | 7790(3) | 4183(2) | 37(1) |
| C41 | 10925(2) | 8620(2) | 2881(2) | 28(1) |
| C42 | 12034(3) | 9207(3) | 3554(2) | 48(1) |
| C43 | 11146(3) | 8692(3) | 2101(2) | 47(1) |
| C44 | 10206(3) | 9206(3) | 3080(2) | 42(1) |
| Cl1 | 4509(2) | 720(4) | -4643(1) | 212(2) |
| C1S | 4735(10) | -489(11) | -4870(7) | 93(4) |

Table 7.18. Anisotropic displacement parameters ($Å^2 \times 10^3$) for **42g•**$CH_2Cl_2$. The anisotropic displacement factor exponent takes the form: $-2\pi^2[h^2a^{*2}U_{11} + ... + 2hka^*b^*U_{12}]$.

| **Atom** | $U_{11}$ | $U_{22}$ | $U_{33}$ | $U_{23}$ | $U_{13}$ | $U_{12}$ |
|---|---|---|---|---|---|---|
| Ag | 30(1) | 29(1) | 24(1) | 10(1) | 10(1) | 19(1) |
| Mo1 | 24(1) | 23(1) | 25(1) | 10(1) | 9(1) | 13(1) |
| Mo2 | 26(1) | 29(1) | 25(1) | 10(1) | 10(1) | 17(1) |
| Mo3 | 26(1) | 27(1) | 21(1) | 9(1) | 8(1) | 16(1) |
| Mo4 | 28(1) | 26(1) | 22(1) | 10(1) | 7(1) | 13(1) |
| P1 | 26(1) | 23(1) | 30(1) | 11(1) | 12(1) | 13(1) |
| P2 | 28(1) | 26(1) | 30(1) | 13(1) | 15(1) | 15(1) |
| P3 | 28(1) | 29(1) | 25(1) | 12(1) | 9(1) | 18(1) |
| P4 | 32(1) | 31(1) | 21(1) | 10(1) | 8(1) | 18(1) |
| O1 | 33(1) | 49(2) | 59(2) | 20(1) | 14(1) | 26(1) |
| O2 | 47(1) | 30(2) | 63(2) | 22(1) | 8(1) | 14(1) |
| O3 | 50(1) | 40(2) | 45(1) | -3(1) | 7(1) | 15(1) |
| O4 | 33(1) | 79(2) | 53(1) | 36(1) | 22(1) | 18(1) |
| O5 | 56(1) | 46(2) | 45(1) | 14(1) | 19(1) | 38(1) |
| O6 | 56(1) | 47(2) | 50(1) | 31(1) | 30(1) | 27(1) |
| O7 | 35(1) | 62(2) | 45(1) | 24(1) | 5(1) | 23(1) |

| | | | | | | |
|---|---|---|---|---|---|---|
| O8 | 47(1) | 44(2) | 41(1) | 8(1) | 22(1) | 21(1) |
| C1 | 31(1) | 31(2) | 35(1) | 13(1) | 12(1) | 16(1) |
| C2 | 30(1) | 28(2) | 37(2) | 12(1) | 8(1) | 13(1) |
| C3 | 32(1) | 40(2) | 37(2) | 13(1) | 11(1) | 19(1) |
| C4 | 27(1) | 50(2) | 36(2) | 18(1) | 10(1) | 19(1) |
| C5 | 38(1) | 37(2) | 30(1) | 14(1) | 13(1) | 24(1) |
| C6 | 35(1) | 36(2) | 34(1) | 14(1) | 11(1) | 20(1) |
| C7 | 36(2) | 37(2) | 30(1) | 14(1) | 10(1) | 17(1) |
| C8 | 33(1) | 37(2) | 31(1) | 15(1) | 13(1) | 15(1) |
| C9 | 53(2) | 36(2) | 29(1) | 10(1) | 17(1) | 27(2) |
| C10 | 40(2) | 44(2) | 26(1) | 10(1) | 9(1) | 21(1) |
| C11 | 49(2) | 45(2) | 30(1) | 21(1) | 17(1) | 29(2) |
| C12 | 42(2) | 38(2) | 34(1) | 19(1) | 22(1) | 18(1) |
| C13 | 40(2) | 47(2) | 30(1) | 14(1) | 21(1) | 26(1) |
| C14 | 57(2) | 39(2) | 37(2) | 10(1) | 9(1) | 36(2) |
| C15 | 52(2) | 60(2) | 42(2) | 21(2) | 19(1) | 46(2) |
| C16 | 47(2) | 55(2) | 41(2) | 14(2) | 1(1) | 36(2) |
| C17 | 71(2) | 52(2) | 31(2) | 20(1) | 15(2) | 45(2) |
| C18 | 56(2) | 40(2) | 50(2) | 26(2) | 20(2) | 34(2) |
| C19 | 41(2) | 30(2) | 30(1) | 5(1) | 0(1) | 10(1) |
| C20 | 39(2) | 40(2) | 24(1) | 0(1) | 2(1) | 24(1) |
| C21 | 32(1) | 44(2) | 20(1) | 8(1) | 6(1) | 17(1) |
| C22 | 36(1) | 45(2) | 25(1) | 14(1) | 4(1) | 24(1) |
| C23 | 28(1) | 48(2) | 31(1) | 12(1) | 4(1) | 17(1) |
| C24 | 43(2) | 34(2) | 47(2) | 24(1) | 6(1) | 16(1) |
| C25 | 62(2) | 37(2) | 34(2) | 23(1) | 15(1) | 18(2) |
| C26 | 44(2) | 37(2) | 59(2) | 30(2) | 20(2) | 14(2) |
| C27 | 47(2) | 27(2) | 43(2) | 12(1) | 3(1) | 9(1) |
| C28 | 55(2) | 29(2) | 46(2) | 15(1) | 16(2) | 22(2) |
| Al1 | 24(1) | 21(1) | 23(1) | 9(1) | 8(1) | 11(1) |
| O9 | 34(1) | 26(1) | 25(1) | 8(1) | 7(1) | 11(1) |
| O10 | 32(1) | 29(1) | 27(1) | 11(1) | 9(1) | 20(1) |
| O11 | 29(1) | 25(1) | 34(1) | 15(1) | 13(1) | 13(1) |
| O12 | 31(1) | 31(1) | 27(1) | 14(1) | 13(1) | 18(1) |
| F1 | 68(1) | 42(1) | 63(1) | 1(1) | 8(1) | 33(1) |
| F2 | 50(1) | 36(1) | 46(1) | -2(1) | -2(1) | 2(1) |
| F3 | 74(2) | 36(1) | 53(1) | 19(1) | 17(1) | 2(1) |
| F4 | 48(1) | 71(2) | 41(1) | 10(1) | -4(1) | 31(1) |
| F5 | 37(1) | 85(2) | 58(1) | 13(1) | 20(1) | 24(1) |
| F6 | 66(1) | 49(1) | 62(1) | 5(1) | -3(1) | 39(1) |
| F7 | 35(1) | 82(2) | 40(1) | 19(1) | 14(1) | 22(1) |
| F8 | 63(1) | 58(2) | 45(1) | 33(1) | 7(1) | 9(1) |
| F9 | 46(1) | 75(2) | 27(1) | 5(1) | 9(1) | 11(1) |

| | | | | | | |
|---|---|---|---|---|---|---|
| F10 | 48(1) | 85(2) | 42(1) | 25(1) | 9(1) | 46(1) |
| F11 | 63(1) | 71(2) | 33(1) | 30(1) | 24(1) | 40(1) |
| F12 | 51(1) | 46(1) | 31(1) | 5(1) | 3(1) | 19(1) |
| F13 | 68(1) | 50(1) | 61(1) | 37(1) | 31(1) | 43(1) |
| F14 | 61(1) | 33(1) | 46(1) | 7(1) | 12(1) | 22(1) |
| F15 | 48(1) | 41(1) | 81(2) | 32(1) | 38(1) | 23(1) |
| F16 | 57(1) | 68(2) | 52(1) | 33(1) | 33(1) | 49(1) |
| F17 | 38(1) | 50(1) | 53(1) | 23(1) | 20(1) | 14(1) |
| F18 | 52(1) | 61(1) | 31(1) | 23(1) | 20(1) | 35(1) |
| F19 | 48(1) | 33(1) | 61(1) | 22(1) | 23(1) | 21(1) |
| F20 | 46(1) | 56(1) | 51(1) | 33(1) | 28(1) | 21(1) |
| F21 | 34(1) | 44(1) | 50(1) | 16(1) | -2(1) | 3(1) |
| F22 | 43(1) | 48(1) | 38(1) | 10(1) | 2(1) | -1(1) |
| F23 | 56(1) | 66(2) | 30(1) | 9(1) | 17(1) | 29(1) |
| F24 | 41(1) | 63(1) | 36(1) | 23(1) | 8(1) | 28(1) |
| F25 | 64(1) | 41(1) | 68(1) | 19(1) | 30(1) | 33(1) |
| F26 | 52(1) | 79(2) | 72(1) | 40(1) | 42(1) | 47(1) |
| F27 | 48(1) | 71(2) | 52(1) | 32(1) | 16(1) | 41(1) |
| F28 | 30(1) | 66(2) | 125(2) | 56(2) | 25(1) | 23(1) |
| F29 | 56(1) | 41(1) | 45(1) | 22(1) | -2(1) | 8(1) |
| F30 | 60(1) | 70(2) | 22(1) | -6(1) | 0(1) | 31(1) |
| F31 | 81(2) | 54(2) | 41(1) | 27(1) | 9(1) | 25(1) |
| F32 | 71(2) | 41(1) | 73(2) | 34(1) | 44(1) | 15(1) |
| F33 | 72(1) | 50(1) | 68(1) | 32(1) | 51(1) | 34(1) |
| F34 | 74(2) | 39(1) | 58(1) | 16(1) | 40(1) | 28(1) |
| F35 | 59(1) | 37(1) | 92(2) | 39(1) | 33(1) | 29(1) |
| F36 | 31(1) | 45(1) | 77(1) | 26(1) | 15(1) | 21(1) |
| C29 | 28(1) | 29(2) | 27(1) | 8(1) | 8(1) | 10(1) |
| C30 | 47(2) | 30(2) | 35(2) | 6(1) | 8(1) | 8(1) |
| C31 | 38(2) | 48(2) | 37(2) | 3(1) | 2(1) | 20(2) |
| C32 | 34(2) | 48(2) | 28(1) | 13(1) | 5(1) | 9(1) |
| C33 | 31(1) | 33(2) | 27(1) | 16(1) | 13(1) | 20(1) |
| C34 | 39(2) | 52(2) | 29(1) | 18(1) | 10(1) | 29(2) |
| C35 | 45(2) | 36(2) | 42(2) | 19(1) | 19(1) | 26(1) |
| C36 | 34(1) | 43(2) | 33(1) | 18(1) | 16(1) | 24(1) |
| C37 | 28(1) | 33(2) | 27(1) | 13(1) | 12(1) | 17(1) |
| C38 | 29(1) | 35(2) | 35(1) | 16(1) | 11(1) | 13(1) |
| C39 | 35(1) | 40(2) | 27(1) | 10(1) | 9(1) | 12(1) |
| C40 | 38(2) | 45(2) | 44(2) | 21(1) | 22(1) | 27(1) |
| C41 | 28(1) | 25(2) | 36(1) | 16(1) | 11(1) | 12(1) |
| C42 | 38(2) | 40(2) | 64(2) | 28(2) | 8(2) | 11(2) |
| C43 | 58(2) | 42(2) | 53(2) | 27(2) | 31(2) | 22(2) |
| C44 | 41(2) | 36(2) | 55(2) | 21(2) | 18(2) | 20(1) |
| Cl1 | 99(2) | 314(5) | 76(1) | -11(2) | -4(1) | 11(2) |
| C1S | 88(7) | 71(8) | 63(6) | 39(5) | 0(5) | -24(6) |

## 7.3.7. $[Au_2\{Cp_2Mo_2(CO)_4(\mu_3,\eta^2:\eta^2:\eta^2\text{-}P_2)\}_2\{Cp_2Mo_2(CO)_4(\mu_4,\eta^2:\eta^2:\eta^1:\eta^1\text{-}P_2)\}_2][(PF_6)_2]\bullet 2C_4H_8O\bullet 2CH_2Cl_2$ (**42h**$\bullet 2C_4H_8O\bullet 2CH_2Cl_2$)

Crystals of **42h**$\bullet 2C_4H_8O\bullet 2CH_2Cl_2$ were obtained from a concentrated THF/$CH_2Cl_2$ solution of **42h** at –28 °C.

Table 7.19. Crystal data and structure refinement for **42h**$\bullet 2C_4H_8O\bullet 2CH_2Cl_2$.

| | |
|---|---|
| Empirical formula | $C_{66}H_{58}Au_2Cl_4F_{12}Mo_8O_{18}P_{10}$ |
| Formula weight | 2980.09 g $mol^{-1}$ |
| Crystal size | $0.22 \times 0.18 \times 0.16$ mm |
| Crystal description | plate |
| Crystal colour | ruby red |
| Crystal system | triclinic |
| Space group | $P\ \bar{1}$ |
| Unit cell dimensions | $a$ = 13.156(1) Å, $\alpha$ = 78.52(1)° |
| | $b$ = 13.930(1) Å, $\beta$ = 64.62(1)° |
| | $c$ = 15.215(1) Å, $\gamma$ = 64.41(1)° |
| Volume | 2271.8(5) $Å^3$ |
| Z, Calculated density | 1, 2.178 Mg $m^{-3}$ |
| Absorption coefficient | 4.658 $mm^{-1}$ |
| F(000) | 1418 |
| Measurement device type | STOE-IPDS diffractometer |
| Measurement method | rotation |
| Temperature | 173(1) K |
| Wavelength | 0.71073 Å |
| Monochromator | graphite |
| $\theta$ range for data collection | 2.79 to 25.93° |
| Index ranges | $-16 \le h \le 16$, $-17 \le k \le 17$, $-17 \le l \le 17$ |
| Reflections collected/ unique | 25284 / 8216 [R(int) = 0.0489] |
| Reflections greater I>2\s(I) | 5655 |
| Absorption correction | analytical |
| Max. and min. transmission | 0.5175 and 0.4826 |
| Refinement method | Full-matrix least-squares on $F^2$ |
| Data / restraints / parameters | 8216 / 0 / 511 |
| Goodness-of-fit on $F^2$ | 0.920 |
| Final R indices [I>2sigma(I)] | R1 = 0.0455, wR2 = 0.1071 |
| R indices (all data) | R1 = 0.0686, wR2 = 0.1131 |
| Largest diff. peak and hole | 1.593 and -0.854 e $Å^{-3}$ |

Table 7.20. Atomic coordinates ($\times 10^4$) and equivalent isotropic displacement parameters ($Å^2 \times 10^3$) for **42h**•$2C_4H_8O$•$2CH_2Cl_2$. $U_{eq}$ is defined as one third of the trace of the orthogonalised $U_{ij}$ tensor.

| **Atom** | **x** | **y** | **z** | $\boldsymbol{U_{eq}}$ |
|---|---|---|---|---|
| Au1 | 7097(1) | 3891(1) | -709(1) | 37(1) |
| Mo1 | 5463(1) | 4517(1) | 2535(1) | 38(1) |
| Mo2 | 4505(1) | 3072(1) | 2156(1) | 36(1) |
| Mo3 | 10808(1) | 2742(1) | -1160(1) | 39(1) |
| Mo4 | 10515(1) | 2375(1) | -2930(1) | 42(1) |
| P1 | 5818(2) | 3902(2) | 943(2) | 35(1) |
| P2 | 4076(2) | 5024(2) | 1687(2) | 37(1) |
| P3 | 9184(2) | 3891(2) | -1829(2) | 39(1) |
| P4 | 9143(2) | 2363(2) | -1148(2) | 40(1) |
| O1 | 6460(10) | 6208(7) | 1228(6) | 82(4) |
| O2 | 8109(7) | 2719(7) | 1828(6) | 67(3) |
| O3 | 3103(8) | 3300(6) | 867(7) | 68(3) |
| O4 | 1945(6) | 4399(6) | 3716(5) | 67(3) |
| O5 | 11134(8) | -42(6) | -2297(8) | 80(4) |
| O6 | 8228(7) | 2456(7) | -3163(6) | 69(3) |
| O7 | 11718(7) | 4512(6) | -2415(6) | 63(3) |
| O8 | 9012(8) | 4446(7) | 460(6) | 75(3) |
| C1 | 5560(10) | 4058(9) | 4050(7) | 52(3) |
| C2 | 4365(9) | 4240(8) | 4196(7) | 48(3) |
| C3 | 3762(11) | 5304(8) | 3967(8) | 62(4) |
| C4 | 4602(16) | 5788(9) | 3671(8) | 82(5) |
| C5 | 5712(13) | 5038(11) | 3735(8) | 68(5) |
| C6 | 6098(10) | 5581(9) | 1667(8) | 55(4) |
| C7 | 7150(9) | 3370(9) | 2080(7) | 48(3) |
| C8 | 4669(12) | 1694(8) | 3301(10) | 65(4) |
| C9 | 4381(13) | 1453(9) | 2586(13) | 76(6) |
| C10 | 5370(12) | 1347(8) | 1692(11) | 70(5) |
| C11 | 6282(11) | 1514(7) | 1845(10) | 61(4) |
| C12 | 5845(11) | 1708(7) | 2836(9) | 59(4) |
| C13 | 3629(9) | 3256(7) | 1307(8) | 45(3) |
| C14 | 2867(9) | 3925(8) | 3160(7) | 47(3) |
| C15 | 11355(10) | 3520(10) | -4051(8) | 64(4) |
| C16 | 10858(11) | 3120(11) | -4470(9) | 70(5) |
| C17 | 11533(10) | 2004(10) | -4546(8) | 65(4) |
| C18 | 12429(10) | 1740(11) | -4174(9) | 70(4) |
| C19 | 12328(9) | 2659(10) | -3880(8) | 63(4) |
| C20 | 10898(9) | 868(9) | -2522(8) | 55(3) |
| C21 | 9049(9) | 2412(7) | -3037(7) | 44(3) |
| C22 | 11542(10) | 963(7) | -641(9) | 54(4) |

| | | | | |
|---|---|---|---|---|
| C23 | 11293(10) | 1626(9) | 70(8) | 59(4) |
| C24 | 12082(10) | 2182(9) | -338(9) | 61(4) |
| C25 | 12826(9) | 1844(8) | -1300(9) | 52(4) |
| C26 | 12521(9) | 1109(7) | -1507(8) | 51(3) |
| C27 | 11354(8) | 3885(8) | -1968(7) | 44(3) |
| C28 | 9659(10) | 3825(8) | -135(8) | 55(3) |
| O9 | -220(30) | 1840(30) | 3490(30) | 291(14) |
| C29 | 530(30) | 2510(20) | 2620(20) | 187(11) |
| C30 | -1030(20) | 2837(19) | 4090(19) | 143(8) |
| C31 | -544(14) | 3468(13) | 4015(13) | 93(4) |
| C32 | 480(20) | 3254(19) | 3115(19) | 148(8) |
| P5 | 6052(3) | 1152(2) | 5722(2) | 57(1) |
| F1 | 5197(9) | 2142(8) | 5337(11) | 160(6) |
| F2 | 5321(14) | 546(8) | 5742(14) | 191(8) |
| F3 | 5210(12) | 1431(15) | 6731(9) | 206(8) |
| F4 | 6828(8) | 1755(7) | 5649(12) | 150(6) |
| F5 | 7035(12) | 804(12) | 4619(9) | 170(6) |
| F6 | 6972(8) | 122(7) | 6003(8) | 120(4) |
| Cl1 | 6368(12) | 1763(8) | 9009(6) | 275(6) |
| Cl2 | 6289(18) | -161(8) | 9008(12) | 363(12) |
| C33 | 6510(30) | 940(20) | 8320(20) | 194(12) |

Table 7.21. Anisotropic displacement parameters ($Å^2 \times 10^3$) for **42h**•$2C_4H_8O$•$2CH_2Cl_2$. The anisotropic displacement factor exponent takes the form: $-2\pi^2[h^2a^{*2}U_{11} + ... + 2hka^*b^*U_{12}]$.

| **Atom** | $U_{11}$ | $U_{22}$ | $U_{33}$ | $U_{23}$ | $U_{13}$ | $U_{12}$ |
|---|---|---|---|---|---|---|
| Au1 | 35(1) | 35(1) | 33(1) | -5(1) | -6(1) | -11(1) |
| Mo1 | 51(1) | 43(1) | 23(1) | 2(1) | -14(1) | -23(1) |
| Mo2 | 39(1) | 33(1) | 35(1) | 5(1) | -16(1) | -14(1) |
| Mo3 | 38(1) | 39(1) | 36(1) | -4(1) | -13(1) | -12(1) |
| Mo4 | 35(1) | 48(1) | 34(1) | -11(1) | -8(1) | -10(1) |
| P1 | 36(1) | 43(1) | 25(1) | -3(1) | -10(1) | -15(1) |
| P2 | 42(1) | 35(1) | 26(1) | 1(1) | -11(1) | -11(1) |
| P3 | 34(1) | 37(1) | 36(1) | -4(1) | -9(1) | -10(1) |
| P4 | 37(1) | 37(1) | 38(1) | -4(1) | -11(1) | -11(1) |
| O1 | 134(8) | 98(6) | 51(5) | 27(4) | -38(5) | -87(6) |
| O2 | 40(4) | 84(5) | 63(5) | 1(4) | -18(4) | -16(4) |
| O3 | 80(5) | 71(5) | 73(6) | 4(4) | -46(5) | -34(4) |
| O4 | 43(4) | 78(5) | 43(4) | 9(4) | -3(3) | -9(4) |
| O5 | 80(6) | 49(5) | 106(8) | -12(4) | -44(5) | -8(4) |
| O6 | 57(5) | 94(6) | 56(5) | -11(4) | -22(4) | -25(4) |
| O7 | 67(5) | 69(5) | 62(5) | 3(4) | -21(4) | -40(4) |
| O8 | 86(6) | 79(5) | 59(5) | -22(4) | -8(5) | -43(5) |

| | | | | | | |
|---|---|---|---|---|---|---|
| C1 | 64(6) | 73(7) | 24(5) | 8(4) | -18(5) | -34(5) |
| C2 | 59(6) | 60(6) | 25(5) | 8(4) | -19(4) | -24(5) |
| C3 | 69(7) | 52(6) | 38(6) | -11(5) | -14(5) | -4(5) |
| C4 | 155(14) | 45(6) | 28(6) | -4(4) | -30(8) | -28(8) |
| C5 | 111(10) | 99(9) | 30(6) | -1(6) | -26(6) | -75(9) |
| C6 | 72(7) | 78(7) | 33(6) | 8(5) | -22(5) | -47(6) |
| C7 | 47(6) | 70(6) | 38(6) | 14(5) | -18(4) | -37(5) |
| C8 | 82(8) | 51(6) | 67(8) | 30(5) | -41(7) | -32(6) |
| C9 | 86(9) | 43(6) | 120(13) | 23(7) | -62(9) | -31(6) |
| C10 | 90(9) | 32(5) | 96(11) | 4(5) | -59(9) | -11(5) |
| C11 | 66(7) | 30(5) | 85(9) | -11(5) | -39(6) | -3(4) |
| C12 | 71(7) | 35(5) | 62(8) | 12(5) | -35(6) | -9(5) |
| C13 | 45(5) | 45(5) | 48(6) | 8(4) | -23(5) | -18(4) |
| C14 | 52(6) | 50(5) | 39(6) | 15(4) | -22(5) | -22(5) |
| C15 | 57(6) | 77(7) | 43(7) | 0(5) | -3(5) | -30(6) |
| C16 | 63(7) | 105(10) | 40(7) | -3(6) | -17(5) | -34(7) |
| C17 | 55(6) | 88(8) | 45(7) | -27(6) | -2(5) | -27(6) |
| C18 | 49(6) | 89(9) | 52(7) | -33(6) | 0(5) | -16(6) |
| C19 | 38(5) | 100(9) | 40(6) | -13(6) | 4(5) | -31(6) |
| C20 | 46(5) | 56(6) | 55(7) | -21(5) | -21(5) | -4(5) |
| C21 | 42(5) | 55(5) | 31(5) | -8(4) | -10(4) | -17(4) |
| C22 | 71(7) | 42(5) | 66(8) | 9(5) | -44(6) | -24(5) |
| C23 | 65(7) | 65(7) | 43(6) | 0(5) | -25(5) | -19(5) |
| C24 | 59(6) | 61(6) | 74(9) | 10(6) | -36(6) | -29(5) |
| C25 | 38(5) | 53(6) | 67(8) | -4(5) | -24(5) | -14(4) |
| C26 | 52(6) | 45(5) | 55(7) | 1(4) | -32(5) | -9(4) |
| C27 | 45(5) | 49(5) | 40(6) | -1(4) | -14(4) | -22(4) |
| C28 | 63(6) | 56(6) | 44(6) | -16(5) | -3(5) | -32(5) |
| P5 | 70(2) | 44(1) | 62(2) | 4(1) | -31(2) | -24(1) |
| F1 | 96(6) | 111(7) | 272(16) | 111(9) | -103(8) | -57(6) |
| F2 | 225(14) | 95(7) | 380(20) | 82(10) | -231(16) | -98(8) |
| F3 | 129(10) | 310(20) | 82(8) | -68(10) | 20(7) | -34(11) |
| F4 | 83(6) | 87(6) | 283(16) | -34(8) | -60(8) | -33(5) |
| F5 | 145(10) | 224(14) | 99(9) | -8(9) | -39(7) | -41(10) |
| F6 | 92(6) | 91(6) | 142(9) | 22(6) | -42(6) | -18(5) |
| Cl1 | 437(15) | 241(8) | 135(6) | -63(6) | 57(8) | -263(11) |
| Cl2 | 740(30) | 210(9) | 470(20) | 151(12) | -500(20) | -278(15) |

## 7.3.8. $[Ag_2\{Cp_2Mo_2(CO)_4(\mu_4,\eta^2:\eta^2:\eta^1:\eta^1\text{-}P_2)\}_2(\eta^2\text{-}NO_2)_2]$ (49)

Crystals of **49** were obtained as dark brown plates by controlled diffusion of a $CH_3CN$ solution of $AgNO_2$ into a $CH_2Cl_2$ solution of **6b** at room temperature in the dark.

Table 7.22. Crystal data and structure refinement for **49**.

| | |
|---|---|
| Empirical formula | $C_{28}H_{20}Ag_2Mo_4N_2O_{12}P_4$ |
| Formula weight | 1299.84 g $mol^{-1}$ |
| Crystal size | 0.120 × 0.080 × 0.060 mm |
| Crystal description | plate |
| Crystal colour | black-brown |
| Crystal system | monoclinic |
| Space group | $P2_1/c$ |
| Unit cell dimensions | $a$ = 9.982(1) Å, $\alpha$ = 90° |
| | $b$ = 10.552(1) Å, $\beta$ = 100.97(1)° |
| | $c$ = 17.578(2) Å, $\gamma$ = 90° |
| Volume | 1817.7(3) $Å^3$ |
| Z, Calculated density | 2, 2.375 Mg $m^{-3}$ |
| Absorption coefficient | 2.632 $mm^{-1}$ |
| F(000) | 1240 |
| Measurement device type | STOE-IPDS |
| Measurement method | rotation |
| Temperature | 173(1) K |
| Wavelength | 0.71073 Å |
| Monochromator | graphite |
| $\theta$ range for data collection | 2.26 to 27.98° |
| Index ranges | $-13 \le h \le 13$, $-13 \le k \le 13$, $-23 \le l \le 23$ |
| Reflections collected / unique | 21303 / 4346 [R(int) = 0.0455] |
| Reflections greater I>2\s(I) | 3528 |
| Absorption correction | numerical |
| Max. and min. transmission | 0.7264 and 0.5913 |
| Refinement method | Full-matrix least-squares on $F^2$ |
| Data / restraints / parameters | 4346 / 0 / 235 |
| Goodness-of-fit on $F^2$ | 0.978 |
| Final R indices [I>2sigma(I)] | R1 = 0.0236, wR2 = 0.0566 |
| R indices (all data) | R1 = 0.0325, wR2 = 0.0581 |
| Largest diff. peak and hole | 0.987 and -0.588 e $Å^{-3}$ |

Table 7.23. Atomic coordinates ($\times 10^4$) and equivalent isotropic displacement parameters ($Å^2 \times 10^3$) for **49**. $U_{eq}$ is defined as one third of the trace of the orthogonalised $U_{ij}$ tensor.

| **Atom** | **x** | **y** | **z** | $U_{eq}$ |
|---|---|---|---|---|
| Ag1 | 1173(1) | 11622(1) | 672(1) | 19(1) |
| Mo1 | 3271(1) | 7762(1) | 758(1) | 14(1) |
| Mo2 | 1118(1) | 7304(1) | 1745(1) | 15(1) |
| P1 | 1515(1) | 9302(1) | 1090(1) | 17(1) |
| P2 | 789(1) | 7831(1) | 306(1) | 17(1) |
| O1 | 3491(3) | 9881(2) | -482(1) | 30(1) |
| O2 | 4823(3) | 9590(2) | 2064(1) | 29(1) |
| O3 | 350(3) | 4743(2) | 846(1) | 39(1) |
| O4 | -2002(3) | 8019(3) | 1417(2) | 36(1) |
| O5 | 2391(3) | 12557(4) | 1875(2) | 49(1) |
| O6 | 3526(3) | 12156(3) | 1016(2) | 37(1) |
| N1 | 3535(3) | 12531(3) | 1693(2) | 33(1) |
| C1 | 5254(3) | 6941(3) | 475(2) | 22(1) |
| C2 | 4152(3) | 6493(3) | -109(2) | 23(1) |
| C3 | 3318(4) | 5693(3) | 241(2) | 26(1) |
| C4 | 3901(4) | 5615(3) | 1051(2) | 24(1) |
| C5 | 5087(3) | 6379(3) | 1195(2) | 22(1) |
| C6 | 3395(3) | 9136(3) | -20(2) | 20(1) |
| C7 | 4236(3) | 8938(3) | 1590(2) | 20(1) |
| C8 | 3016(3) | 7113(4) | 2793(2) | 25(1) |
| C9 | 2182(3) | 6018(4) | 2766(2) | 25(1) |
| C10 | 871(4) | 6402(4) | 2905(2) | 26(1) |
| C11 | 904(4) | 7748(4) | 3009(2) | 27(1) |
| C12 | 2224(4) | 8184(4) | 2937(2) | 28(1) |
| C13 | 644(4) | 5695(3) | 1156(2) | 24(1) |
| C14 | -867(3) | 7755(3) | 1521(2) | 23(1) |

Table 7.24. Anisotropic displacement parameters ($Å^2 \times 10^3$) for **49**. The anisotropic displacement factor exponent takes the form: $-2\pi^2[h^2a^{*2}U_{11} + ... + 2hka^*b^*U_{12}]$.

| **Atom** | $U_{11}$ | $U_{22}$ | $U_{33}$ | $U_{23}$ | $U_{13}$ | $U_{12}$ |
|---|---|---|---|---|---|---|
| Ag1 | 18(1) | 18(1) | 19(1) | 0(1) | -1(1) | 1(1) |
| Mo1 | 14(1) | 14(1) | 15(1) | 1(1) | 2(1) | 0(1) |
| Mo2 | 14(1) | 15(1) | 15(1) | 1(1) | 2(1) | 0(1) |
| P1 | 17(1) | 13(1) | 21(1) | 1(1) | 2(1) | 1(1) |
| P2 | 16(1) | 17(1) | 17(1) | 2(1) | 0(1) | -1(1) |
| O1 | 33(1) | 30(1) | 27(1) | 9(1) | 4(1) | -4(1) |
| O2 | 28(1) | 26(1) | 28(1) | -5(1) | -3(1) | -3(1) |
| O3 | 66(2) | 20(1) | 31(1) | 0(1) | 7(1) | -11(1) |
| O4 | 20(1) | 52(2) | 35(1) | 3(1) | 2(1) | 5(1) |
| O5 | 31(2) | 75(2) | 40(2) | -29(2) | 4(1) | -1(2) |
| O6 | 27(1) | 51(2) | 32(1) | 1(1) | 6(1) | -13(1) |
| N1 | 25(2) | 32(2) | 38(2) | -7(1) | -7(1) | -4(1) |
| C1 | 19(2) | 24(2) | 24(1) | 0(1) | 5(1) | 4(1) |
| C2 | 23(2) | 26(2) | 21(1) | -4(1) | 5(1) | 5(1) |
| C3 | 26(2) | 18(2) | 32(2) | -7(1) | 4(1) | 3(1) |
| C4 | 27(2) | 19(2) | 29(2) | 5(1) | 12(1) | 9(1) |
| C5 | 22(2) | 23(2) | 22(1) | 0(1) | 3(1) | 8(1) |
| C6 | 17(1) | 22(2) | 20(1) | 2(1) | 0(1) | 1(1) |
| C7 | 17(2) | 20(1) | 23(1) | 4(1) | 2(1) | 0(1) |
| C8 | 19(2) | 39(2) | 17(1) | 7(1) | 2(1) | 3(2) |
| C9 | 25(2) | 32(2) | 19(1) | 10(1) | 4(1) | 6(2) |
| C10 | 20(2) | 38(2) | 22(1) | 6(1) | 7(1) | -1(2) |
| C11 | 25(2) | 40(2) | 18(1) | -1(1) | 6(1) | 4(2) |
| C12 | 30(2) | 36(2) | 17(1) | -3(1) | 1(1) | -4(2) |
| C13 | 31(2) | 20(2) | 20(1) | 3(1) | 3(1) | -4(1) |
| C14 | 20(2) | 27(2) | 21(1) | 1(1) | 1(1) | 0(1) |

## 7.3.9. [Au{$Cp_2Mo_2(CO)_4(\mu_3,\eta^2:\eta^2:\eta^1$-$P_2$)}Cl] (50)

Crystals of **50** were obtained by controlled diffusion of a toluene solution of [$Cp_2Mo_2(CO)_4(\mu,\eta^2$-$P_2$)] **6b** into a frozen toluene solution of [(OC)AuCl], which was allowed to thaw gradually, in the dark.

Table 7.25. Crystal data and structure refinement for **50**.

| | |
|---|---|
| Empirical formula | $C_{14}H_{10}AuClMo_2O_4P_2$ |
| Formula weight | 728.46 g $mol^{-1}$ |
| Crystal size | not defined |
| Crystal description | needle |
| Crystal colour | red |
| Crystal system | monoclinic |
| Space group | $P2_1/n$ |
| Unit cell dimensions | $a$ = 8.345(2) Å, $\alpha$ = 90° |
| | $b$ = 23.468(5) Å, $\beta$ = 103.03(3)° |
| | $c$ = 9.278(2) Å, $\gamma$ = 90° |
| Volume | 1770.2(7) $Å^3$ |
| Z, Calculated density | 4, 2.733 Mg $m^{-3}$ |
| Absorption coefficient | 9.905 $mm^{-1}$ |
| F(000) | 1344 |
| Measurement device type | STOE-IPDS |
| Measurement method | rotation |
| Temperature | 203(1) K |
| Wavelength | 0.56087 Å |
| Monochromator | graphite |
| $\theta$ range for data collection | 1.91 to 20.79° |
| Index ranges | $-10 \le h \le 10$, $-29 \le k \le 25$, $-11 \le l \le 11$ |
| Reflections collected / unique | 10844 / 3583 [R(int) = 0.1520] |
| Reflections greater I>2\s(I) | 2614 |
| Absorption correction | none |
| Refinement method | Full-matrix least-squares on $F^2$ |
| Data / restraints / parameters | 3583 / 0 / 217 |
| Goodness-of-fit on $F^2$ | 1.128 |
| Final R indices [I>2sigma(I)] | R1 = 0.1017, wR2 = 0.2568 |
| R indices (all data) | R1 = 0.1264, wR2 = 0.2808 |
| Largest diff. peak and hole | 8.308 and -4.984 e $Å^{-3}$ |

Table 7.26. Atomic coordinates ($\times 10^4$) and equivalent isotropic displacement parameters ($Å^2 \times 10^3$) for **50**. $U_{eq}$ is defined as one third of the trace of the orthogonalised $U_{ij}$ tensor.

| **Atom** | **x** | **y** | **z** | $U_{eq}$ |
|---|---|---|---|---|
| Au | 2984(1) | -559(1) | 2708(1) | 32(3) |
| Mo1 | 3539(2) | 1217(1) | 1480(2) | 24(5) |
| Mo2 | 1827(2) | 1151(1) | 4069(2) | 27(5) |
| Cl | 2493(9) | -1504(2) | 1990(7) | 47(2) |
| P1 | 3162(7) | 384(2) | 3039(6) | 27(1) |
| P2 | 4919(7) | 972(2) | 4113(6) | 30(2) |
| O1 | 820(20) | 467(8) | -560(20) | 47(6) |
| O2 | 6190(20) | 430(7) | 550(20) | 43(5) |
| O3 | 2890(30) | 534(7) | 7130(20) | 57(7) |
| O4 | 3720(20) | 2265(7) | 5450(20) | 54(6) |
| C1 | 1790(30) | 749(7) | 240(20) | 30(6) |
| C2 | 5240(20) | 691(9) | 940(20) | 31(6) |
| C3 | 2550(30) | 760(12) | 5990(20) | 44(8) |
| C4 | 3070(30) | 1837(10) | 4980(20) | 37(7) |
| C5 | 2760(30) | 2185(8) | 1410(30) | 47(8) |
| C6 | 4500(30) | 2153(9) | 1830(30) | 49(8) |
| C7 | 5100(30) | 1922(8) | 670(30) | 36(7) |
| C8 | 3810(40) | 1782(10) | -490(30) | 51(9) |
| C9 | 2330(40) | 1958(11) | -70(30) | 54(9) |
| C10 | -730(30) | 836(9) | 4300(30) | 36(7) |
| C11 | -640(30) | 1424(10) | 4650(20) | 39(7) |
| C12 | -480(30) | 1722(12) | 3400(30) | 53(9) |
| C13 | -560(30) | 1337(10) | 2210(30) | 37(7) |
| C14 | -710(30) | 774(10) | 2810(30) | 41(7) |

Table 7.27. Anisotropic displacement parameters ($Å^2 \times 10^3$) for **50**. The anisotropic displacement factor exponent takes the form: $-2\pi^2[h^2a^{*2}U_{11} + ... + 2hka^*b^*U_{12}]$.

| **Atom** | $U_{11}$ | $U_{22}$ | $U_{33}$ | $U_{23}$ | $U_{13}$ | $U_{12}$ |
|---|---|---|---|---|---|---|
| Au | 48(6) | 9(4) | 43(5) | 1(3) | 18(4) | 0(3) |
| Mo1 | 36(9) | 7(7) | 31(8) | -1(5) | 9(7) | -1(1) |
| Mo2 | 35(9) | 14(8) | 32(9) | -4(6) | 9(7) | 1(1) |
| Cl | 82(4) | 11(2) | 52(3) | -4(2) | -5(2) | 23(3) |
| P1 | 41(3) | 10(2) | 31(2) | 1(2) | 12(2) | 0(2) |
| P2 | 34(3) | 17(2) | 38(3) | -2(2) | 7(2) | 0(2) |
| O1 | 36(9) | 47(10) | 51(10) | -13(8) | -4(8) | -14(7) |
| O2 | 43(9) | 23(7) | 63(11) | -9(7) | 14(8) | 7(6) |
| O3 | 81(15) | 25(9) | 67(13) | 5(8) | 26(11) | 13(8) |
| O4 | 58(11) | 26(9) | 77(12) | -18(8) | 12(10) | -16(8) |
| C1 | 54(13) | 5(8) | 34(10) | 9(7) | 17(10) | 5(8) |
| C2 | 25(1) | 33(11) | 32(10) | 8(8) | 1(8) | 2(8) |
| C3 | 42(13) | 62(16) | 30(11) | 7(11) | 14(10) | 10(11) |
| C4 | 46(13) | 34(12) | 28(10) | -12(8) | 1(9) | -9(9) |
| C5 | 7(17) | 2(8) | 73(16) | 3(9) | 32(14) | 6(9) |
| C6 | 66(17) | 22(11) | 56(14) | -6(1) | 9(13) | -34(11) |
| C7 | 49(13) | 13(9) | 50(12) | 3(8) | 20(10) | -9(8) |
| C8 | 91(19) | 19(11) | 47(14) | 18(9) | 21(14) | -8(11) |
| C9 | 80(19) | 33(13) | 47(14) | 0(1) | 12(13) | 4(13) |
| C10 | 29(11) | 30(11) | 52(13) | 0(1) | 14(10) | -2(8) |
| C11 | 37(12) | 45(13) | 39(12) | -4(1) | 19(10) | 12(10) |
| C12 | 43(14) | 41(14) | 75(18) | -14(12) | 13(13) | 10(10) |
| C13 | 24(11) | 41(12) | 46(12) | 0(10) | 8(9) | 11(8) |
| C14 | 31(11) | 31(12) | 63(15) | -24(10) | 18(11) | 9(9) |

## 7.3.10. $[(Cp''Rh)_2\{Cp_2Mo_2(CO)_4(\mu_4,\eta^2:\eta^2:\eta^1:\eta^1\text{-}P_2)\}(\mu\text{-}Cl)_2][(BF_4)_2]\bullet 1.5CH_2Cl_2$ (**54**$\bullet 1.5CH_2Cl_2$)

Crystals of **54**$\bullet 1.5CH_2Cl_2$ were obtained by controlled diffusion of a THF solution of $[Cp_2Mo_2(CO)_4(\mu,\eta^2\text{-}P_2)]$ **6b** into a $CH_2Cl_2$ solution of $[Cp''Rh(NCCH_3)_2Cl][BF_4]$ at room temperature.

Table 7.28. Crystal data and structure refinement for **54**$\bullet 1.5CH_2Cl_2$.

| | |
|---|---|
| Empirical formula | $C_{41.5}H_{55}B_2Cl_5F_8Mo_2O_4P_2Rh_2$ |
| Formula weight | 1428.37 g $mol^{-1}$ |
| Crystal size | $0.25 \times 0.08 \times 0.04$ mm |
| Crystal description | needle |
| Crystal colour | black |
| Crystal system | monoclinic |
| Space group | $P2_1/n$ |
| Unit cell dimensions | $a$ = 12.559(3) Å, $\alpha$ = 90° |
| | $b$ = 19.653(4) Å, $\beta$ = 96.06(3)° |
| | $c$ = 22.776(5) Å, $\gamma$ = 90° |
| Volume | 5590.2(2) $Å^3$ |
| Z, Calculated density | 4, 1.697 Mg $m^{-3}$ |
| Absorption coefficient | 1.378 $mm^{-1}$ |
| F(000) | 2828 |
| Measurement device type | STOE-IPDS |
| Measurement method | rotation |
| Temperature | 200(1) K |
| Wavelength | 0.71073 Å |
| Monochromator | graphite |
| $\theta$ range for data collection | 1.93 to 24.03° |
| Index ranges | $-13 \le h \le 13$, $-22 \le k \le 22$, $-26 \le l \le 17$ |
| Reflections collected/ unique | 23369 / 7900 [R(int) = 0.0625] |
| Reflections greater I>2\s(I) | 5655 |
| Absorption correction | none |
| Refinement method | Full-matrix least-squares on $F^2$ |
| Data / restraints / parameters | 7900 / 0 / 625 |
| Goodness-of-fit on $F^2$ | 0.884 |
| Final R indices [I>2sigma(I)] | R1 = 0.0360, wR2 = 0.0864 |
| R indices (all data) | R1 = 0.0617, wR2 = 0.0935 |
| Largest diff. peak and hole | 1.141 and -0.893 e $Å^{-3}$ |

Table 7.29. Atomic coordinates ($\times 10^4$) and equivalent isotropic displacement parameters ($Å^2 \times 10^3$) for **54**•1.5$CH_2Cl_2$. $U_{eq}$ is defined as one third of the trace of the orthogonalised $U_{ij}$ tensor.

| **Atom** | **x** | **y** | **z** | $U_{eq}$ |
|---|---|---|---|---|
| Rh1 | 558(1) | 8780(1) | 2329(1) | 21(1) |
| Rh2 | 3325(1) | 9182(1) | 2243(1) | 21(1) |
| Cl1 | 1575(1) | 9649(1) | 1872(1) | 27(1) |
| Cl2 | 2221(1) | 8170(1) | 2224(1) | 28(1) |
| Mo1 | 1960(1) | 10234(1) | 3755(1) | 25(1) |
| Mo2 | 2521(1) | 8745(1) | 4099(1) | 24(1) |
| P1 | 1282(1) | 9203(1) | 3259(1) | 23(1) |
| P2 | 2940(1) | 9352(1) | 3225(1) | 22(1) |
| C1 | 2005(5) | 10764(3) | 2996(3) | 35(2) |
| O1 | 2026(5) | 11115(2) | 2603(3) | 53(1) |
| C2 | 3521(6) | 10429(3) | 3952(3) | 35(2) |
| O2 | 4399(5) | 10562(2) | 4091(3) | 54(2) |
| C3 | 1059(6) | 8672(3) | 4396(3) | 40(2) |
| O3 | 263(5) | 8625(3) | 4580(3) | 62(2) |
| C4 | 2187(6) | 7861(3) | 3679(3) | 36(2) |
| O4 | 2007(5) | 7341(2) | 3468(3) | 58(2) |
| C5 | 1379(7) | 11239(4) | 4131(4) | 51(2) |
| C6 | 1819(7) | 10846(4) | 4622(3) | 50(2) |
| C7 | 1193(7) | 10265(4) | 4664(3) | 44(2) |
| C8 | 347(6) | 10287(4) | 4195(4) | 46(2) |
| C9 | 472(6) | 10890(3) | 3871(4) | 47(2) |
| C10 | 3665(6) | 9197(3) | 4903(3) | 38(2) |
| C11 | 4301(6) | 8908(3) | 4497(3) | 37(2) |
| C12 | 4085(6) | 8207(3) | 4459(3) | 39(2) |
| C13 | 3288(6) | 8050(3) | 4838(3) | 42(2) |
| C14 | 3041(6) | 8677(4) | 5108(3) | 44(2) |
| C15 | -791(5) | 8571(3) | 1645(3) | 27(1) |
| C16 | -1055(5) | 9111(3) | 2038(3) | 28(1) |
| C17 | -1010(5) | 8827(3) | 2611(3) | 29(1) |
| C18 | -678(5) | 8133(3) | 2591(3) | 29(2) |
| C19 | -574(5) | 7963(3) | 1987(3) | 26(1) |
| C20 | -1466(5) | 9813(3) | 1850(3) | 34(2) |
| C21 | -2674(6) | 9805(3) | 1872(4) | 52(2) |
| C22 | -1192(7) | 9979(3) | 1225(4) | 53(2) |
| C23 | -979(6) | 10353(3) | 2292(4) | 51(2) |
| C24 | -356(6) | 7260(3) | 1745(3) | 35(2) |
| C25 | 161(7) | 7316(3) | 1166(3) | 46(2) |
| C26 | -1475(6) | 6929(3) | 1619(4) | 48(2) |
| C27 | 343(6) | 6833(3) | 2196(3) | 43(2) |

| | | | | |
|---|---|---|---|---|
| C270 | 4298(5) | 9657(3) | 1576(3) | 27(1) |
| C28 | 4439(5) | 8941(3) | 1588(3) | 28(2) |
| C29 | 4866(5) | 8722(3) | 2166(3) | 27(1) |
| C30 | 4982(5) | 9325(3) | 2525(3) | 31(2) |
| C31 | 4586(5) | 9891(3) | 2169(3) | 27(1) |
| C32 | 5280(6) | 8025(3) | 2367(4) | 40(2) |
| C33 | 6495(6) | 8045(4) | 2361(4) | 54(2) |
| C34 | 4791(7) | 7475(3) | 1933(4) | 54(2) |
| C35 | 4993(7) | 7872(4) | 2989(4) | 52(2) |
| C36 | 3961(6) | 10091(3) | 1044(3) | 34(2) |
| C37 | 3231(7) | 9713(4) | 586(3) | 48(2) |
| C38 | 5013(6) | 10286(4) | 795(4) | 51(2) |
| C39 | 3416(7) | 10752(3) | 1239(4) | 49(2) |
| C40 | 4219(7) | 5965(4) | 4621(4) | 63(2) |
| Cl3 | 4372(2) | 6439(1) | 3985(1) | 74(1) |
| Cl4 | 5350(2) | 6012(1) | 5143(1) | 86(1) |
| C41 | 8360(20) | 7386(12) | 4441(16) | 135(13) |
| Cl5 | 8186(7) | 6982(3) | 3739(4) | 136(3) |
| Cl6 | 7391(10) | 7315(5) | 4898(6) | 227(7) |
| B1 | 1372(11) | 6844(5) | 5440(5) | 63(3) |
| F1 | 1316(10) | 6953(5) | 4828(4) | 194(6) |
| F2 | 2289(11) | 6591(5) | 5526(10) | 325(12) |
| F3 | 1372(6) | 7484(3) | 5627(3) | 107(2) |
| F4 | 577(8) | 6471(4) | 5500(5) | 169(5) |
| B2 | 7275(12) | 9697(6) | 3801(5) | 78(4) |
| F5 | 6767(13) | 9925(8) | 3299(5) | 310(11) |
| F6 | 6574(6) | 9465(3) | 4182(4) | 121(3) |
| F7 | 7946(14) | 9235(5) | 3740(7) | 316(12) |
| F8 | 7757(6) | 10236(3) | 4051(4) | 112(2) |

Table 7.30. Anisotropic displacement parameters ($Å^2 \times 10^3$) for **54**•1.5$CH_2Cl_2$. The anisotropic displacement factor exponent takes the form: $-2\pi^2[h^2a^{*2}U_{11} + ... + 2hka^*b^*U_{12}]$.

| **Atom** | $U_{11}$ | $U_{22}$ | $U_{33}$ | $U_{23}$ | $U_{13}$ | $U_{12}$ |
|---|---|---|---|---|---|---|
| Rh1 | 17(1) | 26(1) | 20(1) | -2(1) | 1(1) | 0(1) |
| Rh2 | 18(1) | 26(1) | 19(1) | -1(1) | 5(1) | 0(1) |
| Cl1 | 21(1) | 34(1) | 26(1) | 5(1) | 4(1) | 1(1) |
| Cl2 | 20(1) | 28(1) | 37(1) | -5(1) | 4(1) | -1(1) |
| Mo1 | 25(1) | 29(1) | 20(1) | -4(1) | 4(1) | 0(1) |
| Mo2 | 21(1) | 32(1) | 18(1) | 4(1) | 1(1) | -3(1) |
| P1 | 22(1) | 29(1) | 18(1) | -2(1) | 0(1) | -2(1) |
| P2 | 24(1) | 27(1) | 16(1) | 0(1) | 4(1) | 0(1) |
| C1 | 32(5) | 32(3) | 43(5) | -6(3) | 4(3) | -1(3) |

| | | | | | | |
|---|---|---|---|---|---|---|
| O1 | 75(4) | 37(2) | 45(4) | 14(2) | 5(3) | -6(2) |
| C2 | 41(5) | 29(3) | 34(4) | 1(3) | 0(3) | -6(3) |
| O2 | 40(4) | 48(3) | 71(4) | 6(2) | -10(3) | -15(2) |
| C3 | 33(5) | 48(4) | 37(5) | 8(3) | 1(4) | 0(3) |
| O3 | 28(4) | 89(4) | 74(5) | 25(3) | 26(3) | 1(3) |
| C4 | 35(5) | 40(4) | 31(4) | 11(3) | 0(3) | -6(3) |
| O4 | 85(5) | 30(2) | 54(4) | 3(2) | -12(3) | -13(2) |
| C5 | 68(6) | 44(4) | 44(5) | -21(4) | 14(4) | 13(4) |
| C6 | 63(6) | 57(4) | 32(5) | -25(4) | 7(4) | 9(4) |
| C7 | 54(6) | 63(4) | 19(4) | -5(3) | 19(4) | 15(4) |
| C8 | 35(5) | 58(4) | 48(5) | -13(4) | 19(4) | 10(3) |
| C9 | 48(6) | 56(4) | 38(5) | -7(4) | 8(4) | 28(4) |
| C10 | 36(5) | 51(4) | 25(4) | -1(3) | -12(3) | 0(3) |
| C11 | 30(4) | 46(4) | 32(4) | 8(3) | -6(3) | -9(3) |
| C12 | 33(5) | 49(4) | 32(4) | 6(3) | -8(3) | 6(3) |
| C13 | 41(5) | 49(4) | 32(4) | 20(3) | -12(3) | -1(3) |
| C14 | 49(5) | 71(5) | 11(4) | 11(3) | -2(3) | 2(4) |
| C15 | 25(4) | 33(3) | 22(4) | 2(2) | -4(3) | 1(2) |
| C16 | 13(4) | 35(3) | 35(4) | -3(3) | -1(3) | 2(2) |
| C17 | 15(4) | 39(3) | 31(4) | -7(3) | 1(3) | -1(3) |
| C18 | 22(4) | 33(3) | 31(4) | 2(3) | -1(3) | -4(2) |
| C19 | 22(4) | 30(3) | 25(4) | -4(2) | -4(3) | -5(2) |
| C20 | 25(4) | 24(3) | 52(5) | -1(3) | 2(3) | 3(3) |
| C21 | 30(5) | 45(4) | 78(7) | -1(4) | -4(4) | 3(3) |
| C22 | 59(6) | 39(4) | 60(6) | 17(3) | 1(4) | 8(3) |
| C23 | 37(5) | 35(4) | 79(7) | -7(4) | -3(4) | 2(3) |
| C24 | 37(5) | 25(3) | 41(5) | -2(3) | -4(3) | -1(3) |
| C25 | 61(6) | 41(4) | 36(5) | -9(3) | -1(4) | 7(3) |
| C26 | 44(5) | 34(3) | 61(6) | -13(3) | -15(4) | -5(3) |
| C27 | 44(5) | 35(3) | 47(5) | 1(3) | -14(4) | 5(3) |
| C270 | 23(4) | 31(3) | 28(4) | 1(2) | 15(3) | 2(2) |
| C28 | 23(4) | 32(3) | 31(4) | -5(3) | 12(3) | 1(2) |
| C29 | 21(4) | 31(3) | 32(4) | 4(3) | 10(3) | 2(2) |
| C30 | 16(4) | 47(4) | 31(4) | 1(3) | 4(3) | 1(3) |
| C31 | 24(4) | 30(3) | 28(4) | -4(3) | 10(3) | 0(2) |
| C32 | 35(5) | 31(3) | 57(5) | 8(3) | 19(4) | 10(3) |
| C33 | 27(5) | 55(4) | 84(7) | 19(4) | 17(4) | 16(3) |
| C34 | 59(6) | 32(3) | 72(7) | 1(3) | 19(5) | 1(3) |
| C35 | 44(6) | 53(4) | 63(6) | 25(4) | 21(4) | 18(3) |
| C36 | 30(4) | 44(3) | 30(4) | 7(3) | 12(3) | -2(3) |
| C37 | 48(5) | 64(4) | 30(4) | 5(3) | 3(4) | 3(4) |
| C38 | 44(5) | 66(5) | 45(5) | 26(4) | 14(4) | 2(4) |
| C39 | 54(6) | 43(4) | 53(6) | 19(3) | 14(4) | 11(3) |

| | | | | | | |
|---|---|---|---|---|---|---|
| C40 | 57(7) | 56(5) | 76(7) | 2(4) | 6(5) | -5(4) |
| Cl3 | 85(2) | 55(1) | 81(2) | 10(1) | 8(1) | 7(1) |
| Cl4 | 83(2) | 109(2) | 65(2) | -2(1) | -1(1) | -6(1) |
| C41 | 120(20) | 99(16) | 200(40) | -33(18) | 60(20) | -72(16) |
| Cl5 | 194(9) | 89(4) | 118(7) | 24(4) | -18(6) | 1(4) |
| Cl6 | 237(13) | 173(7) | 297(17) | -94(9) | 155(12) | -137(8) |
| B1 | 83(9) | 61(6) | 45(7) | -5(5) | 5(6) | -18(6) |
| F1 | 318(15) | 175(7) | 105(8) | -55(6) | 100(9) | -135(9) |
| F2 | 226(14) | 124(7) | 590(30) | 81(12) | -138(17) | 38(8) |
| F3 | 127(6) | 102(4) | 97(6) | -35(4) | 32(5) | -21(4) |
| F4 | 209(10) | 160(6) | 161(9) | -24(6) | 119(8) | -115(7) |
| B2 | 100(11) | 107(8) | 26(6) | -33(6) | 8(6) | -40(8) |
| F5 | 362(19) | 412(18) | 116(10) | 97(10) | -159(12) | -264(16) |
| F6 | 70(5) | 150(5) | 154(8) | 22(5) | 66(5) | -2(4) |
| F7 | 520(30) | 134(7) | 370(20) | -69(9) | 400(20) | -20(10) |
| F8 | 84(5) | 130(5) | 118(7) | -14(4) | -7(4) | -20(4) |

## 7.3.11. $[(C_{14}H_8)Pt_2\{Cp_2Mo_2(CO)_4(\mu_3,\eta^2:\eta^2:\eta^1\text{-}P_2)\}_2(PEt_3)_4][(PF_6)_2]$ (57)

Crystals of **57** were obtained by controlled diffusion of hexane into a $CH_2Cl_2$ solution of **57** at room temperature.

Table 7.31. Crystal data and structure refinement for **57**.

| | |
|---|---|
| Empirical formula | $C_{66}H_{88}F_{12}Mo_4O_8P_{10}Pt_2$ |
| Formula weight | 2320.99 g $mol^{-1}$ |
| Crystal size | not defined |
| Crystal description | needle |
| Crystal colour | red |
| Crystal system | monoclinic |
| Space group | $P2_1/c$ |
| Unit cell dimensions | $a$ = 21.715(4) Å, $\alpha$ = 90° |
| | $b$ = 28.790(6) Å, $\beta$ = 101.23(3)° |
| | $c$ = 13.933(3) Å, $\gamma$ = 90° |
| Volume | 8544(3) $Å^3$ |
| Z, Calculated density | 4, 1.804 Mg $m^{-3}$ |
| Absorption coefficient | 4.091 $mm^{-1}$ |
| F(000) | 4520 |
| Measurement device type | STOE-IPDS |
| Measurement method | rotation |
| Temperature | 200(1) K |
| Wavelength | 0.71073 Å |
| Monochromator | graphite |
| $\theta$ range for data collection | 3.25 to 31.89° |
| Index ranges | $-29 \le h \le 27$, $-36 \le k \le 39$, $-15 \le l \le 17$ |
| Reflections collected / unique | 67851 / 20435 [R(int) = 0.1461] |
| Reflections greater I>2\s(I) | 8854 |
| Absorption correction | none |
| Refinement method | Full-matrix least-squares on $F^2$ |
| Data / restraints / parameters | 20435 / 0 / 589 |
| Goodness-of-fit on $F^2$ | 0.998 |
| Final R indices [I>2sigma(I)] | R1 = 0.0976, wR2 = 0.2137 |
| R indices (all data) | R1 = 0.2181, wR2 = 0.2633 |
| Largest diff. peak and hole | 6.612 and -1.840 e $Å^{-3}$ |

Table 7.32. Atomic coordinates ($\times 10^4$) and equivalent isotropic displacement parameters ($Å^2 \times 10^3$) for **57**. $U_{eq}$ is defined as one third of the trace of the orthogonalised $U_{ij}$ tensor.

| **Atom** | **x** | **y** | **z** | $U_{eq}$ |
|---|---|---|---|---|
| Pt1 | 3261(1) | -379(1) | 1852(1) | 33(1) |
| Pt2 | 2233(1) | 1177(1) | 3817(1) | 33(1) |
| Mo1 | 2595(1) | -1769(1) | 551(1) | 42(1) |
| Mo2 | 1577(1) | -1425(1) | 1586(1) | 37(1) |
| Mo3 | 286(1) | 1543(1) | 4266(1) | 43(1) |
| Mo4 | 120(1) | 661(1) | 3051(1) | 40(1) |
| P1 | 2539(2) | -1004(1) | 1438(3) | 32(1) |
| P2 | 1925(2) | -1083(2) | 85(4) | 39(2) |
| P3 | 1121(2) | 1067(2) | 3659(3) | 37(2) |
| P4 | 732(2) | 783(2) | 4779(4) | 39(2) |
| P5 | 3867(3) | -798(2) | 3125(4) | 44(2) |
| P6 | 2762(2) | 73(1) | 551(3) | 35(2) |
| P7 | 2092(2) | 1691(1) | 2496(3) | 35(2) |
| P8 | 2472(2) | 730(2) | 5247(4) | 39(2) |
| O1 | 3272(8) | -2149(4) | 2597(10) | 66(6) |
| O2 | 3807(7) | -1260(5) | 210(11) | 65(6) |
| O3 | 619(8) | -1805(5) | -210(10) | 71(6) |
| O4 | 758(7) | -533(5) | 1155(11) | 68(6) |
| O5 | 853(7) | -281(5) | 3314(11) | 63(6) |
| O6 | -671(8) | 291(5) | 4520(13) | 78(7) |
| O7 | 179(7) | 2099(5) | 2300(12) | 70(6) |
| O8 | 1534(7) | 2056(5) | 5198(12) | 71(6) |
| C1 | 3041(9) | -1983(6) | 1876(14) | 41(4) |
| C2 | 3350(11) | -1438(7) | 314(17) | 59(6) |
| C3 | 1005(9) | -1665(6) | 437(14) | 38(4) |
| C4 | 1095(10) | -856(7) | 1306(15) | 51(5) |
| C5 | 578(9) | 84(7) | 3240(14) | 44(5) |
| C6 | -343(9) | 469(6) | 4003(14) | 42(5) |
| C7 | 244(11) | 1886(7) | 3032(17) | 57(6) |
| C8 | 1058(11) | 1856(7) | 4849(16) | 55(5) |
| C9 | 3962(8) | 74(6) | 2064(13) | 37(4) |
| C10 | 4461(9) | -36(6) | 1629(14) | 44(5) |
| C11 | 5040(10) | 220(7) | 1780(16) | 56(6) |
| C12 | 5133(9) | 586(6) | 2343(13) | 41(4) |
| C13 | 4654(10) | 747(7) | 2796(15) | 50(5) |
| C14 | 4063(8) | 509(5) | 2664(13) | 35(4) |
| C15 | 3566(9) | 716(6) | 3068(13) | 40(4) |
| C16 | 3668(8) | 1121(5) | 3639(13) | 35(4) |
| C17 | 3174(9) | 1322(6) | 4005(14) | 46(5) |

| | | | | |
|---|---|---|---|---|
| C18 | 3339(10) | 1715(7) | 4682(15) | 55(5) |
| C19 | 3962(10) | 1924(7) | 4823(16) | 60(6) |
| C20 | 4402(10) | 1717(6) | 4394(14) | 47(5) |
| C21 | 4254(8) | 1342(6) | 3845(13) | 36(4) |
| C22 | 4729(10) | 1135(6) | 3422(14) | 48(5) |
| C23 | 1931(12) | -2365(7) | -109(17) | 66(6) |
| C24 | 2015(11) | -2059(7) | -867(16) | 59(6) |
| C25 | 2633(10) | -2088(7) | -922(16) | 58(6) |
| C26 | 2996(10) | -2382(6) | -208(14) | 50(5) |
| C27 | 2528(10) | -2542(7) | 257(16) | 57(6) |
| C28 | 1012(11) | -1943(8) | 2317(17) | 65(6) |
| C29 | 1611(12) | -2108(9) | 2490(18) | 76(7) |
| C30 | 1977(12) | -1755(7) | 3105(17) | 64(6) |
| C31 | 1570(11) | -1421(8) | 3236(18) | 71(7) |
| C32 | 989(11) | -1522(7) | 2694(17) | 65(6) |
| C33 | -704(10) | 1896(7) | 4218(16) | 53(5) |
| C34 | -212(10) | 2119(7) | 4859(15) | 55(5) |
| C35 | -9(11) | 1793(7) | 5647(17) | 60(6) |
| C36 | -292(11) | 1406(8) | 5388(17) | 66(6) |
| C37 | -739(11) | 1453(8) | 4514(17) | 67(6) |
| C38 | -900(13) | 633(9) | 2048(19) | 82(8) |
| C39 | -606(12) | 1067(8) | 1884(18) | 73(7) |
| C40 | -97(10) | 986(7) | 1472(16) | 57(6) |
| C41 | -56(12) | 483(8) | 1373(18) | 68(7) |
| C42 | -525(11) | 299(8) | 1781(16) | 61(6) |
| C43 | 4347(10) | -1234(7) | 2594(16) | 57(6) |
| C44 | 5000(20) | -1325(15) | 3010(40) | 189(19) |
| C45 | 3409(8) | -1130(5) | 3798(12) | 32(4) |
| C46 | 3734(11) | -1464(7) | 4561(16) | 62(6) |
| C47 | 4420(11) | -492(8) | 4024(17) | 68(6) |
| C48 | 4130(13) | -207(8) | 4707(19) | 84(8) |
| C49 | 2778(9) | -165(6) | -665(14) | 45(5) |
| C50 | 3477(10) | -164(7) | -915(17) | 62(6) |
| C51 | 3085(9) | 660(6) | 475(14) | 44(5) |
| C52 | 2826(12) | 931(8) | -432(19) | 80(7) |
| C53 | 1957(8) | 175(6) | 540(13) | 41(4) |
| C54 | 1822(10) | 282(7) | 1579(15) | 58(6) |
| C55 | 1497(10) | 1496(7) | 1465(16) | 60(6) |
| C56 | 1124(13) | 1871(8) | 750(20) | 88(8) |
| C57 | 2790(10) | 1803(7) | 1974(15) | 51(5) |
| C58 | 2759(12) | 2124(8) | 1142(18) | 80(7) |
| C59 | 1817(9) | 2260(6) | 2773(14) | 44(5) |
| C60 | 2288(10) | 2541(7) | 3524(16) | 60(6) |

| | | | | |
|---|---|---|---|---|
| C61 | 2215(10) | 970(6) | 6276(14) | 48(5) |
| C62 | 2560(11) | 1397(7) | 6761(17) | 65(6) |
| C63 | 2128(9) | 145(6) | 5126(13) | 40(4) |
| C64 | 2311(11) | -124(7) | 4340(16) | 64(6) |
| C65 | 3318(10) | 637(7) | 5733(16) | 57(6) |
| C66 | 3465(12) | 349(8) | 6657(17) | 71(7) |
| P9 | 2602(3) | 8811(2) | 6768(5) | 65(2) |
| F1 | 2379(8) | 8728(5) | 5640(11) | 104(7) |
| F2 | 3101(9) | 9169(6) | 6567(13) | 125(8) |
| F3 | 3056(9) | 8396(5) | 6801(14) | 125(8) |
| F4 | 2126(11) | 9217(5) | 6696(16) | 147(10) |
| F5 | 2084(9) | 8464(5) | 6997(14) | 123(8) |
| F6 | 2837(12) | 8881(5) | 7873(11) | 145(11) |
| P10 | 912(3) | 1147(2) | 8252(5) | 63(2) |
| F7 | 759(8) | 922(6) | 9179(13) | 113(8) |
| F8 | 335(7) | 881(5) | 7571(13) | 103(7) |
| F9 | 1463(7) | 1397(5) | 8895(14) | 107(7) |
| F10 | 1350(6) | 734(4) | 8137(11) | 83(6) |
| F11 | 473(7) | 1564(5) | 8417(11) | 96(6) |
| F12 | 1051(11) | 1389(7) | 7304(14) | 154(10) |

Table 7.33. Anisotropic displacement parameters ($Å^2 \times 10^3$) for **57**. The anisotropic displacement factor exponent takes the form: $-2\pi^2[h^2a^{*2}U_{11} + ... + 2hka^*b^*U_{12}]$.

| **Atom** | $U_{11}$ | $U_{22}$ | $U_{33}$ | $U_{23}$ | $U_{13}$ | $U_{12}$ |
|---|---|---|---|---|---|---|
| Pt1 | 37(1) | 27(1) | 31(1) | -1(1) | 0(1) | -1(1) |
| Pt2 | 42(1) | 24(1) | 33(1) | 0(1) | 7(1) | 0(1) |
| Mo1 | 62(1) | 28(1) | 37(1) | -4(1) | 7(1) | 2(1) |
| Mo2 | 44(1) | 33(1) | 32(1) | 2(1) | 3(1) | -3(1) |
| Mo3 | 50(1) | 36(1) | 41(1) | -3(1) | 7(1) | 8(1) |
| Mo4 | 44(1) | 35(1) | 38(1) | 1(1) | 1(1) | 0(1) |
| P1 | 41(3) | 29(2) | 23(2) | -3(2) | -1(2) | 1(2) |
| P2 | 53(3) | 29(2) | 32(3) | 1(2) | 0(2) | -3(2) |
| P3 | 46(3) | 30(2) | 33(3) | -6(2) | 1(2) | 2(2) |
| P4 | 41(3) | 42(3) | 34(3) | 5(2) | 5(2) | 7(2) |
| P5 | 54(3) | 37(3) | 34(3) | 3(2) | -6(3) | -1(2) |
| P6 | 40(3) | 30(2) | 34(3) | 2(2) | 4(2) | -1(2) |
| P7 | 48(3) | 23(2) | 33(3) | 1(2) | 8(2) | 0(2) |
| P8 | 41(3) | 39(2) | 35(3) | 10(2) | 2(2) | 2(2) |
| O1 | 105(13) | 51(8) | 40(8) | 22(6) | 9(9) | 36(8) |
| O2 | 56(10) | 84(11) | 61(10) | 0(8) | 23(8) | -10(8) |
| O3 | 99(12) | 67(9) | 33(8) | 8(7) | -19(8) | -31(9) |
| O4 | 76(11) | 63(9) | 70(11) | -1(8) | 24(9) | 24(8) |

| | | | | | | |
|---|---|---|---|---|---|---|
| O5 | 58(10) | 57(9) | 67(10) | -4(7) | -4(8) | -7(7) |
| O6 | 65(11) | 79(11) | 85(13) | -2(9) | 6(10) | -8(9) |
| O7 | 74(11) | 61(9) | 74(11) | 29(8) | 13(9) | 14(8) |
| O8 | 56(10) | 56(9) | 99(13) | -30(8) | 9(9) | -12(8) |
| P9 | 87(5) | 48(3) | 59(4) | 6(3) | 12(4) | -1(3) |
| F1 | 118(13) | 99(11) | 81(11) | 5(8) | -15(10) | -10(10) |
| F2 | 149(16) | 111(12) | 114(14) | 24(10) | 21(13) | -69(12) |
| F3 | 173(17) | 49(8) | 139(15) | 3(9) | -3(14) | 22(10) |
| F4 | 210(20) | 68(10) | 190(20) | 38(11) | 109(18) | 53(12) |
| F5 | 127(15) | 102(12) | 130(15) | 40(11) | 2(12) | -29(11) |
| F6 | 290(30) | 86(11) | 50(9) | -31(8) | 8(13) | -40(13) |
| P10 | 57(4) | 72(4) | 53(4) | -7(3) | -5(3) | 0(3) |
| F7 | 108(13) | 135(13) | 96(13) | 17(10) | 23(11) | -24(11) |
| F8 | 71(10) | 112(12) | 117(14) | -12(10) | -7(10) | 2(9) |
| F9 | 62(9) | 83(10) | 167(17) | -10(10) | -2(10) | -3(8) |
| F10 | 65(9) | 75(9) | 106(12) | 16(8) | 8(8) | 15(7) |
| F11 | 94(11) | 81(9) | 105(12) | -12(8) | -3(10) | 22(8) |
| F12 | 190(20) | 185(18) | 96(14) | 53(13) | 52(15) | 45(16) |

## 7.3.12. $[(C_{14}H_8Cl)Pt\{Cp_2Mo_2(CO)_4(\mu_3,\eta^2:\eta^2:\eta^1\text{-}P_2)\}(PEt_3)_2][PF_6]\bullet CH_2Cl_2$ (**59**$\bullet CH_2Cl_2$)

Crystals of **59**$\bullet CH_2Cl_2$ were obtained by controlled diffusion of hexane into a $CH_2Cl_2$ solution of **59** at room temperature.

Table 7.34. Crystal data and structure refinement for **59**$\bullet CH_2Cl_2$.

| | |
|---|---|
| Empirical formula | $C_{41}H_{50}Cl_3F_6Mo_2O_4P_5Pt$ |
| Formula weight | 1368.98 g $mol^{-1}$ |
| Crystal size | $0.10 \times 0.10 \times 0.04$ mm |
| Crystal description | plate |
| Crystal colour | red |
| Crystal system | orthorhombic |
| Space group | $Pca2_1$ |
| Unit cell dimensions | $a$ = 29.581(1) Å, $\alpha$ = 90° |
| | $b$ = 10.433(1) Å, $\beta$ = 90° |
| | $c$ = 16.029(1) Å, $\gamma$ = 90° |
| Volume | 4946.9(2) $Å^3$ |
| Z, Calculated density | 4, 1.838 Mg $m^{-3}$ |
| Absorption coefficient | 3.705 $mm^{-1}$ |
| F(000) | 2680 |
| Measurement device type | STOE-IPDS |
| Measurement method | rotation |
| Temperature | 200(1) K |
| Wavelength | 0.71073 Å |
| Monochromator | graphite |
| $\theta$ range for data collection | 1.87 to 27.10° |
| Index ranges | $-37 \le h \le 37$, $-13 \le k \le 13$, $-20 \le l \le 19$ |
| Reflections collected / unique | 40665 / 10606 [R(int) = 0.0534] |
| Reflections greater I>2\s(I) | 8854 |
| Absorption correction | numerical |
| Max. and min. transmission | 0.8368 and 0.6443 |
| Refinement method | Full-matrix least-squares on $F^2$ |
| Data / restraints / parameters | 10606 / 1 / 559 |
| Goodness-of-fit on $F^2$ | 1.018 |
| Final R indices [I>2sigma(I)] | R1 = 0.0337, wR2 = 0.0804 |
| R indices (all data) | R1 = 0.0397, wR2 = 0.0829 |
| Largest diff. peak and hole | 1.397 and -0.741 e $Å^{-3}$ |

Table 7.35. Atomic coordinates ($\times 10^4$) and equivalent isotropic displacement parameters ($Å^2 \times 10^3$) for **59•**$CH_2Cl_2$. $U_{eq}$ is defined as one third of the trace of the orthogonalised $U_{ij}$ tensor.

| **Atom** | **x** | **y** | **z** | $U_{eq}$ |
|---|---|---|---|---|
| Pt1 | 10796(1) | -2108(1) | 3816(1) | 26(1) |
| Mo1 | 12288(1) | -1963(1) | 3037(1) | 31(1) |
| Mo2 | 11890(1) | 697(1) | 2806(1) | 35(1) |
| P1 | 11484(1) | -1239(1) | 3275(1) | 29(1) |
| P2 | 11694(1) | -1375(2) | 2035(1) | 32(1) |
| P3 | 11055(1) | -1988(2) | 5177(1) | 33(1) |
| P4 | 10502(1) | -2543(2) | 2497(1) | 32(1) |
| Cl1 | 10008(1) | 2246(2) | 3881(2) | 56(1) |
| C1C | 12906(3) | -1260(9) | 2255(6) | 60(2) |
| C2C | 13061(2) | -1726(9) | 3023(6) | 58(2) |
| C3C | 12957(2) | -3042(9) | 3058(6) | 57(2) |
| C4C | 12729(3) | -3377(9) | 2306(5) | 53(2) |
| C5C | 12697(2) | -2288(9) | 1813(5) | 55(2) |
| C6C | 12503(4) | 1414(10) | 3673(7) | 78(3) |
| C7C | 12455(4) | 2223(9) | 2948(8) | 81(3) |
| C8C | 12022(4) | 2833(7) | 2939(7) | 66(2) |
| C9C | 11786(4) | 2465(7) | 3650(6) | 67(3) |
| C10C | 12069(4) | 1648(9) | 4092(6) | 71(3) |
| C15 | 12353(2) | -1487(7) | 4227(4) | 40(1) |
| C16 | 11962(2) | -3555(6) | 3340(4) | 38(1) |
| C17 | 11299(3) | 1347(10) | 2367(7) | 71(3) |
| C18 | 12145(3) | 733(7) | 1664(5) | 59(2) |
| O1 | 12426(2) | -1231(6) | 4911(3) | 60(1) |
| O2 | 11786(2) | -4491(5) | 3495(4) | 59(2) |
| O3 | 10959(3) | 1719(8) | 2137(7) | 103(3) |
| O4 | 12300(3) | 823(6) | 1006(5) | 93(3) |
| C1 | 10202(2) | -2766(6) | 4304(4) | 30(1) |
| C2 | 10143(2) | -4036(6) | 4481(4) | 35(1) |
| C3 | 9743(2) | -4539(7) | 4859(4) | 42(2) |
| C4 | 9393(2) | -3735(7) | 5055(4) | 43(2) |
| C5 | 9430(2) | -2393(6) | 4874(4) | 34(1) |
| C6 | 9839(2) | -1914(6) | 4491(4) | 29(1) |
| C7 | 9867(2) | -592(6) | 4325(4) | 32(1) |
| C8 | 9508(2) | 254(6) | 4488(4) | 33(1) |
| C9 | 9100(2) | -242(7) | 4836(4) | 37(1) |
| C10 | 9073(2) | -1554(8) | 5030(4) | 43(2) |
| C11 | 9518(2) | 1591(7) | 4292(4) | 41(2) |
| C12 | 9151(2) | 2364(8) | 4463(5) | 50(2) |
| C13 | 8759(3) | 1838(9) | 4814(6) | 59(2) |

| | | | | |
|---|---|---|---|---|
| C14 | 8732(2) | 594(8) | 4978(5) | 50(2) |
| C311 | 10638(3) | -2217(8) | 6006(4) | 47(2) |
| C312 | 11328(2) | -460(7) | 5432(5) | 46(2) |
| C313 | 11485(2) | -3197(7) | 5392(4) | 40(1) |
| C314 | 10817(3) | -2128(11) | 6899(5) | 64(3) |
| C315 | 11019(3) | 662(8) | 5362(7) | 66(2) |
| C316 | 11319(3) | -4575(7) | 5310(6) | 52(2) |
| C411 | 9919(2) | -3117(8) | 2471(5) | 49(2) |
| C412 | 10492(2) | -1213(7) | 1753(4) | 44(2) |
| C413 | 10826(2) | -3778(7) | 1966(5) | 43(2) |
| C414 | 9737(3) | -3479(11) | 1619(5) | 68(3) |
| C415 | 10168(3) | -158(9) | 1982(6) | 66(2) |
| C416 | 10803(3) | -5095(7) | 2410(6) | 61(2) |
| P5 | 7936(1) | -4641(2) | 5351(2) | 60(1) |
| F1 | 7707(5) | -4178(15) | 4573(9) | 229(8) |
| F2 | 8169(5) | -5106(17) | 6120(7) | 215(7) |
| F3 | 8156(4) | -3315(8) | 5397(11) | 234(9) |
| F4 | 7547(3) | -4146(8) | 5920(6) | 122(3) |
| F5 | 8346(2) | -5120(6) | 4800(6) | 105(2) |
| F6 | 7692(3) | -5947(8) | 5211(7) | 146(4) |
| C1S | 13642(4) | 2969(11) | 3221(7) | 86(3) |
| Cl1S | 13522(2) | 4090(5) | 2448(3) | 175(3) |
| Cl2S | 13749(1) | 1452(3) | 2818(2) | 84(1) |

Table 7.36. Anisotropic displacement parameters ($Å^2 \times 10^3$) for **59**•$CH_2Cl_2$. The anisotropic displacement factor exponent takes the form: $-2\pi^2[h^2a^{*2}U_{11} + ... + 2hka^*b^*U_{12}]$.

| **Atom** | $U_{11}$ | $U_{22}$ | $U_{33}$ | $U_{23}$ | $U_{13}$ | $U_{12}$ |
|---|---|---|---|---|---|---|
| Pt1 | 26(1) | 27(1) | 26(1) | -3(1) | 0(1) | 2(1) |
| Mo1 | 29(1) | 32(1) | 31(1) | -3(1) | 4(1) | 1(1) |
| Mo2 | 44(1) | 24(1) | 36(1) | -2(1) | 4(1) | -1(1) |
| P1 | 30(1) | 28(1) | 30(1) | 1(1) | -1(1) | 1(1) |
| P2 | 40(1) | 30(1) | 28(1) | -1(1) | -1(1) | 2(1) |
| P3 | 30(1) | 41(1) | 27(1) | -3(1) | -2(1) | 1(1) |
| P4 | 30(1) | 41(1) | 27(1) | -6(1) | -2(1) | 2(1) |
| Cl1 | 57(1) | 38(1) | 74(1) | -2(1) | 6(1) | 1(1) |
| C1C | 44(4) | 64(5) | 72(6) | 2(4) | 20(4) | -8(4) |
| C2C | 39(4) | 72(5) | 65(6) | -19(4) | 9(4) | -14(4) |
| C3C | 42(4) | 76(5) | 53(5) | 0(4) | 9(3) | 27(4) |
| C4C | 41(4) | 59(5) | 57(5) | -12(4) | 18(3) | 12(3) |
| C5C | 39(4) | 83(6) | 43(4) | 1(4) | 16(3) | 11(4) |
| C6C | 93(7) | 73(6) | 68(7) | -9(5) | -12(5) | -27(5) |
| C7C | 102(8) | 60(5) | 81(8) | -11(5) | 14(6) | -41(5) |

| | | | | | | |
|---|---|---|---|---|---|---|
| C8C | 100(7) | 28(3) | 70(6) | -5(4) | -6(5) | 0(4) |
| C9C | 100(7) | 37(3) | 65(7) | -19(4) | -6(5) | 25(4) |
| C10C | 90(7) | 59(5) | 62(6) | -8(4) | -1(5) | -27(5) |
| C15 | 39(3) | 42(4) | 38(4) | -2(3) | -3(3) | -3(3) |
| C16 | 40(3) | 31(3) | 43(4) | -8(3) | 4(3) | 2(3) |
| C17 | 63(5) | 67(6) | 82(7) | 9(5) | -20(5) | 18(5) |
| C18 | 103(7) | 30(3) | 43(4) | 0(3) | 24(4) | -6(4) |
| O1 | 61(3) | 79(4) | 39(3) | -8(3) | -4(2) | -12(3) |
| O2 | 64(3) | 31(2) | 81(4) | -1(2) | 20(3) | -4(2) |
| O3 | 104(6) | 59(4) | 145(9) | 1(5) | -20(6) | 14(4) |
| O4 | 163(8) | 45(3) | 72(5) | 2(3) | 59(5) | -10(4) |
| C1 | 23(2) | 40(3) | 26(3) | 2(2) | 2(2) | -6(2) |
| C2 | 40(3) | 30(3) | 35(3) | 2(2) | -4(2) | -4(2) |
| C3 | 45(3) | 40(3) | 41(4) | 7(3) | -6(3) | -6(3) |
| C4 | 40(3) | 50(4) | 38(4) | 9(3) | 2(3) | -6(3) |
| C5 | 30(3) | 45(3) | 27(3) | 2(3) | -2(2) | -6(2) |
| C6 | 33(3) | 34(3) | 22(3) | 1(2) | -3(2) | 0(2) |
| C7 | 27(3) | 36(3) | 32(3) | -4(2) | 1(2) | -1(2) |
| C8 | 28(3) | 41(3) | 29(3) | -11(2) | -1(2) | 3(2) |
| C9 | 30(3) | 52(4) | 29(3) | -5(3) | -1(2) | 6(3) |
| C10 | 36(3) | 63(4) | 29(3) | -5(3) | 4(2) | -5(3) |
| C11 | 41(3) | 44(3) | 36(4) | -11(3) | -9(3) | 7(3) |
| C12 | 47(4) | 44(4) | 58(5) | -12(3) | -14(3) | 12(3) |
| C13 | 41(4) | 73(5) | 62(5) | -27(4) | -6(3) | 19(4) |
| C14 | 35(3) | 69(5) | 45(4) | -8(4) | -6(3) | 10(3) |
| C311 | 41(3) | 71(5) | 31(3) | -4(3) | 1(3) | 0(3) |
| C312 | 51(4) | 53(4) | 35(4) | -8(3) | -3(3) | -2(3) |
| C313 | 32(3) | 55(4) | 34(3) | 1(3) | -4(3) | 0(3) |
| C314 | 58(5) | 105(8) | 30(4) | 0(4) | 3(3) | -6(5) |
| C315 | 70(6) | 48(4) | 80(7) | -18(4) | 4(5) | -4(4) |
| C316 | 49(4) | 43(4) | 62(5) | 17(3) | -2(3) | 5(3) |
| C411 | 30(3) | 71(5) | 45(4) | -12(4) | -2(3) | -4(3) |
| C412 | 44(3) | 52(4) | 35(4) | 3(3) | -6(3) | 7(3) |
| C413 | 42(3) | 38(3) | 49(4) | -12(3) | 4(3) | 2(3) |
| C414 | 52(4) | 110(8) | 42(5) | -13(5) | -8(4) | -12(5) |
| C415 | 62(5) | 69(6) | 66(6) | 16(5) | 8(4) | 31(4) |
| C416 | 74(5) | 37(4) | 74(6) | -18(4) | 7(4) | -4(4) |
| P5 | 49(1) | 44(1) | 88(2) | 7(1) | 9(1) | -6(1) |
| F1 | 216(12) | 289(17) | 182(12) | 150(12) | 37(10) | 120(12) |
| F2 | 188(11) | 339(19) | 118(8) | -54(10) | -80(7) | 127(12) |
| F3 | 166(8) | 76(5) | 460(20) | -111(9) | 202(12) | -64(6) |
| F4 | 84(4) | 104(5) | 177(9) | 1(5) | 65(5) | 4(4) |
| F5 | 84(4) | 80(4) | 151(7) | -24(4) | 33(4) | -9(3) |
| F6 | 169(8) | 118(6) | 150(8) | -32(6) | 35(7) | -90(6) |
| C1S | 76(6) | 113(9) | 68(7) | 32(6) | 6(5) | 17(6) |
| Cl1S | 204(5) | 161(4) | 162(4) | 91(3) | 83(4) | 120(4) |
| Cl2S | 89(2) | 81(2) | 82(2) | 0(2) | -3(1) | -10(1) |

## 7.3.13. $[Cu(\mu\text{-}Cl)\{Cp_2Cr_2(CO)_4(\mu_4,\eta^2\!:\!\eta^2\!:\!\eta^1\!:\!\eta^1\text{-}P_2)\}]_n$ (66a)

Crystals of **66a** were obtained by controlled diffusion of a $CH_3CN$ solution of CuCl into a $CH_2Cl_2$ solution of $[Cp_2Cr_2(CO)_4(\mu,\eta^2\text{-}P_2)]$ **6a** at room temperature in the dark.

Table 7.37. Crystal data and structure refinement for **66a**.

| | |
|---|---|
| Empirical formula | $C_{14}H_{10}ClCr_2CuO_4P_2$ |
| Formula weight | 507.16 g $mol^{-1}$ |
| Crystal size | $0.400 \times 0.100 \times 0.060$ mm |
| Crystal description | stick |
| Crystal colour | moss green |
| Crystal system | monoclinic |
| Space group | $P2_1/n$ |
| Unit cell dimensions | $a$ = 14.616(2)Å, $\alpha$ = 90° |
| | $b$ = 7.909(1) Å, $\beta$ = 112.10(1)° |
| | $c$ = 16.032(2) Å, $\gamma$ = 90° |
| Volume | 1717.0(3) $Å^3$ |
| Z, Calculated density | 4, 1.962 Mg $m^{-3}$ |
| Absorption coefficient | 2.827 $mm^{-1}$ |
| F(000) | 1000 |
| Measurement device type | STOE-IPDS |
| Measurement method | rotation |
| Temperature | 173(1) K |
| Wavelength | 0.71073 Å |
| Monochromator | graphite |
| $\theta$ range for data collection | 2.98 to 25.86° |
| Index ranges | $-17 \le h \le 17$, $-9 \le k \le 9$, $-19 \le l \le 19$ |
| Reflections collected / unique | 23308 / 3303 [R(int) = 0.0267] |
| Reflections greater I>2\s(I) | 2852 |
| Absorption correction | numerical |
| Max. and min. transmission | 0.8488 and 0.6658 |
| Refinement method | Full-matrix least-squares on $F^2$ |
| Data / restraints / parameters | 3303 / 0 / 217 |
| Goodness-of-fit on $F^2$ | 0.997 |
| Final R indices [I>2sigma(I)] | R1 = 0.0192, wR2 = 0.0501 |
| R indices (all data) | R1 = 0.0237, wR2 = 0.0513 |
| Largest diff. peak and hole | 0.343 and -0.234 e $Å^{-3}$ |

Table 7.38. Atomic coordinates ($\times 10^4$) and equivalent isotropic displacement parameters ($Å^2 \times 10^3$) for **66a**. $U_{eq}$ is defined as one third of the trace of the orthogonalised $U_{ij}$ tensor.

| **Atom** | **x** | **y** | **z** | $U_{eq}$ |
|---|---|---|---|---|
| Cu1 | -49(1) | 1900(1) | 4951(1) | 21(1) |
| Cr1 | -1379(1) | 4834(1) | 6615(1) | 18(1) |
| Cr2 | -2529(1) | 5211(1) | 4620(1) | 18(1) |
| Cl1 | -928(1) | -107(1) | 3872(1) | 24(1) |
| P1 | -1014(1) | 3651(1) | 5414(1) | 19(1) |
| P2 | -896(1) | 6248(1) | 5487(1) | 19(1) |
| O1 | -3518(1) | 4081(2) | 6244(1) | 44(1) |
| O2 | -1632(1) | 8592(2) | 6777(1) | 41(1) |
| O3 | -1843(1) | 4154(3) | 3143(1) | 50(1) |
| O4 | -3365(1) | 1705(2) | 4602(1) | 51(1) |
| C1 | -352(2) | 5165(3) | 8011(1) | 45(1) |
| C2 | -1191(2) | 4287(3) | 8003(1) | 33(1) |
| C3 | -1232(2) | 2734(3) | 7569(1) | 39(1) |
| C4 | -429(2) | 2642(4) | 7303(1) | 54(1) |
| C5 | 117(2) | 4151(5) | 7575(2) | 59(1) |
| C6 | -2725(1) | 4411(3) | 6302(1) | 28(1) |
| C7 | -1550(1) | 7158(3) | 6689(1) | 27(1) |
| C8 | -3516(1) | 7113(3) | 4898(1) | 32(1) |
| C9 | -4088(1) | 5937(3) | 4245(1) | 32(1) |
| C10 | -3823(1) | 6078(3) | 3486(1) | 33(1) |
| C11 | -3072(1) | 7333(3) | 3684(1) | 34(1) |
| C12 | -2884(1) | 7960(2) | 4558(1) | 33(1) |
| C13 | -2087(1) | 4522(3) | 3715(1) | 32(1) |
| C14 | -3023(1) | 3011(2) | 4617(1) | 30(1) |

Table 7.39. Anisotropic displacement parameters ($Å^2 \times 10^3$) for **66a**. The anisotropic displacement factor exponent takes the form: $-2\pi^2[h^2a^{*2}U_{11} + ... + 2hka^*b^*U_{12}]$.

| **Atom** | $U_{11}$ | $U_{22}$ | $U_{33}$ | $U_{23}$ | $U_{13}$ | $U_{12}$ |
|---|---|---|---|---|---|---|
| Cu1 | 22(1) | 16(1) | 25(1) | 0(1) | 10(1) | 1(1) |
| Cr1 | 17(1) | 20(1) | 16(1) | 0(1) | 7(1) | -1(1) |
| Cr2 | 18(1) | 18(1) | 17(1) | 0(1) | 6(1) | 3(1) |
| Cl1 | 27(1) | 19(1) | 22(1) | 1(1) | 3(1) | 0(1) |
| P1 | 19(1) | 18(1) | 19(1) | 0(1) | 8(1) | 4(1) |
| P2 | 19(1) | 18(1) | 21(1) | 1(1) | 10(1) | 0(1) |
| O1 | 24(1) | 76(1) | 35(1) | 5(1) | 14(1) | -9(1) |
| O2 | 59(1) | 25(1) | 45(1) | -10(1) | 25(1) | 2(1) |
| O3 | 47(1) | 81(1) | 24(1) | -3(1) | 14(1) | 22(1) |
| O4 | 44(1) | 25(1) | 68(1) | -3(1) | 3(1) | -8(1) |
| C1 | 49(1) | 50(1) | 20(1) | 6(1) | -6(1) | -20(1) |
| C2 | 39(1) | 42(1) | 18(1) | 6(1) | 13(1) | 1(1) |
| C3 | 52(1) | 31(1) | 27(1) | 11(1) | 7(1) | -6(1) |
| C4 | 70(2) | 65(2) | 25(1) | 18(1) | 15(1) | 44(1) |
| C5 | 21(1) | 116(3) | 36(1) | 40(1) | 6(1) | 10(1) |
| C6 | 27(1) | 37(1) | 22(1) | 0(1) | 11(1) | -3(1) |
| C7 | 29(1) | 32(1) | 22(1) | -5(1) | 11(1) | -2(1) |
| C8 | 30(1) | 34(1) | 32(1) | 0(1) | 10(1) | 18(1) |
| C9 | 18(1) | 34(1) | 42(1) | 6(1) | 8(1) | 8(1) |
| C10 | 27(1) | 37(1) | 24(1) | 1(1) | -2(1) | 12(1) |
| C11 | 32(1) | 34(1) | 35(1) | 17(1) | 11(1) | 13(1) |
| C12 | 29(1) | 20(1) | 41(1) | 3(1) | 4(1) | 9(1) |
| C13 | 27(1) | 42(1) | 22(1) | 0(1) | 6(1) | 10(1) |
| C14 | 28(1) | 25(1) | 31(1) | -3(1) | 3(1) | 2(1) |

## 7.3.14. $[Cu(\mu\text{-}Br)\{Cp_2Cr_2(CO)_4(\mu_4,\eta^2\text{:}\eta^2\text{:}\eta^1\text{:}\eta^1\text{-}P_2)\}]_n$ (66b)

Crystals of **66b** were obtained by controlled diffusion of a $CH_3CN$ solution of CuBr into a $CH_2Cl_2$ solution of $[Cp_2Cr_2(CO)_4(\mu,\eta^2\text{-}P_2)]$ **6a** at room temperature in the dark.

Table 7.40. Crystal data and structure refinement for **66b**.

| | |
|---|---|
| Empirical formula | $C_{14}H_{10}BrCr_2CuO_4P_2$ |
| Formula weight | 551.61 g $mol^{-1}$ |
| Crystal size | $0.460 \times 0.080 \times 0.040$ mm |
| Crystal description | stick |
| Crystal colour | moss green |
| Crystal system | monoclinic |
| Space group | $P2_1/n$ |
| Unit cell dimensions | $a$ = 14.614(1) Å, $\alpha$ = 90° |
| | $b$ = 7.943(1) Å, $\beta$ = 111.72(1)° |
| | $c$ = 16.120(2) Å, $\gamma$ = 90° |
| Volume | 1738.4(3) $Å^3$ |
| Z, Calculated density | 4, 2.108 Mg $m^{-3}$ |
| Absorption coefficient | 4.937 $mm^{-1}$ |
| F(000) | 1072 |
| Measurement device type | STOE-IPDS |
| Measurement method | rotation |
| Temperature | 173(1) K |
| Wavelength | 0.71073 Å |
| Monochromator | graphite |
| $\theta$ range for data collection | 2.90 to 25.85° |
| Index ranges | $-17 \le h \le 17$, $-9 \le k \le 9$, $-19 \le l \le 19$ |
| Reflections collected / unique | 14195 / 3347 [R(int) = 0.0260] |
| Reflections greater I>2\s(I) | 2692 |
| Absorption correction | numerical |
| Max. and min. transmission | 0.8324 and 0.5400 |
| Refinement method | Full-matrix least-squares on $F^2$ |
| Data / restraints / parameters | 3347 / 0 / 217 |
| Goodness-of-fit on $F^2$ | 0.927 |
| Final R indices [I>2sigma(I)] | R1 = 0.0203, wR2 = 0.0475 |
| R indices (all data) | R1 = 0.0281, wR2 = 0.0491 |
| Largest diff. peak and hole | 0.538 and -0.275 e $Å^{-3}$ |

Table 7.41. Atomic coordinates ($\times 10^4$) and equivalent isotropic displacement parameters ($Å^2 \times 10^3$) for **66b**. $U_{eq}$ is defined as one third of the trace of the orthogonalised $U_{ij}$ tensor.

| **Atom** | **x** | **y** | **z** | $U_{eq}$ |
|---|---|---|---|---|
| Br1 | -1002(1) | -4930(1) | 3804(1) | 23(1) |
| Cu1 | 41(1) | -3077(1) | 5025(1) | 21(1) |
| Cr1 | -1380(1) | 101(1) | 6623(1) | 18(1) |
| Cr2 | -2542(1) | -179(1) | 4642(1) | 17(1) |
| P1 | -1016(1) | 1334(1) | 5435(1) | 19(1) |
| P2 | -917(1) | -1255(1) | 5470(1) | 18(1) |
| O1 | -3507(1) | 873(3) | 6289(1) | 40(1) |
| O2 | -1639(1) | -3646(2) | 6740(1) | 39(1) |
| O3 | -1842(1) | 851(3) | 3167(1) | 42(1) |
| O4 | -3346(1) | 3329(2) | 4651(2) | 47(1) |
| C1 | -1231(2) | 2155(3) | 7591(2) | 38(1) |
| C2 | -425(2) | 2251(5) | 7332(2) | 53(1) |
| C3 | 112(2) | 739(6) | 7581(2) | 58(1) |
| C4 | -364(2) | -273(4) | 8007(2) | 45(1) |
| C5 | -1201(2) | 599(3) | 8006(2) | 31(1) |
| C6 | -2718(2) | 545(3) | 6329(2) | 27(1) |
| C7 | -1553(2) | -2220(3) | 6668(2) | 27(1) |
| C8 | -3518(2) | -2096(3) | 4925(2) | 27(1) |
| C9 | -2924(2) | -2910(3) | 4526(2) | 28(1) |
| C10 | -3144(2) | -2210(3) | 3671(2) | 29(1) |
| C11 | -3872(2) | -939(3) | 3537(2) | 29(1) |
| C12 | -4093(1) | -865(3) | 4324(2) | 28(1) |
| C13 | -2090(2) | 494(3) | 3740(2) | 27(1) |
| C14 | -3012(2) | 2023(3) | 4659(2) | 28(1) |

Table 7.42. Anisotropic displacement parameters ($Å^2 \times 10^3$) for **66b**. The anisotropic displacement factor exponent takes the form: $-2\pi^2[h^2a^{*2}U_{11} + ... + 2hka^*b^*U_{12}]$.

| **Atom** | $U_{11}$ | $U_{22}$ | $U_{33}$ | $U_{23}$ | $U_{13}$ | $U_{12}$ |
|---|---|---|---|---|---|---|
| Br1 | 25(1) | 20(1) | 20(1) | -1(1) | 3(1) | 0(1) |
| Cu1 | 20(1) | 18(1) | 24(1) | 0(1) | 9(1) | -1(1) |
| Cr1 | 17(1) | 21(1) | 16(1) | 0(1) | 7(1) | 1(1) |
| Cr2 | 17(1) | 18(1) | 17(1) | 0(1) | 6(1) | -3(1) |
| P1 | 19(1) | 19(1) | 19(1) | -1(1) | 8(1) | -4(1) |
| P2 | 18(1) | 19(1) | 20(1) | -1(1) | 9(1) | 0(1) |
| O1 | 22(1) | 67(1) | 33(1) | -3(1) | 13(1) | 7(1) |
| O2 | 53(1) | 25(1) | 44(1) | 9(1) | 25(1) | -2(1) |
| O3 | 43(1) | 63(1) | 22(1) | 2(1) | 14(1) | -19(1) |
| O4 | 42(1) | 25(1) | 65(1) | 3(1) | 10(1) | 7(1) |
| C1 | 50(1) | 31(1) | 24(1) | -11(1) | 4(1) | 4(1) |
| C2 | 70(2) | 63(2) | 26(1) | -17(1) | 16(1) | -45(2) |
| C3 | 20(1) | 117(3) | 33(2) | -38(2) | 7(1) | -12(2) |
| C4 | 47(2) | 50(2) | 21(1) | -5(1) | -5(1) | 19(1) |
| C5 | 33(1) | 44(2) | 19(1) | -5(1) | 12(1) | -1(1) |
| C6 | 27(1) | 36(1) | 19(1) | 0(1) | 10(1) | 0(1) |
| C7 | 27(1) | 33(1) | 21(1) | 4(1) | 11(1) | 1(1) |
| C8 | 24(1) | 30(1) | 28(1) | 0(1) | 9(1) | -14(1) |
| C9 | 25(1) | 19(1) | 36(1) | -4(1) | 6(1) | -8(1) |
| C10 | 29(1) | 30(1) | 29(1) | -11(1) | 11(1) | -11(1) |
| C11 | 23(1) | 35(1) | 23(1) | -1(1) | 2(1) | -9(1) |
| C12 | 15(1) | 32(1) | 33(1) | -3(1) | 6(1) | -6(1) |
| C13 | 23(1) | 32(1) | 22(1) | -2(1) | 4(1) | -7(1) |
| C14 | 25(1) | 25(1) | 28(1) | 2(1) | 4(1) | -1(1) |

## 7.3.15. [Cu($\mu$-I){$Cp_2Cr_2(CO)_4(\mu_4,\eta^2:\eta^2:\eta^1:\eta^1$-$P_2$)}]$_n$•n$CH_3CN$ (**66c**•n$CH_3CN$)

Crystals of **66c**•n$CH_3CN$ were obtained by controlled diffusion of a $CH_3CN$ solution of CuI into a $CH_2Cl_2$ solution of [$Cp_2Cr_2(CO)_4(\mu,\eta^2$-$P_2)$] **6a** at room temperature in the dark.

Table 7.43. Crystal data and structure refinement for **66c**•n$CH_3CN$.

| | |
|---|---|
| Empirical formula | $C_{16}H_{13}Cr_2CuINO_4P_2$ |
| Formula weight | 639.66 g $mol^{-1}$ |
| Crystal size | 0.300 × 0.060 × 0.040 mm |
| Crystal description | needle |
| Crystal colour | dark green |
| Crystal system | triclinic |
| Space group | $P\ \bar{1}$ |
| Unit cell dimensions | $a$ = 7.980(1) Å, $\alpha$ = 82.06(1) ° |
| | $b$ = 11.485(1) Å, $\beta$ = 81.06(1) ° |
| | $c$ = 11.519(1) Å, $\gamma$ = 76.85(1) ° |
| Volume | 1009.7(2) $Å^3$ |
| Z, Calculated density | 2, 2.104 Mg $m^{-3}$ |
| Absorption coefficient | 3.809 $mm^{-1}$ |
| F(000) | 616 |
| Measurement device type | STOE-IPDS |
| Measurement method | rotation |
| Temperature | 173(1) K |
| Wavelength | 0.71073 Å |
| Monochromator | graphite |
| $\theta$ range for data collection | 1.80 to 25.90° |
| Index ranges | $-9 \le h \le 9$, $-13 \le k \le 13$, $-13 \le l \le 14$ |
| Reflections collected / unique | 6689 / 3006 [R(int) = 0.0998] |
| Reflections greater I>2\s(I) | 2225 |
| Absorption correction | none |
| Refinement method | Full-matrix least-squares on $F^2$ |
| Data / restraints / parameters | 3006 / 0 / 244 |
| Goodness-of-fit on $F^2$ | 0.935 |
| Final R indices [I>2sigma(I)] | R1 = 0.0452, wR2 = 0.1070 |
| R indices (all data) | R1 = 0.0614, wR2 = 0.1122 |
| Largest diff. peak and hole | 0.979 and -0.673 e $Å^{-3}$ |

Table 7.44. Atomic coordinates ($\times 10^4$) and equivalent isotropic displacement parameters ($Å^2 \times 10^3$) for **66c•**n$CH_3CN$. $U_{eq}$ is defined as one third of the trace of the orthogonalised $U_{ij}$ tensor.

| **Atom** | **x** | **y** | **z** | $U_{eq}$ |
|---|---|---|---|---|
| I1 | 535(1) | -6340(1) | 3797(1) | 29(1) |
| Cu1 | 1977(1) | -5042(1) | 4872(1) | 25(1) |
| Cr1 | 4139(1) | -1821(1) | 3553(1) | 21(1) |
| Cr2 | 5733(1) | -3655(1) | 1857(1) | 20(1) |
| P1 | 3578(2) | -3760(2) | 3678(2) | 23(1) |
| P2 | 6142(2) | -3814(2) | 3852(2) | 22(1) |
| O1 | 3741(11) | -1932(7) | 6217(6) | 63(3) |
| O2 | 7672(7) | -1289(6) | 3559(6) | 38(2) |
| O3 | 5610(9) | -6270(6) | 1959(7) | 51(3) |
| O4 | 2312(7) | -3248(6) | 882(5) | 34(2) |
| C1 | 1708(9) | -1184(7) | 2724(8) | 32(3) |
| C2 | 1460(10) | -726(7) | 3815(8) | 35(3) |
| C3 | 2675(10) | 23(8) | 3775(8) | 35(3) |
| C4 | 3666(10) | 19(8) | 2606(8) | 35(3) |
| C5 | 3054(10) | -725(7) | 1973(7) | 31(2) |
| C6 | 3891(11) | -1967(8) | 5211(8) | 36(3) |
| C7 | 6348(10) | -1538(7) | 3556(6) | 26(3) |
| C8 | 7220(10) | -2254(8) | 1005(8) | 33(3) |
| C9 | 6537(9) | -2678(7) | 150(7) | 30(2) |
| C10 | 7242(10) | -3942(8) | 118(7) | 31(3) |
| C11 | 8400(9) | -4269(8) | 1019(7) | 33(3) |
| C12 | 8393(9) | -3275(8) | 1544(7) | 33(3) |
| C13 | 5657(10) | -5280(7) | 1988(7) | 31(3) |
| C14 | 3585(10) | -3370(7) | 1297(7) | 28(2) |
| N1 | -2686(13) | 702(8) | 951(8) | 51(3) |
| C15 | -1700(12) | 1177(9) | 1188(8) | 39(3) |
| C16 | -493(11) | 1801(9) | 1498(9) | 43(3) |

Table 7.45. Anisotropic displacement parameters ($Å^2 \times 10^3$) for **66c**•n$CH_3CN$. The anisotropic displacement factor exponent takes the form: $-2\pi^2[h^2a^{*2}U_{11} + ... + 2hka^*b^*U_{12}]$.

| **Atom** | $U_{11}$ | $U_{22}$ | $U_{33}$ | $U_{23}$ | $U_{13}$ | $U_{12}$ |
|---|---|---|---|---|---|---|
| I1 | 23(1) | 31(1) | 35(1) | -13(1) | -6(1) | -4(1) |
| Cu1 | 23(1) | 26(1) | 27(1) | -2(1) | -5(1) | -7(1) |
| Cr1 | 19(1) | 21(1) | 22(1) | -2(1) | -1(1) | -3(1) |
| Cr2 | 17(1) | 21(1) | 23(1) | -3(1) | -2(1) | -3(1) |
| P1 | 22(1) | 23(1) | 26(1) | 0(1) | -1(1) | -7(1) |
| P2 | 21(1) | 23(1) | 21(1) | 0(1) | -4(1) | -3(1) |
| O1 | 102(6) | 57(5) | 22(4) | -5(3) | -3(3) | -5(4) |
| O2 | 31(3) | 49(4) | 43(4) | -10(3) | -11(2) | -18(3) |
| O3 | 57(4) | 27(4) | 67(5) | -5(3) | -5(3) | -8(3) |
| O4 | 28(3) | 44(4) | 33(3) | -3(3) | -14(2) | -7(2) |
| C1 | 21(4) | 25(4) | 53(5) | -15(4) | -17(3) | 3(3) |
| C2 | 26(4) | 33(5) | 35(4) | -4(3) | 0(3) | 12(3) |
| C3 | 35(4) | 27(4) | 42(5) | -11(4) | -16(3) | 6(3) |
| C4 | 27(4) | 32(4) | 43(5) | 11(4) | -7(3) | -6(3) |
| C5 | 35(4) | 23(4) | 32(4) | -4(3) | -10(3) | 5(3) |
| C6 | 39(5) | 28(4) | 35(5) | -3(4) | 5(3) | -4(3) |
| C7 | 41(5) | 20(4) | 19(4) | -7(3) | -8(3) | -3(3) |
| C8 | 26(4) | 31(4) | 43(5) | -10(4) | 9(3) | -13(3) |
| C9 | 26(4) | 34(4) | 28(4) | 4(3) | 0(3) | -9(3) |
| C10 | 29(4) | 37(5) | 26(4) | -14(3) | 4(3) | -4(3) |
| C11 | 18(4) | 42(5) | 35(4) | -11(4) | 9(3) | -2(3) |
| C12 | 17(4) | 59(6) | 27(4) | -13(4) | 4(3) | -17(3) |
| C13 | 36(4) | 26(5) | 30(4) | -3(3) | -8(3) | -1(3) |
| C14 | 31(4) | 17(4) | 35(4) | -7(3) | 4(3) | -6(3) |
| N1 | 84(6) | 38(5) | 42(5) | 6(4) | -21(4) | -31(4) |
| C15 | 49(5) | 39(5) | 28(5) | -3(4) | -6(3) | -9(4) |
| C16 | 34(5) | 42(5) | 50(6) | -1(4) | -7(4) | -5(4) |

## 7.3.16. $[Ag\{CpMo(CO)_2(\mu_3,\eta^3:\eta^1:\eta^1\text{-}P_3)\}_2]_n[Al\{OC(CF_3)_3\}_4]_n \bullet nCH_2Cl_2$ (71•$nCH_2Cl_2$)

The polymer **71**•$nCH_2Cl_2$ was crystallised from a concentrated $CH_2Cl_2$ solution of **71** at –28 °C.

Table 7.46. Crystal data and structure refinement for **71**•$nCH_2Cl_2$.

| | |
|---|---|
| Empirical formula | $C_{31}H_{12}AgAlCl_2F_{36}Mo_2O_8P_6$ |
| Formula weight | 1779.86 g $mol^{-1}$ |
| Crystal size | 0.480 × 0.100 × 0.040 mm |
| Crystal description | needle |
| Crystal colour | yellow |
| Crystal system | monoclinic |
| Space group | $P2_1/c$ |
| Unit cell dimensions | $a$ = 10.485(1) Å, $\alpha$ = 90° |
| | $b$ = 30.827(3) Å, $\beta$ = 120.75(1)° |
| | $c$ = 19.463(2) Å, $\gamma$ = 90° |
| Volume | 5406.3(12) $Å^3$ |
| Z, Calculated density | 4, 2.187 Mg $m^{-3}$ |
| Absorption coefficient | 1.279 $mm^{-1}$ |
| F(000) | 3416 |
| Measurement device type | STOE-IPDS |
| Measurement method | rotation |
| Temperature | 123(1) K |
| Wavelength | 0.71073 Å |
| Monochromator | graphite |
| $\theta$ range for data collection | 1.80 to 25.28° |
| Index ranges | $-12 \le h \le 12$, $-36 \le k \le 36$, $-23 \le l \le 23$ |
| Reflections collected / unique | 49981 / 9742 [R(int) = 0.1378] |
| Reflections greater I>2\s(I) | 6008 |
| Absorption correction | analytical |
| Max. and min. transmission | 0.9099 and 0.7933 |
| Refinement method | Full-matrix least-squares on $F^2$ |
| Data / restraints / parameters | 9742 / 0 / 784 |
| Goodness-of-fit on $F^2$ | 0.888 |
| Final R indices [I>2sigma(I)] | R1 = 0.0556, wR2 = 0.1296 |
| R indices (all data) | R1 = 0.0899, wR2 = 0.1432 |
| Largest diff. peak and hole | 2.373 and -1.198 e $Å^{-3}$ |

Table 7.47. Atomic coordinates ($\times 10^4$) and equivalent isotropic displacement parameters ($Å^2 \times 10^3$) for **71**•n$CH_2Cl_2$. $U_{eq}$ is defined as one third of the trace of the orthogonalised $U_{ij}$ tensor.

| **Atom** | **x** | **y** | **z** | $U_{eq}$ |
|---|---|---|---|---|
| Ag1 | -2630(1) | 13(1) | 4797(1) | 36(1) |
| Mo1 | 556(1) | -1297(1) | 5470(1) | 31(1) |
| Mo2 | -7840(1) | 248(1) | 2572(1) | 31(1) |
| P1 | -1062(2) | -640(1) | 4843(1) | 38(1) |
| P2 | 818(2) | -686(1) | 4688(1) | 34(1) |
| P3 | 1106(2) | -502(1) | 5853(1) | 36(1) |
| P4 | -5246(2) | 215(1) | 3746(1) | 36(1) |
| P5 | -3058(2) | -186(1) | 5950(1) | 38(1) |
| P6 | -3539(2) | -791(1) | 6300(1) | 39(1) |
| O1 | 3979(7) | -1301(2) | 6773(4) | 50(2) |
| O2 | -297(6) | -1268(2) | 6817(3) | 41(2) |
| O3 | -7867(10) | -763(2) | 2783(4) | 101(3) |
| O4 | -10847(7) | 332(2) | 2562(4) | 51(2) |
| C1 | -952(11) | -1900(2) | 5120(7) | 59(4) |
| C2 | 550(11) | -2039(2) | 5524(6) | 54(3) |
| C3 | 1133(10) | -1924(2) | 5035(5) | 48(3) |
| C4 | 26(10) | -1715(2) | 4348(5) | 49(3) |
| C5 | -1270(10) | -1700(2) | 4394(5) | 50(3) |
| C6 | 2752(10) | -1294(2) | 6318(5) | 38(3) |
| C7 | 54(9) | -1269(2) | 6341(5) | 41(3) |
| C8 | -7543(11) | 797(3) | 1829(5) | 52(3) |
| C9 | -9082(11) | 693(3) | 1478(5) | 50(3) |
| C10 | -9273(10) | 259(3) | 1212(4) | 44(3) |
| C11 | -7901(10) | 88(3) | 1394(5) | 46(3) |
| C12 | -6824(11) | 419(3) | 1777(5) | 50(3) |
| C13 | -7876(11) | -405(3) | 2715(5) | 63(3) |
| C14 | -9732(10) | 297(2) | 2595(4) | 36(2) |
| Al1 | 3680(2) | 1622(1) | -738(1) | 27(1) |
| F1 | 7623(6) | 1642(2) | 205(3) | 74(2) |
| F2 | 8011(6) | 2211(2) | 904(4) | 85(2) |
| F3 | 8946(5) | 1602(2) | 1490(3) | 60(2) |
| F4 | 5276(7) | 1839(2) | 1718(3) | 75(2) |
| F5 | 5916(7) | 2390(1) | 1294(3) | 72(2) |
| F6 | 7615(6) | 1998(2) | 2233(3) | 65(2) |
| F7 | 7130(6) | 1139(1) | 1904(3) | 57(2) |
| F8 | 6807(6) | 953(2) | 755(3) | 70(2) |
| F9 | 4940(6) | 1080(1) | 884(3) | 60(2) |
| F10 | -1589(5) | 1749(2) | -1434(3) | 69(2) |
| F11 | -408(5) | 1575(2) | -2040(3) | 53(2) |

| | | | | |
|---|---|---|---|---|
| F12 | 78(5) | 2179(1) | -1401(3) | 51(2) |
| F13 | -516(5) | 1153(1) | -198(3) | 51(2) |
| F14 | 1504(5) | 839(1) | 9(3) | 45(2) |
| F15 | -382(6) | 880(2) | -1181(3) | 57(2) |
| F16 | 2193(5) | 1606(1) | 795(3) | 46(2) |
| F17 | 2310(5) | 2150(1) | 140(3) | 44(2) |
| F18 | 266(6) | 2009(1) | 114(3) | 55(2) |
| F19 | 5270(7) | 2657(2) | -1985(4) | 76(2) |
| F20 | 3847(8) | 2128(2) | -2666(4) | 75(2) |
| F21 | 5592(6) | 2026(1) | -1456(4) | 60(2) |
| F22 | 1168(7) | 2322(2) | -2847(3) | 74(2) |
| F23 | 1281(6) | 2820(1) | -2048(4) | 67(2) |
| F24 | 2329(7) | 2918(2) | -2741(3) | 75(2) |
| F25 | 5653(6) | 2637(1) | -434(3) | 56(2) |
| F26 | 4256(6) | 3147(1) | -1196(3) | 62(2) |
| F27 | 3569(6) | 2757(1) | -527(3) | 54(2) |
| F28 | 4050(6) | 414(1) | -484(3) | 55(2) |
| F29 | 5944(5) | 378(1) | -621(3) | 52(2) |
| F30 | 3931(6) | 58(1) | -1472(3) | 57(2) |
| F31 | 1733(6) | 1202(1) | -2427(3) | 62(2) |
| F32 | 1989(6) | 555(1) | -2767(3) | 64(2) |
| F33 | 1538(5) | 650(2) | -1816(3) | 61(2) |
| F34 | 6224(6) | 1006(2) | -1492(3) | 58(2) |
| F35 | 4860(6) | 513(1) | -2338(3) | 56(2) |
| F36 | 4192(7) | 1187(1) | -2556(3) | 66(2) |
| O5 | 5107(5) | 1800(1) | 177(3) | 34(2) |
| O6 | 2153(5) | 1444(1) | -706(3) | 32(2) |
| O7 | 3109(5) | 2050(1) | -1405(3) | 33(2) |
| O8 | 4311(5) | 1183(1) | -1033(3) | 31(2) |
| C15 | 6306(8) | 1701(2) | 890(4) | 35(2) |
| C16 | 7737(10) | 1778(3) | 870(6) | 55(3) |
| C17 | 6319(12) | 1986(3) | 1546(5) | 60(3) |
| C18 | 6295(10) | 1210(3) | 1130(6) | 54(3) |
| C19 | 970(8) | 1535(2) | -626(4) | 33(2) |
| C20 | -257(9) | 1757(2) | -1393(5) | 45(3) |
| C21 | 405(9) | 1095(2) | -482(5) | 39(3) |
| C22 | 1439(9) | 1833(2) | 111(5) | 40(3) |
| C23 | 3491(8) | 2416(2) | -1641(4) | 34(2) |
| C24 | 4571(11) | 2307(2) | -1941(6) | 51(3) |
| C25 | 2053(10) | 2625(2) | -2332(5) | 50(3) |
| C26 | 4232(10) | 2750(2) | -945(5) | 45(3) |
| C27 | 3983(8) | 841(2) | -1528(4) | 33(2) |
| C28 | 4475(9) | 414(2) | -1017(5) | 41(3) |

| | | | | |
|---|---|---|---|---|
| C29 | 2294(9) | 805(2) | -2143(5) | 46(3) |
| C30 | 4823(11) | 886(2) | -1980(5) | 48(3) |
| Cl1 | 3097(4) | -3635(1) | -662(2) | 108(2) |
| Cl2 | 5576(3) | -3848(1) | -794(2) | 88(1) |
| C31 | 4109(11) | -3482(3) | -1127(7) | 67(4) |

Table 7.48. Anisotropic displacement parameters ($Å^2 \times 10^3$) for **71**•n$CH_2Cl_2$. The anisotropic displacement factor exponent takes the form: $-2\pi^2[h^2a^{*2}U_{11} + ... + 2hka^*b^*U_{12}]$.

| **Atom** | $U_{11}$ | $U_{22}$ | $U_{33}$ | $U_{23}$ | $U_{13}$ | $U_{12}$ |
|---|---|---|---|---|---|---|
| Ag1 | 43(1) | 24(1) | 45(1) | 3(1) | 25(1) | 1(1) |
| Mo1 | 40(1) | 13(1) | 41(1) | 2(1) | 21(1) | 0(1) |
| Mo2 | 43(1) | 17(1) | 32(1) | 2(1) | 20(1) | 4(1) |
| P1 | 43(1) | 19(1) | 53(1) | 7(1) | 27(1) | 4(1) |
| P2 | 45(1) | 19(1) | 43(1) | 5(1) | 26(1) | 1(1) |
| P3 | 52(1) | 17(1) | 43(1) | -1(1) | 28(1) | -4(1) |
| P4 | 43(1) | 29(1) | 38(1) | 3(1) | 23(1) | 2(1) |
| P5 | 44(1) | 36(1) | 34(1) | 0(1) | 21(1) | -7(1) |
| P6 | 47(1) | 21(1) | 48(1) | -5(1) | 23(1) | -4(1) |
| O1 | 38(3) | 49(3) | 54(4) | 11(3) | 18(3) | 0(3) |
| O2 | 47(3) | 34(3) | 50(3) | 13(2) | 30(3) | 6(2) |
| O3 | 145(7) | 14(3) | 67(5) | 2(3) | -2(5) | -4(3) |
| O4 | 40(3) | 59(3) | 55(4) | -8(3) | 25(3) | -13(3) |
| C1 | 73(7) | 20(3) | 97(8) | -15(4) | 54(6) | -20(4) |
| C2 | 82(7) | 11(3) | 73(6) | -4(3) | 42(6) | -7(3) |
| C3 | 60(5) | 18(3) | 66(6) | -10(3) | 32(5) | 3(3) |
| C4 | 70(6) | 21(3) | 53(5) | -7(3) | 29(5) | -5(3) |
| C5 | 53(5) | 28(4) | 56(5) | -20(4) | 18(4) | -11(3) |
| C6 | 56(5) | 23(3) | 46(5) | 3(3) | 34(5) | -2(3) |
| C7 | 44(5) | 18(3) | 52(5) | 7(3) | 19(4) | -3(3) |
| C8 | 73(6) | 41(4) | 58(6) | 20(4) | 45(5) | 7(4) |
| C9 | 69(6) | 42(4) | 42(5) | 21(4) | 31(5) | 26(4) |
| C10 | 50(5) | 55(5) | 25(4) | 9(3) | 18(4) | 13(4) |
| C11 | 57(5) | 47(4) | 32(4) | 0(3) | 21(4) | 9(4) |
| C12 | 61(6) | 56(5) | 45(5) | 15(4) | 35(5) | 13(4) |
| C13 | 77(7) | 35(4) | 38(5) | -8(4) | 2(5) | 4(4) |
| C14 | 53(5) | 22(3) | 31(4) | -3(3) | 20(4) | -7(3) |
| Al1 | 38(1) | 15(1) | 31(1) | 0(1) | 19(1) | 2(1) |
| F1 | 53(3) | 113(5) | 63(4) | -2(3) | 34(3) | 6(3) |
| F2 | 60(4) | 62(3) | 101(5) | 17(3) | 18(3) | -17(3) |
| F3 | 36(3) | 60(3) | 67(3) | -1(3) | 14(3) | 4(2) |
| F4 | 86(4) | 88(4) | 60(4) | 0(3) | 43(3) | 13(3) |
| F5 | 98(4) | 35(2) | 53(3) | -13(2) | 17(3) | 19(3) |

| | | | | | | |
|---|---|---|---|---|---|---|
| F6 | 78(4) | 56(3) | 32(3) | -9(2) | 7(3) | 12(3) |
| F7 | 62(3) | 41(2) | 43(3) | 10(2) | 9(3) | 10(2) |
| F8 | 74(4) | 44(3) | 70(4) | -14(2) | 20(3) | 21(2) |
| F9 | 56(3) | 39(2) | 64(3) | 12(2) | 16(3) | -9(2) |
| F10 | 39(3) | 93(4) | 74(4) | 30(3) | 28(3) | 21(3) |
| F11 | 57(3) | 53(3) | 43(3) | 4(2) | 21(2) | 1(2) |
| F12 | 63(3) | 33(2) | 65(3) | 20(2) | 38(3) | 18(2) |
| F13 | 58(3) | 49(2) | 61(3) | 5(2) | 42(3) | -6(2) |
| F14 | 65(3) | 22(2) | 52(3) | 5(2) | 33(3) | 2(2) |
| F15 | 66(3) | 56(3) | 49(3) | -12(2) | 29(3) | -28(2) |
| F16 | 66(3) | 33(2) | 39(3) | 1(2) | 27(2) | 1(2) |
| F17 | 61(3) | 21(2) | 61(3) | -5(2) | 38(3) | -2(2) |
| F18 | 74(3) | 33(2) | 82(4) | 0(2) | 58(3) | 10(2) |
| F19 | 120(5) | 41(2) | 122(5) | 5(3) | 101(5) | -8(3) |
| F20 | 141(6) | 41(2) | 74(4) | -4(3) | 77(4) | 3(3) |
| F21 | 70(3) | 39(2) | 96(4) | 6(3) | 60(3) | 9(2) |
| F22 | 85(4) | 47(3) | 43(3) | 8(2) | -2(3) | -5(3) |
| F23 | 63(3) | 38(2) | 88(4) | 18(3) | 31(3) | 20(2) |
| F24 | 111(5) | 41(3) | 65(4) | 26(2) | 39(4) | 2(3) |
| F25 | 60(3) | 36(2) | 66(3) | -5(2) | 27(3) | -16(2) |
| F26 | 94(4) | 18(2) | 83(4) | -4(2) | 51(3) | -6(2) |
| F27 | 78(3) | 41(2) | 62(3) | -15(2) | 50(3) | -5(2) |
| F28 | 83(4) | 35(2) | 64(3) | 10(2) | 49(3) | 6(2) |
| F29 | 55(3) | 36(2) | 55(3) | 5(2) | 21(3) | 12(2) |
| F30 | 84(4) | 15(2) | 67(3) | -5(2) | 36(3) | 0(2) |
| F31 | 67(3) | 32(2) | 59(3) | -4(2) | 12(3) | 16(2) |
| F32 | 74(4) | 38(2) | 53(3) | -22(2) | 14(3) | 5(2) |
| F33 | 46(3) | 47(3) | 89(4) | -22(3) | 33(3) | -8(2) |
| F34 | 67(3) | 50(3) | 78(4) | -8(3) | 52(3) | -2(2) |
| F35 | 86(4) | 38(2) | 64(3) | -6(2) | 53(3) | 12(2) |
| F36 | 118(5) | 38(2) | 64(3) | 9(2) | 62(4) | 10(3) |
| O5 | 39(3) | 24(2) | 39(3) | 0(2) | 19(3) | 3(2) |
| O6 | 40(3) | 22(2) | 41(3) | 3(2) | 26(2) | 2(2) |
| O7 | 43(3) | 17(2) | 38(3) | 3(2) | 20(2) | -1(2) |
| O8 | 37(3) | 20(2) | 35(3) | -5(2) | 17(2) | 0(2) |
| C15 | 36(4) | 28(3) | 30(4) | -1(3) | 10(3) | 0(3) |
| C16 | 57(6) | 50(5) | 49(5) | -1(4) | 21(5) | -1(4) |
| C17 | 74(7) | 41(4) | 42(5) | -4(4) | 14(5) | 13(4) |
| C18 | 55(6) | 37(4) | 54(6) | 7(4) | 16(5) | 6(4) |
| C19 | 37(4) | 25(3) | 40(4) | 4(3) | 22(4) | 2(3) |
| C20 | 47(5) | 42(4) | 46(5) | 9(4) | 24(4) | 11(3) |
| C21 | 47(5) | 40(4) | 38(4) | -2(3) | 27(4) | -9(3) |
| C22 | 58(5) | 25(3) | 52(5) | -2(3) | 38(4) | -2(3) |

| | | | | | | |
|---|---|---|---|---|---|---|
| C23 | 49(4) | 18(3) | 38(4) | 3(3) | 24(4) | -2(3) |
| C24 | 88(7) | 28(4) | 64(6) | 2(4) | 58(6) | -3(4) |
| C25 | 69(6) | 26(3) | 44(5) | 7(3) | 20(4) | -1(4) |
| C26 | 60(6) | 21(3) | 55(5) | -2(3) | 30(5) | -7(3) |
| C27 | 45(4) | 20(3) | 31(4) | -4(3) | 17(3) | 3(3) |
| C28 | 50(5) | 27(3) | 47(5) | -4(3) | 25(4) | 0(3) |
| C29 | 51(5) | 30(4) | 47(5) | -10(3) | 18(4) | 1(3) |
| C30 | 74(6) | 31(4) | 43(5) | -6(3) | 33(5) | 5(4) |
| Cl1 | 87(2) | 136(3) | 129(3) | -56(2) | 75(2) | -22(2) |
| Cl2 | 84(2) | 103(2) | 94(2) | 42(2) | 59(2) | 41(2) |
| C31 | 66(6) | 32(4) | 88(8) | -7(4) | 28(6) | -1(4) |

## 7.3.17. $[Cu_2(\mu\text{-}Cl)_2\{Cp^*Mo(CO)_2(\mu,\eta^3\text{:}\eta^2\text{-}P_3)\}_2]$ (76a)

Crystals of **76a** were obtained from a solution of CuCl and $[Cp^*Mo(CO)_2(\eta^3\text{-}P_3)]$ **7c** in $CH_3CN/CH_2Cl_2$ at –28 °C.

Table 7.49. Crystal data and structure refinement for **76a**.

| | |
|---|---|
| Empirical formula | $C_{24}H_{30}Cl_2Cu_2Mo_2O_4P_6$ |
| Formula weight | 958.18 g $mol^{-1}$ |
| Crystal size | 0.240 × 0.210 × 0.170 mm |
| Crystal description | prism |
| Crystal colour | yellow |
| Crystal system | monoclinic |
| Space group | $P2_1/c$ |
| Unit cell dimensions | $a$ = 13.424(3) Å, $\alpha$ = 90° |
| | $b$ = 9.333(2) Å, $\beta$ = 93.81(3)° |
| | $c$ = 13.772(2) Å, $\gamma$ = 90° |
| Volume | 1721.5(5) $Å^3$ |
| Z, Calculated density | 2, 1.849 Mg $m^{-3}$ |
| Absorption coefficient | 2.393 $mm^{-1}$ |
| F(000) | 944 |
| Measurement device type | STOE-IPDS |
| Measurement method | rotation |
| Temperature | 123(1) K |
| Wavelength | 0.71073 Å |
| Monochromator | graphite |
| $\theta$ range for data collection | 2.64 to 27.43° |
| Index ranges | $-17 \le h \le 17$, $-11 \le k \le 11$, $-16 \le l \le 16$ |
| Reflections collected / unique | 22350 / 3442 [R(int) = 0.0396] |
| Reflections greater I>2\s(I) | 3065 |
| Absorption correction | numerical |
| Max. and min. transmission | 0.5347 and 0.4171 |
| Refinement method | Full-matrix least-squares on $F^2$ |
| Data / restraints / parameters | 3442 / 0 / 181 |
| Goodness-of-fit on $F^2$ | 0.986 |
| Final R indices [I>2sigma(I)] | R1 = 0.0217, wR2 = 0.0550 |
| R indices (all data) | R1 = 0.0251, wR2 = 0.0561 |
| Largest diff. peak and hole | 0.586 and -0.379 e $Å^{-3}$ |

Table 7.50. Atomic coordinates ($\times 10^4$) and equivalent isotropic displacement parameters ($Å^2 \times 10^3$) for **76a**. $U_{eq}$ is defined as one third of the trace of the orthogonalised $U_{ij}$ tensor.

| **Atom** | **x** | **y** | **z** | $U_{eq}$ |
|---|---|---|---|---|
| Mo1 | 2945(1) | 351(1) | 8064(1) | 16(1) |
| Cu1 | 878(1) | -32(1) | 5744(1) | 28(1) |
| Cl1 | -477(1) | 1391(1) | 5709(1) | 33(1) |
| P1 | 1782(1) | -1211(1) | 7017(1) | 23(1) |
| P2 | 2421(1) | 732(1) | 6244(1) | 24(1) |
| P3 | 3241(1) | -1212(1) | 6517(1) | 29(1) |
| O1 | 3672(1) | -2526(2) | 9117(1) | 33(1) |
| O2 | 5094(1) | 1195(2) | 7636(1) | 39(1) |
| C1 | 1563(2) | 1256(2) | 8818(2) | 25(1) |
| C2 | 2034(2) | 2447(2) | 8378(2) | 29(1) |
| C3 | 2987(2) | 2581(2) | 8861(2) | 28(1) |
| C4 | 3113(1) | 1459(2) | 9607(2) | 21(1) |
| C5 | 2217(1) | 654(2) | 9566(1) | 20(1) |
| C6 | 510(2) | 830(3) | 8626(2) | 41(1) |
| C7 | 1540(3) | 3480(3) | 7641(2) | 51(1) |
| C8 | 3675(2) | 3803(3) | 8710(2) | 48(1) |
| C9 | 3956(2) | 1313(3) | 10362(2) | 37(1) |
| C10 | 1976(2) | -527(2) | 10287(2) | 34(1) |
| C11 | 3423(2) | -1495(2) | 8711(2) | 22(1) |
| C12 | 4315(2) | 868(2) | 7776(2) | 24(1) |

Table 7.51. Anisotropic displacement parameters ($Å^2 \times 10^3$) for **76a**. The anisotropic displacement factor exponent takes the form: $-2\pi^2[h^2a^{*2}U_{11} + ... + 2hka^*b^*U_{12}]$.

| **Atom** | $U_{11}$ | $U_{22}$ | $U_{33}$ | $U_{23}$ | $U_{13}$ | $U_{12}$ |
|---|---|---|---|---|---|---|
| Mo1 | 14(1) | 18(1) | 16(1) | -1(1) | 1(1) | 0(1) |
| Cu1 | 24(1) | 32(1) | 28(1) | 4(1) | -8(1) | -1(1) |
| Cl1 | 35(1) | 32(1) | 31(1) | -5(1) | -10(1) | 9(1) |
| P1 | 22(1) | 22(1) | 23(1) | 1(1) | -4(1) | -3(1) |
| P2 | 24(1) | 29(1) | 19(1) | 4(1) | 0(1) | -5(1) |
| P3 | 24(1) | 37(1) | 25(1) | -12(1) | 0(1) | 5(1) |
| O1 | 38(1) | 26(1) | 37(1) | 4(1) | -1(1) | 8(1) |
| O2 | 21(1) | 45(1) | 51(1) | -10(1) | 12(1) | -8(1) |
| C1 | 19(1) | 35(1) | 22(1) | -8(1) | 3(1) | 7(1) |
| C2 | 36(1) | 27(1) | 24(1) | 1(1) | 5(1) | 14(1) |
| C3 | 34(1) | 18(1) | 32(1) | -6(1) | 15(1) | -3(1) |
| C4 | 18(1) | 22(1) | 24(1) | -8(1) | 2(1) | 2(1) |
| C5 | 21(1) | 21(1) | 18(1) | -4(1) | 5(1) | -1(1) |
| C6 | 20(1) | 62(2) | 42(2) | -18(1) | 0(1) | 4(1) |
| C7 | 75(2) | 42(1) | 35(2) | 5(1) | 1(2) | 31(1) |
| C8 | 60(2) | 28(1) | 61(2) | -11(1) | 32(2) | -18(1) |
| C9 | 24(1) | 48(1) | 38(1) | -21(1) | -6(1) | 8(1) |
| C10 | 49(1) | 29(1) | 27(1) | -1(1) | 13(1) | -10(1) |
| C11 | 20(1) | 24(1) | 22(1) | -5(1) | 1(1) | 1(1) |
| C12 | 22(1) | 26(1) | 24(1) | -5(1) | 2(1) | -1(1) |

## 7.3.18. $[Cu_2(\mu\text{-}Br)_2\{Cp^*Mo(CO)_2(\mu,\eta^3:\eta^2\text{-}P_3)\}_2]$ (76b)

Crystals of **76b** were obtained by controlled diffusion of a $CH_3CN$ solution of CuBr into a $CH_2Cl_2$ solution of $[Cp^*Mo(CO)_2(\eta^3\text{-}P_3)]$ **7c** at room temperature in the dark.

Table 7.52. Crystal data and structure refinement for **76b**.

| | |
|---|---|
| Empirical formula | $C_{24}H_{30}Br_2Cu_2Mo_2O_4P_6$ |
| Formula weight | 1047.08 g $mol^{-1}$ |
| Crystal size | $0.220 \times 0.170 \times 0.110$ mm |
| Crystal description | prism |
| Crystal colour | yellow |
| Crystal system | orthorhombic |
| Space group | *Pbca* |
| Unit cell dimensions | $a$ = 9.623(1) Å, $\alpha$ = 90° |
| | $b$ = 13.209(1) Å, $\beta$ = 90° |
| | $c$ = 27.265(2) Å, $\gamma$ = 90° |
| Volume | 3465.6(4) $Å^3$ |
| Z, Calculated density | 4, 2.007 Mg $m^{-3}$ |
| Absorption coefficient | 4.530 $mm^{-1}$ |
| F(000) | 2032 |
| Measurement device type | STOE-IPDS |
| Measurement method | rotation |
| Temperature | 173(1) K |
| Wavelength | 0.71073 Å |
| Monochromator | graphite |
| $\theta$ range for data collection | 3.08 to 25.95° |
| Index ranges | $-11 \le h \le 11$, $-16 \le k \le 16$, $-33 \le l \le 33$ |
| Reflections collected / unique | 30268 / 3352 [R(int) = 0.0396] |
| Reflections greater I>2\s(I) | 3044 |
| Absorption correction | analytical |
| Max. and min. transmission | 0.6140 and 0.3265 |
| Refinement method | Full-matrix least-squares on $F^2$ |
| Data / restraints / parameters | 3352 / 0 / 181 |
| Goodness-of-fit on $F^2$ | 1.044 |
| Final R indices [I>2sigma(I)] | R1 = 0.0227, wR2 = 0.0583 |
| R indices (all data) | R1 = 0.0255, wR2 = 0.0592 |
| Largest diff. peak and hole | 0.633 and -0.286 e $Å^{-3}$ |

Table 7.53. Atomic coordinates ($\times 10^4$) and equivalent isotropic displacement parameters ($Å^2 \times 10^3$) for **76b**. $U_{eq}$ is defined as one third of the trace of the orthogonalised $U_{ij}$ tensor.

| **Atom** | **x** | **y** | **z** | $U_{eq}$ |
|---|---|---|---|---|
| Mo1 | -327(1) | 2099(1) | -1482(1) | 20(1) |
| Br1 | -1448(1) | 4175(1) | 281(1) | 38(1) |
| Cu1 | 13(1) | 4305(1) | -430(1) | 35(1) |
| P1 | -685(1) | 3904(1) | -1217(1) | 29(1) |
| P2 | 1156(1) | 3064(1) | -885(1) | 26(1) |
| P3 | 1219(1) | 3676(1) | -1616(1) | 35(1) |
| O1 | 2454(2) | 1088(1) | -1847(1) | 43(1) |
| O2 | -1172(2) | 2801(1) | -2546(1) | 42(1) |
| C1 | -2334(2) | 1704(2) | -1015(1) | 27(1) |
| C2 | -1177(2) | 1201(2) | -791(1) | 26(1) |
| C3 | -628(2) | 499(2) | -1141(1) | 23(1) |
| C4 | -1441(2) | 572(2) | -1582(1) | 25(1) |
| C5 | -2501(2) | 1320(2) | -1500(1) | 27(1) |
| C6 | -3311(3) | 2413(2) | -754(1) | 42(1) |
| C7 | -750(3) | 1292(2) | -263(1) | 34(1) |
| C8 | 498(3) | -266(2) | -1035(1) | 31(1) |
| C9 | -1327(3) | -120(2) | -2020(1) | 34(1) |
| C10 | -3706(3) | 1548(2) | -1835(1) | 39(1) |
| C11 | 1455(2) | 1477(2) | -1723(1) | 29(1) |
| C12 | -839(2) | 2545(2) | -2162(1) | 28(1) |

Table 7.54. Anisotropic displacement parameters ($Å^2 \times 10^3$) for **76b**. The anisotropic displacement factor exponent takes the form: $-2\pi^2[h^2a^{*2}U_{11} + ... + 2hka^*b^*U_{12}]$.

| **Atom** | $U_{11}$ | $U_{22}$ | $U_{33}$ | $U_{23}$ | $U_{13}$ | $U_{12}$ |
|---|---|---|---|---|---|---|
| Mo1 | 21(1) | 18(1) | 20(1) | 0(1) | 0(1) | -1(1) |
| Br1 | 33(1) | 36(1) | 45(1) | -15(1) | 8(1) | -3(1) |
| Cu1 | 38(1) | 34(1) | 35(1) | -11(1) | -2(1) | 3(1) |
| P1 | 33(1) | 21(1) | 33(1) | -3(1) | -6(1) | 4(1) |
| P2 | 25(1) | 26(1) | 29(1) | -5(1) | -3(1) | 0(1) |
| P3 | 42(1) | 29(1) | 33(1) | 0(1) | 6(1) | -13(1) |
| O1 | 36(1) | 42(1) | 52(1) | 4(1) | 16(1) | 10(1) |
| O2 | 50(1) | 48(1) | 27(1) | 5(1) | -5(1) | 2(1) |
| C1 | 24(1) | 25(1) | 33(1) | 2(1) | 5(1) | -2(1) |
| C2 | 27(1) | 24(1) | 26(1) | 3(1) | 2(1) | -4(1) |
| C3 | 26(1) | 18(1) | 26(1) | 2(1) | -1(1) | -4(1) |
| C4 | 26(1) | 21(1) | 28(1) | 1(1) | -1(1) | -5(1) |
| C5 | 24(1) | 26(1) | 31(1) | 4(1) | -2(1) | -5(1) |
| C6 | 32(1) | 41(1) | 54(2) | -4(1) | 14(1) | 3(1) |
| C7 | 41(1) | 35(1) | 25(1) | 1(1) | 1(1) | -6(1) |
| C8 | 31(1) | 23(1) | 40(1) | 3(1) | -6(1) | 2(1) |
| C9 | 41(1) | 29(1) | 32(1) | -6(1) | -3(1) | -5(1) |
| C10 | 27(1) | 41(1) | 47(2) | 6(1) | -11(1) | -1(1) |
| C11 | 32(1) | 27(1) | 29(1) | 4(1) | 2(1) | -2(1) |
| C12 | 29(1) | 27(1) | 28(1) | -1(1) | 0(1) | -1(1) |

## 7.3.19. $[Cu(\mu\text{-}I)\{Cp^*Mo(CO)_2(\mu_3,\eta^3:\eta^1:\eta^1\text{-}P_3)\}]_n$ (77)

Crystals of **77** were obtained by controlled diffusion of $Et_2O$ into a mixture of CuI and $[Cp^*Mo(CO)_2(\eta^3\text{-}P_3)]$ **7c** (100 mg, 0.26 mmol), dissolved in $CH_3CN/CH_2Cl_2$, at –28 °C.

Table 7.55. Crystal data and structure refinement for **77**.

| | |
|---|---|
| Empirical formula | $C_{12}H_{15}CuIMoO_2P_3$ |
| Formula weight | 570.54 g $mol^{-1}$ |
| Crystal size | 0.290 × 0.180 × 0.130 mm |
| Crystal description | prism |
| Crystal colour | orange to red |
| Crystal system | monoclinic |
| Space group | *C*2/*c* |
| Unit cell dimensions | $a$ = 21.372(2) Å, $\alpha$ = 90° |
| | $b$ = 15.333(1) Å, $\beta$ = 132.09(1)° |
| | $c$ = 14.831(1) Å, $\gamma$ = 90° |
| Volume | 3607.0(7) $Å^3$ |
| Z, Calculated density | 8, 2.101 Mg $m^{-3}$ |
| Absorption coefficient | 3.849 $mm^{-1}$ |
| F(000) | 2176 |
| Measurement device type | STOE-IPDS |
| Measurement method | rotation |
| Temperature | 173(1) K |
| Wavelength | 0.71073 Å |
| Monochromator | graphite |
| $\theta$ range for data collection | 1.85 to 25.86° |
| Index ranges | $-26 \le h \le 26$, $-18 \le k \le 18$, $-18 \le l \le 18$ |
| Reflections collected / unique | 20361 / 3435 [R(int) = 0.0566] |
| Reflections greater I>2\s(I) | 2926 |
| Absorption correction | analytical |
| Max. and min. transmission | 0.6765 and 0.4698 |
| Refinement method | Full-matrix least-squares on $F^2$ |
| Data / restraints / parameters | 3435 / 0 / 181 |
| Goodness-of-fit on $F^2$ | 1.171 |
| Final R indices [I>2sigma(I)] | R1 = 0.0720, wR2 = 0.1996 |
| R indices (all data) | R1 = 0.0778, wR2 = 0.2017 |
| Largest diff. peak and hole | 4.528 and -1.471 e $Å^{-3}$ |

Table 7.56. Atomic coordinates ($\times 10^4$) and equivalent isotropic displacement parameters ($Å^2 \times 10^3$) for **77**. $U_{eq}$ is defined as one third of the trace of the orthogonalised $U_{ij}$ tensor.

| **Atom** | **x** | **y** | **z** | $U_{eq}$ |
|---|---|---|---|---|
| I1 | 10057(1) | 2629(1) | 1059(1) | 32(1) |
| Mo1 | 7450(1) | 5104(1) | -293(1) | 19(1) |
| Cu1 | 9128(1) | 2551(1) | 1620(2) | 27(1) |
| P1 | 8116(2) | 3653(2) | 660(3) | 24(1) |
| P2 | 7424(2) | 4134(2) | 1128(3) | 30(1) |
| P3 | 6767(2) | 3653(2) | -667(3) | 25(1) |
| O1 | 6012(7) | 6014(7) | -568(11) | 45(4) |
| O2 | 8943(7) | 5959(7) | 2240(10) | 46(3) |
| C1 | 6545(8) | 5699(8) | -423(12) | 27(4) |
| C2 | 8391(9) | 5661(9) | 1335(12) | 29(4) |
| C3 | 7514(8) | 4758(7) | -1750(11) | 21(3) |
| C4 | 6739(8) | 5181(10) | -2361(12) | 31(4) |
| C5 | 6950(9) | 6067(9) | -1902(12) | 29(4) |
| C6 | 7834(9) | 6145(8) | -1015(12) | 28(4) |
| C7 | 8200(8) | 5315(9) | -892(11) | 27(4) |
| C8 | 7591(11) | 3832(9) | -2056(14) | 38(5) |
| C9 | 5879(10) | 4863(13) | -3428(14) | 48(5) |
| C10 | 6323(12) | 6801(11) | -2422(17) | 49(6) |
| C11 | 8310(12) | 6975(11) | -418(16) | 50(6) |
| C12 | 9116(9) | 5138(13) | -192(16) | 48(5) |

Table 7.57. Anisotropic displacement parameters ($Å^2 \times 10^3$) for **77**. The anisotropic displacement factor exponent takes the form: $-2\pi^2[h^2a^{*2}U_{11} + ... + 2hka^*b^*U_{12}]$.

| **Atom** | $U_{11}$ | $U_{22}$ | $U_{33}$ | $U_{23}$ | $U_{13}$ | $U_{12}$ |
|---|---|---|---|---|---|---|
| I1 | 30(1) | 40(1) | 27(1) | 5(1) | 20(1) | 3(1) |
| Mo1 | 24(1) | 16(1) | 19(1) | 0(1) | 16(1) | 0(1) |
| Cu1 | 26(1) | 24(1) | 27(1) | 0(1) | 17(1) | -1(1) |
| P1 | 31(2) | 18(2) | 25(2) | 3(1) | 20(2) | 2(1) |
| P2 | 51(2) | 24(2) | 30(2) | 1(1) | 33(2) | 0(1) |
| P3 | 31(2) | 19(2) | 28(2) | -1(1) | 21(2) | -3(1) |
| O1 | 48(6) | 33(5) | 69(8) | 6(5) | 46(6) | 8(5) |
| O2 | 49(6) | 41(6) | 32(6) | -5(5) | 21(6) | -13(5) |
| C1 | 33(7) | 22(6) | 33(7) | 6(5) | 25(6) | 3(5) |
| C2 | 37(7) | 26(7) | 24(7) | -5(5) | 20(6) | -8(5) |
| C3 | 40(7) | 11(5) | 25(6) | 2(4) | 27(6) | 0(5) |
| C4 | 28(6) | 47(8) | 22(7) | 9(6) | 18(6) | 0(6) |
| C5 | 44(8) | 27(7) | 25(7) | 7(5) | 27(7) | 12(6) |
| C6 | 52(8) | 15(6) | 28(7) | -4(5) | 32(7) | -6(5) |
| C7 | 27(6) | 40(7) | 21(6) | 1(5) | 19(6) | -3(5) |
| C8 | 60(9) | 27(7) | 43(9) | -4(6) | 41(8) | 5(6) |
| C9 | 35(8) | 74(12) | 25(8) | -3(8) | 16(7) | -3(8) |
| C10 | 69(11) | 38(9) | 56(10) | 24(8) | 49(10) | 27(8) |
| C11 | 70(11) | 39(9) | 52(10) | -13(7) | 46(10) | -24(8) |
| C12 | 32(8) | 67(11) | 46(9) | 9(8) | 27(8) | -2(7) |

## 7.3.20. $[Ag_2\{Cp^*Mo(CO)_2(\mu,\eta^3:\eta^2\text{-}As_3)\}_2\{Cp^*Mo(CO)_2(\mu_3,\eta^3:\eta^2:\eta^2\text{-}As_3)\}_2][\langle Al\{OC(CF_3)_3\}_4\rangle_2]\bullet 2.5CH_2Cl_2$ (**81**•2.5$CH_2Cl_2$)

Crystals of **81**•2.5$CH_2Cl_2$ were obtained from concentrated $CH_2Cl_2$ solutions of **81** at –28 °C.

Table 7.58. Crystal data and structure refinement for **81**•2.5$CH_2Cl_2$.

| | |
|---|---|
| Empirical formula | $C_{82.5}H_{65}Ag_2Al_2As_{12}Cl_5F_{72}Mo_4O_{16}$ |
| Formula weight | 4410.10 g $mol^{-1}$ |
| Crystal size | 0.510 × 0.190 × 0.080 mm |
| Crystal description | prism |
| Crystal colour | yellow |
| Crystal system | monoclinic |
| Space group | *C*2/*c* |
| Unit cell dimensions | $a$ = 36.467(2) Å, $\alpha$ = 90° |
| | $b$ = 18.221(1) Å, $\beta$ = 103.43(1)° |
| | $c$ = 20.434(1) Å, $\gamma$ = 90° |
| Volume | 13206(1) $Å^3$ |
| Z, Calculated density | 4, 2.218 Mg $m^{-3}$ |
| Absorption coefficient | 3.914 $mm^{-1}$ |
| F(000) | 8420 |
| Measurement device type | Oxford Diffraction Xcalibur 3 CCD |
| Measurement method | 4 omega scans, 1°/frame |
| Temperature | 100(1) K |
| Wavelength | 0.71073 Å |
| Monochromator | graphite |
| $\theta$ range for data collection | 4.02 to 25.00° |
| Index ranges | $-41 \le h \le 43$, $-21 \le k \le 20$, $-23 \le l \le 18$ |
| Reflections collected / unique | 28407 / 10531 [R(int) = 0.0450] |
| Reflections greater I>2\s(I) | 8080 |
| Absorption correction | integration |
| Max. and min. transmission | 0.297 and 0.671 |
| Refinement method | Full-matrix least-squares on $F^2$ |
| Data / restraints / parameters | 10531 / 0 / 889 |
| Goodness-of-fit on $F^2$ | 1.045 |
| Final R indices [I>2sigma(I)] | R1 = 0.0798, wR2 = 0.2036 |
| R indices (all data) | R1 = 0.0964, wR2 = 0.2228 |
| Largest diff. peak and hole | 1.952 and -1.210 e $Å^{-3}$ |

Table 7.59. Atomic coordinates ($\times 10^4$) and equivalent isotropic displacement parameters ($Å^2 \times 10^3$) for **81**•2.5$CH_2Cl_2$. $U_{eq}$ is defined as one third of the trace of the orthogonalised $U_{ij}$ tensor.

| **Atom** | **x** | **y** | **z** | $U_{eq}$ |
|---|---|---|---|---|
| Ag1 | 20(1) | 5616(1) | 3476(1) | 37(1) |
| Mo1 | 1160(1) | 4890(1) | 2920(1) | 29(1) |
| Mo2 | 302(1) | 7282(1) | 5121(1) | 33(1) |
| As1 | 508(1) | 4512(1) | 3199(1) | 32(1) |
| As2 | 561(1) | 5721(1) | 2703(1) | 30(1) |
| As3 | 527(1) | 4576(1) | 2050(1) | 32(1) |
| As4 | 433(1) | 5964(1) | 4716(1) | 34(1) |
| As5 | -221(1) | 6499(1) | 4328(1) | 35(1) |
| As6 | 1(1) | 6007(1) | 5421(1) | 38(1) |
| Al1 | 1737(1) | 61(2) | 8172(2) | 31(1) |
| C1C | 1263(3) | 5134(7) | 3897(7) | 43(3) |
| C2C | 1208(3) | 3818(7) | 3142(7) | 42(3) |
| C3C | -92(4) | 7608(8) | 5609(7) | 57(4) |
| C4C | 639(4) | 7040(6) | 6018(7) | 40(3) |
| C10 | 1802(4) | 4963(7) | 3032(7) | 41(3) |
| C11 | 1650(3) | 4582(6) | 2415(6) | 36(3) |
| C12 | 1416(3) | 5076(6) | 1961(6) | 34(3) |
| C13 | 1413(3) | 5762(6) | 2288(6) | 35(3) |
| C14 | 1647(3) | 5709(6) | 2947(6) | 29(2) |
| C15 | 2107(4) | 4698(9) | 3615(7) | 49(3) |
| C16 | 1773(4) | 3834(7) | 2256(7) | 46(3) |
| C17 | 1253(4) | 4924(8) | 1227(6) | 46(3) |
| C18 | 1233(3) | 6457(7) | 1961(7) | 42(3) |
| C19 | 1775(3) | 6341(8) | 3425(7) | 47(3) |
| C20 | 673(5) | 7723(7) | 4403(7) | 56(4) |
| C21 | 308(5) | 7948(8) | 4145(7) | 55(4) |
| C22 | 201(4) | 8435(7) | 4629(7) | 50(3) |
| C23 | 510(4) | 8471(7) | 5203(6) | 45(3) |
| C24 | 813(4) | 8030(7) | 5063(7) | 45(3) |
| C25 | 911(6) | 7292(9) | 4033(10) | 81(6) |
| C26 | 82(6) | 7861(10) | 3431(8) | 85(6) |
| C27 | -151(5) | 8888(10) | 4506(10) | 86(6) |
| C28 | 546(5) | 8970(7) | 5793(7) | 54(4) |
| C29 | 1199(4) | 7989(8) | 5495(8) | 60(4) |
| C111 | 2196(4) | 900(8) | 9306(7) | 54(4) |
| C112 | 2118(4) | 655(9) | 9996(8) | 58(4) |
| C113 | 2635(5) | 948(9) | 9409(8) | 64(4) |
| C114 | 2007(7) | 1649(8) | 9098(9) | 86(7) |
| C121 | 2159(3) | -1280(7) | 7995(6) | 40(3) |

| | | | | |
|---|---|---|---|---|
| C122 | 2179(4) | -1798(8) | 8602(7) | 48(3) |
| C123 | 2550(4) | -904(7) | 8075(7) | 44(3) |
| C124 | 2065(4) | -1747(7) | 7331(7) | 51(3) |
| C131 | 1592(3) | 962(7) | 6931(6) | 40(3) |
| C132 | 1560(5) | 340(9) | 6399(7) | 62(4) |
| C133 | 1893(4) | 1527(8) | 6836(8) | 59(4) |
| C134 | 1209(4) | 1349(10) | 6839(14) | 90(7) |
| C141 | 1004(4) | -322(8) | 8462(7) | 49(3) |
| C142 | 1146(7) | -880(18) | 9100(2) | 156(14) |
| C143 | 765(15) | -82(2) | 7931(16) | 210(30) |
| C144 | 835(15) | 26(5) | 88500(3) | 430(70) |
| O1C | 1330(2) | 5294(6) | 4463(4) | 48(2) |
| O1 | 2071(3) | 373(5) | 8847(5) | 66(3) |
| O2C | 1250(3) | 3199(5) | 3255(5) | 49(2) |
| O2 | 1880(3) | -791(5) | 7964(5) | 51(2) |
| O3 | 1708(4) | 695(5) | 7550(5) | 67(3) |
| O3C | -301(3) | 7821(7) | 5894(6) | 69(3) |
| O4 | 1287(3) | -9(6) | 8300(6) | 71(3) |
| O4C | 849(3) | 6949(6) | 6512(5) | 66(3) |
| F11 | 1755(3) | 748(6) | 9992(7) | 93(3) |
| F12 | 2194(3) | -55(5) | 10090(5) | 73(3) |
| F13 | 2322(3) | 1017(5) | 10514(4) | 71(3) |
| F14 | 2767(4) | 1563(6) | 9758(6) | 102(4) |
| F15 | 2724(4) | 973(6) | 8818(6) | 101(4) |
| F16 | 2805(2) | 388(5) | 9742(4) | 62(2) |
| F17 | 1633(4) | 1542(7) | 8867(7) | 124(6) |
| F18 | 2133(6) | 1964(6) | 8645(6) | 150(8) |
| F19 | 2030(4) | 2096(5) | 9631(5) | 96(4) |
| F21 | 1897(3) | -2273(5) | 8489(5) | 67(2) |
| F22 | 2164(3) | -1424(5) | 9147(4) | 69(2) |
| F23 | 2494(3) | -2195(4) | 8739(4) | 63(2) |
| F24 | 2509(3) | -302(5) | 7678(5) | 72(3) |
| F25 | 2804(2) | -1342(5) | 7897(6) | 73(3) |
| F26 | 2695(2) | -680(4) | 8695(5) | 59(2) |
| F27 | 2139(3) | -1350(5) | 6838(4) | 83(3) |
| F28 | 2277(3) | -2356(4) | 7392(4) | 61(2) |
| F29 | 1715(3) | -1941(5) | 7184(5) | 68(3) |
| F31 | 1354(5) | 534(6) | 5820(5) | 137(6) |
| F32 | 1902(3) | 113(5) | 6360(5) | 78(3) |
| F33 | 1388(3) | -254(5) | 6575(5) | 74(3) |
| F34 | 2227(2) | 1275(6) | 7048(8) | 106(4) |
| F35 | 1838(4) | 1693(7) | 6165(6) | 110(4) |
| F36 | 1855(2) | 2143(4) | 7161(5) | 67(2) |

| | | | | |
|---|---|---|---|---|
| F37 | 931(3) | 848(6) | 6827(10) | 139(7) |
| F38 | 1125(3) | 1817(5) | 6367(7) | 114(5) |
| F39 | 1207(3) | 1733(6) | 7440(8) | 101(4) |
| F41 | 508(4) | -1169(12) | 8029(8) | 160(8) |
| F42 | 956(4) | -1014(8) | 7479(5) | 111(4) |
| F43 | 508(5) | -68(14) | 7526(9) | 172(9) |
| F44 | 877(5) | -1035(8) | 9373(6) | 126(5) |
| F45 | 1456(4) | -720(8) | 9411(6) | 106(4) |
| F46 | 1165(5) | -1571(6) | 8538(9) | 137(6) |
| F47 | 424(5) | 24(13) | 8757(17) | 245(14) |
| F48 | 995(3) | 314(8) | 9459(6) | 101(4) |
| F49 | 740(8) | 841(11) | 8378(11) | 203(14) |
| C1S | 1431(5) | 2881(10) | 4882(8) | 68(4) |
| Cl1S | 1024(1) | 3357(3) | 4899(2) | 78(1) |
| Cl2S | 1817(1) | 3505(4) | 4902(3) | 96(2) |
| C2S | 0 | 798(4) | 7500 | 320(12) |
| Cl3S | 347(8) | 7360(10) | 7394(9) | 189(10) |

Table 7.60. Anisotropic displacement parameters ($Å^2 \times 10^3$) for **81**•2.5$CH_2Cl_2$. The anisotropic displacement factor exponent takes the form: $-2\pi^2[h^2a^{*2}U_{11} + ... + 2hka^*b^*U_{12}]$.

| **Atom** | $U_{11}$ | $U_{22}$ | $U_{33}$ | $U_{23}$ | $U_{13}$ | $U_{12}$ |
|---|---|---|---|---|---|---|
| Ag1 | 40(1) | 40(1) | 33(1) | -6(1) | 12(1) | -2(1) |
| Mo1 | 27(1) | 33(1) | 29(1) | -1(1) | 8(1) | (1) |
| Mo2 | 40(1) | 31(1) | 29(1) | -3(1) | 6(1) | -2(1) |
| As1 | 31(1) | 35(1) | 33(1) | 4(1) | 11(1) | 2(1) |
| As2 | 30(1) | 31(1) | 31(1) | -1(1) | 9(1) | 2(1) |
| As3 | 29(1) | 35(1) | 33(1) | -5(1) | 8(1) | (1) |
| As4 | 34(1) | 34(1) | 35(1) | -3(1) | 9(1) | -(1) |
| As5 | 33(1) | 40(1) | 31(1) | -5(1) | 7(1) | 1(1) |
| As6 | 43(1) | 41(1) | 31(1) | -2(1) | 13(1) | -7(1) |
| Al1 | 34(2) | 29(2) | 31(2) | -1(1) | 8(1) | 2(1) |
| C1C | 34(6) | 48(7) | 47(8) | 10(6) | 7(6) | 13(5) |
| C2C | 36(6) | 40(7) | 51(8) | 5(6) | 10(6) | 0(5) |
| C3C | 59(9) | 56(8) | 51(8) | -17(7) | 4(7) | 7(7) |
| C4C | 52(7) | 27(6) | 44(8) | -7(5) | 16(6) | -17(5) |
| C10 | 43(7) | 36(7) | 44(7) | -5(5) | 9(6) | -3(5) |
| C11 | 35(6) | 39(6) | 42(7) | -5(5) | 25(5) | 4(5) |
| C12 | 26(5) | 41(6) | 37(6) | -3(5) | 9(5) | -9(5) |
| C13 | 26(5) | 36(6) | 47(7) | -2(5) | 14(5) | -1(5) |
| C14 | 27(5) | 30(5) | 36(6) | -10(5) | 16(5) | -3(4) |
| C15 | 35(7) | 71(9) | 40(7) | 4(7) | 4(6) | 4(6) |
| C16 | 47(7) | 47(7) | 54(8) | -1(6) | 35(6) | 6(6) |
| C17 | 41(7) | 58(8) | 42(7) | -2(6) | 18(6) | -4(6) |

| | | | | | | |
|---|---|---|---|---|---|---|
| C18 | 38(6) | 36(6) | 49(7) | 17(5) | 5(6) | 3(5) |
| C19 | 29(6) | 58(8) | 53(8) | -15(7) | 5(6) | 0(6) |
| C20 | 91(12) | 38(7) | 54(8) | -11(6) | 47(9) | -16(7) |
| C21 | 82(11) | 48(8) | 31(7) | 4(6) | 2(7) | -16(8) |
| C22 | 56(8) | 42(7) | 44(7) | 6(6) | -4(6) | 1(6) |
| C23 | 60(8) | 32(6) | 42(7) | -9(5) | 10(6) | -9(6) |
| C24 | 50(7) | 42(7) | 46(7) | 8(6) | 18(6) | -11(6) |
| C25 | 119(15) | 55(10) | 89(13) | -13(9) | 65(12) | -35(10) |
| C26 | 132(16) | 69(11) | 42(8) | 1(8) | -6(9) | -60(11) |
| C27 | 89(13) | 54(10) | 94(14) | -8(9) | -18(11) | 28(9) |
| C28 | 81(10) | 43(7) | 39(7) | -12(6) | 15(7) | -19(7) |
| C29 | 47(8) | 49(8) | 81(11) | 9(8) | 5(7) | -19(7) |
| C111 | 62(9) | 43(7) | 50(8) | -15(6) | -3(7) | 4(7) |
| C112 | 40(7) | 61(9) | 73(10) | -14(8) | 12(7) | 6(7) |
| C113 | 90(12) | 59(9) | 46(8) | -9(7) | 18(8) | -23(9) |
| C114 | 160(20) | 32(8) | 46(9) | -14(7) | -21(11) | 15(10) |
| C121 | 36(6) | 42(7) | 41(7) | -5(5) | 7(5) | -1(5) |
| C122 | 57(8) | 50(8) | 40(7) | 5(6) | 18(6) | -13(7) |
| C123 | 46(7) | 31(6) | 60(9) | 9(6) | 20(6) | -4(5) |
| C124 | 72(10) | 37(7) | 41(7) | -12(6) | 7(7) | 15(7) |
| C131 | 35(6) | 41(7) | 45(7) | 9(6) | 10(5) | -3(5) |
| C132 | 93(12) | 51(9) | 37(8) | 3(6) | 3(8) | -11(8) |
| C133 | 58(9) | 46(8) | 70(10) | -5(7) | 12(8) | -8(7) |
| C134 | 25(7) | 59(10) | 180(20) | -19(14) | 23(1) | -17(7) |
| C141 | 51(8) | 49(8) | 50(8) | -1(6) | 21(6) | 3(6) |
| C142 | 65(14) | 140(30) | 280(40) | 10(30) | 70(20) | -59(16) |
| C143 | 360(60) | 220(40) | 110(20) | -90(30) | 150(30) | -200(40) |
| C144 | 230(50) | 800(150) | 350(70) | -470(90) | 270(50) | -360(80) |
| O1C | 48(5) | 69(6) | 26(5) | -6(4) | 7(4) | 4(5) |
| O1 | 70(7) | 46(5) | 65(7) | -30(5) | -19(5) | 19(5) |
| O2C | 50(5) | 42(5) | 57(6) | 15(4) | 19(4) | 16(4) |
| O2 | 45(5) | 38(5) | 66(6) | -16(4) | 5(4) | 10(4) |
| O3 | 130(10) | 31(5) | 48(6) | 9(4) | 36(6) | 11(5) |
| O3C | 70(7) | 81(8) | 65(7) | -22(6) | 34(6) | 9(6) |
| O4 | 76(7) | 56(6) | 103(9) | -27(6) | 65(7) | -20(5) |
| O4C | 70(7) | 62(7) | 47(6) | 22(5) | -24(5) | -22(5) |
| F11 | 71(6) | 87(7) | 137(10) | -21(7) | 55(7) | 18(5) |
| F12 | 79(6) | 61(6) | 95(7) | 6(5) | 51(6) | 0(5) |
| F13 | 97(7) | 67(6) | 46(5) | -11(4) | 14(5) | 11(5) |
| F14 | 116(9) | 87(8) | 119(9) | -52(7) | 55(7) | -55(7) |
| F15 | 164(12) | 85(7) | 77(7) | 1(6) | 72(8) | -23(7) |
| F16 | 47(4) | 89(7) | 50(5) | -5(5) | 10(4) | -1(4) |
| F17 | 140(11) | 92(8) | 103(9) | -53(7) | -45(9) | 68(8) |
| F18 | 32(2) | 48(6) | 70(8) | 8(6) | 21(11) | 23(10) |
| F19 | 152(11) | 57(6) | 67(6) | -26(5) | 0(6) | 20(6) |
| F21 | 75(6) | 56(5) | 79(6) | 0(4) | 35(5) | -30(4) |
| F22 | 90(6) | 75(6) | 51(5) | -16(4) | 35(5) | -14(5) |

| | | | | | | |
|---|---|---|---|---|---|---|
| F23 | 76(6) | 46(4) | 62(5) | 8(4) | 7(4) | 6(4) |
| F24 | 94(7) | 48(5) | 83(7) | 9(4) | 36(5) | -19(5) |
| F25 | 45(5) | 68(6) | 121(8) | -11(5) | 46(5) | -10(4) |
| F26 | 55(5) | 40(4) | 75(6) | -11(4) | 3(4) | -8(4) |
| F27 | 145(10) | 65(6) | 39(5) | 2(4) | 24(5) | -17(6) |
| F28 | 78(6) | 39(4) | 68(5) | -9(4) | 23(4) | 10(4) |
| F29 | 65(6) | 58(5) | 68(6) | -30(4) | -15(4) | 4(4) |
| F31 | 249(18) | 75(7) | 48(6) | -7(5) | -46(8) | 17(9) |
| F32 | 119(9) | 66(6) | 66(6) | -16(5) | 59(6) | -7(6) |
| F33 | 63(5) | 48(5) | 103(8) | -11(5) | 1(5) | -13(4) |
| F34 | 38(5) | 63(6) | 214(14) | -28(7) | 24(6) | -3(4) |
| F35 | 167(12) | 89(8) | 99(8) | 25(7) | 84(9) | -18(8) |
| F36 | 59(5) | 35(4) | 100(7) | 4(4) | 1(5) | -13(4) |
| F37 | 42(5) | 63(7) | 300(20) | 8(9) | 5(8) | -6(5) |
| F38 | 87(8) | 44(5) | 168(12) | 15(6) | -62(8) | 5(5) |
| F39 | 83(7) | 61(6) | 178(13) | -8(7) | 71(8) | 9(5) |
| F41 | 119(11) | 240(20) | 116(11) | -31(12) | 10(9) | -110(13) |
| F42 | 146(11) | 146(12) | 40(5) | -23(6) | 20(6) | 10(9) |
| F43 | 109(11) | 280(30) | 128(13) | 91(16) | 25(10) | 18(13) |
| F44 | 176(14) | 132(11) | 95(9) | -1(8) | 84(9) | -60(10) |
| F45 | 108(10) | 134(11) | 69(7) | 15(7) | 7(6) | -16(8) |
| F46 | 208(16) | 48(6) | 189(15) | 5(8) | 117(13) | -3(8) |
| F47 | 100(12) | 220(20) | 460(40) | -30(20) | 160(20) | 41(13) |
| F48 | 101(8) | 128(10) | 84(8) | -49(7) | 42(7) | -14(7) |
| F49 | 34(3) | 141(15) | 171(18) | 86(14) | 140(20) | 160(20) |
| C1S | 80(11) | 70(10) | 54(9) | 1(8) | 18(8) | 19(9) |
| Cl1S | 68(3) | 98(3) | 74(3) | -9(2) | 31(2) | -2(2) |
| Cl2S | 55(2) | 140(5) | 83(3) | 2(3) | 1(2) | -5(3) |
| C2S | 16(9) | 40(40) | 800(400) | 0 | 250(160) | 0 |
| Cl3S | 32(3) | 119(12) | 129(13) | -2(10) | 62(16) | 80(15) |

## 7.3.21. $[Ag\{Cp^*Fe(\mu_3,\eta^5:\eta^2:\eta^1\text{-}P_5)\}_2]_n[Al\{OC(CF_3)_3\}_4]_n \bullet nCH_2Cl_2$ (**83**•$nCH_2Cl_2$)

The polymer **83**•$nCH_2Cl_2$ was crystallised from a concentrated $CH_2Cl_2$ solution of **83** at –28 °C.

Table 7.61. Crystal data and structure refinement for **83**•$nCH_2Cl_2$.

| | |
|---|---|
| Empirical formula | $C_{37}H_{32}AgAlCl_2F_{36}Fe_2O_4P_{10}$ |
| Formula weight | 1851.78 g $mol^{-1}$ |
| Crystal size | $0.200 \times 0.100 \times 0.050$ mm |
| Crystal description | needle |
| Crystal colour | dark brown |
| Crystal system | monoclinic |
| Space group | $P2_1/n$ |
| Unit cell dimensions | $a$ = 10.524(2) Å, $\alpha$ = 90° |
| | $b$ = 32.471(7) Å, $\beta$ = 90.31(3)° |
| | $c$ = 18.221(4) Å, $\gamma$ = 90° |
| Volume | 6226(2) $Å^3$ |
| Z, Calculated density | 4, 1.975 Mg $m^{-3}$ |
| Absorption coefficient | 1.275 $mm^{-1}$ |
| F(000) | 3624 |
| Measurement device type | STOE-IPDS |
| Measurement method | 4 omega scans, 1°/frame |
| Temperature | 150(1) K |
| Wavelength | 0.71073 Å |
| Monochromator | graphite |
| $\theta$ range for data collection | 1.68 to 26.07° |
| Index ranges | $-12 \le h \le 11$, $-39 \le k \le 40$, $-20 \le l \le 22$ |
| Reflections collected / unique | 44498 / 11596 [R(int) = 0.1176] |
| Reflections greater I>2\s(I) | 7101 |
| Absorption correction | numerical |
| Max. and min. transmission | 0.9280 and 0.7244 |
| Refinement method | Full-matrix least-squares on $F^2$ |
| Data / restraints / parameters | 11596 / 5 / 839 |
| Goodness-of-fit on $F^2$ | 1.028 |
| Final R indices [I>2sigma(I)] | R1 = 0.0954, wR2 = 0.2534 |
| R indices (all data) | R1 = 0.1321, wR2 = 0.2861 |
| Largest diff. peak and hole | 1.286 and -1.469 e $Å^{-3}$ |

Table 7.62. Atomic coordinates ($\times 10^4$) and equivalent isotropic displacement parameters ($Å^2 \times 10^3$) for **83**•n$CH_2Cl_2$. $U_{eq}$ is defined as one third of the trace of the orthogonalised $U_{ij}$ tensor.

| **Atom** | **x** | **y** | **z** | $U_{eq}$ |
|---|---|---|---|---|
| Ag | 2473(1) | 55(1) | 4846(1) | 64(1) |
| Fe1 | 4966(1) | 1118(1) | 4562(1) | 57(1) |
| Fe2 | -29(1) | 250(1) | 7060(1) | 57(1) |
| P11 | 4230(3) | 632(1) | 5413(1) | 62(1) |
| P12 | 2833(3) | 891(1) | 4677(2) | 67(1) |
| P13 | 3648(3) | 903(1) | 3603(2) | 69(1) |
| P14 | 5451(3) | 617(1) | 3640(2) | 66(1) |
| P15 | 5809(3) | 471(1) | 4751(2) | 62(1) |
| P21 | 849(3) | 74(1) | 5928(1) | 63(1) |
| P22 | -787(3) | 454(1) | 5899(1) | 64(1) |
| P23 | -2140(3) | 174(1) | 6629(2) | 71(1) |
| P24 | -1252(3) | -351(1) | 7111(2) | 75(1) |
| P25 | 577(3) | -419(1) | 6663(2) | 71(1) |
| C111 | 4648(12) | 1759(2) | 4438(7) | 76(3) |
| C112 | 5771(13) | 1640(3) | 4065(6) | 74(3) |
| C113 | 6634(10) | 1466(2) | 4598(5) | 63(2) |
| C114 | 6040(10) | 1482(2) | 5291(5) | 60(2) |
| C115 | 4810(11) | 1659(2) | 5192(6) | 65(2) |
| C116 | 3482(14) | 1959(3) | 4112(9) | 102(4) |
| C117 | 6013(16) | 1704(3) | 3278(6) | 97(4) |
| C118 | 7937(11) | 1322(3) | 4427(7) | 74(3) |
| C119 | 6620(11) | 1356(3) | 6006(6) | 68(2) |
| C120 | 3901(12) | 1743(3) | 5805(8) | 88(3) |
| C211 | -237(10) | 812(2) | 7618(5) | 63(2) |
| C212 | 1011(9) | 773(3) | 7364(5) | 59(2) |
| C213 | 1588(10) | 415(3) | 7663(6) | 64(2) |
| C214 | 645(11) | 234(3) | 8149(6) | 69(3) |
| C215 | -480(10) | 475(3) | 8117(6) | 67(2) |
| C216 | -1129(12) | 1147(3) | 7481(7) | 78(3) |
| C217 | 1612(13) | 1080(3) | 6848(6) | 84(3) |
| C218 | 2919(10) | 282(4) | 7583(8) | 86(3) |
| C219 | 892(15) | -125(4) | 8634(7) | 89(4) |
| C220 | -1636(13) | 400(4) | 8553(7) | 86(3) |
| Al1 | 3751(3) | 1740(1) | 24(2) | 59(1) |
| O1 | 4397(8) | 1268(2) | 191(4) | 77(2) |
| O2 | 4234(8) | 1915(2) | -818(4) | 81(2) |
| O3 | 4223(11) | 2070(2) | 687(4) | 103(3) |
| O4 | 2167(9) | 1711(4) | 27(7) | 132(4) |
| C1 | 4617(12) | 944(3) | 607(6) | 78(3) |

| | | | | |
|---|---|---|---|---|
| C2 | 4859(11) | 1874(3) | -1467(5) | 70(3) |
| C3 | 964(13) | 1741(4) | -178(11) | 107(5) |
| C4 | 4569(10) | 2413(2) | 1009(6) | 65(2) |
| C11 | 3800(50) | 572(6) | 298(13) | 228(19) |
| C12 | 4310(40) | 968(5) | 1348(11) | 390(40) |
| C13 | 5948(18) | 838(7) | 569(11) | 430(50) |
| C21 | 4798(18) | 1414(4) | -1727(7) | 101(4) |
| C22 | 4316(17) | 2144(4) | -2028(8) | 104(4) |
| C23 | 6297(18) | 1973(5) | -1346(11) | 114(5) |
| C31 | 746(18) | 1924(5) | -1020(10) | 109(5) |
| C32 | 390(20) | 1313(5) | -229(12) | 119(5) |
| C33 | 250(20) | 2027(7) | 290(20) | 213(17) |
| C41 | 3745(15) | 2480(4) | 1702(7) | 90(4) |
| C42 | 4387(13) | 2780(3) | 495(7) | 77(3) |
| C43 | 5930(17) | 2374(7) | 1232(11) | 130(7) |
| F111 | 2589(13) | 657(5) | 704(13) | 212(8) |
| F112 | 3850(30) | 569(4) | -352(7) | 278(14) |
| F113 | 4310(30) | 237(3) | 590(7) | 343(17) |
| F121 | 4106(12) | 645(3) | 1784(4) | 143(4) |
| F122 | 3173(18) | 1212(4) | 1458(7) | 187(7) |
| F123 | 4940(30) | 1277(5) | 1707(7) | 264(12) |
| F131 | 6337(16) | 653(11) | 1192(16) | 490(30) |
| F132 | 6667(14) | 1202(7) | 630(12) | 272(12) |
| F133 | 6182(19) | 662(5) | -118(9) | 238(11) |
| F211 | 5009(14) | 1379(2) | -2440(4) | 159(5) |
| F212 | 5635(10) | 1179(2) | -1377(5) | 122(3) |
| F213 | 3669(10) | 1261(2) | -1597(5) | 119(3) |
| F221 | 3224(13) | 1988(3) | -2281(7) | 164(5) |
| F222 | 5034(13) | 2218(3) | -2612(5) | 150(4) |
| F223 | 4003(10) | 2517(2) | -1742(5) | 121(3) |
| F231 | 6721(9) | 1837(4) | -751(8) | 154(4) |
| F232 | 6994(12) | 1863(3) | -1908(8) | 177(5) |
| F233 | 6376(10) | 2392(3) | -1338(6) | 145(4) |
| F311 | 1200(14) | 1668(3) | -1492(6) | 161(4) |
| F312 | -324(12) | 2029(4) | -1142(7) | 150(4) |
| F313 | 1472(11) | 2281(3) | -987(8) | 164(5) |
| F321 | 1160(20) | 1081(3) | -583(8) | 223(8) |
| F322 | -693(17) | 1306(4) | -528(9) | 204(7) |
| F323 | 227(12) | 1157(3) | 464(7) | 147(4) |
| F331 | -994(12) | 1968(6) | 280(11) | 240(9) |
| F332 | 562(17) | 1921(5) | 1042(7) | 189(7) |
| F333 | 443(16) | 2405(3) | 206(7) | 181(5) |
| F411 | 4192(16) | 2758(3) | 2136(5) | 178(6) |

| | | | | |
|---|---|---|---|---|
| F412 | 2591(10) | 2603(3) | 1501(7) | 155(5) |
| F413 | 3599(8) | 2133(2) | 2079(4) | 102(2) |
| F421 | 5330(8) | 2790(2) | -19(4) | 98(2) |
| F422 | 3336(9) | 2759(2) | 129(5) | 119(3) |
| F423 | 4364(11) | 3144(2) | 816(5) | 124(3) |
| F431 | 6595(14) | 2224(7) | 699(10) | 273(13) |
| F432 | 6074(10) | 2146(5) | 1820(6) | 175(6) |
| F433 | 6396(15) | 2745(8) | 1430(9) | 280(14) |
| C1S | 530(20) | 1543(8) | 2467(12) | 158(8) |
| Cl1S | 715(5) | 1517(1) | 3420(3) | 136(2) |
| Cl2S | -1042(6) | 1376(2) | 2198(4) | 177(2) |

Table 7.63. Anisotropic displacement parameters ($Å^2 \times 10^3$) for **83**•n$CH_2Cl_2$. The anisotropic displacement factor exponent takes the form: $-2\pi^2[h^2a^{*2}U_{11} + ... + 2hka^*b^*U_{12}]$.

| **Atom** | $U_{11}$ | $U_{22}$ | $U_{33}$ | $U_{23}$ | $U_{13}$ | $U_{12}$ |
|---|---|---|---|---|---|---|
| Ag | 81(1) | 42(1) | 69(1) | -3(1) | -16(1) | 1(1) |
| Fe1 | 84(1) | 29(1) | 58(1) | -(1) | -20(1) | 1(1) |
| Fe2 | 75(1) | 36(1) | 60(1) | -4(1) | -17(1) | -2(1) |
| P11 | 86(2) | 35(1) | 65(1) | 35(9) | -12(1) | -0(1) |
| P12 | 80(2) | 43(1) | 78(2) | -5(1) | -18(1) | 4(1) |
| P13 | 95(2) | 46(1) | 67(2) | -4(1) | -27(2) | -4(1) |
| P14 | 90(2) | 43(1) | 66(2) | -9(1) | -14(1) | -3(1) |
| P15 | 83(2) | 33(1) | 70(2) | -1(1) | -17(1) | 4(1) |
| P21 | 82(2) | 47(1) | 61(1) | -9(1) | -13(1) | 2(1) |
| P22 | 85(2) | 45(1) | 61(1) | -5(1) | -20(1) | 2(1) |
| P23 | 77(2) | 59(1) | 77(2) | -10(1) | -18(2) | -4(1) |
| P24 | 93(2) | 52(1) | 79(2) | 0(1) | -15(2) | -19(1) |
| P25 | 95(2) | 38(1) | 81(2) | -5(1) | -19(2) | 3(1) |
| C111 | 109(8) | 27(4) | 92(7) | 6(4) | -35(7) | 8(4) |
| C112 | 120(9) | 36(4) | 65(6) | 6(4) | -32(6) | -13(5) |
| C113 | 93(7) | 32(4) | 64(6) | 2(3) | -15(5) | -3(4) |
| C114 | 88(6) | 34(4) | 58(5) | -2(3) | -19(5) | -1(4) |
| C115 | 96(7) | 34(4) | 67(6) | -6(4) | -15(5) | -2(4) |
| C116 | 120(10) | 51(5) | 134(12) | 29(6) | -45(9) | 10(6) |
| C117 | 162(13) | 57(6) | 70(7) | 15(5) | -17(8) | -24(7) |
| C118 | 85(7) | 50(5) | 87(7) | -4(5) | 1(6) | -13(5) |
| C119 | 87(7) | 56(5) | 61(6) | -4(4) | -18(5) | -4(5) |
| C120 | 102(8) | 57(6) | 105(9) | -27(6) | 5(7) | 0(5) |
| C211 | 91(7) | 35(4) | 64(5) | -11(3) | -20(5) | 5(4) |
| C212 | 71(6) | 42(4) | 65(6) | -5(4) | -7(5) | -4(4) |
| C213 | 80(6) | 49(4) | 64(6) | -4(4) | -13(5) | 3(4) |
| C214 | 93(7) | 43(4) | 72(6) | 0(4) | -25(6) | -4(4) |
| C215 | 81(6) | 53(5) | 68(6) | -12(4) | -8(5) | -1(4) |
| C216 | 102(8) | 50(5) | 83(7) | -17(5) | -25(6) | 20(5) |

| | | | | | | |
|---|---|---|---|---|---|---|
| C217 | 128(1) | 52(5) | 71(6) | -2(4) | 0(7) | -38(6) |
| C218 | 70(6) | 85(7) | 104(9) | -26(6) | -22(7) | 12(5) |
| C219 | 125(10) | 70(6) | 70(7) | 13(5) | -20(7) | 11(6) |
| C220 | 103(9) | 79(7) | 75(7) | -3(6) | 8(7) | -16(6) |
| Al1 | 74(2) | 38(1) | 65(2) | -2(1) | -14(1) | 5(1) |
| O1 | 115(6) | 41(3) | 76(4) | -1(3) | -5(4) | 12(3) |
| O2 | 112(6) | 54(4) | 78(5) | 3(3) | -12(5) | 9(4) |
| O3 | 205(10) | 46(3) | 59(4) | -2(3) | -18(6) | -8(5) |
| O4 | 67(5) | 195(12) | 135(9) | 46(8) | -9(6) | 22(6) |
| C1 | 117(9) | 48(5) | 70(6) | 8(4) | 4(6) | 20(5) |
| C2 | 100(8) | 53(5) | 56(6) | -6(4) | 3(6) | -9(5) |
| C3 | 75(8) | 82(8) | 165(15) | -31(9) | -10(9) | 4(6) |
| C4 | 87(6) | 37(4) | 69(6) | -8(4) | -18(5) | 1(4) |
| C11 | 500(60) | 79(11) | 98(14) | -10(10) | -10(20) | 30(20) |
| C12 | 990(120) | 75(11) | 107(15) | 34(11) | 140(30) | 200(30) |
| C13 | 106(17) | 570(80) | 630(100) | 530(90) | -40(40) | -50(30) |
| C21 | 159(14) | 73(7) | 70(8) | -19(6) | 6(9) | -22(9) |
| C22 | 150(13) | 70(7) | 91(9) | -3(6) | -1(10) | -19(8) |
| C23 | 132(13) | 94(10) | 116(12) | -19(9) | 20(12) | -30(9) |
| C31 | 119(12) | 89(9) | 118(12) | 8(8) | -4(10) | 23(9) |
| C32 | 139(14) | 93(10) | 125(14) | -18(10) | -27(12) | 10(10) |
| C33 | 114(15) | 114(15) | 410(50) | -130(20) | 20(20) | -18(11) |
| C41 | 125(11) | 69(7) | 75(7) | -6(6) | 11(8) | 2(7) |
| C42 | 106(9) | 44(5) | 80(7) | -10(4) | -4(7) | -9(5) |
| C43 | 101(11) | 182(18) | 107(12) | 75(12) | -5(11) | 1(12) |
| F111 | 158(11) | 150(11) | 330(20) | 64(14) | 43(13) | -28(9) |
| F112 | 600(40) | 121(9) | 108(9) | 8(7) | -64(15) | -162(16) |
| F113 | 830(50) | 49(5) | 153(10) | 17(5) | 162(19) | 84(12) |
| F121 | 253(12) | 97(6) | 80(5) | 29(4) | 2(7) | 16(7) |
| F122 | 319(19) | 113(8) | 130(9) | 28(6) | 87(12) | 61(10) |
| F123 | 520(40) | 181(14) | 92(8) | -29(8) | -76(14) | 90(18) |
| F131 | 166(13) | 69(5) | 610(50) | 540(50) | 110(20) | 180(20) |
| F132 | 117(9) | 44(3) | 260(20) | 120(20) | -56(12) | -24(14) |
| F133 | 300(20) | 194(13) | 223(15) | 107(12) | 156(15) | 157(15) |
| F211 | 337(17) | 78(5) | 61(4) | -19(4) | 13(7) | -31(7) |
| F212 | 190(9) | 74(4) | 103(6) | 6(4) | 20(6) | 42(5) |
| F213 | 175(8) | 63(4) | 119(6) | -8(4) | -32(6) | -33(5) |
| F221 | 203(11) | 113(7) | 176(11) | 7(6) | -108(10) | -21(7) |
| F222 | 272(14) | 105(6) | 73(5) | 15(4) | -1(7) | -39(7) |
| F223 | 177(8) | 60(4) | 128(7) | 18(4) | -26(6) | 3(4) |
| F231 | 105(7) | 191(11) | 165(11) | 19(9) | -41(7) | 1(7) |
| F232 | 174(10) | 119(7) | 238(14) | 11(8) | 110(10) | 7(7) |
| F233 | 147(8) | 126(7) | 164(9) | -39(7) | 30(7) | -58(6) |
| F311 | 238(13) | 116(7) | 128(8) | -8(6) | 14(9) | 19(8) |
| F312 | 145(9) | 145(9) | 160(10) | 5(7) | -54(8) | 8(7) |
| F313 | 157(9) | 104(7) | 232(14) | 50(8) | -26(9) | -20(6) |
| F321 | 400(20) | 85(6) | 182(12) | -47(7) | 58(15) | 13(10) |

| | | | | | | |
|---|---|---|---|---|---|---|
| F322 | 240(15) | 149(10) | 221(15) | 30(10) | -97(13) | -108(11) |
| F323 | 173(10) | 115(7) | 154(10) | 18(6) | 4(8) | -18(6) |
| F331 | 112(8) | 291(19) | 320(20) | -142(17) | 30(11) | 42(10) |
| F332 | 227(15) | 241(16) | 98(7) | -23(8) | -5(9) | -27(12) |
| F333 | 311(17) | 66(5) | 167(10) | -8(6) | 18(11) | 10(7) |
| F411 | 354(18) | 86(5) | 96(6) | -43(5) | 68(9) | -53(8) |
| F412 | 139(8) | 131(8) | 196(11) | 63(8) | 70(8) | 57(7) |
| F413 | 133(6) | 85(4) | 89(5) | 13(4) | 8(5) | -3(4) |
| F421 | 125(6) | 82(4) | 86(5) | 20(3) | 3(5) | 3(4) |
| F422 | 128(6) | 90(5) | 139(7) | 46(5) | -41(6) | 7(4) |
| F423 | 218(10) | 50(3) | 104(5) | -9(3) | -3(6) | -19(5) |
| F431 | 157(10) | 430(30) | 228(15) | 218(19) | 98(12) | 183(16) |
| F432 | 122(7) | 282(15) | 120(8) | 115(9) | -26(6) | 0(8) |
| F433 | 180(13) | 490(30) | 174(13) | 172(18) | -97(12) | -215(18) |
| C1S | 133(15) | 190(20) | 156(18) | 33(15) | 38(14) | -26(14) |
| Cl1S | 134(3) | 107(3) | 165(4) | 4(3) | -7(3) | -4(2) |
| Cl2S | 151(4) | 224(7) | 155(5) | 53(5) | -3(4) | -17(4) |

## 7.3.22. $[Cu_{20}(\mu\text{-}Cl)_{16}(\mu_3\text{-}Cl)_4\{(Cp^*Mo)_2(\mu_7,\eta^6{:}\eta^6{:}\eta^1{:}\eta^1{:}\eta^1{:}\eta^1\text{-}P_6)\}_3\{(Cp^*Mo)_2(\mu_7,\eta^6{:}\eta^6{:}\eta^2{:}\eta^1{:}\eta^1{:}\eta^1\text{-}P_6)\}(NCCH_3)_{12}]_n \bullet 2nCH_2Cl_2$ (**88**•$2nCH_2Cl_2$)

Crystals of **88**•$2nCH_2Cl_2$ were obtained by controlled diffusion of $Et_2O$ into a mixture of CuCl and $[(Cp^*Mo)_2(\mu,\eta^6\text{-}P_6)]$ **11c**, dissolved in $CH_3CN/CH_2Cl_2$, at room temperature in the dark.

Table 7.64. Crystal data and structure refinement for **88**•$2nCH_2Cl_2$.

| | |
|---|---|
| Empirical formula | $C_{26.5}H_{40}Cl_6Cu_5Mo_2N_3P_6$ |
| Formula weight | 1308.72 g $mol^{-1}$ |
| Crystal size | 0.240 × 0.220 × 0.180 mm |
| Crystal description | prism |
| Crystal colour | yellow to brown |
| Crystal system | triclinic |
| Space group | $P\ \bar{1}$ |
| Unit cell dimensions | $a$ = 10.552(1) Å, $\alpha$ = 69.64(1)° |
| | $b$ = 13.816(1) Å, $\beta$ = 89.68(1)° |
| | $c$ = 16.568(2) Å, $\gamma$ = 71.62(1)° |
| Volume | 2134.3(4) $Å^3$ |
| Z, Calculated density | 2, 2.036 Mg $m^{-3}$ |
| Absorption coefficient | 3.637 $mm^{-1}$ |
| F(000) | 1282 |
| Measurement device type | STOE-IPDS |
| Measurement method | rotation |
| Temperature | 123(1) K |
| Wavelength | 0.71073 Å |
| Monochromator | graphite |
| $\theta$ range for data collection | 2.17 to 26.85° |
| Index ranges | $-13 \le h \le 13$, $-17 \le k \le 16$, $-20 \le l \le 20$ |
| Reflections collected / unique | 19226 / 8490 [R(int) = 0.0310] |
| Reflections greater I>2\s(I) | 6477 |
| Absorption correction | analytical |
| Max. and min. transmission | 0.6156 and 0.5052 |
| Refinement method | Full-matrix least-squares on $F^2$ |
| Data / restraints / parameters | 8490 / 0 / 434 |
| Goodness-of-fit on $F^2$ | 0.962 |
| Final R indices [I>2sigma(I)] | R1 = 0.0389, wR2 = 0.0974 |
| R indices (all data) | R1 = 0.0526, wR2 = 0.1013 |
| Largest diff. peak and hole | 2.641 and -0.885 e $Å^{-3}$ |

Table 7.65. Atomic coordinates ($\times 10^4$) and equivalent isotropic displacement parameters ($Å^2 \times 10^3$) for **88**•2n$CH_2Cl_2$. $U_{eq}$ is defined as one third of the trace of the orthogonalised $U_{ij}$ tensor.

| **Atom** | **x** | **y** | **z** | $U_{eq}$ |
|---|---|---|---|---|
| Mo1 | -1143(1) | -922(1) | 2717(1) | 15(1) |
| Mo2 | 1524(1) | -1362(1) | 2843(1) | 15(1) |
| Cu1 | 617(1) | -2998(1) | 1033(1) | 26(1) |
| Cu2 | -287(1) | 1553(1) | 3480(1) | 30(1) |
| Cu3 | -499(1) | 2897(1) | 4414(1) | 24(1) |
| Cu4 | 870(1) | 5357(1) | 4249(1) | 25(1) |
| Cu5 | -489(1) | 2251(1) | 909(1) | 25(1) |
| Cl1 | -1307(1) | -2182(1) | -10(1) | 29(1) |
| Cl2 | 2269(1) | -2604(1) | 114(1) | 30(1) |
| Cl3 | 1344(1) | 2230(1) | 3695(1) | 26(1) |
| Cl4 | -2244(1) | 2811(1) | 3560(1) | 26(1) |
| Cl5 | -994(1) | 4748(1) | 4254(1) | 22(1) |
| P1 | 391(1) | -2214(1) | 2028(1) | 21(1) |
| P2 | 86(1) | -477(1) | 1329(1) | 30(1) |
| P3 | -110(1) | 579(1) | 2039(1) | 39(1) |
| P4 | -4(1) | -95(1) | 3501(1) | 35(1) |
| P5 | 291(1) | -1804(1) | 4181(1) | 23(1) |
| P6 | 484(1) | -2873(1) | 3411(1) | 18(1) |
| Cu6 | -201(3) | 1460(2) | 705(2) | 29(1) |
| N1 | 2464(4) | 4371(3) | 3971(3) | 25(1) |
| N2 | 1189(6) | -4615(4) | 1389(4) | 43(2) |
| N3 | -936(7) | 3484(5) | 1337(4) | 31(2) |
| C1 | -3296(4) | 357(4) | 2378(3) | 17(1) |
| C2 | -3199(4) | -325(4) | 1874(3) | 17(1) |
| C3 | -2979(4) | -1418(4) | 2465(3) | 18(1) |
| C4 | -2959(4) | -1411(4) | 3327(3) | 16(1) |
| C5 | -3159(4) | -313(3) | 3274(3) | 16(1) |
| C6 | -3648(5) | 1587(3) | 2020(3) | 21(1) |
| C7 | -3416(5) | 78(4) | 895(3) | 23(1) |
| C8 | -2876(5) | -2402(4) | 2239(4) | 22(1) |
| C9 | -2862(5) | -2371(4) | 4147(3) | 20(1) |
| C10 | -3318(5) | 84(4) | 4015(3) | 23(1) |
| C11 | 3329(4) | -709(3) | 2684(3) | 17(1) |
| C12 | 3420(4) | -1382(4) | 3584(3) | 18(1) |
| C13 | 3624(4) | -2479(4) | 3623(3) | 19(1) |
| C14 | 3662(4) | -2479(4) | 2759(3) | 20(1) |
| C15 | 3481(4) | -1384(4) | 2176(3) | 17(1) |
| C16 | 3228(5) | 478(4) | 2352(3) | 20(1) |
| C17 | 3406(5) | -1025(4) | 4336(3) | 23(1) |

| | | | | |
|---|---|---|---|---|
| C18 | 3906(5) | -3478(4) | 4446(3) | 23(1) |
| C19 | 3965(5) | -3476(4) | 2519(4) | 24(1) |
| C20 | 3545(5) | -1024(4) | 1213(3) | 22(1) |
| C21 | 3248(5) | 3828(4) | 3701(4) | 26(1) |
| C22 | 4261(6) | 3118(6) | 3376(6) | 50(2) |
| C23 | 1659(8) | -5486(6) | 1394(5) | 52(3) |
| C24 | 2260(10) | -6616(6) | 1427(7) | 71(3) |
| C25 | -1252(9) | 4158(6) | 1601(6) | 38(3) |
| C26 | -1727(13) | 5058(8) | 1910(8) | 65(4) |

Table 7.66. Anisotropic displacement parameters ($Å^2 \times 10^3$) for **88**•2n$CH_2Cl_2$. The anisotropic displacement factor exponent takes the form: $-2\pi^2[h^2a^{*2}U_{11} + ... + 2hka^*b^*U_{12}]$.

| **Atom** | $U_{11}$ | $U_{22}$ | $U_{33}$ | $U_{23}$ | $U_{13}$ | $U_{12}$ |
|---|---|---|---|---|---|---|
| Mo1 | 12(1) | 12(1) | 20(1) | -5(1) | 5(1) | -5(1) |
| Mo2 | 12(1) | 12(1) | 21(1) | -5(1) | 4(1) | -5(1) |
| Cu1 | 30(1) | 24(1) | 26(1) | -11(1) | 6(1) | -8(1) |
| Cu2 | 25(1) | 20(1) | 49(1) | -16(1) | 6(1) | -10(1) |
| Cu3 | 23(1) | 24(1) | 29(1) | -14(1) | 6(1) | -10(1) |
| Cu4 | 26(1) | 17(1) | 30(1) | -8(1) | 9(1) | -8(1) |
| Cu5 | 29(1) | 19(1) | 27(1) | -8(1) | 7(1) | -9(1) |
| Cl1 | 26(1) | 36(1) | 27(1) | -12(1) | 5(1) | -12(1) |
| Cl2 | 28(1) | 38(1) | 27(1) | -11(1) | 7(1) | -14(1) |
| Cl3 | 22(1) | 32(1) | 35(1) | -21(1) | 12(1) | -15(1) |
| Cl4 | 20(1) | 24(1) | 37(1) | -15(1) | 1(1) | -6(1) |
| Cl5 | 26(1) | 17(1) | 25(1) | -8(1) | 5(1) | -10(1) |
| P1 | 17(1) | 26(1) | 22(1) | -12(1) | 5(1) | -7(1) |
| P2 | 18(1) | 29(1) | 30(1) | 4(1) | 5(1) | -6(1) |
| P3 | 17(1) | 17(1) | 70(1) | 1(1) | 5(1) | -6(1) |
| P4 | 17(1) | 30(1) | 74(1) | -36(1) | 10(1) | -9(1) |
| P5 | 17(1) | 34(1) | 24(1) | -16(1) | 6(1) | -9(1) |
| P6 | 16(1) | 15(1) | 23(1) | -7(1) | 5(1) | -7(1) |
| Cu6 | 28(2) | 24(2) | 31(2) | -3(1) | 5(1) | -10(1) |
| N1 | 26(2) | 20(2) | 27(2) | -5(2) | 9(2) | -9(2) |
| N2 | 59(3) | 22(2) | 42(3) | -9(2) | -5(3) | -10(2) |
| N3 | 41(3) | 26(3) | 27(3) | -12(2) | 6(3) | -12(3) |
| C1 | 11(2) | 19(2) | 20(2) | -6(2) | 3(2) | -5(2) |
| C2 | 13(2) | 16(2) | 23(2) | -7(2) | 3(2) | -6(2) |
| C3 | 11(2) | 18(2) | 27(3) | -11(2) | 5(2) | -6(2) |
| C4 | 11(2) | 17(2) | 20(2) | -5(2) | 5(2) | -6(2) |
| C5 | 12(2) | 16(2) | 20(2) | -8(2) | 4(2) | -3(2) |
| C6 | 17(2) | 13(2) | 28(3) | -6(2) | 6(2) | -1(2) |

| | | | | | | |
|---|---|---|---|---|---|---|
| C7 | 24(2) | 23(2) | 20(2) | -5(2) | 3(2) | -9(2) |
| C8 | 19(2) | 19(2) | 31(3) | -12(2) | 4(2) | -6(2) |
| C9 | 20(2) | 16(2) | 24(3) | -5(2) | 8(2) | -8(2) |
| C10 | 24(2) | 24(2) | 22(2) | -11(2) | 7(2) | -7(2) |
| C11 | 12(2) | 16(2) | 24(2) | -8(2) | 5(2) | -6(2) |
| C12 | 11(2) | 19(2) | 23(2) | -7(2) | 6(2) | -5(2) |
| C13 | 10(2) | 18(2) | 26(3) | -5(2) | 3(2) | -5(2) |
| C14 | 12(2) | 18(2) | 28(3) | -9(2) | 5(2) | -4(2) |
| C15 | 13(2) | 19(2) | 21(2) | -6(2) | 6(2) | -8(2) |
| C16 | 17(2) | 16(2) | 31(3) | -10(2) | 6(2) | -9(2) |
| C17 | 22(2) | 25(2) | 24(3) | -12(2) | 3(2) | -9(2) |
| C18 | 21(2) | 16(2) | 28(3) | -3(2) | 3(2) | -6(2) |
| C19 | 23(2) | 18(2) | 32(3) | -10(2) | 6(2) | -7(2) |
| C20 | 21(2) | 26(2) | 20(2) | -8(2) | 8(2) | -10(2) |
| C21 | 21(2) | 23(2) | 37(3) | -11(2) | 6(2) | -10(2) |
| C22 | 30(3) | 52(4) | 79(5) | -42(4) | 19(3) | -10(3) |
| C23 | 64(5) | 40(4) | 45(4) | -10(3) | -6(4) | -15(3) |
| C24 | 83(6) | 36(4) | 90(7) | -23(4) | -12(5) | -14(4) |
| C25 | 47(5) | 31(4) | 40(4) | -12(3) | 24(4) | -18(3) |
| C26 | 102(9) | 43(5) | 80(7) | -43(5) | 63(7) | -42(5) |

## 7.3.23. $[Ag\{(Cp^*Mo)_2(\mu_3,\eta^6{:}\eta^6{:}\eta^2\text{-}P_6)\}_2][Al\{OC(CF_3)_3\}_4] \bullet CH_2Cl_2$ (**90**$\bullet CH_2Cl_2$)

The complex **90**$\bullet CH_2Cl_2$ was crystallised from a 1:2 mixture of $Ag[Al\{OC(CF_3)_3\}_4]$ and $[(Cp^*Mo)_2(\mu,\eta^6\text{-}P_6)]$ **11c**, dissolved in $CH_2Cl_2$, at –28 °C.

Table 7.67. Crystal data and structure refinement for **90**$\bullet CH_2Cl_2$.

| | |
|---|---|
| Empirical formula | $C_{57}H_{62}AgAlF_{36}Cl_2Mo_4O_4P_{12}$ |
| Formula weight | 2456.22 g $mol^{-1}$ |
| Crystal size | 0.180 × 0.150 × 0.060 mm |
| Crystal description | plate |
| Crystal colour | orange to red |
| Crystal system | monoclinic |
| Space group | *C*2/*c* |
| Unit cell dimensions | $a$ = 36.624(2) Å, $\alpha$ = 90° |
| | $b$ = 16.249(1) Å, $\beta$ = 101.54(1)° |
| | $c$ = 14.622(1) Å, $\gamma$ = 90° |
| Volume | 8525.3(10) $Å^3$ |
| Z, Calculated density | 4, 1.914 Mg $m^{-3}$ |
| Absorption coefficient | 1.217 $mm^{-1}$ |
| F(000) | 4808 |
| Measurement device type | STOE-IPDS |
| Measurement method | rotation |
| Temperature | 123(1) K |
| Wavelength | 0.71073 Å |
| Monochromator | graphite |
| $\theta$ range for data collection | 1.89 to 25.75° |
| Index ranges | $-44 \le h \le 43$, $-19 \le k \le 19$, $-17 \le l \le 17$ |
| Reflections collected/ unique | 30283 / 7872 [R(int) = 0.0704] |
| Reflections greater I>2\s(I) | 6055 |
| Absorption correction | numerical |
| Max. and min. transmission | 0.9193 and 0.7925 |
| Refinement method | Full-matrix least-squares on $F^2$ |
| Data / restraints / parameters | 7872 / 0 / 400 |
| Goodness-of-fit on $F^2$ | 1.032 |
| Final R indices [I>2sigma(I)] | R1 = 0.1015, wR2 = 0.2351 |
| R indices (all data) | R1 = 0.1223, wR2 = 0.2519 |
| Largest diff. peak and hole | 3.416 and -1.862 e $Å^{-3}$ |

Table 7.68. Atomic coordinates ($\times 10^4$) and equivalent isotropic displacement parameters ($Å^2 \times 10^3$) for **90**•$CH_2Cl_2$. $U_{eq}$ is defined as one third of the trace of the orthogonalised $U_{ij}$ tensor.

| **Atom** | **x** | **y** | **z** | $U_{eq}$ |
|---|---|---|---|---|
| Ag1 | 2500 | 2500 | 0 | 34(1) |
| Mo1 | 3164(1) | 1228(1) | 2417(1) | 18(1) |
| Mo2 | 2456(1) | 1123(1) | 2558(1) | 16(1) |
| P1 | 2646(1) | 1165(2) | 981(2) | 24(1) |
| P2 | 2701(1) | 2371(2) | 1828(2) | 24(1) |
| P3 | 2872(1) | 2307(2) | 3346(2) | 25(1) |
| P4 | 2982(1) | 1111(2) | 4032(2) | 27(1) |
| P5 | 2924(1) | -22(2) | 3225(2) | 27(1) |
| P6 | 2757(1) | -10(2) | 1705(2) | 25(1) |
| C1 | 3786(3) | 919(7) | 3041(8) | 30(2) |
| C2 | 3753(3) | 1796(7) | 2962(7) | 27(2) |
| C3 | 3643(3) | 1998(6) | 1991(7) | 26(2) |
| C4 | 3614(3) | 1247(6) | 1472(7) | 26(2) |
| C5 | 3699(3) | 586(6) | 2120(8) | 27(2) |
| C6 | 3932(4) | 455(9) | 3931(9) | 43(3) |
| C7 | 3856(3) | 2412(9) | 3759(9) | 45(3) |
| C8 | 3622(3) | 2859(7) | 1585(9) | 35(3) |
| C9 | 3538(4) | 1186(8) | 432(8) | 39(3) |
| C10 | 3729(4) | -312(7) | 1852(10) | 39(3) |
| C11 | 1899(3) | 1802(6) | 2682(8) | 26(2) |
| C12 | 1823(3) | 1277(6) | 1877(8) | 26(2) |
| C13 | 1877(3) | 441(6) | 2182(7) | 20(2) |
| C14 | 1995(3) | 452(6) | 3186(7) | 21(2) |
| C15 | 2009(3) | 1286(6) | 3492(7) | 24(2) |
| C16 | 1841(4) | 2724(7) | 2689(11) | 46(3) |
| C17 | 1665(3) | 1558(8) | 893(8) | 38(3) |
| C18 | 1790(3) | -300(7) | 1572(9) | 35(3) |
| C19 | 2057(3) | -293(7) | 3811(8) | 34(3) |
| C20 | 2090(4) | 1580(8) | 4492(8) | 38(3) |
| Cl1 | 4606(4) | 1504(8) | 2389(8) | 178(4) |
| C21 | 5000 | 2310(40) | 2500 | 190(20) |
| Al1 | 0 | -1702(3) | -2500 | 27(1) |
| O1 | -363(4) | -1096(9) | -2995(8) | 84(5) |
| O2 | -133(4) | -2320(10) | -1696(9) | 97(5) |
| C22 | -241(5) | -2772(11) | -1066(13) | 67(4) |
| C23 | -632(4) | -625(10) | -3377(11) | 54(4) |
| C24 | -436(9) | -3678(19) | -2430(20) | 121(9) |
| C25 | -940(20) | -1030(40) | -4610(50) | 230(20) |
| C26 | -629(10) | -1980(20) | -500(30) | 128(10) |

| | | | | |
|---|---|---|---|---|
| C27 | -767(12) | -120(30) | -2310(30) | 139(11) |
| F1 | -642(11) | 730(20) | -3020(20) | 260(14) |
| F2 | 68(6) | -2145(14) | 283(15) | 168(8) |
| F3 | -1216(10) | -300(20) | -4160(20) | 245(13) |
| F5 | -255(7) | -125(13) | -4302(15) | 163(7) |
| F6 | -723(8) | -3023(17) | -2351(19) | 206(10) |
| F7 | -804(8) | -2071(18) | -3770(20) | 212(10) |
| F8 | -284(10) | -1380(20) | -570(20) | 252(14) |
| F9 | -252(8) | -4126(18) | -1250(20) | 213(11) |
| F10 | -449(11) | -2350(20) | 260(30) | 266(15) |
| F11 | -525(8) | -123(15) | -1762(18) | 179(8) |
| F12 | -1083(12) | 240(30) | -2870(30) | 281(16) |
| F13 | 164(9) | -3484(18) | 10(20) | 215(11) |
| F14 | -833(11) | -2270(30) | -1520(30) | 280(16) |
| F15 | 363(13) | -3070(30) | -660(30) | 322(19) |
| F16 | -852(6) | -3127(14) | -1242(15) | 157(7) |
| F17 | -1157(8) | -1354(16) | -4060(20) | 181(9) |
| F18 | -674(9) | -1018(17) | -4970(20) | 203(11) |
| F19 | -1004(13) | -710(30) | -2220(30) | 320(20) |
| F20 | -1059(11) | -1490(20) | -2940(30) | 279(16) |
| F21 | -202(12) | 460(20) | -3160(30) | 303(19) |
| F22 | -417(14) | -3630(30) | -20(30) | 330(20) |
| F23 | -719(13) | 310(30) | -4550(30) | 315(19) |

Table 7.69. Anisotropic displacement parameters ($Å^2 \times 10^3$) for **90**•$CH_2Cl_2$. The anisotropic displacement factor exponent takes the form: $-2\pi^2[h^2a^{*2}U_{11} + ... + 2hka^*b^*U_{12}]$.

| **Atom** | $U_{11}$ | $U_{22}$ | $U_{33}$ | $U_{23}$ | $U_{13}$ | $U_{12}$ |
|---|---|---|---|---|---|---|
| Ag1 | 29(1) | 47(1) | 25(1) | 19(1) | 3(1) | 1(1) |
| Mo1 | 22(1) | 17(1) | 14(1) | 1(1) | 2(1) | 0(1) |
| Mo2 | 22(1) | 14(1) | 13(1) | 1(1) | 3(1) | 1(1) |
| P1 | 27(1) | 28(1) | 15(1) | -1(1) | 3(1) | -1(1) |
| P2 | 29(1) | 17(1) | 24(1) | 5(1) | 3(1) | -1(1) |
| P3 | 29(1) | 22(1) | 23(1) | -7(1) | 5(1) | -3(1) |
| P4 | 29(1) | 37(2) | 15(1) | 3(1) | 1(1) | 0(1) |
| P5 | 27(1) | 22(1) | 31(1) | 11(1) | 5(1) | 5(1) |
| P6 | 28(1) | 19(1) | 29(1) | -6(1) | 7(1) | 0(1) |
| C1 | 23(5) | 35(6) | 31(5) | 3(4) | 5(5) | 0(4) |
| C2 | 21(5) | 37(6) | 23(5) | -3(4) | 4(4) | -4(4) |
| C3 | 25(5) | 22(5) | 31(5) | 1(4) | 7(4) | -4(4) |
| C4 | 25(5) | 28(5) | 26(5) | 0(4) | 11(4) | -1(4) |
| C5 | 21(5) | 26(5) | 33(5) | 2(4) | 6(4) | 2(4) |

| | | | | | | |
|---|---|---|---|---|---|---|
| C6 | 32(6) | 59(8) | 34(6) | 10(6) | 1(5) | 12(6) |
| C7 | 28(6) | 56(8) | 46(7) | -19(6) | 0(6) | -13(5) |
| C8 | 34(6) | 26(5) | 47(7) | 9(5) | 11(5) | -6(4) |
| C9 | 40(7) | 49(7) | 31(6) | -1(5) | 15(5) | 3(5) |
| C10 | 40(7) | 28(6) | 53(7) | -1(5) | 16(6) | 5(5) |
| C11 | 29(5) | 19(5) | 33(5) | 0(4) | 15(5) | 4(4) |
| C12 | 24(5) | 23(5) | 31(5) | 5(4) | 6(4) | 5(4) |
| C13 | 21(5) | 20(5) | 21(5) | -1(4) | 5(4) | 2(4) |
| C14 | 20(5) | 21(5) | 22(5) | 3(4) | 6(4) | -4(4) |
| C15 | 25(5) | 31(5) | 20(5) | -5(4) | 12(4) | -6(4) |
| C16 | 39(7) | 20(5) | 83(10) | -4(6) | 25(7) | 4(5) |
| C17 | 34(6) | 48(7) | 31(6) | 14(5) | 4(5) | 5(5) |
| C18 | 33(6) | 28(6) | 43(6) | -15(5) | 5(5) | -5(4) |
| C19 | 33(6) | 31(6) | 37(6) | 17(5) | 5(5) | 0(5) |
| C20 | 36(6) | 52(7) | 28(6) | -15(5) | 12(5) | -8(5) |
| Al1 | 16(2) | 31(2) | 32(2) | 0 | 1(2) | 0 |
| O1 | 75(8) | 117(11) | 56(7) | 0(7) | 0(6) | 71(8) |
| O2 | 99(10) | 122(12) | 69(8) | 38(8) | 15(8) | -60(9) |

## 7.3.24. [{Cu($\mu$-I)}$_3${(Cp*Mo)$_2$($\mu_3$,$\eta^3$:$\eta^3$:$\eta^1$-P$_3$)($\mu$,$\eta^2$-PS)} {(Cp*Mo)$_2$($\mu_3$,$\eta^3$:$\eta^3$:$\eta^1$-P$_3$)($\mu_3$,$\eta^2$:$\eta^2$:$\eta^1$-PS)}]$_n$ (92c)

Crystals of **92c** were obtained by controlled diffusion of a $CH_3CN$ solution of CuI into a $CH_2Cl_2$ solution of [(Cp*Mo)$_2$($\mu$,$\eta^3$-P$_3$)($\mu$,$\eta^2$-PS)] **91** at room temperature.

Table 7.70. Crystal data and structure refinement for **92c**.

| | |
|---|---|
| Empirical formula | $C_{40}H_{60}Cu_3I_3Mo_4P_8S_2$ |
| Formula weight | 1807.89 g mol$^{-1}$ |
| Crystal size | 0.520 × 0.200 × 0.160 mm |
| Crystal description | rod |
| Crystal colour | dark red |
| Crystal system | triclinic |
| Space group | $P\ \overline{1}$ |
| Unit cell dimensions | $a$ = 10.836(1) Å, $\alpha$ = 76.31(1)° |
| | $b$ = 15.791(2) Å, $\beta$ = 76.56(1)° |
| | $c$ = 18.157(2) Å, $\gamma$ = 70.87(1)° |
| Volume | 2811.1(5) Å$^3$ |
| Z, Calculated density | 2, 2.136 Mg m$^{-3}$ |
| Absorption coefficient | 3.954 mm$^{-1}$ |
| F(000) | 1732 |
| Measurement device type | STOE-IPDS |
| Measurement method | rotation |
| Temperature | 173(1) K |
| Wavelength | 0.71073 Å |
| Monochromator | graphite |
| $\theta$ range for data collection | 2.02 to 25.89° |
| Index ranges | $-13 \le h \le 13$, $-19 \le k \le 19$, $-22 \le l \le 22$ |
| Reflections collected / unique | 32095 / 10172 [R(int) = 0.0277] |
| Reflections greater I>2\s(I) | 9330 |
| Absorption correction | analytical |
| Max. and min. transmission | 0.5755 and 0.2381 |
| Refinement method | Full-matrix least-squares on F$^2$ |
| Data / restraints / parameters | 10172 / 0 / 541 |
| Goodness-of-fit on F$^2$ | 1.034 |
| Final R indices [I>2sigma(I)] | R1 = 0.0266, wR2 = 0.0678 |
| R indices (all data) | R1 = 0.0296, wR2 = 0.0691 |
| Largest diff. peak and hole | 1.838 and -1.493 e Å$^{-3}$ |

Table 7.71. Atomic coordinates ($\times 10^4$) and equivalent isotropic displacement parameters ($Å^2 \times 10^3$) for **92c**. $U_{eq}$ is defined as one third of the trace of the orthogonalised $U_{ij}$ tensor.

| **Atom** | **x** | **y** | **z** | $U_{eq}$ |
|---|---|---|---|---|
| I1 | 7668(1) | 5585(1) | 1992(1) | 42(1) |
| I2 | 6329(1) | 8480(1) | 1186(1) | 37(1) |
| I3 | 5718(1) | 7457(1) | 3576(1) | 34(1) |
| Mo1 | 1960(1) | 6961(1) | 1457(1) | 17(1) |
| Mo2 | 1566(1) | 6429(1) | 2980(1) | 17(1) |
| Mo3 | 5882(1) | 1563(1) | 2956(1) | 19(1) |
| Mo4 | 3581(1) | 1520(1) | 2701(1) | 22(1) |
| Cu1 | 7745(1) | 7171(1) | 2148(1) | 47(1) |
| Cu2 | 5522(1) | 6841(1) | 2361(1) | 55(1) |
| Cu3 | 6025(1) | 8816(1) | 2538(1) | 36(1) |
| S1 | 709(1) | 8054(1) | 2357(1) | 23(1) |
| S2 | 5318(1) | 1929(1) | 1655(1) | 33(1) |
| P1 | 3514(1) | 6852(1) | 2262(1) | 25(1) |
| P2 | 3615(1) | 5498(1) | 2109(1) | 27(1) |
| P3 | 1645(1) | 5487(1) | 2076(1) | 25(1) |
| P4 | -238(1) | 7144(1) | 2245(1) | 21(1) |
| P5 | 5525(1) | 228(1) | 2736(1) | 29(1) |
| P6 | 4610(1) | 466(1) | 3907(1) | 31(1) |
| P7 | 3824(1) | 1912(1) | 3867(1) | 28(1) |
| P8 | 4305(1) | 2914(1) | 2341(1) | 29(1) |
| C1 | 2563(3) | 7980(2) | 360(2) | 25(1) |
| C2 | 3425(3) | 7083(2) | 285(2) | 26(1) |
| C3 | 2630(4) | 6538(2) | 232(2) | 25(1) |
| C4 | 1279(4) | 7093(2) | 276(2) | 26(1) |
| C5 | 1233(3) | 7977(2) | 371(2) | 25(1) |
| C6 | 2963(4) | 8799(3) | 376(2) | 37(1) |
| C7 | 4912(4) | 6771(3) | 225(2) | 35(1) |
| C8 | 3140(4) | 5576(3) | 82(2) | 38(1) |
| C9 | 135(4) | 6817(3) | 183(2) | 38(1) |
| C10 | 21(4) | 8786(3) | 397(2) | 34(1) |
| C11 | 2389(4) | 5784(2) | 4147(2) | 25(1) |
| C12 | 1690(4) | 5214(2) | 4024(2) | 25(1) |
| C13 | 319(3) | 5721(2) | 4045(2) | 23(1) |
| C14 | 178(3) | 6615(2) | 4168(2) | 22(1) |
| C15 | 1455(3) | 6651(2) | 4234(2) | 23(1) |
| C16 | 3814(4) | 5477(3) | 4257(2) | 35(1) |
| C17 | 2288(4) | 4221(2) | 3974(2) | 33(1) |
| C18 | -765(4) | 5357(2) | 3983(2) | 29(1) |
| C19 | -1089(4) | 7373(2) | 4280(2) | 28(1) |

| | | | | |
|---|---|---|---|---|
| C20 | 1735(4) | 7438(3) | 4427(2) | 32(1) |
| C21 | 8188(3) | 1298(2) | 2567(2) | 27(1) |
| C22 | 7953(3) | 831(2) | 3340(2) | 26(1) |
| C23 | 7244(3) | 1495(2) | 3821(2) | 22(1) |
| C24 | 7037(3) | 2374(2) | 3345(2) | 23(1) |
| C25 | 7606(3) | 2251(2) | 2571(2) | 25(1) |
| C26 | 8986(4) | 870(3) | 1878(2) | 42(1) |
| C27 | 8452(4) | -182(2) | 3617(3) | 37(1) |
| C28 | 6874(4) | 1303(3) | 4682(2) | 32(1) |
| C29 | 6396(4) | 3275(2) | 3617(2) | 35(1) |
| C30 | 7690(4) | 3000(3) | 1884(2) | 40(1) |
| C31 | 1835(4) | 2212(3) | 1993(2) | 32(1) |
| C32 | 2387(4) | 1292(3) | 1868(2) | 32(1) |
| C33 | 2175(4) | 707(3) | 2588(2) | 31(1) |
| C34 | 1481(3) | 1268(3) | 3157(2) | 30(1) |
| C35 | 1259(4) | 2194(3) | 2793(2) | 30(1) |
| C36 | 1748(5) | 3062(3) | 1389(3) | 44(1) |
| C37 | 2996(5) | 1000(3) | 1096(3) | 46(2) |
| C38 | 2502(4) | -319(3) | 2714(3) | 45(1) |
| C39 | 966(4) | 941(3) | 3990(2) | 42(1) |
| C40 | 446(4) | 3017(3) | 3152(3) | 43(1) |

Table 7.72. Anisotropic displacement parameters ($Å^2 \times 10^3$) for **92c**. The anisotropic displacement factor exponent takes the form: $-2\pi^2[h^2a^{*2}U_{11} + ... + 2hka^*b^*U_{12}]$.

| **Atom** | $U_{11}$ | $U_{22}$ | $U_{33}$ | $U_{23}$ | $U_{13}$ | $U_{12}$ |
|---|---|---|---|---|---|---|
| I1 | 35(1) | 32(1) | 63(1) | -17(1) | -9(1) | -7(1) |
| I2 | 29(1) | 46(1) | 36(1) | -9(1) | -10(1) | -4(1) |
| I3 | 27(1) | 41(1) | 37(1) | -11(1) | -4(1) | -13(1) |
| Mo1 | 16(1) | 19(1) | 18(1) | -3(1) | -3(1) | -6(1) |
| Mo2 | 16(1) | 19(1) | 18(1) | -3(1) | -3(1) | -6(1) |
| Mo3 | 18(1) | 20(1) | 19(1) | -4(1) | -3(1) | -7(1) |
| Mo4 | 20(1) | 25(1) | 24(1) | -6(1) | -5(1) | -9(1) |
| Cu1 | 21(1) | 40(1) | 88(1) | -22(1) | -13(1) | -9(1) |
| Cu2 | 21(1) | 67(1) | 88(1) | -36(1) | -7(1) | -15(1) |
| Cu3 | 34(1) | 30(1) | 49(1) | -17(1) | -9(1) | -7(1) |
| S1 | 25(1) | 20(1) | 25(1) | -6(1) | -3(1) | -7(1) |
| S2 | 31(1) | 49(1) | 22(1) | -4(1) | -5(1) | -16(1) |
| P1 | 18(1) | 33(1) | 25(1) | -4(1) | -4(1) | -11(1) |
| P2 | 23(1) | 25(1) | 28(1) | -4(1) | -3(1) | -1(1) |
| P3 | 30(1) | 20(1) | 25(1) | -5(1) | -3(1) | -9(1) |
| P4 | 16(1) | 26(1) | 22(1) | -3(1) | -4(1) | -7(1) |
| P5 | 27(1) | 25(1) | 38(1) | -11(1) | -8(1) | -8(1) |

| | | | | | | |
|---|---|---|---|---|---|---|
| P6 | 33(1) | 33(1) | 29(1) | 3(1) | -7(1) | -17(1) |
| P7 | 23(1) | 38(1) | 28(1) | -14(1) | -1(1) | -10(1) |
| P8 | 28(1) | 22(1) | 39(1) | 1(1) | -14(1) | -8(1) |
| C1 | 26(2) | 27(2) | 18(2) | 3(1) | -2(1) | -10(1) |
| C2 | 24(2) | 34(2) | 15(1) | 0(1) | 1(1) | -8(1) |
| C3 | 28(2) | 30(2) | 16(2) | -5(1) | -2(1) | -8(1) |
| C4 | 29(2) | 32(2) | 18(2) | -5(1) | -5(1) | -8(1) |
| C5 | 27(2) | 26(2) | 18(2) | 3(1) | -5(1) | -7(1) |
| C6 | 41(2) | 33(2) | 39(2) | 2(2) | -7(2) | -18(2) |
| C7 | 25(2) | 41(2) | 31(2) | 0(2) | 1(2) | -8(2) |
| C8 | 42(2) | 36(2) | 35(2) | -15(2) | -3(2) | -5(2) |
| C9 | 35(2) | 56(2) | 32(2) | -13(2) | -11(2) | -18(2) |
| C10 | 31(2) | 31(2) | 32(2) | 1(1) | -8(2) | -2(2) |
| C11 | 29(2) | 29(2) | 20(2) | -1(1) | -9(1) | -9(1) |
| C12 | 30(2) | 25(2) | 19(2) | -1(1) | -4(1) | -10(1) |
| C13 | 25(2) | 26(2) | 17(1) | -2(1) | -2(1) | -10(1) |
| C14 | 23(2) | 25(2) | 17(1) | -2(1) | -2(1) | -8(1) |
| C15 | 28(2) | 28(2) | 17(1) | -3(1) | -5(1) | -11(1) |
| C16 | 28(2) | 38(2) | 38(2) | -3(2) | -11(2) | -7(2) |
| C17 | 42(2) | 25(2) | 32(2) | -1(1) | -9(2) | -11(2) |
| C18 | 32(2) | 33(2) | 25(2) | -3(1) | -1(2) | -17(2) |
| C19 | 26(2) | 30(2) | 27(2) | -7(1) | 0(1) | -7(1) |
| C20 | 36(2) | 35(2) | 30(2) | -10(2) | -7(2) | -14(2) |
| C21 | 17(2) | 37(2) | 29(2) | -11(1) | -4(1) | -8(1) |
| C22 | 20(2) | 27(2) | 30(2) | -6(1) | -8(1) | -6(1) |
| C23 | 21(2) | 25(2) | 25(2) | -4(1) | -7(1) | -9(1) |
| C24 | 21(2) | 23(2) | 29(2) | -5(1) | -6(1) | -10(1) |
| C25 | 21(2) | 32(2) | 26(2) | -3(1) | -5(1) | -15(1) |
| C26 | 27(2) | 60(3) | 40(2) | -25(2) | 4(2) | -10(2) |
| C27 | 32(2) | 27(2) | 51(2) | -7(2) | -16(2) | -1(2) |
| C28 | 36(2) | 43(2) | 24(2) | -3(2) | -9(2) | -19(2) |
| C29 | 35(2) | 28(2) | 49(2) | -15(2) | -10(2) | -9(2) |
| C30 | 42(2) | 49(2) | 32(2) | 6(2) | -7(2) | -27(2) |
| C31 | 26(2) | 41(2) | 34(2) | -5(2) | -16(2) | -12(2) |
| C32 | 26(2) | 45(2) | 32(2) | -15(2) | -9(2) | -13(2) |
| C33 | 23(2) | 37(2) | 43(2) | -12(2) | -8(2) | -15(2) |
| C34 | 20(2) | 40(2) | 37(2) | -8(2) | -7(2) | -14(2) |
| C35 | 20(2) | 37(2) | 38(2) | -12(2) | -8(2) | -8(1) |
| C36 | 41(2) | 53(3) | 44(2) | 6(2) | -23(2) | -20(2) |
| C37 | 46(3) | 67(3) | 39(2) | -27(2) | -8(2) | -21(2) |
| C38 | 36(2) | 35(2) | 72(3) | -15(2) | -12(2) | -16(2) |
| C39 | 30(2) | 61(3) | 39(2) | -7(2) | -3(2) | -23(2) |
| C40 | 27(2) | 48(2) | 60(3) | -24(2) | -10(2) | -5(2) |

## 7.3.25. $[Ag\{(Cp^*Mo)_2(\mu_3,\eta^3:\eta^3:\eta^1\text{-}P_3)(\mu,\eta^2\text{-}PS)\}\{(Cp^*Mo)_2(\mu_3,\eta^3:\eta^3:\eta^1\text{-}P_3)(\mu_3,\eta^2:\eta^2:\eta^1\text{-}PS)\}]_n[Al\{OC(CF_3)_3\}_4]_n \bullet 0.25nC_7H_8$ (**94**$\bullet 0.25nC_7H_8$)

Crystals of **94**$\bullet 0.25nC_7H_8$ were obtained by controlled diffusion of a toluene solution of $[(Cp^*Mo)_2(\mu,\eta^3\text{-}P_3)(\mu,\eta^2\text{-}PS)]$ **91** into a $CH_2Cl_2$ solution of $Ag[Al\{OC(CF_3)_3\}_4]$ at room temperature in the dark.

Table 7.73. Crystal data and structure refinement for **94**$\bullet 0.25nC_7H_8$.

| | |
|---|---|
| Empirical formula | $C_{115.5}H_{124}Ag_2Al_2F_{72}Mo_8O_8P_{16}S_4$ |
| Formula weight | 4669.13 g $mol^{-1}$ |
| Crystal size | $0.220 \times 0.120 \times 0.080$ mm |
| Crystal description | needle |
| Crystal colour | brown to black |
| Crystal system | orthorhombic |
| Space group | *Pnma* |
| Unit cell dimensions | $a$ = 45.899(2) Å, $\alpha$ = 90° |
| | $b$ = 33.486(1) Å, $\beta$ = 90° |
| | $c$ = 22.478(1) Å, $\gamma$ = 90° |
| Volume | 34548(2) $Å^3$ |
| Z, Calculated density | 8, 1.795 Mg $m^{-3}$ |
| Absorption coefficient | 1.112 $mm^{-1}$ |
| F(000) | 18312 |
| Measurement device type | STOE-IPDS |
| Measurement method | rotation |
| Temperature | 110(1) K |
| Wavelength | 0.71073 Å |
| Monochromator | graphite |
| $\theta$ range for data collection | 1.58 to 24.12° |
| Index ranges | $-35 \le h \le 52$, $-38 \le k \le 37$, $-23 \le l \le 17$ |
| Reflections collected / unique | 80287 / 24594 [R(int) = 0.1459] |
| Reflections greater I>2\s(I) | 10464 |
| Absorption correction | none |
| Refinement method | Full-matrix least-squares on $F^2$ |
| Data / restraints / parameters | 24594 / 0 / 929 |
| Goodness-of-fit on $F^2$ | 1.176 |
| Final R indices [I>2sigma(I)] | R1 = 0.1091, wR2 = 0.2666 |
| R indices (all data) | R1 = 0.1847, wR2 = 0.2875 |
| Largest diff. peak and hole | 2.563 and -1.663 e $Å^{-3}$ |

Table 7.74. Atomic coordinates ($\times 10^4$) and equivalent isotropic displacement parameters ($Å^2 \times 10^3$) for **94**•0.25n$C_7H_8$. $U_{eq}$ is defined as one third of the trace of the orthogonalised $U_{ij}$ tensor.

| **Atom** | **x** | **y** | **z** | $U_{eq}$ |
|---|---|---|---|---|
| Ag1 | 1683(1) | 5201(1) | 3997(1) | 38(1) |
| Ag2 | 3541(1) | 5226(1) | 2833(1) | 40(1) |
| Mo1 | 1261(1) | 4726(1) | 5801(1) | 49(1) |
| Mo2 | 1479(1) | 5455(1) | 5960(1) | 45(1) |
| Mo3 | 1174(1) | 4889(1) | 2326(1) | 44(1) |
| Mo4 | 953(1) | 5599(1) | 2609(1) | 49(1) |
| Mo5 | 2707(1) | 4960(1) | 3959(1) | 36(1) |
| Mo6 | 2603(1) | 5638(1) | 3377(1) | 37(1) |
| Mo7 | 4417(1) | 5118(1) | 3784(1) | 42(1) |
| Mo8 | 4284(1) | 5885(1) | 3933(1) | 42(1) |
| S1 | 1764(1) | 4840(2) | 6185(3) | 55(2) |
| S2 | 1332(2) | 5514(2) | 1841(3) | 57(2) |
| S3 | 2417(1) | 4983(1) | 3027(2) | 47(2) |
| S4 | 4597(1) | 5652(2) | 3119(3) | 58(2) |
| P1 | 1510(1) | 5101(2) | 5030(2) | 52(2) |
| P2 | 1069(2) | 5323(2) | 5156(3) | 61(2) |
| P3 | 969(1) | 5294(2) | 6088(3) | 60(2) |
| P4 | 1422(1) | 4974(2) | 6773(2) | 48(2) |
| P5 | 1353(1) | 5292(1) | 3137(2) | 43(2) |
| P6 | 946(1) | 5014(2) | 3388(3) | 51(2) |
| P7 | 671(1) | 4986(2) | 2607(3) | 58(2) |
| P8 | 918(2) | 5313(2) | 1593(3) | 63(2) |
| P9 | 2651(1) | 5603(1) | 4452(2) | 45(2) |
| P10 | 3074(1) | 5567(1) | 4054(3) | 48(2) |
| P11 | 3033(1) | 5237(1) | 3218(2) | 43(2) |
| P12 | 2216(1) | 5215(1) | 3791(2) | 39(2) |
| P13 | 3984(1) | 5420(1) | 3381(2) | 42(2) |
| P14 | 3930(1) | 5329(1) | 4336(2) | 44(2) |
| P15 | 4349(1) | 5422(1) | 4753(2) | 48(2) |
| P16 | 4785(1) | 5637(2) | 3956(3) | 56(2) |
| C1 | 900(7) | 4276(7) | 6040(14) | 85(8) |
| C2 | 1153(6) | 4112(6) | 6208(11) | 61(6) |
| C3 | 1313(7) | 4045(7) | 5707(14) | 83(8) |
| C4 | 1170(7) | 4179(7) | 5212(14) | 87(8) |
| C5 | 929(8) | 4302(8) | 5384(15) | 98(9) |
| C6 | 640(9) | 4404(9) | 6387(18) | 126(12) |
| C7 | 1228(8) | 3978(8) | 6825(15) | 107(10) |
| C8 | 1615(8) | 3837(8) | 5750(15) | 102(9) |
| C9 | 1289(10) | 4116(10) | 4563(18) | 133(12) |

| | | | | |
|---|---|---|---|---|
| C10 | 680(10) | 4490(11) | 4980(20) | 148(14) |
| C11 | 1580(5) | 6085(5) | 5583(9) | 47(5) |
| C12 | 1835(5) | 5924(5) | 5765(10) | 50(5) |
| C13 | 1836(5) | 5868(5) | 6385(10) | 54(5) |
| C14 | 1562(5) | 6002(5) | 6590(11) | 58(6) |
| C15 | 1397(6) | 6140(6) | 6105(11) | 64(6) |
| C16 | 1507(6) | 6226(6) | 4958(10) | 59(6) |
| C17 | 2099(6) | 5868(6) | 5372(11) | 69(6) |
| C18 | 2076(6) | 5724(6) | 6805(11) | 63(6) |
| C19 | 1463(7) | 6051(7) | 7233(13) | 86(8) |
| C20 | 1103(6) | 6346(6) | 6127(12) | 71(6) |
| C21 | 1479(5) | 4341(5) | 2504(9) | 48(5) |
| C22 | 1569(5) | 4515(5) | 1979(9) | 44(5) |
| C23 | 1341(5) | 4469(5) | 1567(10) | 48(5) |
| C24 | 1094(5) | 4276(5) | 1845(9) | 46(5) |
| C25 | 1185(5) | 4195(5) | 2428(10) | 57(5) |
| C26 | 1662(5) | 4281(5) | 3063(10) | 54(5) |
| C27 | 1864(6) | 4671(6) | 1842(11) | 67(6) |
| C28 | 1341(6) | 4589(6) | 913(11) | 69(6) |
| C29 | 830(6) | 4143(6) | 1571(11) | 64(6) |
| C30 | 1022(5) | 3944(5) | 2893(10) | 59(6) |
| C31 | 998(5) | 6245(5) | 2996(10) | 49(5) |
| C32 | 767(6) | 6050(6) | 3299(11) | 59(6) |
| C33 | 549(6) | 5962(6) | 2866(11) | 61(6) |
| C34 | 646(6) | 6113(6) | 2299(11) | 64(6) |
| C35 | 929(6) | 6278(6) | 2404(11) | 67(6) |
| C36 | 1262(6) | 6414(6) | 3293(11) | 65(6) |
| C37 | 747(6) | 5976(6) | 3939(11) | 71(6) |
| C38 | 252(7) | 5810(8) | 2978(14) | 98(9) |
| C39 | 476(7) | 6144(7) | 1732(14) | 92(8) |
| C40 | 1101(6) | 6501(6) | 1919(11) | 69(6) |
| C41 | 2999(6) | 4571(6) | 4594(11) | 63(6) |
| C42 | 2975(6) | 4366(6) | 4092(11) | 67(6) |
| C43 | 2663(5) | 4271(5) | 4040(10) | 58(6) |
| C44 | 2530(6) | 4433(6) | 4507(12) | 73(7) |
| C45 | 2724(5) | 4616(5) | 4863(10) | 58(5) |
| C46 | 3271(10) | 4726(11) | 4850(20) | 157(15) |
| C47 | 3145(9) | 4203(9) | 3628(17) | 123(11) |
| C48 | 2533(9) | 4029(9) | 3598(17) | 130(12) |
| C49 | 2209(13) | 4373(13) | 4690(20) | 184(19) |
| C50 | 2696(11) | 4804(11) | 5433(19) | 155(15) |
| C51 | 2610(5) | 6339(5) | 3340(9) | 45(5) |
| C52 | 2750(5) | 6195(5) | 2822(10) | 56(5) |

| | | | | |
|---|---|---|---|---|
| C53 | 2551(5) | 6000(5) | 2489(9) | 44(5) |
| C54 | 2282(5) | 5994(4) | 2776(9) | 41(4) |
| C55 | 2320(5) | 6215(5) | 3340(9) | 47(5) |
| C56 | 2736(6) | 6603(6) | 3836(12) | 76(7) |
| C57 | 3071(8) | 6259(8) | 2641(16) | 109(10) |
| C58 | 2591(6) | 5822(6) | 1886(11) | 74(7) |
| C59 | 1986(5) | 5851(6) | 2563(11) | 63(6) |
| C60 | 2090(6) | 6317(6) | 3782(11) | 69(6) |
| C61 | 4250(5) | 6530(5) | 3534(10) | 49(5) |
| C62 | 3971(5) | 6436(5) | 3819(10) | 58(5) |
| C63 | 4041(6) | 6388(6) | 4442(11) | 61(6) |
| C64 | 4344(6) | 6458(6) | 4532(11) | 63(6) |
| C65 | 4466(5) | 6536(5) | 3989(11) | 57(5) |
| C66 | 4302(6) | 6635(6) | 2897(12) | 73(7) |
| C67 | 3684(8) | 6419(8) | 3566(15) | 101(9) |
| C68 | 3813(7) | 6319(8) | 4927(14) | 99(9) |
| C69 | 4482(8) | 6453(8) | 5118(14) | 98(9) |
| C70 | 4774(6) | 6644(6) | 3857(12) | 69(6) |
| C71 | 4751(7) | 4602(7) | 3923(15) | 91(8) |
| C72 | 4438(6) | 4468(6) | 4116(12) | 68(6) |
| C73 | 4292(7) | 4451(7) | 3620(14) | 81(7) |
| C74 | 4423(8) | 4554(8) | 3210(15) | 90(8) |
| C75 | 4690(7) | 4653(6) | 3283(12) | 75(7) |
| C76 | 5001(16) | 4644(16) | 4370(30) | 250(30) |
| C77 | 4434(16) | 4361(16) | 4800(30) | 250(30) |
| C78 | 4012(18) | 4333(19) | 3400(40) | 280(40) |
| C79 | 4339(12) | 4581(13) | 2530(20) | 189(19) |
| C80 | 4940(14) | 4765(14) | 2900(30) | 220(20) |
| Al2 | 2177(2) | 7500 | 979(4) | 52(2) |
| F1 | 1728(6) | 6412(6) | 1171(11) | 143(7) |
| F6 | 2087(9) | 6146(10) | 702(17) | 209(12) |
| F10 | 1813(9) | 6125(9) | 328(16) | 215(12) |
| F22 | 2224(13) | 6519(13) | 1150(20) | 300(20) |
| O4 | 2179(7) | 7500 | 1770(13) | 93(8) |
| O5 | 2535(8) | 7500 | 818(14) | 102(9) |
| O6 | 2020(6) | 7097(5) | 719(11) | 110(7) |
| C84 | 2064(7) | 7500 | 2268(14) | 48(7) |
| C85 | 2820(20) | 7500 | 890(40) | 190(30) |
| C86 | 1903(7) | 6775(7) | 403(13) | 78(7) |
| C110 | 1976(17) | 6406(16) | 930(30) | 169(19) |
| C116 | 3550(10) | 7500 | 4260(20) | 86(11) |
| C117 | 3298(11) | 7500 | 3970(20) | 97(12) |
| C118 | 3301(9) | 7500 | 3340(17) | 71(9) |

| | | | | |
|---|---|---|---|---|
| C119 | 3562(10) | 7500 | 3020(20) | 82(11) |
| C120 | 3801(11) | 7500 | 3320(20) | 93(12) |
| C121 | 3821(11) | 7500 | 3960(20) | 89(11) |
| C122 | 4081(14) | 7500 | 4380(30) | 140(20) |
| Al1 | 2634(2) | 7500 | 6463(4) | 48(2) |
| F47 | 2021(9) | 7130(9) | 7568(18) | 210(12) |
| O1 | 2494(7) | 7500 | 7171(14) | 92(8) |
| O2 | 2367(8) | 7500 | 5921(15) | 112(9) |
| O3 | 2833(5) | 7071(5) | 6387(9) | 92(6) |
| C82 | 2129(7) | 7500 | 5652(14) | 46(7) |
| C83 | 3016(8) | 6769(8) | 6226(16) | 103(9) |
| C111 | 2413(13) | 7334(11) | 7670(20) | 180(20) |
| C115 | 2210(15) | 6960(15) | 7920(30) | 175(19) |
| Al3 | 413(3) | 7500 | 8369(6) | 78(3) |
| O7 | 422(12) | 7500 | 9190(20) | 182(16) |
| O8 | 762(9) | 7500 | 8093(15) | 112(9) |
| O9 | 223(9) | 7082(9) | 8113(17) | 183(12) |
| C88 | 1008(16) | 7500 | 7880(30) | 139(19) |
| C89 | 85(9) | 6754(9) | 7836(17) | 112(10) |
| C114 | 310(20) | 6560(20) | 7300(40) | 310(40) |
| Al4 | -146(4) | 7500 | 4353(7) | 101(4) |
| O11 | 74(10) | 7500 | 3769(19) | 141(12) |
| O12 | -70(7) | 7091(7) | 4691(14) | 148(9) |
| C91 | 176(9) | 7500 | 3240(18) | 73(10) |
| C92 | -28(15) | 6719(15) | 5100(30) | 210(20) |
| F16 | 3439(8) | 6921(9) | 6110(17) | 203(12) |
| F23 | 3399(12) | 7234(10) | 5740(20) | 263(19) |
| F31 | 3455(9) | 6425(10) | 6214(18) | 232(14) |
| F45 | 3338(12) | 6600(14) | 6850(20) | 290(20) |
| F49 | 3370(7) | 6988(8) | 6812(14) | 179(10) |
| F3 | 1881(7) | 6896(7) | 2475(14) | 180(9) |
| F13 | 2191(8) | 6816(7) | 2169(14) | 197(11) |
| F14 | 1689(11) | 7131(10) | 2000(20) | 250(15) |
| F41 | -253(13) | 6445(12) | 4270(20) | 302(19) |
| F46 | 125(9) | 6431(9) | 4234(16) | 223(13) |
| C123 | -23(15) | 6183(16) | 4720(30) | 200(20) |
| F2 | 1710(7) | 7091(6) | 5738(13) | 169(9) |
| F4 | 2417(7) | 7182(6) | 2806(13) | 169(9) |
| F5 | 2124(10) | 7500 | 8531(19) | 184(14) |
| F7 | 2058(9) | 6909(9) | 6101(17) | 226(13) |
| F8 | 2140(10) | 6875(11) | 5280(20) | 279(17) |
| F9 | 455(9) | 6947(9) | 3279(16) | 221(13) |
| F11 | 2797(9) | 6918(9) | 1265(17) | 225(13) |

| | | | | |
|---|---|---|---|---|
| F12 | 1096(9) | 6951(9) | 8341(17) | 225(13) |
| F15 | 2975(10) | 6265(10) | 6927(18) | 250(15) |
| F17 | 16(9) | 6943(9) | 2867(17) | 231(13) |
| F18 | 598(11) | 7500 | 3900(20) | 203(16) |
| F19 | 2921(15) | 7500 | 7920(30) | 280(20) |
| F20 | 2538(8) | 7103(8) | 8420(16) | 206(11) |
| F21 | -901(14) | 7500 | 5070(30) | 270(20) |
| F24 | 2358(10) | 6564(10) | 29(19) | 254(15) |
| F25 | 3105(9) | 6731(9) | 5306(17) | 235(14) |
| F26 | 3092(8) | 6161(8) | 5883(15) | 207(11) |
| F27 | 423(12) | 7117(11) | 10380(20) | 302(19) |
| F28 | 2966(9) | 7202(8) | 5298(17) | 207(12) |
| F29 | 2669(7) | 6598(8) | 5436(14) | 198(11) |
| F30 | -911(9) | 6939(9) | 4541(17) | 239(13) |
| F32 | 2895(15) | 7500 | -180(30) | 280(20) |
| F33 | 13(13) | 7500 | 10210(20) | 240(20) |
| F34 | 2203(8) | 7100(7) | -338(15) | 203(11) |
| F35 | 2053(10) | 6576(10) | -498(19) | 259(15) |
| F36 | -177(8) | 7500 | 2510(16) | 156(11) |
| F37 | 2297(16) | 7500 | 4810(30) | 290(30) |
| F38 | -795(13) | 7500 | 3030(30) | 250(20) |
| F39 | 181(9) | 6383(9) | 8616(16) | 230(13) |
| F40 | 1465(11) | 7023(11) | 770(20) | 281(17) |
| F42 | 2565(12) | 6541(13) | 6890(20) | 310(20) |
| F43 | -1121(10) | 7123(9) | 3465(18) | 236(14) |
| F44 | -631(13) | 7006(12) | 3550(20) | 300(20) |
| F48 | 1298(13) | 7187(11) | 7360(20) | 290(20) |
| F50 | 2262(3) | 6824(3) | 7186(7) | 132(4) |
| F51 | 2132(17) | 7500 | 3300(30) | 300(30) |
| F52 | 207(14) | 5280(13) | 5060(20) | 340(20) |
| F53 | 2692(10) | 6297(10) | 6179(19) | 255(15) |
| F54 | 952(14) | 6844(14) | 7590(30) | 330(20) |
| C90 | -778(13) | 7500 | 4040(30) | 125(16) |
| C112 | 2749(9) | 6835(9) | 7734(17) | 117(10) |
| C113 | -192(12) | 7031(12) | 7230(20) | 164(16) |

Table 7.75. Anisotropic displacement parameters ($Å^2 \times 10^3$) for **94**•0.25n$C_7H_8$. The anisotropic displacement factor exponent takes the form: $-2\pi^2[h^2a^{*2}U_{11} + ... + 2hka^*b^*U_{12}]$.

| **Atom** | $U_{11}$ | $U_{22}$ | $U_{33}$ | $U_{23}$ | $U_{13}$ | $U_{12}$ |
|---|---|---|---|---|---|---|
| Ag1 | 35(1) | 50(1) | 29(1) | 1(1) | -2(1) | -1(1) |
| Ag2 | 34(1) | 56(1) | 31(1) | 0(1) | -2(1) | 0(1) |
| Mo1 | 50(1) | 67(1) | 32(1) | 6(1) | 3(1) | -3(1) |
| Mo2 | 45(1) | 59(1) | 32(1) | 5(1) | 1(1) | 5(1) |
| Mo3 | 43(1) | 55(1) | 34(1) | 4(1) | -9(1) | -7(1) |
| Mo4 | 40(1) | 57(1) | 50(1) | 9(1) | -12(1) | -3(1) |
| Mo5 | 32(1) | 46(1) | 31(1) | 4(1) | -3(1) | -1(1) |
| Mo6 | 35(1) | 48(1) | 30(1) | 6(1) | -2(1) | -1(1) |
| Mo7 | 30(1) | 62(1) | 34(1) | 2(1) | -1(1) | 1(1) |
| Mo8 | 33(1) | 59(1) | 34(1) | 1(1) | 0(1) | -3(1) |
| S1 | 49(4) | 69(3) | 48(3) | 2(2) | 2(3) | 10(3) |
| S2 | 63(4) | 66(3) | 43(3) | 11(2) | -5(3) | -13(3) |
| S3 | 45(4) | 56(3) | 41(3) | 2(2) | -8(3) | -3(2) |
| S4 | 49(4) | 74(3) | 51(4) | 10(3) | 11(3) | 2(3) |
| P1 | 55(4) | 70(3) | 31(3) | 2(2) | 1(3) | -1(3) |
| P2 | 59(5) | 74(3) | 51(4) | 10(3) | -5(4) | 4(3) |
| P3 | 40(4) | 83(4) | 58(4) | 5(3) | 3(4) | 7(3) |
| P4 | 48(4) | 68(3) | 29(3) | 8(2) | 5(3) | 1(3) |
| P5 | 36(3) | 55(3) | 38(3) | 4(2) | -4(3) | 0(2) |
| P6 | 44(4) | 63(3) | 47(3) | 9(3) | 4(3) | 0(3) |
| P7 | 40(4) | 64(3) | 69(4) | 9(3) | -11(4) | -9(3) |
| P8 | 71(5) | 72(3) | 47(4) | 13(3) | -21(4) | -7(3) |
| P9 | 47(4) | 48(2) | 40(3) | 1(2) | -2(3) | 0(2) |
| P10 | 40(4) | 54(3) | 50(4) | 6(2) | -11(3) | -3(2) |
| P11 | 31(3) | 58(3) | 41(3) | 7(2) | -1(3) | 3(2) |
| P12 | 32(3) | 53(2) | 33(3) | 4(2) | -6(3) | -5(2) |
| P13 | 31(3) | 60(3) | 34(3) | -2(2) | -5(3) | -2(2) |
| P14 | 38(3) | 61(3) | 33(3) | 2(2) | 4(3) | -3(2) |
| P15 | 49(4) | 62(3) | 34(3) | 3(2) | -3(3) | -2(2) |
| P16 | 26(3) | 77(3) | 64(4) | 6(3) | -1(3) | -8(2) |

# 8. Acknowledgements

At this point, I would like to express my gratitude to:

- Prof. Manfred Scheer for giving me the opportunity to work in his research group on such an interesting and well-supervised project. The entire experience was highly rewarding, both academically and personally.
- Prof. Henri Brunner and co-workers for the warm welcome and invaluable assistance, which ensured a smooth transition from Karlsruhe to Regensburg.
- My parents, Helen and Gregory, and my sister, Rebekah. Without their unconditional support, the pursuit of a chemical career would have been unthinkable.
- Helene and Helmut Neumann for offering me a home away from home.
- Dr. Manfred Zabel and Ms. Sabine Stemfhuber for their patience in measuring and solving the 'exemplary' crystals I delivered.
- The NMR departments of the universities of Karlsruhe (Dr. Eberhard Matern, Ms. Helga Berberich, Ms. Sibylle Schneider) and Regensburg (Dr. Thomas Burgemeister, Mr. Fritz Kastner, Ms. Annette Schramm, Ms. Georgine Stühler) for their competent and continuous support. I am especially thankful to Mr. Kastner for pushing the AVANCE400 to its limits.
- The MS departments of the universities of Karlsruhe (Mr. Dieter Müller) and Regensburg (Dr. K. K. Mayer, Mr. Josef Kiermaier, Mr. Wolfgang Söllner) for their skill and cooperation. I am deeply indebted to Mr. Kiermaier for not banning me from the TSQ 7000 and happily accepting my teflonate samples.
- The microanalytical laboratories of the universities of Karlsruhe (Ms. Sabine Lude) and Regensburg (Mr. H. Schüller, Ms. B. Baumann, Ms. W. Krutina) for their precision and attention to detail.
- Prof. Ingo Krossing and co-workers (in particular, Marcin, Ines) for theoretical calculations, much assistance with the silver teflonate salt and the enjoyable company during the Karlsruhe era.
- Dr. Marek Sierka for theoretical calculations.

- Prof. Hellmut Eckert and co-workers (Dr. Gunther Brunklaus, Dr. Long Zhang) for the measurement of MAS NMR spectra in Münster.
- Prof. Eike Brunner and Dipl. Phys. Christian Gröger for the measurement of MAS NMR spectra in Regensburg.
- Dr. Joachim Wachter for the $As_n$- and $P_mS_n$-complexes and for generally looking after us.
- The good people in Supplies and in the Electronics, Mechanical and Glass workshops of the universities of Karlsruhe and Regensburg.
- Members of the Scheer group: Petra Lugauer for much technical assistance and garden produce, Walter Meier (the master of 'Leberkäse'), Manfred 'Musch' Muschiol (the Crystal King), Barbara Treitinger, Karin Kilgert, Elisabeth 'Lizzy' Ederer, Naziha Muschiol, Thomas 'Schotti' Schottenhammer for not missing a party, Ariane 'Ari' Adolf for being a good friend and flatmate, Ulf Vogel for his expertise, good flatmate properties and pronounced multicultural appreciation, the highly reliable Karl-Christian 'Kalle' Schwan (the Karlsruhe Administrator), Christian Kuntz for taking on the solvent-box, for his bicycle skills, for amusing stories concerning the Golf 4, seeded bread and organic beer, and for being an all-round good lad, Alexander 'Alex' Ebner for keeping a photographic record of the most embarrassing moments of everybody, Andreas 'Andi' Lange (the Regensburg Administrator) for keeping the 'solvents' full, Roger 'Der Organisator' Merkle for, well, organising stuff, Brian Wegley for his quiet, subtly humorous character and for buying a laser printer, which he let me use for guess what, Shining Deng and the secret of eternal youth, Kathrin Bratz for making the best Mo2P2, Christian Keck, Miriam Eberl for not training Karate on us and for eating lunch at a relaxed rate, Cornelia 'Conny' Dreher for revealing the benefits of living close to the Czech border, Hannes Krauss for being a nice guy, Christian Eisenhut for demonstrating that the microwave works, on a daily basis, Andrea Schindler, Michael Pronold, Fabian Dielmann, Stefan Almstätter, Patrick Schwarz.
- Former members of the Scheer group: 'Graf' Gabor Balazs for being a good flatmate, friend, chemist and marathon running-partner at all times, Brian Johnson for discussions and for visiting me in the hospital after my shoulder operation, Daniel Himmel for having a father in the wine

business, Dr. Sergei Konchenko for chemical advice and gifts, as well as international musical exchanges, Dr. Alexander Virovets for crystallographic rescue, Dr. Rajiv Trivedi for the tea breaks, Dr. Shouzhong Zhan, Dr. Junfeng Bai, Johann, Nikolai, Anton.

- Prof. Dieter Fenske, Prof. Hansgeorg Schnöckel, Dr. Udo Radius, Dr. Stephie Dehnen and their co-workers and former co-workers (particularly, Sven Koenig, Christian Nietschke, Christian Zimmermann, Maryam Shafaei-Fallah, Donna Nikolova, Alex Rothenberg, Markus Wunder, Bettina Bechlars, Jürgen Zeller, Thomas Schaub, Simon Dürr, Jean Vollet, Ralf Burgert, Katerina Weiss, Gregor Stösser, Jochen Steiner) for the pleasant time in Karlsruhe. Many thanks to Ralf and Katerina for the ESI-MS spectra.
- Florian Krauss and Thomas Rossmeier for interesting discussions about chemistry, politics, the future…
- Laurent Chouvet, Burcu Panya, Markus Busch, Marianne Neumann and Dominik Harz for their friendship through the years.

Last but not least, I would like to thank Rosi for her patience, understanding, support and artistic talent and for being a part of my life.